

2

AFWAL-TR-86- 2024



ASSESSMENT OF REMAINING LUBRICANT LIFE

Robert E. Kauffman  
Wendell E. Rhine

University of Dayton Research Institute  
300 College Park Avenue  
Dayton, OH 45469-0001

DTIC  
SELECTED  
MAR 03 1987  
S D

November 1986

Final Report for Period 15 November 1983 to 15 December 1985

Approved for Public Release; Distribution unlimited

AD-A177 186

DTIC FILE COPY


AERO PROPULSION LABORATORY  
AIR FORCE WRIGHT AERONAUTICAL LABORATORIES  
AIR FORCE SYSTEMS COMMAND  
WRIGHT-PATTERSON AIR FORCE BASE, OHIO 45433-6563


87 3 2 024

NOTICE

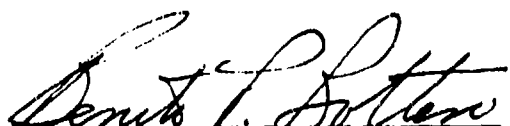
When Government drawings, specifications, or other data are used for any purpose other than in connection with a definitely related Government procurement operation, the United States Government thereby incurs no responsibility nor any obligation whatsoever; and the fact that the Government may have formulated, furnished, or in any way supplied the said drawings, specifications, or other data, is not to be regarded by implication or otherwise as in any manner licensing the holder or any other person or corporation, or conveying any rights or permission to manufacture, use, or sell any patented invention that may in any way be related thereto.

This technical report has been reviewed and is approved for publication.

  
\_\_\_\_\_  
G. A. BEANE, IV  
Project Engineer  
Lubrication Branch

  
\_\_\_\_\_  
HOWARD F. JONES  
Chief, Lubrication Branch  
Fuels and Lubrication Division

FOR THE COMMANDER:

  
\_\_\_\_\_  
BENITO P. BOTTERI, Assistant Chief  
Fuels and Lubrication Division  
Aero Propulsion Laboratory

If your address has changed, if you wish to be removed from our mailing list, or if addressee is no longer employed by your organization, please notify AFWAL/POSL, Wright-Patterson Air Force Base, Ohio 45433-6563 to help maintain a current mailing list.

Copies of this report should not be returned unless return is required by security considerations, contractual obligations, or notice on a specific document.

REPORT DOCUMENTATION PAGE				
1a. REPORT SECURITY CLASSIFICATION <b>UNCLASSIFIED</b>		1b. RESTRICTIVE MARKINGS <b>AD-A177186</b>		
2a. SECURITY CLASSIFICATION AUTHORITY		3. DISTRIBUTION/AVAILABILITY OF REPORT Approved for public release; Distribution unlimited		
2b. DECLASSIFICATION/DOWNGRADING SCHEDULE				
4. PERFORMING ORGANIZATION REPORT NUMBER(S)  UDRI-TR-86-14		5. MONITORING ORGANIZATION REPORT NUMBER(S)  AFWAL-TR-86-2024		
6a. NAME OF PERFORMING ORGANIZATION University of Dayton Research Institute		6b. OFFICE SYMBOL (If applicable)	7a. NAME OF MONITORING ORGANIZATION  Aero Propulsion Laboratory (AFWAL/POSL)	
6c. ADDRESS (City, State and ZIP Code) 300 College Park Drive Dayton, OH 45469		7b. ADDRESS (City, State and ZIP Code) Air Force Wright Aeronautical Laboratories Wright-Patterson Air Force Base, OH 45433-6503		
8a. NAME OF FUNDING/SPONSORING ORGANIZATION Aero Propulsion Laboratory		8b. OFFICE SYMBOL (If applicable) AFWAL/POSL	8. PROCUREMENT INSTRUMENT IDENTIFICATION NUMBER  F33615-83-C-2317	
8c. ADDRESS (City, State and ZIP Code) Air Force Wright Aeronautical Laboratories Wright-Patterson Air Force Base, OH 45433-6563		10. SOURCE OF FUNDING NOS.		
		PROGRAM ELEMENT NO. 62203F	PROJECT NO. 3048	TASK NO. 06
				WORK UNIT NO. 31
11. TITLE (Include Security Classification) Assessment of Remaining Lubricant Life				
12. PERSONAL AUTHOR(S) Robert E. Krauffman and Wendell E. Rhine				
13a. TYPE OF REPORT Final Technical		13b. TIME COVERED FROM Nov 83 TO Dec 85	14. DATE OF REPORT (Yr., Mo., Day) November 1986	15. PAGE COUNT 354
16. SUPPLEMENTARY NOTATION				
17. COSATI CODES			18. SUBJECT TERMS (Continue on reverse if necessary and identify by block number)	
FIELD	GROUP	SUB. GR.		
11	08		Remaining Lubricant Life Antioxidant Capacity	
21	05		Oil Analysis Turbine Engine Lubricating Oils	
			Cyclic Voltammetry Differential Scanning Calorimetry	
19. ABSTRACT (Continue on reverse if necessary and identify by block number)				
<p>An investigation was conducted in order to develop a remaining lubricant life assessment test (RLLAT) for MIL-L-7808 lubricating oils. The RLLAT would enable the Air Force to reduce material and labor costs by eliminating scheduled oil changes. The investigation was performed in three tasks.</p> <p>In Task 1 analytical procedures capable of performing remaining lubricant life (RLL) assessments of MIL-L-7808 lubricating oils were identified and evaluated. Of the numerous analytical procedures identified in Task 1, procedures based on cyclic voltammetry, differential scanning calorimetry (DSC), and chemical stressing were determined to be the best candidates for development into a RLLAT.</p> <p>In Task 2, a RLLAT was developed from the reductive-cyclic voltammetric (RCV) technique and a microcomputer based data acquisition system. The RLLAT based on the RCV technique and data acquisition system (RLLAT-RCV) was rapid (total analysis time less than 30</p>				
20. DISTRIBUTION/AVAILABILITY OF ABSTRACT UNCLASSIFIED/UNLIMITED <input type="checkbox"/> SAME AS RPT. <input checked="" type="checkbox"/> DTIC USERS <input type="checkbox"/>			21. ABSTRACT SECURITY CLASSIFICATION Unclassified	
22a. NAME OF RESPONSIBLE INDIVIDUAL G. A. Beane IV		22b. TELEPHONE NUMBER (Include Area Code) 513-255-7463	22c. OFFICE SYMBOL AFWAL/POSL	

18. (Concluded)  
Hydroperoxide Decomposition                      Free Radical Traps

19. (Concluded)  
seconds), inexpensive (less than \$3,000), and base-level in operation and RLL assessments. The development of RLLAT from the DSC techniques were limited by the high instrumental costs (greater than \$20,000). The development of RLLAT from the chemical stressing techniques were limited by the toxicity and instability of the required reagents and the difficult interpretation of the techniques' results.

In Task 3, the applicability of the RLLAT-RCV to different types of lubricating oils was demonstrated. The results in Task 3 also showed that the RLLAT-RCV could be used to detect engines experiencing severe wear in addition to being used to eliminate scheduled oil changes.

FOREWORD

This report describes the research conducted by personnel of the University of Dayton Research Institute on Contract No. F33615-83-C-2317 entitled Assessment of Remaining Lubricant Life. The work reported herein was performed during the period of 15 November 1983 to 15 December 1985 and was supported by the Aero Propulsion Laboratory, Air Force Wright Aeronautical Labs, Wright Patterson Air Force Base, Ohio. The effort was monitored by Mr. G.A. Beane IV of the Aero Propulsion Laboratory whose advice and direction were significant in the successful completion of this effort.

The authors are indebted to Mr. Michael A. Keller and James D. Wolf of the Research Institute for their assistance in characterizing the stressed oil samples and in writing the computer program used to control the data acquisition system.

Accession For	
NTIS CRA&I	<input checked="" type="checkbox"/>
DTIC TAB	<input type="checkbox"/>
Unannounced	<input type="checkbox"/>
Justification	
By	
Distribution/	
Availability Codes	
Dist	Availability or Special
A-1	



## TABLE OF CONTENTS

SECTION	PAGE
I INTRODUCTION	1
II RESULTS AND DISCUSSION	3
1. TASK 1. IDENTIFICATION OF REMAINING LUBRICANT LIFE ASSESSMENT TEST CANDIDATES	3
a. Introduction	3
b. Voltammetric Techniques	4
(1) Introduction	4
(2) Effect of Solvent Type	10
(3) Effect of Working Electrode	18
(4) Effect of Electrolyte	18
(5) Effect of Scan Rate	18
(6) Effect of Additives	20
(7) Effect of Formulation	20
(8) Calibration Curves of Antioxidants in MIL-L-7808 Oil	24
(9) Effect of Successive Scans on Voltammograms of MIL-L-7808 Oils	27
(10) Effect of Oxidation Products	27
(11) Effect of Organic Peroxides on the Voltammograms of the MIL-L- 7808 Lubricating Oils	38
(12) Effect of Pyridine on the Voltammograms of the MIL-L-7808 Lubricating Oils	38
(13) Summary of the Voltammetric Techniques	47
c. Thermal Stressing Techniques	47
(1) Introduction	47
(2) Effect of Sample Size	49
(3) Effect of Analysis Temperature	51
(4) Summary of HP-DSC Technique	54
d. Chemical Stressing Techniques	54
(1) Introduction	54
(2) Colorimetric Method	54
(a) Introduction	54
(b) Effect of BDN Solution/Cumene Hydroperoxide Ratio	58
(c) Effect of Sample Size	59
(d) Effect of Antioxidant Type	61
(e) Effect of Formulation	63
(f) Analysis of Laboratory Stressed TEL-4005 Oil Samples	63
(g) Summary of Colorimetric Method	66

TABLE OF CONTENTS (CONTINUED)

SECTION		PAGE
II	(3) Modified Ford Method	66
	(a) Introduction	66
	(b) Effect of Type of Easily Oxidizable Substrate	69
	(c) Effect of Hexadecane	71
	(d) Effect of AIBN Solution Concentration	73
	(e) Effect of AIBN Solution and Benzaldehyde Quantities	73
	(f) Effect of Oxygen Purge	73
	(g) Effect of Oil Sample Size	74
	(h) Modified Ford Method	74
	(i) Effect of Time on the AIBN Solution	77
	(j) Effect of Formulation	79
	(k) Analysis of Thermally Oxidized TEL-4005 Oil Samples	79
	(l) Summary of the Modified Ford Method	83
e.	Hydroperoxide Measurements	83
	(1) Introduction	83
	(2) Iodine Liberation Techniques	86
	(3) Cyclic Voltammetric Techniques	88
	(a) Introduction	88
	(b) Thin Film Mercury Working Electrode	88
	(c) Glassy Carbon Working Electrode	89
	(4) Summary of Alkyl Hydroperoxide Detection Techniques	94
f.	Permanganatometric Method	94
	(1) Introduction	94
	(2) Effect of $KMnO_4$ Concentration	95
	(3) Effect of Reaction Time	96
	(4) Summary of Permanganatometric Method	96
g.	Electrical Property Measurements	97
	(1) Introduction	97
	(2) Comparison of the Electrical Property Measuring Systems Used by UDRI and the COBRA	98
	(3) Effect of Oxidative Degradation	100
	(4) Relationship Between $V_I/V$ and COBRA Readings	100
	(5) Effect of Formulation	102
	(6) Summary of Electrical Property Measurements	102

TABLE OF CONTENTS (CONTINUED)

SECTION		PAGE
II	h. Fluorescence Spectrophotometry	105
	(1) Introduction	105
	(2) Effect of Formulation	105
	(3) Effect of Oxidative Degradation	107
	(4) Summary of Fluorescence Spectrophotometry	107
	i. Comparison of Identified Analytical Procedures	109
2.	TASK 2. DEVELOPMENT OF REMAINING LUBRICANT LIFE ASSESSMENT TEST CANDIDATES	111
	a. Introduction	111
	b. Voltammetric Techniques	113
	(1) Introduction	113
	(2) Cyclic Voltammetric Analyses of the MIL-L-7808 Oils	114
	(3) Effect of Dilution Solvent Amount	124
	(4) Effect of Electrode Configuration	124
	(5) Effect of Antioxidant Type	125
	(6) Reductive-Cyclic Voltammetric Analyses of the MIL-L-7808 Oils	129
	(7) Linearizing the Reductive-Cyclic Voltammetric Plots	129
	(8) Effect of Organic Base	137
	(9) Effect of Successive Scanning Cycles	142
	(10) Determination of the Mathematical Relationship Between the RLL of MIL-L-7808 Oils and the RCV Results	152
	(11) Effect of Formulation	158
	(12) Summary of the Reductive-Cyclic Voltammetric Technique	158
	c. Thermal Stressing Technique	160
	(1) Introduction	160
	(2) High Pressure-Differential Scanning Calorimetry	160
	(a) Introduction	160
	(b) High Pressure-Differential Scanning Calorimetric Analyses of the MIL-L-7808 Oils	162
	(c) Linearizing the HP-DSC Onset of Oxidation Time Plots	171

TABLE OF CONTENTS (CONTINUED)

SECTION	PAGE
II	
(d) Linearizing the HP-DSC Onset of Reaction Time Plots	171
(3) Sealed Pan-Differential Scanning Calorimetry	178
(a) Introduction	178
(b) Effect of Sample Pan	178
(c) Effect of Sample Size	179
(d) Effect of Oxidizing Substances	182
(e) Effect of Oxidizing Atmosphere	184
(f) Effect of Initial Temperature	188
(g) Sealed Pan-Differential Scanning Calorimetric Analyses of the MIL-L-7808 Oils	188
(h) Linearizing the SP-DSC Onset of Oxidation Time Plots	199
(4) Comparison of the SP-DSC and HP-DSC Techniques	201
d. Chemical Stressing Technique	203
(1) Introduction	203
(2) Effect of Sample Temperature	204
(3) Effect of Cumene Hydroperoxide Concentration	206
(4) Colorimetric Analyses of MIL-L- 7808 Oils	207
(5) Linearizing the Colorimetric BDN Decoloration Induction Time Plots	214
e. Comparison of Remaining Lubricant Life Assessment Test Candidates	217
3. TASK 3. EVALUATION OF REMAINING LUBRICANT LIFE ASSESSMENT TEST BASED ON THE REDUCTIVE-CYCLIC VOLTAMMETRIC TECHNIQUE	219
a. Introduction	219
b. Effect of Stressing Temperature	219
c. Effect of Oil Formulation	220
d. Analysis of Used MIL-L-7808 Oils	223
e. Analysis of Authentic Used MIL-L- 7808 and MIL-L-23699 Oils	231
f. Effect of Oil Addition	235
g. Summary of RLLAT Based on RCV	242

TABLE OF CONTENTS (CONCLUDED)

SECTION	PAGE
III CONCLUSIONS AND RECOMMENDATIONS	245
APPENDIX A: PREPARATION AND CHARACTERIZATION OF STRESSED MIL-L-7808 OIL SAMPLES	248
APPENDIX B: EQUIPMENT AND PROCEDURES	301
REFERENCES	320

## LIST OF ILLUSTRATIONS

FIGURE		PAGE
1	Typical Triangular Waveform (a) Used by Cyclic Voltammetry and a Typical Current-Potential Curve (Voltammogram) (b) Produced by Cyclic Voltammetry (Reproduced from Reference 1). E = Potential and i = Current.	8
2	Voltammograms for the Basestock (A) and Fresh TEL-4005 Oil (B) in Acetonitrile with a Platinum Working Electrode.	11
3	Voltammograms of the Fresh TEL-4005 and an Used MIL-L-7808 Oil Sample (J79 Engine; 450 Hours Since Oil Change) in Acetonitrile with a Platinum Working Electrode.	12
4	Voltammograms of 100 and 200 $\mu$ l Samples of the Fresh TEL-4005 Oil in Acetonitrile with a Platinum Working Electrode.	14
5	Voltammogram of a 200 $\mu$ l Sample of the Fresh TEL-4005 Oil in Propylene Carbonate with a Platinum Working Electrode.	15
6	Voltammogram of a 200 $\mu$ l Sample of the Fresh TEL-4005 Oil in Methanol with a Platinum Working Electrode.	16
7	Voltammogram of a 200 $\mu$ l Sample of the Fresh TEL-4005 Oil in Acetone with a Platinum Working Electrode.	17
8	Effect of the Working Electrode Type on the Voltammogram of the Fresh TEL-4005 Oil: GCE=Glassy Carbon Electrode, PTE=Platinum Electrode, and AUE=Gold Electrode.	19
9	Effect of the Scan Rate (mV/sec) on the Voltammogram of the Fresh TEL-4005 Oil in Acetone with a Glassy Carbon Working Electrode.	21
10	Voltammograms of the Fresh TEL-4001, TEL-4002, and TEL-4003 Lubricating Oils in Acetone with a Glassy Carbon Working Electrode.	22
11	Voltammograms of the Fresh TEL-4004, TEL-4005, and TEL-4006 Lubricating Oils in Acetone with a Glassy Carbon Working Electrode.	23

LIST OF ILLUSTRATIONS (CONTINUED)

FIGURE		PAGE
12	Effect of Successive Additions of 1% DODPA and PANA Solutions on the Voltammograms Produced by a Glassy Carbon Working Electrode in Acetone.	25
13	Calibration Curves for the Oxidation and Reduction Waves of PANA and DODPA.	26
14	First and Fifth Scan Voltammograms of the Fresh TEL-4001 and TEL-4002 Oils in Acetone with a Glassy Carbon Working Electrode.	28
15	First and Fifth Scan Voltammograms of the Fresh TEL-4003 and TEL-4004 Oils in Acetone with a Glassy Carbon Working Electrode.	29
16	First and Fifth Scan Voltammograms of the Fresh TEL-4005 and TEL-4006 Oils in Acetone with a Glassy Carbon Working Electrode.	30
17	Effect of Successive Additions of a 1% PANA Solution in the Presence of 1% DODPA and 0.3% PANA on the First and Fifth Scan Voltammograms Produced by a Glassy Carbon Working Electrode in Acetone.	31
18	Voltammograms of Fresh and Stressed TEL-4005 Oils in Acetone with a Glassy Carbon Working Electrode.	33
19	First and Fifth Scan Voltammograms of 24 Hours Stressed TEL-4005 Oil in Acetone with a Glassy Carbon Working Electrode.	34
20	First and Fifth Scan Voltammograms of 48 and 72 Hours Stressed TEL-4005 Oils in Acetone with a Glassy Carbon Working Electrode.	35
21	First and Fifth Scan Voltammograms of 96-168 Hours Stressed TEL-4005 Oils in Acetone with a Glassy Carbon Working Electrode.	36
22	First and Fifth Scan Voltammograms of 192-240 Hours Stressed TEL-4005 Oils in Acetone with a Glassy Carbon Working Electrode.	37
23	Effect of Benzoyl Peroxide on the Voltammogram of the Fresh TEL-4005 Oil in Acetone Using a Glassy Carbon Working Electrode.	39

LIST OF ILLUSTRATIONS (CONTINUED)

FIGURE		PAGE
24	Effect of Benzoyl Peroxide on the Voltammogram of the Fresh TEL-4001 Oil in Acetone Using a Glassy Carbon Working Electrode.	40
25	Effect of Successive Additions of the 5% Pyridine in Acetone Solution on the Voltammogram of the Fresh TEL-4005 Oil in Acetone Using a Glassy Carbon Working Electrode.	42
26	Effect of the 5% Pyridine in Acetone Solution on the Voltammograms of the Fresh TEL-4001 and TEL-4002 Oils in Acetone Using a Glassy Carbon Working Electrode.	43
27	Effect of the 5% Pyridine in Acetone Solution on the Voltammograms of the Fresh TEL-4003 and TEL-4004 Oils in Acetone Using a Glassy Carbon Working Electrode.	44
28	Effect of 5% Pyridine in Acetone Solution on the Voltammograms of the Fresh TEL-4005 and TEL-4006 Oils in Acetone Using a Glassy Working Electrode.	45
29	Reduced Scan Voltammograms of the 16 and 24 Hours Stressed TEL-4005 Oils in the Presence of Pyridine Using a Glassy Carbon Working Electrode.	46
30	Plots of the 280 mV Reduction and 630 mV Oxidation Waves' Heights (1st and 4th Scan) versus the Stressing Time for TEL-4005 Oil.	48
31	HP-DSC Thermogram of the TEL-4005 Oil Produced Using a 5 $\mu$ l Sample, a Heating Rate of 10°C/Minute, and an Oxygen Pressure of 500 psi.	50
32	HP-DSC Thermogram of the TEL-4005 Oil Produced Using a 1 $\mu$ l Sample, a Heating Rate of 10°C/Minute, and an Oxygen Pressure of 500 psi.	52
33	HP-DSC Thermograms of the Uninhibited Ester Base-stock, the Fresh TEL-4001 and TEL-4005 Oils, and the Authentic Used (F-25 and R-30) MIL-L-7808 Oil Samples Produced Using a 1 $\mu$ l Sample, Isothermal Temperature of 230°C, and an Oxygen Pressure of 100 psi.	53

LIST OF ILLUSTRATIONS (CONTINUED)

FIGURE		PAGE
34	Effect of Antioxidant Concentration on the Decoloration Rate of a BDN Solution (Reproduced from Reference 18).	56
35	Effect of Sample Size on the % Absorbance of the BDN Solution versus Reaction Time (25°C) Plots for the TEL-4004 Oil.	60
36	Effect of Antioxidant Type on the % Absorbance of the BDN Solution versus Reaction Time (25°C) Plots for PANA and DODPA.	62
37	Plots of the % Absorbance of the BDN Solution versus Reaction Time for the Fresh TEL-4001 through TEL-4006 MIL-L-7808 Oils.	64
38	Plots of the % Absorbance of the BDN Solution versus Reaction Time for the Fresh and Stressed (19-137 Hours) TEL-4005 Oils.	65
39	Plots of Oxygen Absorption versus Time of AIBN Stressing at 60°C for Automotive Engine Oils ( $\tau$ =Induction Time) (Reproduced from Reference 21).	68
40	Plots of Oxygen Absorption versus Reaction Time of AIBN Stressing at 60°C of Easily Oxidized Substances (No MIL-L-7808 Oil Present).	70
41	Plots of Oxygen Absorption versus Reaction Time of AIBN Stressing at 60°C of Fresh and Oxidatively Stressed TEL-4005 Oils.	72
42	Effect of Oxygen Purge on the Oxygen Absorption versus Reaction Time of AIBN Stressing at 60°C of Benzaldehyde.	75
43	The Effect of Sample Size (TEL-4005 Oil) on the Oxygen Absorption versus Reaction Time of AIBN Stressing at 60°C of Benzaldehyde.	76
44	The Effect of AIBN Solution Aging Time on the Oxygen Absorption versus Reaction Time of AIBN Stressing at 60°C for the TEL-4005 Oil.	78

LIST OF ILLUSTRATIONS (CONTINUED)

FIGURE		PAGE
45	Plots of Oxygen Absorption Versus Reaction Time of AIBN Stressing at 60°C for the Different MIL-L-7808 Oils.	80
46	Plots of Oxygen Absorption versus Reaction Time of AIBN Stressing at 60°C for the Fresh and Oxidatively Stressed TEL-4005 Oils.	81
47	Plot of Induction Time (AIBN at 60°C) versus Thermal Oxidation Stressing Time for the TEL-4005 Oils (Stable Life Ends at 96 Hours).	82
48	Hydroperoxide (-OOH: ■ and ○ = Initial Amige Concentrations of $7.0 \times 10^{-4}$ and $2.9 \times 10^{-3}$ M, Respectively) Formation and Amine Antioxidant (AH: □ and ○ = Initial Concentrations of $7.0 \times 10^{-4}$ and $2.9 \times 10^{-3}$ M, Respectively) Consumption in the Inhibited Autoxidation of Pentaerythrityl Tetraheptanoate (Reproduced from Reference 20).	85
49	Plots of Total Peroxide and Hydroperoxide Concentrations versus Stressing Time of TEL-4005 Oils.	87
50	Voltammograms of Hydroperoxides Present in New and Laboratory Stressed TEL-4005 Lubricating Oils in Acetone Using a Hg-AUE Electrode.	90
51	Voltammograms of 50, 100, 150, and 200 $\mu$ l Samples of Benzoic Peroxide (A) and Cumene Hydroperoxide (B) in Acetone Using a Glassy Carbon Working Electrode.	92
52	Voltammograms of Hydroperoxides in New and Laboratory Stressed (24-144 Hours) TEL-4005 Lubricating Oils in Acetone Using a Glassy Carbon Working Electrode.	93
53	Schematic of Electrical Circuit Used to Measure Electrical Properties of Oil Samples.	99
54	Plots of the $V_I/V$ Ratio for 10, 100, and 1000 Hz Inputs versus Stressing Time for Fresh and Stressed (24-120 Hours) TEL-4005 Oil Samples.	101
55	Plot of the COBRA Reading versus the Reciprocal of the $V_I/V$ Ratio for the Fresh and Stressed (0-120 Hours) TEL-4005 Oils Using an Input of 10 Hz.	103

LIST OF ILLUSTRATIONS (CONTINUED)

FIGURE		PAGE
56	Effect of Formulation on the Fluorescence of Fresh MIL-L-7808 Lubricating Oils.	106
57	Effect of Oxidation Degradation on the Fluorescence of MIL-L-7808 Lubricating Oils.	108
58	Single Scan Voltammograms of Fresh and Stressed (19-137 Hours at 370°F) TEL-4001 MIL-L-7808 Oils in Acetone Using a Glassy Carbon Working Electrode.	115
59	Single Scan Voltammograms of Fresh and Stressed (16-234 Hours at 370°F) TEL-4002 MIL-L-7808 Oils in Acetone Using a Glassy Carbon Working Electrode.	116
60	Single Scan Voltammograms of Fresh and Stressed (16-304 Hours at 370°F) TEL-4003 MIL-L-7808 Oils in Acetone Using a Glassy Carbon Working Electrode.	117
61	Single Scan Voltammograms of Fresh and Stressed (16-263 Hours at 370°F) TEL-4004 MIL-L-7808 Oils in Acetone Using a Glassy Carbon Working Electrode.	118
62	Single Scan Voltammograms of Fresh and Stressed (19-194 Hours at 370°F) TEL-4005 MIL-L-7808 Oils in Acetone Using a Glassy Carbon Working Electrode.	119
63	Single Scan Voltammograms of Fresh and Stressed (19-408 Hours at 370°F) TEL-4006 MIL-L-7808 Oils in Acetone Using a Glassy Carbon Working Electrode.	120
64	First and Fifth Scan Voltammograms of Fresh TEL-5001 MIL-L-7808 Oil in Acetone Using a Glassy Carbon Working Electrode.	122
65	First and Fifth Scan Voltammograms of Fresh TEL-5002 MIL-L-7808 Oil in Acetone Using a Glassy Carbon Working Electrode.	123
66	Reductive Voltammograms of Different Antioxidants and Antioxidant Combinations in Acetone Containing Pyridine Using a Glassy Carbon Working Electrode.	126

## LIST OF ILLUSTRATIONS (CONTINUED)

FIGURE		PAGE
67	First and Steady State Scan Voltammograms of PANA and PANA with DODPA Antioxidant Systems in Acetone Using a Glassy Carbon Working Electrode.	127
68	First and Steady State Scan Voltammograms of Octyl-PANA and Octyl-PANA with DODPA Antioxidant Systems in Acetone Using a Glassy Carbon Working Electrode.	128
69	Reductive Voltammograms of Fresh and Stressed (19-137 Hours at 370°F) TEL-4001 MIL-L-7808 Oils in Acetone Containing Pyridine Using a Glassy Carbon Working Electrode.	130
70	Reductive Voltammograms of Fresh and Stressed (16-234 Hours at 370°F) TEL-4002 MIL-L-7808 Oils in Acetone Containing Pyridine Using a Glassy Carbon Working Electrode.	131
71	Reductive Voltammograms of Fresh and Stressed (16-313 Hours at 370°F) TEL-4003 MIL-L-7808 Oils in Acetone Containing Pyridine Using a Glassy Carbon Working Electrode.	132
72	Reductive Voltammograms of Fresh and Stressed (16-263 Hours at 370°F) TEL-4004 MIL-L-7808 Oils in Acetone Containing Pyridine Using a Glassy Carbon Working Electrode.	133
73	Reductive Voltammograms of Fresh and Stressed (19-194 Hours at 370°F) TEL-4005 MIL-L-7808 Oils in Acetone Containing Pyridine Using a Glassy Carbon Working Electrode.	134
74	Reductive Voltammograms of Fresh and Stressed (19-408 Hours at 370°F) TEL-4006 MIL-L-7808 Oils in Acetone Containing Pyridine Using a Glassy Carbon Working Electrode.	135
75	Plots of Reduction Wave (C) Height in the Presence of Pyridine Versus Stressing Time (370°F) for the TEL-4001 through TEL-4006 MIL-L-7808 Oils.	136
76	Semi-Logarithmic Plots of the Reduction Wave (C) Height in the Presence of Pyridine Versus Stressing Time (370°F) for the TEL-4001 through TEL-4006 MIL-L-7808 Oils.	138

LIST OF ILLUSTRATIONS (CONTINUED)

FIGURE		PAGE
77	Effects of the Amount (0-90 $\mu$ l) of a 5% Pyridine Solution on the Reductive Voltammograms of the TEL-4003 MIL-L-7808 Oil in Acetone Using a Glassy Carbon Working Electrode.	139
78	Effects of the Amount (0-90 $\mu$ l) of a 5% Pyridazine Solution on the Reductive Voltammograms of the TEL-4003 MIL-L-7808 Oil in Acetone Using a Glassy Carbon Working Electrode.	140
79	Effects of the Amount (0-120 $\mu$ l) of a 5% 2,2' Dipyrldyl Solution on the Reductive Voltammograms of the TEL-4003 MIL-L-7808 Oil in Acetone Using a Glassy Carbon Working Electrode.	141
80	First (F), Second (S), and Steady State Reduction Waves of the Fresh and Stressed (16-234 Hours at 370°F) TEL-4002 MIL-L-7808 Oils and of the Blank.	144
81	Plots of the First, Second, and Steady State Reduction Wave Heights Versus Stressing Time (370°F) for the TEL-4001 MIL-L-7808 Oil.	147
82	Plots of the First, Second, and Steady State Reduction Wave Heights Versus Stressing Time (370°F) for the TEL-4002 MIL-L-7808 Oil.	148
83	Plots of the First, Second, and Steady State Reduction Wave Heights Versus Stressing Time (370°F) for the TEL-4006 MIL-L-7808 Oils.	149
84	Plots of the ln of the First, Second, and Steady State Reduction Wave Heights Versus Stressing Time (370°F) for the TEL-4001 Oil.	151
85	Plots of the ln of the First, Second, and Steady State Reduction Wave Heights Versus Stressing Time (370°F) for the TEL-4002 Oil.	153
86	Plots of the ln of the First, Second, and Steady State Reduction Wave Heights Versus Stressing Time (370°F) for the TEL-4006 Oil.	154
87	Plots of the Inverse and Inverse Squared of the Steady State Reduction Wave Height Versus Stressing Time (370°F) for the TEL-4002 Oil.	156

LIST OF ILLUSTRATIONS (CONTINUED)

FIGURE		PAGE
88	Plots of the ln of the Steady State Reduction Wave Height and Percent Lubricant Life Versus Hours of Remaining Lubricant Life at 370°F for the TEL-4001, TEL-4002, and TEL-4006 Oils.	157
89	Plots of the ln of the Reduction Wave Heights and Percent Remaining Life of the Reductive-Cyclic Voltammetric Technique Versus Hours of Remaining Life at 370°F for the Fresh and Stressed MIL-L-7808 Oils.	159
90	HP-DSC Thermogram of Fresh TEL-4003 MIL-L-7808 Oil Demonstrating Procedures Used to Determine the Onset of Oxidation Time, Onset of Reaction Time, and Preoxidation Period.	161
91	Plots of the HP-DSC Onset of Oxidation Time Versus Stressing Time at 370°F for the TEL-4001 through TEL-4006 MIL-L-7808 Oils.	170
92	Plots of the ln of the Onset of Oxidation Time Versus Stressing Time at 370°F for the TEL-4001 through TEL-4006 MIL-L-7808 Oils.	172
93	Plots of the Inverse of the Onset of Oxidation Time Versus Stressing Time at 370°F for the TEL-4001 through TEL-4006 MIL-L-7808 Oils.	173
94	Plots of the Inverse Squared of the Onset of Oxidation Time Versus Stressing Time at 370°F for the TEL-4001 through TEL-4006 MIL-L-7808 Oils.	174
95	Plots of the HP-DSC Onset of Reaction Time Versus Remaining Lubricant Life at 370°F for the Fresh and Stressed MIL-L-7808 Oils.	176
96	Plots of the ln of the HP-DSC Onset of Reaction Time Versus Remaining Lubricant Life at 370°F for the Fresh and Stressed MIL-L-7808 Oils.	177
97	SP-DSC Thermogram of Fresh TEL-4006 MIL-L-7808 Oil Performed in the Stainless Steel Capsule.	180
98	Effect of Sample Size on the SP-DSC (in air) Thermogram (250°C) of a Stressed (194 Hours at 370°F) TEL-4006 MIL-L-7808 Oil.	181
99	Effect of Fresh TEL-4004 MIL-L-7808 Oil on the Thermogram (90°C - Isothermal) of a 10 Percent Cumene Hydroperoxide in Benzaldehyde Solution.	183

LIST OF ILLUSTRATIONS (CONTINUED)

FIGURE		PAGE
100	Effects of Fresh TEL-4004 and TEL-4005 MIL-L-7808 Oils on the Thermogram (250°C - Isothermal) of a Aged (180 Hours at 370°F) TEL-4005 MIL-L-7808 Oil.	185
101	Effect of an Oxygen Atmosphere on the SP-DSC Thermograms (250°C) of Fresh and Stressed (194 Hours at 370°F) TEL-4006 MIL-L-7808 Oils.	186
102	Effect of Oxygen Pressure on the Thermogram (250°C - Isothermal) of the Fresh TEL-4006 MIL-L-7808 Oil.	187
103	Effect of Initial Temperature on the SP-DSC (in Oxygen) Thermogram of a Stressed (305 Hours at 370°F) TEL-4006 MIL-L-7808 Oil.	189
104	SP-DSC Thermogram (230°C - 3°C/Min.) of the Fresh TEL-4006 MIL-L-7808 Oil Demonstrating the Determination of the Onset of Oxidation Time.	190
105	SP-DSC (in Oxygen) Thermograms (230°C - 3°C/Min.) of Fresh and Stressed (19-116 Hours at 370°F) TEL-4001 MIL-L-7808 Oils.	192
106	SP-DSC (in Oxygen) Thermograms (230°C - 3°C/Min.) of the Fresh and Stressed (16-213 Hours at 370°F) TEL-4002 MIL-L-7808 Oils.	193
107	SP-DSC (in Oxygen) Thermograms (230°C - 3°C/Min.) of the Fresh and Stressed (16-360 Hours at 370°F) TEL-4003 MIL-L-7808 Oils.	194
108	SP-DSC (in Oxygen) Thermograms (230°C - 3°C/Min.) of the Fresh and Stressed (16-213 Hours at 370°F) TEL-4004 MIL-L-7808 Oils.	195
109	SP-DSC (in Oxygen) Thermograms (230°C - 3°C/Min.) of the Fresh and Stressed (19-166 Hours at 370°F) TEL-4005 MIL-L-7808 Oils.	196
110	SP-DSC (in Oxygen) Thermograms (230°C - 3°C/Min.) of the Fresh and Stressed (19-380 Hours at 370°F) TEL-4006 MIL-L-7808 Oils.	197
111	Plots of the SP-DSC (in Oxygen) Onset of Oxidation Time Versus Stressing Time at 370°F for the Fresh and Stressed MIL-L-7808 Oils.	198

LIST OF ILLUSTRATIONS (CONTINUED)

FIGURE		PAGE
112	Plots of the ln of the SP-DSC Onset of Oxidation Time Versus Hours of Remaining Lubricant Life at 370°F for the Fresh and Stressed MIL-L-7808 Oils.	200
113	Plots of the Percent BDN Absorbance Versus Reaction Time at 35°C for the Fresh and Stressed TEL-4001 and TEL-4006 Oils.	205
114	Plots of the Percent BDN Absorbance Versus Reaction Time at 35°C for the Fresh and Stressed (19-148 Hours at 370°F) TEL-4001 Oils.	208
115	Plots of the Percent BDN Absorbance Versus Reaction Time at 35°C for the Fresh and Stressed (16-234 Hours at 370°F) TEL-4002 Oils.	209
116	Plots of the Percent BDN Absorbance Versus Reaction Time at 35°C for the Fresh and Stressed (16-352 Hours at 370°F) TEL-4003 Oils.	210
117	Plots of the Percent BDN Absorbance Versus Reaction Time at 35°C for the Fresh and Stressed (16-241 Hours at 370°F) TEL-4004 Oils.	211
118	Plots of the Percent BDN Absorbance Versus Reaction Time at 35°C for the Fresh and Stressed (19-166 Hours at 370°F) TEL-4005 Oils.	212
119	Plots of the Percent BDN Absorbance Versus Reaction Time at 35°C for the Fresh and Stressed (19-354 Hours at 370°F) TEL-4006 Oils.	213
120	Plots of the BDN Decoloration Induction Time Versus Stressing Time at 370°F for the TEL-4001 through TEL-4006 MIL-L-7808 Oils.	215
121	Plots of the Log of the BDN Decoloration Induction Time Versus Hours of Remaining Lubricant Life at 370°F for the Fresh and Stressed MIL-L-7808 Oils.	216
122	Plots of the ln of the Reduction Wave Height and Percent Remaining Life of the Reductive-Cyclic Voltammetric Technique Versus Hours of Remaining Lubricant Life at 392°F for the Fresh and Stressed MIL-L-7808 Oils.	221

LIST OF ILLUSTRATIONS (CONTINUED)

FIGURE		PAGE
123	Cyclic (First Scan and Steady State) and Reductive-Cyclic Voltammograms of a Candidate MIL-L-27502 Oil in Acetone Using a GCE Electrode.	222
124	Cyclic (First Scan) Voltammograms of the Fresh TEL-4004 Oil and the OP-232-1, OP-232-4, and OP-232-6 MIL-L-7808 Oil Samples in Acetone Using a GCE Electrode.	224
125	Cyclic (First Scan) Voltammograms of the OP-232-7, OP-232-8, and OP-232-9 MIL-L-7808 Oil Samples in Acetone Using a GCE Electrode.	225
126	Cyclic (First Scan) Voltammograms of the OP-232-10, OP-232-11, and OP-232-12 MIL-L-7808 Oil Samples in Acetone Using a GCE Electrode.	226
127	Cyclic (First Scan) Voltammograms of the OP-232-26 and OP-232-29 MIL-L-7808 Oil Samples in Acetone Using a GCE Electrode.	227
128	Cyclic (First Scan) Voltammograms of the OP-232-33, OP-232-34, and OP-232-43 MIL-L-7808 Oil Samples in Acetone Using a GCE Electrode.	228
129	Plots of the $\ln$ of the Reduction Wave Height and Percent Remaining Life of the Reductive-Cyclic Voltammetry Technique and the Fe Concentration (ppm) Versus Hours Since Oil Change for the Used Lubricating Oil Samples.	232
130	Plots of the $\ln$ of the Reduction Wave Height and Percent Remaining Life of the Reductive-Cyclic Voltammetry Technique and the Fe Concentration (ppm) Versus Hours Since Oil Change for the Used Lubricating Oil Samples.	233
131	Plots of the $\ln$ of the Reduction Wave Height and Percent Remaining Life of the Reductive-Cyclic Voltammetry Technique and the Fe Concentration (ppm) Versus Hours Since Oil Change for the Used Lubricating Oil Samples.	234
132	Plots of the RCV Wave Height and COBRA Reading Versus Stressing Time (347°F) for the DIL-1 Oil Samples.	237

LIST OF ILLUSTRATIONS (CONTINUED)

FIGURE		PAGE
133	Plots of the RCV Wave Height and COBRA Reading Versus Stressing Time (347°F) for the DIL-2 Oil Samples.	238
134	Plots of the RCV Wave Height and COBRA Reading Versus Stressing Time (347°F) for the DIL-3 Oil Samples.	239
135	Plots of the RCV Wave Height and COBRA Reading Versus Stressing Time (347°F) for the DIL-4 Oil Samples.	240
136	Plots of the ln of the RCV Wave Height Versus Stressing Time at 347°F and 370°F for the DIL-1 through DIL-4 Oil Samples.	243
A-1	Plots of the COBRA Reading, Viscosity (40°C), Total Acid Number (TAN), and Mg Concentration Versus Stressing Time at 370°F for the TEL-4001 MIL-L-7808 Oil.	249
A-2	Plots of the COBRA Reading, Viscosity (40°C), Total Acid Number (TAN), and Mg Concentration Versus Stressing Time at 370°F for the TEL-4002 MIL-L-7808 Oil.	250
A-3	Plots of the COBRA Reading, Viscosity (40°C), Total Acid Number (TAN), and Mg Concentration Versus Stressing Time at 370°F for the TEL-4003 MIL-L-7808 Oil.	251
A-4	Plots of the COBRA Reading, Viscosity (40°C), Total Acid Number (TAN), and Mg Concentration Versus Stressing Time at 370°F for the TEL-4004 MIL-L-7808 Oil.	252
A-5	Plots of the COBRA Reading, Viscosity (40°C), Total Acid Number (TAN), and Mg Concentration Versus Stressing Time at 370°F for the TEL-4005 MIL-L-7808 Oil.	253
A-6	Plots of the COBRA Reading, Viscosity (40°C), Total Acid Number (TAN), and Mg Concentration Versus Stressing Time at 370°F for the TEL-4006 MIL-L-7808 Oil.	254

LIST OF ILLUSTRATIONS (CONTINUED)

FIGURE		PAGE
A-7	Plots of the COBRA Reading, Viscosity (40°C), Total Acid Number (TAN), and Mg Concentration Versus Stressing Time at 392°F for the TEL-4001 MIL-L-7808 Oil.	258
A-8	Plots of the COBRA Reading, Viscosity (40°C), Total Acid Number (TAN), and Mg Concentration Versus Stressing Time at 392°F for the TEL-4002 MIL-L-7808 Oil.	259
A-9	Plots of the COBRA Reading, Viscosity (40°C), Total Acid Number (TAN), and Mg Concentration Versus Stressing Time at 392°F for the TEL-4003 MIL-L-7808 Oil.	260
A-10	Plots of the COBRA Reading, Viscosity (40°C), Total Acid Number (TAN), and Mg Concentration Versus Stressing Time at 392°F for the TEL-4004 MIL-L-7808 Oil.	261
A-11	Plots of the COBRA Reading, Viscosity (40°C), Total Acid Number (TAN), and Mg Concentration Versus Stressing Time at 392°F for the TEL-4005 MIL-L-7808 Oil.	262
A-12	Plots of the COBRA Reading, Viscosity (40°C), Total Acid Number (TAN), and Mg Concentration Versus Stressing Time at 392°F for the TEL-4006 MIL-L-7808 Oil.	263
A-13	Plots of the COBRA Reading, Viscosity (40°C), Total Acid Number (TAN), and Mg Concentration Versus Stressing Time at 370°F for the TEL-5001 MIL-L-7808 Oil.	266
A-14	Plots of the COBRA Reading, Viscosity (40°C), Total Acid Number (TAN), and Mg Concentration versus Stressing Time at 370°F for the TEL-5002 MIL-L-7808 Oil.	267
A-15	Gas Chromatograms of the Fresh and Stressed (16-263 Hours at 370°F) TEL-4004 MIL-L-7808 Oils.	269
A-16	Gas Chromatograms of the Fresh and Stressed (19-137 Hours at 370°F) TEL-4001 MIL-L-7808 Oils.	271
A-17	Gas Chromatograms of the Fresh and Stressed (19-354 Hours at 370°F) TEL-4006 MIL-L-7808 Oils.	272

LIST OF ILLUSTRATIONS (CONTINUED)

FIGURE		PAGE
A-18	Gas Chromatogram of the Fresh TEL-5002 MIL-L-7808 Oil.	273
A-19	Gas Chromatogram of the Fresh TEL-5001 MIL-L-7808 Oil.	274
A-20	The Plots of the Percent (by Weight) of the Antioxidants, PANA and DODPA, of the ln of the Percent (by Weight) of DODPA, and of the Total Acid Number (TAN) versus Stressing Time at 370°F for the TEL-4002 MIL-L-7808 Oil.	276
A-21	Plots of Percent (by Weight) of Antioxidants, PANA and DODPA, of the ln of the Percent (by Weight) of DODPA, and of the Total Acid Number (TAN) versus Stressing Time at 370°F for the TEL-4003 MIL-L-7808 Oil.	277
A-22	Plots of Percent (by Weight) of Antioxidants, PANA and DODPA, of the ln of Percent (by Weight) of DODPA, and of the Total Acid Number (TAN) versus Stressing Time at 370°F for the TEL-4004 MIL-L-7808 Oil.	278
A-23	Plots of Percent (by Weight) of Antioxidants, PANA and DODPA, of the ln of Percent (by Weight) of DODPA, and of the Total Acid Number (TAN) versus Stressing Time at 370°F for the TEL-4005 MIL-L-7808 Oil.	279
A-24	Plots of Percent (by Weight) of Antioxidants, Octyl-PANA and DODPA, of the ln of Percent (by Weight) of DODPA, and of the Total Acid Number (TAN) versus Stressing Time at 370°F for the TEL-4001 MIL-L-7808 Oil.	281
A-25	Plots of Weight Fractions of Antioxidants, Octyl-PANA, DODPA, and Unknown (Retention Time = 1.9 Minutes), and of the ln of Weight Fraction of Unknown versus Stressing Time at 370°F for the TEL-4001 MIL-L-7808 Oil.	283
A-26	Plots of Percent (by Weight) of Antioxidants, Octyl-PANA and DODPA, of the ln of Percent of DODPA, of the Mg Concentration, and of the Total Acid Number (TAN) versus Stressing Time at 370°F for the TEL-4006 MIL-L-7808 Oil.	284

LIST OF ILLUSTRATIONS (CONTINUED)

FIGURE		PAGE
A-27	Plots of Weight Fractions of Antioxidants, Octyl-PANA, DODPA, and Unknown (Retention Time = 5.0 Minutes), and of the ln of the Weight Fraction of the Unknown versus Stressing Time at 370°F for the TEL-4006 MIL-L-7808 Oil.	286
A-28	Plots of Percent (by Weight) of Antioxidants, Phenothiazine and DODPA, of the ln of Percent (by Weight) of DODPA, and of Total Acid Number (TAN) versus Stressing Time at 370°F for the TEL-5001 MIL-L-7808 Oil.	287
A-29	Plots of Percent (by Weight) of the Antioxidants, Octyl-PANA and DODPA, of the ln of Percent (by Weight) of DODPA, and of Total Acid Number (TAN) versus Stressing Time at 370°F for the TEL-5002 MIL-L-7808 Oil.	289
A-30	Plots of Percent (by Weight) of the Antioxidants, PANA and DODPA, of the ln of the Percent (by Weight) of DODPA, and of the Total Acid Number (TAN) versus Stressing Time at 392°F for the TEL-4002 MIL-L-7808 Oil.	291
A-31	The Plots of the Percent (by Weight) of the Antioxidants, PANA and DODPA, of the ln of the Percent (by Weight) of DODPA, and of the Total Acid Number (TAN) versus Stressing Time at 392°F for the TEL-4003 MIL-L-7808 Oil.	292
A-32	Plots of Percent (by Weight) of Antioxidants, PANA and DODPA, of the ln of Percent (by Weight) of DODPA, and of the Total Acid Number (TAN) versus Stressing Time at 392°F for the TEL-4004 MIL-L-7808 Oil.	293
A-33	Plots of Percent (by Weight) of Antioxidants, PANA and DODPA, of the ln of Percent (by Weight) of DODPA, and of the Total Acid Number (TAN) versus Stressing Time at 392°F for the TEL-4005 MIL-L-7808 Oil.	294
A-34	Plots of Percent (by Weight) of Antioxidants, Octyl-PANA and DODPA, of the ln of Percent (by Weight) of DODPA, and of the Total Acid Number (TAN) versus Stressing Time at 392°F for the TEL-4001 MIL-L-7808 Oil.	295

LIST OF ILLUSTRATIONS (CONCLUDED)

FIGURE		PAGE
A-35	Plots of Percent (by Weight) of Antioxidants, Octyl-PANA and DODPA, of the ln of Percent (by Weight) of DODPA, and of the Total Acid Number (TAN) versus Stressing Time at 392°F for the TEL-4006 MIL-L-7808 Oil.	296
A-36	Plots of Weight Fraction of Unknown (Retention Time = 1.9 Minutes) and of the ln of Weight Fraction of Unknown versus Stressing Time at 392°F for the TEL-4001 MIL-L-7808 Oil.	297
A-37	Plots of Weight Fraction of Unknown (Retention Time = 5.0 Minutes) and of the ln of the Weight Fraction of the Unknown versus Stressing Time at 392°F for the TEL-4006 MIL-L-7808 Oil.	298
B-1	Viscosity versus Stressing Time (175°C) Plot for the TEL-4005 Oil.	306
B-2	Computer Program Used to Acquire Data and Calculate the Remaining Lubricant Life on the Apple IIe Microcomputer.	314

LIST OF TABLES

TABLE		PAGE
1	CRITERIA FOR REMAINING LUBRICANT LIFE ASSESSMENT TEST CANDIDATES	5
2	SUMMARY OF IDENTIFIED ANALYTICAL TECHNIQUES	6
3	EFFECT OF FORMULATION ON $V_I/V$ PRODUCED BY 10 AND 1000 HZ INPUTS	104
4	COMPARISON OF CANDIDATES' POTENTIALS FOR DEVELOPMENT INTO LUBRICANT LIFE ASSESSMENT TESTS	110
5	STABLE LIVES (370°F) AND ANTIOXIDANT CONCENTRATIONS OF MIL-L-7808 OILS	112
6	OIL STABILITY OF TEL-4001 MIL-L-7808 OIL	163
7	OIL STABILITY OF TEL-4002 MIL-L-7808 OIL	164
8	OIL STABILITY OF TEL-4003 MIL-L-7808 OIL	165
9	OIL STABILITY OF TEL-4004 MIL-L-7808 OIL	166
10	OIL STABILITY OF TEL-4005 MIL-L-7808 OIL	167
11	OIL STABILITY OF TEL-4006 MIL-L-7808 OIL	168
12	SUMMARY OF SP-DSC AND HP-DSC TECHNIQUES	202
13	SUMMARY OF REMAINING LUBRICANT LIFE ASSESSMENT TEST CANDIDATES	218
14	REDUCTIVE-CYCLIC VOLTAMMETRIC RESULTS FOR MIL-L-7808 OILS	230
A-1	BREAKPOINTS OF PHYSICAL PROPERTY VERSUS STRESSING TIME PLOTS FOR 370°F	256
A-2	BREAKPOINTS OF PHYSICAL PROPERTY VERSUS STRESSING TIME PLOTS FOR 392°F	264
B-1	IODINE LIBERATION METHODS I, II AND III	310

## ABBREVIATIONS AND SYMBOLS

### ABBREVIATIONS

AFWAL/POSL	Air Force Wright Aeronautical Labs, Aero Propulsion Laboratory
AIBN	Azobisisobutyronitrile-Free Radical Initiator
AUE	Gold Working Electrode
BDN	Bis[4-(dimethylamino) dithiobenzil] Nickel Complex-Laser Dye
COBRA	Complete Oil Breakdown Rate Analyzer
CV	Cyclic Voltammetry
DODPA	Diocetyldiphenyl Amine
DSC	Differential Scanning Calorimetry
F	Failure Oil Sample
GCE	Glassy Carbon Working Electrode
H	Hit Oil Sample
Hg-AUE	Mercury Film on Gold Working Electrode
HP-DSC	High Pressure-Differential Scanning Calorimetry
ln	Natural Logarithm
log	Logarithm
octyl-PANA	N-(p-octylphenyl)- $\alpha$ -naphthyl Amine
PANA	N-phenyl- $\alpha$ -naphthyl Amine
PTE	Platinum Working Electrode
RCV	Reductive-Cyclic Voltammetry
RLL	Remaining Lubricant Life
RLLAT	Remaining Lubricant Life Assessment Test
RLLAT-RCV	Remaining Lubricant Life Assessment Test Based on Reductive-Cyclic Voltammetry
SOAP	Spectrometric Oil Analysis Program

ABBREVIATIONS AND SYMBOLS (CONTINUED)

SP-DSC	Sealed Pan-Differential Scanning Calorimetry
TAN	Total Acid Number
TEAP	Tetraethylammonium Perchlorate
THF	Tetrahydrofuran
UDRI	University of Dayton Research Institute
$V_I/V$	Voltage Drop Across Resistor/Voltage Drop Across the Sample Cell of UDRI Electrical Property Measuring System

CHEMICAL SYMBOLS

Ag	Silver
AgCl	Silver Chloride
Fe	Iron
$KMnO_4$	Potassium Permanganate
KOH	Potassium Hydroxide
$LiClO_4$	Lithium Perchlorate
Mg	Magnesium
N	Nitrogen
P	Phosphorous

QUANTITY SYMBOLS

$^{\circ}C$	Degree Celsius
cc	Cubic Centimeter
cs	Centistokes
$^{\circ}F$	Degree Fahrenheit
g	Gram

ABBREVIATIONS AND SYMBOLS (CONCLUDED)

hr	Hour
Hz	Hertz
ml	Milliliter
mV	Millivolt
nm	Nanometer
ppm	Parts Per Million
psi	Pounds per Square Inch
sec	Second
µA	Microamp
µl	Microliter
V	Volt

## SECTION I INTRODUCTION

While lubricating and cooling the oil-wetted components of the turbine engine, the lubricating oil experiences various environmental stresses which cause the oil's basestock to undergo thermal and oxidative degradation. As long as the lubricant is adequately protected by an antioxidant system, the oxidative degradation of the oil's basestock and the changes in the lubricating oil's properties are minimal. Since the antioxidants are depleted with engine operating time, they eventually become ineffective allowing large changes to occur in the physical properties of the lubricant. The large changes in the physical properties of the lubricant signify the end of its stable life and result in excessive oil degradation, coking, component wear and eventual failure of the engine. The length of engine operating time from the time a lubricant is sampled until the end of its stable life is referred to as "Remaining Lubricant Life."

To ensure that a lubricant is not used past the end of its stable life, the Air Force uses scheduled oil changes. Because the scheduled oil changes are inherently conservative, lubricants with remaining lubricant lives are discarded. Therefore, the ability to assess the remaining lubricant life of an oil sample would eliminate the need for scheduled oil changes providing savings in material and labor costs to the Air Force.

However, the only tests currently available to the Air Force for assessing remaining lubricant life are long term stability tests. The analytical techniques used to detect changes in the physical properties (viscosity, total acid number, volatility, etc.) of a lubricant during the long term stability tests are incapable of assessing remaining lubricant life.

Therefore, research was conducted to develop a remaining lubricant life assessment test suitable for use by the Air Force. The work reported herein was performed in three tasks. In the first task, analytical techniques capable of performing remaining

lubricant life assessments were identified, optimized, and initially evaluated. In the second task, the best analytical techniques were developed into remaining lubricant life assessment test candidates. Performance criteria were then used to evaluate the suitability of each test candidate for use by the Air Force. In the third task, the selected candidate was developed into a remaining lubricant life assessment test.

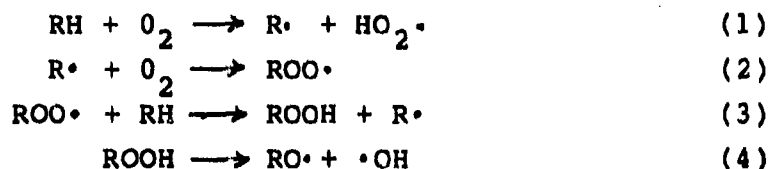
The results and discussion of the remaining lubricant life assessment test candidates are presented in Section II, while Section III discusses the conclusions and recommendations derived from the research conducted. The preparation and characterization of the stressed MIL-L-7808 oils used in the development of the remaining lubricant life assessment test candidates are discussed in Appendix A. The equipment and procedures used to develop the remaining lubricant life assessment test candidates are discussed in Appendix B.

SECTION II  
RESULTS AND DISCUSSION

1. TASK 1. IDENTIFICATION OF REMAINING LUBRICANT LIFE  
ASSESSMENT TEST CANDIDATES

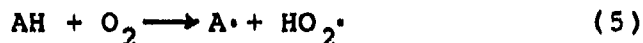
a. Introduction

The objective of Task 1 was to identify, optimize, and initially evaluate analytical techniques capable of assessing the remaining lubricant lives (RLL) of MIL-L-7808 lubricating oils. The RLL of a MIL-L-7808 oil is dependent upon the amount of antioxidant capacity remaining in the oil sample to inhibit the autoxidation of the oil's ester basestock (RH) which occurs by the following reaction scheme:

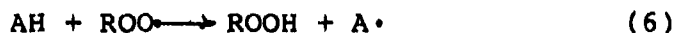


The primary inhibition reactions of the antioxidant systems (AH) used in MIL-L-7808 oils are the following reactions:

Direct Oxidation [Inhibits Reaction (1)]



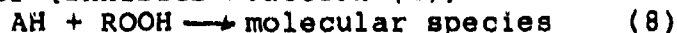
Free Radical Trap [Inhibits Reaction (3)]



Recombination [Inhibits Reaction (3)]



Hydroperoxide Decomposer [Inhibits Reaction (4)]



Due to the variety of inhibition reactions, the literature search was used to identify a wide range of analytical procedures with RLL assessing capabilities. The analytical procedures identified during the literature search can be categorized into two main groups. The first group contains analytical techniques which determine the concentration of each antioxidant species present in the oil sample. The antioxidant concentrations are then used to calculate the RLL value.

The second group contains analytical techniques which directly determine the amount of antioxidant capacity remaining in the sample to inhibit a particular autoxidation reaction (Reactions 3-4) of the ester basestock. Thus the success of each analytical technique in the second group is dependent upon the importance of the corresponding inhibition reaction (Reactions 5-8) to the RLL of the oil sample.

Once an analytical technique was identified, it was evaluated using the criteria summarized in Table 1. If the identified procedure could be modified to use a sample size less than 5 cc and an analysis time less than 10 minutes, the technique's RLL assessing capabilities were studied. Ester basestocks (uninhibited), fresh MIL-L-7808 lubricating oils (obtained from AFWAL/POSL), a set of laboratory stressed oil samples produced from a MIL-L-7808 oil, and authentic used MIL-L-7808 oil samples were used to optimize and evaluate the identified analytical procedures' RLL assessing capabilities.

A summary of the analytical procedures that were identified and initially evaluated in Task 1 is presented in Table 2. The analytical techniques are listed in the order of their ranking as remaining lubricant life assessment test (RLLAT) candidates.

The studies used to optimize and evaluate the potentials of the various analytical procedures for development into RLLAT candidates are described herein. The analytical procedures are discussed in the same order as in Table 2.

#### b. Voltammetric Techniques

##### (1) Introduction

Electroanalytical methods based on current-voltage-time relationships at micro-electrodes are referred to as voltammetry. Usually the potential is varied linearly with time and the current is recorded as a function of the potential. When the starting and ending potentials are identical and the potential waveform is triangular (Figure 1a), the experiment is

TABLE 1

CRITERIA FOR REMAINING LUBRICANT  
LIFE ASSESSMENT TEST CANDIDATES

COST

Instrumental	Less Than \$2,000
Operational	As Low As Possible

OPERATIONAL PARAMETERS

Sample Size	Less Than 5 cc
Analysis Time	Less Than 10 Minutes
Ease of Operation	Base-Level
Sample Preparation	Minimal
Analysis of Results	Base Level

TABLE 2

SUMMARY OF IDENTIFIED ANALYTICAL TECHNIQUES

<u>Type of Technique</u>	<u>Specific Technique</u>	<u>Basis of Technique</u>	<u>Oil Property Measured by Technique</u>
Voltammetric	Voltammetry-reduction only Scan from +1.0V to 0.0V	Quantify generated antioxidant species and oil's potential to generate new antioxidant species	Measures concentration of antioxidant species thought to be responsible for lubricant's oxidative stability.
	Cyclic Voltammetry Scan between 0.0V and +1.0V	Detect and approximate concentration of original antioxidant and generated antioxidant species	Estimates degree of antioxidant depletion
	Scan between 0.0V and -1.0V	Approximate concentration of hydroperoxide	Estimates degree of lubricant degradation
Thermal Stressing	High Pressure-Differential Scanning Calorimetry (HP-DSC)	Uses thermal-oxidative stressing to rapidly degrade oil samples then quantifies energy and time of exothermic reaction that occurs at the end of the oil's induction period	Measures total oxidative stability of lubricant. Energy of exothermic reaction may also be related to oxidative stability
	High Pressure-Differential Thermal Analyzer(HP-DTA)	Uses thermal-oxidative stressing to rapidly degrade oil samples then detects time of exothermic reaction that occurs at the end of the oil's induction period	Measures total oxidative stability of lubricant
Chemical Stressing	Colorimetric Method	Uses cumene hydroperoxide to deplete antioxidant species and then detects decoloration of reaction system that occurs at the end of the oil's induction period.	Measures hydroperoxide decomposing capacity of antioxidant species
	Modified Ford Method	Uses generated free radicals to deplete antioxidant species and then detects rapid pressure decrease of reaction system that occur's at the end of the oil's induction period.	Measures radical trapping capacity of antioxidant species

TABLE 2

## SUMMARY OF IDENTIFIED ANALYTICAL TECHNIQUES (CONCLUDED)

Other Methods Investigated	Specific Technique	Basis of Technique	Oil Property Measured by Technique
Titration	Iodometric Hydroperoxide and Peroxide Determinations.	Measures amount of KI converted to I <sub>2</sub> to determine concentration of hydroperoxides and peroxides.	Estimates degree of lubricant degradation.
	Permanganatometric Measurements.	Measures concentration of species oxidizable in oil sample, e.g. antioxidants and degradation products.	Estimates degree of lubricant degradation.
Electrochemical	Conductivity Measurements (COBRA).	Measures change in oil sample's conductivity caused by degradation products.	Estimates degree of lubricant degradation.
Spectrophotometric	Fluorescence Measurements.	Measures decrease in oil sample's fluorescence caused by degradation products and antioxidant products.	Estimates degree of lubricant degradation.
Feasible Methods Not Investigated	Detection of Volatiles (High Pressure)	Basis of Technique	Oil Property Measured by Technique
		Uses thermal-oxidative stressing to rapidly degrade oil sample, then detects volatiles that are produced at end of oil's induction period.	Measures total oxidative stability of lubricant.
Spectroscopic (Emission)	High Pressure-Chemiluminescence Detection Method.	Uses thermal-oxidative stressing to rapidly degrade oil sample, then detects increase in chemiluminescence that occurs at end of oil's induction period.	Measures total oxidative stability of lubricant.
		Uses thermal-oxidative stressing to rapidly degrade oil sample, then detects large change in oil's electrical properties that occurs at end of oil's induction period.	Measures total oxidative stability of lubricant.
Electrochemical	High Pressure - COBRA Detection Method.		Measures total oxidative stability of lubricant.

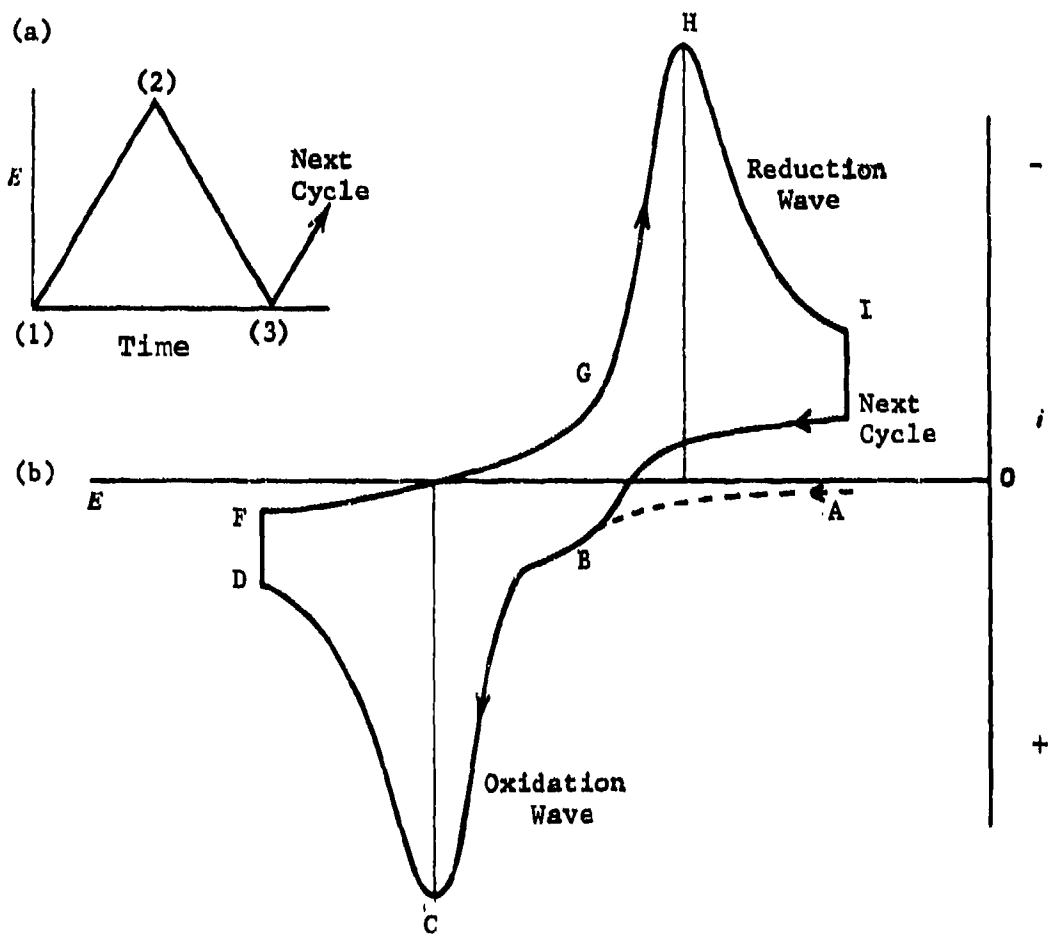


Figure 1. Typical Triangular Waveform (a) Used by Cyclic Voltammetry and a Typical Current-Potential Curve (Voltammogram) (b) Produced by Cyclic Voltammetry (Reproduced from Reference 1).  $E$  = Potential and  $i$  = Current.

usually called cyclic voltammetry and a voltammograph of the type shown in Figure 1b is produced.

Initially (Point A in Figure 1b), the rate of the electrochemical reaction is so slow that virtually no current flows through the cell. As the voltage is increased (Point 1 to Point 2 in Figure 1a), the electroactive species at the micro-electrode's surface begin to oxidize producing the anodic rise (Point B in Figure 1b) in the current. As the potential increases further, the decrease in the electroactive species' concentration at the electrode surface and the exponential increase of the oxidation rate lead to a maximum (Point C in Figure 1b) in the current-potential curve. The current then decreases to the diffusion-limited anodic current value (Point D in Figure 1b). The produced peak is referred to as the oxidation wave. The direction of applied voltage is then reversed (Point F in Figure 1b) and becomes more cathodic with time (Point 2 to Point 3 in Figure 1a). When the voltage becomes sufficiently cathodic, the oxidized species at the surface of the micro-electrode begin to reduce producing the cathodic rise (Point G in Figure 1b) in the current. Again a maximum current is obtained (Point H in Figure 1b), and the current decreases with decreasing potential until the cycle is completed or a new cycle is initiated (Point I in Figure 1b). The produced peak is referred to as the reduction wave.

Although cyclic voltammetry has been used extensively in the analysis of secondary aromatic amines (Reference 1), it has not been used to analyze the aromatic amine antioxidants of MIL-L-7808 lubricating oils. However, cyclic voltammetry was identified as a possible RLLAT candidate because it requires sample sizes less than 1 cc, is simple to operate, requires less than 20 seconds to perform an analysis, and requires very inexpensive instrumentation (less than \$900).

To obtain preliminary data on cyclic voltammetry, samples of fresh TEL-4005 oil, its ester basestock, and a used MIL-L-7808 oil were sent to Bioanalytical Systems for analysis.

The cyclic voltammograms of the basestock and fresh MIL-L-7808 oil and of the fresh MIL-L-7808 oil and used MIL-L-7808 oil sample are shown in Figures 2 and 3, respectively.

As seen in Figure 2, the basestock (A) produces no discernible peaks, while the fresh MIL-L-7808 oil (B) produces a large oxidation wave (1) and two smaller reduction waves (2) and (3). Also, the sizes of the oxidation and reduction waves of the cyclic voltammograms decrease with engine operating time (Figure 3). Therefore, the observed peaks were assigned to the oxidation, then reduction, of the antioxidants present in the MIL-L-7808 oils. Consequently, cyclic voltammetry was deemed capable of RLL analyses.

Therefore, the effects of different experimental parameters on the capability of cyclic voltammetry to assess RLL by quantifying the antioxidants in MIL-L-7808 oils and by alternative methods were studied. The experimental parameters studied during this investigation included solvent type, working electrode type, electrolyte type, scan rate, multiple scans, additive interferences, formulation dependency, and oxidation product interferences. The effects of organic bases and free radical initiators on the cyclic voltammograms of fresh and laboratory stressed MIL-L-7808 oils were also studied.

#### (2) Effect of Solvent Type

In the preliminary work performed by Bioanalytical Services, acetonitrile was used as the solvent and tetraethylammonium perchlorate (TEAP) was used as the electrolyte. Although acetonitrile is commonly used in cyclic voltammetry, it is fairly toxic and can be absorbed through the skin. Therefore, a study was performed to find a more suitable, less toxic, solvent system for use in the cyclic voltammetry technique. The solvents acetonitrile, acetone, ethanol, methanol, and propylene carbonate were used as received. A 200  $\mu$ l sample of TEL-4005 MIL-L-7808 lubricating oil was added to 10 ml of solvent for this study. A platinum working electrode in combination with a

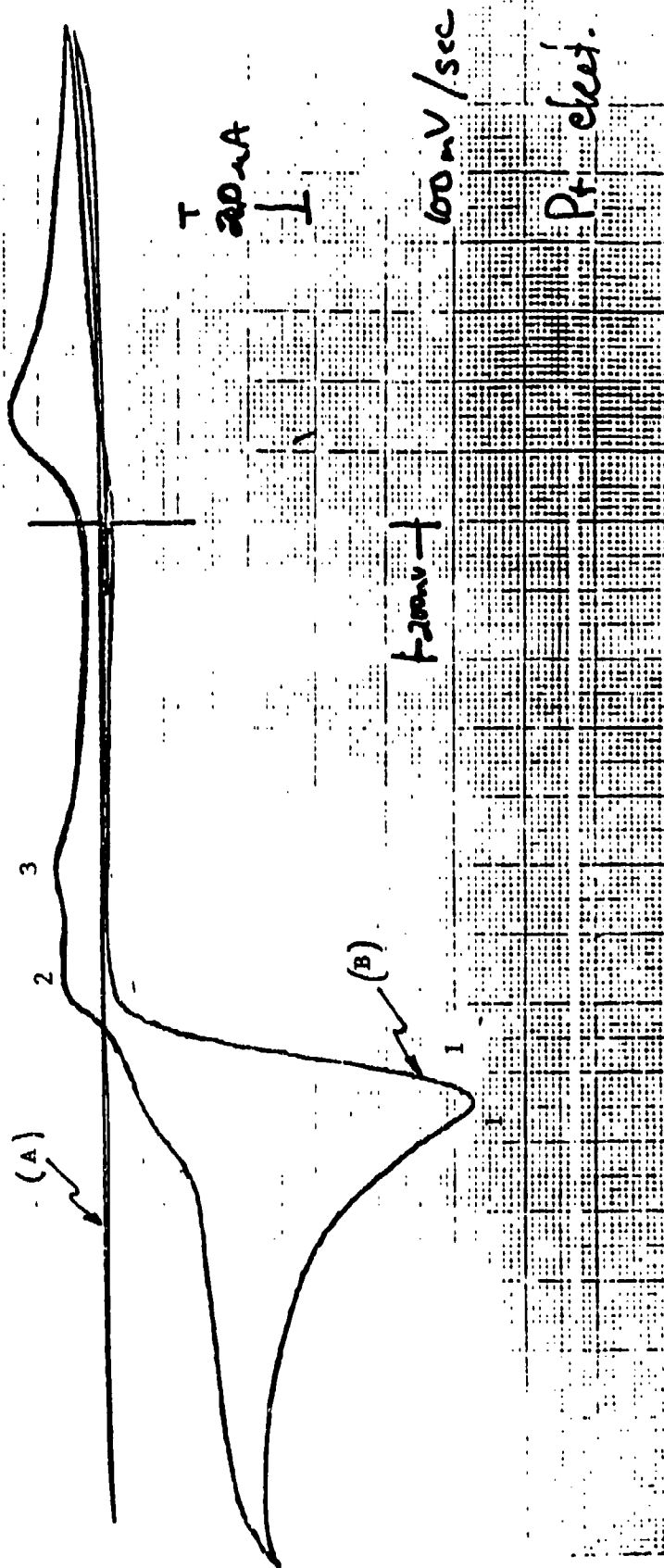


Figure 2. Voltammograms for the Basestock (A) and Fresh TEL-4005 Oil (B) in Acetonitrile With a Platinum Working Electrode.

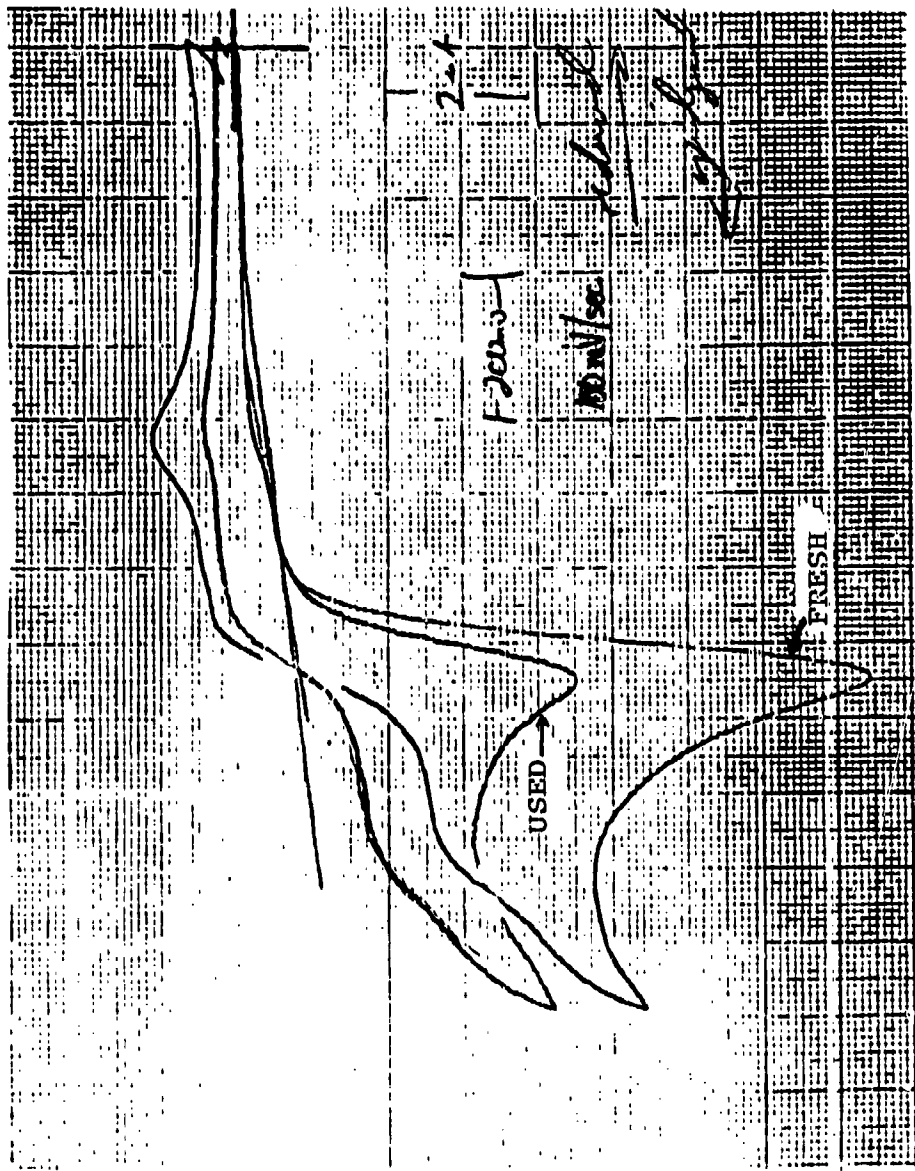


Figure 3. Voltammograms of the Fresh TEL-4005 and an Used MIL-L-7808 Oil Sample (J79 Engine; 450 Hours Since Oil Change) in Acetonitrile With a Platinum Working Electrode.

platinum wire auxiliary electrode and a Ag/AgCl reference electrode were used to produce the voltammograms. A rate of 250 mV/sec was used to scan the voltage range of -0.1 to +1.9 volts. Therefore one complete scan (-0.1 V to +1.9 V then back to 0.1 V) took approximately 16 seconds to complete.

The TEAP electrolyte was soluble enough to produce a concentration of 0.1 M in all of the solvents except ethanol. The TEAP electrolyte did not have sufficient solubility in ethanol to produce a voltammogram, and consequently, ethanol was not studied.

The voltammograms produced in acetonitrile for the solvent and the 100 and 200  $\mu$ l samples of the TEL-4005 oil are shown in Figure 4. The oxidation wave (A in Figure 4) is produced by the oxidation of the antioxidants while the reduction waves (B and C in Figure 4) are produced by the reduction of the oxidized products of the antioxidants.

In Figures 5 and 6 the voltammograms produced in propylene carbonate and methanol for the solvent and the 200  $\mu$ l sample of the TEL-4005 oil are shown. Even though propylene carbonate is a commonly used solvent in cyclic voltammetry, the oxidation wave (A in Figure 5) is very weak compared to the wave obtained using acetonitrile (Figure 4) and the reduction waves are not observed. As illustrated in Figure 6, the voltammogram for the oil sample in methanol does not contain any peaks that can be assigned to the antioxidants.

Figure 7 shows the voltammograms produced in acetone for the solvent and the 200  $\mu$ l sample of the TEL-4005 oil. The oxidation wave (A in Figure 7) is much stronger in acetone than in acetonitrile (Figure 4). The reduction waves (B and C in Figure 7) are also observed.

Since acetone is a very common solvent, less expensive than acetonitrile, and basically nontoxic, acetone was used for the rest of the following work.

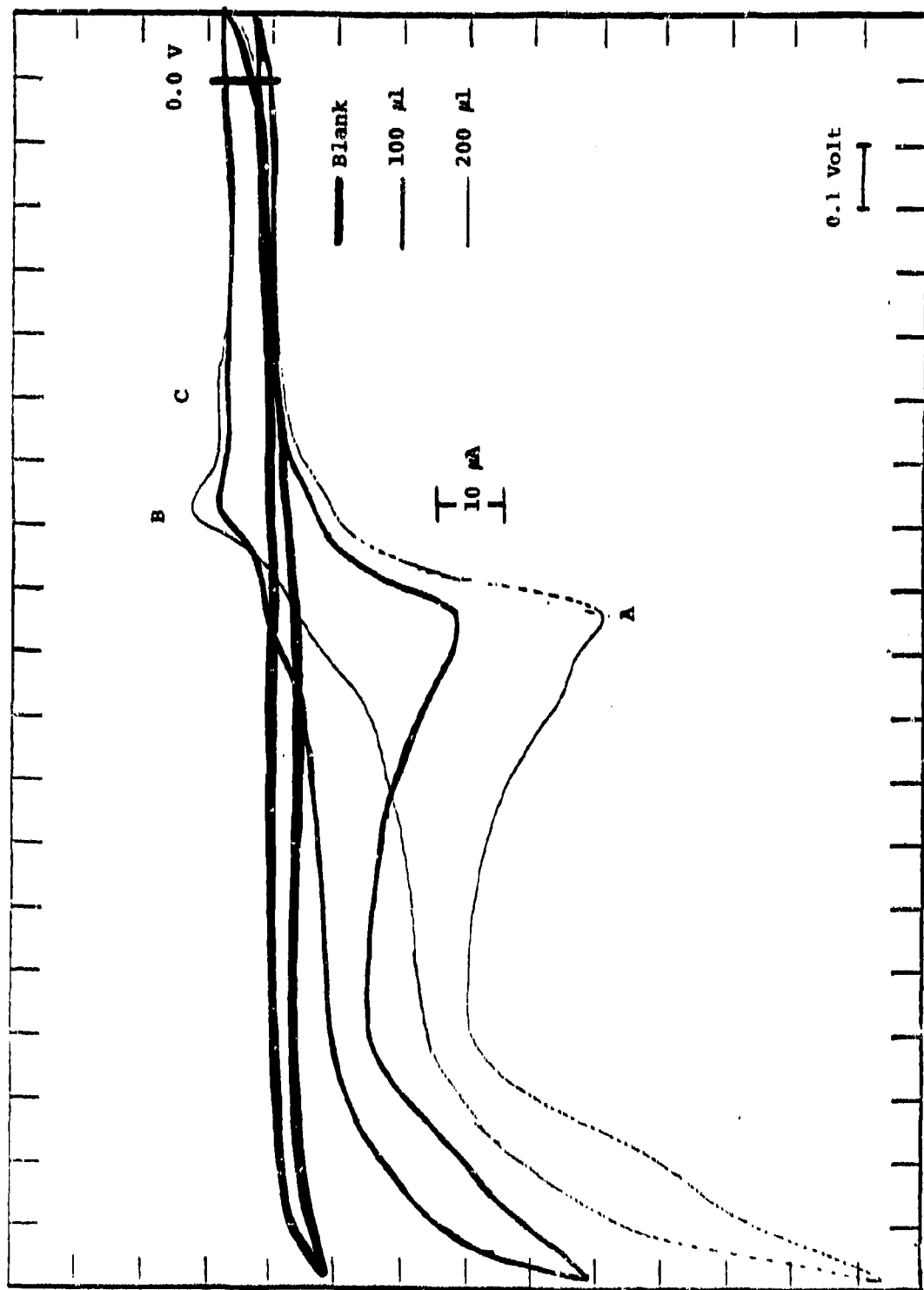


Figure 4. Voltammograms of 100 and 200  $\mu$ l Samples of the Fresh TEL-4005 Oil in Acetonitrile with a Platinum Working Electrode.

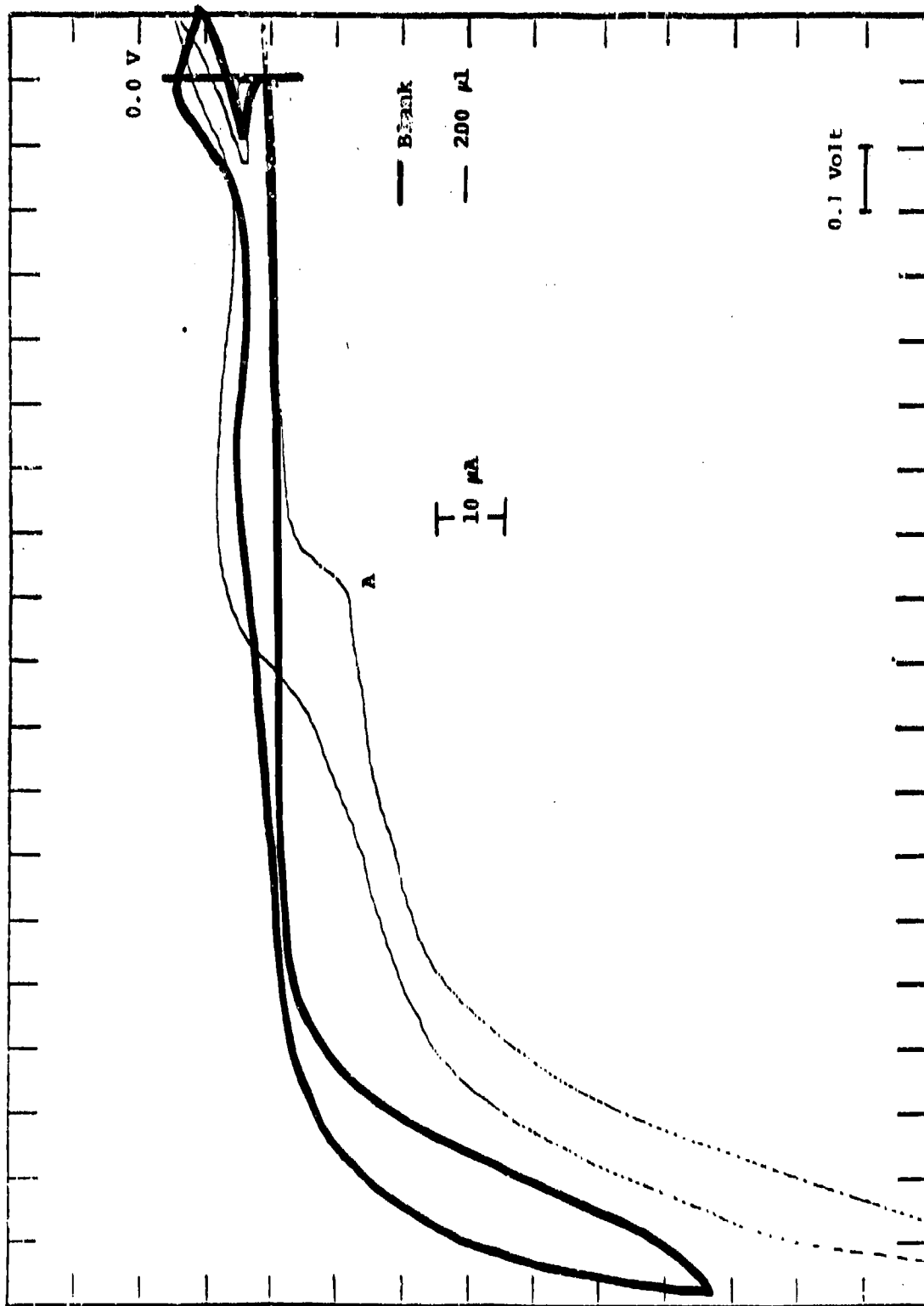


Figure 5. Voltammogram of a 200  $\mu\text{l}$  Sample of the Fresh TEL-4005 Oil in Propylene Carbonate with a Platinum Working Electrode.

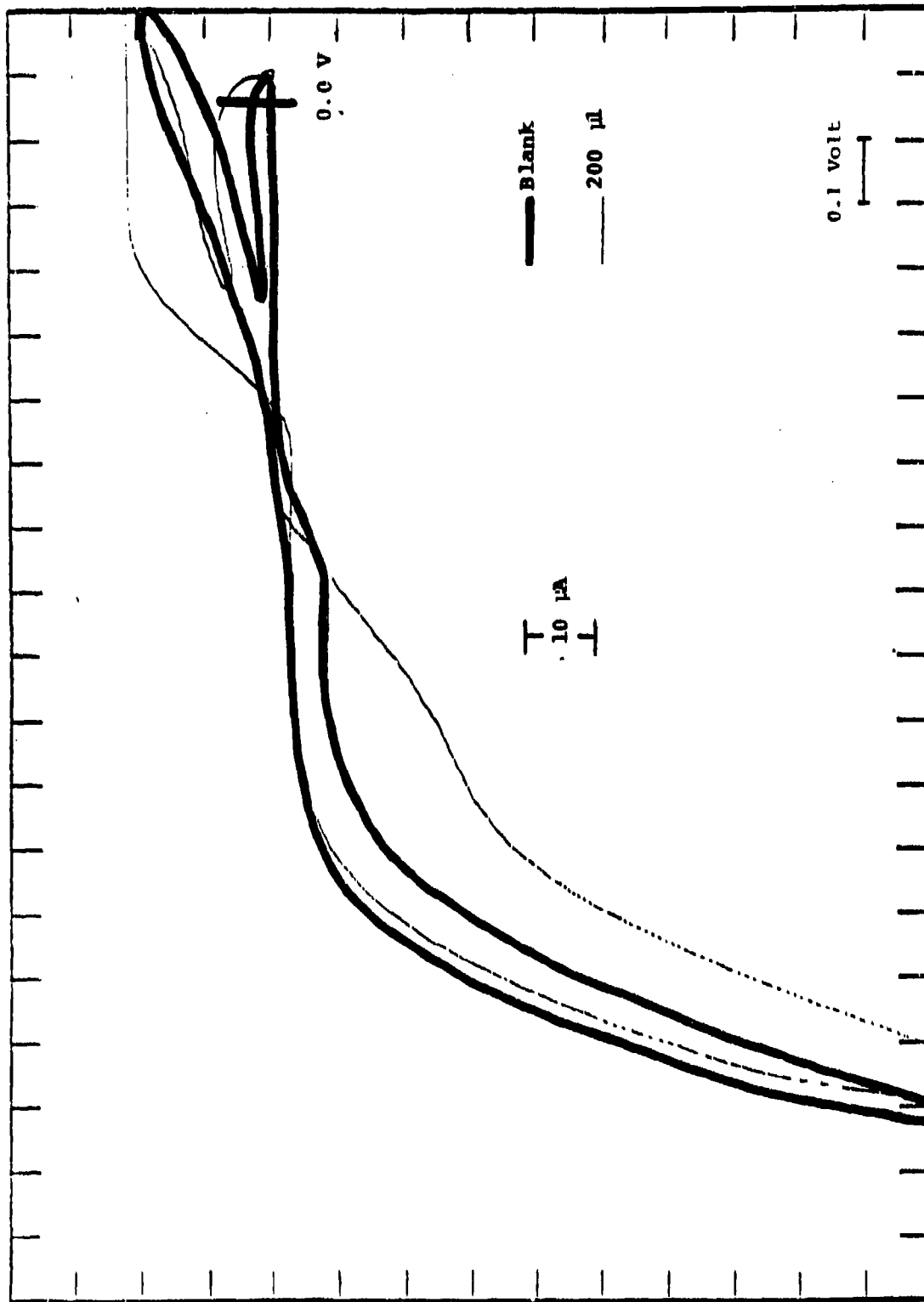


Figure 6. Voltammogram of a 200  $\mu\text{l}$  Sample of the Fresh TEL-4005 Oil in Methanol with a Platinum Working Electrode.

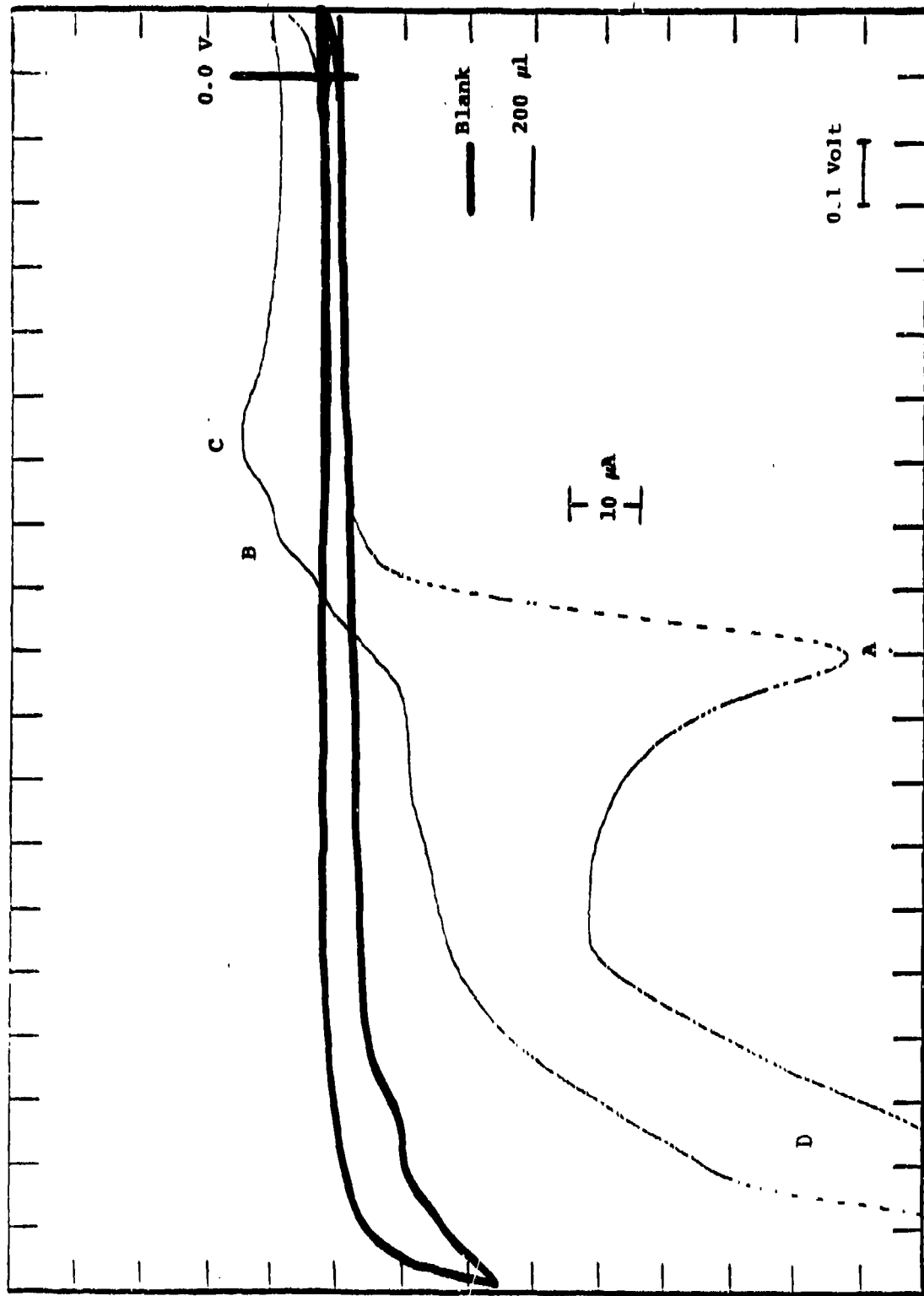


Figure 7. Voltammogram of a 200  $\mu\text{l}$  Sample of the Fresh TEL-4005 Oil in Acetone with a Platinum Working Electrode.

### (3) Effect of Working Electrode

In order to determine the best working electrode for use in acetone, carbon paste, glassy carbon, platinum and gold working electrodes were studied. A scan rate of 250 mV/sec was used but the voltage range was reduced to -0.3 V to +1.4 V in order to eliminate the peaks produced by the TEAP electrolyte (D in Figure 7).

The carbon paste electrode disintegrated in the acetone before a single scan could be completed. The voltammograms produced by the glassy carbon, gold, and platinum voltammetry electrodes are shown in Figure 8. As illustrated in Figure 8, the glassy carbon electrode produces the best resolved reduction waves (B) and (C) and produces the largest oxidation wave (A).

The glassy carbon electrode is ideally suited for routine determinations due to its high mechanical stability and the simple polishing procedure required to clean the surface of the electrode. The polishing procedure requires only a couple minutes to complete. Therefore, the glassy carbon electrode was used for the following work.

### (4) Effect of Electrolyte

In an attempt to further decrease the cost per sample of the cyclic voltammetry technique,  $\text{LiClO}_4$  was studied as an electrolyte. Besides its lower cost,  $\text{LiClO}_4$  can be obtained in anhydrous form, is very soluble in acetone (137 g/100 g of acetone) and has a lower molecular weight than TEAP so that less  $\text{LiClO}_4$  is needed to produce a 0.1 M solution. The results for 0.1 M solutions of  $\text{LiClO}_4$  and TEAP in acetone were identical. Therefore,  $\text{LiClO}_4$  was used as the electrolyte for the following work.

### (5) Effect of Scan Rate

To determine the effect of the scan rate, voltammograms were produced using scan rates of 750, 500, and

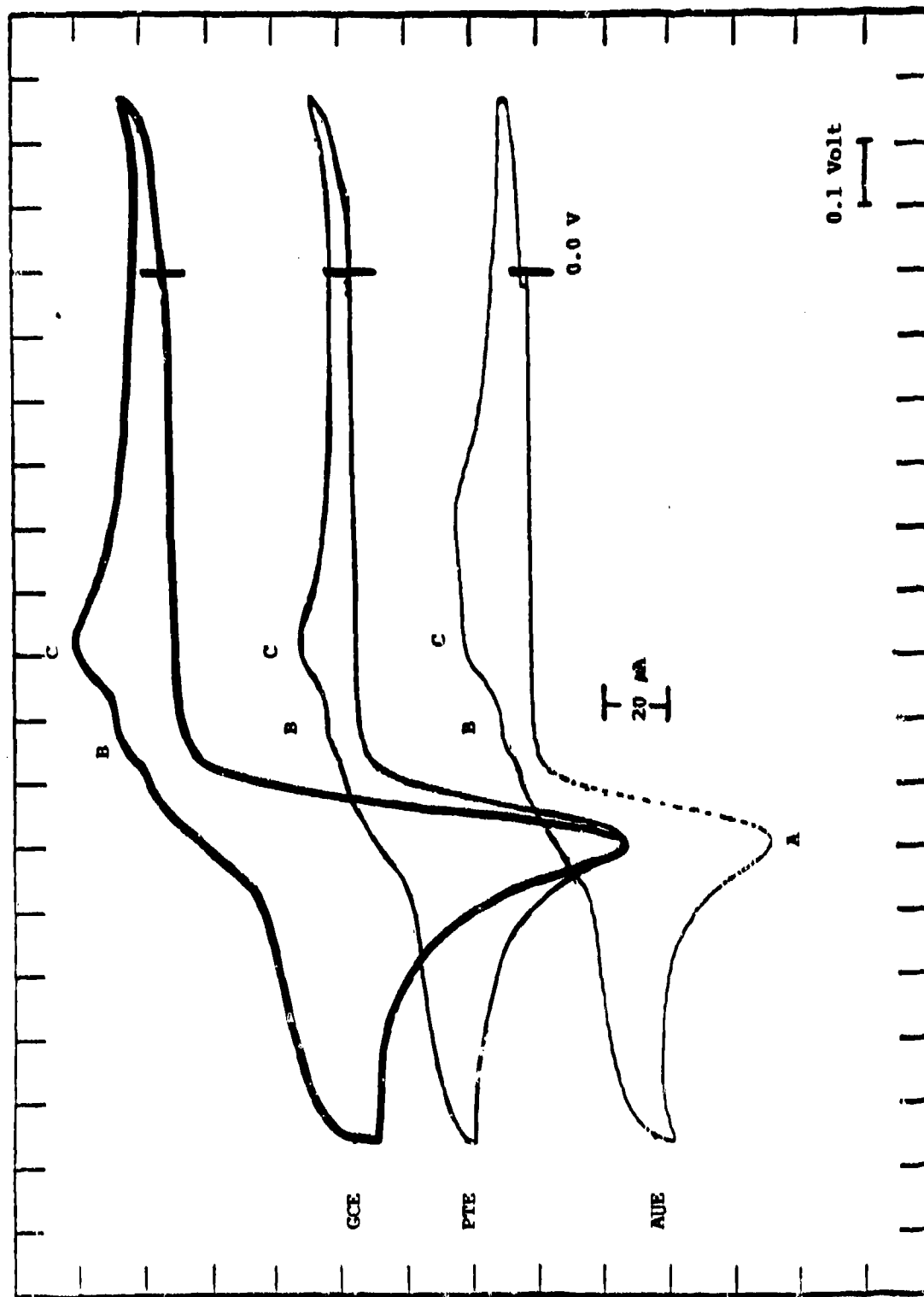


Figure 8. Effect of the Working Electrode Type on the Voltammogram of the Fresh TEL-4005 Oil: GCE=Glassy Carbon Electrode, PTE=Platinum Electrode, and AUE=Gold Electrode.

250 mV/sec. As illustrated in Figure 9, the oxidation wave (A) increases in intensity and shifts to a higher potential as the scan rate is increased. The optimum resolution of the reduction waves (B and C in Figure 9) are obtained with a scan rate of 500 mV/sec. At the higher scan rate of 750 mV/sec, the reduction waves (B and C in Figure 9) are greater in intensity but are broader and less defined. Also, the background increases with the scan rate. Thus, a scan rate of 500 mV/sec was used for the following research.

#### (6) Effect of Additives

To determine if additives other than the antioxidants are contributing to the voltammograms of the MIL-L-7808 lubricating oils, the voltammograms of quinizarin (anticorrosion), tricresylphosphate (TCP) (antiwear), and TCP's degradation products (o- and p-cresol) were compared to the voltammogram of the blank. None of the compounds studied produced oxidation or reduction waves in the range of -0.3 V to 1.4 V.

#### (7) Effect of Formulation

To determine the effects of formulation on the antioxidant determinations by cyclic voltammetry, the voltammograms for the six different MIL-L-7808 lubricating oils, TEL-4001 through TEL-4006 oils (obtained from AFWAL/POSL), were recorded and are shown in Figures 10 and 11. The voltammograms are displayed using a scale of 0.2 V/inch instead of 0.1 V/inch so that they could be combined into two figures, instead of six separate ones, to facilitate comparison.

As illustrated in Figures 10 and 11, all six MIL-L-7808 oils appear to contain similar antioxidants (waves occur at similar potentials), but only the TEL-4002 and TEL-4004 oils contain similar ratios of antioxidants (voltammograms of similar shape). Of the lubricating oils studied, the TEL-4001 oil appears to have the lowest concentration of antioxidants (smallest

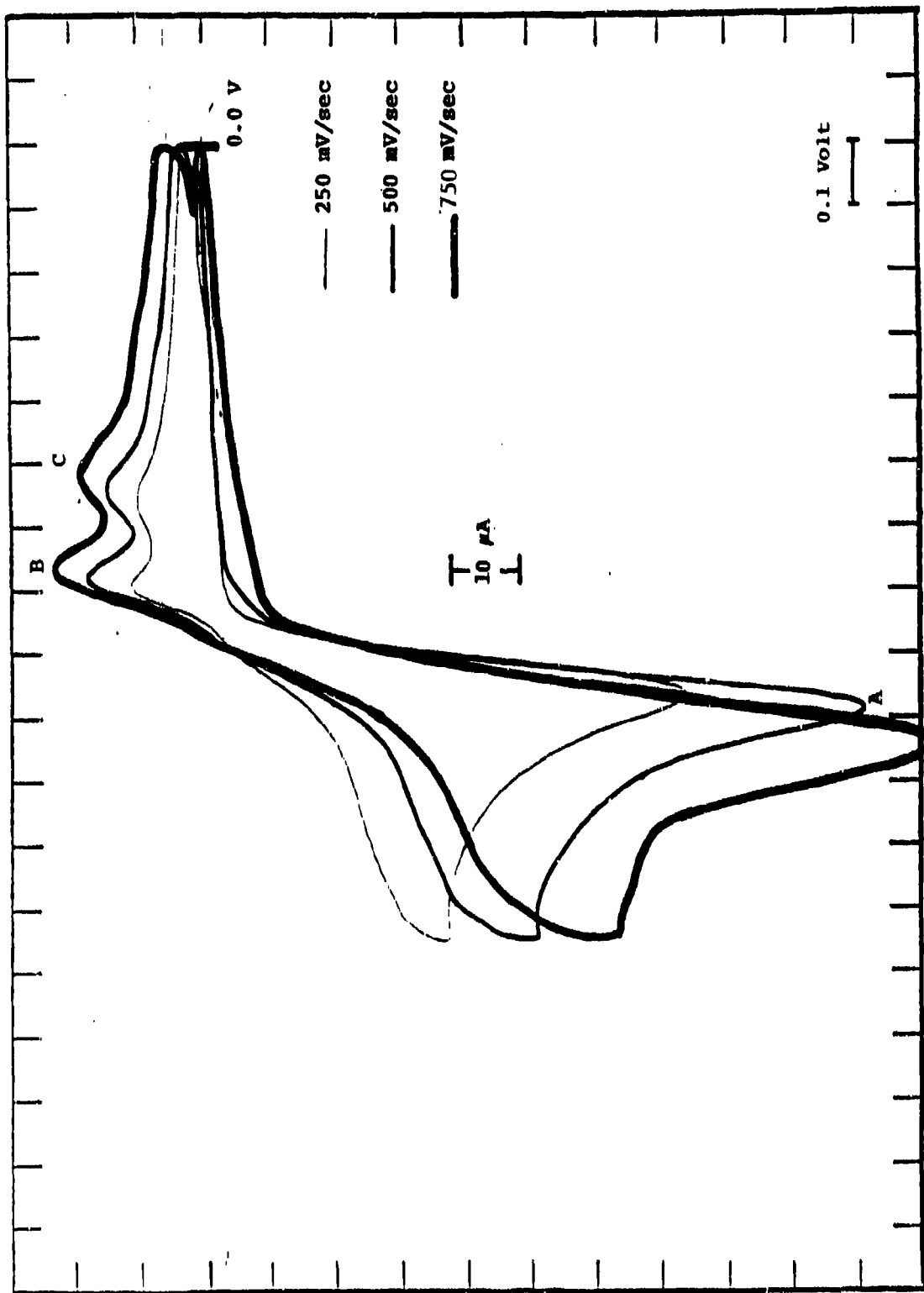


Figure 9. Effect of the Scan Rate (mV/sec) on the Voltammogram of the Fresh TEL-4005 Oil in Acetone with a Glassy Carbon Working Electrode.

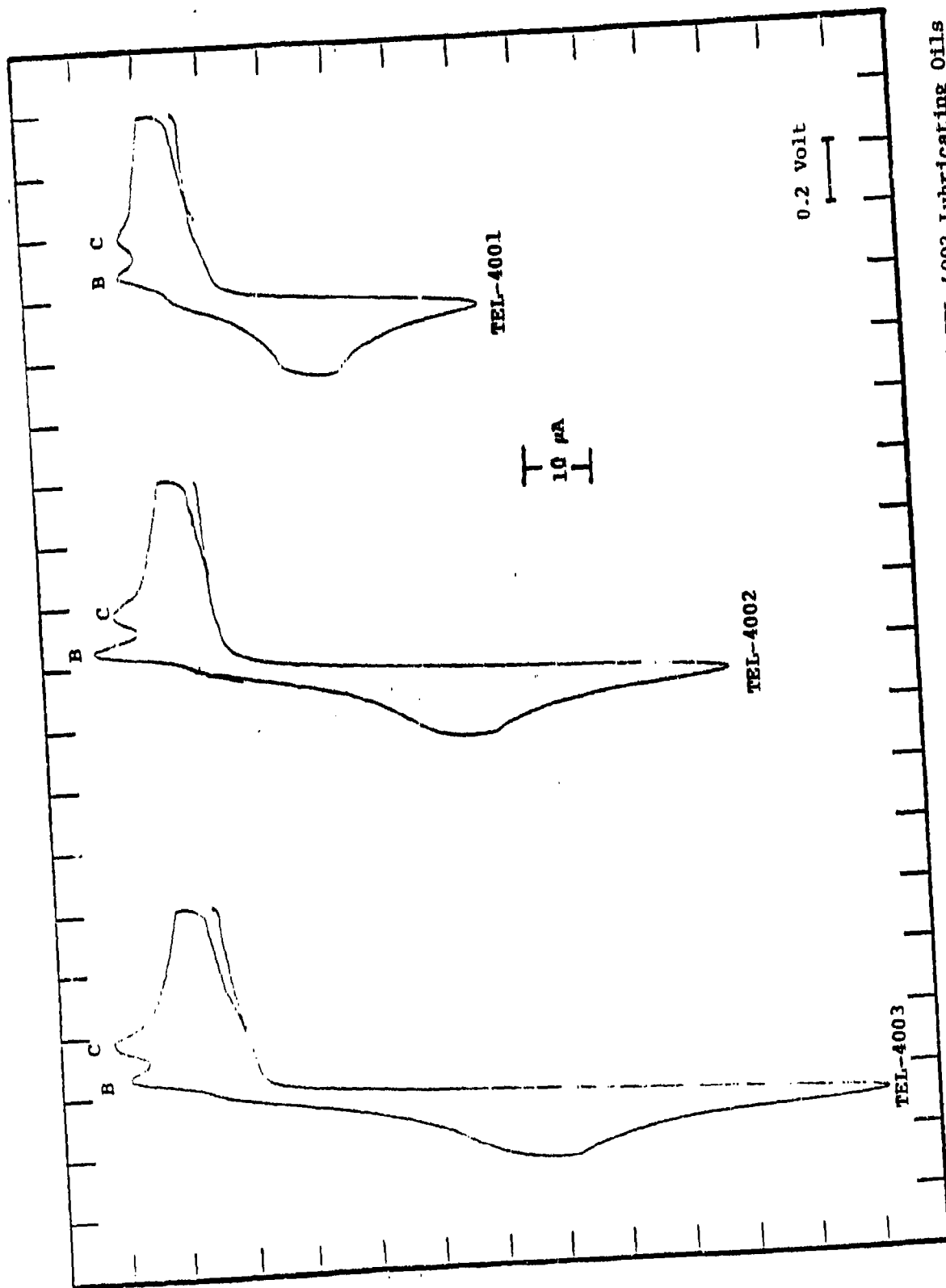


Figure 10. Voltammograms of the Fresh TEL-4001, TEL-4002, and TEL-4003 Lubricating Oils in Acetone with a Glassy Carbon Working Electrode.

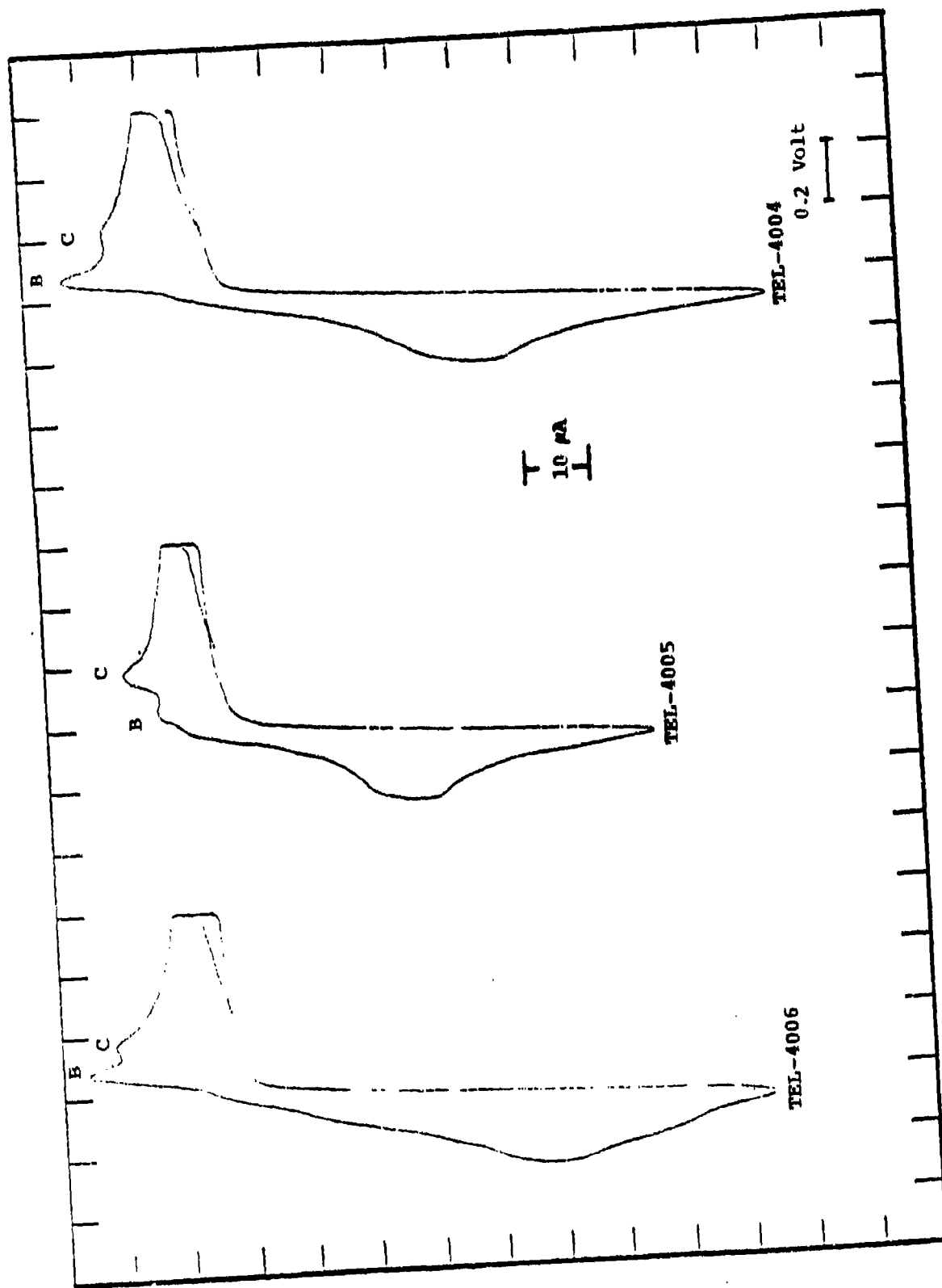


Figure 11. Voltammograms of the Fresh TEL-4004, TEL-4005, and TEL-4006 Lubricating Oils in Acetone with a Glassy Carbon Working Electrode.

waves) while TEL-4003 oil appears to have the highest concentration (largest waves).

(8) Calibration Curves of Antioxidants in MIL-L-7808 Oil

In order that calibration curves could be produced for the antioxidants in a MIL-L-7808 oil, a gas chromatographic analysis using a thermionic specific detector [sensitive only to compounds containing N (antioxidants) and P] was performed on TEL-4005 oil. It was determined that the antioxidants used in TEL-4005 oil are N-phenyl- $\alpha$ -naphthylamine (PANA) and dioctyl-diphenyl amine (DODPA).

To quantify the DODPA and PANA in the TEL-4005 MIL-L-7808 oil, cyclic voltammograms were produced for sequential additions of 20 and 40  $\mu$ l of 1% solutions of DODPA and PANA to 10 ml of acetone (Figure 12). The calibration curves produced by this procedure are shown in Figure 13 for both the oxidation and reduction waves of PANA and DODPA. Since the cyclic voltammetric responses are dependent on concentration (molarity) and antioxidant concentrations are usually given in percent weight, the responses were plotted versus both concentration and percent weight of antioxidant.

As illustrated in Figure 13, the oxidation waves are twice as sensitive to PANA as to DODPA, but the reduction waves of PANA and DODPA are of similar sensitivities.

Due to the different sensitivities of the oxidation waves to DODPA and PANA, their ratio must be known before a total concentration of antioxidant can be determined. For instance, in Figure 11 the TEL-4005 oil appears to contain much less total antioxidant than the TEL-4004 oil, but if the ratio of DODPA/PANA is greater for the TEL-4005 oil than for the TEL-4004 oil, they may have similar total concentrations of antioxidants.

Thus, it appears that the reduction waves of the cyclic voltammograms are better suited for quantifying the antioxidants in the MIL-L-7808 oils. The response of the reduction waves is similar for PANA and DODPA (Figure 13) and two reduction

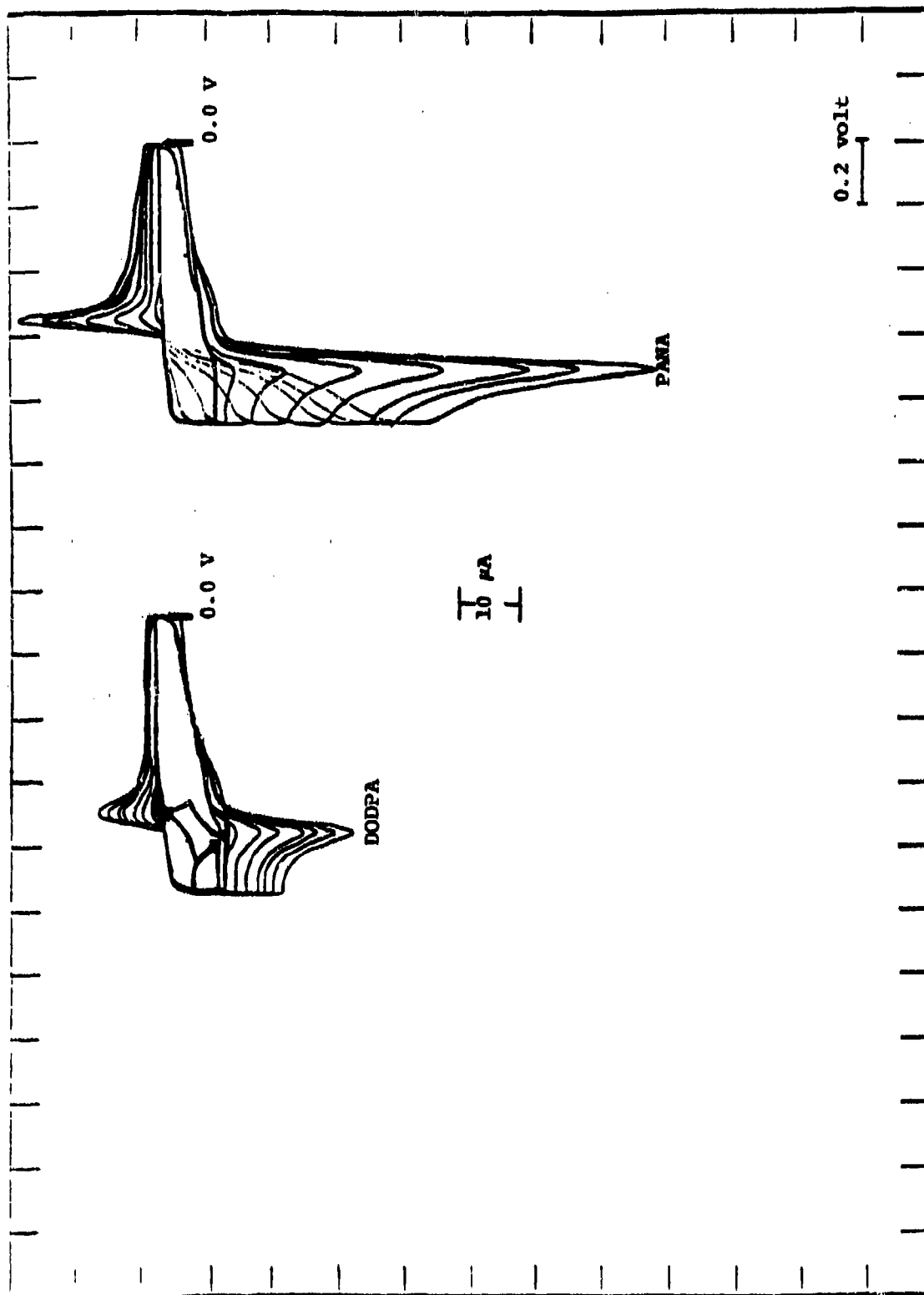


Figure 12. Effect of Successive Additions of 1% DODPA and PANA Solutions on the Voltammograms Produced by a Glassy Carbon Working Electrode in Acetone.

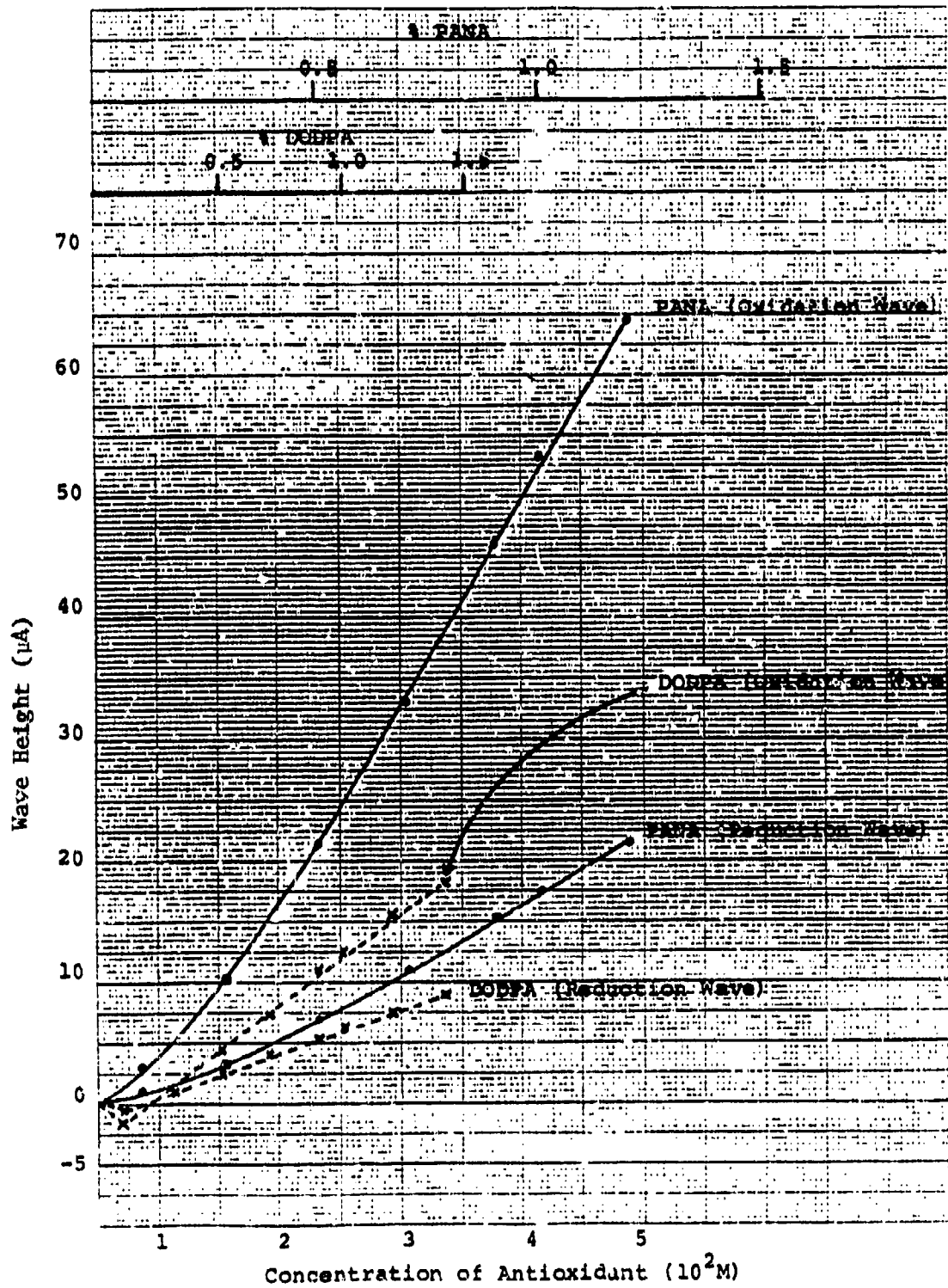


Figure 13. Calibration Curves for the Oxidation and Reduction Waves of PANA and DODPA.

waves are produced by TEL-4005 oil, presumably for DODPA and PANA (Figure 2) (DODPA and PANA produce one combined oxidation wave).

(9) Effect of Successive Scans on Voltammograms of MIL-L-7808 Oils

To determine the effects of electrochemical oxidation on the voltammograms of the different MIL-L-7808 oils, the voltammograms produced by successive scans were studied. By studying the voltammograms of successive scans, new compounds produced by the electrochemical oxidation of the antioxidants could be observed. The cyclic voltammograms produced by the first and fifth scans for each MIL-L-7808 oil are shown in Figures 14-16.

As seen in Figures 14-16, the oxidation wave (A) at 800 mV of each oil is decreased for the fifth scan in comparison to the first scan. However, the reduction waves of each oil increase for the fifth scan as compared to the first scan. In addition to the oxidation wave at 800 mV seen in the voltammogram of the first scan, new oxidation waves between 550 and 800 mV (B in Figures 14-16) are present in the voltammogram of the fifth scan. New oxidation waves, similar to those seen in Figures 14-16, were also present in the fifth scan voltammograms of different PANA/DODPA mixtures (Figure 17).

Therefore, regardless of the MIL-L-7808 oil's formulation, new compounds, which oxidize between 550-800 mV, are produced by the electrochemical oxidation of the antioxidants.

(10) Effect of Oxidation Products

It has been determined by high pressure differential scanning calorimetry (Reference 2) that, with equal concentrations of original antioxidants, oxidized oil has a longer induction period than fresh oil. It has also been reported (Reference 3) that the reaction mixture produced by chemically or thermally oxidizing PANA has more antioxidant capability than the original PANA. Therefore, to determine if cyclic voltammetry was able to detect the antioxidants' reaction products which increase the stability of oxidized oil samples,

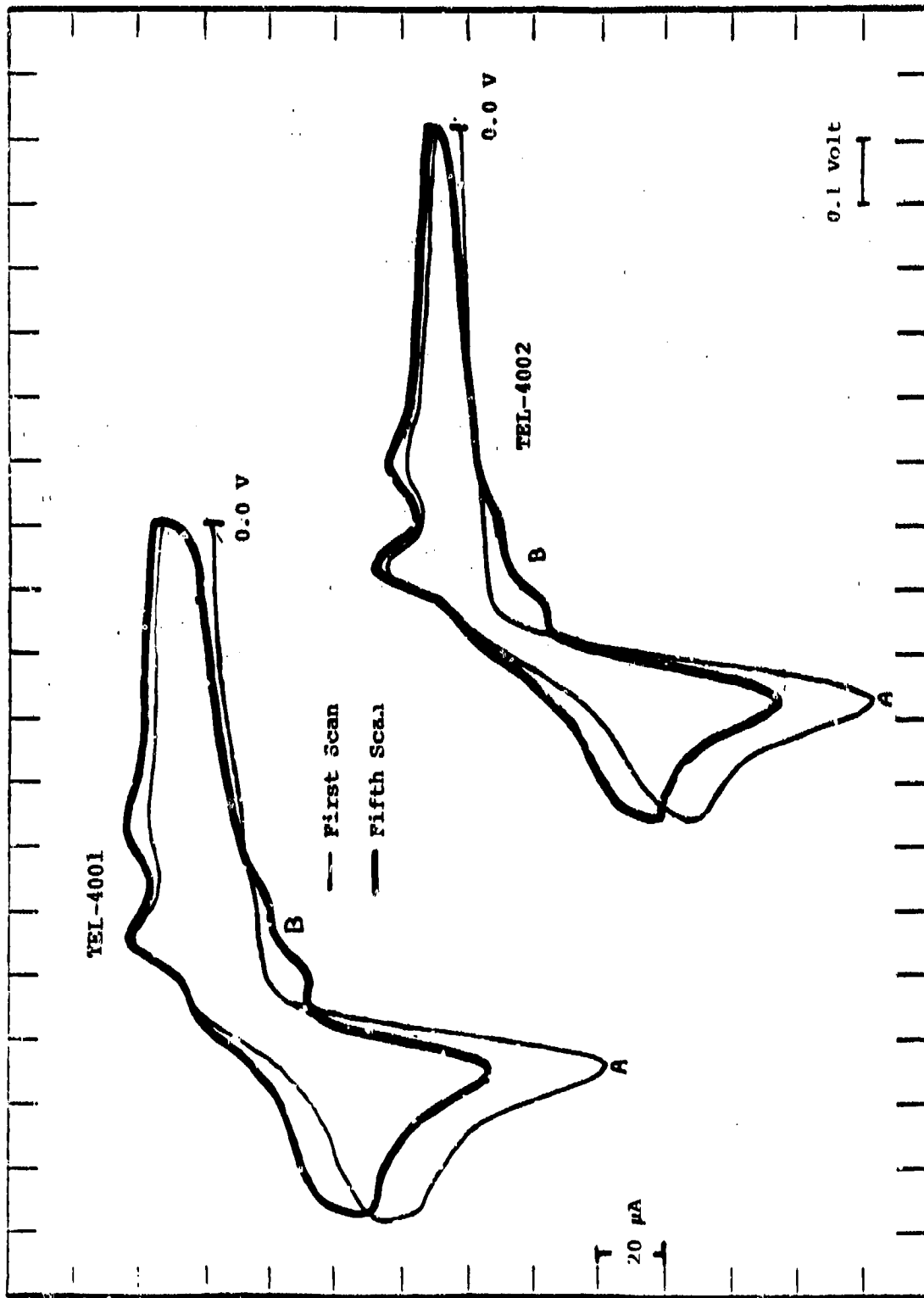


Figure 14. First and Fifth Scan Voltammograms of the Fresh TEL-4001 and TEL-4002 Oils in Acetone with a Glassy Carbon Working Electrode.

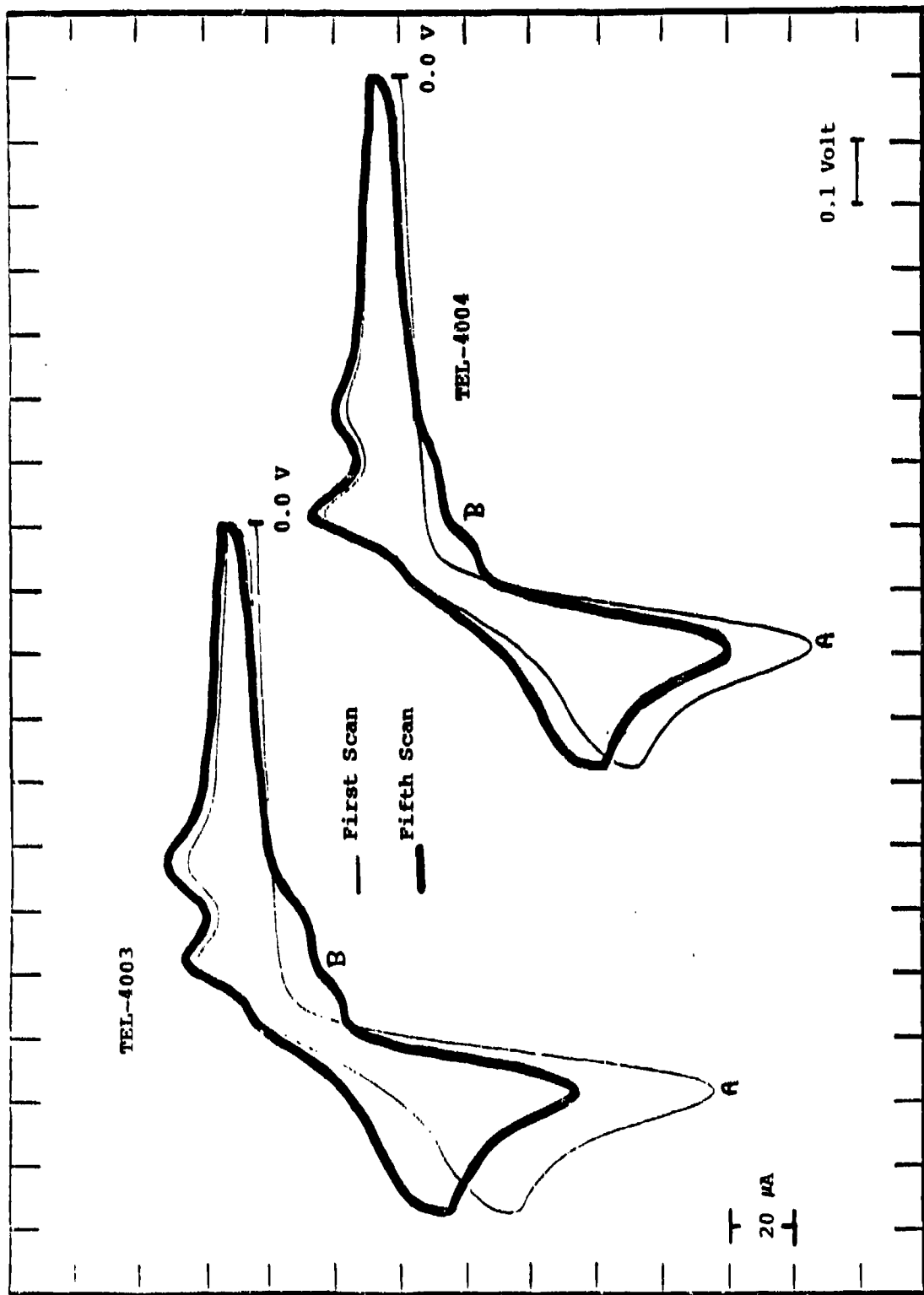


Figure 15. First and Fifth Scan Voltammograms of the Fresh TEL-4003 and TEL-4004 Oils in Acetone with a Glassy Carbon Working Electrode.

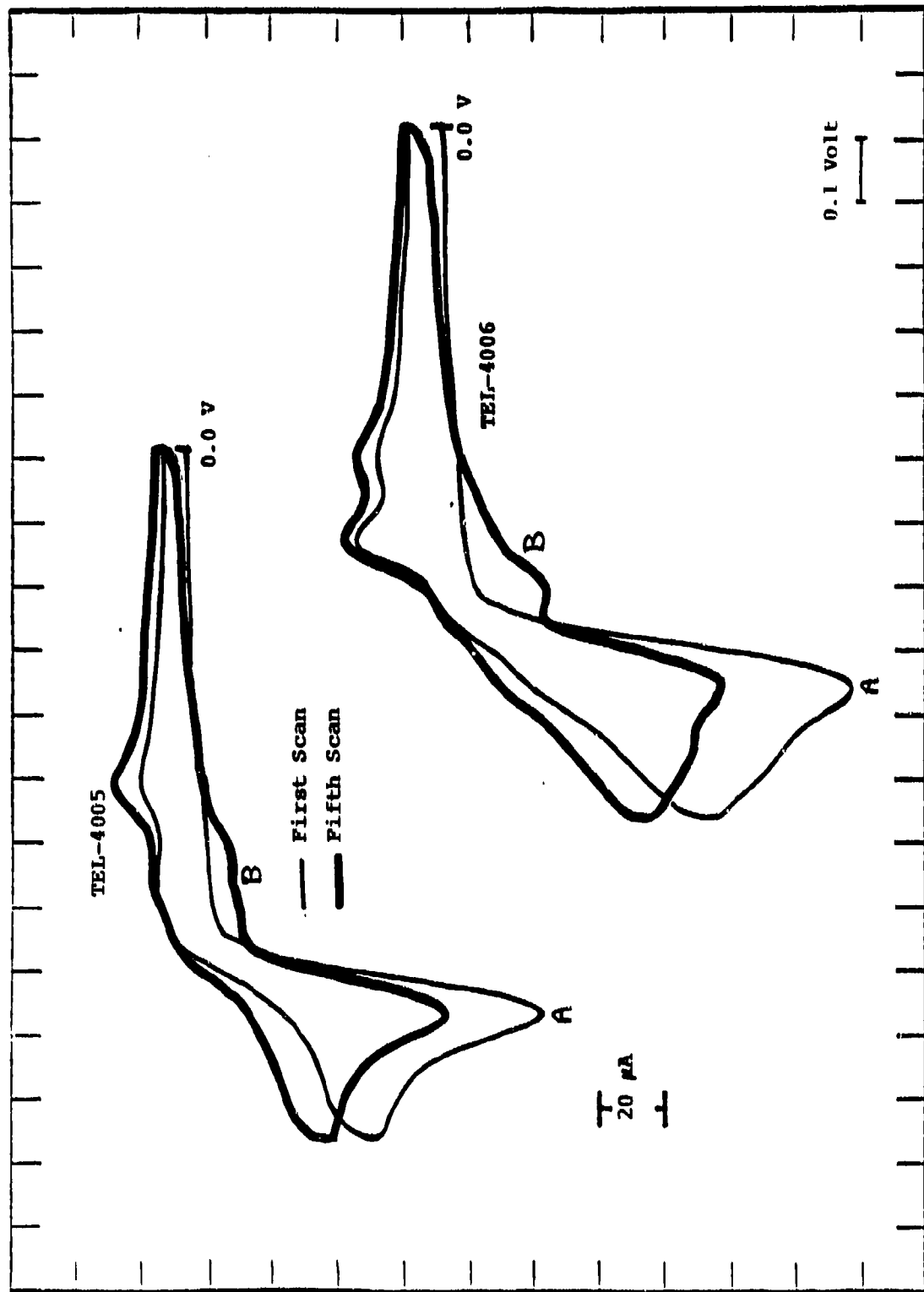


Figure 16. First and Fifth Scan Voltammograms of the Fresh TEL-4005 and TEL-4006 Oils in Acetone with a Glassy Carbon Working Electrode.

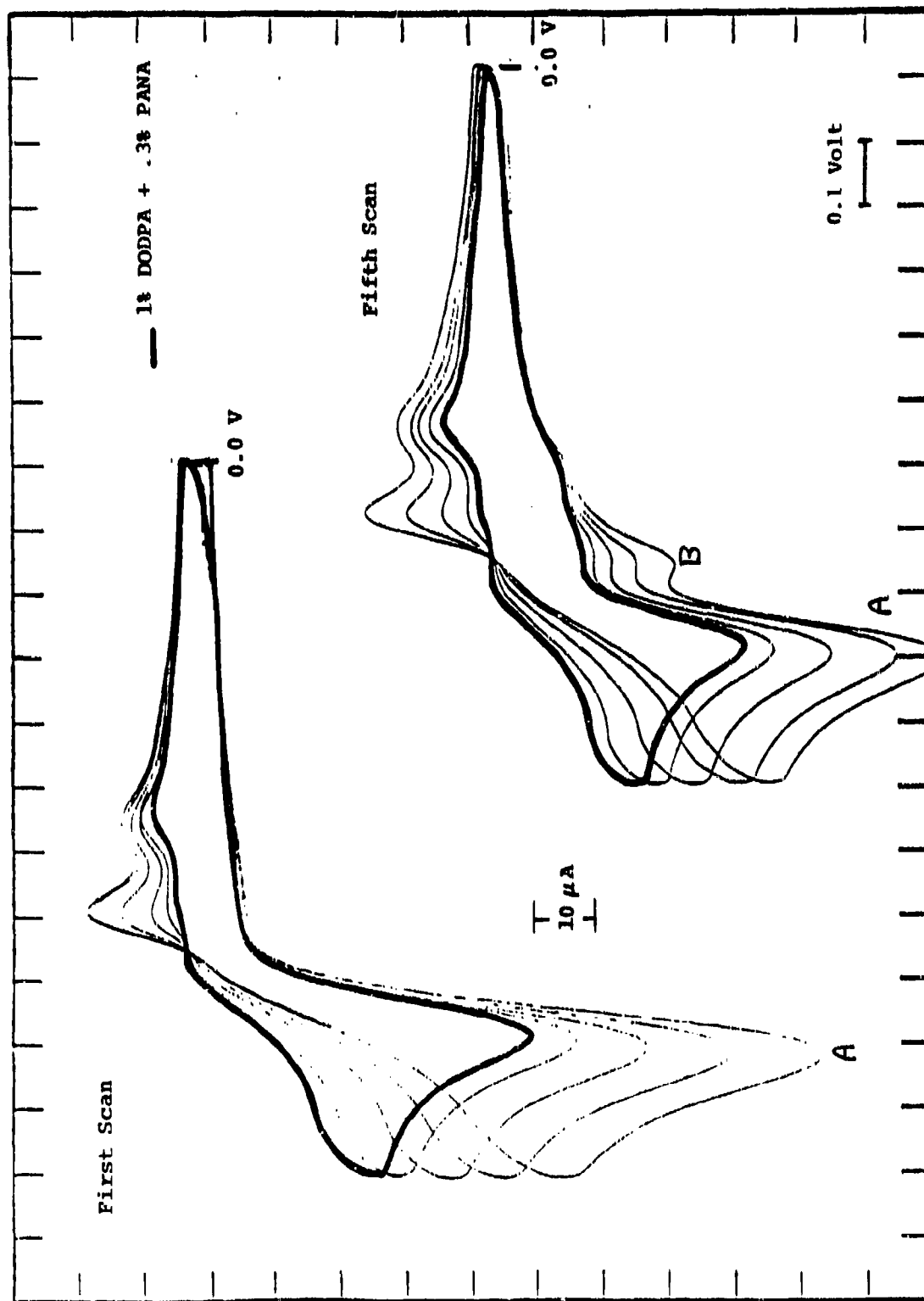


Figure 17. Effect of Successive Additions of a 1% PANa Solution in the Presence of 1% DODPA and 0.3% PANa on the First and Fifth Scan Voltammograms Produced by a Glassy Carbon Working Electrode in Acetone.

TEL-4005 oil heated at 175°C with a flow rate of 10 l/hr was sampled every 16-24 hours to produce samples of increasingly oxidized oil. Each oil was then analyzed by single scan and multiscan cyclic voltammetry. The first scan voltammograms of the fresh and stressed TEL-4005 oil samples are shown in Figure 18.

As seen in Figure 18, the oxidation wave produced by PANA and DODPA (A) decreases with stressing time, especially during the first 72 hours. The reduction waves also decrease but go through a complex series of changes.

As expected, the stressed (thermal oxidation) TEL-4005 oil samples contain species that are similar to those produced by electrochemical oxidation, i.e., oxidation waves at 550-800 mV in the voltammograms of the stressed oil samples (Figure 18) and in the fifth scan voltammograms of the fresh oils (Figures 14-16).

During the thermal oxidative stressing, the oxidation waves at 550-800 mV increase during the first 72 hours, stay constant for the next 72 hours, and then decrease in size with additional stressing time. Thus, the production rate of the new species decreases with increasing stressing time relative to the consumption rate of the new species. Thus, the ability of multiscan cyclic voltammetry to produce the new species should decrease as the thermal oxidative stressing time of the oil sample increases. To verify this idea, first and fifth scan voltammograms were produced for the stressed TEL-4005 oil samples and are shown in Figures 19-22.

As seen in Figures 19-22, the broad oxidation waves produced at 550-800 mV by the fifth scan decrease with increasing stressing time relative to the oxidation waves produced by the first scan.

Therefore, by comparing the 550-800 mV oxidation waves of the first and fifth scans of used oil samples, it may be

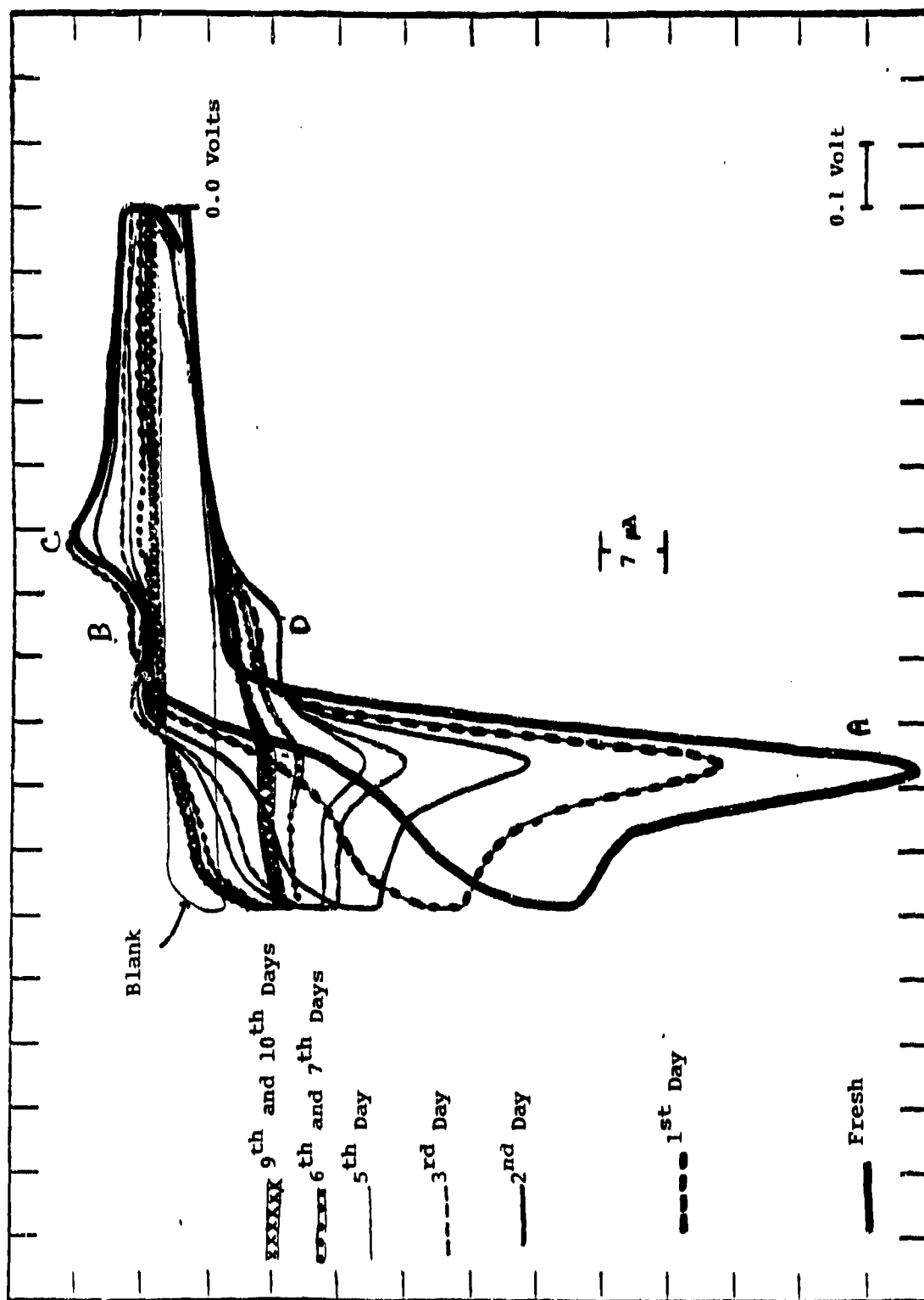


Figure 18. Voltammograms of Fresh and Stressed TEL-4005 Oils in Acetone with a Glassy Carbon Working Electrode.

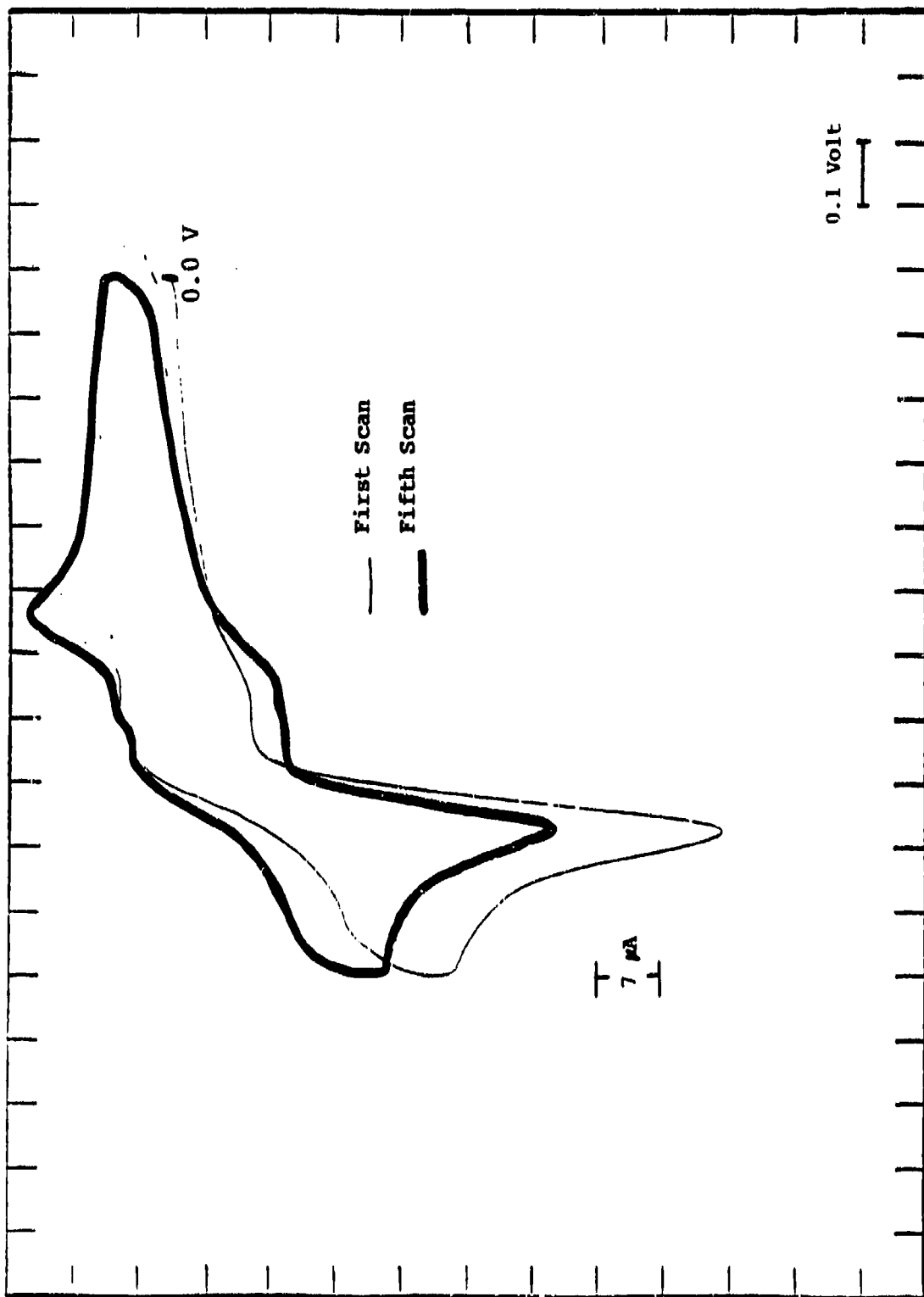


Figure 19. First and Fifth Scan Voltammograms of 24 Hours Stressed TEL-4005 Oil in Acetone with a Glassy Carbon Working Electrode.

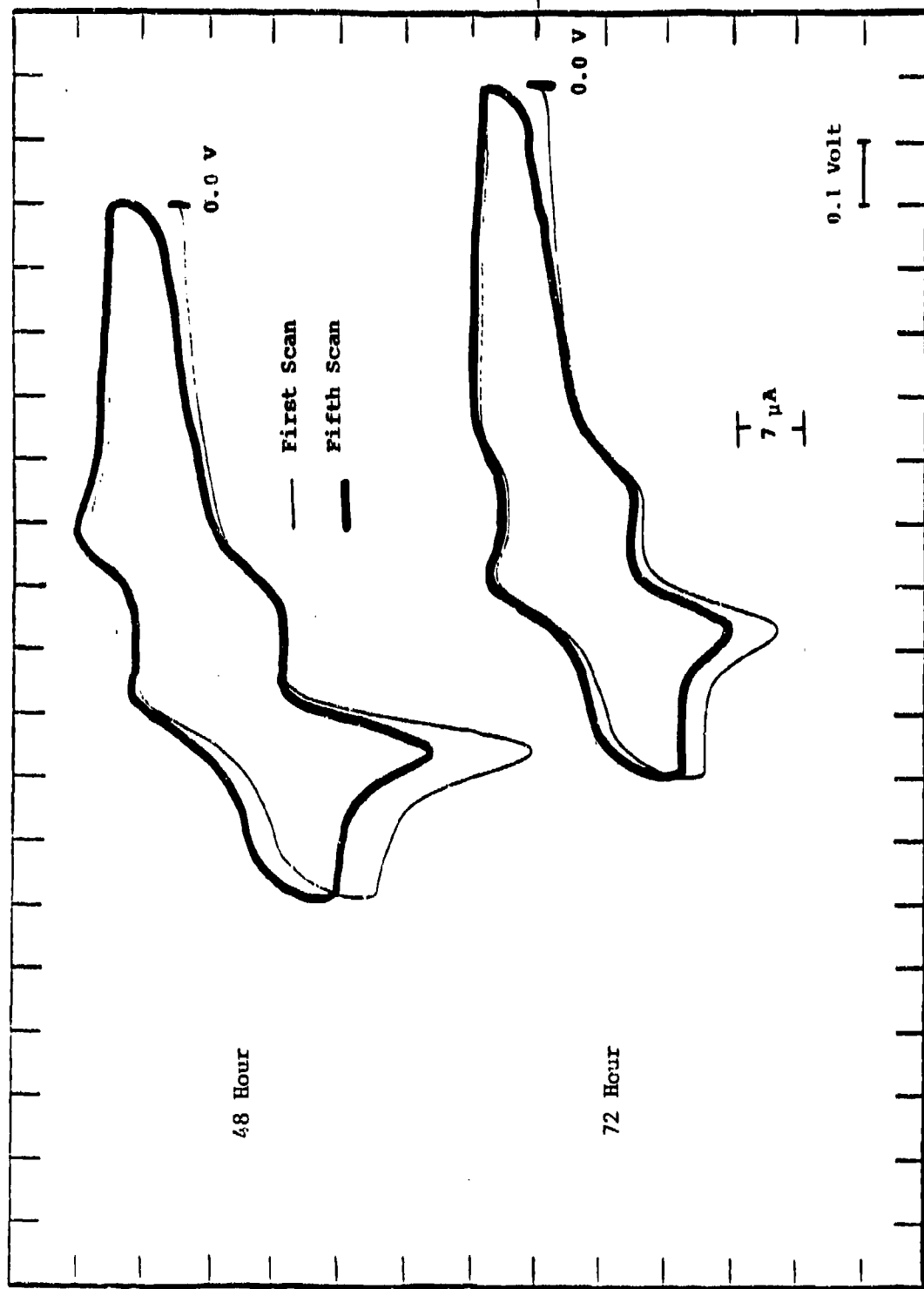


Figure 20. First and Fifth Scan Voltammograms of 48 and 72 Hours Stressed TEL-4005 Oils in Acetone with a Glassy Carbon Working Electrode.

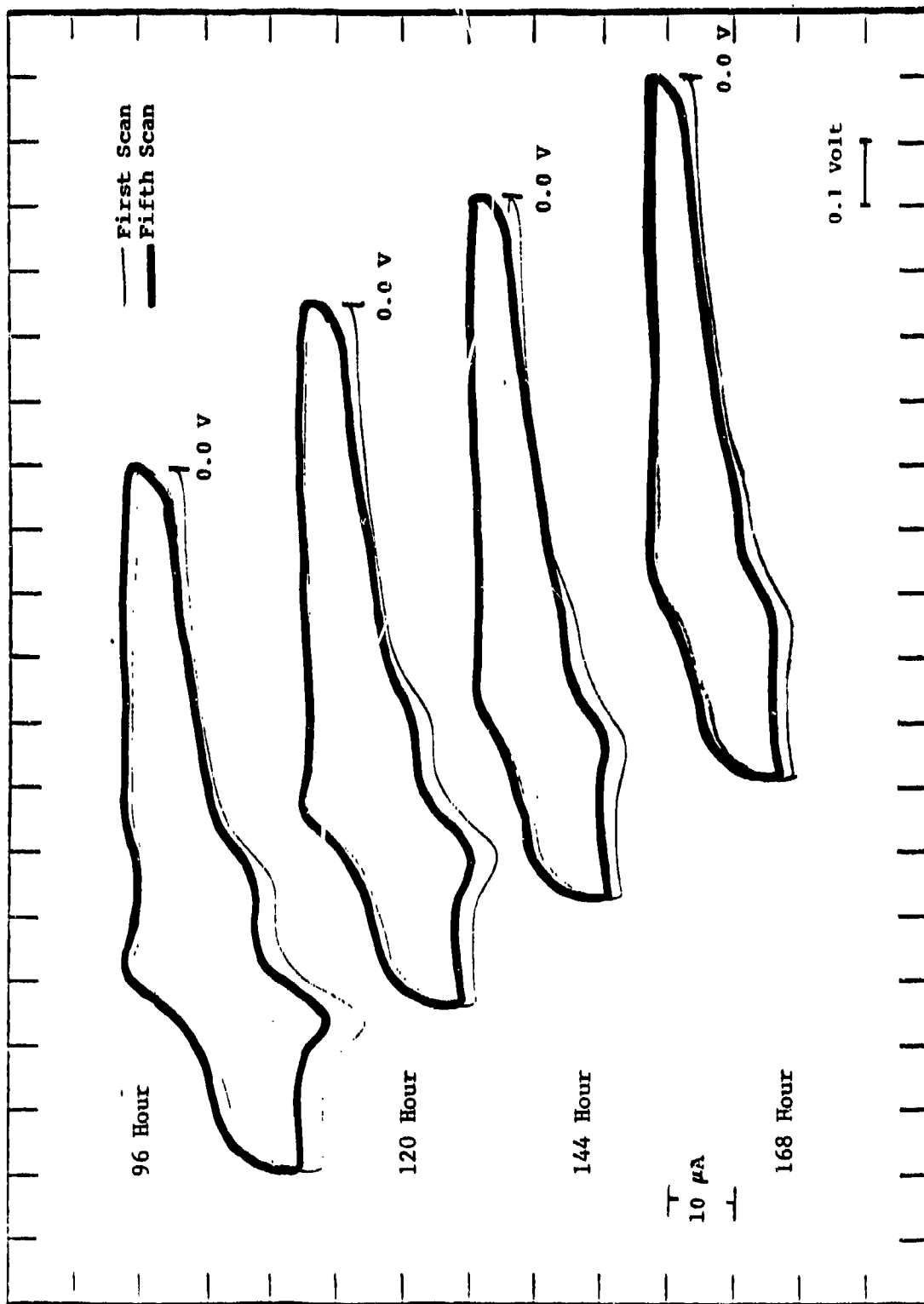


Figure 21. First and Fifth Scan Voltammograms of 96-168 Hours Stressed TEL-4005 Oils in Acetone with a Glassy Carbon Working Electrode.

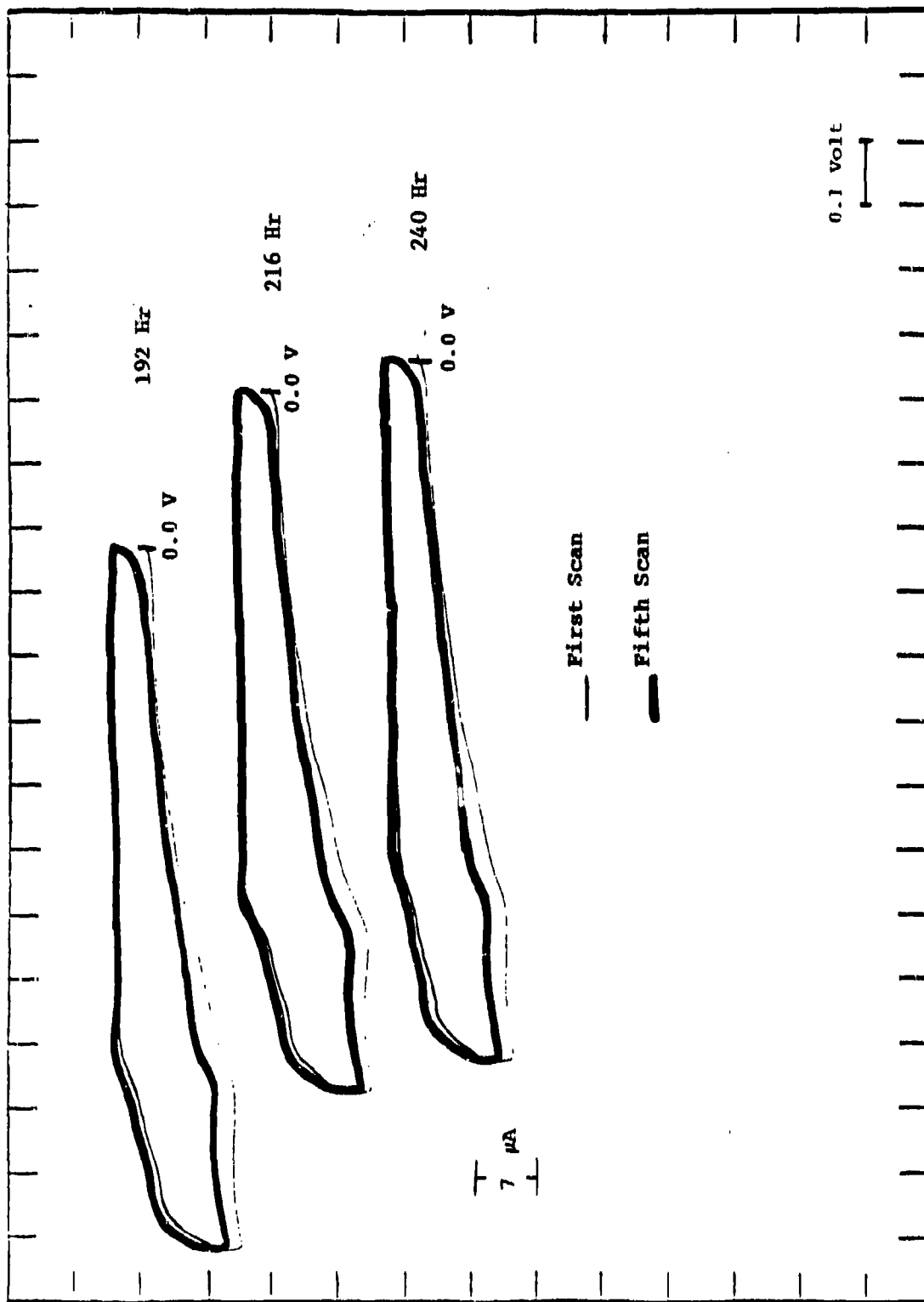


Figure 22. First and Fifth Scan Voltammograms of 192-240 Hours Stressed TEL-4005 Oils in Acetone with a Glassy Carbon Working Electrode.

possible to relate the increase or decrease in the oxidation wave at 550-800 mV to the RLL of a MIL-L-7808 oil.

(11) Effect of Organic Peroxides on the Voltammograms of the MIL-L-7808 Lubricating Oils

In an attempt to combine chemical stressing with cyclic voltammetry for the development of a RLLAT candidate, organic peroxides (benzoyl peroxide and dicumene peroxide) and a free radical initiator, azobisisobutyronitrile (AIBN) were added to the diluted oil sample prior to cyclic voltammetric analysis. The cyclic voltammograms of the MIL-L-7808 oils (200  $\mu$ l) diluted with 10 ml of acetone (0.1M LiClO<sub>4</sub>) were obtained at a scan rate of 500 mV/sec using a GCE as the working electrode.

The addition of dicumene peroxide or the free radical initiator, AIBN, did not affect the cyclic voltammograms of the MIL-L-7808 oils. However, the addition of benzoyl peroxide to the TEL-4005 oil produced a new oxidation peak (A in Figure 23) at 780 mV which is not reproduced during the second scan. The TEL-4002 through TEL-4004 oils gave similar results in the presence of benzoyl peroxide. However the cyclic voltammogram of the TEL-4006 oil was not affected by the addition of benzoyl peroxide and the cyclic voltammogram of the TEL-4001 oil (Figure 24) showed a different response to the presence of benzoyl peroxide than did the TEL-4002 through TEL-4005 oils.

Therefore, these particular chemical stressing, cyclic voltammetric methods were eliminated as possible RLLAT candidates.

(12) Effect of Pyridine on the Voltammograms of the MIL-L-7808 Lubricating Oils

It has been reported that pyridine (Reference 4) and other organic bases (Reference 5) react with the electrochemical oxidation products of aromatic amines. The mechanism by which organic bases (:B) are thought to alter the oxidation products of aromatic amines (Ar<sub>2</sub>NH) is as follows:



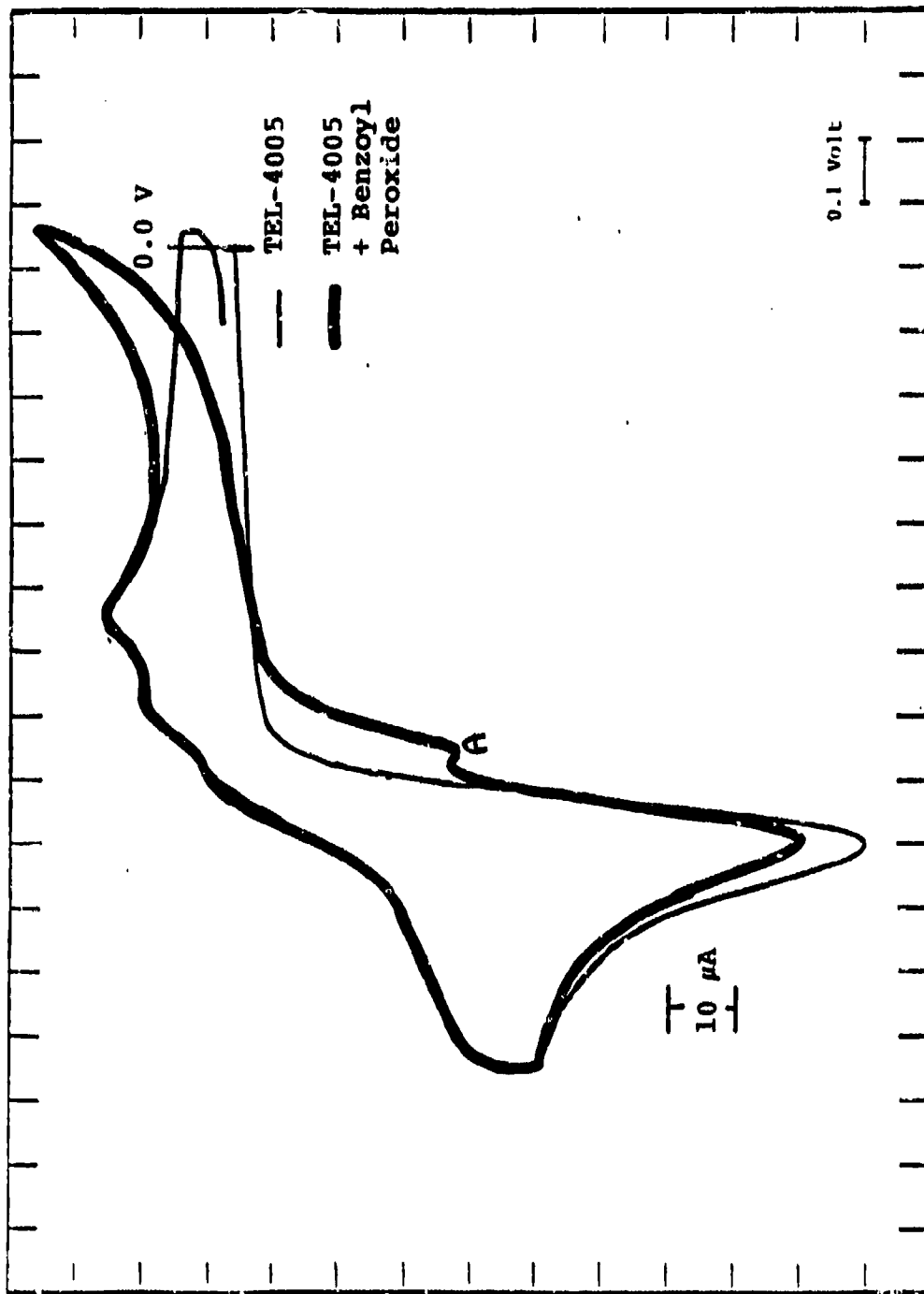


Figure 23. Effect of Benzoyl Peroxide on the Voltammogram of the Fresh TEL-4005 OIL in Acetone Using a Glassy Carbon Working Electrode.

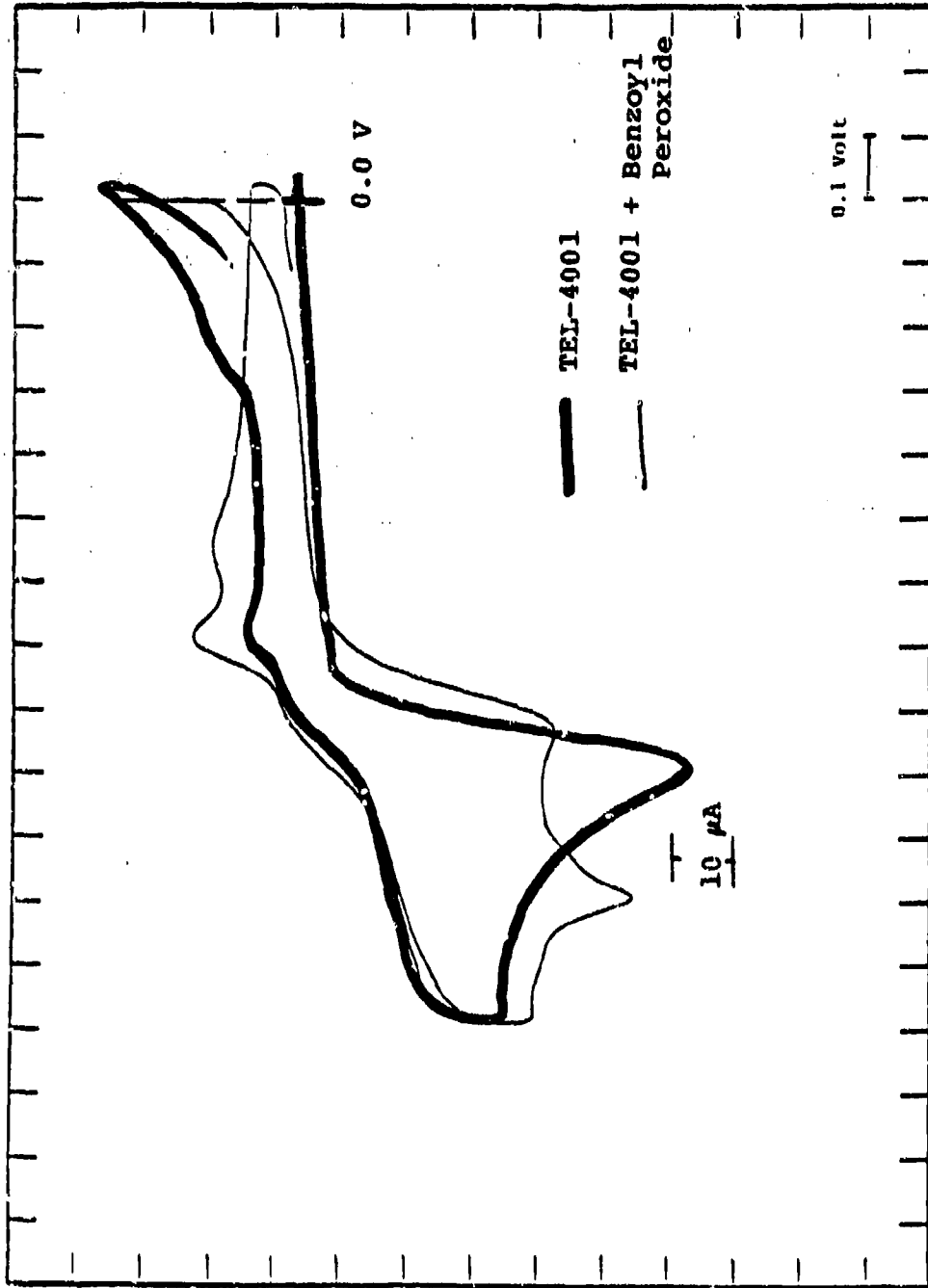
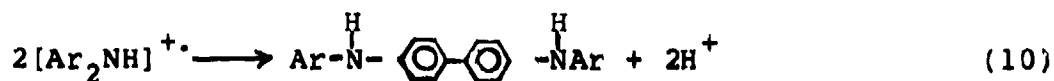


Figure 24. Effect of Benzoyl Peroxide on the Voltammogram of the Fresh TEL-4001 Oil in Acetone Using a Glassy Carbon Working Electrode.



To study the effects of pyridine, voltammograms of the TEL-4005 oil were recorded after each 10  $\mu\text{l}$  addition of a 5 percent pyridine in acetone solution. As seen in Figure 25, the first 10  $\mu\text{l}$  addition has a small effect on the voltammogram of the TEL-4005 oil. However, the second and third 10  $\mu\text{l}$  additions of pyridine cause the oxidation wave (Figure 25) to shift to a lower oxidation potential and eliminate the reduction waves between 500 and 800 mV. In addition to the effects on the original oxidation and reduction waves produced by the TEL-4005 oil, a new reduction wave at 290 mV is produced (Figure 25).

To determine the effect of pyridine on the voltammograms of all the MIL-L-7808 lubricating oils, 30  $\mu\text{l}$  of the 5 percent pyridine in acetone solution was added to 200  $\mu\text{l}$  of each oil dissolved in 10 ml of acetone (0.1M  $\text{LiClO}_4$ ). The voltammograms of the different lubricating oils before and after the addition of the pyridine are shown in Figures 26-28. As seen in Figures 26-28 every oil produces a reduction wave between 200-300 mV in the presence of pyridine.

Therefore, the voltammograms of the stressed TEL-4005 oil samples were recorded after the addition of 30  $\mu\text{l}$  of the 5 percent pyridine in acetone solution. The voltage scan was limited to 0.7 V to 0.0 V to eliminate the large oxidation wave at 800 mV. The reduced scan allows the small oxidation wave at 630 mV and the reduction wave between 200-300 mV to be the major peaks of the voltammogram so that the changes in their respective intensities can be detected more accurately. The voltammogram of TEL-4005 oil in the absence of pyridine was used as the blank signal. An example of the voltammograms produced in this manner are shown in Figure 29.

The plots of the 630 mV oxidation wave's and the 280 mV reduction wave's intensities versus stressing time shown

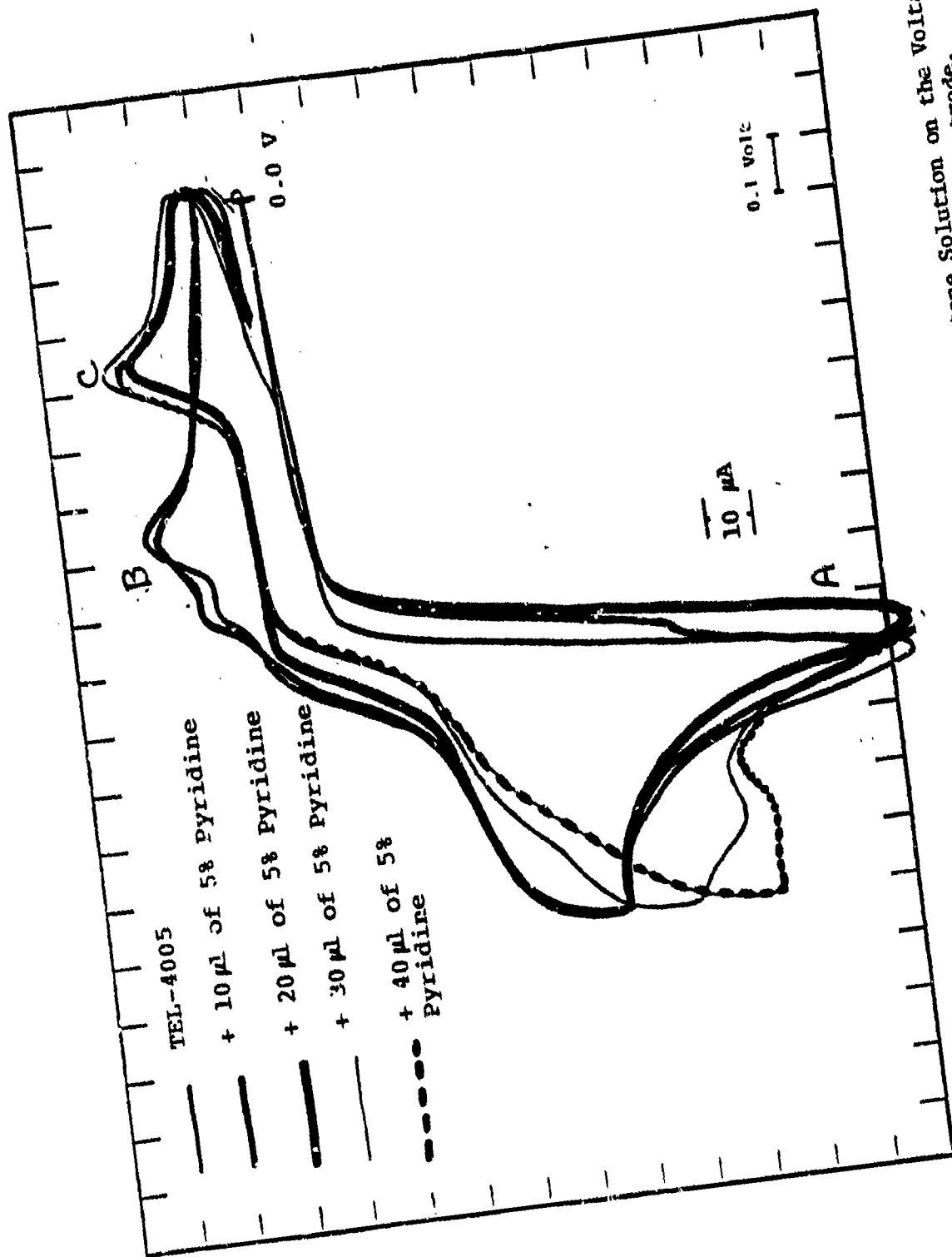


Figure 25. Effect of Successive Additions of the 5% Pyridine in Acetone Solution on the Voltammogram of the Fresh TEL-4005 Oil in Acetone Using a Glassy Carbon Working Electrode.

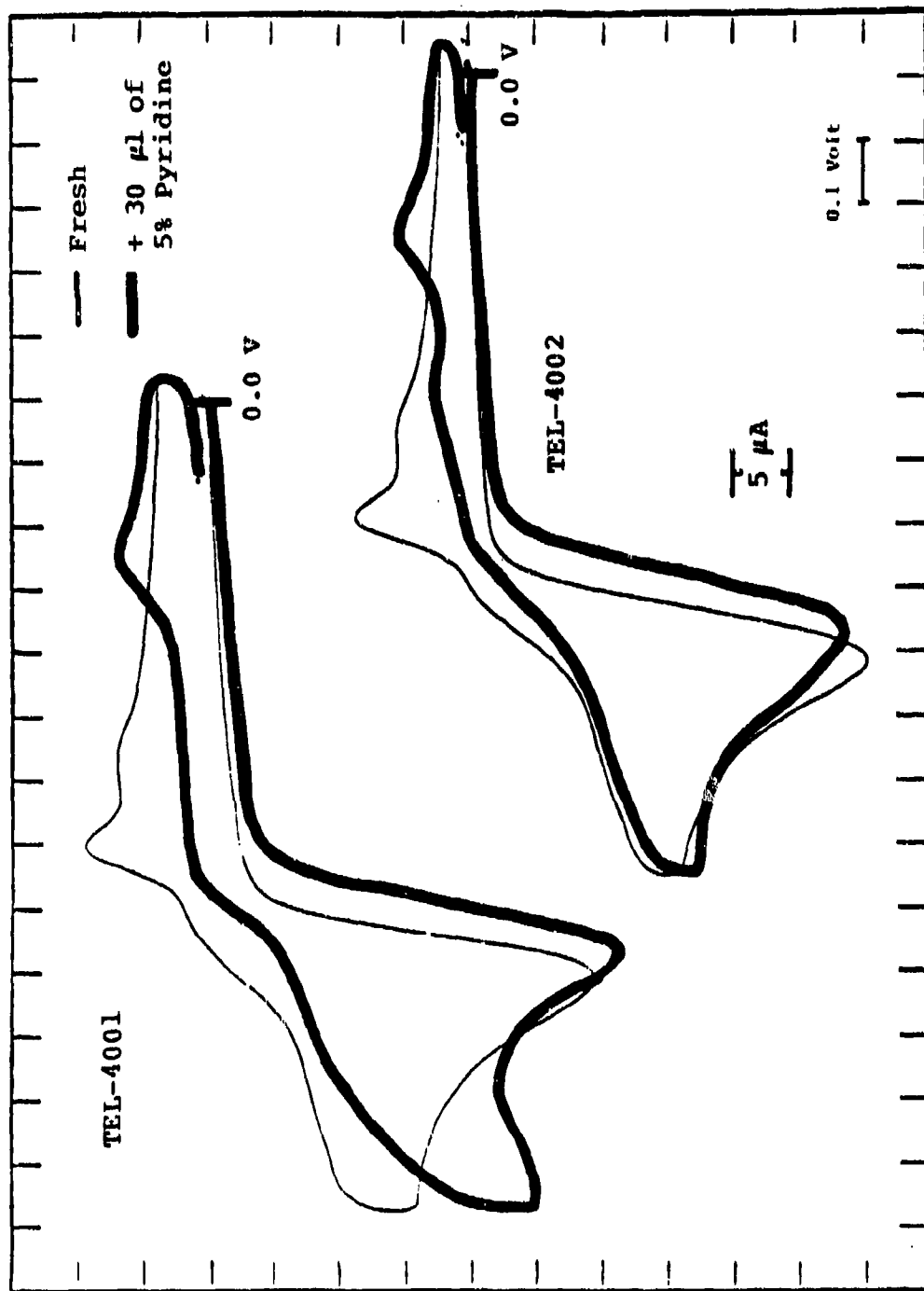


Figure 26. Effect of the 5% Pyridine in Acetone Solution on the Voltammograms of the Fresh TEL-4001 and TEL-4002 Oils in Acetone Using a Glassy Carbon Working Electrode.

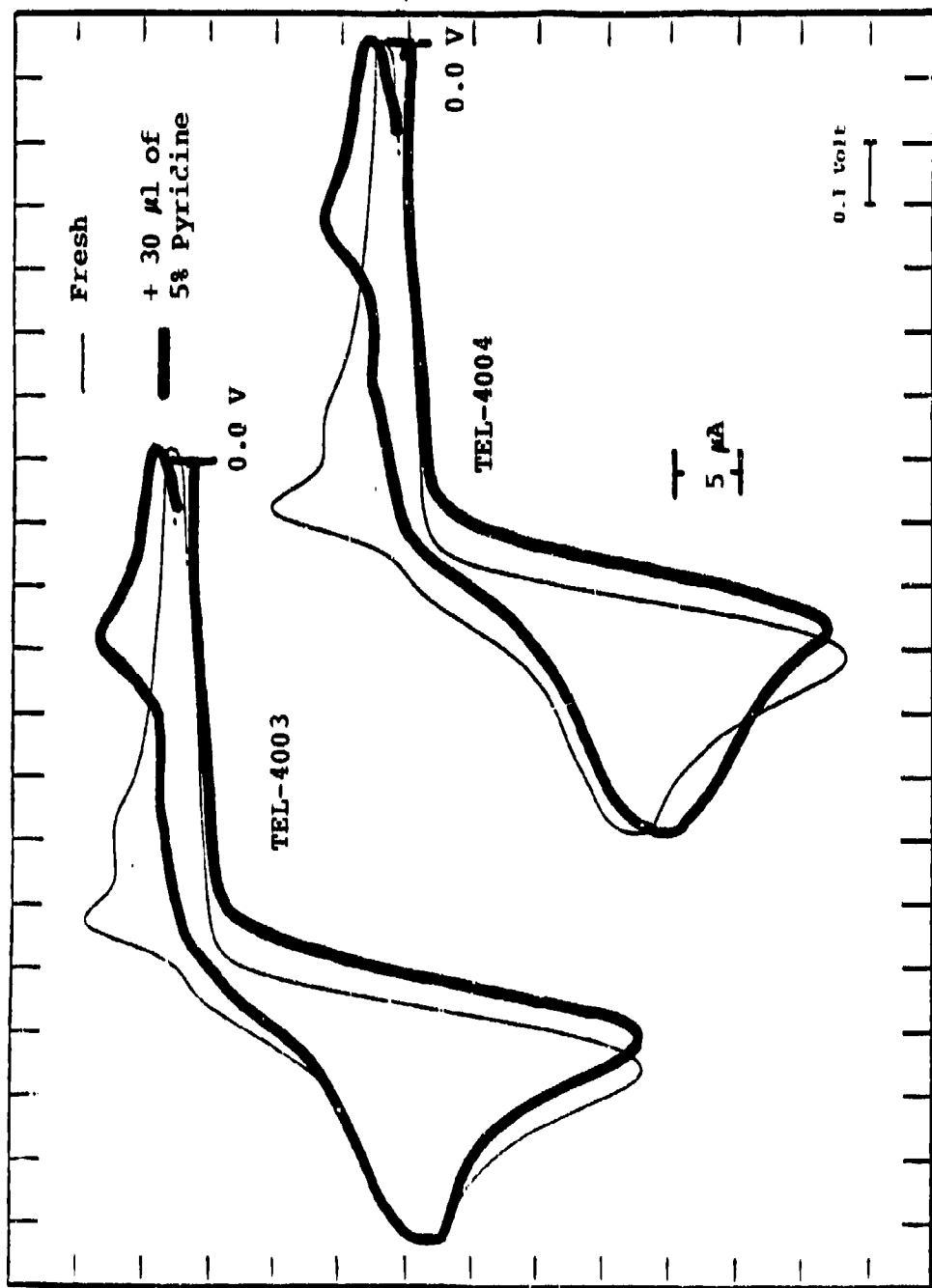


Figure 27. Effect of the 5% Pyridine in Acetone Solution on the Voltammograms of the Fresh TEL-4003 and TEL-4004 Oils in Acetone Using a Glassy Carbon Working Electrode.

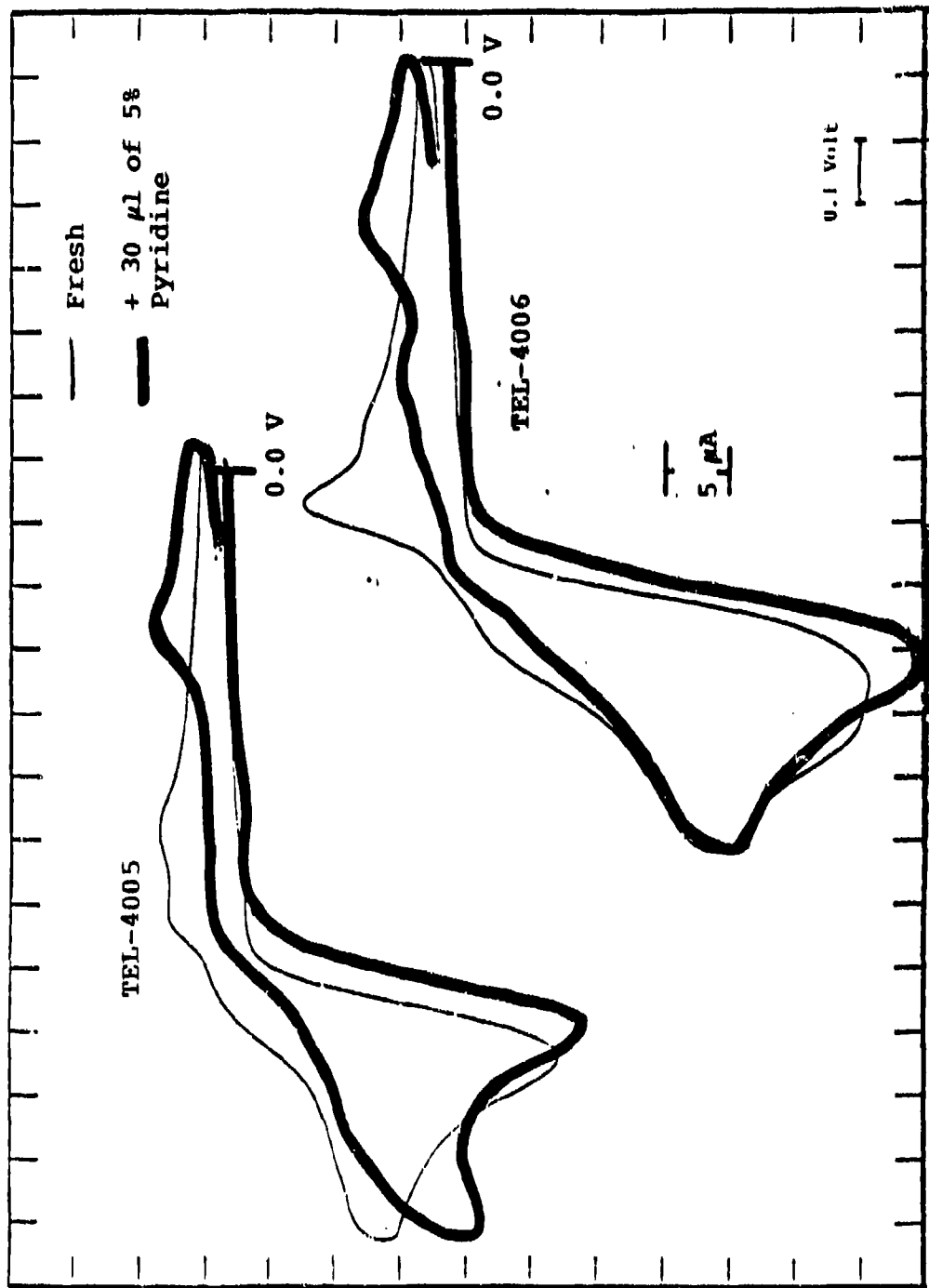


Figure 28. Effect of 5% Pyridine in Acetone Solution on the Voltammograms of the Fresh TEL-4005 and TEL-4005 Oils in Acetone Using a Glassy Carbon Working Electrode.

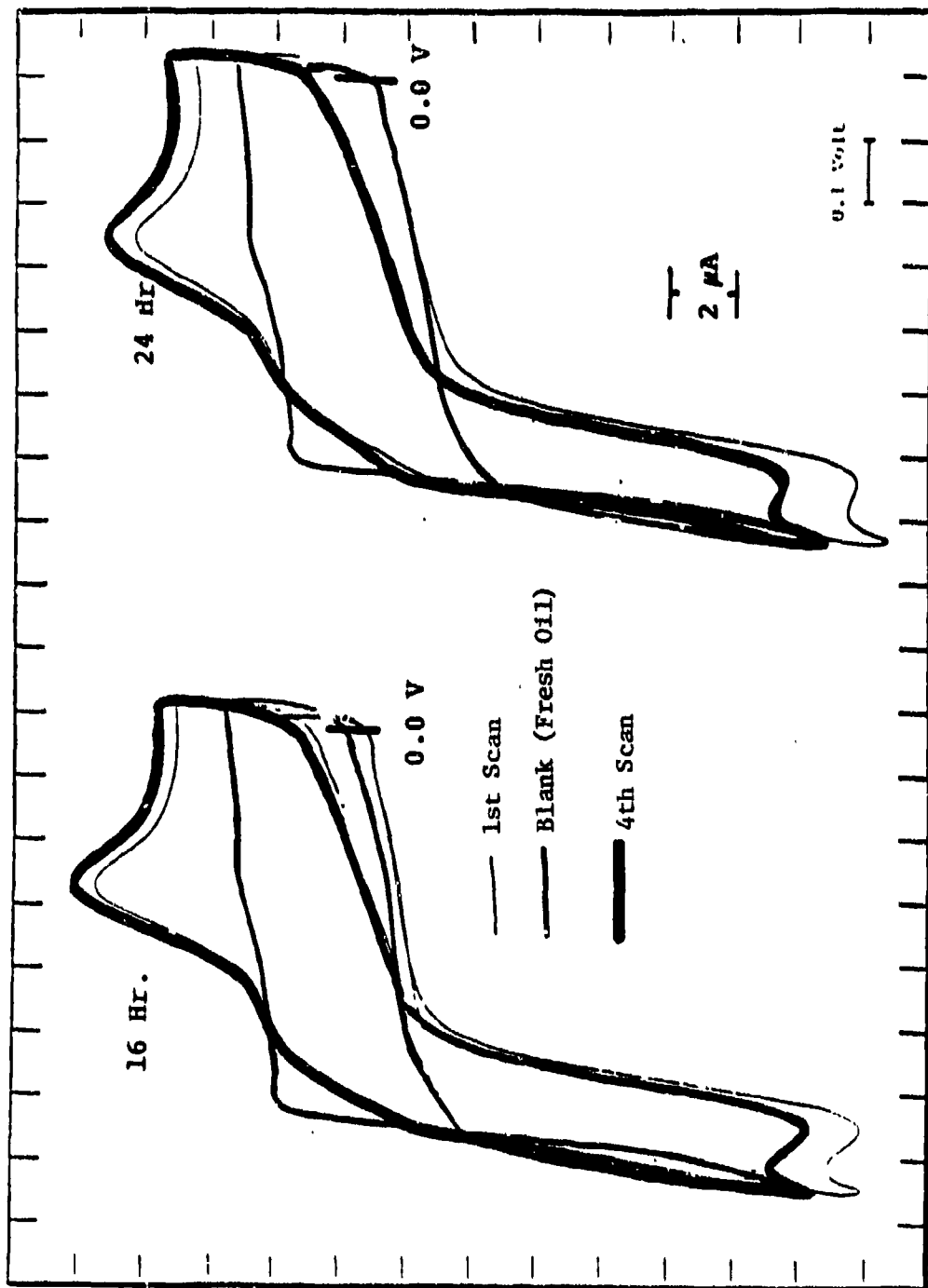


Figure 29. Reduced Scan Voltammograms of the 16 and 24 Hours Stressed TEL-4005 Oils in the Presence of Pyridine Using a Glassy Carbon Working Electrode.

in Figure 30 are smooth curves up to the end of the stable life of the TEL-4005 oil [96 hours determined from the breakpoint of the viscosity versus stressing time plot (Appendix (B))] and should be suitable for curve fitting techniques. The results of the first and steady state scan (fourth or higher) for each wave are similar.

### (13) Summary of the Voltammetric Techniques

The voltammetric techniques developed during the initial study require less than 200  $\mu$ l of sample, require less than 30 seconds to perform (sample preparation and analysis), and are easy and inexpensive to operate. The results of the voltammetric techniques can be used to quantify the antioxidants in MIL-L-7808 oils and to detect the antioxidants' reaction products in thermally-oxidized MIL-L-7808 oil samples. The results of the voltammetric techniques involving the antioxidants' reaction products in the presence of pyridine (Figure 30) appear to be directly related to the RLL of the fresh and stressed TEL-4005 oils.

Therefore, the initial study of the voltammetric techniques indicated that the voltammetric techniques were well suited for development into a RLLAT candidate.

#### c. Thermal Stressing Techniques

##### (1) Introduction

In complete contrast to the voltammetric techniques, numerous analytical procedures based on thermal stressing techniques have been reported (References 6-17) which are capable of assessing the RLL of lubricating oils. The thermal stressing techniques use thermal-oxidative stressing to deplete the antioxidants (Reaction 5) present in the lubricating oil. Once the antioxidants become ineffective, the basestock of the lubricating oil rapidly degrades (Reactions 1-4). The different thermal stressing techniques then use various methods to detect the "onset time" (isothermal conditions) or "onset temperature" (ramped temperature conditions) at which the rapid degradation of

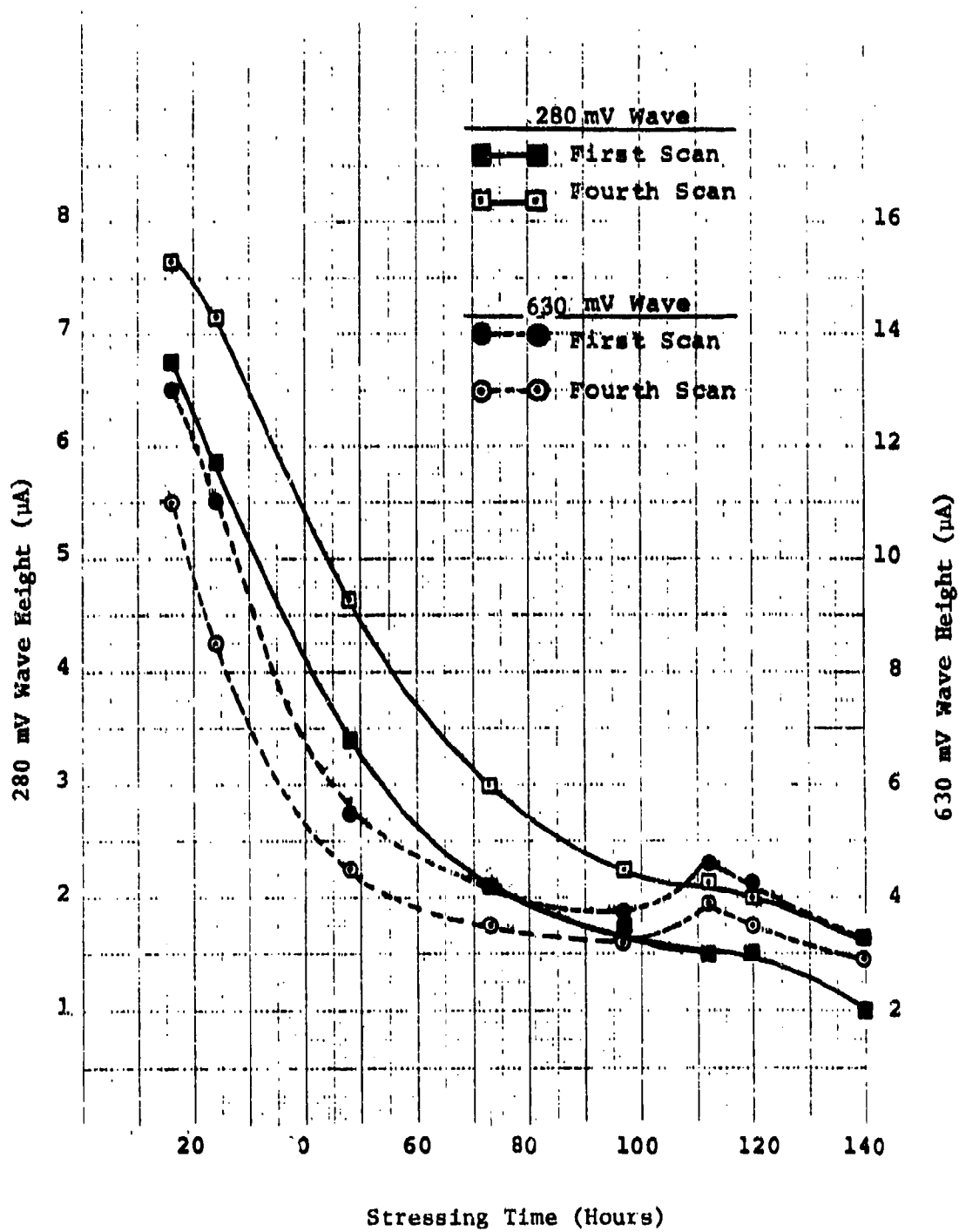


Figure 30. Plots of the 280 mV Reduction and 630 mV Oxidation Waves' Heights (1st and 4th Scan) versus the Stressing Time for TEL-4005 Oil.

the basestock begins. The onset time or temperature is then used to assess the RLL of the oil sample.

Of the various methods that have been used to detect the rapid degradation of the basestock, e.g., chemiluminescence (Reference 6), gas evolution rate (References 7 and 8), weight loss (Reference 9), oxygen uptake (Reference 10), and molecular weight distribution (Reference 11), the methods which detect changes in the sample's temperature, differential thermal analysis, or measure the amount of heat generated or absorbed by the sample, differential scanning calorimetry (DSC), have been used to assess the RLL of MIL-L-7808 type oils. It has been reported (Reference 16) that the use of high pressure (>100 psi) inside the DSC cell's analysis chamber was required to reduce formulation effects and evaporation of the MIL-L-7808 oils. The use of high oxygen pressure also increases the peak size and onset definition of the DSC signal.

Although high pressure-DSC (HP-DSC) has been used to assess the RLL of lubricating oils, the onset times of the HP-DSC analyses for fresh and slightly stressed oils were over 30 minutes. Since one of the RLLAT criteria (Table 1) is an analysis time of less than 10 minutes, the experimental conditions of the reported HP-DSC studies (References 12-17) had to be modified.

Therefore, an investigation was performed to determine the HP-DSC experimental conditions that result in onset times of 10 minutes or less. The experimental conditions of sample size and analysis temperature were evaluated using an uninhibited ester basestock and fresh and authentic used MIL-L-7808 oils.

## (2) Effect of Sample Size

The sample size experiments were run using heating rates of 10°C/min., an oxygen pressure of 500 psi and sample sizes of 1 and 5  $\mu$ l of fresh TEL-4005 oil. As shown in Figure 31, the onset time (exotherm) of the sample size of 5  $\mu$ l was approximately 22 minutes and the oxidation reaction was

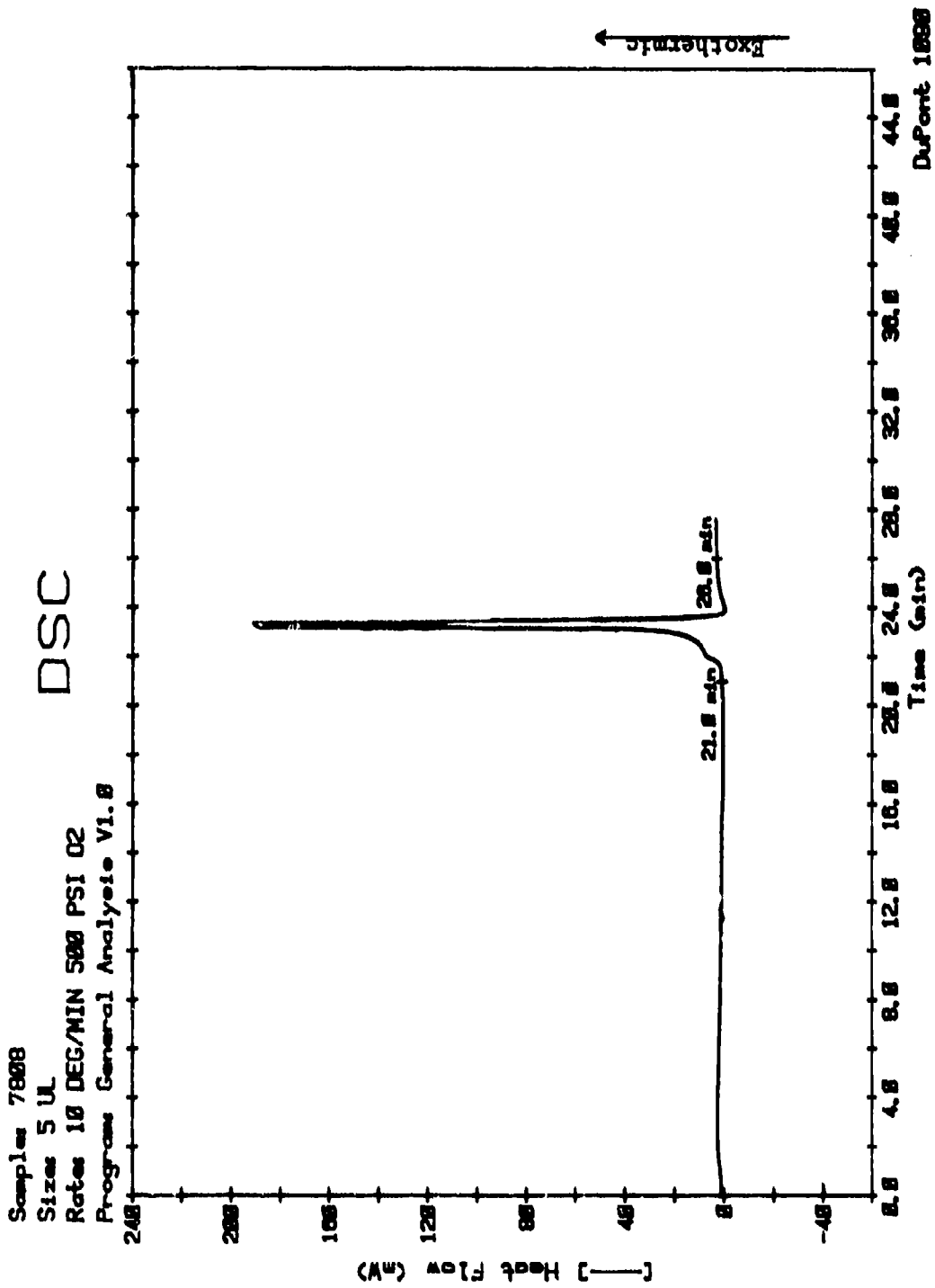


Figure 31. HP-DSC Thermogram of the TEL-4005 Oil Produced Using a 5  $\mu$ l Sample, a Heating Rate of 10°C/Minute, and an Oxygen Pressure of 500 psi.

complete after 28 minutes. Figure 32 shows that the onset time was reduced to less than 16 minutes by reducing the sample size to 1  $\mu$ l. Thus, 1  $\mu$ l samples were used for the temperature study.

### (3) Effect of Analysis Temperature

In the HP-DSC analysis of MIL-L-7808 type oils (Reference 17), an analysis temperature of 250°C resulted in onset times of approximately 30 minutes for fresh oils. Also the onset time of 16 minutes in Figure 32 translates into an onset temperature (dashed line) of 250°C. Thus, the analysis temperature study was initiated at 250°C. The analysis temperature study was run under isothermal conditions because the HP-DSC results for the MIL-L-7808 type oils (References 16-17) showed that onset times were better suited for RLL assessments than onset temperatures.

When the 1  $\mu$ l sample of the TEL-4005 oil was analyzed at 250°C under 500 psi of oxygen, the exothermic reaction occurred at 6 minutes and was so rapid that the sample ignited and the sample pan melted. Consequently, the analysis temperature and oxygen pressure were varied to identify a combination which produced onset times of approximately 10 minutes for fresh MIL-L-7808 oils and which inhibited ignition of the oil sample. An analysis temperature of 230°C and an oxygen pressure of 100 psi were the best analysis conditions identified by the initial HP-DSC analyses of the MIL-L-7808 oils.

When the 1  $\mu$ l samples of the TEL-4001 and TEL-4005 oils were analyzed isothermally at 230°C under an oxygen pressure of 100 psi, onset times of 13.6 and 14.1 minutes, respectively, were produced (Figure 33). The uninhibited basestock had an onset time of less than 1 minute (Figure 33). The authentic used oil samples, F-25 and R-30, had intermediate onset times (Figure 33).

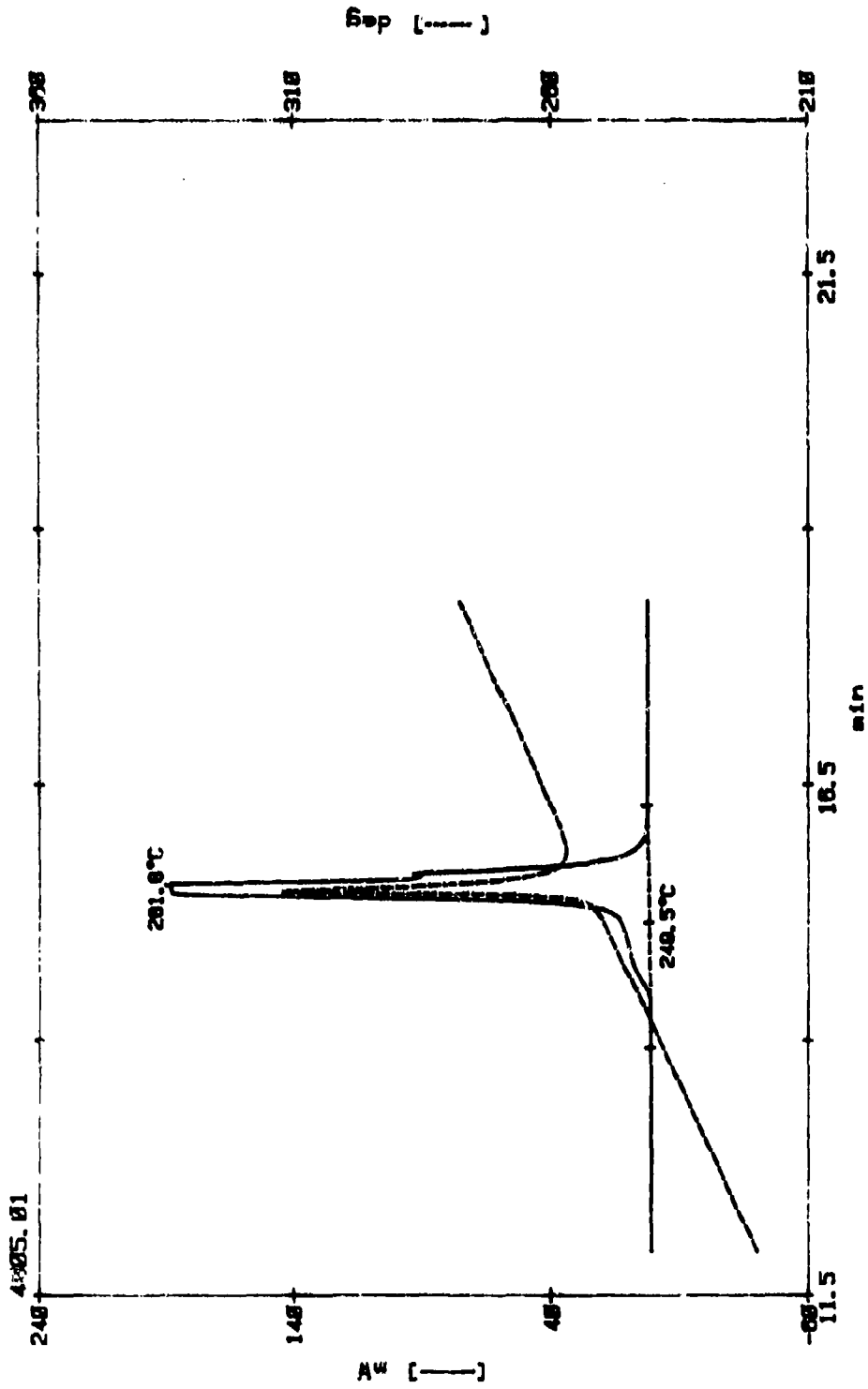


Figure 32. HP-DSC Thermogram of the TEL-4005 Oil Produced Using a 1  $\mu$ l Sample, a Heating Rate of 10°C/Minute, and an Oxygen Pressure of 500 psi.

# DSC

Size: 1 UL  
 Rate: ISO 230C 100 PSI 02  
 Program: General Analysis V1.0

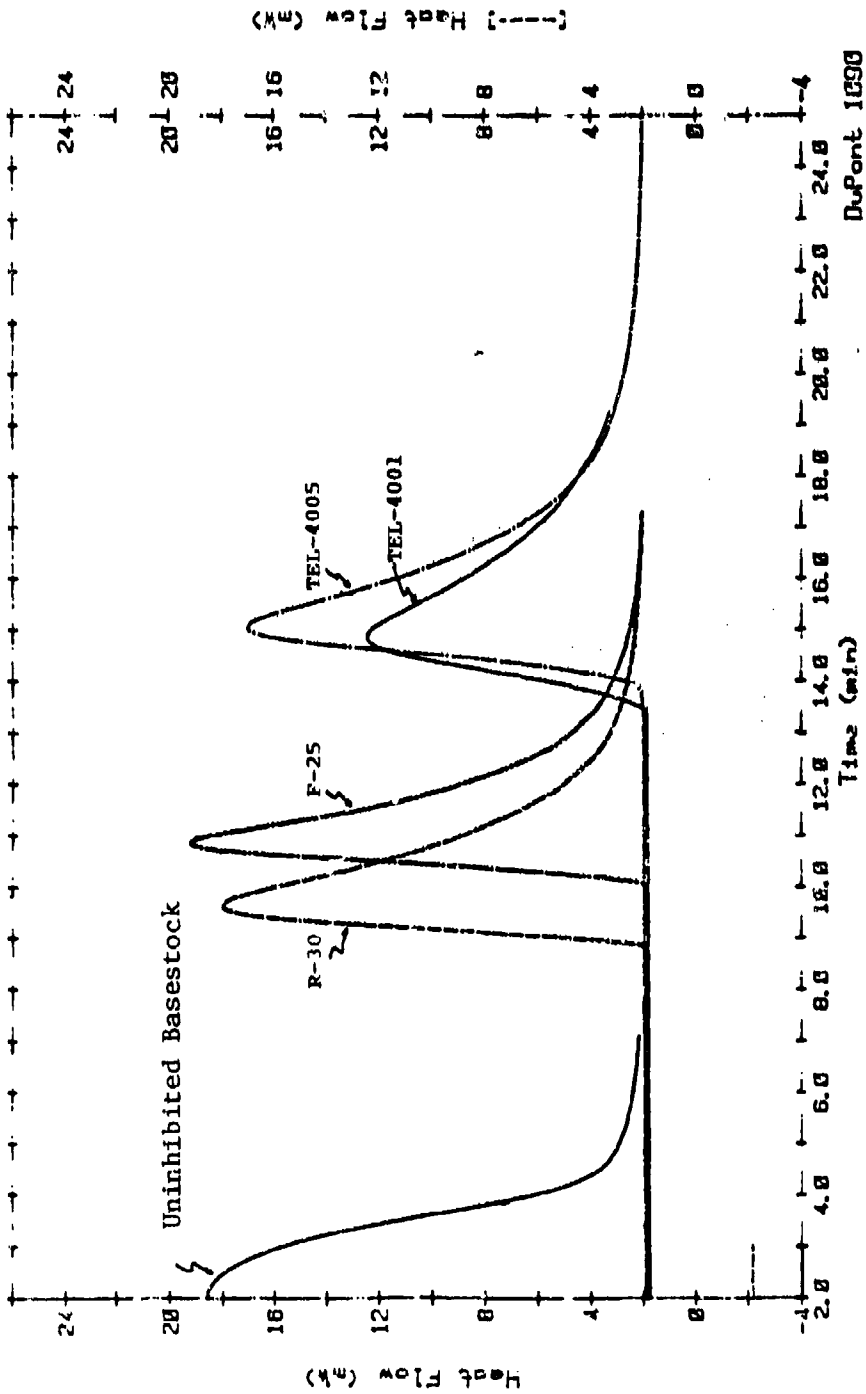


Figure 33. HP-DSC Thermograms of the Uninhibited Ester Basestock, the Fresh TEL-4001 and TEL-4005 Oils, and the Authentic Used (F-25 and R-30) MIL-L-7808 Oil Samples Produced Using a 1  $\mu$ l Sample, Isothermal Temperature of 230°C, and an Oxygen Pressure of 100 psi.

#### (4) Summary of HP-DSC Technique

Although the experimental conditions capable of producing onset times of 10 minutes for fresh MIL-L-7808 oil samples were not identified by the initial study, it was shown that the HP-DSC technique has the potential for assessing the RLL of MIL-L-7808 oils in less than 10 minutes. The HP-DSC analyses use 1  $\mu$ l samples, do not require sample preparation, and are moderately easy to perform.

Therefore, the initial study of the HP-DSC technique and the results reported by other researchers (References 6-17) indicate that thermal stressing techniques were well-suited for development into a RLLAT candidate, but that optimization studies of the techniques' experimental conditions were needed.

#### d. Chemical Stressing Technique

##### (1) Introduction

In an attempt to develop stressing techniques that do not employ the elevated temperatures and oxygen pressures used by thermal stressing techniques, chemical stressing techniques were investigated. The two chemical stressing techniques identified as having potential for development into RLLAT candidates are referred to as the colorimetric method (Reference 18) and the Ford method (References 19-21).

##### (2) Colorimetric Method

###### (a) Introduction

During research with laser dye solutions, researchers at the Mitsubishi Electric Corporation (Reference 18) observed that the dark green solutions of bis [4-(dimethylamino) dithiobenzil] nickel (BDN) in tetrahydrofuran (THF) faded with time. From this observation the researchers at the Mitsubishi Electric Corporation developed a stressing technique that uses the oxidation of tetrahydrofuran (THF) as a "radical generator" and uses the decoloration rate of the BDN to estimate the relative efficiencies of various antioxidants. The BDN complex has

hydroperoxide decomposing, free radical trapping, and UV stabilizing capacities (Reference 22), and thus, the BDN is capable of measuring the inhibition efficiencies of different types of antioxidants.

The Mitsubishi chemical stressing technique is based on the competition between the BDN complex and the added antioxidants to react with the "radicals" generated by the oxidation of THF. As the BDN reacts, the solution becomes colorless, and thus, the reaction rate of the BDN can be measured by its decoloration rate. Consequently, the decoloration rate of the BDN solution in the presence of an antioxidant is dependent upon the ability of the added antioxidant to stop the BDN from reacting with the THF generated "radicals". Since the inhibiting capability of the added antioxidant is dependent on its efficiency and concentration, the decoloration rate of the BDN solution decreases as the concentration of the antioxidant increases (Figure 34).

The efficiencies of various antioxidants relative to diphenylamine were determined by the BDN decoloration rate and compared favorably with those obtained for the autoxidation of tetraline (Reference 18). Since the Mitsubishi chemical stressing technique is based upon the decoloration of BDN at 25°C by THF, it does not have the thermal or pressure requirements of the thermal stressing techniques. Also, since the decoloration of BDN is used to determine the efficiency of the added antioxidant, inexpensive spectrophotometers are used.

However, the greatest advantage of the Mitsubishi chemical stressing technique was the fact that it uses the rate of BDN decoloration as compared to the induction time determined by the HP-DSC technique. Since the rate of BDN decoloration is constant throughout the test (Figure 34), the antioxidant capacity of an used oil sample could be determined in only a few minutes and the test time would be independent of the used oil sample's RLL. In comparison, the test times of the HP-DSC technique (Figure 33) ranged from approximately 1 minute for

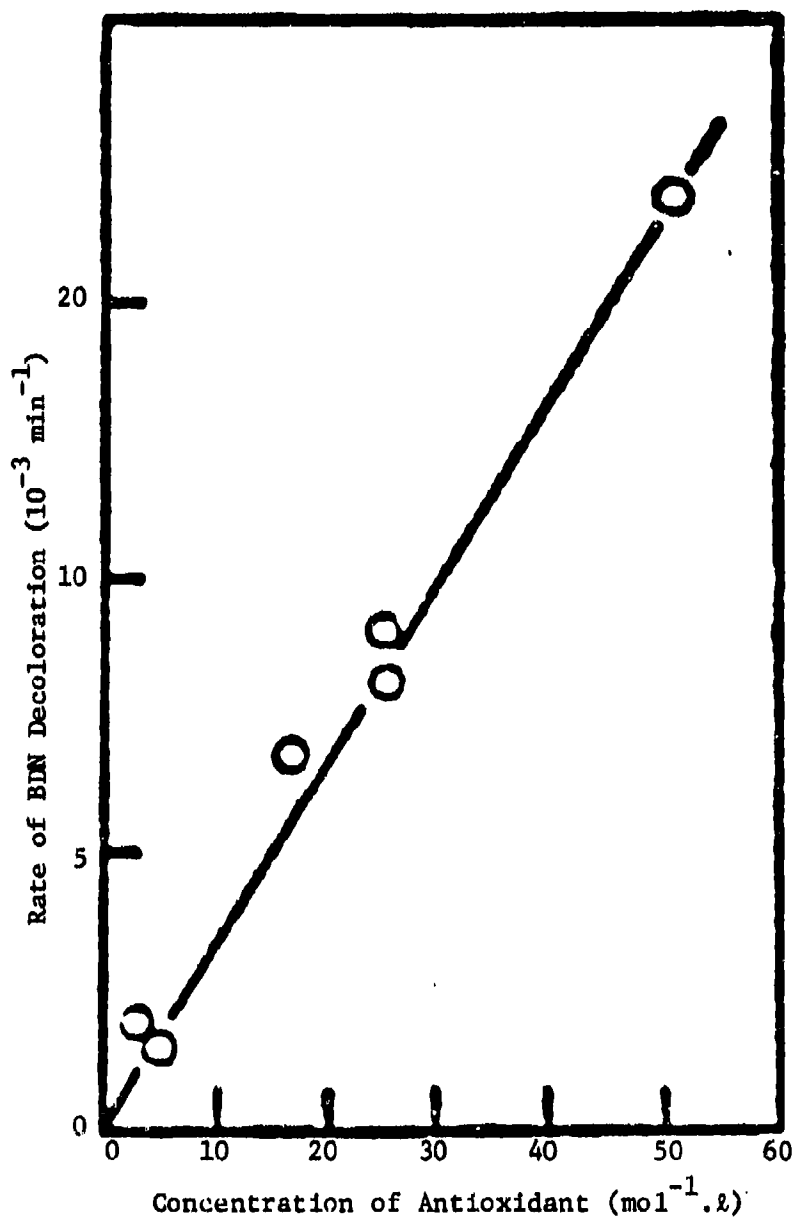


Figure 34. Effect of Antioxidant Concentration on the Decoloration Rate of a BDN Solution (Reproduced from Reference 18).

the uninhibited basestock to over 14 minutes for the fresh TEL-4005 oil.

Although the Mitsubishi chemical stressing technique termed the THF as a "radical generator", our preliminary research indicated that the THF was simply a source of hydroperoxides, and therefore, the Mitsubishi method determines the hydroperoxide decomposing capabilities (Reaction 8) of antioxidants, not their free radical trapping capabilities (Reactions 6 and 7). To determine if the hydroperoxide decomposing capabilities of the antioxidant species present in used MIL-L-7808 lubricating oils could be used to assess the oils' RLL, an initial investigation was performed.

However, before the Mitsubishi method was evaluated, several modifications were made in the method to improve its ease of operation and to decrease its instrumental and operational costs. The first modification was to replace the unstabilized THF (which contains an unknown, constantly increasing hydroperoxide concentration) with cumene hydroperoxide (80% purity). The cumene hydroperoxide is a stable liquid at room temperature.

The second modification was to use the 632.8 nm wavelength instead of the 1100 nm wavelength (Reference 18) to monitor the decoloration of the green BDN solution. By choosing the 632.8 nm wavelength, an inexpensive, safe He-Ne laser can be used, eliminating the need for an expensive near-infrared spectrophotometer. A third modification, although minor, was to change the solvent system from 1,2-dichloroethane to toluene. Toluene was favored as the solvent over 1,2-dichloroethane because BDN is more soluble in toluene and because toluene is a lower health risk than 1,2-dichloroethane.

The analytical procedure which was derived from the Mitsubishi chemical stressing method is termed the colorimetric method.

Before the colorimetric method could be evaluated, the experimental parameters had to be optimized. The effects of the BDN solution/cumene hydroperoxide ratio, the oil sample size, and antioxidant type on the decoloration rate of the BDN solution were studied. The optimized BDN colorimetric method was then used to determine the effects of the fresh TEL-4001 through TEL-4006 MIL-L-7808 oils and of the laboratory stressed TEL-4005 oils on the decoloration rate of the BDN solution.

(b) Effect of BDN Solution/Cumene Hydroperoxide Ratio

To obtain the greatest difference possible between the blank and a fresh MIL-L-7808 oil, the decoloration rate of the BDN solution in the presence of the blank sample should be very rapid (slope of plot approaching  $\infty$ ). Therefore, a study was conducted to determine the BDN solution/cumene hydroperoxide ratio which produced the fastest rate of decoloration (greatest slope). The amount of BDN solution was held at 1.5 ml while the amount of the cumene hydroperoxide was varied from 0.25 to 2.0 ml.

The decoloration rate of the BDN solution increased as the amount of cumene hydroperoxide was increased from 0.25 to 1.0 ml. Amounts higher than 1 ml of cumene hydroperoxide had little effect on the decoloration rate of the BDN solution. Thus, it was determined that 1.5 ml of BDN solution and 1.0 ml of cumene hydroperoxide produced the greatest slope for the blank.

(c) Effect of Sample Size

In addition to a rapid decoloration rate for the blank, the decoloration rate of the fresh oil samples should be very slow (slope of plot approaching zero) to increase the colorimetric method's sensitivity to different degrees of RLL. Therefore, a study was conducted to determine the minimum amount of oil sample which produces the slowest decoloration rate for the BDN solution.

To determine the effect of oil sample size on the decoloration rate of the BDN solution, 10 to 30  $\mu$ l samples of TEL-4004 oil were added to 1.5 ml of BDN solution and 1.0 ml of cumene hydroperoxide. The percent absorbance of the BDN solution was plotted versus reaction time for the different samples sizes of the TEL-4004 oil and the blank sample as shown in Figure 35.

The plots of the percent absorbance of the BDN solution versus reaction time in Figure 35 show that addition of the TEL-4004 oil greatly decreases the decoloration rate of the BDN solution and that the decoloration rate decreases with increasing sample size.

Although increasing the sample size decreases the BDN solution's decoloration rate, the effects of the oil sample's color, which darkens with stressing time, also increases. To determine the effect of the oil sample's color on the colorimetric method, the TEL-4005 oil sample taken at 140 hours (stable life ended at 96 hours), which was the darkest of the stressed oil samples, was added in amounts of 10, 20, and, 30  $\mu$ l to 1.5 ml of BDN solution and 1.0 ml of cumene hydroperoxide.

The stressed oil sample's color was found to affect the initial absorbance of the BDN solution but did not affect the slope of the BDN decoloration plot. The effect of the sample's color on the initial point of the plot decreases the colorimetric method's ease of operation since the starting point has to be adjusted for every used oil sample.

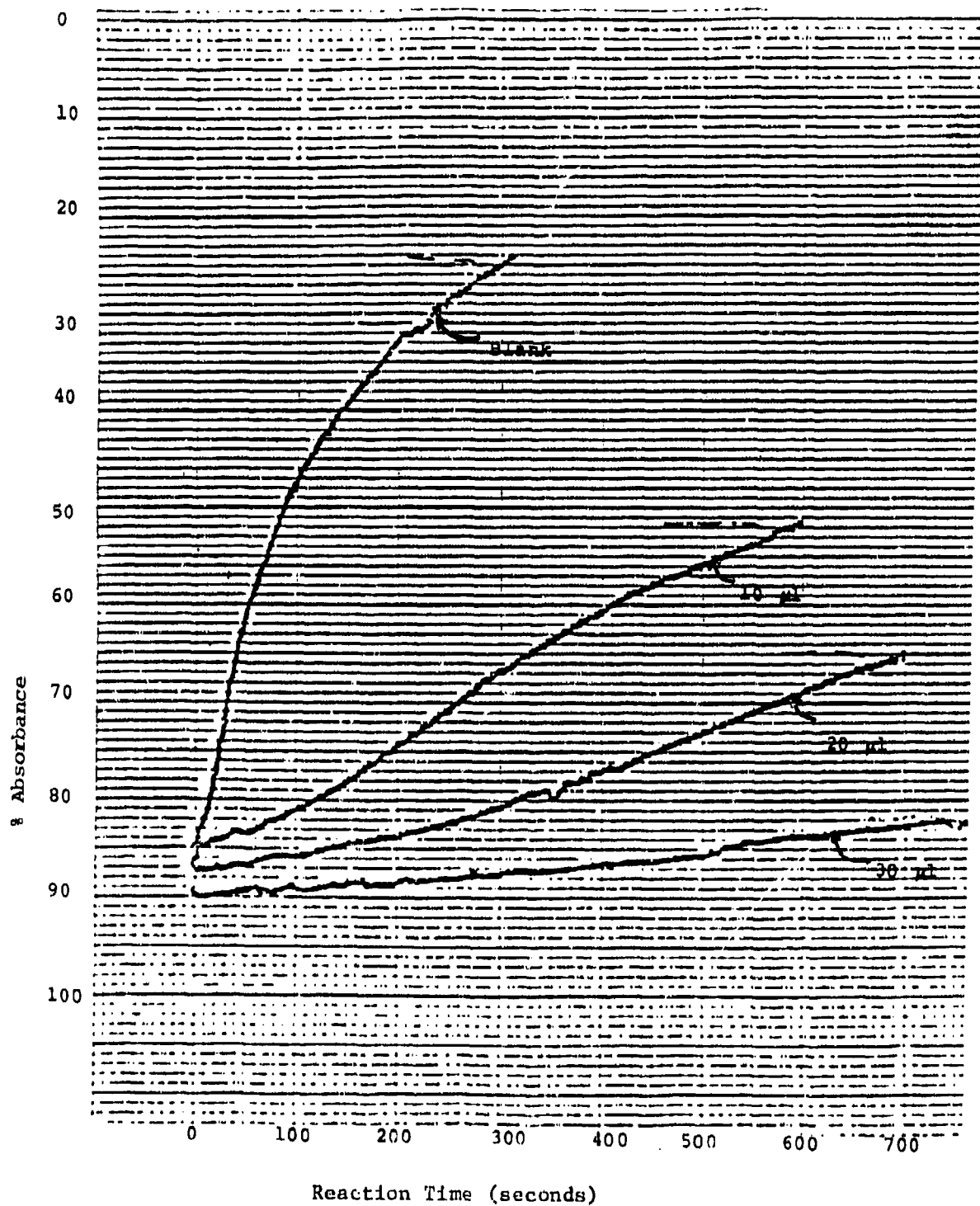


Figure 35. Effect of Sample Size on the % Absorbance of the BDN Solution versus Reaction Time (25°C) Plots For the TEL-4004 011.

Since the rate of decoloration was similar for the blank and the different sample sizes of the stressed TEL-4005 oil sample, the results indicated that the antioxidants are depleted in the stressed oil sample to the point that they can no longer decompose hydroperoxides. These results were expected since the stressed oil sample was taken 40 hours after the end of the TEL-4005 oil's stable life.

The results from the initial investigation into the effects of sample size were inconclusive since the effects of sample size on the decoloration rate and on the initial point of the BDN absorbance plot differ in direction and are deemed similar in importance. Therefore, a 30  $\mu$ l oil sample size was arbitrarily chosen for the initial evaluation of the colorimetric method.

#### (d) Effect of Antioxidant Type

To determine if PANA and DODPA (antioxidants in TEL-4005 oil) are effective hydroperoxide decomposers, i.e., inhibit the decoloration of the BDN solution, 1 and 2% solutions of each antioxidant were prepared in toluene and then added in 30  $\mu$ l quantities to 1.5 ml of the BDN solution and 1 ml of cumene hydroperoxide in a 1 dram vial. The plots of the percent absorbance of the BDN solution versus reaction time for PANA and DODPA are shown in Figure 36.

The results in Figure 36 show that both PANA and DODPA are effective hydroperoxide decomposers since PANA and DODPA significantly decrease the decoloration rate of the BDN solution relative to the blank. The results in Figure 36 also indicate that DODPA is a better hydroperoxide decomposer than PANA, i.e., BDN solution decoloration slower in presence of DODPA than in presence of PANA. Therefore, the colorimetric method is sensitive to the depletions of both PANA and DODPA.

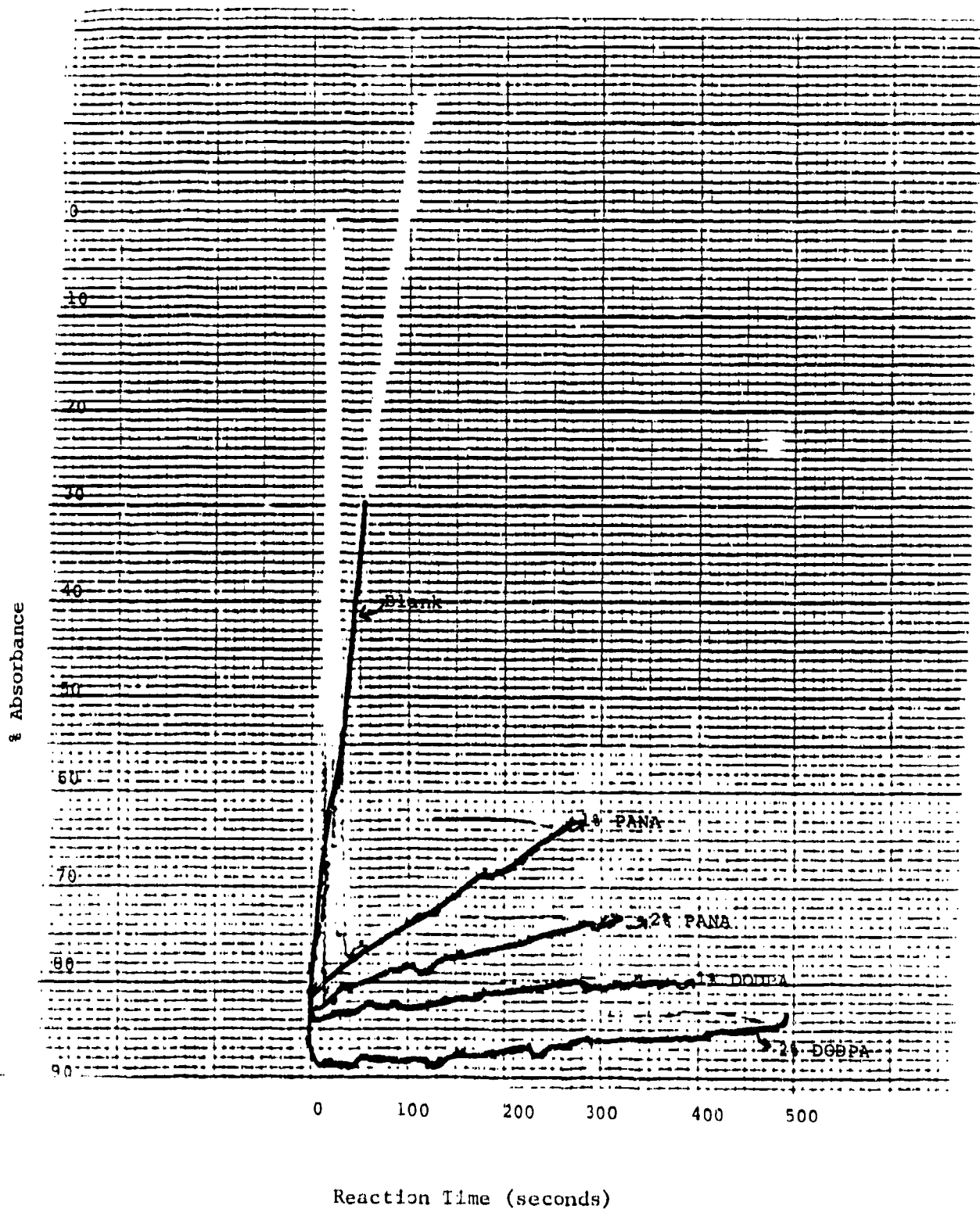


Figure 36. Effect of Antioxidant Type on the % Absorbance of the BDN Solution versus Reaction Time (25°C) Plots for PANA and DODPA.

(e) Effect of Formulation

To determine the effect of formulation on the rate of BDN solution decoloration, the rates of the TEL-4001 through TEL-4006 MIL-L-7808 lubricating oils were determined. The resulting plots of the percent absorbance of the BDN solution versus reaction time for the MIL-L-7808 lubricating oils are shown in Figure 37.

As expected the rates of BDN solution decoloration for the TEL-4001 through TEL-4006 oils shown in Figure 37 were different. The different decoloration rates were expected since cyclic voltammetry showed that the MIL-L-7808 oils contain differing concentrations of antioxidants (Figures 10 and 11). The TEL-4001 through TEL-4005 oils produce similar rates of BDN solution decoloration, while the TEL-4006 oil produces a much slower rate of decoloration. Thus, the antioxidant system in the TEL-4006 oil is a more effective hydroperoxide decomposer than those of the other MIL-L-7808 oils.

(f) Analysis of Laboratory Stressed  
TEL-4005 Oil Samples

In order to determine the colorimetric method's capability to distinguish between differing degrees of thermal-oxidative degradation, the series of stressed TEL-4005 oil samples were studied. The plots of the percent absorbance of the BDN solution versus reaction time for each oil sample are shown in Figure 38.

The results in Figure 38 show that the colorimetric method is capable of distinguishing between oil samples of differing RLL. However, the induction period (period of time before rapid decoloration occurs), not the rate of BDN solution decoloration, is capable of RLL assessments. The other factor eliminating the rate of BDN solution decoloration for assessing RLL is that the initial rates of BDN solution decoloration for the stressed oil samples are much slower than those of the fresh oils.

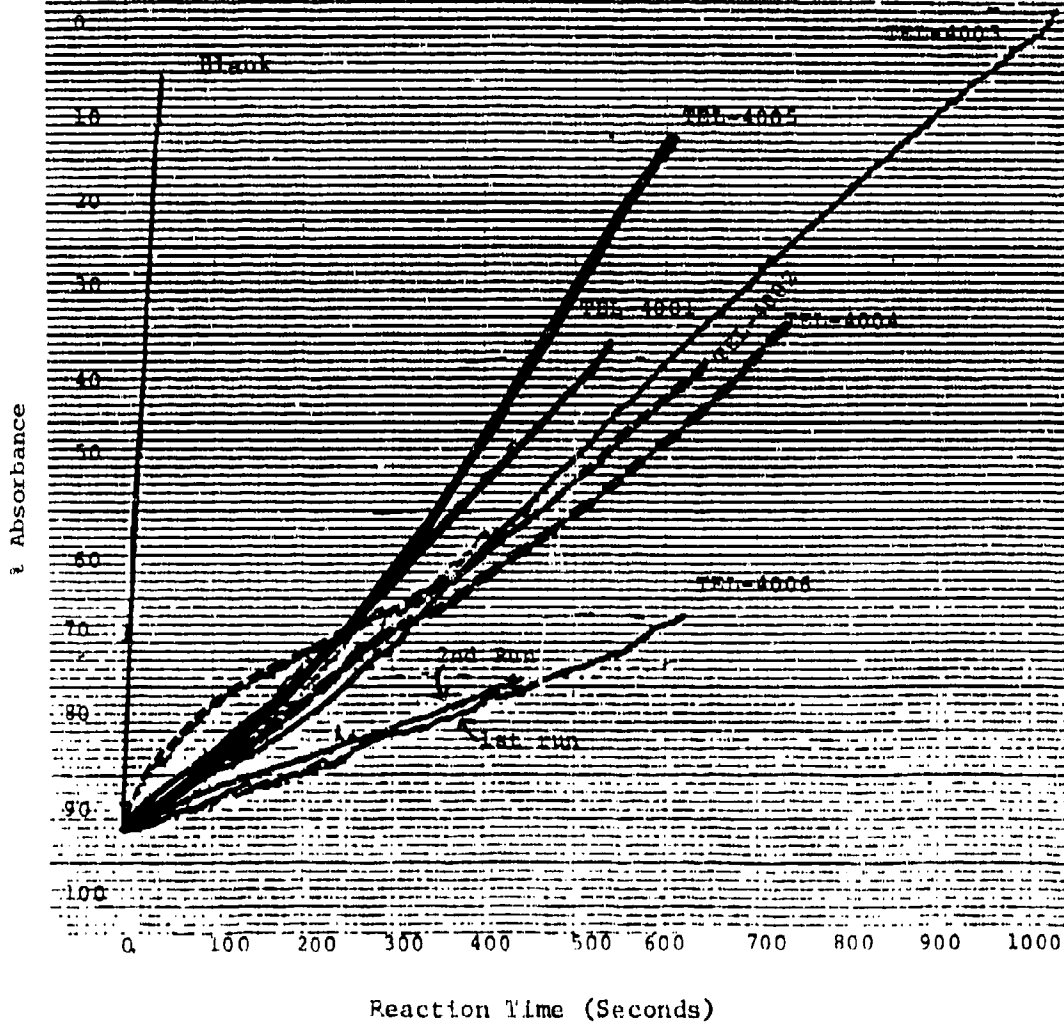


Figure 37. Plots of the % Absorbance of the BDN Solution versus Reaction Time for the Fresh TEI-4001 through TEI-4006 MIL-L-7808 Oils.

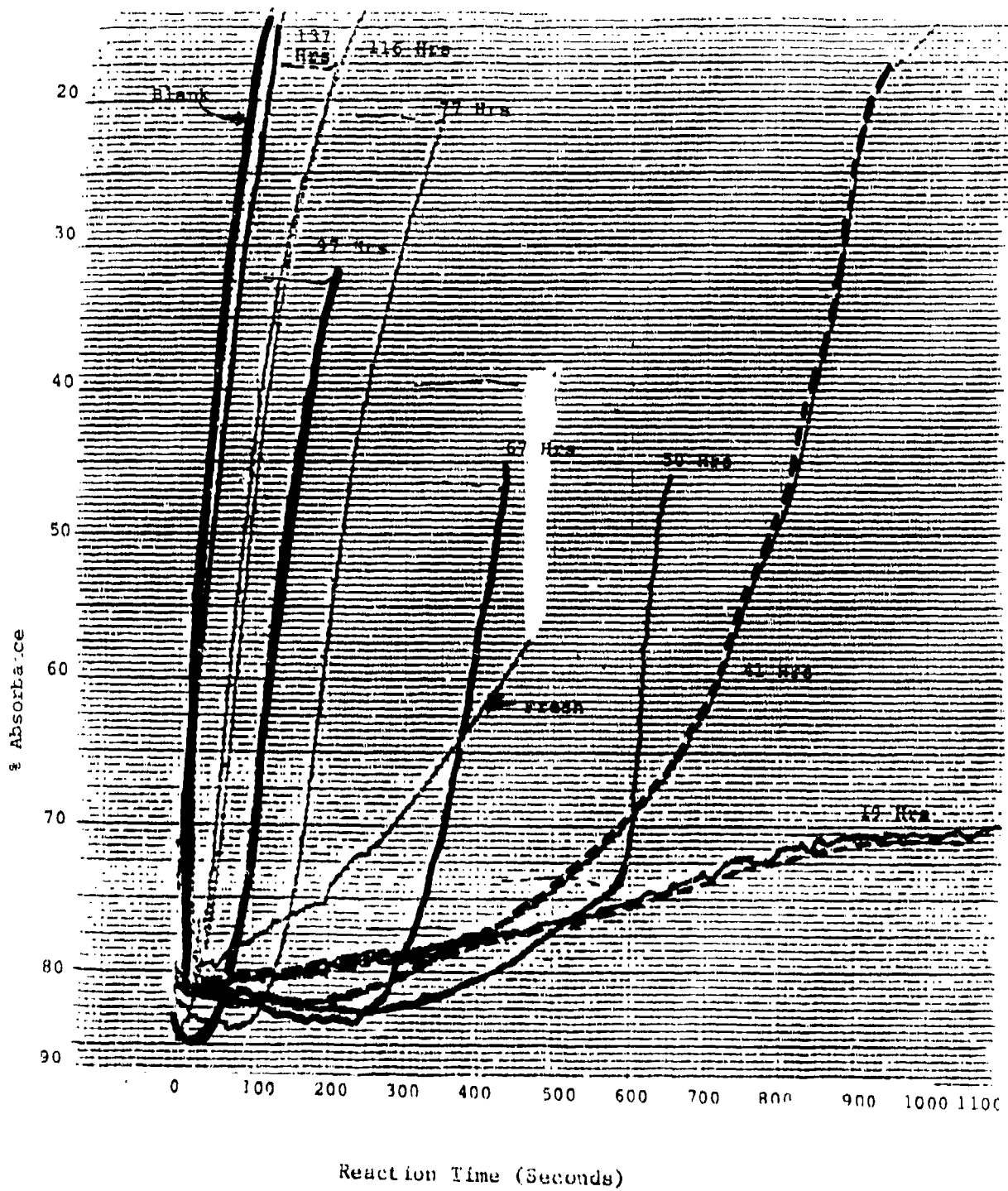


Figure 38. Plots of the % Absorbance of the BDN Solution versus Reaction Time for the Fresh and Stressed (19-137 Hours) TEL-4005 Oils.

Because the colorimetric method must use an induction period to assess the RLL of MIL-L-7808 oil samples, the method's main advantage over the thermal stressing techniques is eliminated. The colorimetric method had the advantage over induction period methods (thermal stressing) because it required only a few minutes of analysis time regardless of the oil sample's RLL. In contrast, the analysis time required by induction period methods varies from less than 1 minute to over 15 minutes depending on the oil sample's RLL.

#### (g) Summary of Colorimetric Method

The results of its initial evaluation indicated that the colorimetric method has potential for development into a RLLAT candidate. The colorimetric method requires only 30  $\mu$ l of the oil sample, can be performed using inexpensive equipment, is moderately easy to operate, and has RLL assessment capabilities. However, the experimental parameters needed to be modified to obtain analysis times of less than 10 minutes and the mathematical relationship between the results of the colorimetric method and the RLL of an oil sample needed to be better established.

Although the potential of the colorimetric method for development into a RLLAT is lower than those of the voltammetric and thermal stressing techniques, the colorimetric method is suitable for development into a RLLAT and was further evaluated in Task 2.

### (3) Modified Ford Method

#### (a) Introduction

Researchers at the Ford Motor Company have developed a method (References 19-21) which titrates the antioxidant species in diluted oil samples with peroxy radicals ( $\text{ROO}\cdot$  in Reaction 2) produced by the thermal decomposition of the free radical initiator, azobisisobutyronitrile (AIBN) at  $60^\circ\text{C}$ . The AIBN thermally decomposes to produce free radicals ( $\text{R}\cdot$ ) at a known and constant rate:



(12)

The free radicals then combine with oxygen to produce peroxy radicals in the same manner as in Reaction 2. The free radical reactions are performed in a model hydrocarbon oxidation system containing cyclohexene as an oxidizing substrate and n-hexadecane as a hydrocarbon solvent.

In the absence of antioxidants, the cyclohexene oxidizes rapidly (Reactions 2-4) and the resulting oxygen consumption is monitored by recording the pressure change in a closed reaction system. In the presence of antioxidants, the oxidation of the cyclohexene is suppressed as the antioxidant species are consumed (Reaction 6 and 7) through reaction with the peroxy radicals produced by AIBN. Once the antioxidant species lose their efficiency, the cyclohexene oxidizes rapidly absorbing oxygen. The length of time before the rapid oxygen consumption begins (induction time) has been related to the RLL of automotive engine oil samples (Reference 21). The oxygen absorption versus AIBN reaction time curves for the automotive engine oil samples are presented in Figure 39.

Thus, the Ford method measures the free radical trapping capabilities (Reactions 6 and 7) of the antioxidants in the oil samples. The Ford method also is sensitive to "natural inhibitors" present in the ester basestock and the antioxidant species generated in the lubricating oil during use. However, the results of the Ford method are independent of the hydroperoxide decomposing capabilities (Reaction 8) of the antioxidants (colorimetric method). Therefore, an initial investigation was performed to determine the potential of the Ford chemical stressing method as a RLLAT candidate.

However, before the Ford method could be evaluated, several modifications in the method were needed to meet the time and ease of operation requirements for a RLLAT. As seen in Figure 39, the induction time of the new oil is approximately 50 minutes, but the test had to be run for 90 minutes to obtain the induction time by extrapolation. Also the test

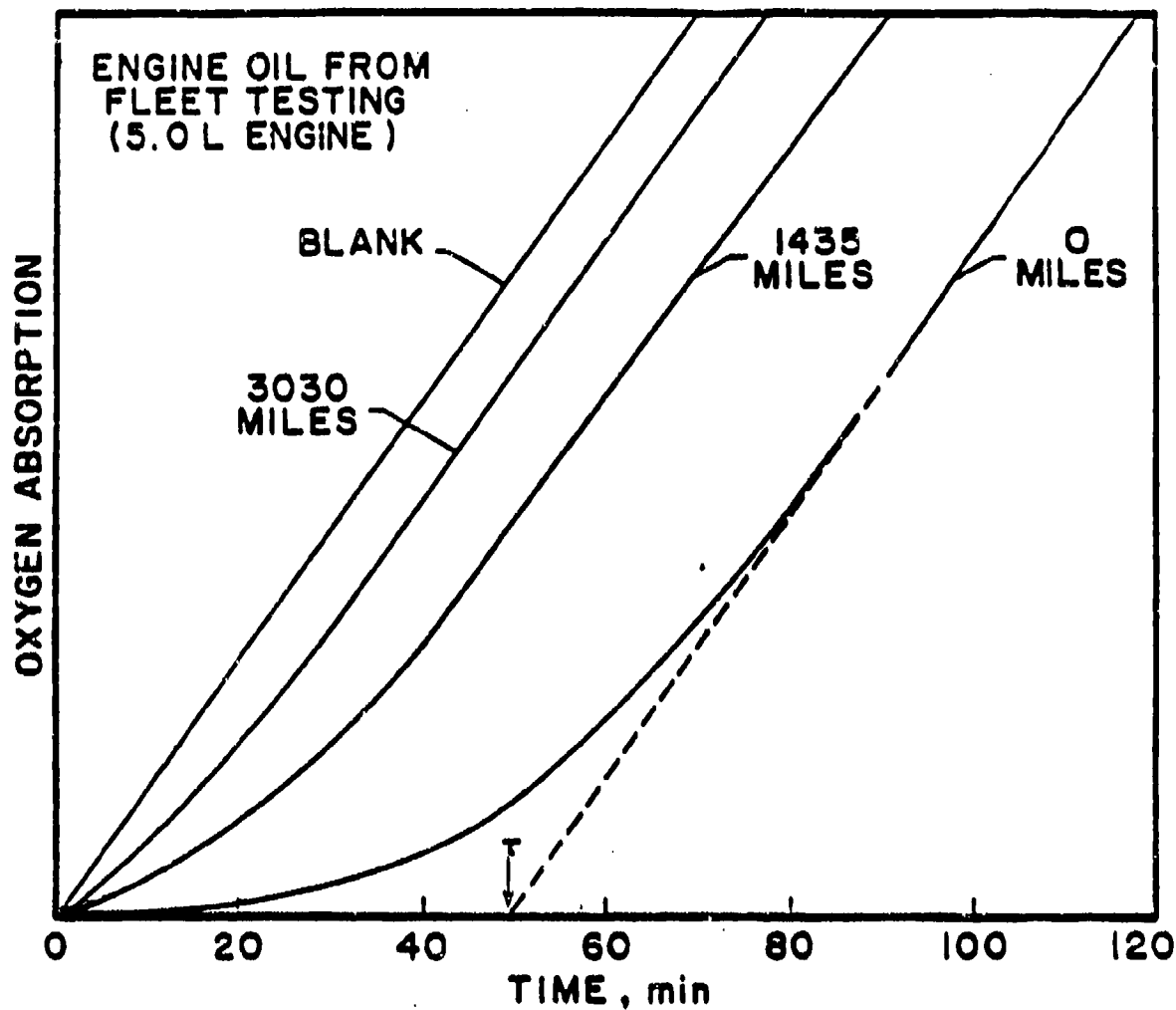


Figure 39. Plots of Oxygen Absorption versus Time of AIBN Stressing at 60°C for Automotive Engine Oils ( $\tau$ =Induction Time) (Reproduced from Reference 21).

system was allowed to equilibrate for 15 minutes before starting the test. Since the time requirements for RLLAT are 10 minutes or less, studies were undertaken to decrease the total test time (equilibration plus induction times) of the Ford method from the original 105 minutes to the required 10 minutes. The experimental parameters studied included the type of easily oxidizable substrate; the quantity, the aging time, and the concentration of the AIBN solution; the quantity of hydrocarbon solvent; and the quantity of the oil sample.

In order to improve the ease of operation of the modified Ford method, the effect of eliminating the oxygen purge and the effects of using a specified pressure drop in place of the rate of pressure drop for determining the induction time were studied. The modified Ford method was then evaluated with the fresh (TEL-4001 to TEL-4006), laboratory stressed (TEL-4005), and authentic used MIL-L-7808 lubricating oils.

(b) Effect of Type of Easily Oxidizable Substrate

Because the Ford method was designed to take approximately 2 hours to complete for new oils and the RLLAT should take 10 minutes or less to complete, modifications in the Ford method were necessary. Another problem with the Ford chemical stressing method is shown in Figure 39. Due to the gradual change in the rate of oxygen absorption as the induction period ends, the test must be run 10-40 minutes longer than the actual induction period so that an extrapolation can be carried out to determine the induction period. In addition to increasing the time of the test, the necessity of extrapolation to determine the induction time reduces the potential of the Ford method for development into an easy to operate, base-level RLLAT. Therefore, the effect of the type of easily oxidizable substrate on the rate of oxygen absorption was studied.

The results in Figure 40 (no MIL-L-7808 oil present) show that benzaldehyde is clearly the easiest oxidizable substrate tested. The stability of the cyclohexene is due to the fact that it is stabilized with 0.01% BHT. Since a supply of

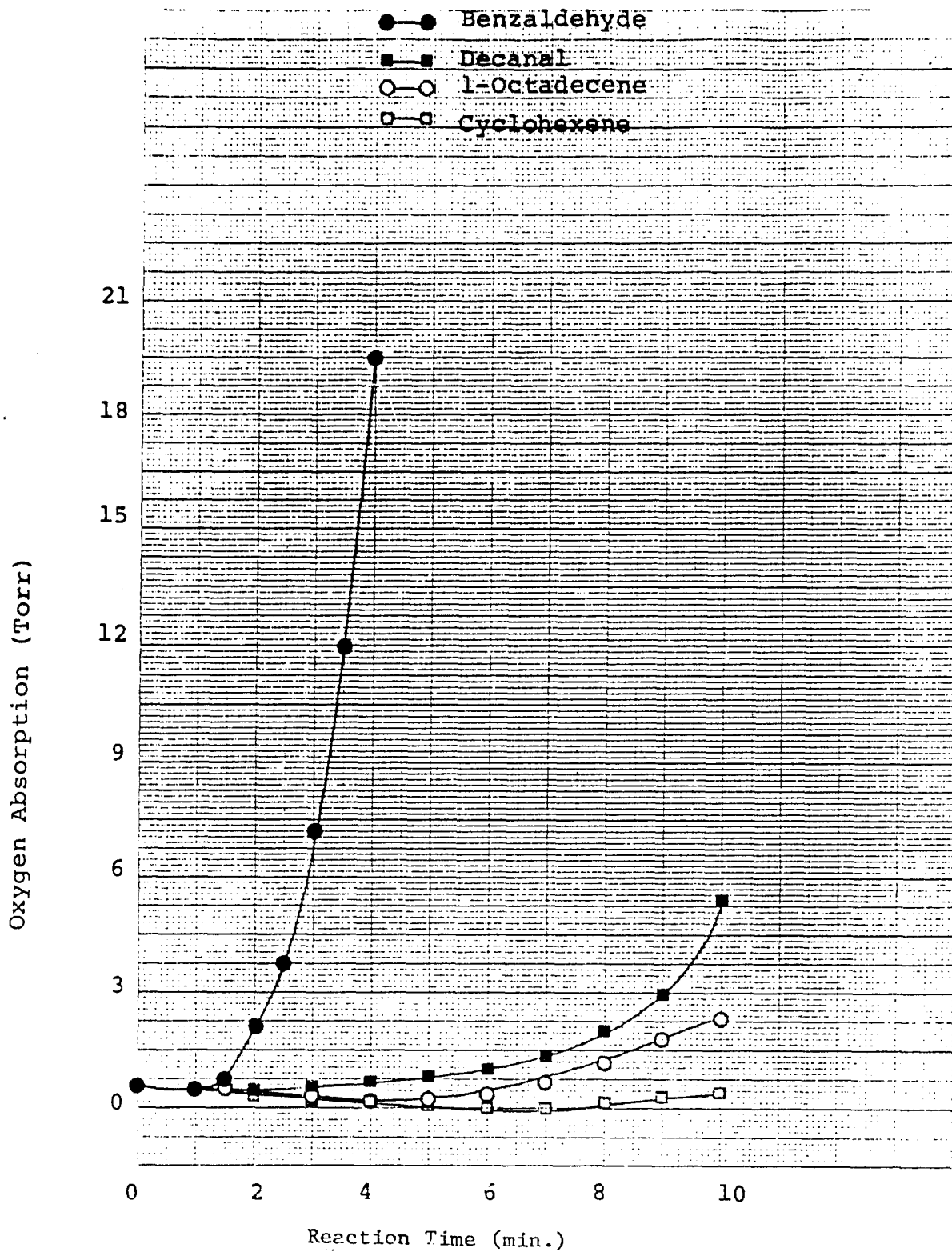


Figure 40. Plots of Oxygen Absorption Versus Reaction Time of AIBN Stressing at 50°C of Easily Oxidized Substances (No MIL-L-7808 Oil Present).

unstabilized cyclohexene could not be found, no further work was performed with cyclohexene.

To test the ability of the benzaldehyde reaction system to differentiate between MIL-L-7808 oils with varying degrees of oxidative degradation, 100  $\mu$ l samples of fresh TEL-4005 oil and TEL-4005 oils stressed 72 and 144 hours (stable life ended at 96 hours) were added to the reaction system prior to the addition of the AIBN initiator.

However, the addition of the oil samples to the benzaldehyde reaction system resulted in a pressure increase, not a pressure decrease (oxygen absorption), before and after the AIBN addition. Therefore, the order of addition was changed so that the oil sample, AIBN in chlorobenzene, and hexadecane were added to the 25 ml flask, purged with oxygen, equilibrated, and then the benzaldehyde injected through the septum to start the reaction. The data presented in Figure 41 was collected using this order of addition.

As seen in Figure 41, the modified Ford method with benzaldehyde differentiates between the fresh and stressed TEL-4005 oil samples. The rate of oxygen absorption is much slower than desired, and the induction time for the fresh TEL-4005 oil is over 20 minutes. Therefore, further research was conducted to shorten the induction period and to increase the rate of oxygen absorption after the end of the induction period.

#### (c) Effect of Hexadecane

In order to simplify the modified Ford method and increase the rate of oxygen absorption, the effect of eliminating the hexadecane from the reaction system was studied. In one system, hexadecane (9 ml) and 0.2 M AIBN in chlorobenzene (0.5 ml) were used while in another system only 0.2 M AIBN in chlorobenzene (9 ml) was used. The elimination of hexadecane shortened the time before the oxygen absorption became rapid from 4 to 2 minutes, sharpened the transition period, and increased the rate of oxygen absorption. Therefore, eliminating hexadecane

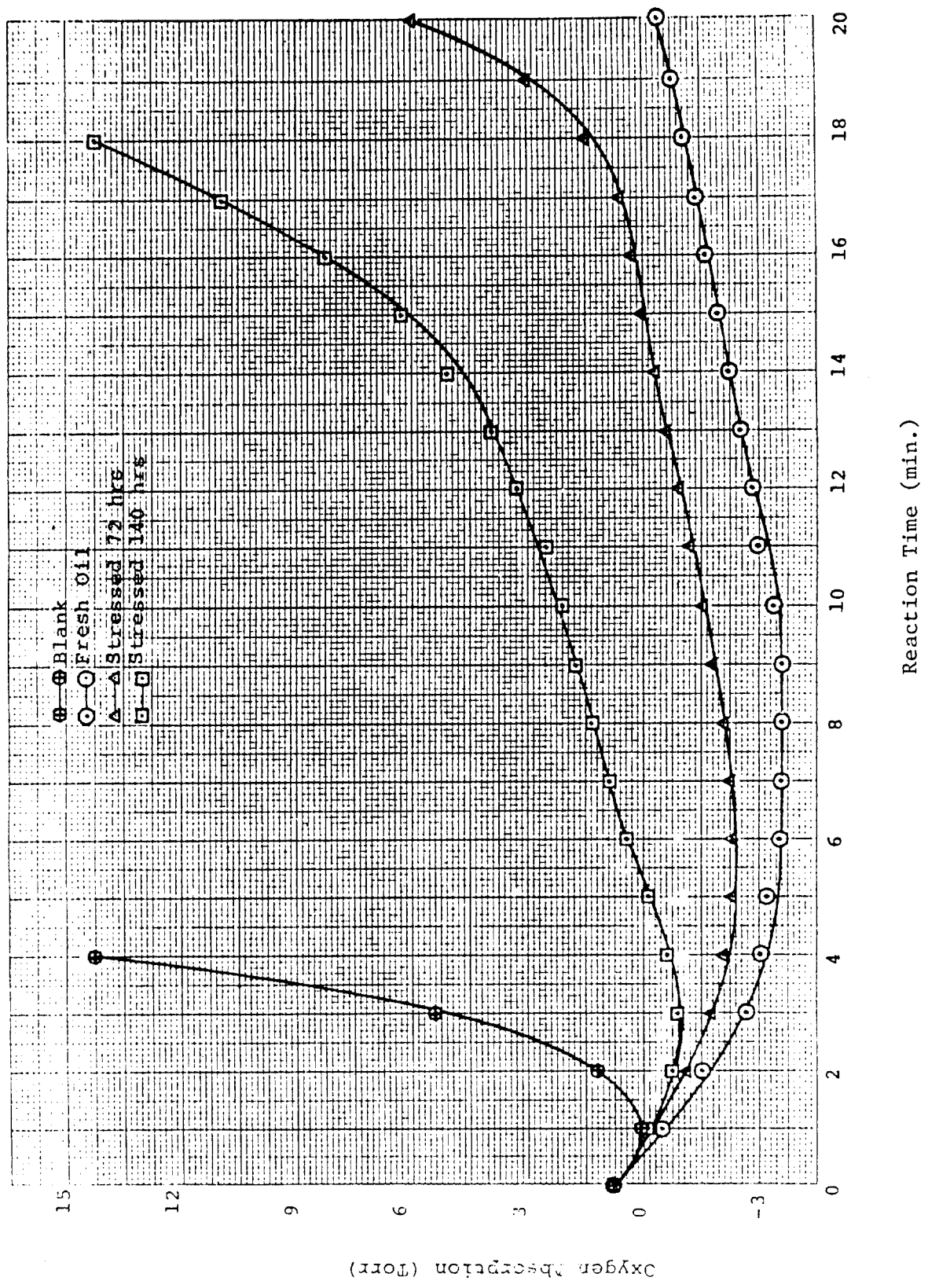


Figure 41. Plots of Oxygen Absorption versus Reaction Time of AIBN Stressing at 60°C of Fresh and Oxidatively Stressed TEL-4005 Oils.

not only simplified the modified Ford method but also produced a shorter, better defined induction time.

(d) Effect of AIBN Solution Concentration

In an attempt to increase the rate of oxygen absorption, the effect of increasing the concentration of the AIBN solution from 0.2 M to 0.5 M was investigated. Although the rate of oxygen absorption was increased and the induction time shortened, the 0.5 M AIBN solution was stable for less than 24 hours with precipitation occurring overnight. Due to this instability, the 0.2 M AIBN was used in all of the following work.

(e) Effect of AIBN Solution and Benzaldehyde Quantities

In an attempt to decrease the equilibration time while increasing the oxygen absorption, different combinations of the AIBN solution and benzaldehyde were investigated. It was found that decreasing the quantity of AIBN solution from 9 ml to 4 ml, decreased the equilibration time from 5 minutes to 2 minutes without significantly affecting the rate of oxygen absorption. Decreasing the quantity of benzaldehyde from 1 to 0.5 ml also did not affect the rate of oxygen absorption significantly but did produce a sharper transition period. Further decreases in the quantities of the AIBN solution and benzaldehyde decreased the rate of oxygen absorption without significantly affecting the equilibration or transition period. Therefore, all further work was performed using 4 ml of the 0.2 M AIBN solution and 0.5 ml of benzaldehyde and a equilibration time of two minutes.

(f) Effect of Oxygen Purge

In an effort to simplify the chemical stressing method further, the effect of eliminating the oxygen purge was investigated. The 0.2 M AIBN in chlorobenzene (4.0 ml) was pipetted into the 25 ml flask, allowed to equilibrate for 2 minutes, and then benzaldehyde (0.5 ml) was injected through the

septum. The plots of oxygen absorption versus reaction time, with and without an oxygen purge, are shown in Figure 42.

Although the time at which the oxygen absorption begins is similar for each system, the oxygen purge results in a much sharper transition period and faster pressure decrease. These results were expected since air is only approximately one-fifth oxygen. Taking this into account (Air Adjusted in Figure 42) the absorption of oxygen is similar for the two systems. Thus, oxygen purges were used for the rest of the studies in order to enhance the pressure changes.

#### (g) Effect of Oil Sample Size

Since the induction time of the fresh TEL-4005 oil was approximately 30 minutes using a 100  $\mu$ l sample, research was conducted to find the amount of a MIL-L-7808 lubricating oil that would produce an induction time of approximately 10 minutes. The results for 50, 20 and 10  $\mu$ l samples of the TEL-4005 oil are shown in Figure 43.

As seen in Figure 43, the induction time decreases proportionally with sample size. Although the 10  $\mu$ l sample gave a shorter induction period than the 20  $\mu$ l sample (Figure 43), the 20  $\mu$ l sample size was chosen for the optimum procedure, since it would allow for better differentiation of the stressed samples (longer induction periods).

#### (h) Modified Ford Method

The modified Ford method involves pipetting 20  $\mu$ l of MIL-L-7808 lubricating oil and 4 ml of the 0.2 M AIBN chlorobenzene solution into the 25 ml flask. Oxygen is then bubbled rapidly through the reaction solution for 1 minute, and then the reaction solution is allowed to equilibrate for 2 minutes with stirring. Benzaldehyde (0.5 ml) is then injected through the stopper using a 2 ml syringe to start the analysis period.

The other major modification used by the modified Ford method is the manner in which the induction period

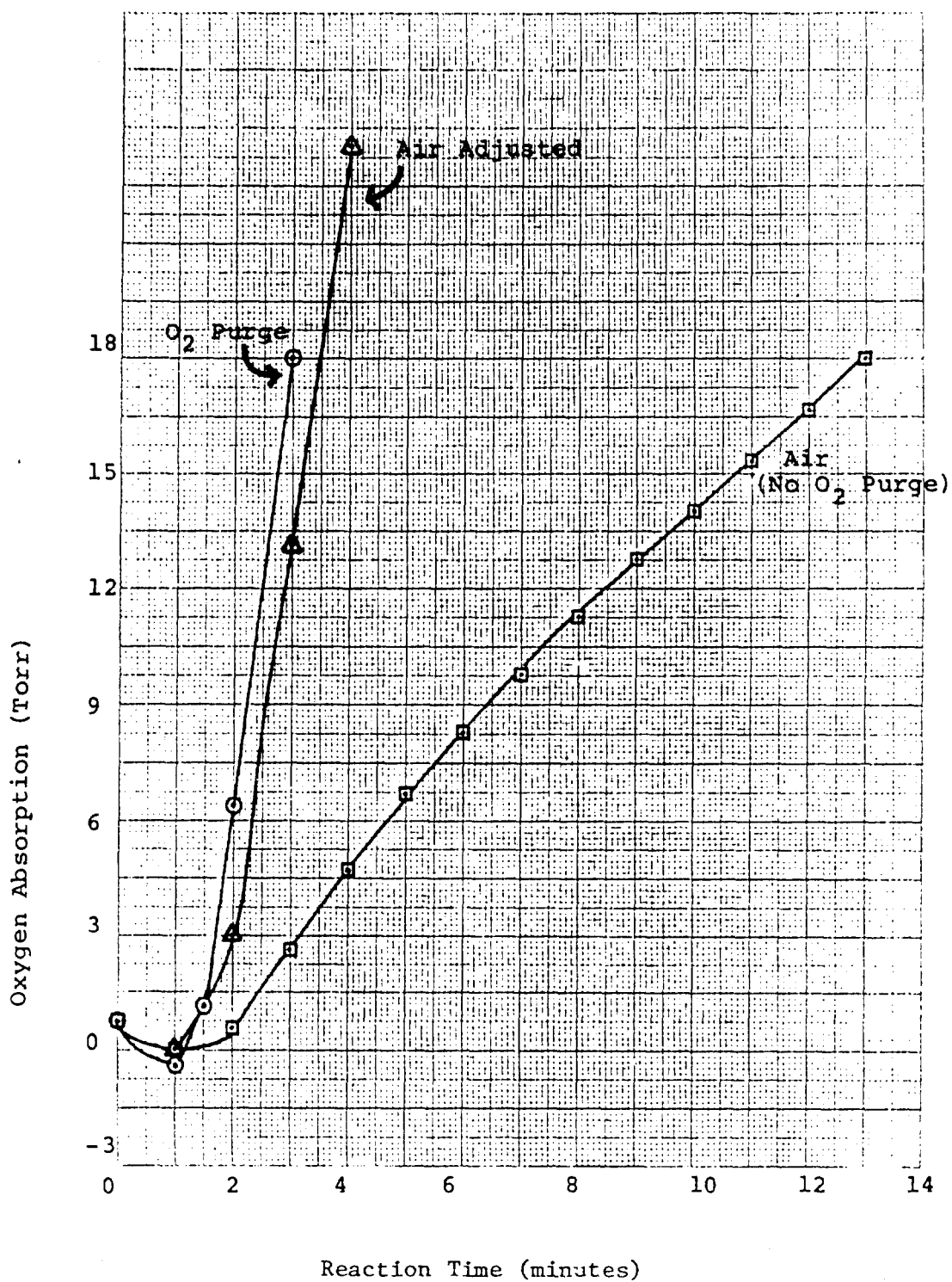


Figure 42. Effect of Oxygen Purge on the Oxygen Absorption versus Reaction Time of AIBN Stressing at 60°C of Benzaldehyde.

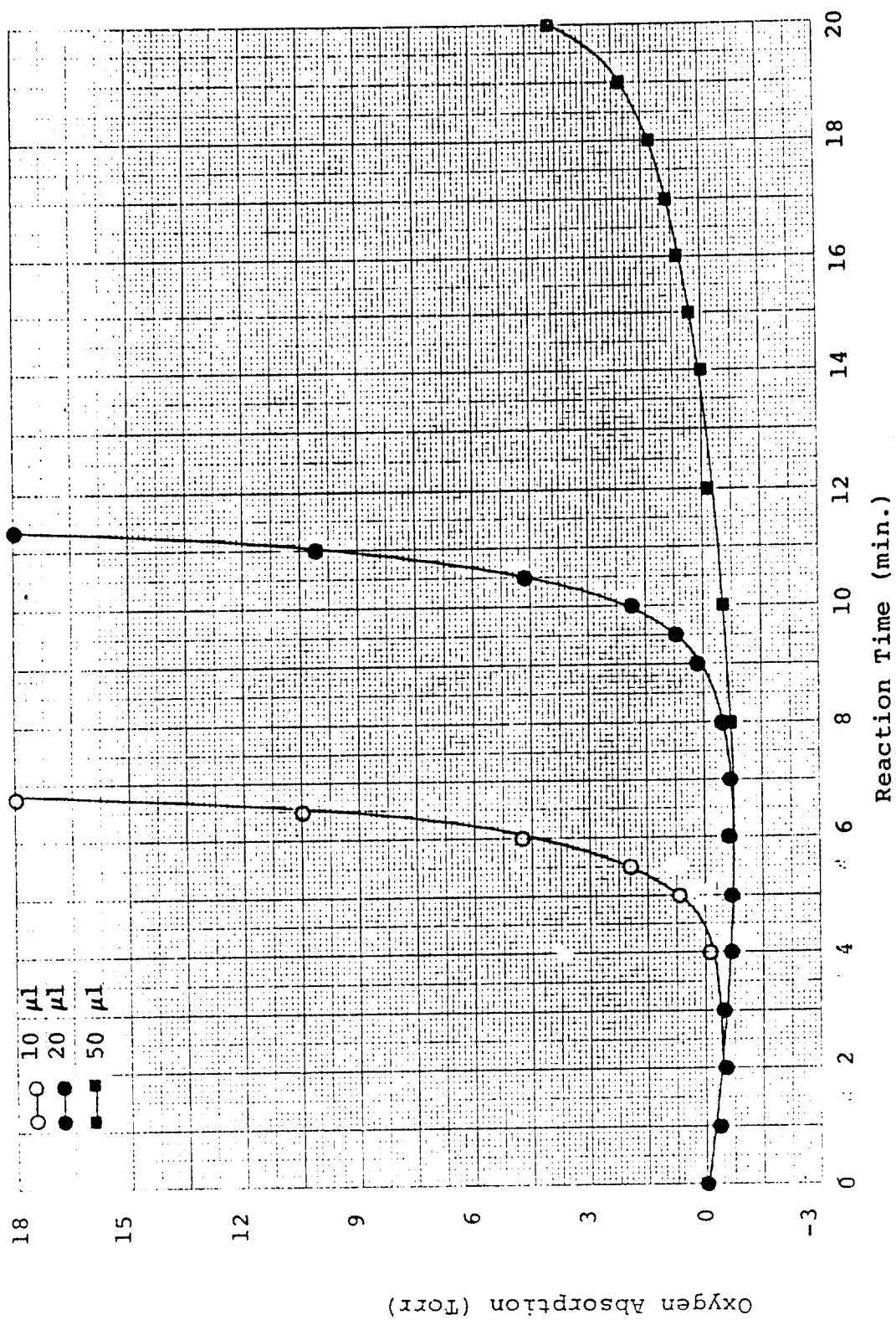


Figure 43. The Effect of Sample Size (TEL-4005 Oil) on the Oxygen Absorption versus Reaction Time of AIBN Stressing at 60°C of Benzaldehyde.

is determined. Instead of using extrapolation techniques as illustrated in Figure 39, the induction time for this work is defined as the length of time required for the oxygen absorption to result in a pressure decrease of 18 torr. The main advantage of defining the induction period in this manner is that it eliminates any need for interpretation by the analyst, thus shortening the total time and ease of operation of the technique.

(i) Effect of Time on the AIBN Solution

Due to its ability to thermally produce free radicals at relatively low temperatures (60°C), the AIBN in solid form requires refrigeration when not in use. To determine the effect of aging on the AIBN solution, the modified Ford method was performed on the TEL-4005 lubricating oil using a freshly prepared AIBN solution and AIBN solutions which had been allowed to sit at room temperature for 1 day, 1 week, 2 weeks, and 1 month. The plots of oxygen absorption versus reaction time for the freshly prepared and aged AIBN solutions are shown in Figure 44.

The plots in Figure 44 show that the main effect of aging on the AIBN solution occurs in the first 24 hours. During the first 24 hours the induction time produced by the AIBN increases, indicating a decrease in the concentration of free radicals produced by AIBN. After 24 hours, the produced induction periods are fairly constant for AIBN solutions aged up to 2 weeks.

However, after 2 weeks the effect of aging on the AIBN solution increases with time resulting in less defined, longer induction periods. Also a precipitate was observed in the one month aged AIBN solution.

These results indicate that the ability of the AIBN solution to produce free radicals at 60°C decreases with aging times. Although, the long term instability of the AIBN solution limits the suitability of the modified Ford method for development into a RLLAT, refrigeration of the AIBN solution or

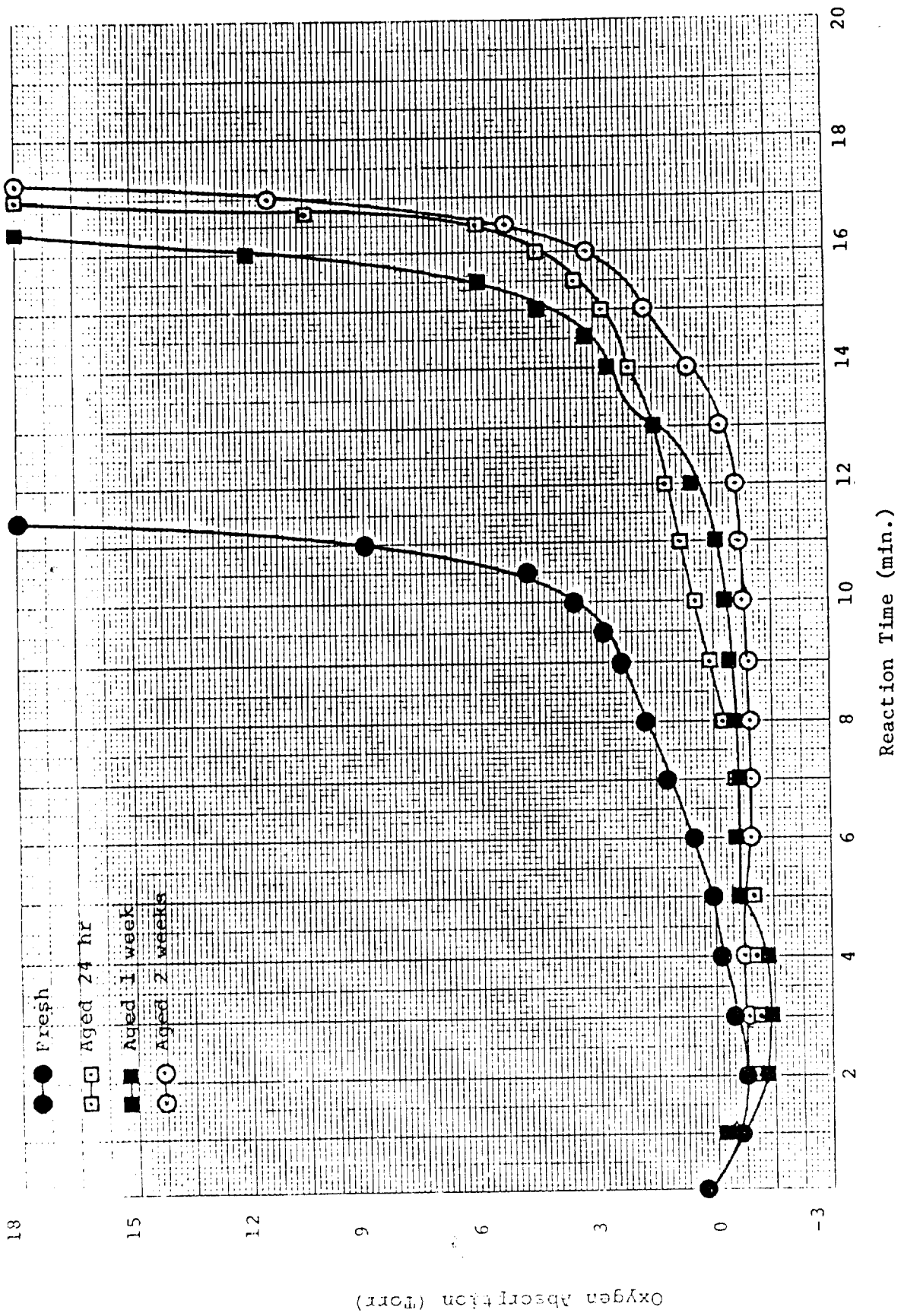


Figure 44. The Effect of AIBN Solution Aging Time on the Oxygen Absorption versus Reaction Time of AIBN Stressing at 60°C for the TEL-4005 Oil.

using solid AIBN in place of the AIBN solution could be used to eliminate the instability problem.

(j) Effect of Formulation

To determine the effects of formulation on the induction periods determined by the modified Ford method, the induction periods of the TEL-4001 through TEL-4006 MIL-L-7808 lubricating oils were determined. The resulting plots of oxygen absorption versus reaction time for the MIL-L-7808 lubricating oils are shown in Figure 45.

As expected, the TEL-4001 through TEL-4006 oils produce different induction periods (Figure 45). The different induction periods were expected, since each oil was shown by cyclic voltammetry to contain differing concentrations of antioxidants (Figures 10 and 11). The main problem with the wide range of induction periods produced by the different fresh MIL-L-7808 oils is that the experimental conditions required to obtain induction periods of less than 10 minutes for the TEL-4004 oil would greatly decrease the modified Ford method's capability to assess the RLL of stressed oil samples.

(k) Analysis of Thermally Oxidized TEL-4005 Oil Samples

In order to determine the modified Ford method's capability to assess RLL, the series of stressed TEL-4005 oils were studied. The plots of oxygen absorption versus reaction time for the oil samples are shown in Figure 46.

The results in Figure 46 show that the modified Ford method is capable of distinguishing between oil samples of differing degrees of thermal oxidation and that the AIBN induction time decreases as the thermal oxidative stressing time increases. Thus, the results of the modified Ford method are related to the RLL of the stressed TEL-4005 oil samples.

However, the plot of the AIBN induction time (oxygen absorption of 18 torr) versus the thermal-oxidative stressing time shown in Figure 47 is not a smooth curve. The

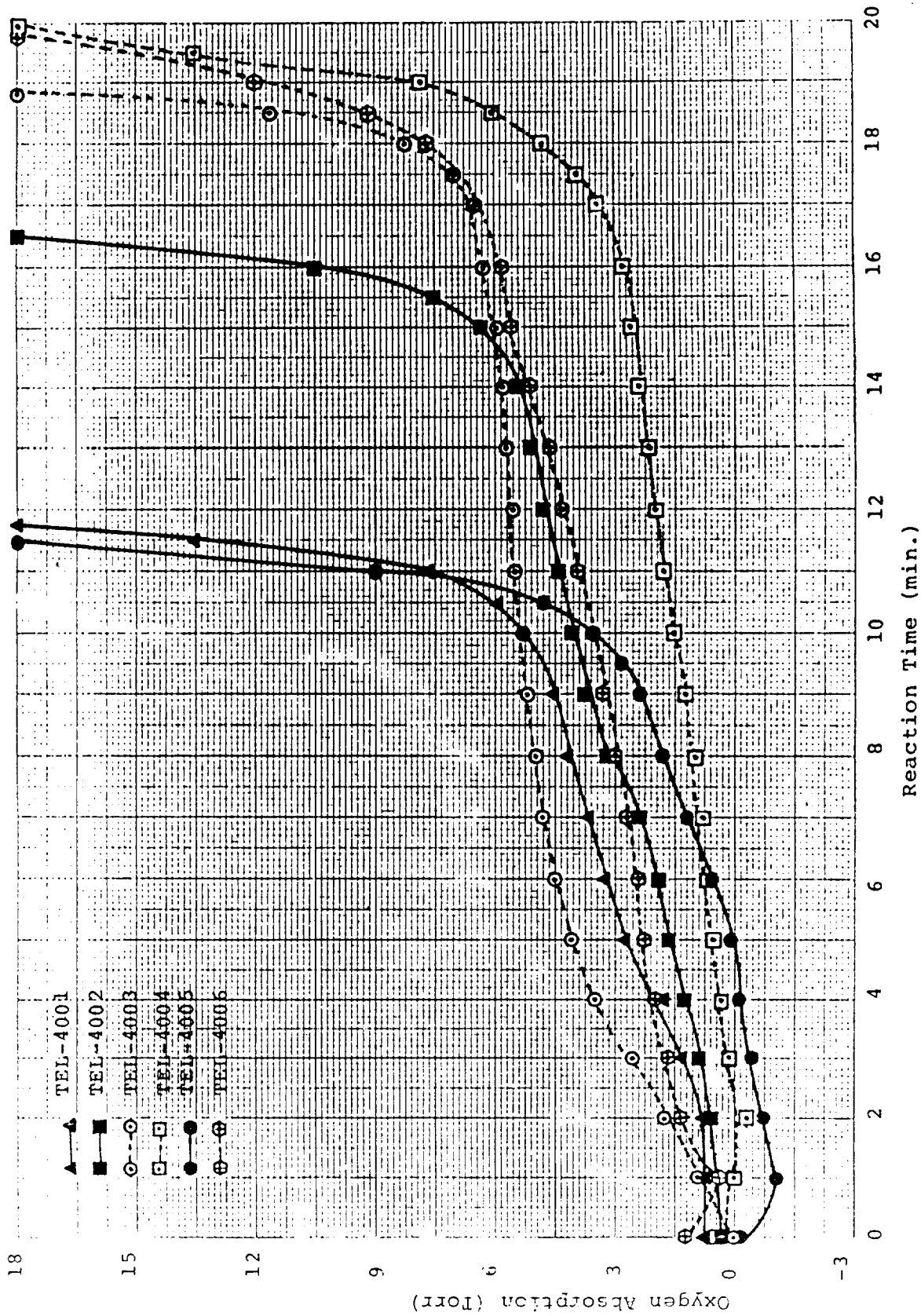


Figure 45. Plots of Oxygen Absorption Versus Reaction Time of AIBN Stressing at 60°C for the Different MIL-L-7808 Oils.

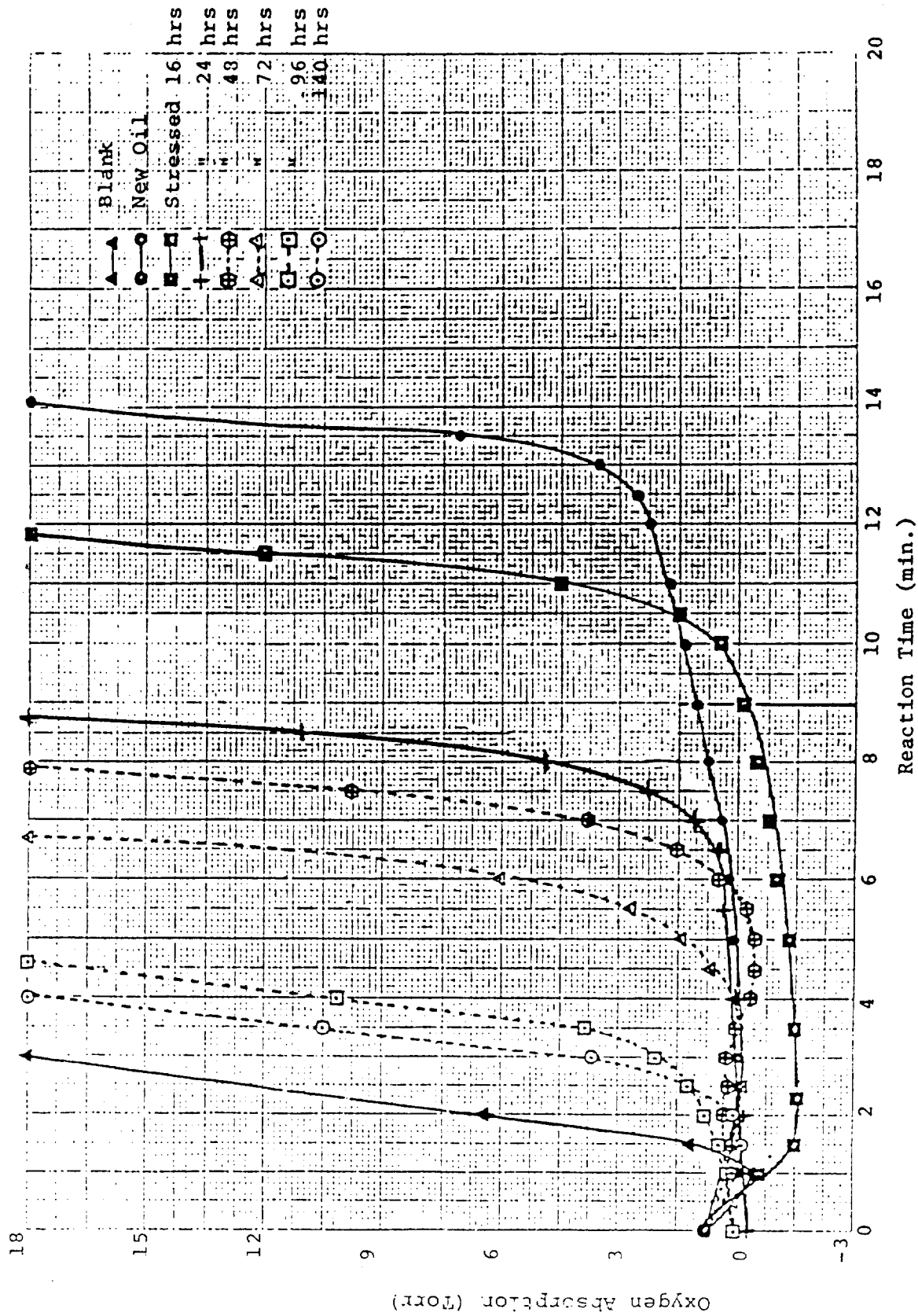


Figure 46. Plots of Oxygen Absorption Versus Reaction Time of AIBN Stressing at 60°C for the Fresh and Oxidatively Stressed TEL-4005 Oils.

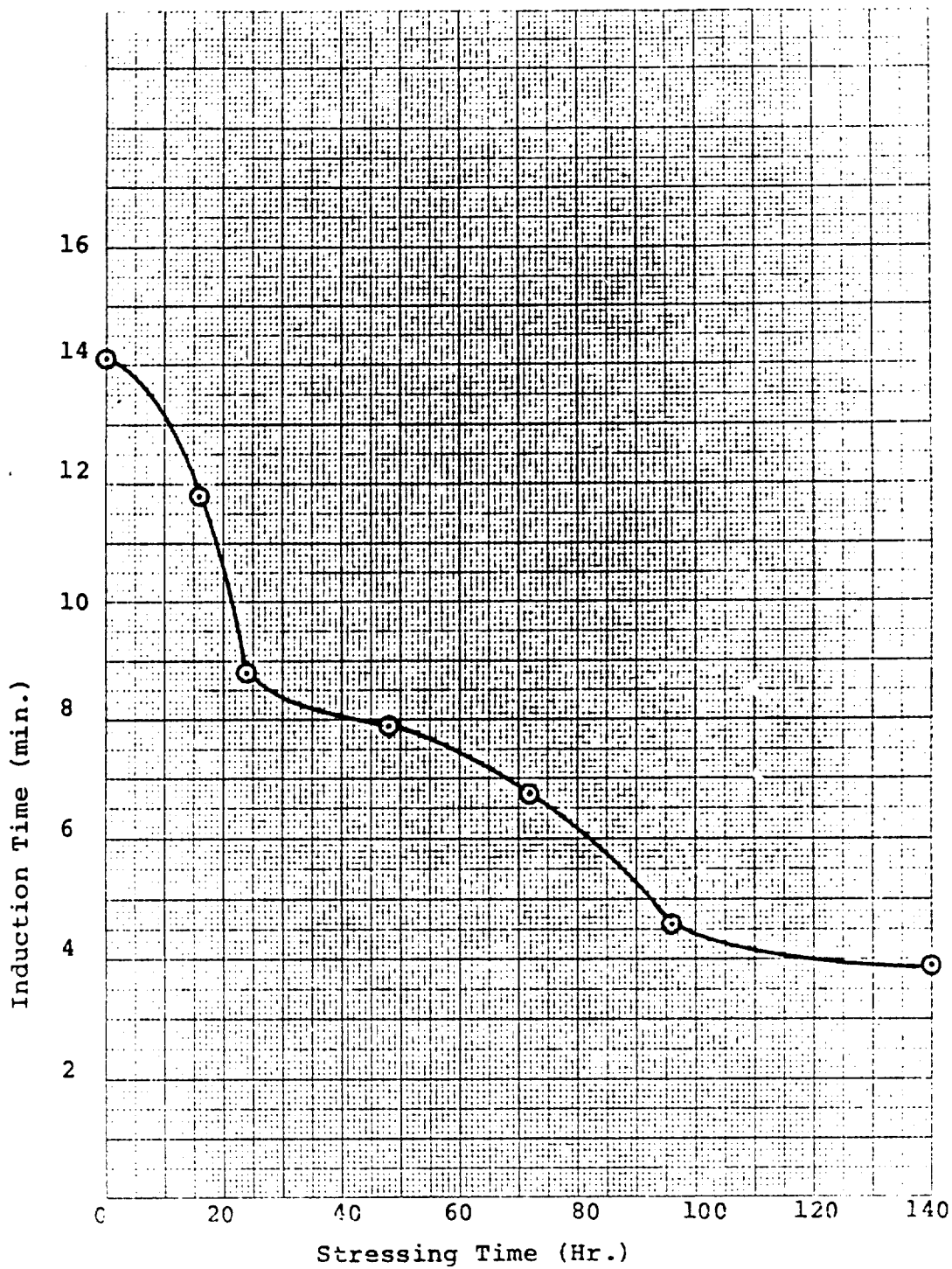


Figure 47. Plot of Induction Time (AIBN at 60°C) versus Thermal Oxidation Stressing Time for the TEL-4005 Oils (Stable Life Ends at 96 Hours).

plot appears to be made up of two separate curves. The first curve is from 0 to 24 hours of thermal-oxidative stressing time and indicates a rapid decrease in the AIBN induction periods of the stressed samples. The second curve is from 24 to 96 hours of thermal-oxidative stressing time and indicates a much slower decrease in the AIBN induction periods of the stressed samples.

#### (1) Summary of the Modified Ford Method

The results of its initial evaluation indicate that the modified Ford method has limited potential for development into a RLLAT candidate. Although the modified Ford method requires only 20  $\mu$ l of the oil sample, can be performed using inexpensive equipment, and has RLL assessment capabilities, the modified Ford method is hard to operate and the age of the AIBN initiator solution affects the RLL assessments. Also, the AIBN induction times range from 12 to 20 minutes for the different MIL-L-7808 oils and the modified Ford method requires a 2 minute oxygen purge and temperature equilibration time prior to the analysis time.

Therefore, the modified Ford method was eliminated from further consideration as a RLLAT candidate.

#### e. Hydroperoxide Measurements

##### (1) Introduction

The primary oxidation product of the ester basestock is the hydroperoxide (ROOH in Reaction 3). Hydroperoxides are also produced by interaction between free radical trapping antioxidants and peroxide radicals (Reaction 6). The generated hydroperoxides are then depleted by thermal decomposition (Reaction 4). Thus, a steady state concentration is obtained for the hydroperoxides during the initial stages of an MIL-L-7808 lubricating oil's stable life.

However, as the oxidation time of the MIL-L-7808 lubricating oil increases, the antioxidants' concentrations decrease allowing the production rate of the hydroperoxide to increase (Reaction 3). Since the depletion rate of the

hydroperoxides remains fairly constant (Reaction 4 controlled mainly by temperature), the concentration of hydroperoxides slowly increases with oxidation time. Once the stable life of the MIL-L-7808 oil ends, the production of the hydroperoxides is no longer inhibited and becomes very rapid resulting in a dramatic increase in the hydroperoxide's concentration. Consequently, the concentration of the hydroperoxides is inversely proportional to the concentration of the antioxidants in the MIL-L-7808 oil (Figure 48).

Although numerous analytical techniques have been developed for determining the concentration of organic peroxides, the iodine liberation methods are the most popular. Of the iodine liberation methods, the set of methods developed by Mair and Graupner (Reference 23) appear to have the best potential for development into a RLLAT candidate.

The methods are based upon the peroxide oxidation of sodium iodide in isopropanol. Since sodium iodide is not oxidized by air when dissolved in isopropanol, the need for blank determinations is eliminated. The set of methods developed by Mair and Graupner are also capable of distinguishing between different types of organic peroxides. Method I stoichiometrically determines peracids and hydroperoxides, method II stoichiometrically determines those of method I plus peresters, ketone peroxides, and aldehyde peroxides, while method III stoichiometrically determines all organic peroxides regardless of their structure, including di-tert-alkyl peroxides.

In addition to the well-established iodine liberation methods, electrochemical techniques have been used to determine the concentration of hydroperoxides in various compounds (References 24 and 25). Of these electrochemical techniques, a cyclic voltammetric technique which employs a

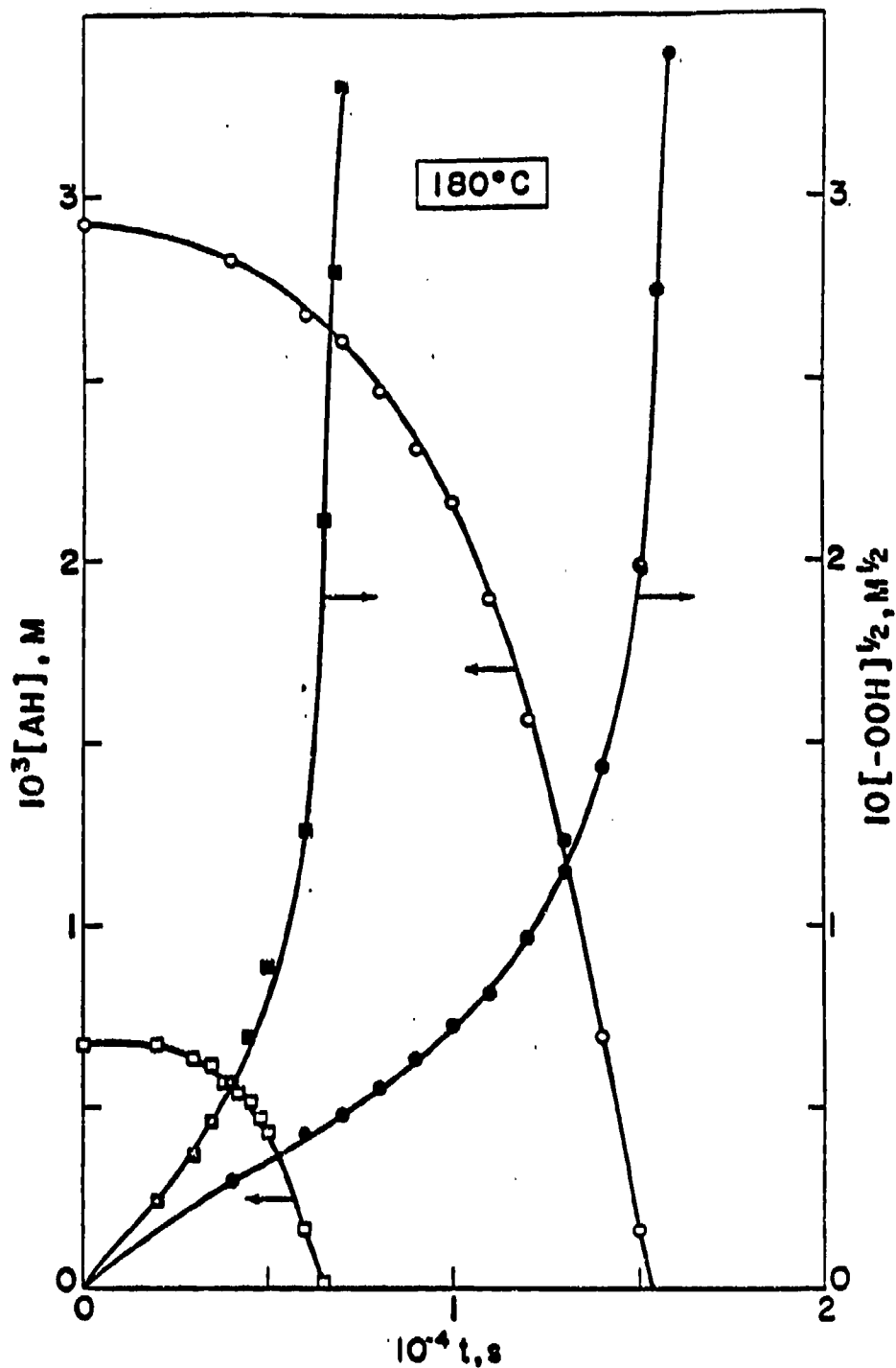


Figure 48. Hydroperoxide ( $-OOH$ : ■ and ● = Initial Amine Concentrations of  $7.0 \times 10^{-4}$  and  $2.9 \times 10^{-3}$  M, Respectively) Formation and Amine Antioxidant (AH: □ and ○ = Initial Concentrations of  $7.0 \times 10^{-4}$  and  $2.9 \times 10^{-3}$  M, Respectively) Consumption in the Inhibited Autoxidation of Pentaerythrityl Tetraheptanoate (Reproduced from Reference 20).

platinum working electrode (Reference 25) appears to be the best suited technique for development into a RLLAT candidate.

Therefore, in order to evaluate the different techniques' potentials as RLLAT candidates, an investigation was conducted to compare the hydroperoxide and peroxide determinations of the selected iodine liberation methods and of the cyclic voltammetric techniques using platinum, glassy carbon, and thin film mercury on gold working electrodes.

## (2) Iodine Liberation Techniques

In order to evaluate the RLL assessment capabilities of the different iodine liberation techniques, the samples of TEL-4005 lubricating oil stressed for 0 to 144 hours (stable life ended at 96 hours) were analyzed. The results of the different iodine liberation techniques are plotted versus stressing time in Figure 49.

The results in Figure 49 show that the organic peroxides present in the stressed MIL-L-7808 oil samples are determined stoichiometrically by methods II and III, but not by method I. These results indicate that the organic peroxides present in stressed oil samples are less than 5 percent hydroperoxides, and instead, appear to be perester-ketone type peroxides.

To confirm these results cumene hydroperoxide was analyzed by method I and produced stoichiometric results after less than three minutes of reaction time. Also, dicumene peroxide did not liberate any detectable amounts of iodine by method I, even after 30 minutes of reaction time, but liberated stoichiometric amounts of iodine by methods II and III.

Even though they make up less than 5 percent of the stressed oil samples' peroxide contents, the concentration of the hydroperoxides determined by method I increases almost linearly

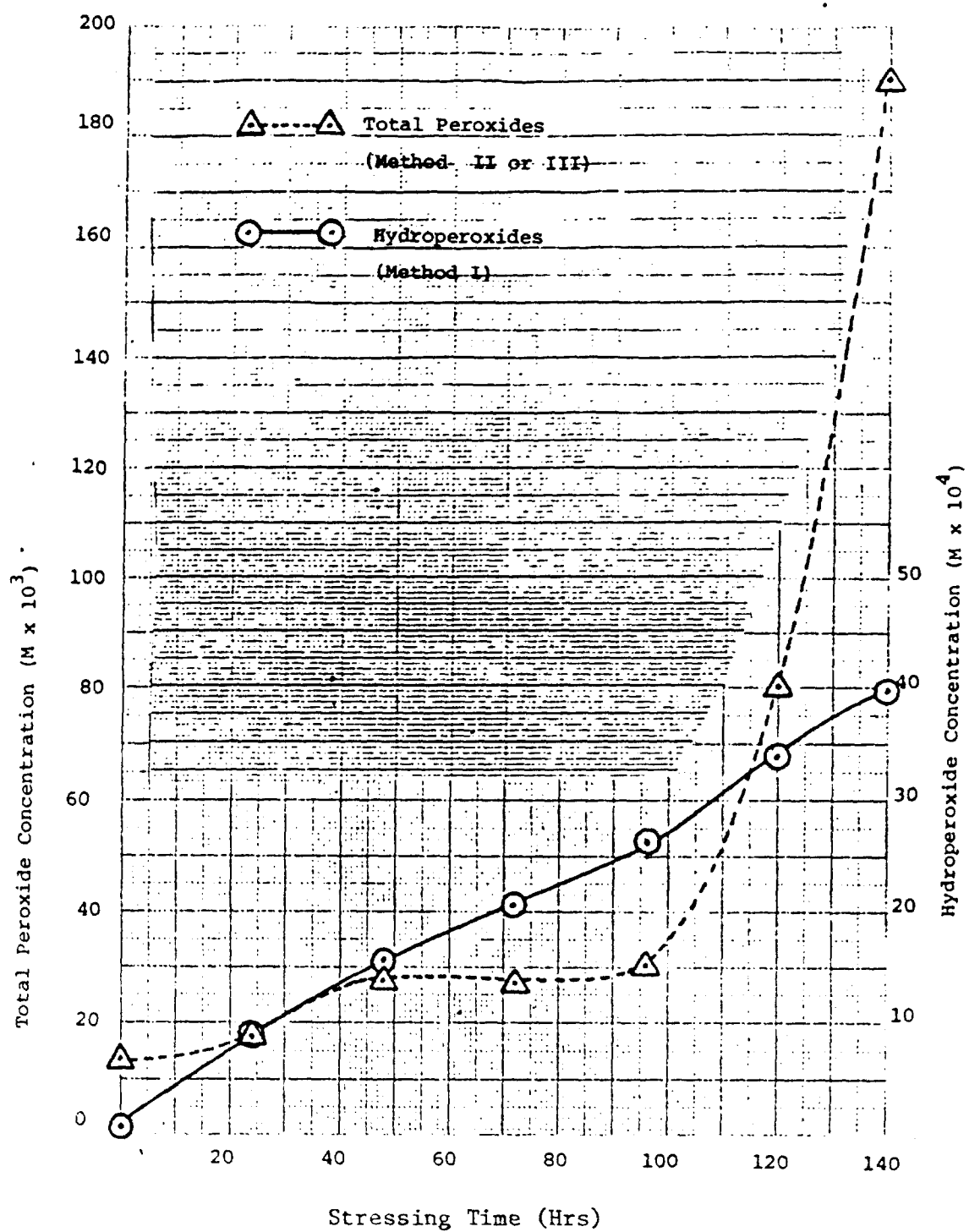


Figure 49. Plots of Total Peroxide and Hydroperoxide Concentrations Versus Stressing Time of TEL-4005 Oils.

with stressing time up to 96 hours (end of TEL-4005 oil's stable life). After the stable life ends, the hydroperoxides increase at a slightly faster rate. In contrast to the hydroperoxides, the total peroxide content determined by methods II or III are independent of the stressing time between 24 and 96 hours, after which time they increase rapidly.

Thus, since method I was the only iodine liberation technique which could be performed in less than 10 minutes and the hydroperoxide's concentration appeared to be related to the RLL of the TEL-4005 oils, method I was selected as the iodine liberation method with the most potential for development into a RLLAT candidate.

### (3) Cyclic Voltammetric Techniques

#### (a) Introduction

In order to evaluate the capability of cyclic voltammetry to determine the concentration of organic peroxides in used MIL-L-7808 oils, the effect of the type of working electrode on the cyclic voltammetry's peroxide determinations was investigated. For this study platinum, glassy carbon, and thin film mercury (gold substrate) working electrodes were studied. Although the reported cyclic voltammetric technique (Reference 25) employed a platinum working electrode, the platinum electrode could only be used to -0.4 V due to its high sensitivity to impurities in the solvent system, and thus, was eliminated from further consideration.

#### (b) Thin Film Mercury Working Electrode

The next working electrode studied was the thin film mercury on gold (Hg-AUE) electrode. The Hg-AUE electrode's surface is similar to that of the dropping mercury electrode of polarography which has been successfully used in various hydroperoxide determinations (Reference 24).

Although the Hg-AUE electrode was unable to detect 13 solutions of benzoyl peroxide, cumene hydroperoxide and dicumene peroxide, it was able to detect oxidatively generated species in the laboratory stressed oil samples. The generated species produced broad reduction waves from 0.0 to -1.7 V (Figure 50). At a potential of -0.1 V, an additional reduction wave is produced for the stressed oil samples (96-144 hours in Figure 50) taken after the stable life of the TEL-4005 oil had ended.

The reducible species are believed to be hydroperoxides even though the Hg-AUE electrode could not detect cumene hydroperoxide. The hydroperoxide concentrations determined by cyclic voltammetry are estimated to be in the  $10^{-3}$  M range (method I determined the hydroperoxide concentrations to range from 0.1 to  $4.0 \times 10^{-3}$  M). The concentration of hydroperoxides determined by cyclic voltammetry can only be estimated due to the broadness of the reduction waves and because the reduction waves did not reach a maximum value before the impurities in the solvent system began to reduce at -1.7 V. By plotting the current at a specific voltage, e.g. -1.5 V, versus the stressing time of the oil samples, one could produce a calibration curve to aid in the assessment of RLL, even though the actual hydroperoxide concentrations are unknown.

The reduction peaks at -0.1 V can not be used to assess RLL since the species responsible for the peak are only detected after the stable life has ended. Also, the reduction peak at -0.1 V would be unreliable since it appears to be produced by a specific hydroperoxide which may not be produced by all of the different MIL-L-7808 oils' ester basestocks.

#### (c) Glassy Carbon Working Electrode

The last working electrode investigated for the cyclic voltammetric determinations of hydroperoxides is the

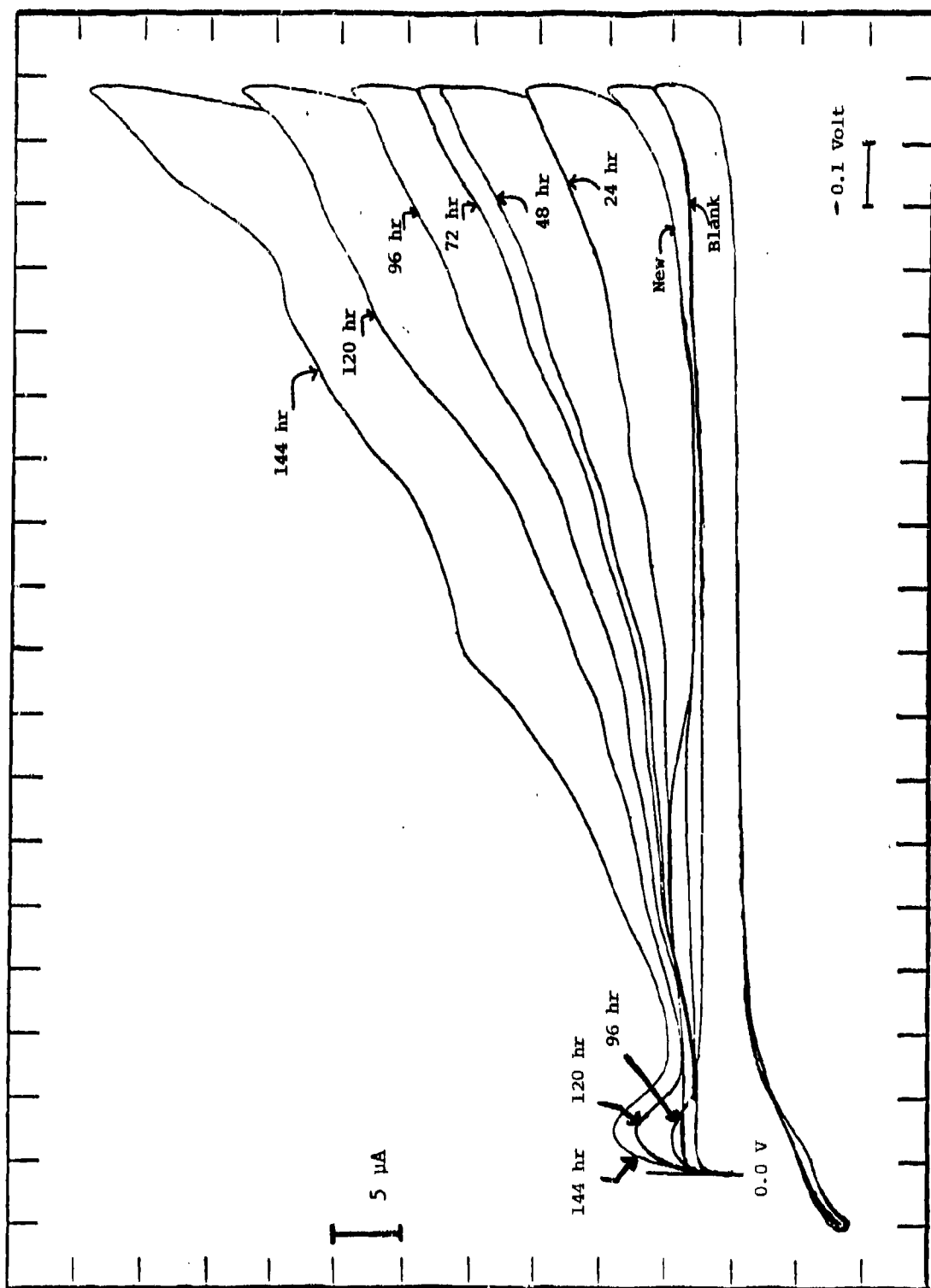


Figure 50. Voltammograms of Hydroperoxides Present in New and Laboratory Stressed TEL-4005 Lubricating Oils in Acetone Using a Hg-AUE Electrode.

glassy carbon (GCE) electrode. Although no work has been published on the use of GCE electrodes for hydroperoxide determinations, the GCE electrode was able to detect benzoylperoxide (A) and cumene hydroperoxide (B) (Figure 51), but not dicumene peroxide. In fact, due to the high stability of dicumene peroxide, no electrochemical technique has been able to detect it. The Mair and Graupner's iodometric method is one of the few techniques capable of quantitatively analyzing for dicumene peroxide.

The GCE electrode was then used to analyze the laboratory stressed TEL-4005 oils for hydroperoxide content. The voltammograms produced by the glassy carbon electrode are shown in Figure 52, and except for the reduction wave at  $-0.1$  V, (Figure 50), the voltammograms produced by the Hg-AUE and GCE electrodes are very similar. Even though the voltammogram of cumene hydroperoxide (Figure 51) produced by the GCE electrode has a maximum, the voltammograms of the stressed oil samples do not possess a maximum (Figure 52). As with the Hg-AUE voltammograms, the plots of the current produced by the GCE electrode at a specific voltage versus the stressing time of the oil sample could be used to aid in RLL assessments.

The main advantage of the glassy carbon electrode over the Hg-AUE electrode is that the GCE electrode can be used to determine the concentration of antioxidants present in the oil sample ( $0.0$  to  $1.5$  V) (Figure 8) but the Hg-AUE electrode can not be used above  $0.2$  V (oxidation of Hg). Also the GCE electrode is much easier to maintain than the Hg-AUE electrode.

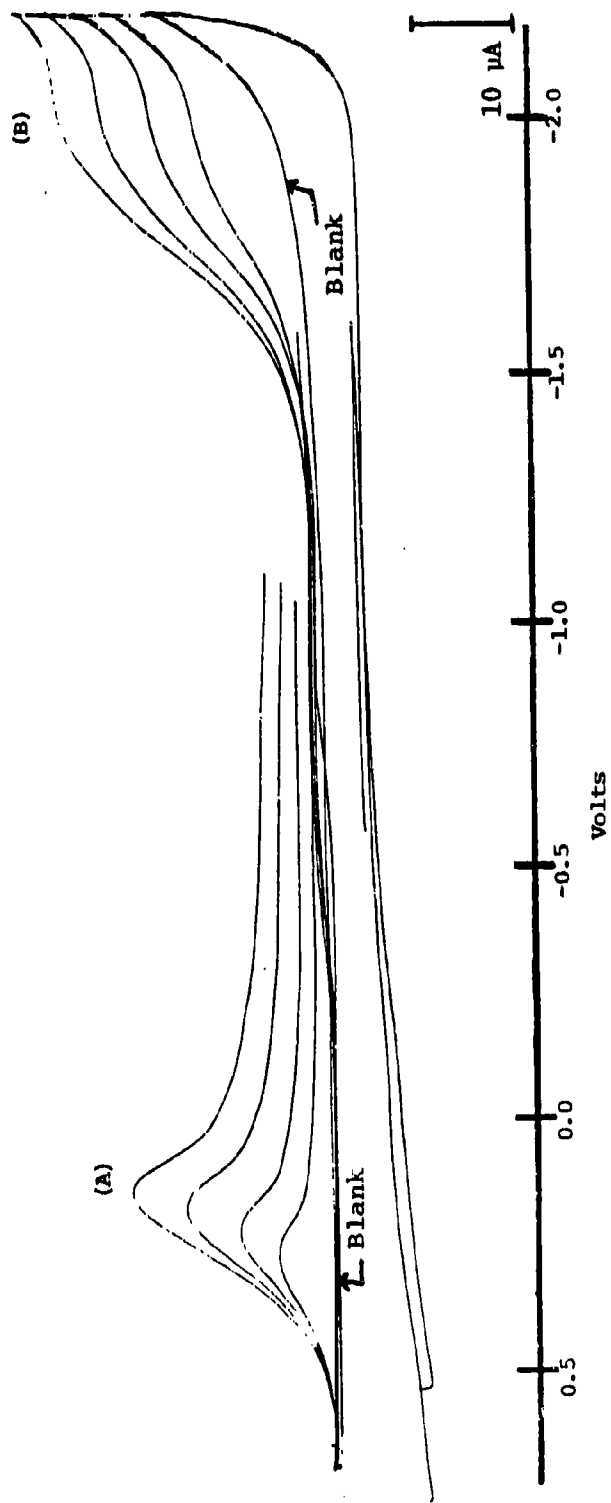


Figure 51. Voltammograms of 50, 100, 150, and 200  $\mu\text{l}$  Samples of Benzoic Peroxide (A) and Cumene Hydroperoxide (B) in Acetone Using a Glassy Carbon Working Electrode.

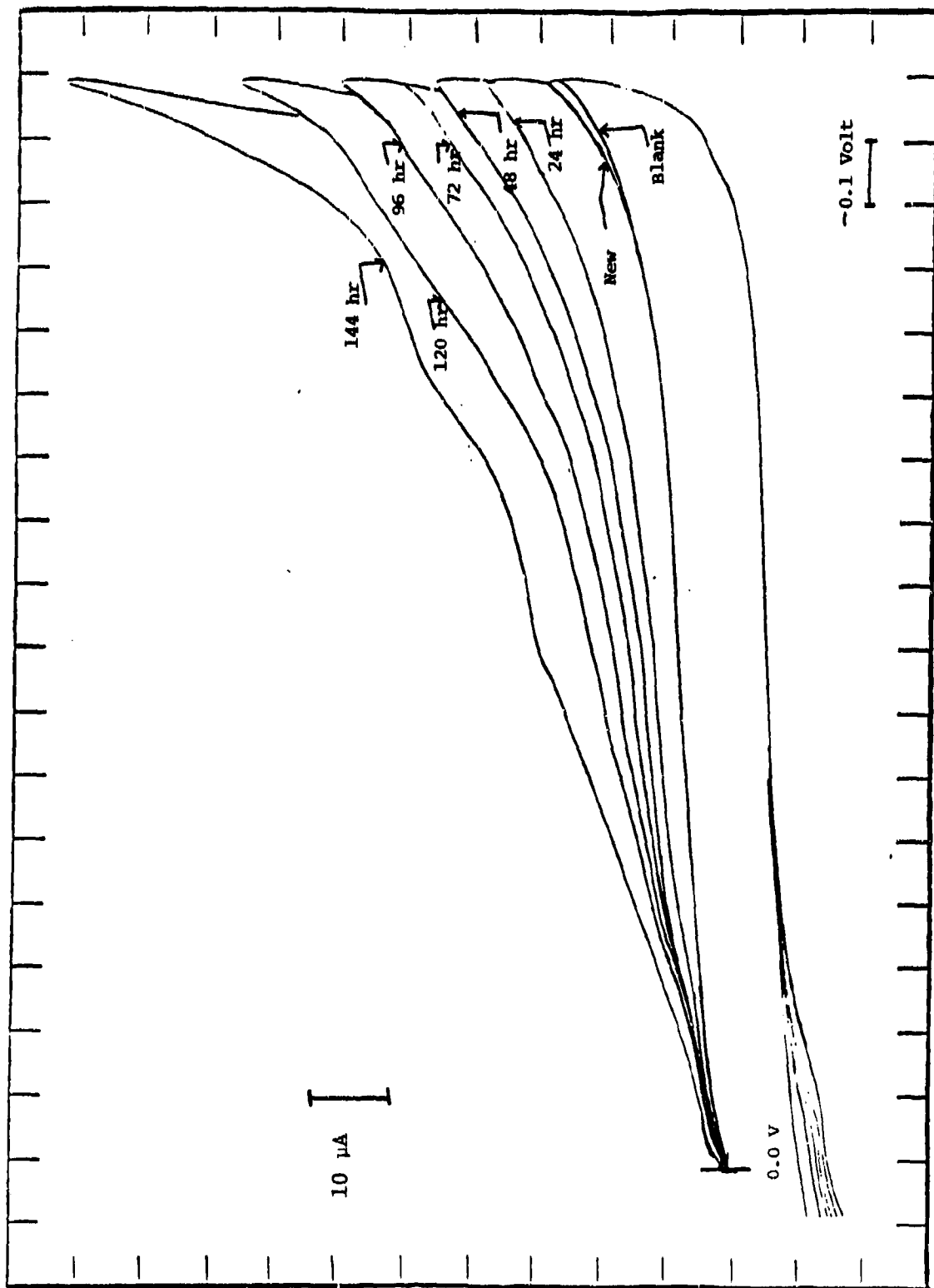


Figure 52. Voltammograms of Hydroperoxides in New and Laboratory Stressed (24-144 Hours) TEL-4005 Lubricating Oils in Acetone Using a Glassy Carbon Working Electrode.

#### (4) Summary of Alkyl Hydroperoxide Detection Techniques

The initial investigation indicated that the alkyl hydroperoxide detection techniques have limited potential for development into RLLAT. The broad voltammograms (Figures 50 and 52) indicate that numerous hydroperoxides are produced by the ester basestock of the TEL-4005 oil and that the produced hydroperoxides have a wide range of reduction potentials. Since the different MIL-L-7808 oils use a variety of ester basestocks, the number of different hydroperoxides produced by the various ester basestocks and the range of their respective reduction potentials will be great causing the results of the iodine liberation and cyclic voltammetric hydroperoxide analyses to be formula dependent.

Consequently, the alkyl hydroperoxide results are better suited for degree of oxidative degradation estimations than for RLL assessments.

##### f. Permanganatometric Method

###### (1) Introduction

In addition to the colorimetric and modified Ford chemical stressing techniques, a chemical stressing technique which uses the strong oxidant, potassium permanganate ( $\text{KMnO}_4$ ), has been reported (References 26 and 27) and is referred to as the permanganatometric method. Acidic  $\text{KMnO}_4$  solutions were used to determine the oxidation stability of fresh and oxidized samples of hydrocarbon fuels and lubricants. As the hydrocarbon fuel or lubricant becomes increasingly oxidized, the amount of  $\text{KMnO}_4$  which reacts with the sample increases.

However, in unrelated work,  $\text{KMnO}_4$  has been used to oxidize amine antioxidants (Reference 28). Also the hydrocarbon fuels and lubricants analyzed by the permanganatometric method contained less than 0.003% of a hindered phenol antioxidant, while the MIL-L-7808 oils to be tested employ an ester basestock and 1-2% of amine antioxidants.

Therefore, an investigation was carried out to determine if the presence of amine antioxidants or ester basestocks hinder the permanganatometric method's RLL assessments. The effects of  $\text{KMnO}_4$  concentration and the reaction time on the permanganatometric method's results were studied.

#### (2) Effect of $\text{KMnO}_4$ Concentration

To determine the effect of the  $\text{KMnO}_4$  concentration on the permanganatometric method's RLL assessments, fresh and stressed (96 hours) TEL-4005 oils were reacted with 0.1 and 0.01 M  $\text{KMnO}_4$  solutions for 30 minutes. The reacted solutions were then titrated with a 0.02 M sodium thiosulfate solution to determine the quantity of unreacted  $\text{KMnO}_4$  remaining in solution.

When the 0.1 M  $\text{KMnO}_4$  solution was reacted for 30 minutes with the fresh and stressed TEL-4005 oil samples, the same amount of unreacted  $\text{KMnO}_4$  solution was present in both reacted solutions. However, when the 0.01 M  $\text{KMnO}_4$  solution was reacted for thirty minutes with the fresh and stressed oil samples, the reacted solution of the stressed oil contained twice the amount of unreacted  $\text{KMnO}_4$  as the reacted solution of the fresh oil.

### (3) Effect of Reaction Time

Since the initial tests indicated that the permanganatometric method had the ability to distinguish between oil samples of varying degrees of oxidation, research was conducted to shorten the reaction time from thirty minutes to less than ten minutes. In order to shorten the reaction time, vigorous stirring with a magnetic stirrer was used to keep the oil sample dispersed in the aqueous  $\text{KMnO}_4$  solution to increase the interaction between the two phases.

After 30, 15, and 10 minutes of stirring, the fresh and oxidized oil samples required  $3.5 \pm 0.2$  ml of titrant, i.e., reacted solutions contained the same amounts of unreacted  $\text{KMnO}_4$ . Once the stirring time was shortened to less than 5 minutes, the fresh oil still required  $3.5 \pm 0.2$  ml of titrant but the oxidized oil required  $7.0 \pm 2.0$  ml. Thus, the amount of titrant required by the fresh oil was not dependent on the reaction time, while the amount of titrant required by the stressed oil decreased with time. Therefore, it appears that the species reacting with the  $\text{KMnO}_4$  are of nearly equal concentrations in the fresh and oxidized oil samples, but for some unknown reason, the species in the fresh oil react at a faster rate than those in the oxidized oil. Since the antioxidants are of lower concentration in the oxidized oil sample than in the fresh oil, species other than antioxidants must be reacting with the  $\text{KMnO}_4$ .

### (4) Summary of Permanganatometric Method

The initial evaluation indicated that the permanganatometric method has very limited RLL assessing capabilities and is very sensitive to small variations in the

experimental procedure. Therefore, the permanganatometric method is not suited for development into a RLLAT and was eliminated from further consideration.

#### g. Electrical Property Measurements

##### (1) Introduction

When the ester basestocks of MIL-L-7808 lubricating oils undergo thermal-oxidative degradation, they produce polar compounds which affect the electrical properties of the oils. Several authors (References 29-36) have reported that there is a direct relationship between the degree of oxidative degradation and the electrical properties of the lubricant. The Air Force currently uses the Complete Oil-Breakdown-Rate Analyzer (COBRA) to monitor the condition of used MIL-L-7808 and MIL-L-23699 lubricating oils (References 35 and 36). This device is believed to determine the electrical properties of lubricants which can be measured in less than 5 minutes using very inexpensive, easy to operate instrumentation, and thus, would be suitable for development into a RLLAT. However, most of these studies were designed to detect large changes in the lubricant's degree of oxidative degradation. It has also been reported that the electrical property measurements of the COBRA are formula dependent (References 35 and 36).

Therefore, an investigation was conducted to determine the potential of electrical property measurements for development into a RLLAT. The effect of formulation and oxidative degradation on the combined resistance and capacitance of fresh and laboratory stressed MIL-L-7808 lubricating oils were studied. The relationship between the resistance and the COBRA measurements of the laboratory stressed MIL-L-7808 lubricating oils were also determined.

(2) Comparison of the Electrical Property Measuring Systems Used by UDRI and COBRA

In the electrical property measuring system used by UDRI, the ratio of  $V_I/V$  (Figure 53) is related to the frequency of the input waveform, the capacitances and resistances of the voltage meters, and the resistance ( $R_x$ ) and  $C_x$ , of the oil filled sample cell. Since all of the quantities are known except for  $R_x$  and  $C_x$ , the  $V_I/V$  ratio can be used to approximate  $R_x$  and  $C_x$ .

At a very high frequency, e.g. 1000 Hz, the ratio of  $V_I/V$  is related to the capacitance of the oil sample, and at a very low frequency, e.g. 10 Hz, the ratio  $V_I/V$  is related to the resistance of the oil sample. Therefore, the resistance and capacitance measurements of fresh and oxidatively degraded oils were performed with waveform inputs of 10 and 1000 Hz.

In order to monitor the frequency dependence of MIL-L-7808 oils, the input waveform of the electrical property measuring system used by UDRI was designed with two important characteristics. First, a d.c. voltage was eliminated from the input, because the lubricant polarized when subjected to a d.c. voltage causing the readings to drift with time. The second characteristic of the input was that its waveform was a sine wave. In this manner, the response of the lubricant was dependent on only one frequency component.

In contrast to the electrical property measuring system used by UDRI, the COBRA instrument employs a square wave input, a d.c. offset, and several frequency components. The drift during the initial phase of the COBRA measurement is most likely due to the d.c. offset. The drift was eliminated when the d.c. offset was set to zero.

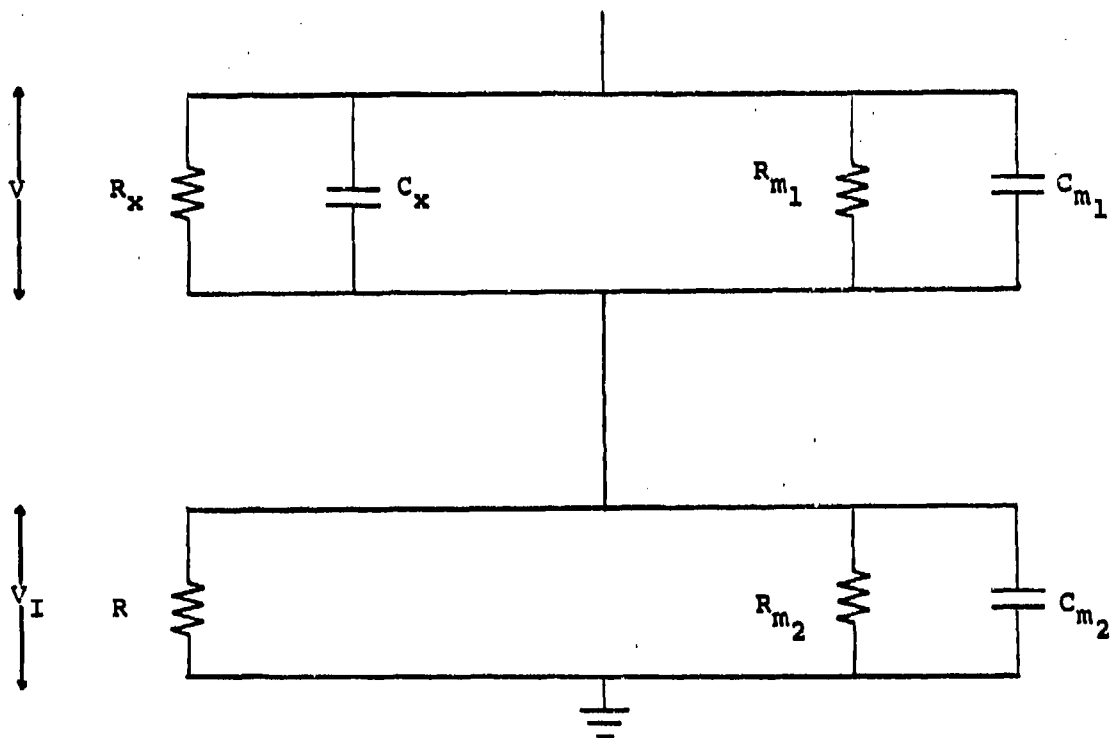


Figure 53. Schematic of Electrical Circuit Used to Measure Electrical Properties of Oil Samples.

- $R_{m1}$  and  $C_{m1}$  = Resistance and Capacitance of Voltage Meter 1, Respectively
- $R_{m2}$  and  $C_{m2}$  = Resistance and Capacitance of Voltage Meter 2, Respectively
- $R$  = Current Sensing Resistor
- $R_x$  and  $C_x$  = Resistance and Capacitance of Sample Cell, Respectively
- $V$  = Voltage Drop Across Measurement Cell
- $V_I$  = Voltage Drop Across Current Sensing Resistor

### (3) Effect of Oxidative Degradation

To determine the effects of oxidative degradation on the combined resistance and capacitance of MIL-L-7808 lubricating oils, the TEL-4005 oil samples which had been stressed for 24 to 120 hours (stable life ended at 96 hours) were analyzed with 10, 100 and 1000 Hz sine wave inputs. The plots of  $V_I/V$  versus stressing time for the inputs of 10, 100, 1000 Hz are shown in Figure 54.

The plots of  $V_I/V$  versus stressing time for a 10 Hz input in Figure 54 decrease rapidly with stressing time indicating that the resistance of the MIL-L-7808 oil decreases rapidly with stressing time. The resistance of the oil samples are decreased by the polar compounds produced by the oxidative degradation of the ester basestock.

As the frequency of the input is increased from 10 Hz to 1000 Hz, the effect on the  $V_I/V$  ratio due to resistance decreases, while the effect of capacitance increases. As seen in Figure 54, the effect of oxidative degradation on the  $V_I/V$  ratio is small for 1000 Hz inputs in comparison to the effect seen for 10 Hz inputs. Therefore, it appears that the capacitance of the MIL-L-7808 oils is affected to a much lesser degree by oxidative degradation than the resistance of the oil.

### (4) Relationship between $V/V_I$ and COBRA Readings

Since the COBRA instrument is thought to measure conductivity, the inverse of the resistance measurements obtained by the 10 Hz input for the stressed MIL-L-7808 oil samples should be proportional to the oils' respective COBRA readings. The plot of  $V/V_I$  (inverse of  $V_I/V$ ) for a 10 Hz input versus the COBRA

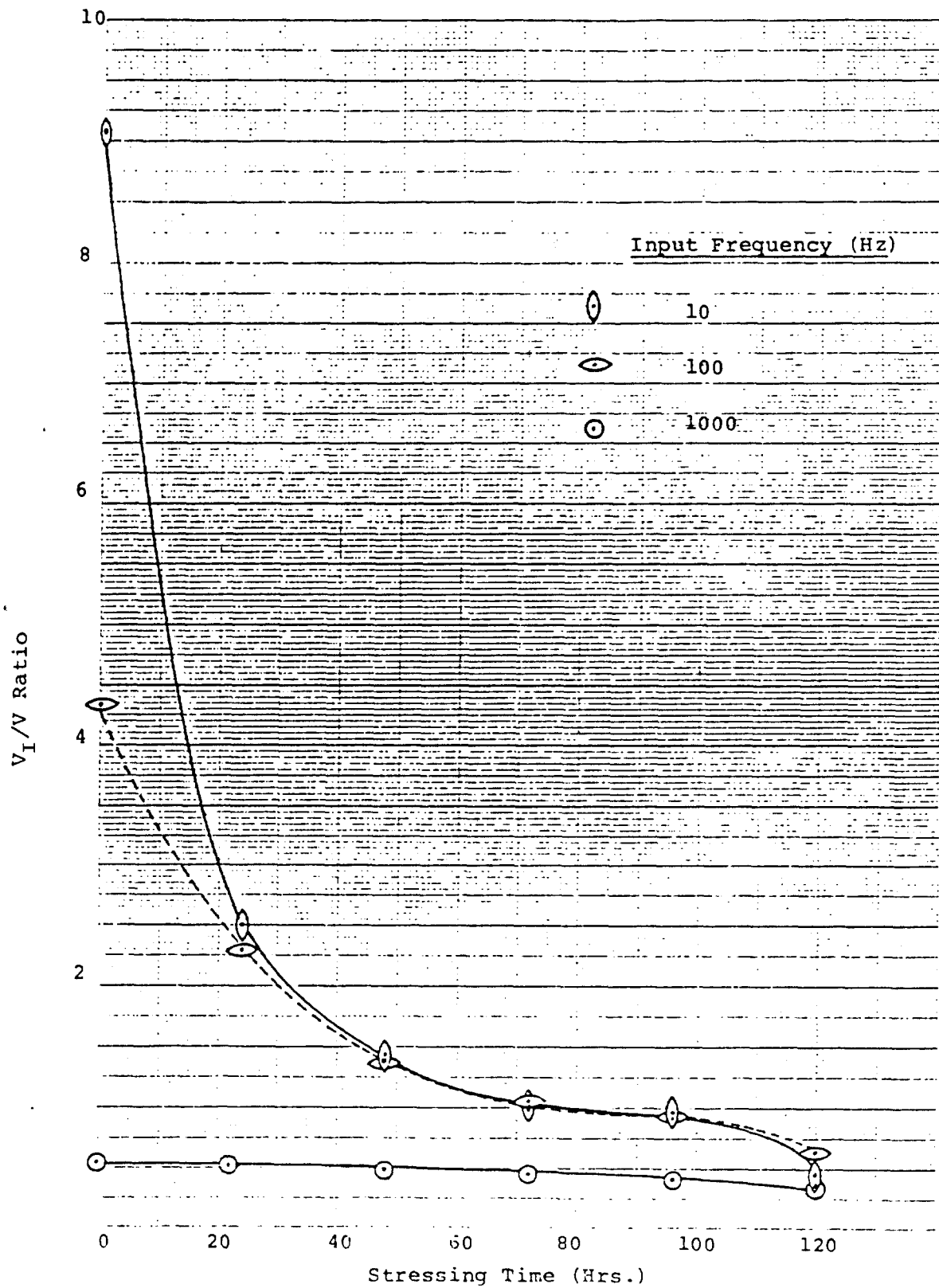


Figure 54. Plots of the  $V_I/V$  Ratio for 10, 100 and 1000 Hz Inputs Versus Stressing Time for Fresh and Stressed (24 to 120 Hours) TEL-4005 Oils.

reading for the fresh and stressed TEL-4005 oil samples is shown in Figure 55.

The plot of  $V/V_I$  at 10 Hz versus the COBRA readings shows that there is a very strong correlation (straight line with a slope of 1.1) between the  $V/V_I$  and the COBRA measurements when resistance is the main component of the  $V/V_I$  ratio. Therefore, it appears that the COBRA instrument measures the conductivity of used MIL-L-7808 oil samples.

#### (5) Effect of Formulation

To determine the effect of formulation on the resistance and capacitance of fresh MIL-L-7808 lubricating oils, the  $V_I/V$  ratios of fresh TEL-4001, TEL-4004, TEL-4005 and TEL-4006 MIL-L-7808 oils were determined at 10 and 1000 Hz. The results are presented in Table 3.

The results presented in Table 3 show that the  $V_I/V$  ratio produced by a 10 Hz input is more affected by formulation than the  $V_I/V$  ratio produced by the 1000 Hz input. Thus, formulation affects the resistance component of the  $V_I/V$  ratio to a greater extent than the capacitance component.

#### (6) Summary of Electrical Property Measurements

The initial investigation indicated that the electrical property measurements have limited potential for development into RLLAT. The measurements based on resistance (or conductance by the COBRA) are sensitive to changes in the oxidative degradation of oil samples but are also formula dependent. In contrast, the measurements based on capacitance are not formula dependent but are also not sensitive to changes in the oxidative degradation of the oil samples.

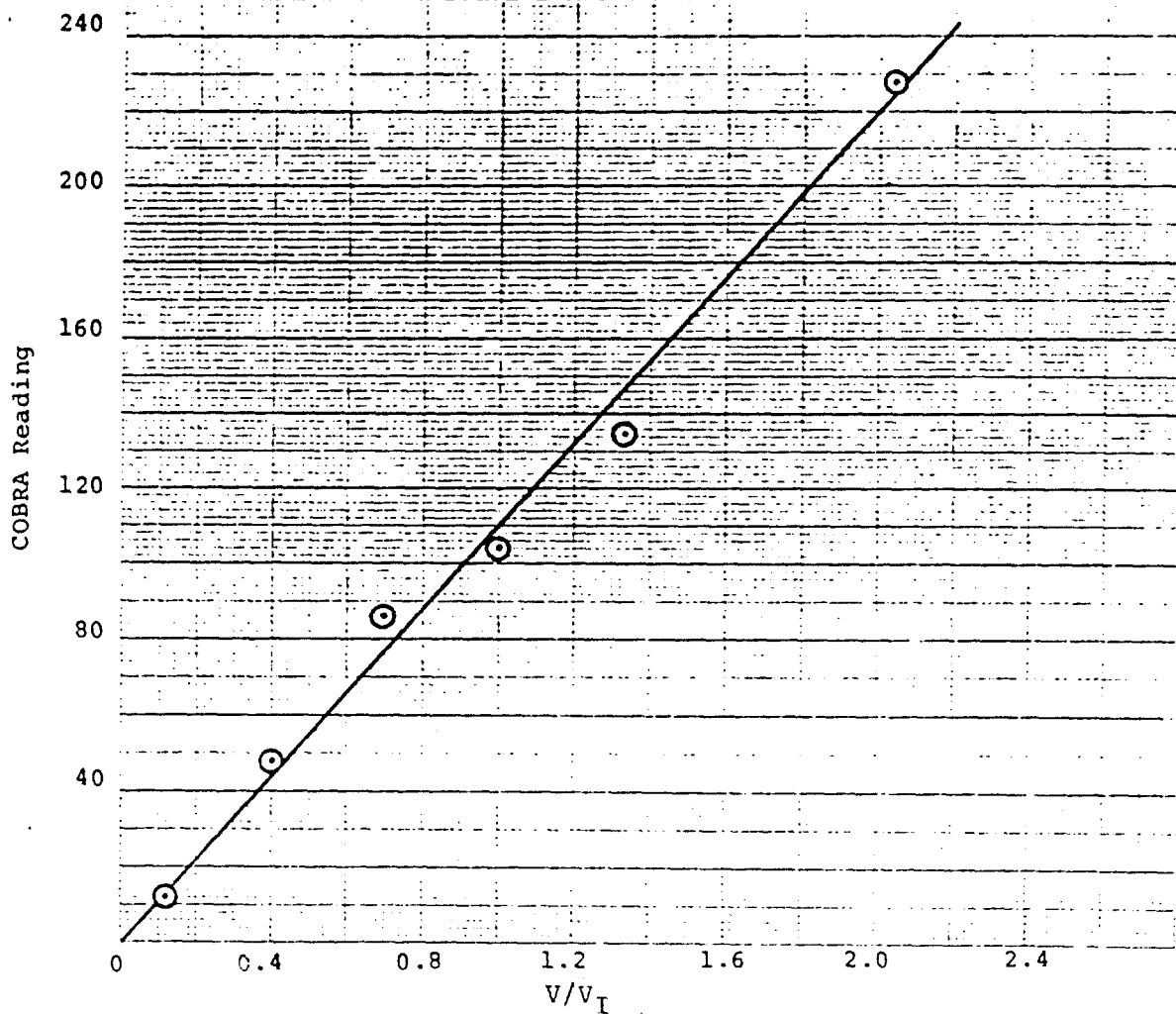


Figure 55. Plot of the COBRA Reading versus the Reciprocal of the  $V_I/V$  Ratio for the Fresh and Stressed (0-120 Hours) TEL-4005 Oils Using an Input of 10 Hz.

TABLE 3  
EFFECT OF FORMULATION ON  $V_I/V$  PRODUCED BY 10 AND 1000 Hz INPUTS

MIL-L-7808 OIL

	$V_I/V$	
	10 Hz	1000 Hz
TEL-4001	8.32	.529
TEL-4004	10.85	.528
TEL-4005	9.08	.529
TEL-4006	7.39	.569

Consequently, the electrical property measurements are better suited for degree of oxidative degradation estimations than for RLL assessments.

#### h. Fluorescence Spectrophotometry

##### (1) Introduction

The technique of fluorescence spectrophotometry has been used extensively for determining the oxidative degradation of mineral oils and hydrocarbon lubricating oils (References 37-41). Therefore, an investigation was conducted to determine if fluorescence measurements could be used to assess the RLL of used MIL-L-7808 lubricating oils. The effect of formulation on the fluorescence of fresh MIL-L-7808 oils was also studied.

##### (2) Effect of Formulation

To determine the effect of formulation on the fluorescence of fresh MIL-L-7808 lubricating oils, the TEL-4003, TEL-4005, and TEL-4006 oils were tested. The plots of the intensity of fluorescence versus emission wavelength for the fresh TEL-4003, TEL-4005, and TEL-4006 oils are shown in Figure 56.

The plots in Figure 56 indicate that formulation has a very strong effect on the fluorescence of MIL-L-7808 oils. The intensity of the fluorescence produced by the TEL-4006 oil is only 30% of that produced by the TEL-4003 oil. Whether the

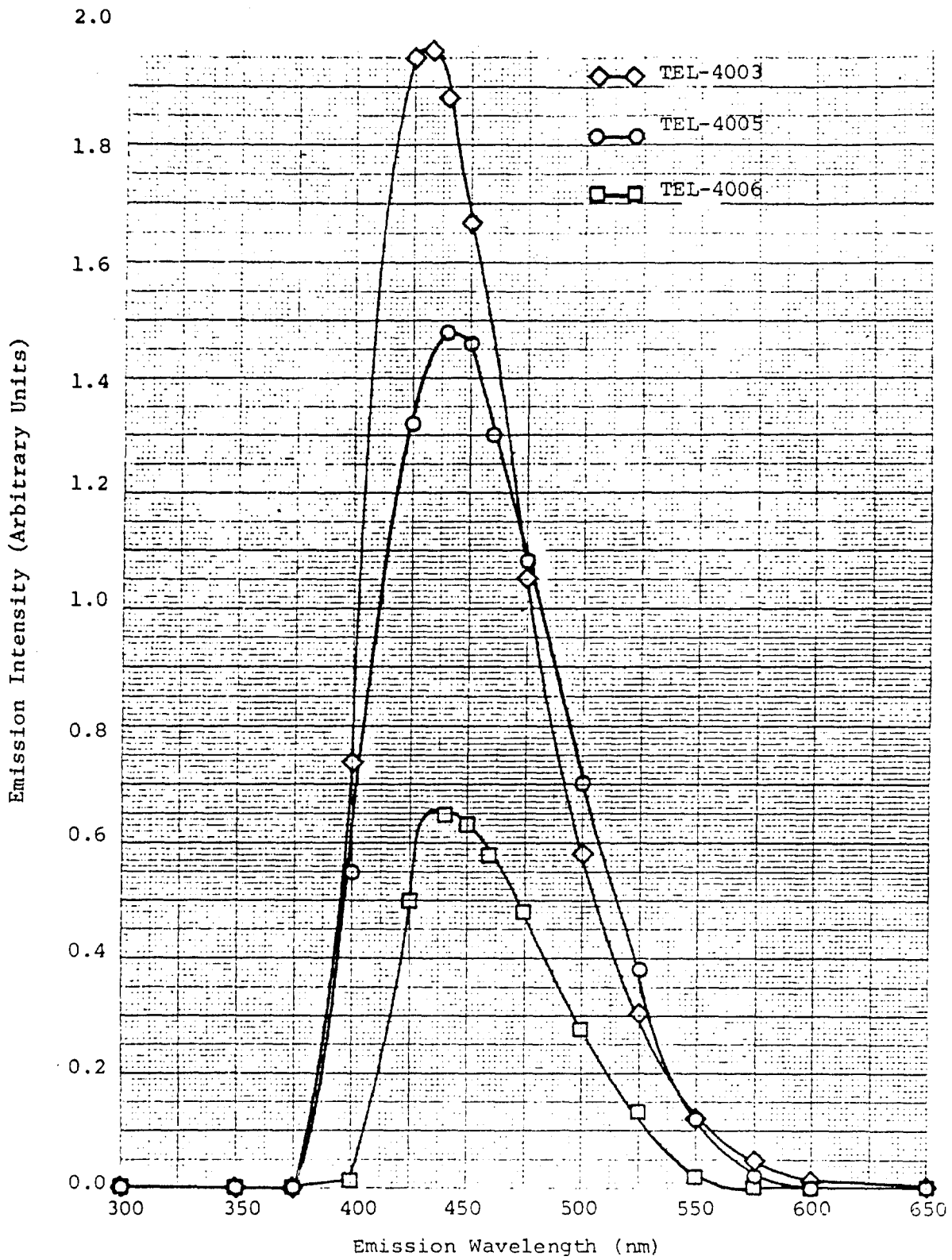


Figure 56. Effect of Formulation on the Fluorescence of Fresh MIL-L-7808 Lubricating Oils.

differences in the MIL-L-7808 oils' fluorescence intensities are due to antioxidant, ester basestock, or other formulation differences was not determined.

### (3) Effect of Oxidative Degradation

To determine the effect of oxidative degradation on the fluorescence of MIL-L-7808 oils, fresh and slightly degraded (stressed 24 hours) TEL-4005 oils were tested. The plots of the intensity of fluorescence versus emission wavelength for the fresh and slightly degraded (LS-24) oils are shown in Figure 57.

The plots in Figure 57 show that the fluorescence is extremely sensitive to oxidative degradation. The fluorescence of LS-24 is approximately  $3 \times 10^{-3}$  as intense as the fresh lubricant. The oil samples degraded longer than 24 hours did not produce detectable levels of fluorescence on the MK-1 spectrophotometer. Therefore, their fluorescences were less than  $10^{-5}$  as intense as the fresh oil. Whether the darkening of the oil sample or the loss of fluorescing species through oxidative degradation of the oil was responsible for the reduced fluorescence was not determined.

### (4) Summary of Fluorescence Spectrophotometry

The initial investigation indicated that fluorescence spectrophotometry has very limited potential for development into a RLLAT. Fluorescence spectrophotometry is very formula dependent and is extremely sensitive to small changes in the oxidative degradation of the oil samples.

Consequently, fluorescence spectrophotometry is not suited for RLL assessments or degree of oxidative degradation estimations.

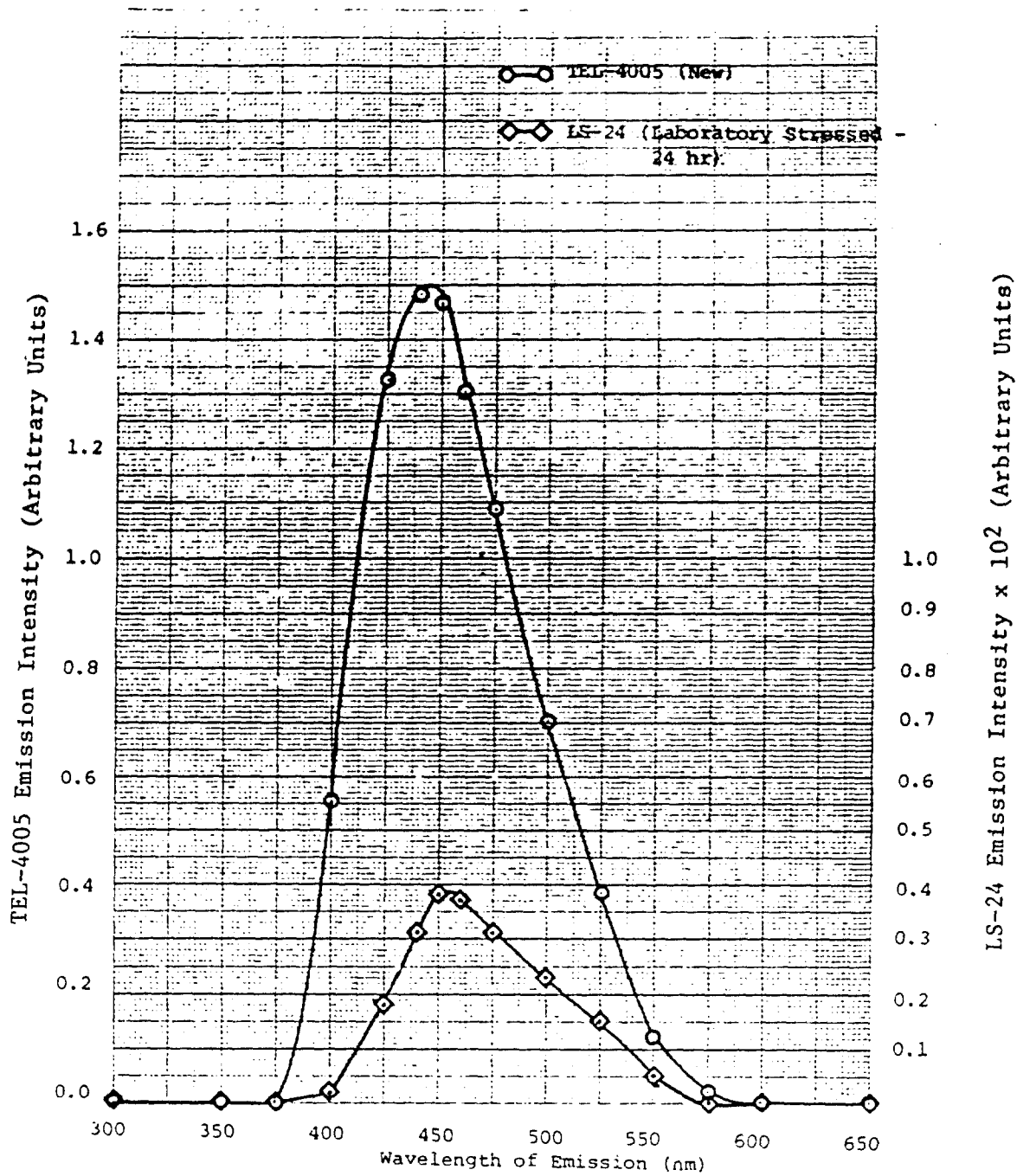


Figure 57. Effect of Oxidation Degradation on the Fluorescence of MIL-L-7808 Lubricating Oils.

### i. Comparison of Identified Analytical Procedures

During Task 1, various analytical procedures were identified and initially evaluated for development into a RLLAT candidate. As previously listed in Table 2, the analytical techniques with potential for development into RLLAT candidates were categorized into three main groups: voltammetric, thermal stressing, and chemical stressing. The analytical techniques which have been investigated but do not have potential for development into RLLAT candidates or those which have been identified, but not investigated, were also included in Table 2. The characteristics used to evaluate the potentials of the analytical techniques for development into RLLAT are listed in Table 4.

Of the techniques listed in Table 2, the voltammetric techniques were ranked first for development into a RLLAT due to their ease of operation and very short analysis times. Although the relationship between the data produced by the voltammetric technique and the RLL of MIL-L-7808 oils had not been fully established, the preliminary results presented in Figure 30 indicated that there was a strong correlation between the two values.

Thermal stressing techniques were ranked in front of the chemical stressing techniques, because thermal techniques do not require the toxic chemicals used by the chemical stressing techniques and because the thermal techniques are much easier to operate. The only advantage of the chemical stressing techniques over the thermal stressing techniques was instrumental cost (Table 4). For this reason, the low cost high pressure-differential thermal analysis (HP-DTA) technique was included in Table 4.

TABLE 4  
COMPARISON OF CANDIDATES' POTENTIALS FOR DEVELOPMENT INTO LUBRICANT LIFE ASSESSMENT TESTS

Type of Technique	Advantages	Disadvantages
Voltammetric	<ul style="list-style-type: none"> <li>- Analysis time: 2 to 10 seconds.</li> <li>- Easy to operate.</li> <li>- Low cost - less than \$2,000.</li> <li>- Relationship between RLL and results of technique indicated for MIL-L-7808 oils.</li> <li>- Obtain supplemental information to aid in RLL assessments.</li> </ul>	<ul style="list-style-type: none"> <li>- Requires sample dilution.</li> </ul>
Thermal Stressing	<ul style="list-style-type: none"> <li>- No sample preparation.</li> <li>- Relationship between RLL and results of technique established for MIL-L-7808 oils by other researchers.</li> <li>- HP-DTA: Lower cost-less than \$3,000.</li> </ul>	<ul style="list-style-type: none"> <li>- Analysis time - 1 to 20 minutes.</li> <li>- HP-DSC: Higher cost-greater than \$20,000.</li> </ul>
Chemical Stressing	<ul style="list-style-type: none"> <li>- Low cost-less than \$3,000.</li> <li>- Relationship between RLL and results of technique established for various lubricants by other researchers.</li> </ul>	<ul style="list-style-type: none"> <li>- Requires extensive sample preparation</li> <li>- Requires use of unstable, toxic chemicals.</li> <li>- Hard to operate.</li> <li>- Analysis time - 1 to 20 minutes.</li> <li>- Degree of oil degradation affects results.</li> </ul>
Other Methods	<ul style="list-style-type: none"> <li>- Low cost-less than \$3,000.</li> </ul>	<ul style="list-style-type: none"> <li>- Unable to assess RLL.</li> </ul>
Feasible Methods	<ul style="list-style-type: none"> <li>- Used by other researchers in long and short term oxidation tests.</li> </ul>	<ul style="list-style-type: none"> <li>- Offer no apparent advantage over thermal stressing techniques.</li> </ul>

## 2. TASK 2. DEVELOPMENT OF REMAINING LUBRICANT LIFE ASSESSMENT TEST CANDIDATES

### a. Introduction

During Task 1 of this investigation, the analytical procedures based on voltammetric, thermal stressing, and chemical stressing techniques were identified as having potential for development into RLLAT. In Task 2 of this investigation, sets of fresh and thermally-oxidized MIL-L-7808 oil samples were used to develop RLLAT candidates from the identified analytical procedures.

The development of the RLLAT candidates was performed in two steps. In the first step, the experimental parameters of the analytical procedures were optimized using the fresh TEL-4001 through TEL-4006, TEL-5001, and TEL-5002 MIL-L-7808 lubricating oils. When optimized, the experimental parameters enabled the analytical procedures to analyze fresh MIL-L-7808 oil, regardless of formulation, in less than 10 minutes and to differentiate between stressed MIL-L-7808 oil samples, regardless of the degree of oxidative degradation.

In the second step of the developmental research, laboratory stressed samples of the TEL-4001 through TEL-4006, TEL-5001, and TEL-5002 MIL-L-7808 lubricating oils were prepared using Federal Test Method Standard 791 Method 5307.1 at 370°F. The stressed MIL-L-7808 oil samples were characterized by measuring the samples' physical properties (viscosity, total acid number, COBRA, and Mg concentration) and antioxidant concentrations. The physical properties and antioxidant concentrations of the oil samples were then plotted versus stressing time to determine the end of each MIL-L-7808 oil's stable life as described in Appendix A. The stable life and antioxidant system determined in Appendix A for each MIL-L-7808 oil are listed in Table 5.

The sets of fresh and stressed TEL-4001 through TEL-4006 MIL-L-7808 oils were then analyzed by each optimized analytical procedure to establish the mathematical relationships between the results of each procedure and the RLL of MIL-L-7808 oils. The

TABLE 5  
 STABLE LIVES (370°F) AND ANTIOXIDANT  
 CONCENTRATIONS OF MIL-L-7808 OILS

<u>MIL-L-7808 Oil</u>	<u>Stable Life at 370°F<sup>a</sup></u> (Hours)	<u>Antioxidant Concentrations<sup>b</sup></u> (% Weight)
TEL-4001	105	Octyl-PANA (0.7%) DODPA (0.7%) UNK
TEL-4002	175	PANA (0.9%) DODPA (1.1%)
TEL-4003	240	PANA (1.0%) DODPA (1.7%)
TEL-4004	205	PANA (1.2%) DODPA (1.2%)
TEL-4005	155	PANA (0.4%) DODPA (1.6%)
TEL-4006	320	Octyl-PANA (1.4%) DODPA (0.3%) UNK
TEL-5001	240	PTZ (0.3%) DODPA (1.3%)
TEL-5002	110	Octyl-PANA (1.3%) DODPA (1.3%)

<sup>a</sup> Stable life determined from breakpoints of viscosity (40°C) and total acid number plots (Appendix A)

<sup>b</sup> PANA = N-Phenyl- $\alpha$ -naphthylamine  
 DODPA = Dioctyldiphenyl amine  
 Octyl-PANA = N-(p-Octylphenyl)- $\alpha$ -naphthylamine  
 PTZ = Phenothiazine  
 UNK = Unknown nitrogen or phosphorous containing compound  
 percent weight could not be determined.

potential of each candidate for development into a RLLAT was then evaluated based on the criteria listed in Table 1 and its RLL assessing capabilities.

The studies used to develop and evaluate the different RLLAT candidates are described herein. The candidates are discussed in the order of their potentials for development into a RLLAT: voltammetric >thermal stressing >chemical stressing.

b. Voltammetric Techniques

(1) Introduction

As the results of Task 1 indicated, the voltammetric techniques, in particular, the reductive-cyclic voltammetric technique, are well-suited for development into a RLLAT candidate. In contrast to the chemical and thermal stressing techniques, the voltammetric techniques require less than 1 minute to perform so that optimization studies of the voltammetric experimental parameters were not required. However, the effects of successive scans and pyridine on the voltammetric analyses of MIL-L-7808 oils were not understood. Also, the mathematical relationships between the results of the voltammetric techniques and the RLL of the MIL-L-7808 oils had not been established.

Therefore, a series of studies were performed to develop the different voltammetric techniques into RLLAT candidates. Cyclic voltammetric analyses of the fresh and stressed (370°F) MIL-L-7808 oils were performed in order to further characterize the stressed oils and to evaluate the cyclic voltammetric techniques' capabilities to assess RLL. The effects of the dilution solvent amount, electrode configuration, and different organic bases on the cyclic voltammetric analyses of the different MIL-L-7808 lubricating oils were studied. The effects of antioxidant type, scan direction, and number of scans on the reductive-cyclic voltammetric analyses in the presence of organic bases were also studied. In addition to these studies, the initial attempts to linearize the plots of the reductive-cyclic voltammetric result versus stressing time at 370°F and to develop

a data acquisition system for the reductive-cyclic voltammetric technique were performed.

(2) Cyclic Voltammetric Analyses of the MIL-L-7808 Oils

Cyclic voltammetric (CV) analyses were used to determine the degree of degradation of each MIL-L-7808 lubricating oil sample stressed at 370°F. The CV analyses of the stressed TEL-4001 through TEL-4006 MIL-L-7808 oil samples were accomplished by producing single scan voltammograms for each set of degraded MIL-L-7808 lubricating oils as shown in Figures 58-63.

The single scan voltammograms of the MIL-L-7808 oils show similar changes with increasing stressing time. For every MIL-L-7808 oil, the oxidation waves assigned to the original antioxidants (A in Figures 58-63) decrease with stressing time. However, as the oxidation wave (A) in Figure 63 of the TEL-4006 oil decreases, it splits into two oxidation waves, (A1) and (A2). The oxidation wave at the lower potential (A1) corresponds to the oxidation waves (A in Figures 58-62) produced by the other MIL-L-7808 lubricating oils. The higher potential oxidation wave (A2) decreases at a slower rate than the (A1) oxidation wave (Figure 63).

The single scan voltammograms of stressed MIL-L-7808 oils also exhibit an oxidation wave (B in Figures 58-63) which is at a lower potential than the oxidation wave assigned to the original antioxidants (A in Figures 58-63). Oxidation wave (B) is not present in the voltammograms of the fresh MIL-L-7808 lubricating oils (Figures 58-63). Oxidation wave (B) rapidly increases in size during the first 16-24 hours of stressing, as oxidation wave (A) (original antioxidants) rapidly decreases in size. After 24 hours of stressing, oxidation wave (B) decreases with stressing time. Therefore, the oxidation wave (B) is assigned to antioxidant species generated by the oxidation of the original antioxidants.

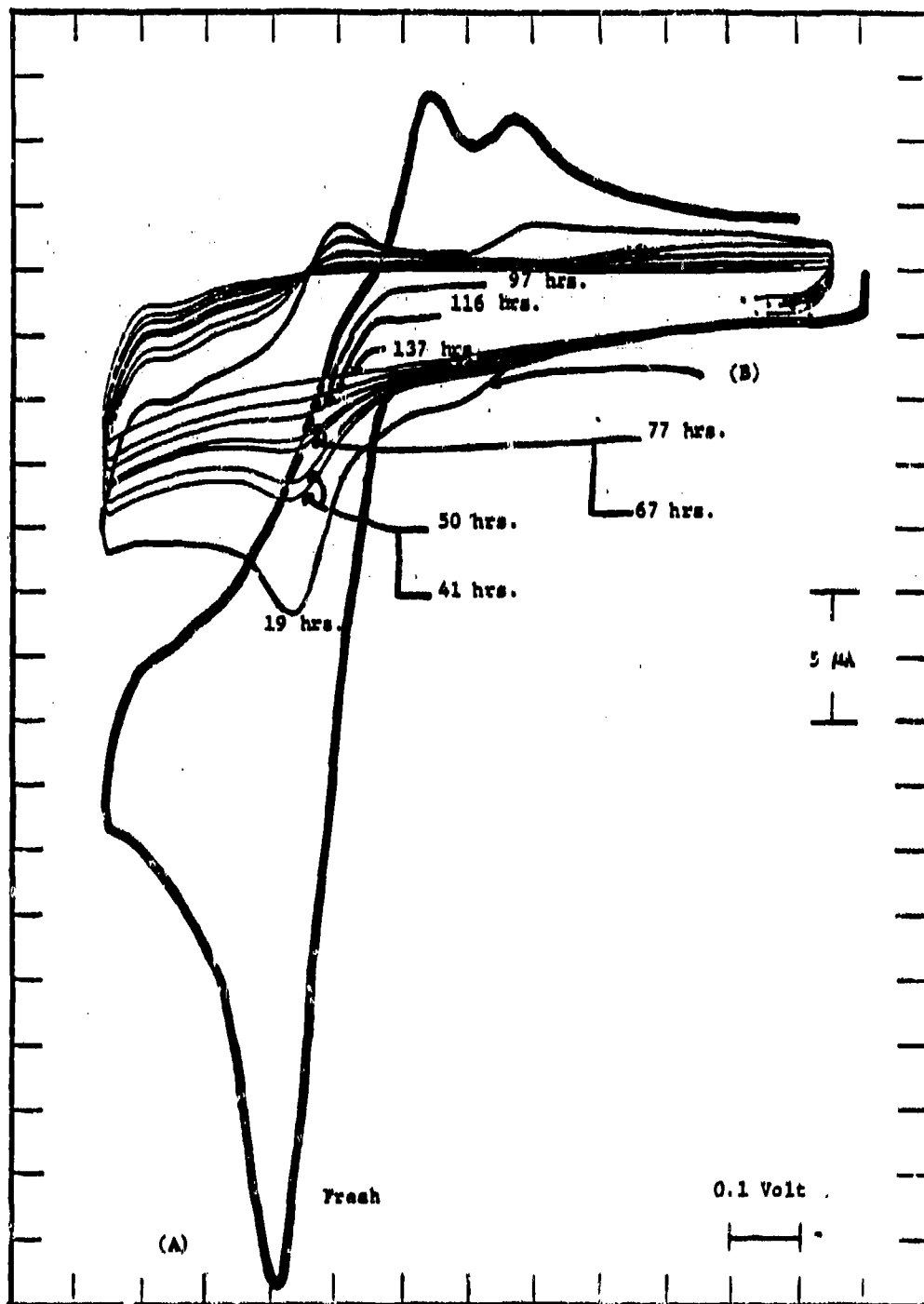


Figure 58. Single Scan Voltammograms of Fresh and Stressed (19-137 Hours at 370°F) TEL-4001 MIL-L-7808 Oils in Acetone Using a Glassy Carbon Working Electrode.

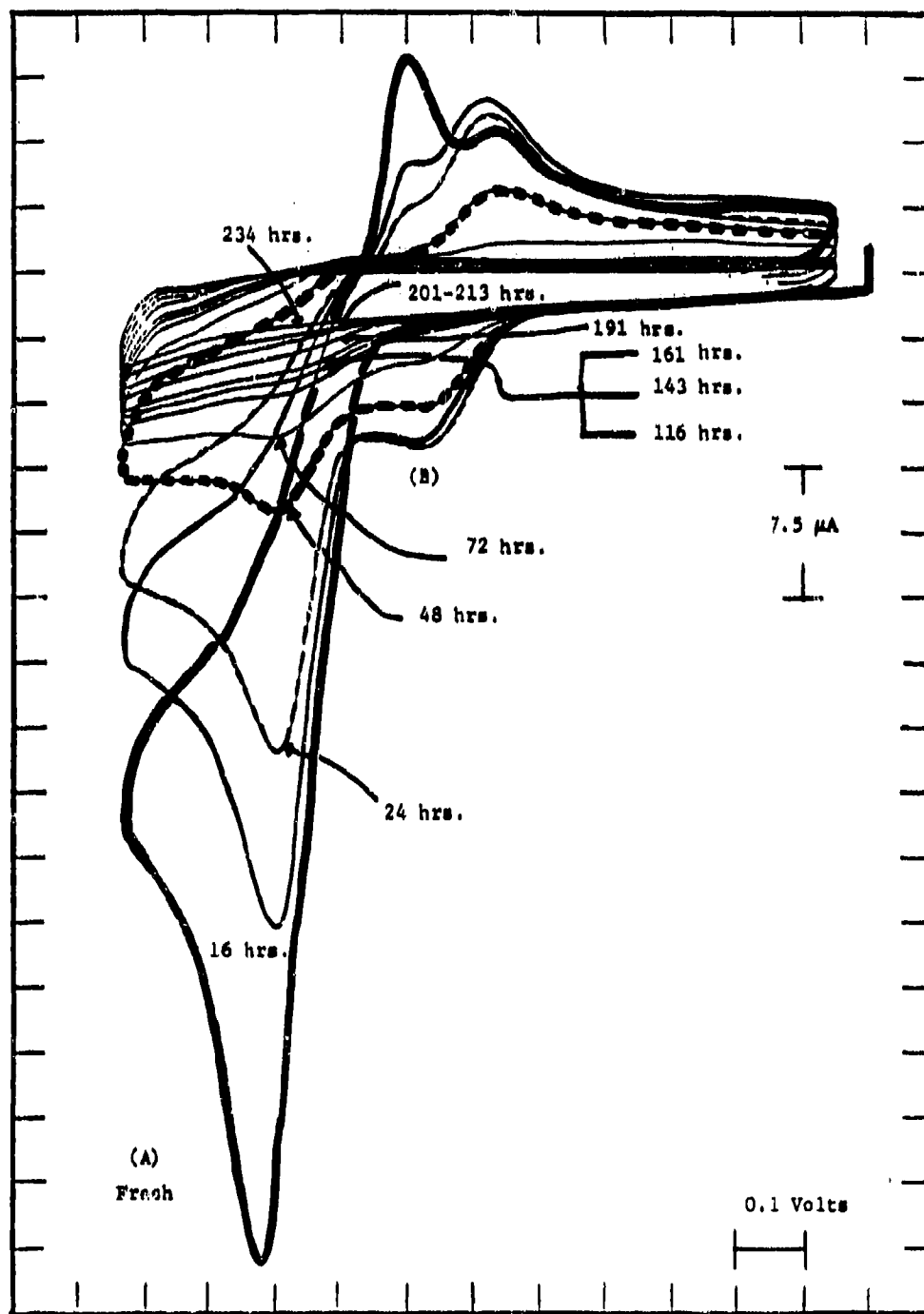


Figure 59. Single Scan Voltammograms of Fresh and Stressed (16-234 Hours at 370°F) TEL-4002 MIL-L-7808 Oils in Acetone Using a Glassy Carbon Working Electrode.

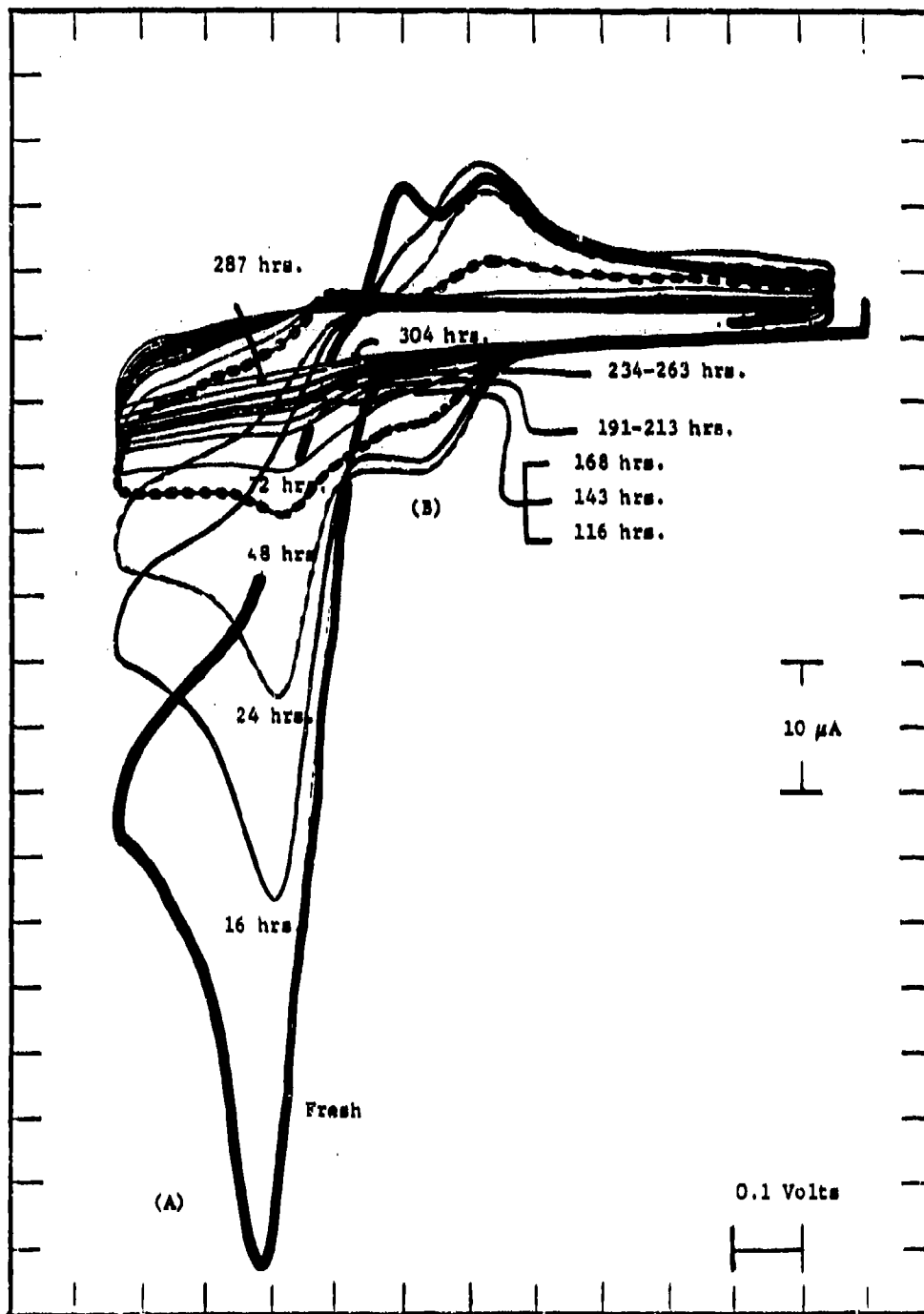


Figure 60. Single Scan Voltammograms of Fresh and Stressed (16-304 Hours at 370°F) TEL-4003 MIL-L-7808 Oils in Acetone Using a Glassy Carbon Working Electrode.

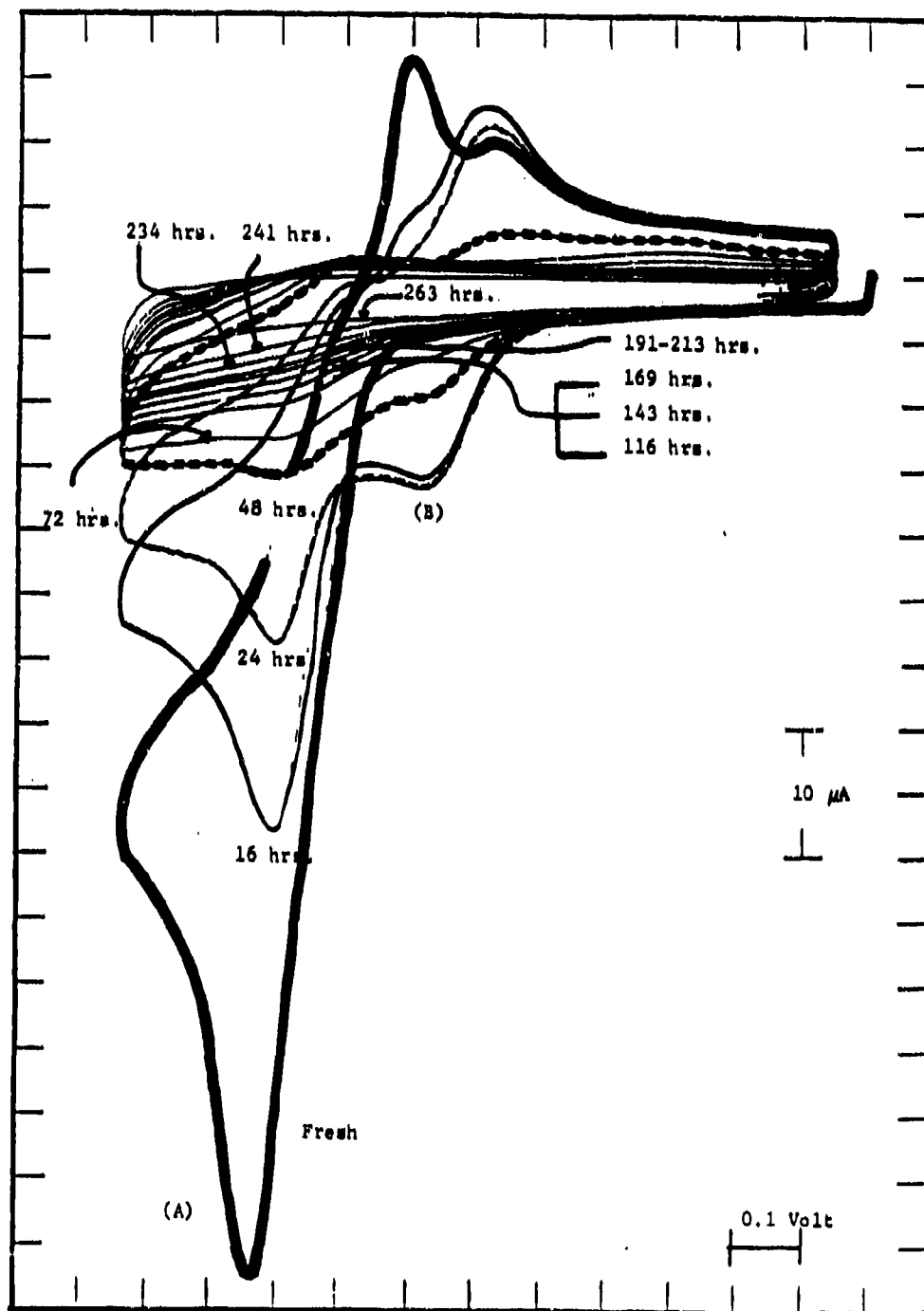


Figure 61. Single Scan Voltammograms of Fresh and Stressed (16-263 Hours at 370°F) TEL-4004 MIL-L-7808 Oils in Acetone Using a Glassy Carbon Working Electrode.

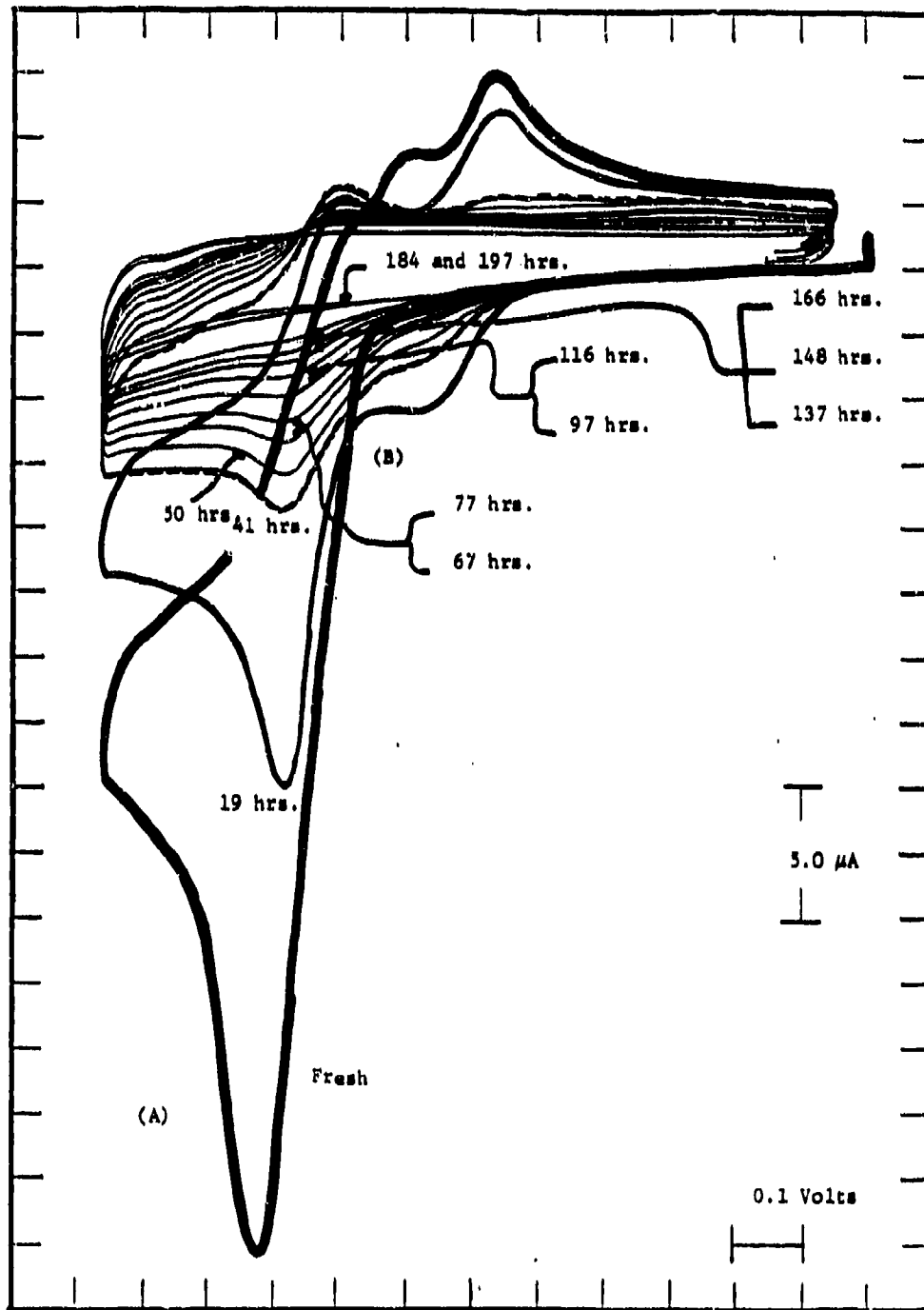


Figure 62. Single Scan Voltammograms of Fresh and Stressed (19-194 Hours at 370°F) TEL-4005 MIL-L-7808 Oils in Acetone Using a Glassy Carbon Working Electrode.

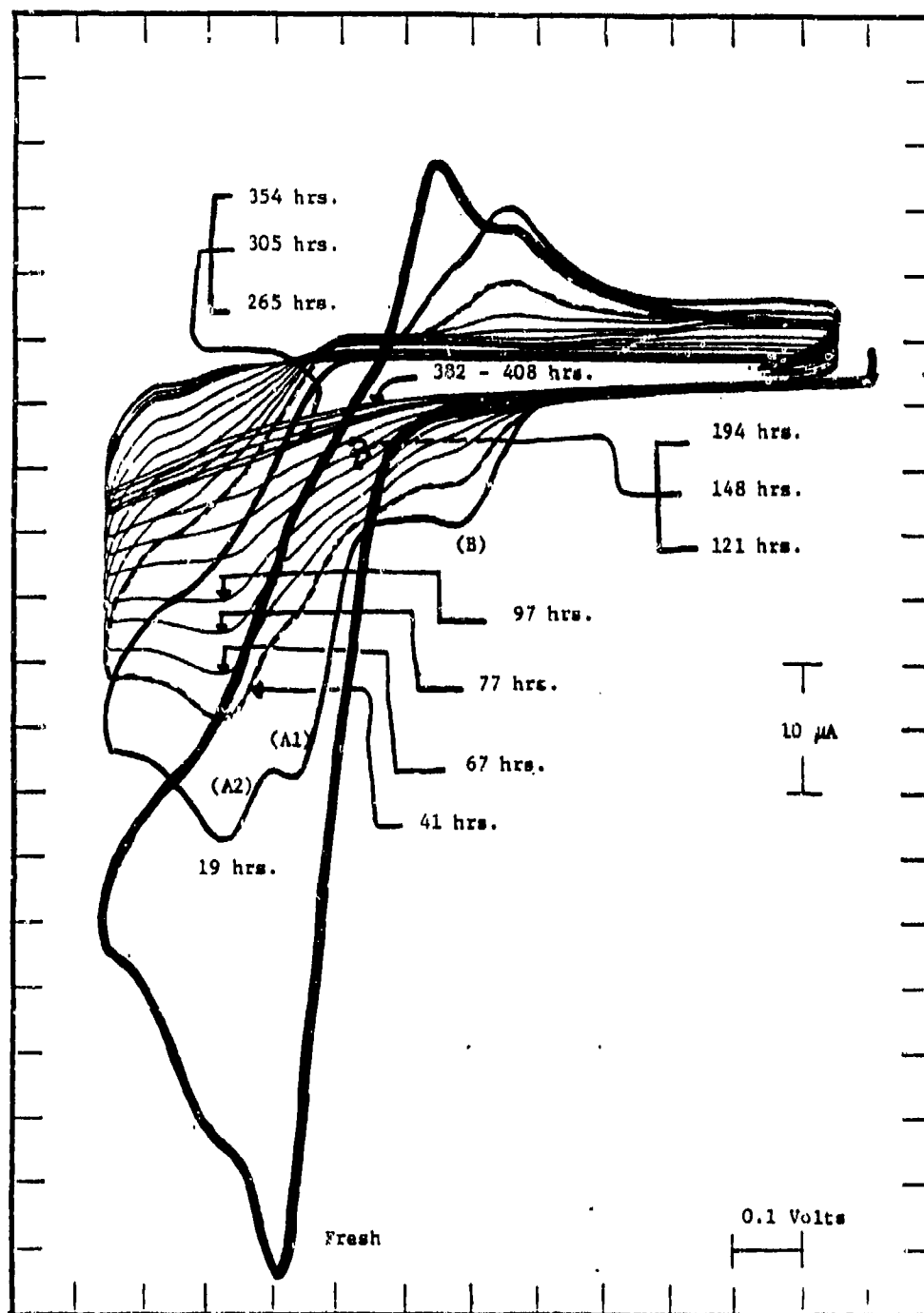


Figure 63. Single Scan Voltammograms of Fresh and Stressed (19-408 Hours at 370°F) TEL-4006 MIL-L-7808 Oils in Acetone Using a Glassy Carbon Working Electrode.

To further test the RLL assessing capabilities of the single scan CV analyses, two additional MIL-L-7808 oils, TEL-5001 and TEL-5002, were analyzed. The single and fifth scan voltammograms of the fresh TEL-5001 and TEL-5002 oils are shown in Figures 64 and 65.

As seen in Figure 64, the single and fifth scan voltammograms of the fresh TEL-5001 oil are very different from those produced by the fresh TEL-4001 through TEL-4006 oils (Figures 58-63) and the fresh TEL-5002 oil (Figure 65). First, an oxidation wave (B) (Figure 64) is produced by the first scan of the fresh TEL-5001 oil which is not produced by the first scans of the fresh TEL-4001 through TEL-4006 oils (Figures 58-63) and fresh TEL-5002 oil (Figure 65). Second, repetitive scanning as represented by the fifth scan voltammogram in Figure 64 does not produce any new species or increase the size of the oxidation wave (B) for the fresh TEL-5001 oil. Repetitive scanning increased the size of the oxidation wave (B) for the fresh TEL-5002 oil (Figure 65) and the fresh TEL-4001 through TEL-4006 oils (Figures 14-16).

Although, the results of Task 1 indicated that the height of oxidation wave (B) (Figure 58-63) could be mathematically related to the RLL of MIL-L-7808 oils (Figure 30), the fresh TEL-5001 oil contains an oxidation wave (B in Figure 64) at the same potential as the stressed TEL-4001 through TEL-4006 (B in Figure 58-63) and TEL-5002 oils (B in Figure 65). The oxidation wave (B) (Figure 64) produced by the TEL-5001 oil is assigned to the sulfur component of the phenothiazine type antioxidant used in the oil (Table 5).

Therefore, the height of oxidation wave (B) is formula dependent and cannot be used for RLL assessments. Consequently, the remaining development studies of the voltammetric techniques concentrated on the voltammetric technique

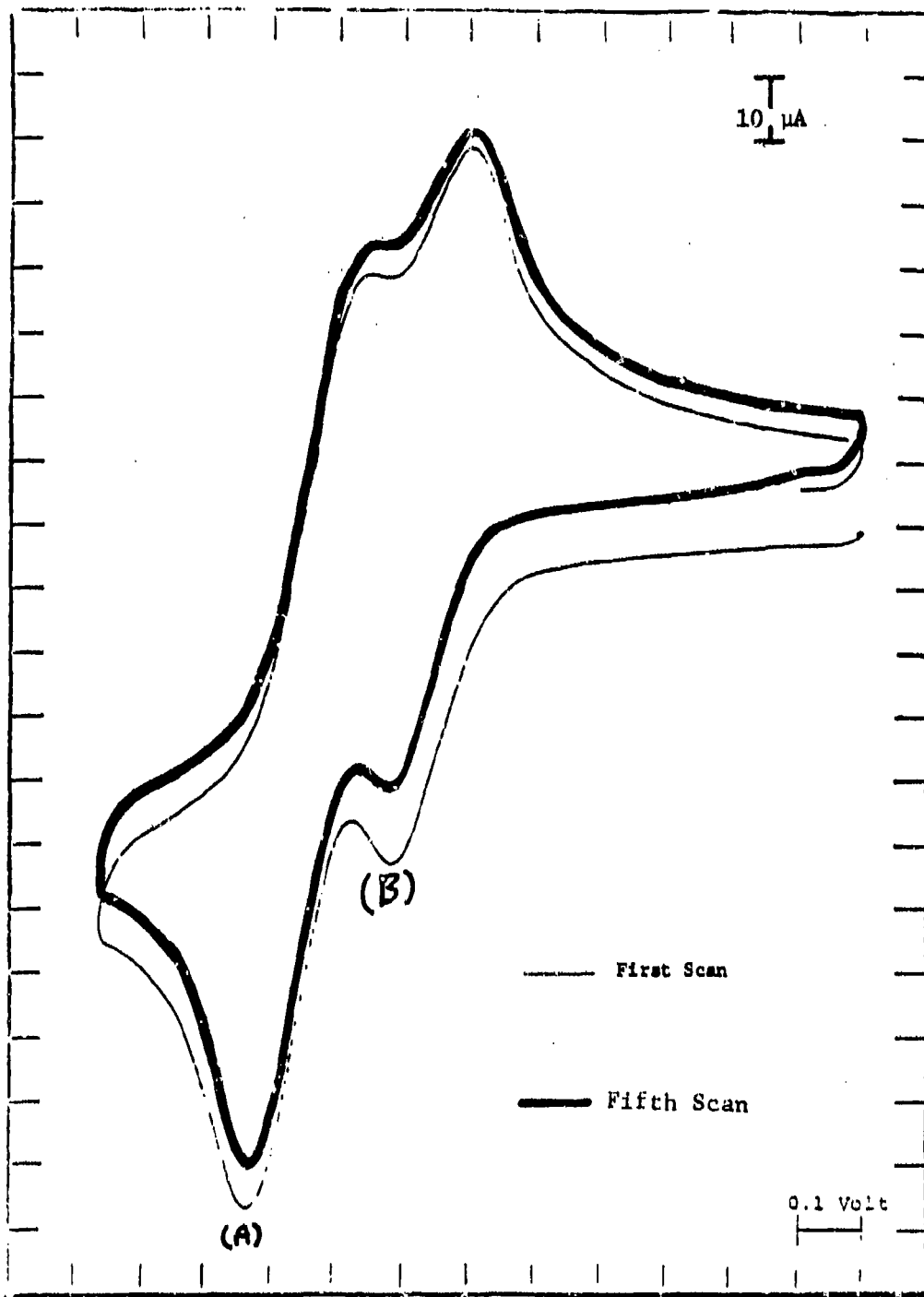


Figure 64. First and Fifth Scan Voltammograms of Fresh TEL-5001 MIL-L-7808 Oil in Acetone Using a Glassy Carbon Working Electrode.

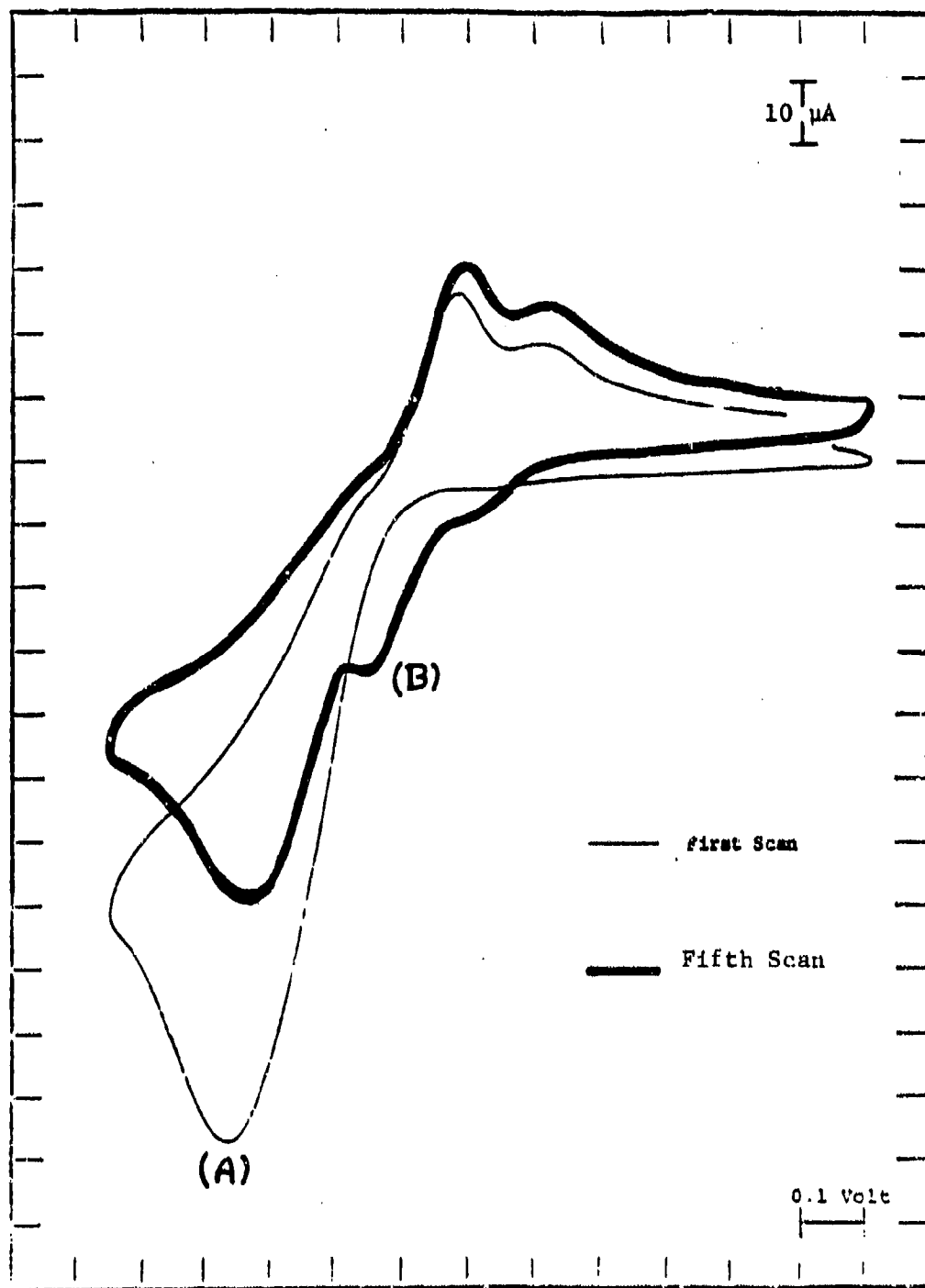


Figure 65. First and Fifth Scan Voltammograms of Fresh TEL-5002 MIL-L-7808 Oil in Acetone Using a Glassy Carbon Working Electrode.

in the presence of pyridine, the reductive-cyclic voltammetric technique (RCV).

### (3) Effect of Dilution Solvent Amount

The requirement of sample dilution prior to analysis limits the suitability of RCV for development into a RLLAT since it results in increased solvent storage and waste disposal problems. Therefore a study was conducted to determine the effect of the dilution solvent amount on the results of the RCV analyses. The ratio of sample to dilution solvent was 1:50 in all cases.

To test the effect of solvent amount, 100, 150, and 200  $\mu$ l samples of TEL-4004 MIL-L-7808 oil were diluted with 5, 7.5 and 10 ml of diluent, respectively, and then analyzed in a 20 ml scintillation vial. The voltammograms showed that reducing the solvent amount from 10 to 5 ml had no effect on the RCV analyses of the TEL-4004 oils. Diluent amounts of less than 5 ml could not be analyzed in the 20 ml scintillation vial.

### (4) Effect of Electrode Configuration

Since the diluent amount was limited to 5 ml by the 20 ml scintillation vial, the use of smaller vials was investigated. However, in order that the smaller vials could be tested, the electrodes had to be taken out of the electrode holder provided with the CV-1B Voltammetry Electronics Control Module. The working, reference, and auxiliary electrodes were bound together with two O-rings to perform the RCV analyses in the smaller vials. The electrodes were arranged so that the reference electrode rested on the bottom of the vial. The voltammograms for 100  $\mu$ l of the TEL-4004 oil in 5 ml of diluent were identical with and without the electrode holder indicating that the electrode configuration has no effect on the RCV analyses.

In order that the diluent amount could be lowered further, the 20 ml scintillation vial was replaced by a 7 ml scintillation vial. The diluent amount could be reduced to 2.5 ml (50  $\mu$ l oil sample) in the 7 ml scintillation vial. This further

reduction in diluent amount had no effect on the RCV analyses of the TEL-4004 oil.

#### (5) Effect of Antioxidant Type

In an attempt to obtain a better understanding of the RCV technique in the presence of organic bases, the effects of pyridine on the reductive voltammograms of PANA, octyl-PANA, and DODPA [antioxidants used in TEL-4001 through TEL-4006 oils (Table 5)] and on the mixtures of PANA with DODPA and octyl-PANA with DODPA were studied. The reductive voltammograms were produced in acetone containing 5% pyridine by applying 1.0 V to the working electrode, and immediately scanning at 500 mV/sec to 0.0 V. The oxidation wave (A in Figures 14-16) was eliminated to increase the size of the reduction wave (C in Figure 66).

The reductive voltammograms of the antioxidants and antioxidant mixtures in Figure 66 show that the reduction waves (C) produced by MIL-L-7808 oils are produced by the antioxidant mixtures, but not by the individual antioxidants.

The first and steady state (fifth-tenth scans) voltammograms of PANA, octyl-PANA, and their respective DODPA mixtures are shown in Figures 67 and 68. Although, PANA and octyl-PANA are electrochemically oxidized to produce new species (B in Figures 67 and 68) which have an oxidation potential similar to those found in stressed MIL-L-7808 oils (B in Figures 58-63), PANA and octyl-PANA do not produce the reduction wave (C in Figure 66) in the presence of pyridine in contrast to the MIL-L-7808 oils (Figures 26-28). However, when the PANA with DODPA and octyl-PANA with DODPA mixtures are electrochemically oxidized, they produced species similar to those produced by PANA and octyl-PANA, (B in Figures 67 and 68) but they also produced new species (D in Figures 67 and 68) which are not produced by PANA and octyl-PANA.

These results indicate that the RCV analyses in the presence of pyridine are insensitive to PANA, octyl-PANA, DODPA and their individual oxidation products. The RCV technique is solely dependent on the new antioxidant species generated in the

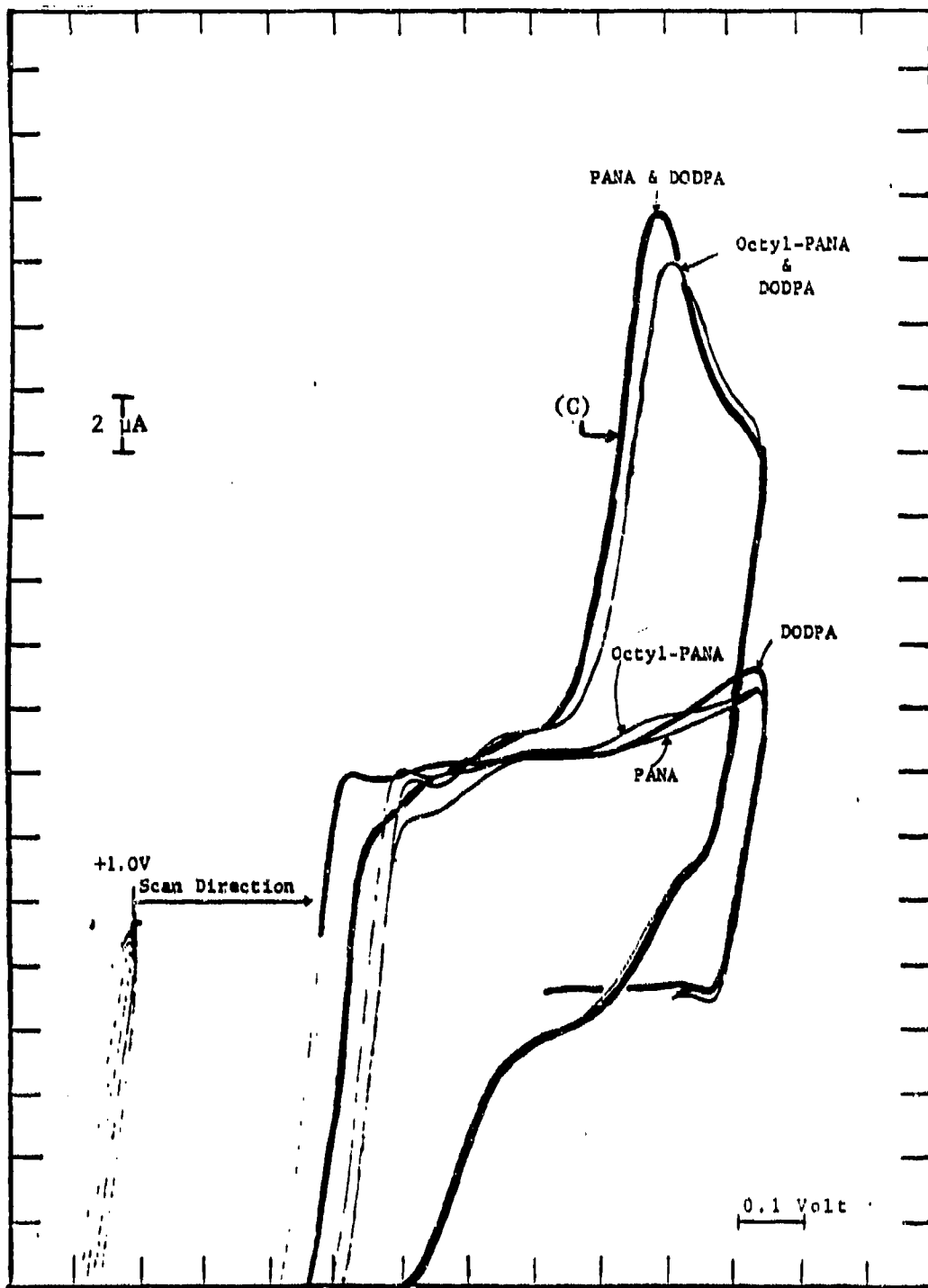


Figure 66. Reductive Voltammograms of Different Antioxidants and Antioxidant Combinations in Acetone Containing Pyridine Using a Glassy Carbon Working Electrode.

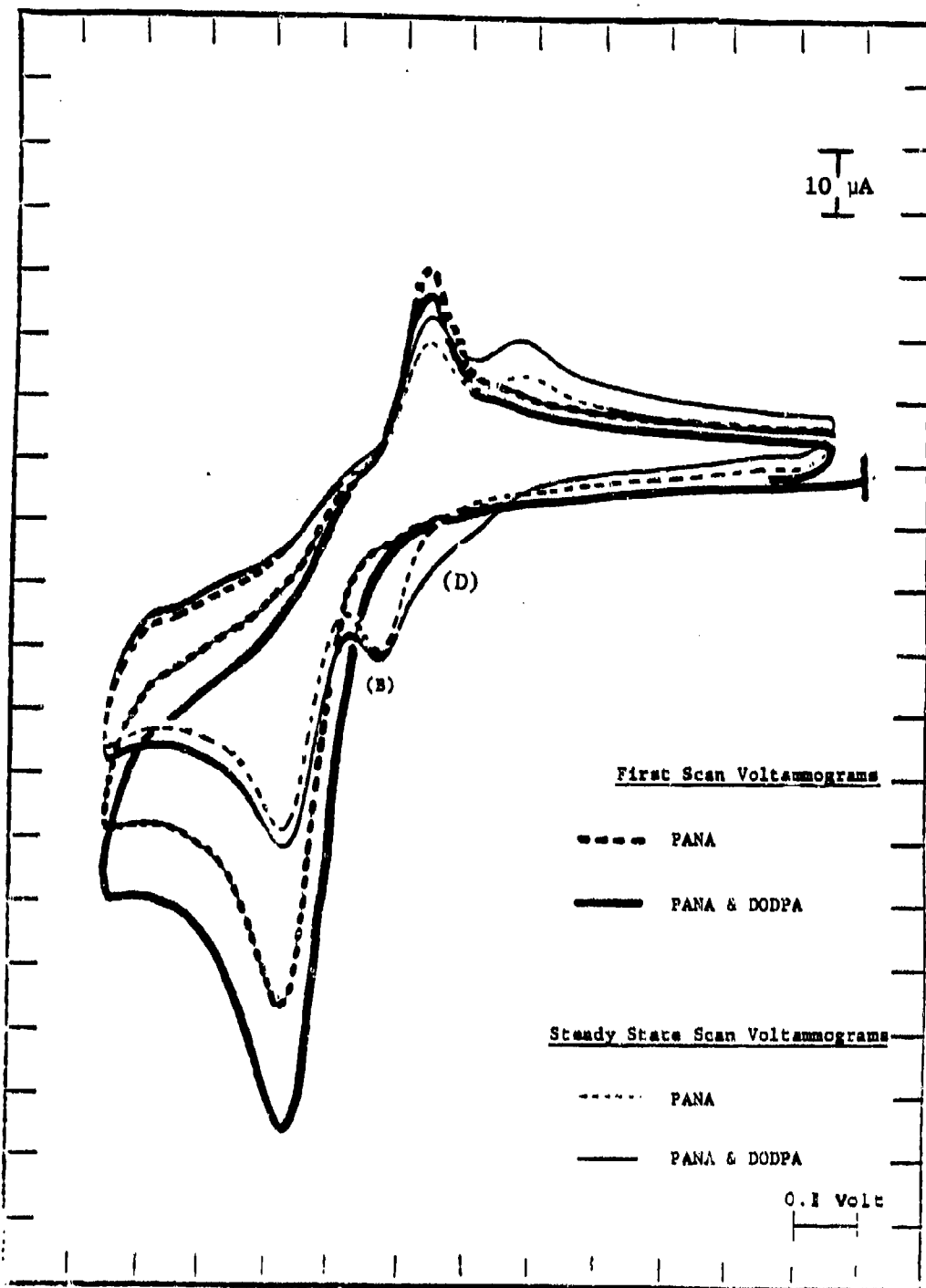


Figure 67. First and Steady State Scan Voltammograms of PANA and PANA with DODPA Antioxidant Systems in Acetone Using a Glassy Carbon Working Electrode.

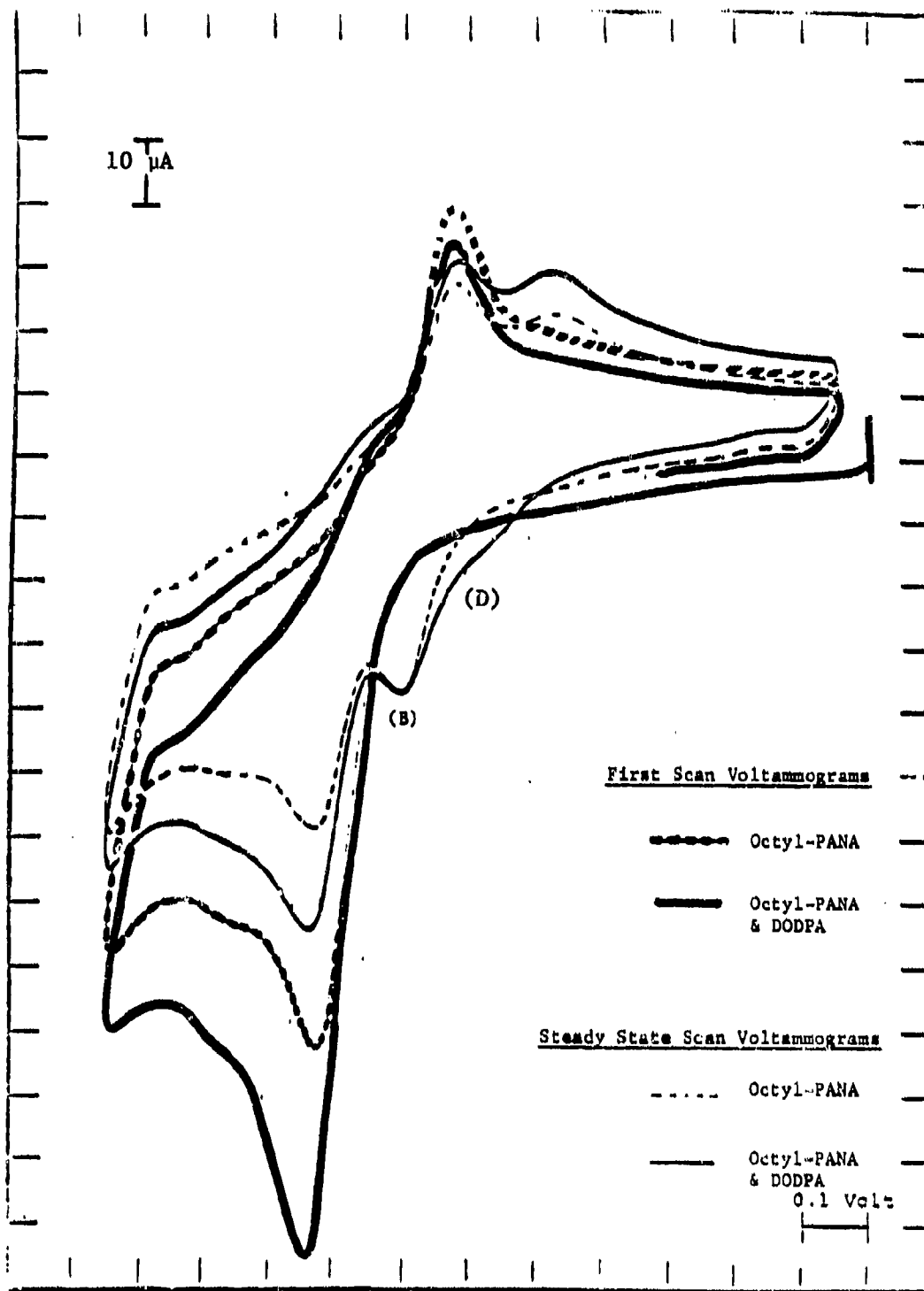


Figure 68. First and Steady State Scan Voltammograms of Octyl-PANA and Octyl-PANA with DODPA Antioxidant Systems in Acetone Using a Glassy Carbon Working Electrode.

presence of PANA or octyl-PANA with DODPA. These results are consistent with Figure 30 which showed that the concentration of the generated antioxidation species and the reduction wave (Figure 29) were related.

(6) Reductive-Cyclic Voltammetric Analyses of the MIL-L-7808 Oils

To evaluate the capabilities of the RCV technique to assess the RLL of stressed MIL-L-7808 lubricating oils, RCV analyses of the fresh and stressed TEL-4001 through TEL-4006 MIL-L-7808 oils were performed. The reductive voltammograms of the fresh and stressed TEL-4001 through TEL-4006 oils are shown in Figures 69-74. The reductive voltammograms were obtained in the same manner as Figure 66.

To evaluate the RCV technique's capability to assess RLL, the peak heights of the reduction waves (C) in Figures 69-74 were plotted versus stressing time for the TEL-4001 through TEL-4006 lubricating oils as shown in Figure 75. During the first 16 hours of stressing, the reduction waves (C in Figures 69-74) increased for the TEL-4002 and TEL-4004 oils, but decreased rapidly for the other MIL-L-7808 oils (Figure 75). During the next 24 to 75 hours, the reduction waves decreased rapidly for all of the MIL-L-7808 oils. The reduction waves then decreased at a slower, fairly constant rate until the ends of the oils' stable lives (Figure 75). The reduction waves of the TEL-4001 through TEL-4006 oils decreased at a similar rate in the latter stages of oxidation. The TEL-4001 through TEL-4006 oils decreased to a similar peak height (0.25-0.40  $\mu\text{A}$ ) at the end of each oil's stable life (stable life defined in Appendix A).

(7) Linearizing the Reductive-Cyclic Voltammetric Plots

As shown in Figure 75, the reduction wave (C) heights of the MIL-L-7808 oils decrease at a very fast rate in the early stages of oxidation. The rates at which the reduction wave heights decrease then become fairly constant up to the ends of the

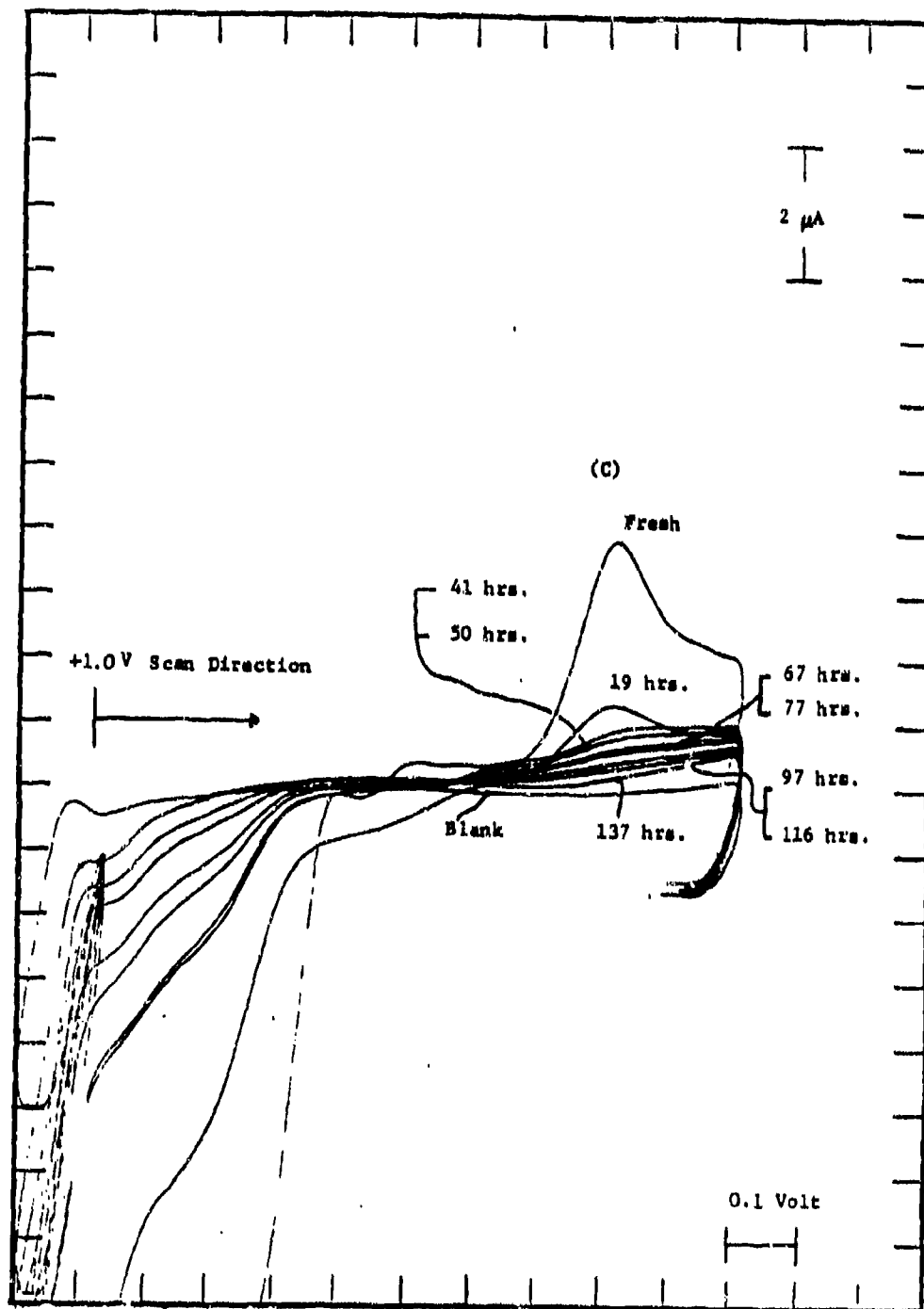


Figure 69. Reductive Voltammograms of Fresh and Stressed (19-137 Hours at 370°F) TEL-4001 MIL-L-7808 Oils in Acetone Containing Pyridine Using a Glassy Carbon Working Electrode.

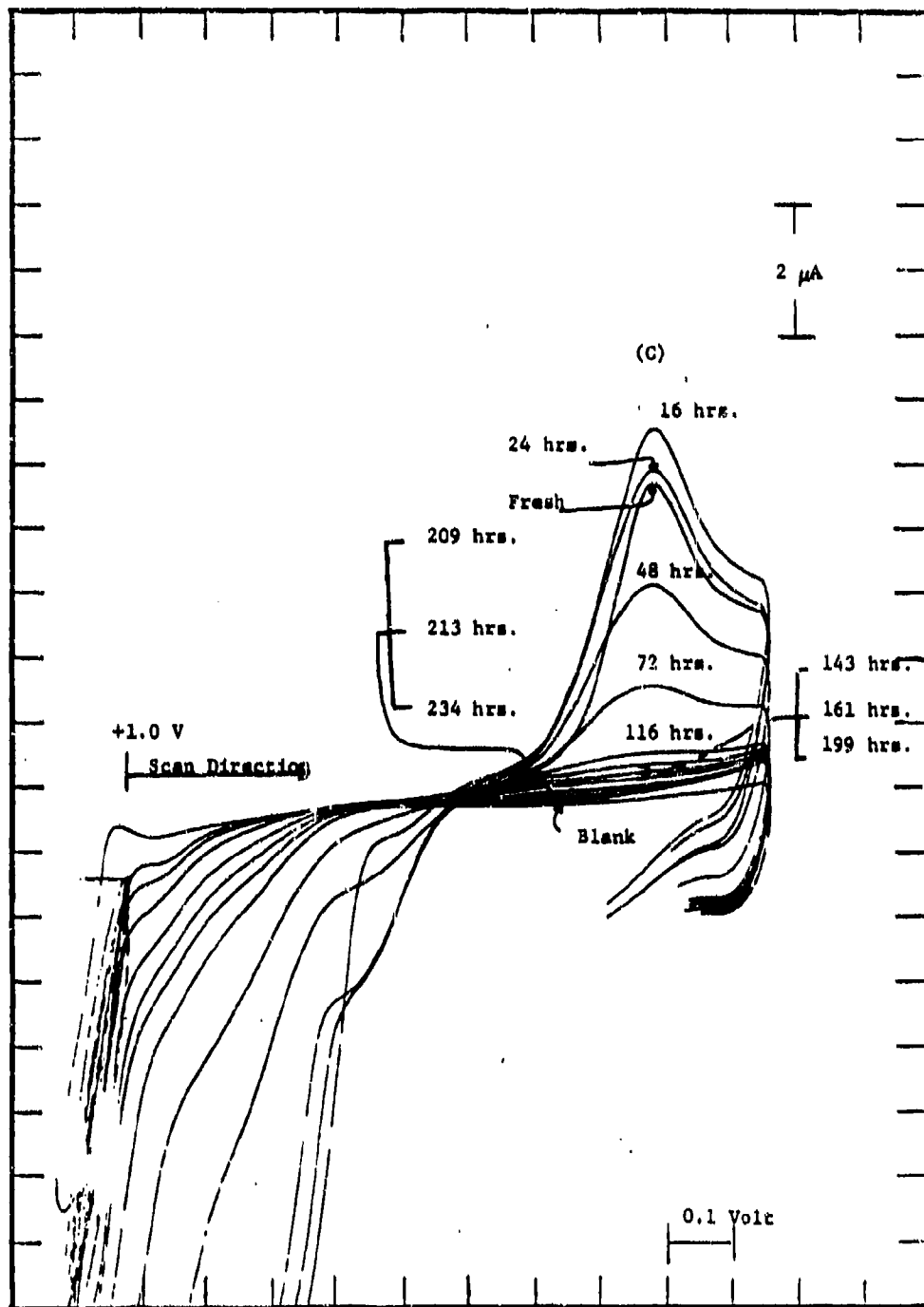


Figure 70. Reductive Voltammograms of Fresh and Stressed (16-234 Hours at 370°F) TEL-4002 MIL-L-7808 Oils in Acetone Containing Pyridine Using a Glassy Carbon Working Electrode.

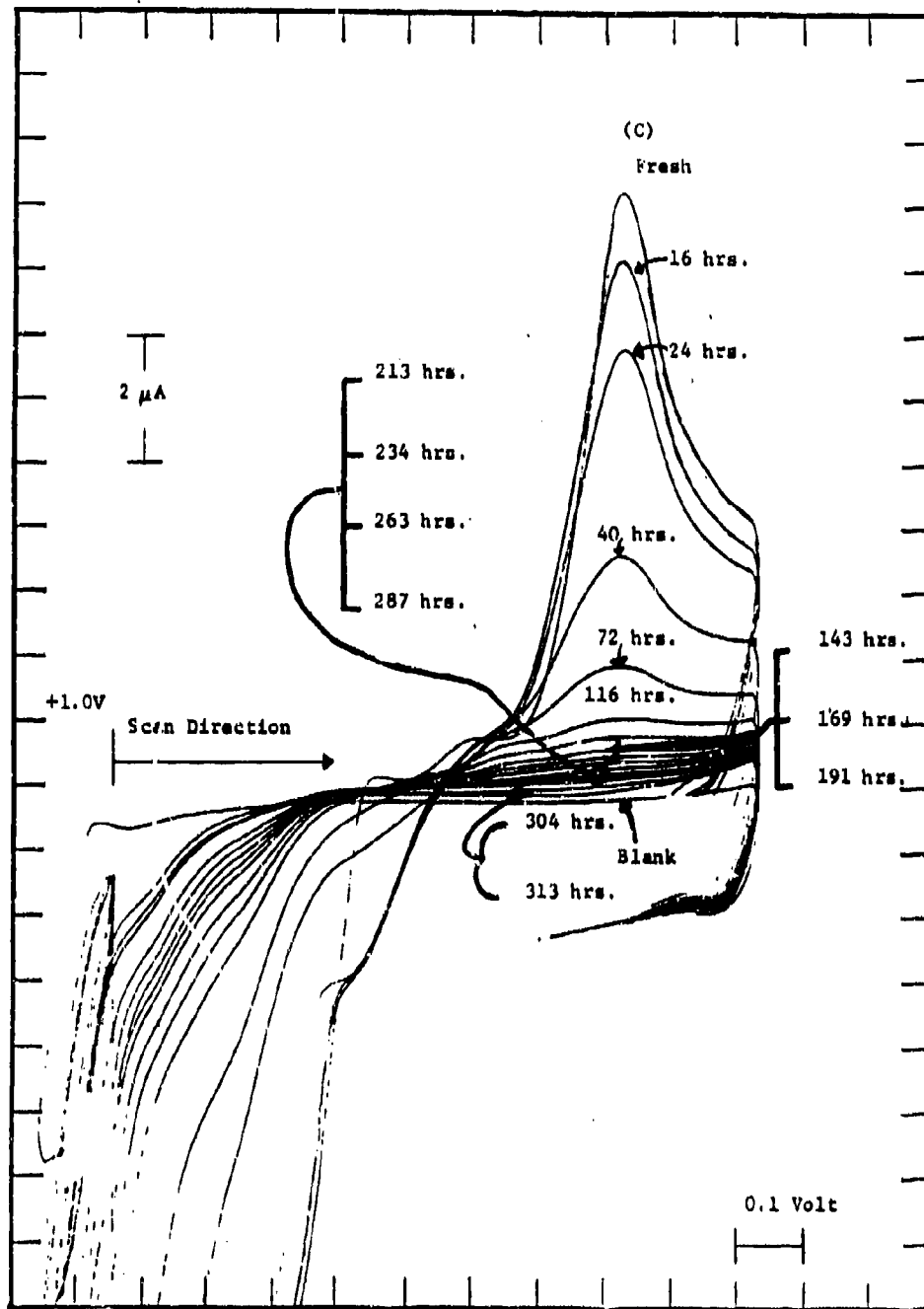


Figure 71. Reductive Voltammograms of Fresh and Stressed (16-313 Hours at 370°F) TEL-4003 MIL-L-7808 Oils in Acetone Containing Pyridine Using a Glassy Carbon Working Electrode.

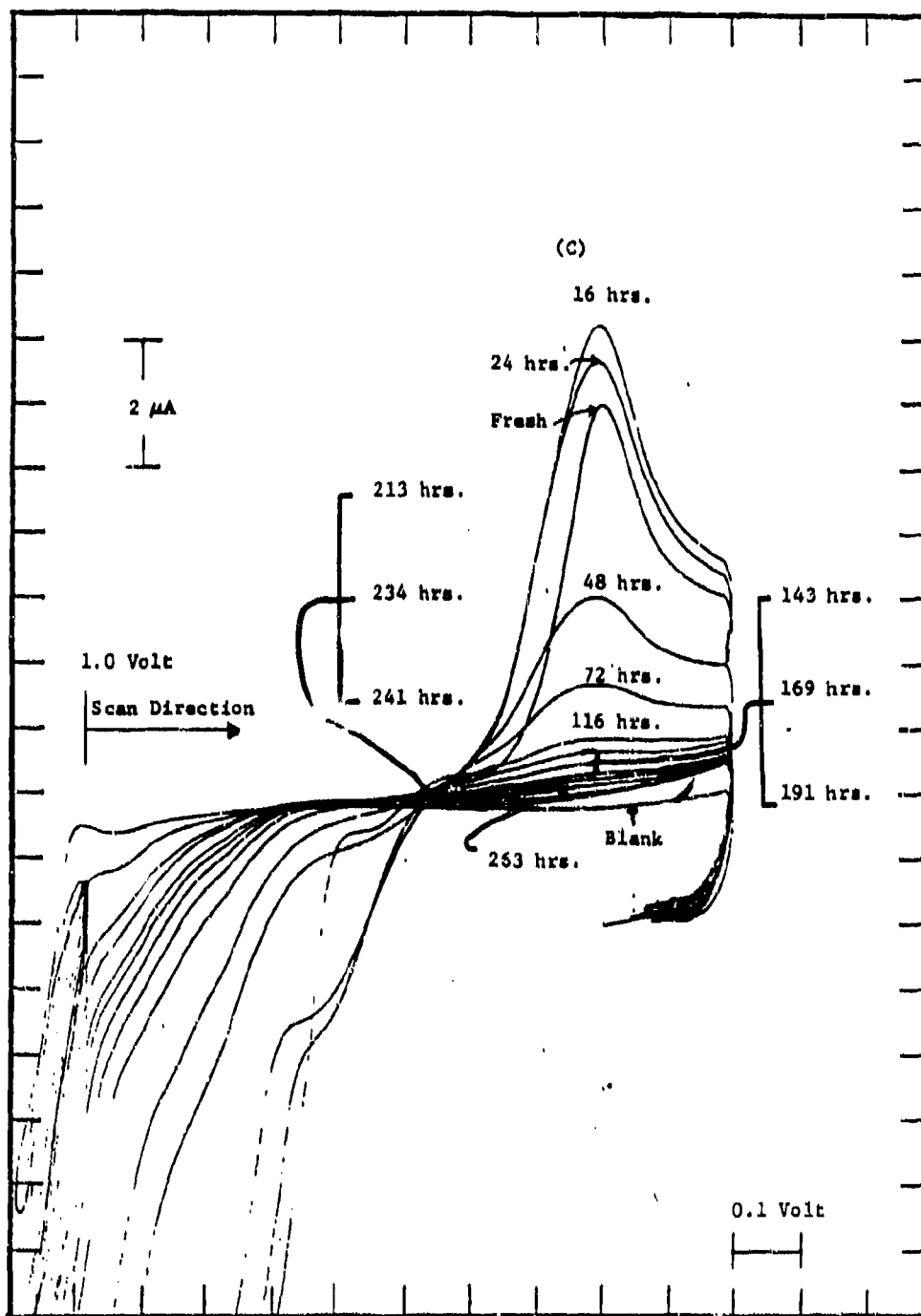


Figure 72. Reductive Voltammograms of Fresh and Stressed (16-263 Hours at 370°F) TEL-4004 MIL-L-7808 Oils in Acetone Containing Pyridine Using a Glassy Carbon Working Electrode.

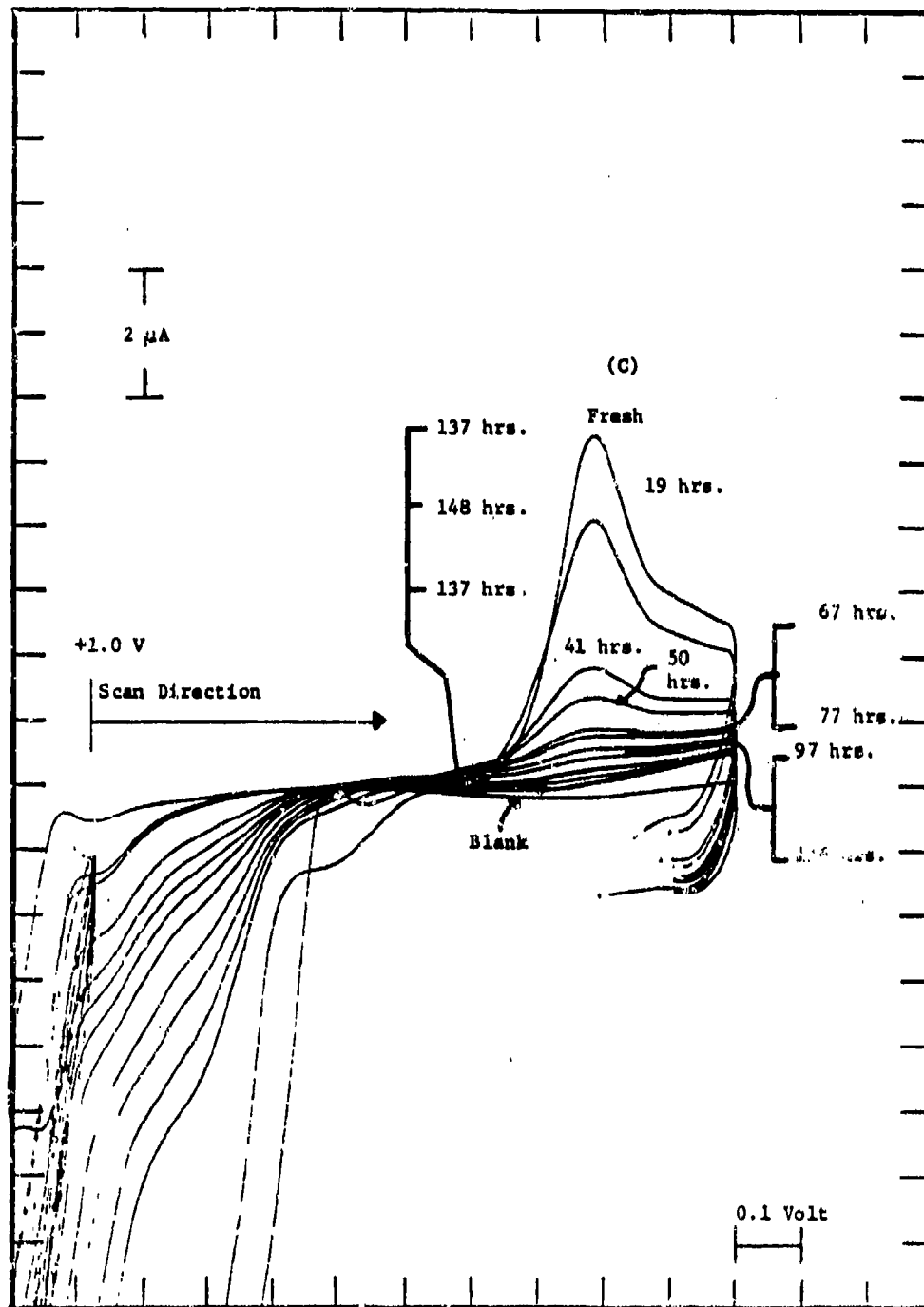


Figure 73. Reductive Voltammograms of Fresh and Stressed (19-194 Hours at 370°F) TEL-4005 MIL-L-7808 Oils in Acetone Containing Pyridine Using a Glassy Carbon Working Electrode.

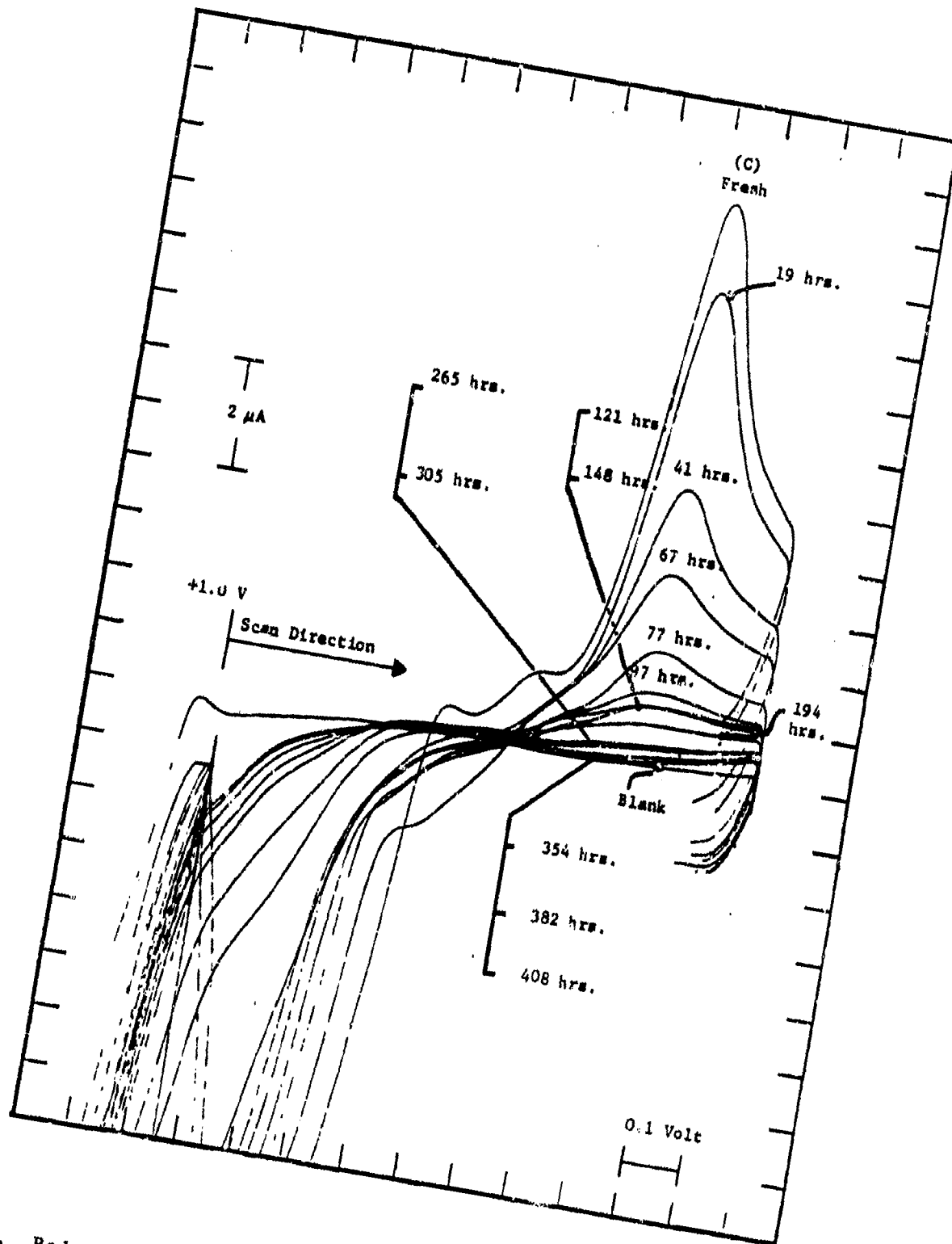


Figure 74. Reductive Voltammograms of Fresh and Stressed (19-408 Hours at 370°F) TEL-4006 MIL-L-7808 Oils in Acetone Containing Pyridine Using a Glassy Carbon Working Electrode.

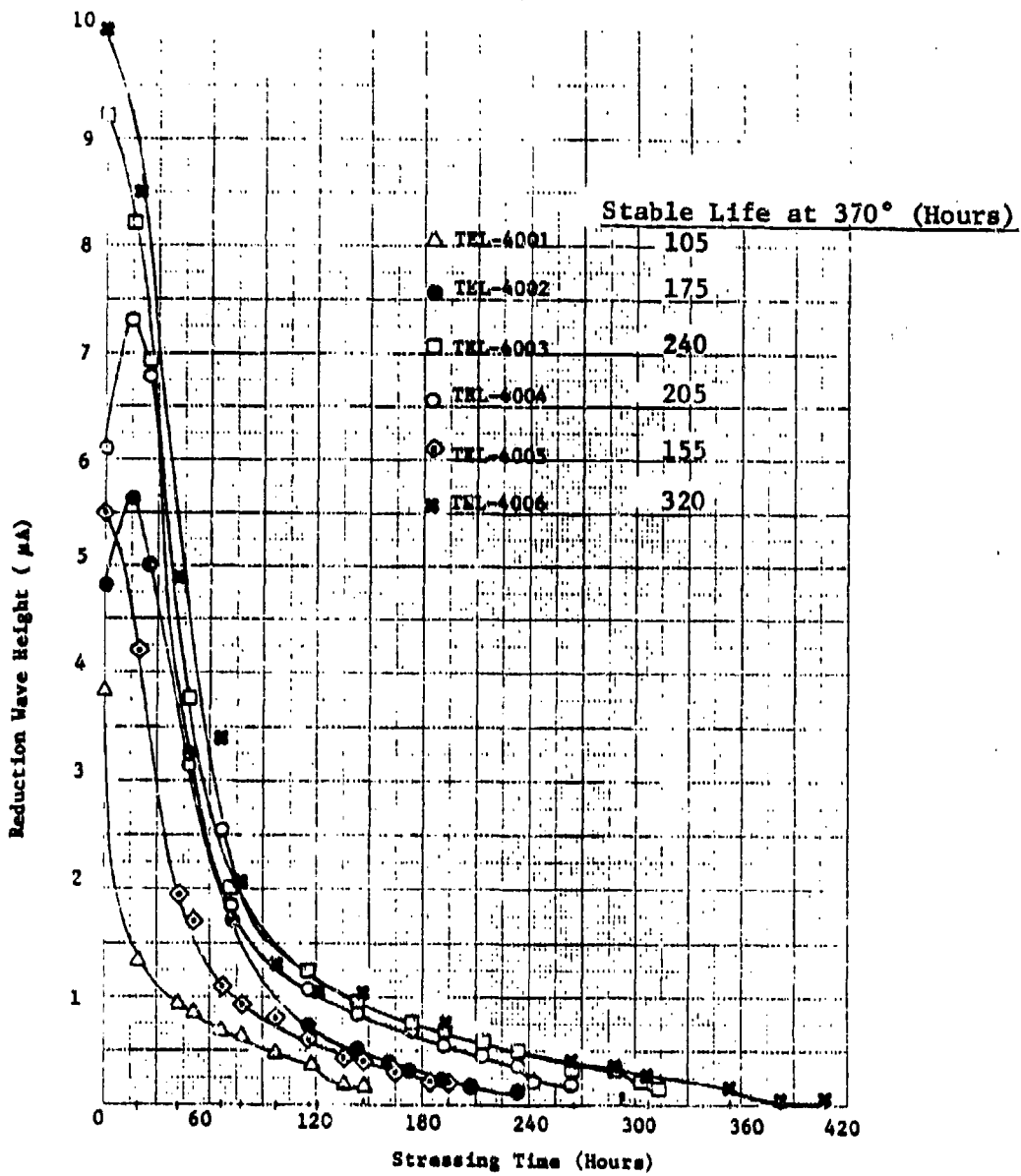


Figure 75. Plots of Reduction Wave (C) Height in the Presence of Pyridine Versus Stressing Time (370°F) for the TEL-4001 Through TEL-4006 MIL-L-7808 Oils.

oils' stable lives. The shape of the plots cause the RCV technique to be sensitive to small changes in the oil's RLL during the early periods of oxidation and insensitive to small changes in the oil's RLL during the latter periods of oxidation, when the RLL assessments become more important. Also, the estimation of the RLL is difficult because of the nonlinearity of the plots. Therefore, an initial study designed to linearize the plots of the reduction wave height versus stressing time at 370°F was conducted.

It has been reported (Reference 42) that the depletion of the original antioxidants in lubricating oils is a first order reaction. If the depletion of the generated antioxidant species (species reduction wave C in Figures 69-74 is assigned) is also first order, then the log of the reduction wave height versus stressing time at 370°F plots for the TEL-4001 through TEL-4006 should be linear. As seen in Figure 76, the semi-log plots of the TEL-4001 through TEL-4006 oils appear to consist of two linear regions with the transition period occurring at nearly the same reduction wave height (10-15  $\mu$ A) for each MIL-L-7808 oil.

#### (8) Effect of Organic Base

To gain a better understanding of the results of the RCV technique employing pyridine, the effects of different organic bases on the reductive voltammograms of the fresh TEL-4003 oil were studied and the resulting reductive voltammograms are shown in Figures 77-79 for pyridine, pyridazine, and 2,2' dipyridyl. The organic bases pyrazine and quinoxaline did not affect the reductive voltammogram of the fresh TEL-4003 oil.

The Figures 78 and 79 show that pyridazine and 2,2' dipyridyl produce changes similar to pyridine (Figure 77) in the reductive voltammograms of the fresh TEL-4003 oil. It takes 90-120  $\mu$ l of 2,2' dipyridyl (5% in acetone) to produce the same effect as 60  $\mu$ l of pyridine and pyridazine (5% in acetone). The original reduction waves (D) are inhibited and the new reduction waves (C) are enhanced in the presence of the organic bases (Figures 77-79).

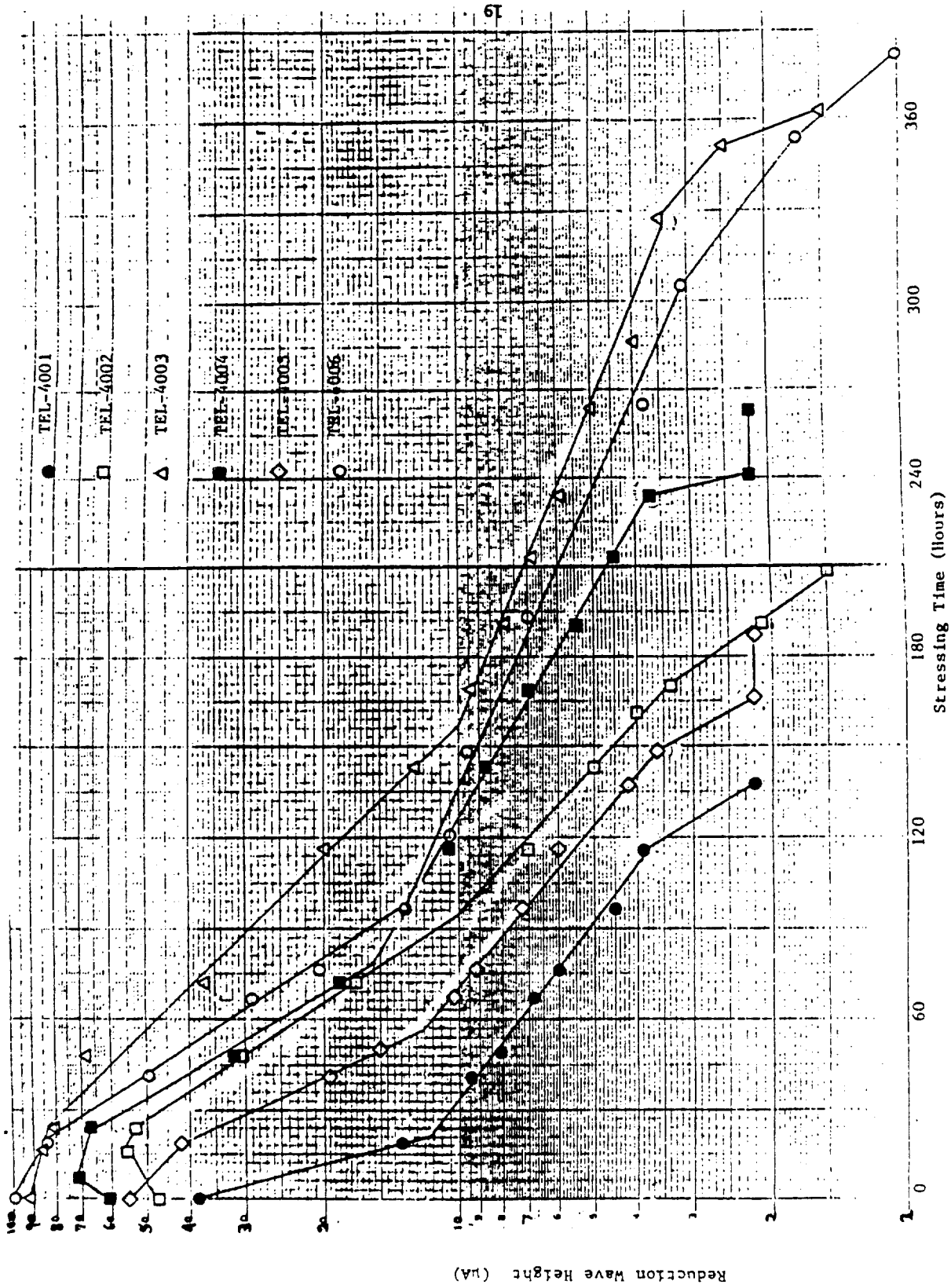


Figure 76. Semi-Logarithmic Plots of the Reduction Wave (C) Height in the Presence of Pyridine Versus Stressing Time (370°F) for the TEL-4001 Through TEL-4006 MIL-L-7808 Oils.

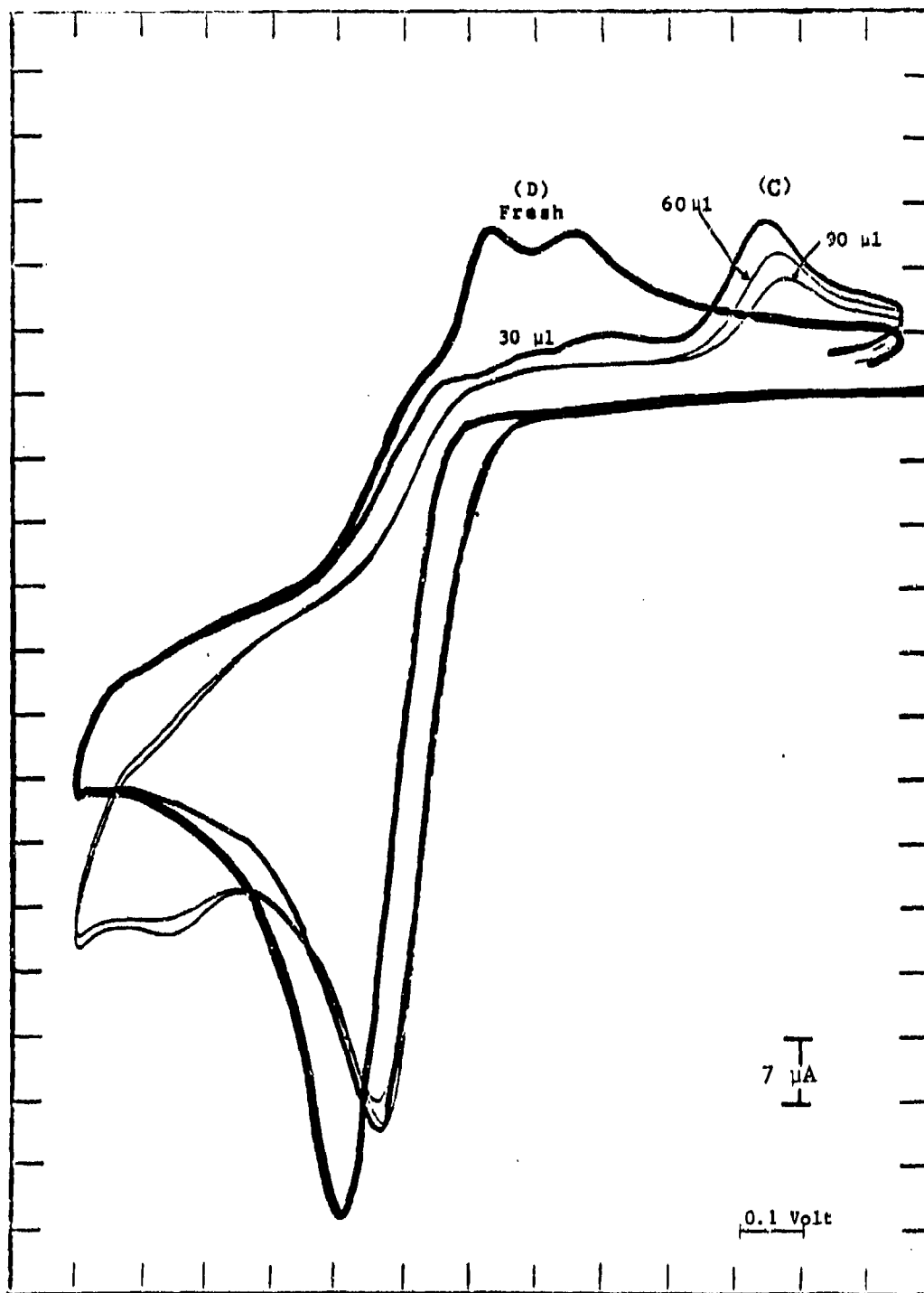


Figure 77. Effects of the Amount (0-90  $\mu\text{l}$ ) of a 5% Pyridine Solution on the Reductive Voltammograms of the TEL-4003 MIL-L-7808 Oil in Acetone Using a Glassy Carbon Working Electrode.

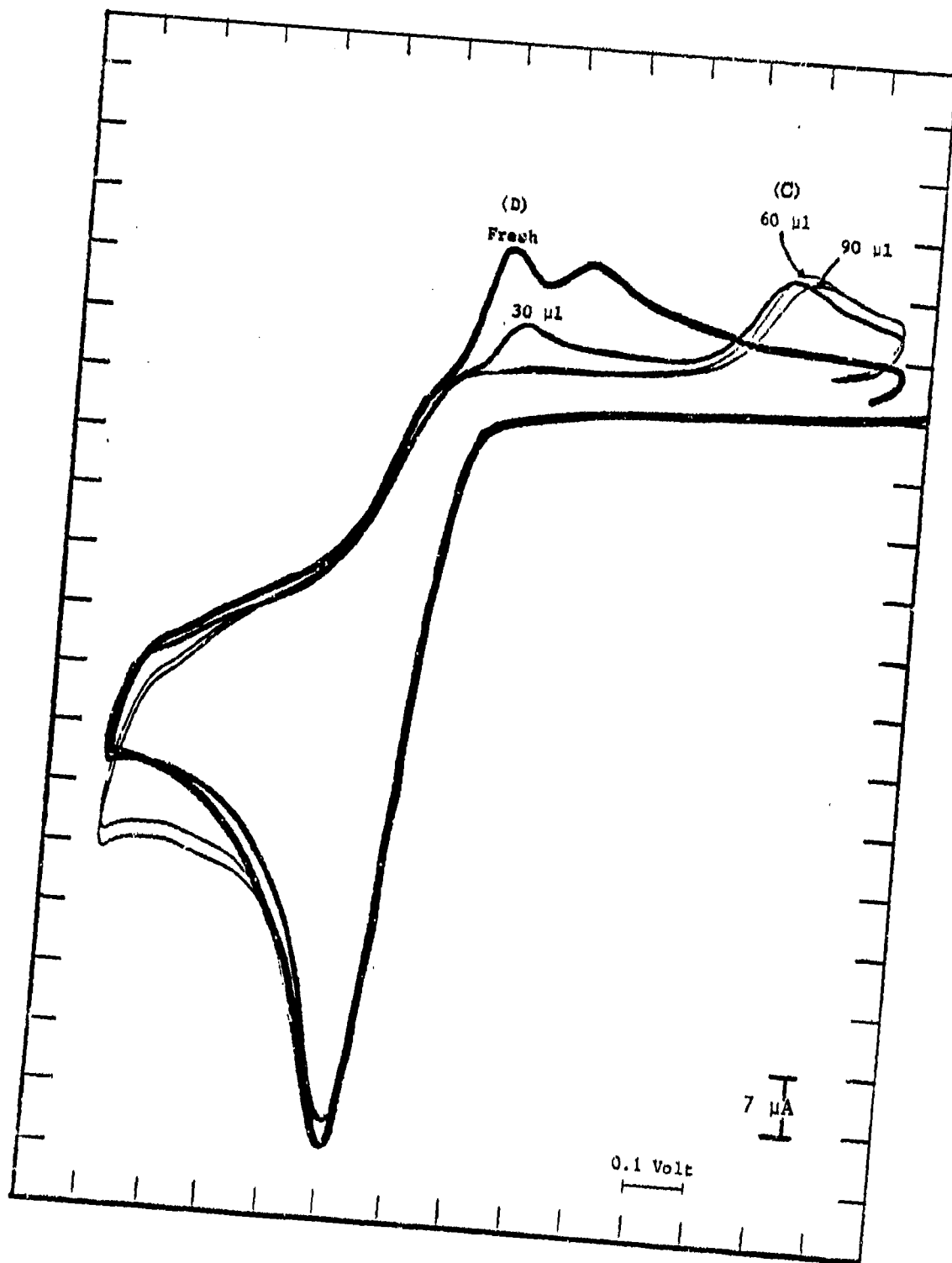


Figure 78. Effects of the Amount (0-90  $\mu$ l) of a 5% Pyridazine Solution on the Reductive Voltammograms of the TEL-4003 MIL-L-7808 Oil in Acetone Using a Glassy Carbon Working Electrode.

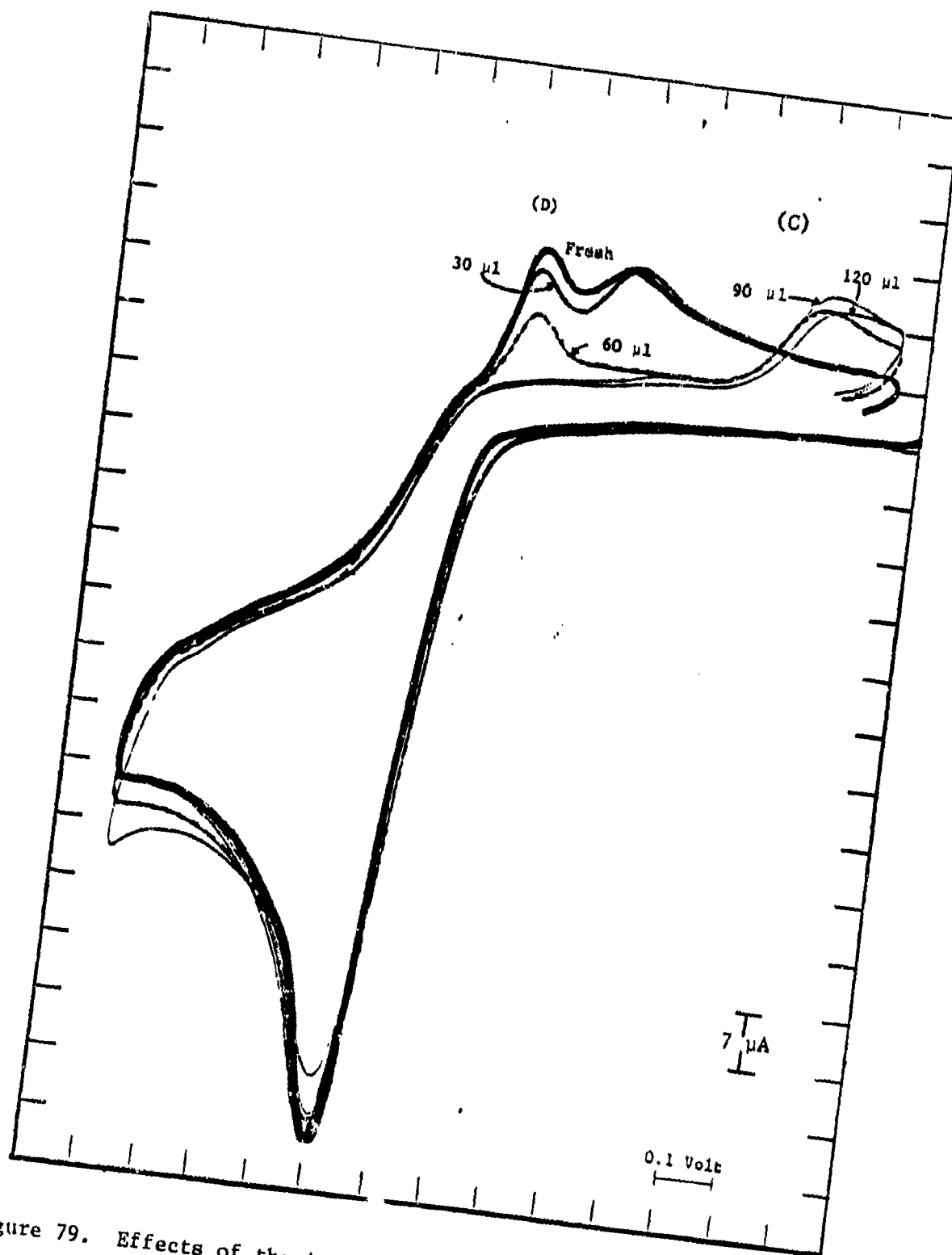


Figure 79. Effects of the Amount (0-120  $\mu\text{l}$ ) of a 5% 2,2' Dipyridyl Solution on the Reductive Voltammograms of the TEL-4003 MIL-L-7808 Oil in Acetone Using a Glassy Carbon Working Electrode.

The effects of the organic bases appear to be related to their respective basicities. The weaker bases pyrazine and quinoxaline have no effect on the reductive voltammograms. The stronger bases, pyridine, pyridazine, and 2,2' dipyridyl inhibit the original reduction waves (D) and enhance the new reduction waves (C) (Figures 77-79).

The results in Figures 77 and 78 indicate that pyridazine is better suited for the RCV technique than pyridine since the height of the reduction wave for pyridazine is less dependent on the organic base/antioxidant ratio than for pyridine, i.e., as the amount of base is increased the reduction wave height decreases for pyridine but remains fairly constant for pyridazine. Also pyridazine is much safer to work with than pyridine. Pyridazine does not have the flammability, odor, and irritant problems associated with pyridine.

Therefore, the remaining developmental work on the RCV technique was performed with a 0.1 M  $\text{LiClO}_4$  in acetone solution containing 375 ppm of pyridazine.

#### (9) Effect of Successive Scanning Cycles

Since the log of the reduction wave height versus stressing time plots for the TEL-4001 through TEL-4006 MIL-L-7808 oils were not linear, the effect of successive scanning cycles on the reduction wave heights was studied. To determine the concentration of the antioxidant species generated during the thermal-oxidative stressing of the oil samples (oxidation wave B in Figures 58-63), the RCV analyses were started at a working electrode potential of 0.6 V and scanned to 0.0 V. To determine the capability of the RCV technique to generate similar antioxidant species from the oil sample, the RCV analyses were started at a working electrode potential of 0.0 V and then cycled between 0.0 V and 1.0 V for over ten cycles. The heights of the reduction waves were then compared to determine the effects of successive scanning on the RCV technique's results.

In order that the effect of successive scanning cycles on the RCV technique could be studied, a data acquisition

system based on a Apple IIe microcomputer was used because the X-Y recorder on which the previous RCV analyses were displayed was better suited for single sweep than multisweep voltammograms and for qualitative than quantitative analyses. Although the Apple IIe data acquisition system was more expensive than a strip chart recorder, it was in the price range of a X-Y recorder and the incorporation of the Apple IIe microcomputer into the RCV technique greatly increases the ease of operation and diagnostic capabilities of the RCV technique.

The Apple IIe computer was programmed to run the CV-1B module, sample the output of the working electrode, subtract out the blank wave height to determine the heights of the selected reduction peaks, and perform other required mathematical manipulations. Once a mathematical relationship between the height of the reduction waves and the RLL of MIL-L-7808 oils was established, the microcomputer could be programmed to readout in percent RLL. Therefore, the incorporation of the microcomputer greatly increased the ease of operation of the RCV technique suitable for base-level operation.

To study the effects of the successive scanning cycles on the RCV results, the fresh and stressed (370°F) oil samples of the TEL-4001, TEL-4002, and TEL-4006 MIL-L-7808 lubricating oil samples were analyzed. The reduction waves for the series of TEL-4002 oil samples and the blank are shown in Figure 80. The heights for the first (scan from 0.6 to 0.0V), second (first cycle between 0.0 to 1.0 V) and steady state (sixth to ninth cycles between 0.0 to 1.0 V) waves were plotted versus stressing time for the TEL-4001, TEL-4002, and TEL-4006 oils and are shown in Figures 81-83. The integrations of the reduction waves showed decreasing correlation with increasing stressing time, and thus, were not plotted.

The heights of the first wave (scan from 0.6 to 0.0 V) plotted in Figures 81-83 are only dependent upon the concentration of the new antioxidant species generated during the thermal-oxidation (370°F) of the MIL-L-7808 oil samples. As

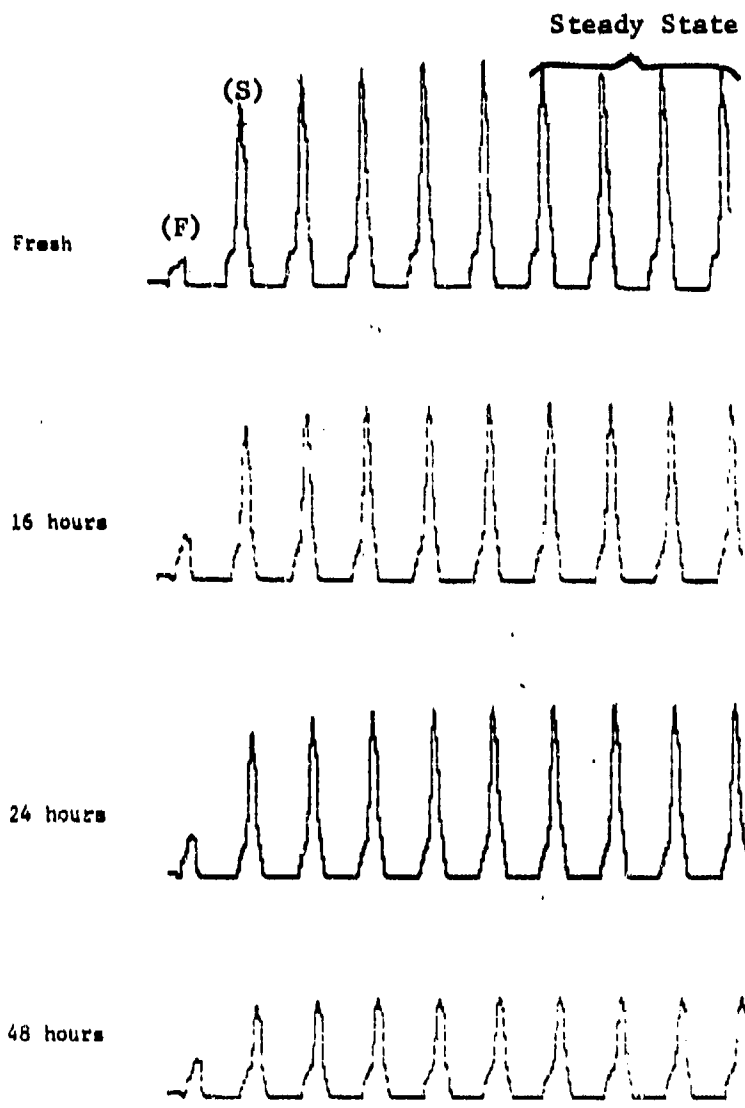


Figure 80. First (F), Second (S), and Steady State Reduction Waves of the Fresh and Stressed (16-234 Hours at 370°F) TEL-4002 MIL-L-7808 Oils and of the Blank.

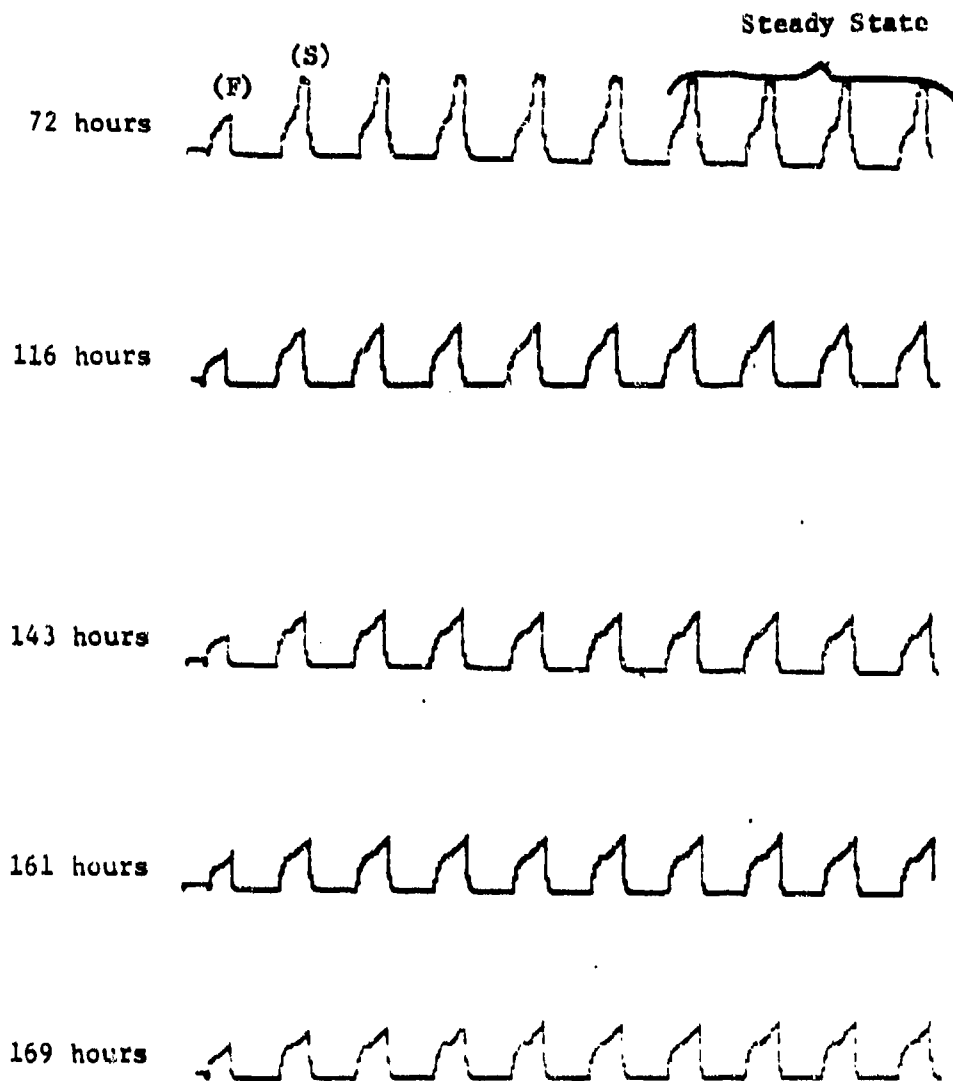


Figure 80. First (F), Second (S), and Steady State Reduction Waves of the Fresh and Stressed (16-234 Hours at 370°F) TEL-4002 MIL-L-7808 Oils and of the Blank. (Continued)

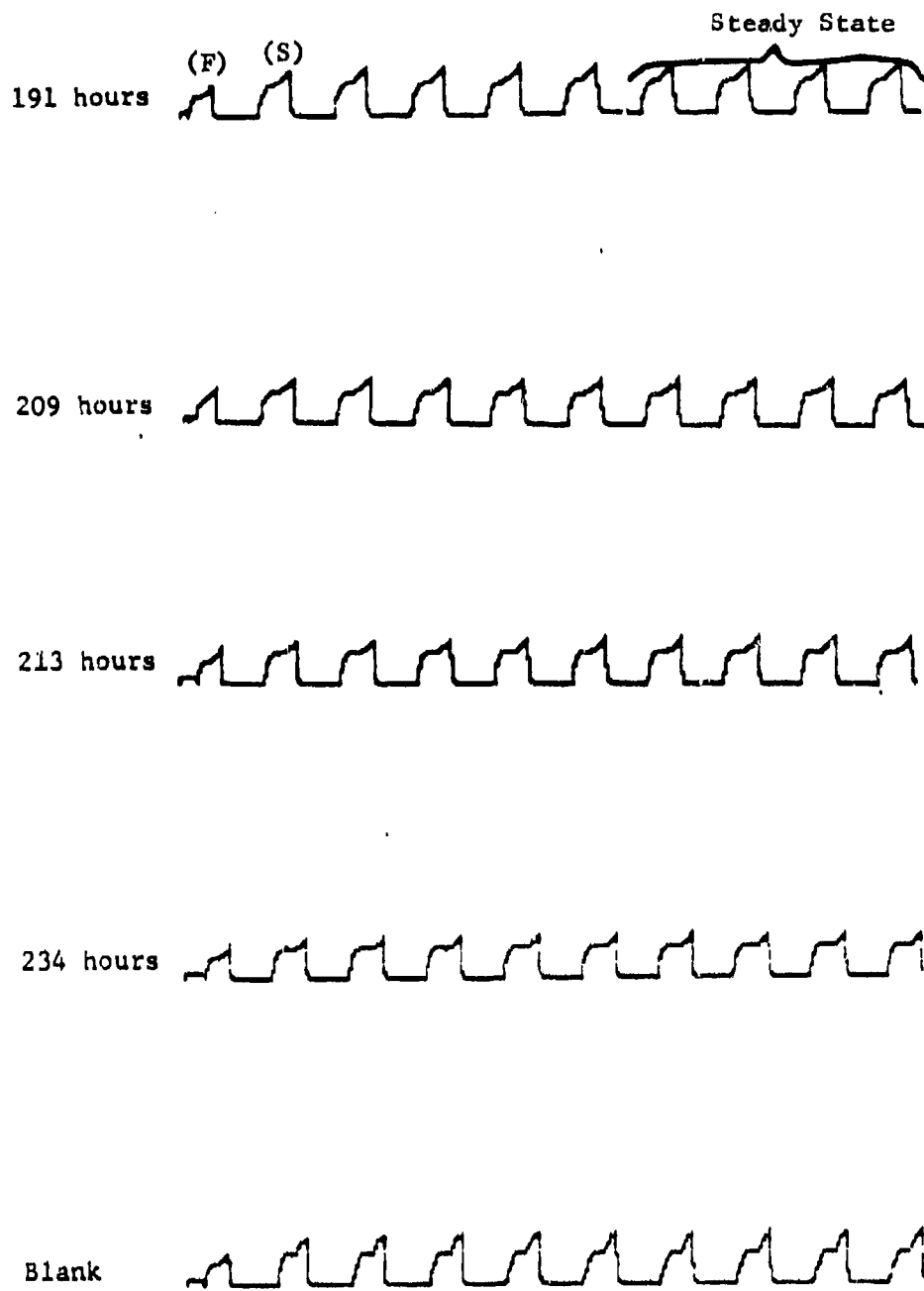


Figure 80. First (F), Second (S), and Steady State Reduction Waves of the Fresh and Stressed (16-234 Hours at 370°F) TEL-4002 MIL-L-7808 Oils and of the Blank. (Concluded)

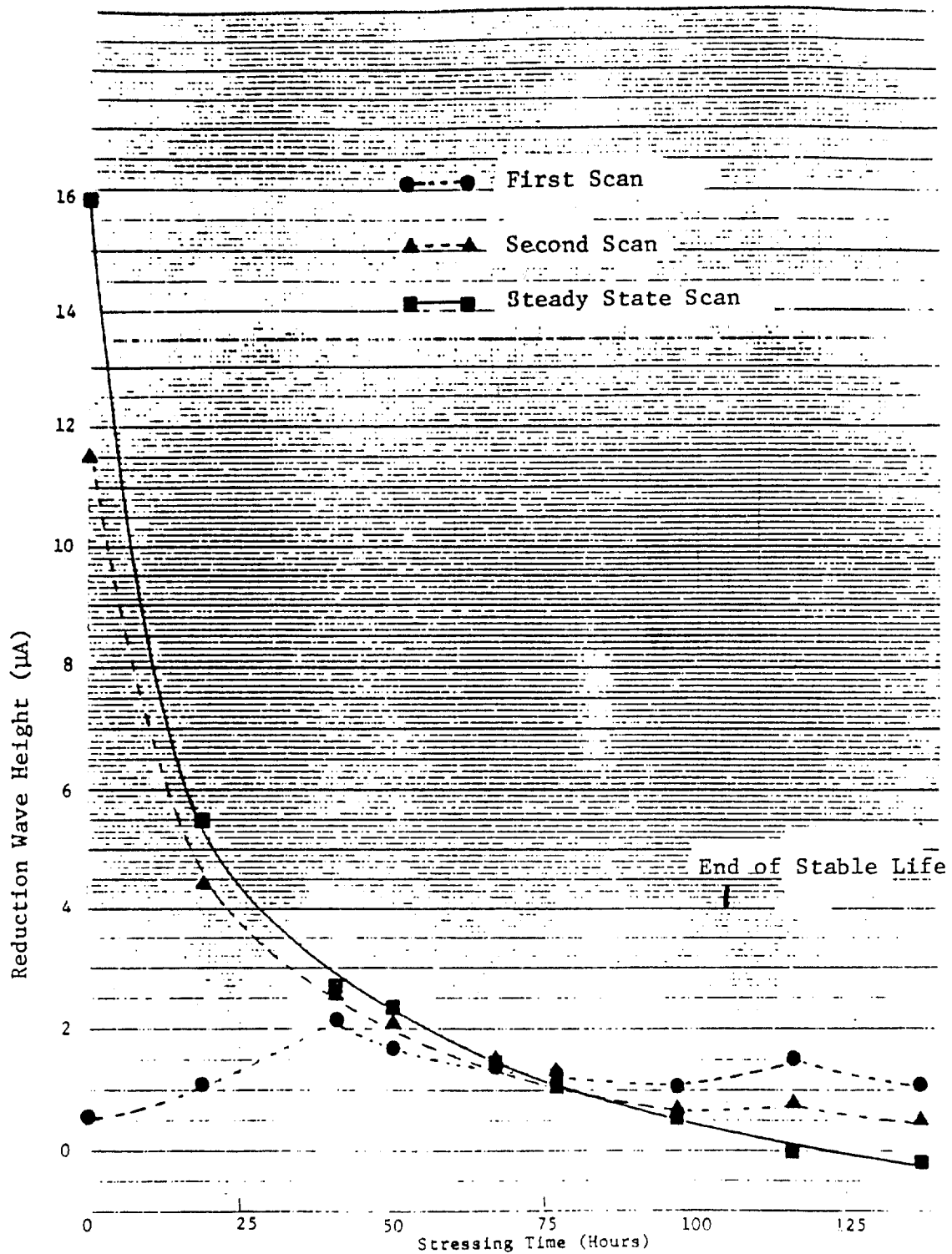


Figure 81. Plots of the First, Second, and Steady State Reduction Wave Heights Versus Stressing Time (370°F) for the TEL-4001 MIL-L-7808 Oil.

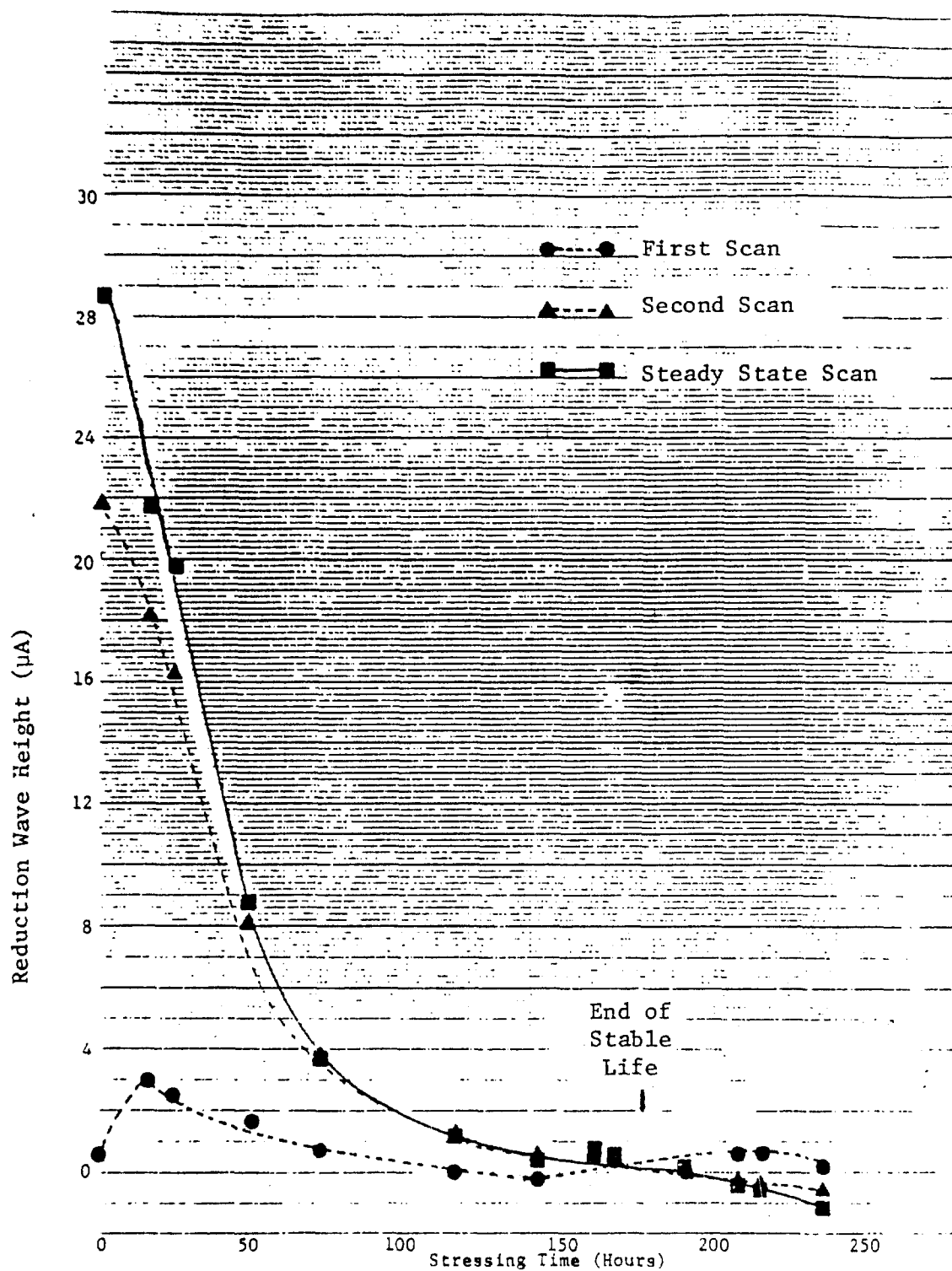


Figure 82. Plots of the First, Second, and Steady State Reduction Wave Heights Versus Stressing Time (370°F) for the TEL-4002 MIL-L-7808 Oil.

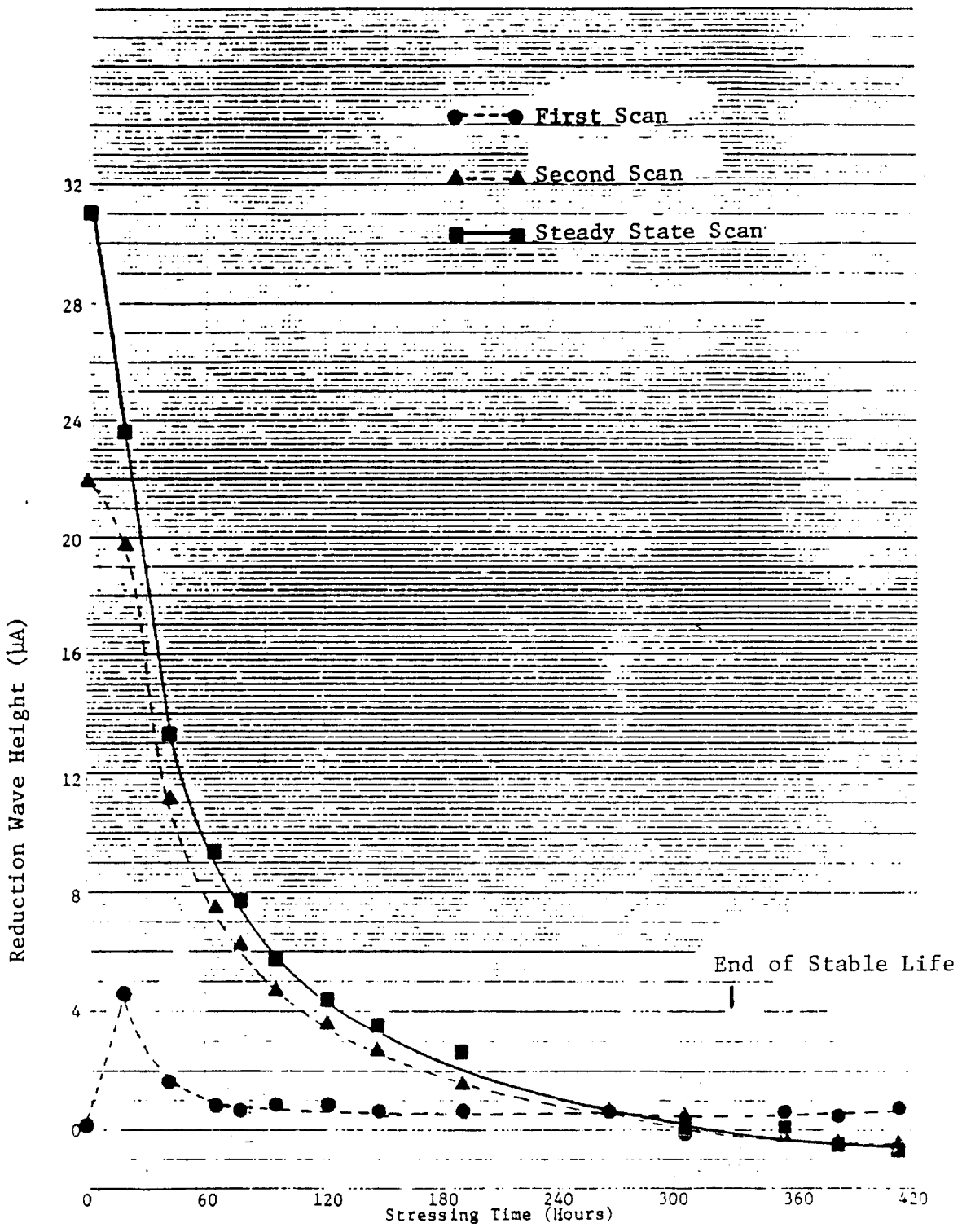


Figure 83. Plots of the First, Second, and Steady State Reduction Wave Heights Versus Stressing Time (370°F) for the TEL-4006 MIL-L-7808 Oil.

expected, the concentrations of the generated antioxidant species are minimal in the fresh oils, increase during the initial stages of oxidation, and then decrease with increasing stressing time (Figures 81-83). However, the reduction wave heights of the generated species become constant several hours prior to the ends of the TEL-4002 and TEL-4006 oils' stable lives. Also, the reduction wave heights remained constant or even increased after the stable lives of the studied MIL-L-7808 oils had ended. Therefore, the heights of the first wave for the different MIL-L-7808 oils, which represent the concentration of the antioxidant species generated by thermal oxidation, show only a limited correlation with stressing time, and consequently, are not related to the RLL of the oil samples.

The heights of the reduction waves produced by the first cycle between 0.0 and 1.0 V (second wave in Figures 81-83) and the sixth through ninth cycles (steady state waves in Figures 81-83) are only slightly dependent on the concentration of the generated antioxidants in the stressed oil samples. The heights of the second and steady state reduction waves are mainly dependent on the species produced during the electrochemical oxidation of the original antioxidants. In contrast to the first waves of the Figures 81-83 and the semilog plot of the reduction wave height versus stressing time at 370°F for the TEL-4002 oil shown in Figure 76, the heights of the second and steady state cycle reduction waves in Figures 81-83 decrease with increasing stressing time.

Although the plots of the second and steady state reduction wave heights versus stressing time in Figures 82-84 are similar in shape, the heights of the steady state waves are greater than the heights of the second waves, especially for the fresh oils. The differences between the heights of the second and steady state waves decrease with stressing time and become negligible as the oils approach the ends of their respective stable lives.

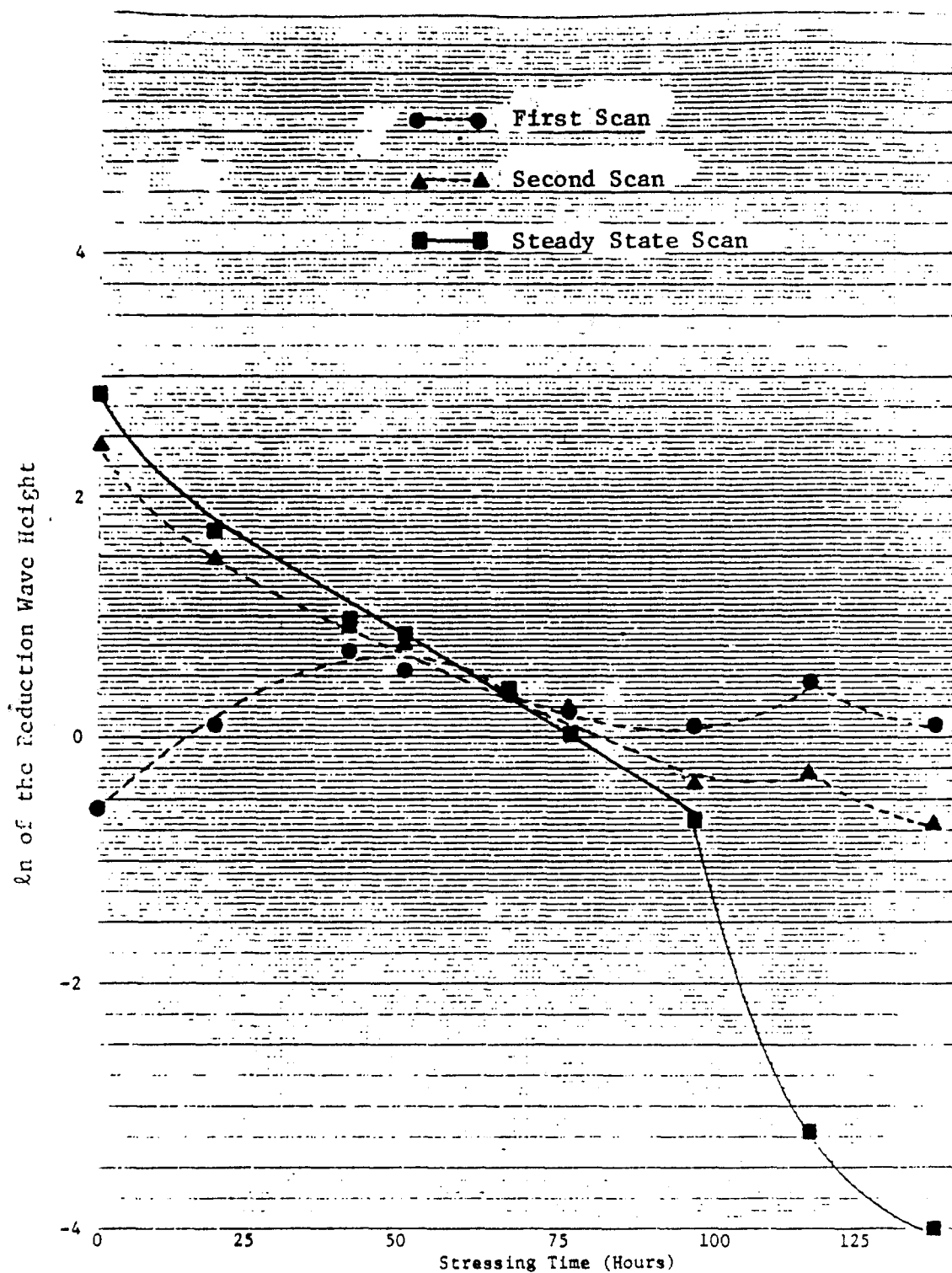


Figure 84. Plots of the  $\ln$  of the First, Second, and Steady State Reduction Wave Heights Versus Stressing Time (370°F) for the TEL-4001 Oil.

Therefore, the plots of the second and steady state reduction wave heights versus stressing time were used to develop the mathematical relationships capable of assessing the RLL of MIL-L-7808 lubricating oils.

(10) Determination of the Mathematical Relationship Between the RLL of MIL-L-7808 Oils and the RCV Results

As shown in Figure 76, the initial attempts to linearize the RCV technique's results by plotting the log of the reduction wave heights were only partially successful. Therefore, the most common kinetic equations, those for zero through third rate reactions, were applied to the plots of the second and steady state reduction wave heights versus stressing time at 370°F for the TEL-4001, TEL-4002, and TEL-4006 MIL-L-7808 lubricating oils.

If the depletion reaction of the antioxidant species is zero order, equation (1), where (A) equals the concentration of the antioxidant species,  $(A_0)$  equals the maximum concentration of the antioxidant species, k equals the rate constant, and t equals time, then the plot of the second

$$(A) = (A_0) - kt \quad (1)$$

and steady state reduction wave heights versus stressing time should be linear. As seen in Figures 81-83, none of the plots are linear.

If the depletion reaction of the antioxidant species is first order (as reported in Reference 42), equation (2), then plotting the natural log of the second

$$\ln(A) = \ln(A_0) - kt \quad (2)$$

and steady state reduction wave heights versus stressing time should be linear. As seen in Figures 84-86, the plots of the natural log of the steady state reduction wave heights versus

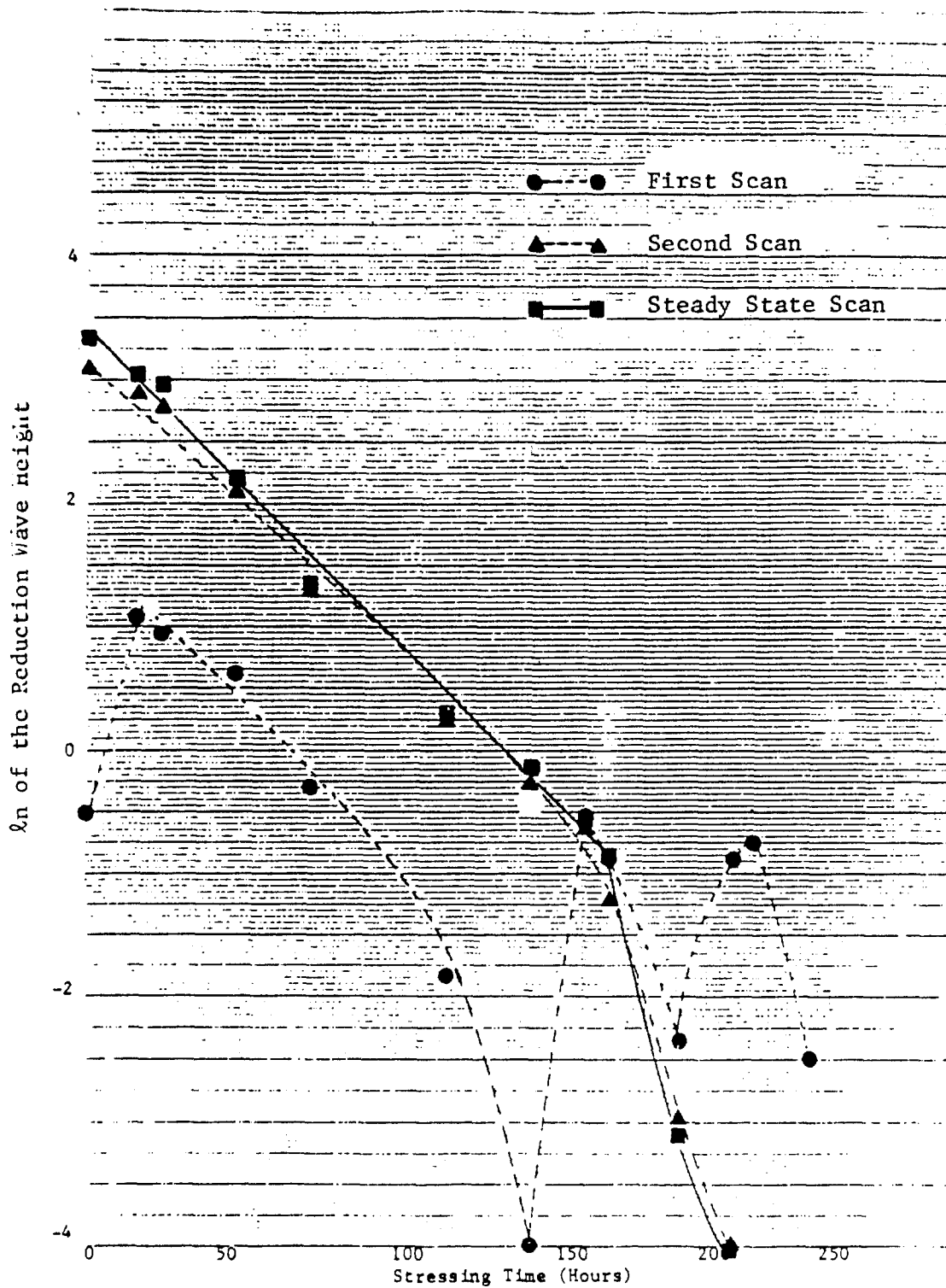


Figure 85. Plots of the  $\ln$  of the First, Second, and Steady State Reduction Wave Heights Versus Stressing Time ( $370^{\circ}\text{F}$ ) for the TEL-4002 Oil.

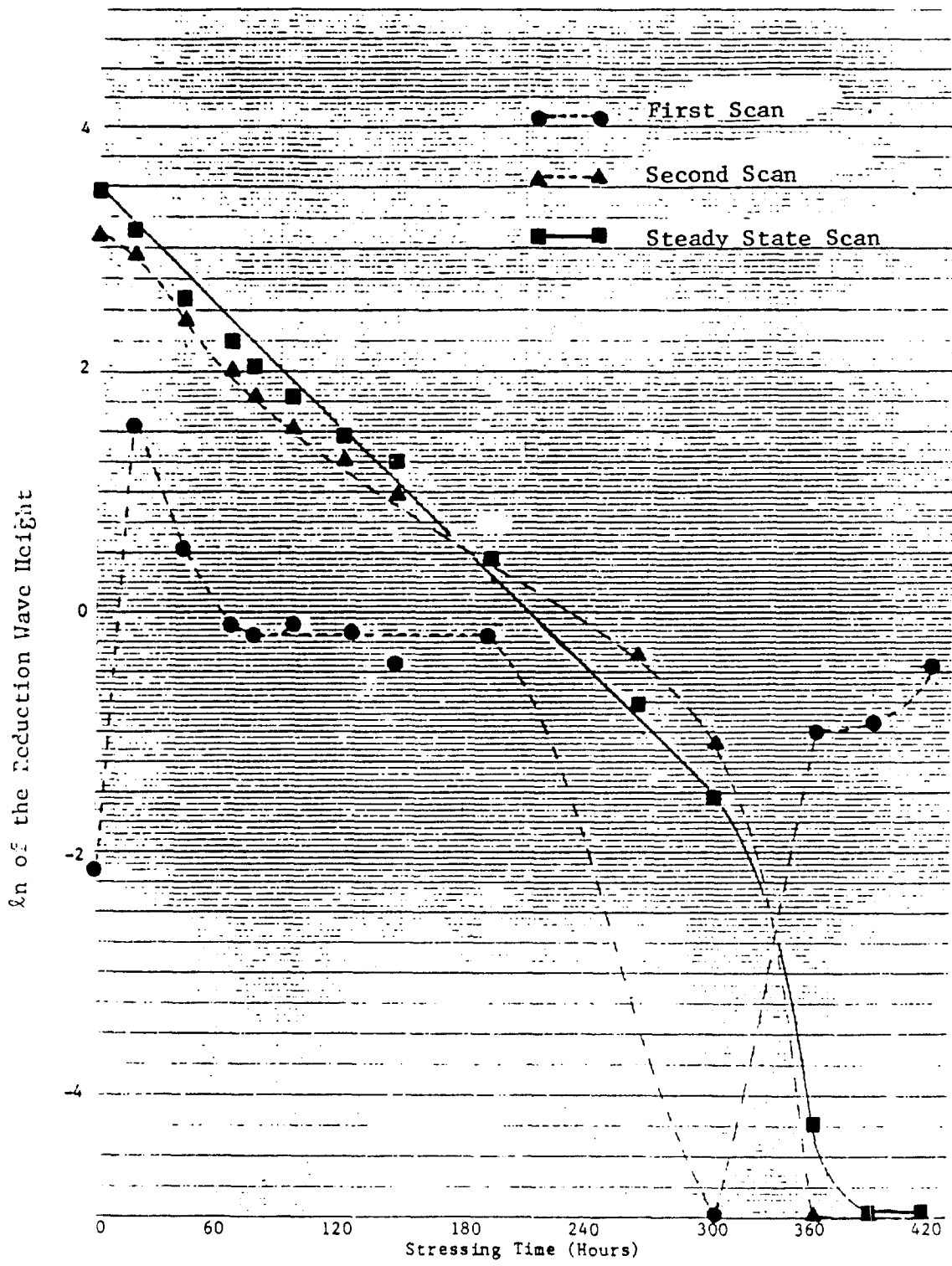


Figure 86. Plots of the  $\ln$  of the First, Second, and Steady State Reduction Wave Heights Versus Stressing Time ( $370^{\circ}\text{F}$ ) for the TEL-4006 Oil.

stressing time are fairly linear for the TEL-4001, TEL-4002, and TEL-4006 oils prior to the end of their respective stable lives.

If the depletion reaction of the antioxidant species is second or third order, equations (3) and (4),

$$\frac{1}{(\bar{A})} = \left(\frac{1}{\bar{A}_0}\right) + kt \quad (3)$$

$$\left(\frac{1}{\bar{A}}\right)^2 = \left(\frac{1}{\bar{A}_0}\right)^2 + kt \quad (4)$$

respectively, then plotting the inverse or inverse squared of the steady state reduction wave height versus stressing time should produce linear plots. As seen in Figure 87, the plots for the TEL-4002 oil are clearly nonlinear.

Therefore, it appears that the depletion reaction of the antioxidant species is first order. To better compare the results of the TEL-4001, TEL-4002, and TEL-4006 lubricating oils, the natural logs of the steady state reduction wave heights for the fresh and stressed oil samples of each MIL-L-7808 oil were plotted against the same time scale. The plots were then shifted so that they intersected at -0.750, which is the natural log value at which the stable lives of the TEL-4001, TEL-4002, and TEL-4006 oils ended.

The ln value of the fresh TEL-4006 oil's steady state reduction wave height is 3.44 and is defined as 100 percent lubricant life. Since the plots of the ln values of the steady state reduction wave height versus stressing time are linear for the studied MIL-L-7808 oils, the ln of the reduction wave heights can be assigned percent RLL values (Figure 88). Therefore, the mathematical relationship between the steady state reduction wave heights and the percent RLL of MIL-L-7808 oils is given in equation (5).

$$\% \text{ RLL} = \frac{\ln \text{ of the reduction wave height} + 0.750}{3.44} \times 100 \quad (5)$$

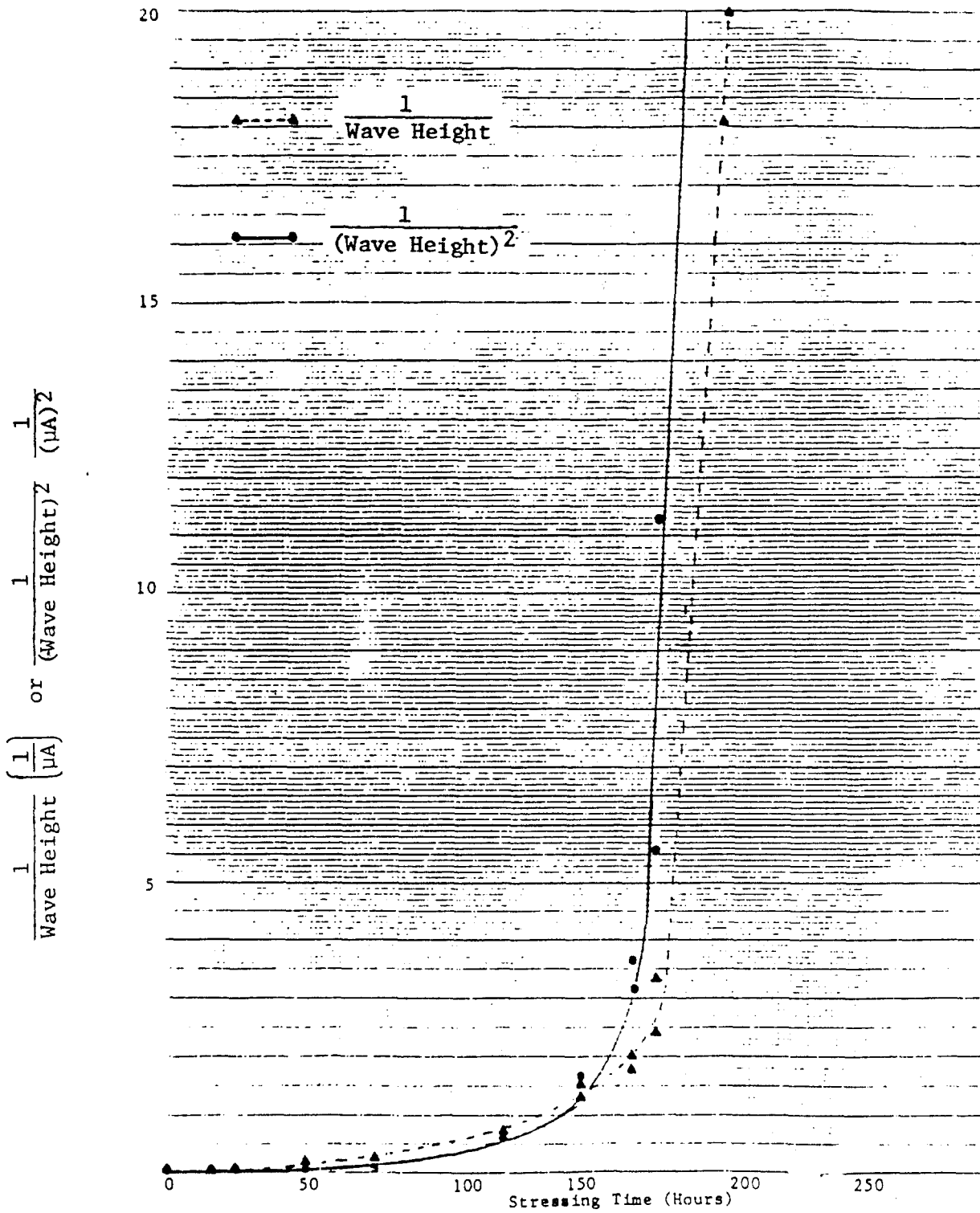


Figure 87. Plots of the Inverse and Inverse Squared of the Steady State Reduction Wave Height Versus Stressing Time (370°F) for the TEL-4002 Oil.

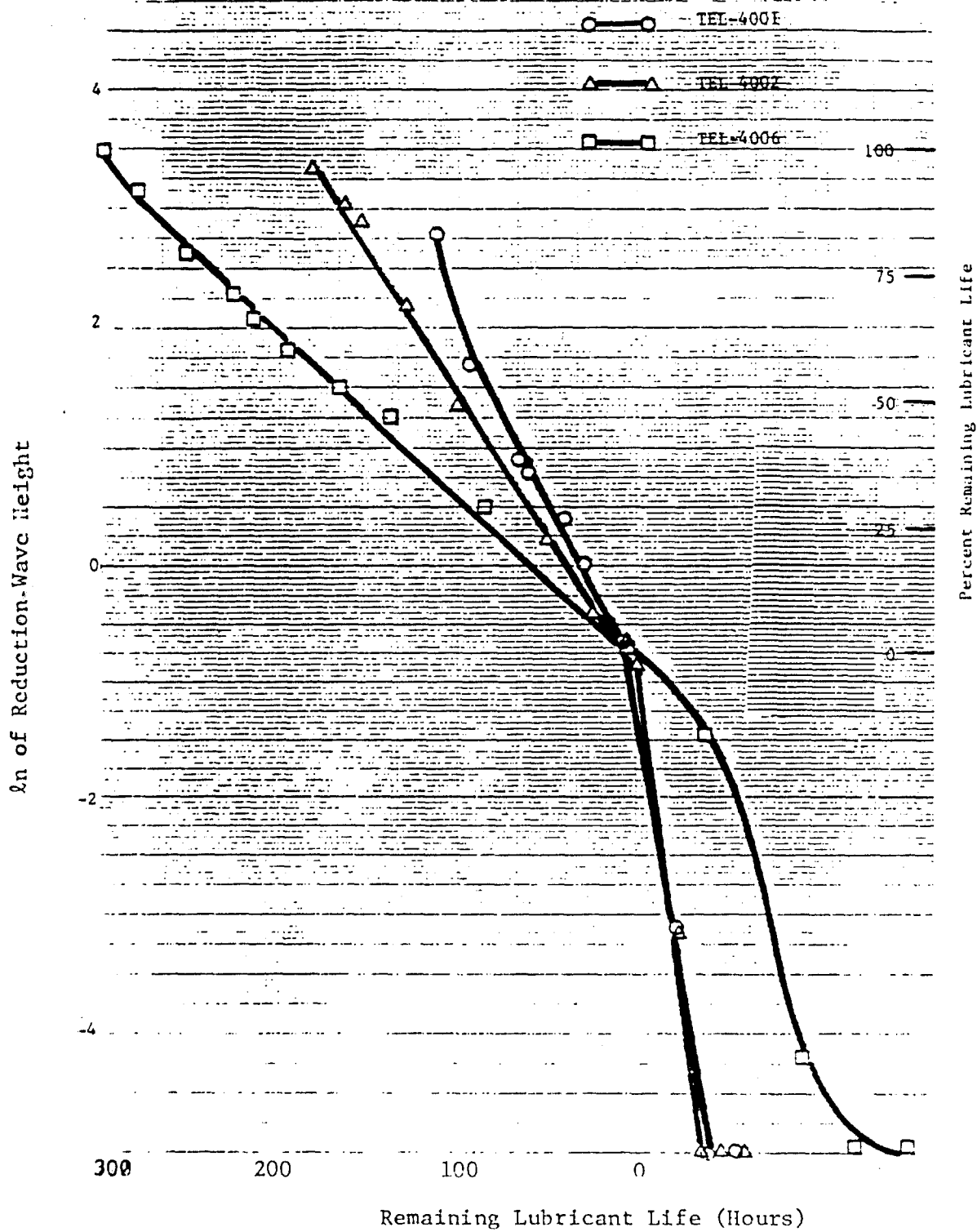


Figure 88. Plots of the  $\ln$  of the Steady State Reduction Wave Height and Percent Lubricant Life Versus Hours of Remaining Lubricant Life at  $370^{\circ}\text{F}$  for the TEL-4001, TEL-4002, and TEL-4006 Oils.

However, as seen in Figure 88, the slopes of the TEL-4001, TEL-4002, and TEL-4006 oils' plots are different which makes the assignment of RLL in hours to a single oil sample extremely difficult unless the oil's formulation and stressing temperature are known. For example, an oil sample with a  $\ln$  value of 2.00, could have anywhere from 195 to 90 hours of RLL.

#### (11) Effect of Formulation

To determine the effects of formulation on the RCV technique's capability to assess the RLL of MIL-L-7808 lubricating oils, the sets of fresh and stressed TEL-4001 through TEL-4006, TEL-5001, and TEL-5002 MIL-L-7808 oils were analyzed. The RLL plots for the MIL-L-7808 oils are shown in Figure 89.

The results in Figure 89 show that the  $\ln$  plots of the reduction wave heights versus remaining hours of lubricant life are essentially linear for all of the MIL-L-7808 oils. The only nonlinearity displayed by the  $\ln$  plots occurs during the early stages of oxidation, especially for the TEL-5001 oil. Although previous cyclic voltammetric analyses indicated that new species were not generated (Figure 64), the % RLL of the TEL-5001 oil as determined by the RCV technique increases during the early stages of oxidation. These results suggest that the generation of the new species with antioxidant capacity does occur for the TEL-5001 oil, in contradiction to the cyclic voltammograms in Figure 64.

The results in Figure 89 also show that regardless of formulation, the reduction wave height of  $0.5 \mu\text{A}$  ( $\ln$  value =  $-0.70$ ) can be assigned the value of 0% RLL. Once the assignment of 100 percent RLL is given to the  $\ln$  value of the fresh TEL-4006 oil, 3.44, % RLL can be made from the RCV results since the  $\ln$  plots are linear.

#### (12) Summary of the Reductive-Cyclic Voltammetric Technique

The RLLAT candidate developed from the RCV technique met all of the criteria listed in Table 1 and was capable of RLL assessments regardless of the MIL-L-7808 lubricating oil's

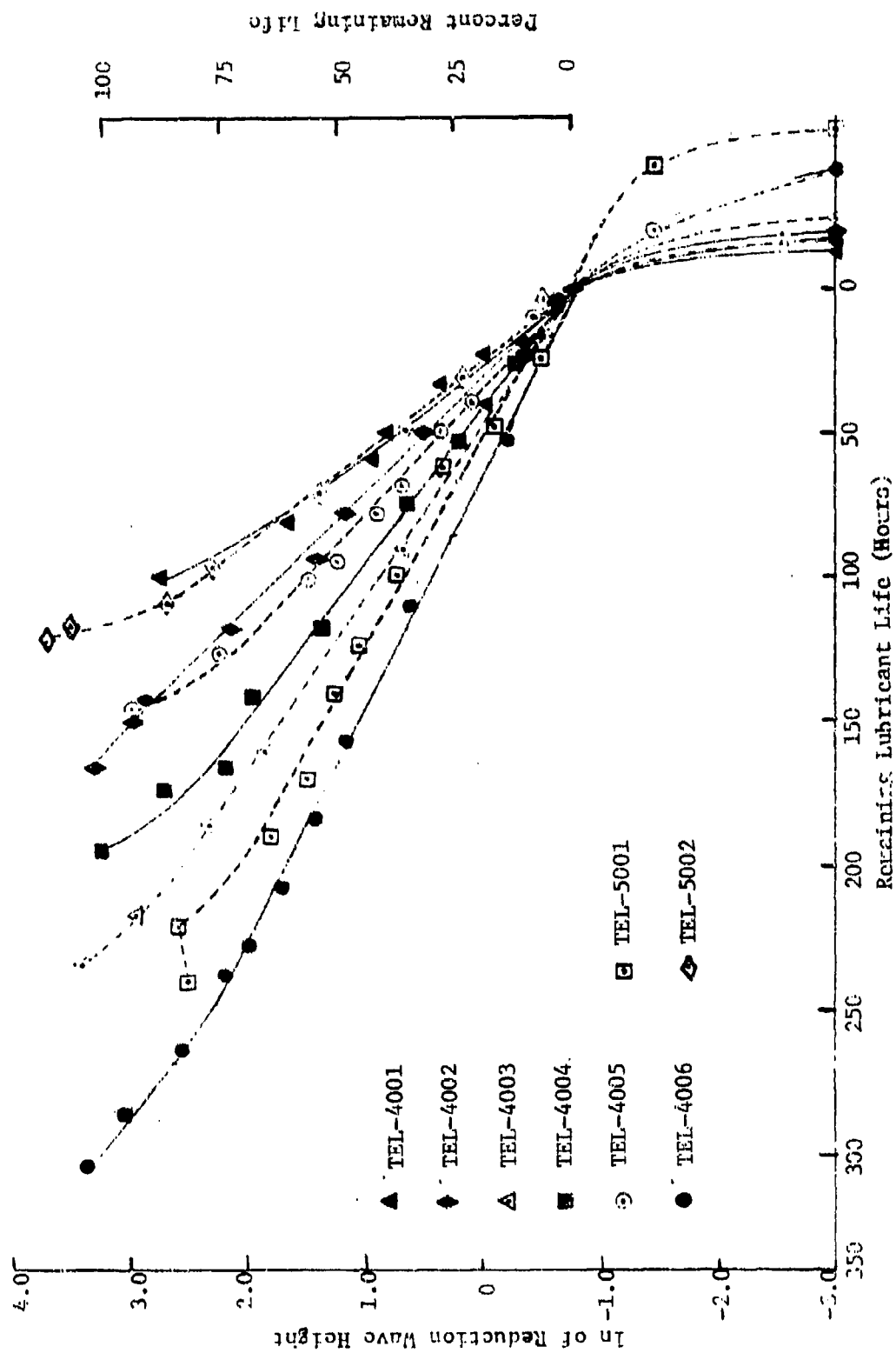


Figure 89. Plots of the ln of the Reduction Wave Heights and Percent Remaining Life of the Reductive-Cyclic Voltammetric Technique Versus Hours of Remaining Lubricant Life at 370°F for the Fresh and Stressed MIL-L-7808 Oils.

formulation. The incorporation of the Apple IIe microcomputer based data acquisition system made the RCV technique base-level in operation and in interpretation of the results.

Therefore, the RCV technique combined with the Apple IIe microcomputer based data acquisition system is very well-suited for development into a RLLAT.

### c. Thermal Stressing Technique

#### (1) Introduction

As the results of Task 1 indicated, the thermal stressing techniques based on high pressure-differential scanning calorimetry (HP-DSC) are well suited for development into a RLLAT candidate. In contrast to the voltammetric techniques, the analysis times of the thermal stressing techniques were greater than 10 minutes. In addition to the HP-DSC technique, a sealed pan-DSC (SP-DSC) technique was investigated in an attempt to eliminate the pressure requirements of the HP-DSC technique.

#### (2) High-Pressure-Differential Scanning Calorimetry

##### (a) Introduction

Before the potential of HP-DSC for development into a RLLAT candidate could be evaluated, the experimental conditions of the HP-DSC had to be changed in order to obtain onset of oxidation times (Figure 90) of less than 10 minutes for all of the MIL-L-7808 oils. An investigation showed that increasing the temperature from 230° to 250°C resulted in onset of oxidation times of less than 11 minutes for all of the MIL-L-7808 lubricating oils. Since the temperature was increased, the pressure was increased from 100 to 200 psig to decrease any effects of volatilization.

To fully evaluate the potential of HP-DSC as a RLLAT candidate, sets of fresh and laboratory stressed (370°F) oil samples were prepared for the TEL-4001 through TEL-4006 MIL-L-7808 lubricating oils. Each set contained seven samples ranging from fresh and slightly degraded oil samples to oil samples taken just after the stable life had ended. The six sets of oil samples were

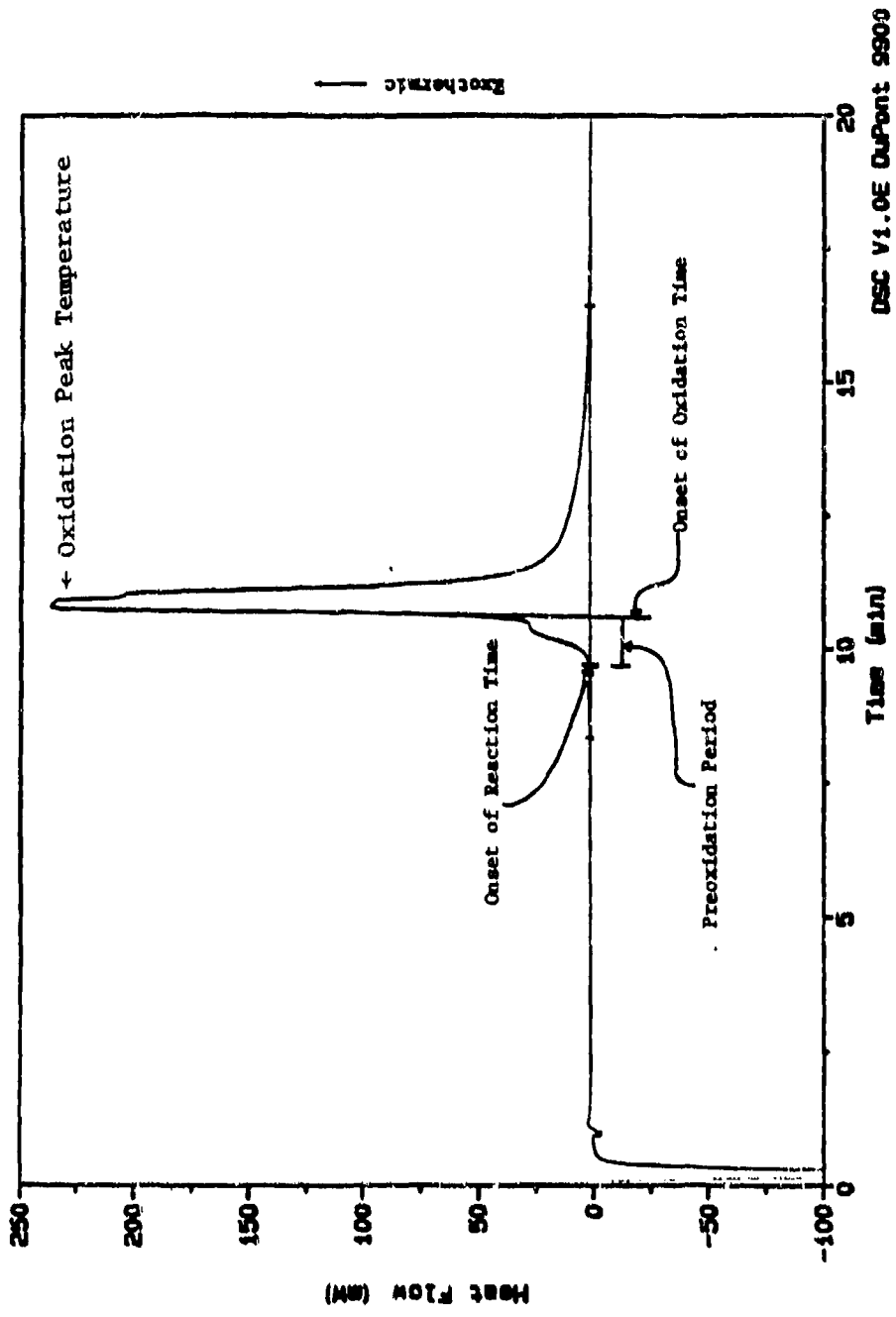


Figure 90. HP-DSC Thermogram of Fresh TEL-4003 MIL-L-7808 Oil Demonstrating Procedures Used to Determine the Onset of Oxidation Time, Onset of Reaction Time, and Preoxidation Period.

sent to DuPont for analysis on the 9000/9900 Thermal Analyzer system. The oil samples were analyzed and the onset of oxidation time, onset of reaction time, oxidation peak temperature, and peak energy (Figure 90) for each oil sample were recorded. The onset of oxidation times and onset of reaction times for each set of MIL-L-7808 lubricating oils were then plotted versus the stressing times at 370°F to determine the relationships which exist between the HP-DSC results and RLL of MIL-L-7808 oils.

(b) High Pressure-Differential Scanning  
Calorimetric Analyses of the MIL-L-7808 Oils

Six sets of oil samples representing the TEL-4001 through TEL-4006 MIL-L-7808 lubricating oils in various degrees of RLL were sent to DuPont for HP-DSC analysis. The sample designation codes (corresponding stressing time at 370°F), onset of oxidation times, oxidation peak temperature (maximum temperature of sample), and peak energies for the TEL-4001 through TEL-4006 MIL-L-7808 oils are listed in Tables 6 through 11, respectively. In each set, designation A represents a fresh oil, E represents a sample taken a few hours prior to the end of the oil's stable life at 370°F, and F and G represent samples taken after the end of the oil's stable life. The stable lives as determined by viscosity (40°C) and total acid number breakpoints (Appendix A) are also listed in Tables 6 through 11.

Although it has been suggested (Reference 43) that the peak energies of the thermograms may be related to the oxidative stability of the oil samples, Tables 6-11 indicate that there is no correlation between the peak energy and the RLL of a used MIL-L-7808 lubricating oil. The data in Tables 6 and 10 also show that the reproducibilities of the peak energies are poor.

In contrast to the peak energies, the onset of oxidation times listed in Tables 6-11 are related to the RLL of the MIL-L-7808 oils. The data for 5A and 5E listed in Table 10 shows that the standard deviation is fairly constant (~20 seconds). Since the standard deviation is constant, but the onset of oxidation times decrease with increasing stressing time, the

TABLE 6  
OIL STABILITY OF TEL-4001 MIL-L-7808 OIL

Sample Designation Code	250°C - 200 psig O <sub>2</sub>		Peak Energy (J/g)
	Onset Oxidation Time (min)	Oxidation Peak Temp (°C)	
1A (Fresh)	6.32	263	5532
	6.37	262	4223
1B (19 Hours)*	3.80	261	7320
	3.12	260	6266
1C (41 Hours)	2.64	260	5497
	2.96	259	4805
1D (67 Hours)	1.84	260	5704
	1.76	257	4095
1E (97 Hours)	1.52	259	6983
	1.48	274	4269
1F (116 Hours)	0.96	257	5645
	1.00	258	6941
1G (137 Hours)	1.00	257	5881
	1.04	257	6459

\*Stressing Time at 370°F.  
Stable Life = 105 Hours.

TABLE 7  
OIL STABILITY OF TEL-4002 MIL-L-7808 OIL

Sample Designation Code	250°C - 200 psig O <sub>2</sub>		Peak Energy (J/g)
	Onset Oxidation Time (min)	Oxidation Peak Temp (°C)	
2A. (Fresh)	6.4	262	4915
2B (16 Hours)*	6.85	263	3817
2C (48 Hours)	2.5	260	6552
2D (116 Hours)	1.52	259	6520
2E (161 Hours)	1.44	258	5977
2F (191 Hours)	1.08	260	7142
2G (213 Hours)	0.64	259	6787

\*Stressing time at 370°F.  
Stable Life = 175 hours.

TABLE 8  
OIL STABILITY OF TEL-4003 MIL-L-7808 OIL

Sample Designation Code	250°C - 200 psig O <sub>2</sub>		Peak Energy (J/g)
	Onset Oxidation Time (min)	Oxidation Peak Temp (°C)	
2A (Fresh)	10.65	260	4011
3B (24 Hours)*	11.70	260	6335
3C (72 Hours)	6.75	259	5911
3D (143 Hours)	3.10	257	4838
3E (234 Hours)	2.3	259	5653
3F (287 Hours)	2.4	258	7851
3G (352 Hours)	1.85	257	7697

\*Stressing Time at 370°F.  
Stable Life = 240 Hours.

TABLE 9  
OIL STABILITY OF TEL-4004 MIL-L-7808 OIL

Sample Designation Code	250°C - 200 psig O <sub>2</sub>		Peak Energy (J/g)
	Onset Oxidation Time (min)	Oxidation Peak Temp (°C)	
4A (Fresh)	7.90	261	3208
4B (16 Hours)*	7.50	259	3047
4C (48 Hours)	5.70	257	2793
4D (116 Hours)	2.30	259	4190
4E (169 Hours)	2.55	258	3896
4F (213 Hours)	1.80	257	5211
4G (241 Hours)	1.00	259	3789

\*Stressing Time at 370°F.  
Stable Life = 205 Hours.

TABLE 10  
OIL STABILITY OF TEL-4005 MIL-L-7808 OIL

Sample Designation Code	250°C - 200 psig O <sub>2</sub>		Peak Energy (J/g)
	Onset Oxidation Time (min)	Oxidation Peak Temp (°C)	
5A-1 (Fresh)	4.96	258	2016
-2	5.75	266	3013
-3	5.5	263	2614
-4	5.5	264	5549
Mean X	<u>5.45</u>	<u>263</u>	<u>2846</u>
Std. Dev.	<u>+0.3</u>	<u>+3.4</u>	<u>+2189</u>
5B (19 Hours)*	5.4	265	6044
5C (50 Hours)	2.4	262	4034
5D (97 Hours)	1.6	260	6953
5E-1 (137 Hours)	1.2	260	7939
-2	1.5	259	6339
-3	1.0	259	6841
Mean X	<u>1.2</u>	<u>259</u>	<u>7040</u>
Std. Dev.	<u>+0.3</u>	<u>+0.6</u>	<u>+818</u>
5F (166 Hours)	1.2	259	6475
5G (187 Hours)	1.0	260	5084

\*Stressing Time at 370°F.  
Stable Life = 155 Hours.

TABLE 11  
OIL STABILITY OF TEL-4006 MIL-L-7808 OIL

Sample Designation Code	250°C - 200 psig O <sub>2</sub>		Peak Energy (J/g)
	Onset Oxidation Time (min)	Oxidation Peak Temp (°C)	
6A (Fresh)	10.8	265	4749
6B (19 Hours)*	8.4	264	5285
6C (67 Hours)	6.2	267	2438
6D (148 Hours)	2.5	261	4648
6E (265 Hours)	1.65	259	5277
6F (354 Hours)	1.7	258	6901
6G (382 Hours)	1.7	258	2702

\*Stressing Time at 370°F.

Stable Life = 320 Hours.

percent error of the analyses for the TEL-4005 oil increases from 5% to 30% with increasing stressing time.

To initially study the relationships which exist between the HP-DSC onset of oxidation times and the remaining useful lives of the MIL-L-7808 oils, the onset of oxidation time for each oil sample was plotted versus its corresponding stressing time at 370°F. The plots for the TEL-4001 through TEL-4006 MIL-L-7808 oils are shown in Figure 91.

The plots of the MIL-L-7808 oils' onset of oxidation times in Figure 91, show that the oxidative stabilities of the fresh MIL-L-7808 oils and the rate at which they decrease with stressing time at 370°F, decrease in the order: TEL-4003 ~ TEL-4006 > TEL-4004 > TEL-4002 ~ TEL-4005 > TEL-4001. The order of oxidative stabilities are in fair agreement with the results of the 370°F stressing results.

However, the high temperature (250°C) conditions of the HP-DSC technique reduce the sensitivity of the HP-DSC technique to small changes in the oxidative stabilities of the MIL-L-7808 oils in the latter stages of their stable lives. For instance, the onset of oxidation times are similar for the TEL-4006 oil samples taken 60 hours prior to and 60 hours after the end of the TEL-4006 oil's stable life at 370°F.

Another problem in predicting RLL from the HP-DSC data is that the onset of oxidation time for the TEL-4001 oil with 0% RLL is 1.0 minute, while the onset of oxidation time for the TEL-4003 oil with 0% RLL is 2.4 minutes (Figure 91). The 2.4 minute onset of oxidation time corresponds to the TEL-4001 oil which was stressed for only 41 hours at 370°F (stable life = 105 hours). Therefore, the assignment of 0% RLL to a particular onset of oxidation time is not straight forward.

Since HP-DSC measures both the antioxidant capacity and the oxidative stability of the ester basestock and the RCV results indicate that the antioxidant capacities of the oils with 0% RLL are similar, the oxidative stabilities of the ester basestocks used in the MIL-L-7808 oils, which are expected

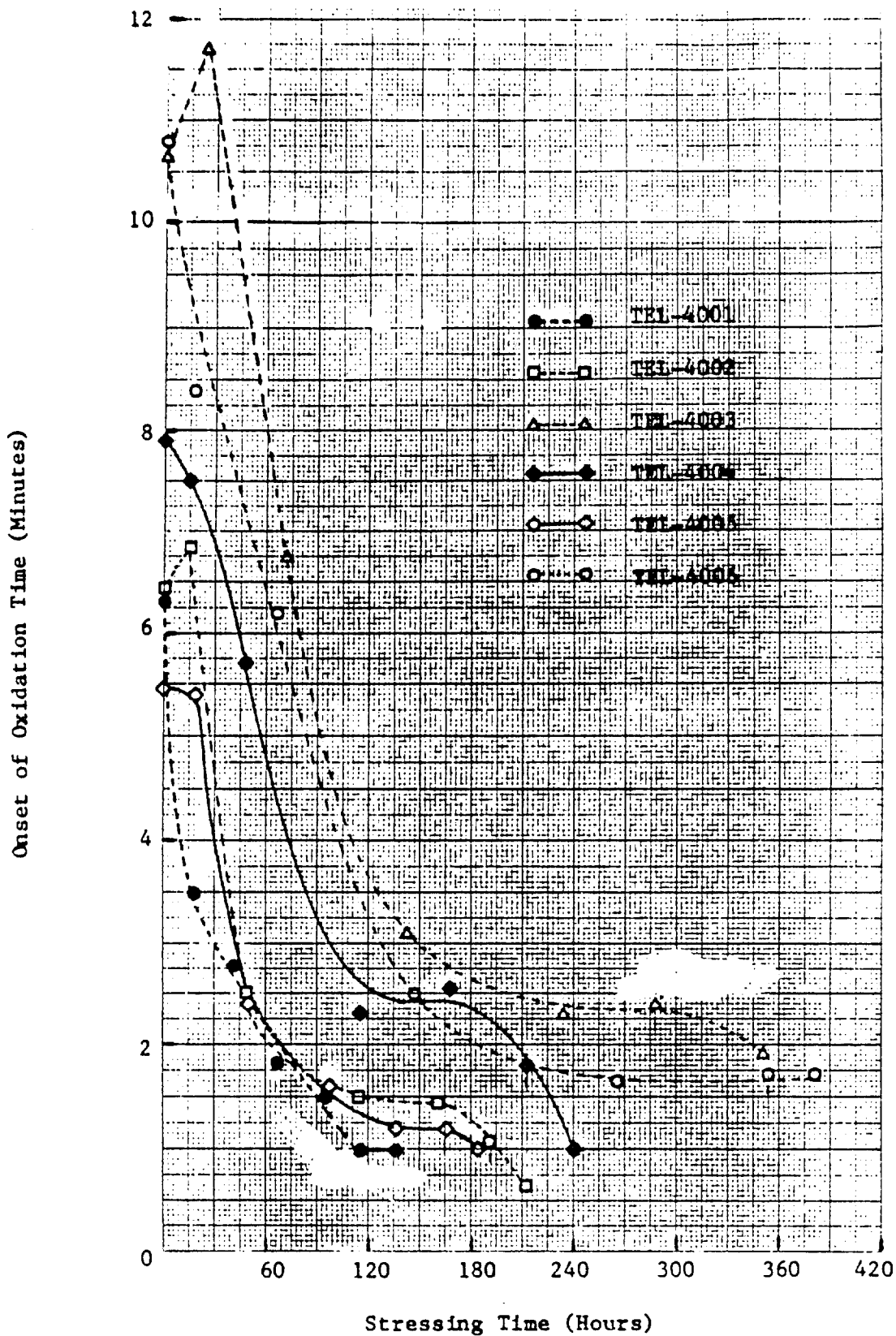


Figure 91. Plots of the HP-DSC Onset of Oxidation Time Versus Stressing Time at 370°F for the TEL-4001 Through TEL-4006 MIL-L-7808 Oils.

to be different, appear to be complicating the interpretation of the HP-DSC results.

Another problem in assessing RLL from the HP-DSC data is that the onset of oxidation time for the TEL-4002 and TEL-4003 oils increase during the initial stages of oxidation (Figure 91). Similar results have been reported for the HP-DSC analyses of MIL-L-7808 type oils (References 2 and 17) and were attributed to the thermal-oxidative generation of new antioxidant species [CV analyses (Figures 58-63) also identified the presence of new antioxidant species in the stressed MIL-L-7808 oils]. The increase in oxidative stabilities complicates the RLL assessment of slightly degraded lubricants.

(c) Linearizing the HP-DSC Onset of Oxidation Time Plots

In an attempt to better understand the relationships between the onset of oxidation time and the RLL of a MIL-L-7808 oil, the  $\ln$ , inverse, and inverse squared of the onset of oxidation time representing first, second, and third order reactions, respectively, were plotted versus stressing time at 370°F. The plots of the TEL-4001 through TEL-4006 oils are shown in Figures 92-94.

Although none of the different mathematical relationships produce linear plots, the  $\ln$  of the onset of oxidation time versus stressing time plots appear to be the most linear. Again, the increase in the oxidative stability of the oils during early oxidation and the insensitivity to differences in the oxidation stabilities of badly degraded oils limits the linearity, and consequently, the RLL assessing capabilities of the HP-DSC results.

(d) Linearizing the HP-DSC Onset of Reaction Time Plots

Since it appeared that the different oxidation stabilities of the ester basestocks used in the MIL-L-7808 oils were affecting the RLL assessment capabilities of the HP-DSC technique, the HP-DSC results were reanalyzed. Instead of using

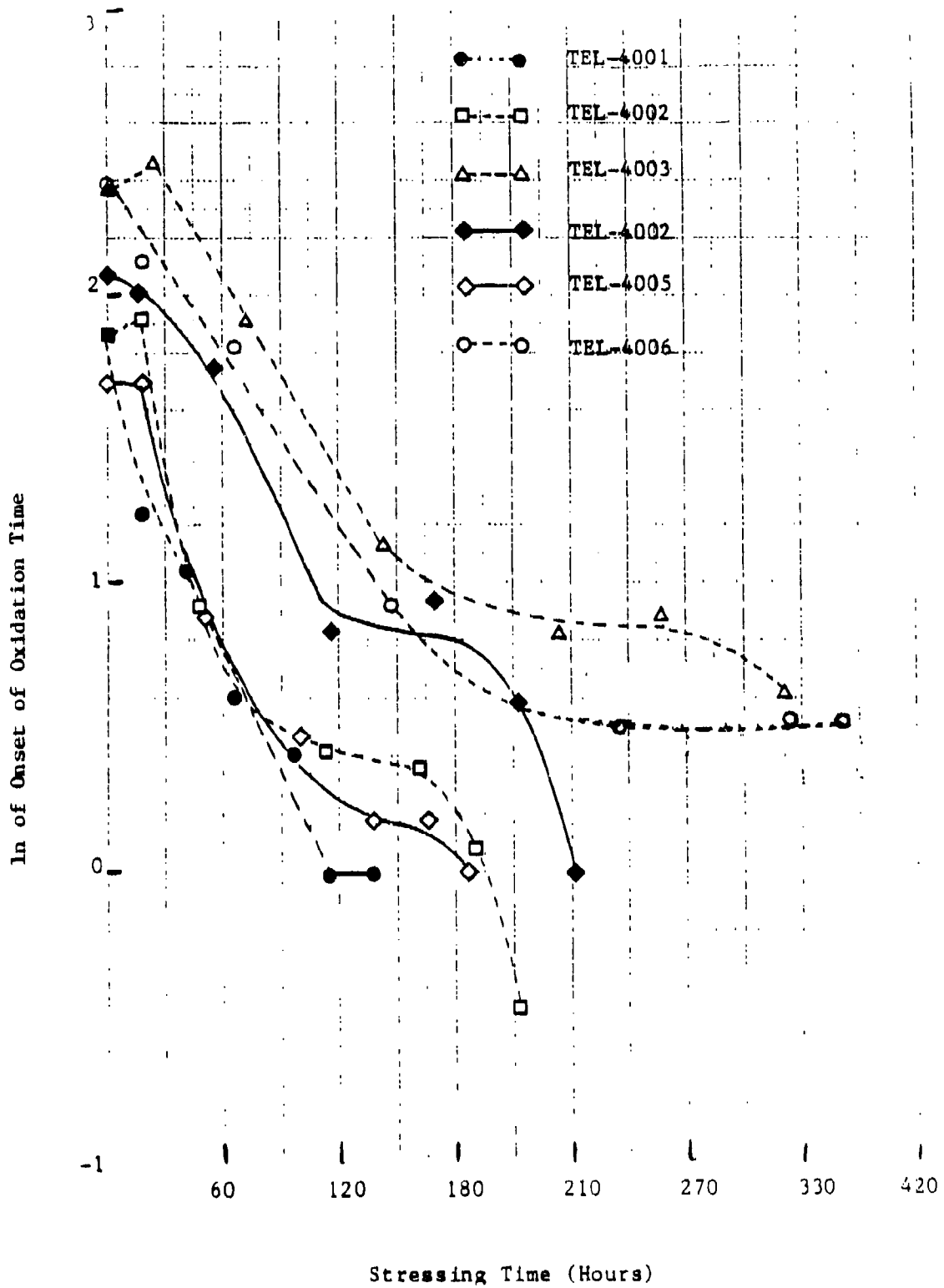


Figure 92. Plots of the ln of the Onset of Oxidation Time Versus Stressing Time at 370°F for the TEL-4001 Through TEL-4006 MIL-L-7808 Oils.

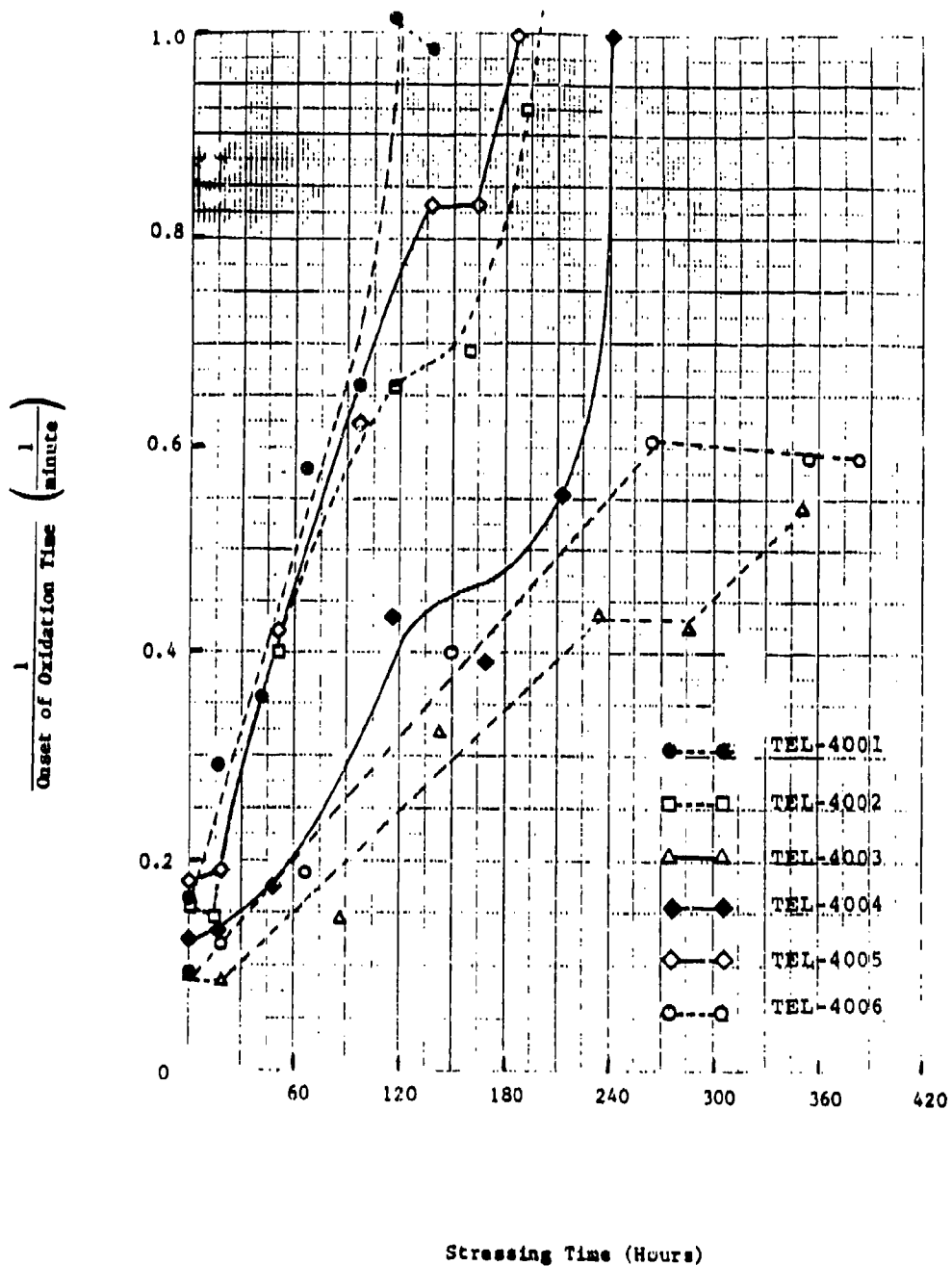


Figure 93. Plots of the Inverse of the Onset of Oxidation Time Versus Stressing Time at 370°F for the TEL-4001 Through TEL-4006 MIL-L-7808 Oils.

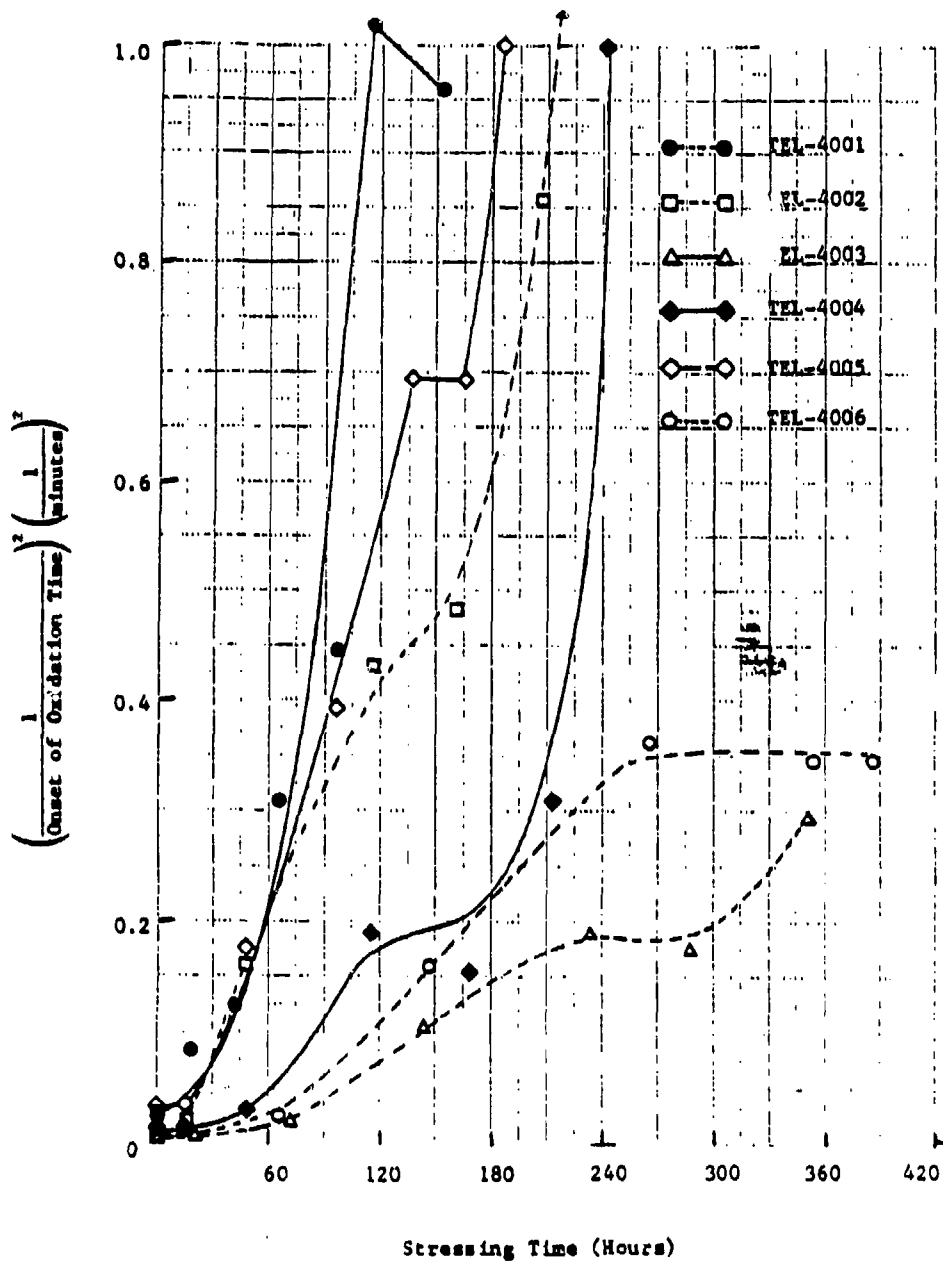


Figure 94. Plots of the Inverse Squared of the Onset of Oxidation Time Versus Stressing Time at 370°F for the TEL-4001 Through TEL-4006 MIL-L-7808 Oils.

the onset of oxidation time determined from the large exothermic peak in Figure 90 produced by the oxidation of the ester basestock, the onset of reaction time determined from the initiation of the small exothermic peak in Figure 90 was used. It was postulated that the initiation of the small exothermic peak in Figure 90 occurred when the antioxidant capacity of the oil sample was depleted, and thus, was independent of the ester basestock.

To determine the RLL assessing capabilities of the onset of reaction times, the onset of reaction times for the MIL-L-7808 oils were plotted versus hours of remaining lubricant life as shown in Figure 95. Although the preoxidation period decreased with increasing stressing time, the preoxidation period was very formula dependent and decreased in a random manner, and thus, was eliminated from further consideration.

The plots of the onset of reaction times for the TEL-4001 through TEL-4006 oils versus remaining hours of lubricant life shown in Figure 95 indicate that the onset of reaction time is strongly related to RLL.

In contrast to the onset of oxidation times (Figure 92) which vary from 2.5 to 1.0 minutes at the ends of the MIL-L-7808 oils' stable lives, the onset of reaction times (Figure 95) vary only from 1.1 to 0.9 minutes at the ends of the MIL-L-7808 oils' stable lives, and thus, a 0% RLL value can be assigned.

In an attempt to obtain a linear relationship between the onset of reaction time and RLL, the  $\ln$  values of the onset of reaction times were plotted versus remaining hours of lubricant life as shown in Figure 96.

The  $\ln$  plots of the onset of reaction times shown in Figure 96 are linear after the first hours of stressing down to a  $\ln$  value of approximately 0.2 (onset of reaction time = 1.2 minutes). Therefore, if 0% RLL is assigned to a  $\ln$  value of 0.2 and 100% RLL to a  $\ln$  value to 2.20 (fresh TEL-4006 oil),

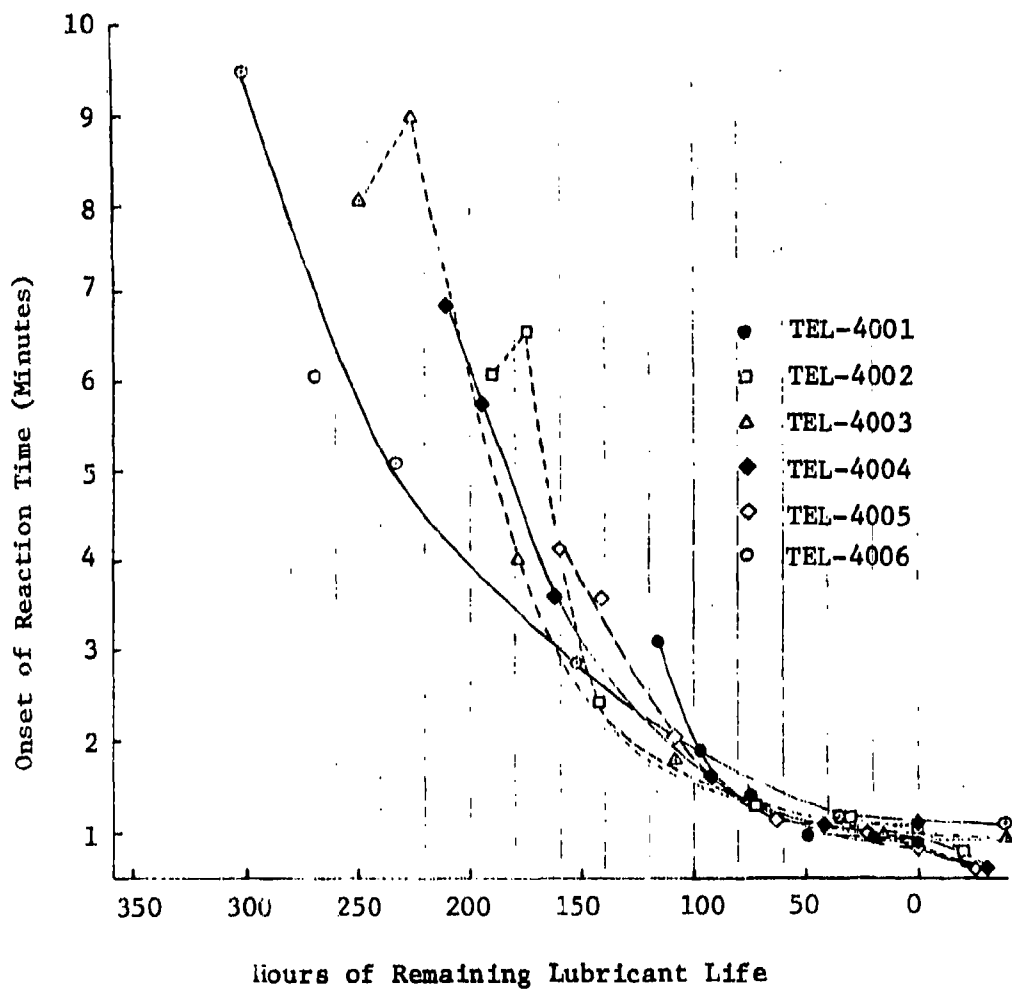


Figure 95. Plots of the HP-DSC Onset of Reaction Time Versus Remaining Lubricant Life at 370°F for the Fresh and Stressed MIL-L-7808 Oils.

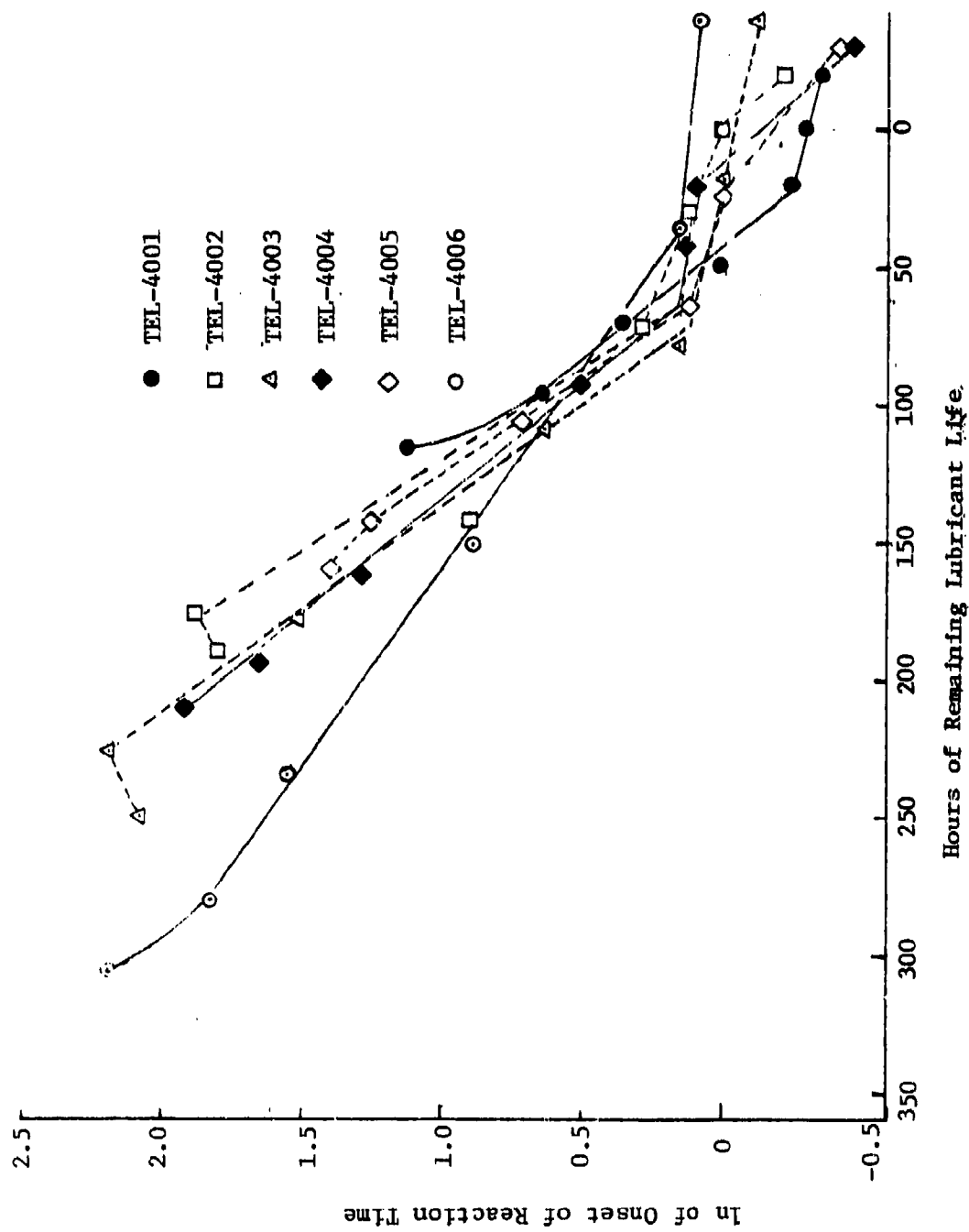


Figure 96. Plots of the ln of the HP-DSC Onset of Reaction Time Versus Remaining Lubricant Life at 370°F for the Fresh and Stressed MIL-L-7808 Oils.

percent RLL can be determined from the  $\ln$  values of the onset of reaction times.

However, the onset of reaction times result in conservative 0% RLL assessments for the MIL-L-7808 oils. The 0% RLL occur approximately 60 hours prior to the ends of the MIL-L-7808 oils' stable lives. Although an analysis temperature lower than 250°C would be expected to decrease the conservative nature of the HP-DSC results, a lower analysis temperature would result in analysis times greater than the criteria time limit (Table 1) of 10 minutes.

In spite of the conservative nature of the onset of reaction times, they make the HP-DSC technique suitable for development into a RLLAT. In fact, the conservative nature of the onset of reaction times may be advantageous in that it provides the analyst with a safety buffer for incorrect RLL assessments.

### (3) Sealed Pan-Differential Scanning Calorimetry

#### (a) Introduction

In addition to the HP-DSC studies, a sealed pan-DSC (SP-DSC) technique was developed which eliminated the high pressure requirements of the HP-DSC technique. The effects of the sample pan, sample size, atmosphere, oxidizing agents, initial temperature, and heating rates on the analysis times of the SP-DSC were studied to obtain analysis times of less than ten minutes. To fully evaluate the SP-DSC technique, sets of fresh and stressed (370°F) MIL-L-7808 lubricating oils, TEL-4001 through TEL-4006, were analyzed. The onset of oxidation times and the peak heights were recorded for each oil sample. The onset of oxidation time was then plotted versus stressing time at 370°F for each oil sample to determine the relationships which exist between the SP-DSC results and the RLL of the MIL-L-7808 oil samples.

#### (b) Effect of Sample Pan

Two types of sample pans were studied during the SP-DSC investigation. The first sample pan investigated was a

high pressure (200 psi internal pressure), sealable pan consisting of two threaded, stainless steel capsules which are sealed with a copper ring. When the DSC analyses were run using the stainless steel capsules, small (less than 0.25 mW) endothermic baseline shifts (Figure 97) were produced, in complete contrast to the large (greater than 200 mW) exothermic peaks (Figure 90) produced by the HP-DSC technique. However, when hermetically sealable pans (withstand 50 psi internal pressure), consisting of two sealable aluminum pans, were used for the DSC analysis, a small (less than 5 mW) exothermic peak was produced in agreement with the HP-DSC results.

It is well known that during long term oxidation studies, steel catalyzes oil oxidation (Reference 44). Therefore, since the HP-DSC technique uses aluminum pans, it appears that the stainless steel surface of the high pressure, threaded pans is reacting with the oil sample causing the differences between the HP-DSC and SP-DSC results.

Due to the apparent reaction between the stainless steel surface of the high pressure, threaded pan and the oil sample, the high cost of the threaded, stainless steel pan (\$300) makes it unsuitable for routine use, and consequently, for use in a RLLAT.

Therefore, all of the development research on the SP-DSC technique was performed using the hermetically-sealed aluminum pans.

#### (c) Effect of Sample Size

To determine the effect of sample size on the SP-DSC results, sample sizes of 0.2 to 2.0  $\mu$ l were used for a stressed TEL-4006 oil sample (stressed 194 hours at 370°F). Although sample sizes larger than 1.5  $\mu$ l did not produce discernable DSC signals, the thermograms in Figure 98 indicate that the air inside the hermetically sealed pan is adequate to produce a discernible DSC signal for oil sample sizes of less than 1.5  $\mu$ l. In fact, the produced DSC signal is greatest for the 0.2  $\mu$ l sample, indicating that sample sizes, smaller than 0.2  $\mu$ l would

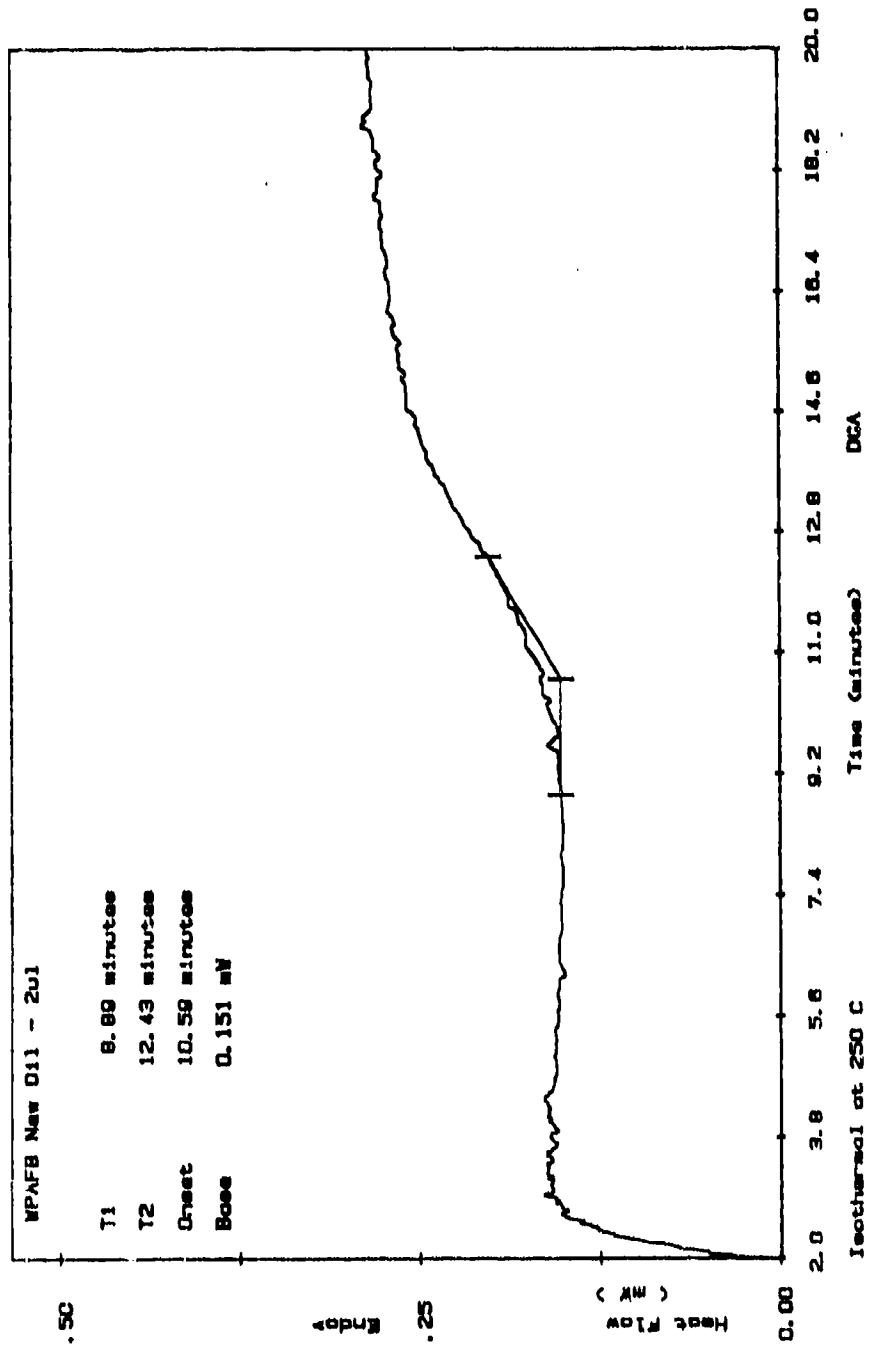


Figure 97. SP-DSC Thermogram of Fresh TEL-4006 MIL-L-7808 Oil Performed in the Stainless Steel Capsule.

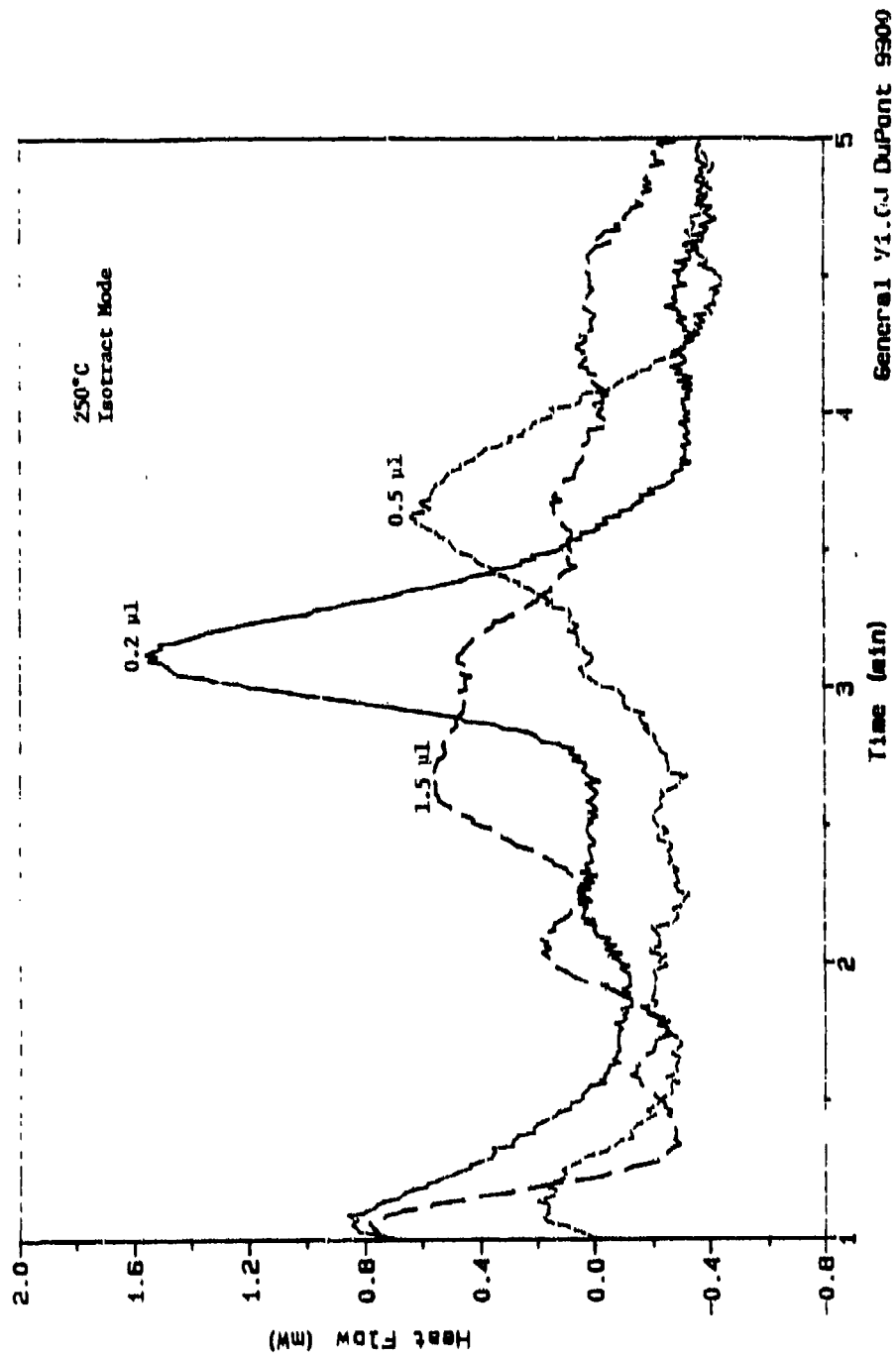


Figure 98. Effect of Sample Size on the SP-DSC (in air) Thermogram (250°C) of a Stressed (194 Hours at 370°F) TEL-4006 MIL-L-7808 Oil.

yield even larger DSC signals. However, 0.2  $\mu$ l is the smallest sample that could be dispensed with accuracy. Therefore, unless stated otherwise, 0.2  $\mu$ l samples were used during the rest of the SP-DSC study.

(d) Effect of Oxidizing Substances

Although the exotherms produced by the stressed TEL-4006 oil sample (Figure 98) are easily discernible, no discernible peaks were produced by the fresh or slightly stressed (less than 100 hours at 370°F) TEL-4006 oil samples. The fresh TEL-4001 and TEL-4005 oil samples also did not produce discernible peaks. Thus, it appeared that a catalyst was needed to produce discernible peaks for fresh and slightly stressed MIL-L-7808 oil samples. Therefore, oxidizing substances were added to the oil sample in the DSC pan prior to analysis. The first oxidizing substance tested was  $\text{LiClO}_4$ , but no discernible peaks were produced for the fresh TEL-4006 oil.

The next oxidizing substance studied was cumene hydroperoxide. A 10 percent solution of cumene hydroperoxide was prepared in benzaldehyde (easily oxidizable substance). A 1  $\mu$ l sample of the cumene hydroperoxide/benzaldehyde solution was placed in the DSC pan and hermetically sealed. The exotherm produced by the solution is shown in Figure 99. Although, the presence of fresh TEL-4006 oil inhibited the exotherm produced by the cumene hydroperoxide/benzaldehyde solution (Figure 99), a later discernible peak was not produced. Since the size of the exotherm is dependent upon numerous factors, e.g., cumene hydroperoxide concentration, amount of cumene hydroperoxide/benzaldehyde solution, sample size of oil, etc., the size of the exotherm could not be used for reliable RLL assessments.

The next oxidizing substances studied were the hydroperoxides present in an aged TEL-4005 oil sample (Figure 49) which had been stressed 180 hours at 370°F and had 0 percent remaining lubricant life (stable life at 370°F=155 hours). The exotherm produced at 250°C (isothermal) by the aged TEL-4005 oil

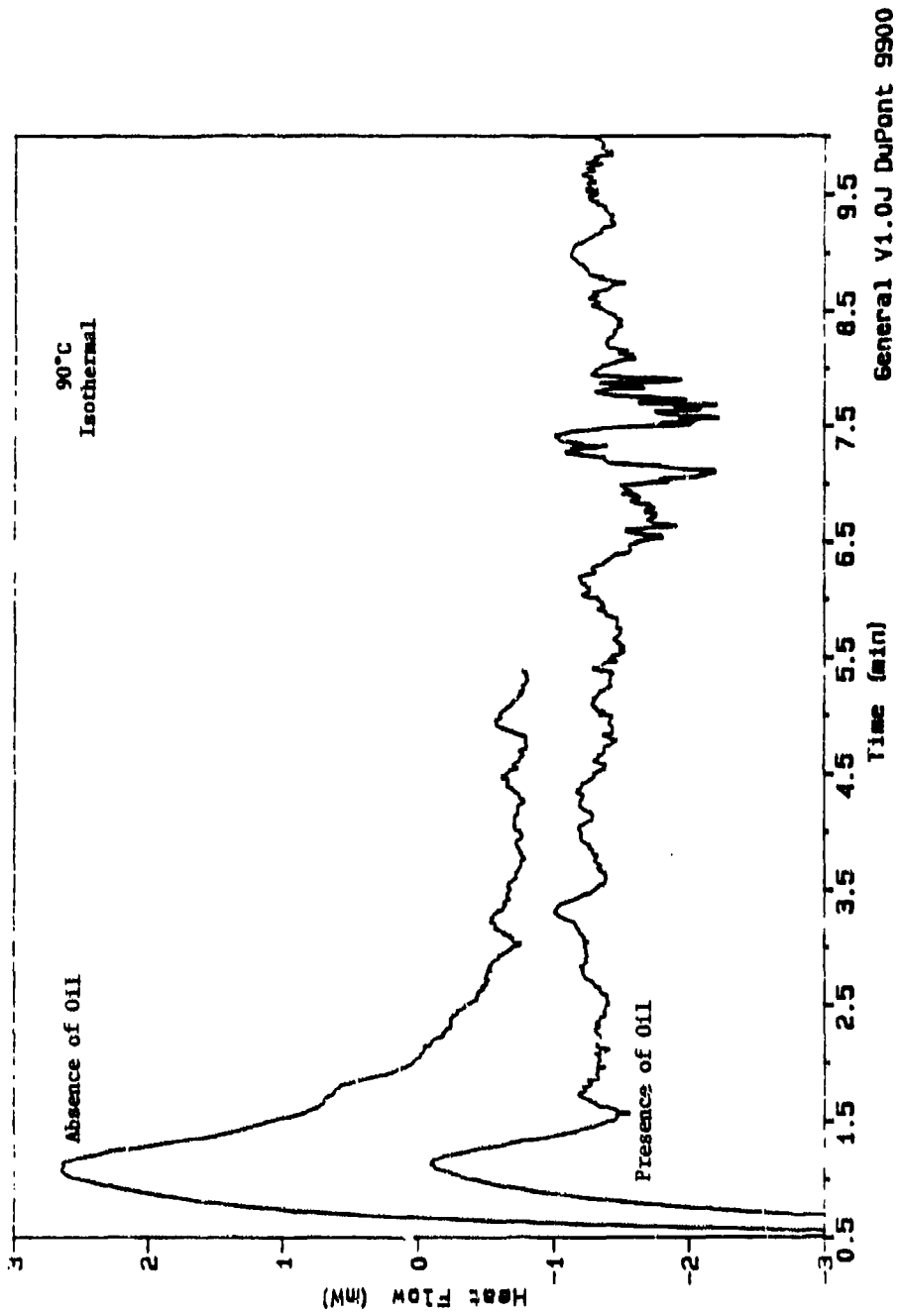


Figure 99. Effect of Fresh TEL-4004 MIL-L-7808 Oil on the Thermogram (90°C - Isothermal) of a 10 Percent Cumene Hydroperoxide in Benzaldehyde Solution.

sample is shown in Figure 100. Although the addition of fresh TEL-4005 and TEL-4004 oils inhibited the exotherm of the aged TEL-4005 oil (Figure 100), stressed TEL-4005 and TEL-4004 oils had no effect on the exotherm produced by the aged TEL-4005 sample.

(e) Effect of Oxidizing Atmosphere

To test the effect of an oxidizing atmosphere on the SP-DSC results, the DSC pans were sealed under an atmosphere of oxygen inside a glove bag. The exotherms for a stressed TEL-4006 oil sample (194 hours at 370°F) produced under air and oxygen atmospheres at 250°C (isothermal) are shown in Figure 101. The presence of oxygen shortened the onset of oxidation time from 2.7 minutes to 0.8 minutes and increased the size of the exotherm. The presence of oxygen also produced a discernible exotherm for fresh TEL-4006 oil (Figure 101).

Although the exotherm produced in the oxygen atmosphere is larger than the exotherm produced in the air atmosphere, it is much smaller than the exotherm produced under 200 psi of oxygen at 250°C (Figure 102). Thus, it appears that the oxygen atmosphere sealed in the DSC pan is sufficient to initiate the oxidation of the oil sample, but is not enough to produce the complete oxidation of the oil sample, as obtained under 200 psi in the HP-DSC technique. In the sealed pan of the SP-DSC technique the fresh TEL-4006 oil sample was still a liquid and only slightly darkened after analysis (incomplete oxidation), but the oil was completely oxidized in the open pan of the HP-DSC resulting in a dark brown solid.

Therefore, the results of the SP-DSC technique using the oxygen atmosphere should be similar to those obtained from the onset of reaction times (Figure 90) of the HP-DSC produced exotherms (Figure 96), and thus, the RLL assessments of the SP-DSC technique should be affected very little by the formulation differences of the TEL-4001 through TEL-4006 MIL-L-7808 lubricating oils.

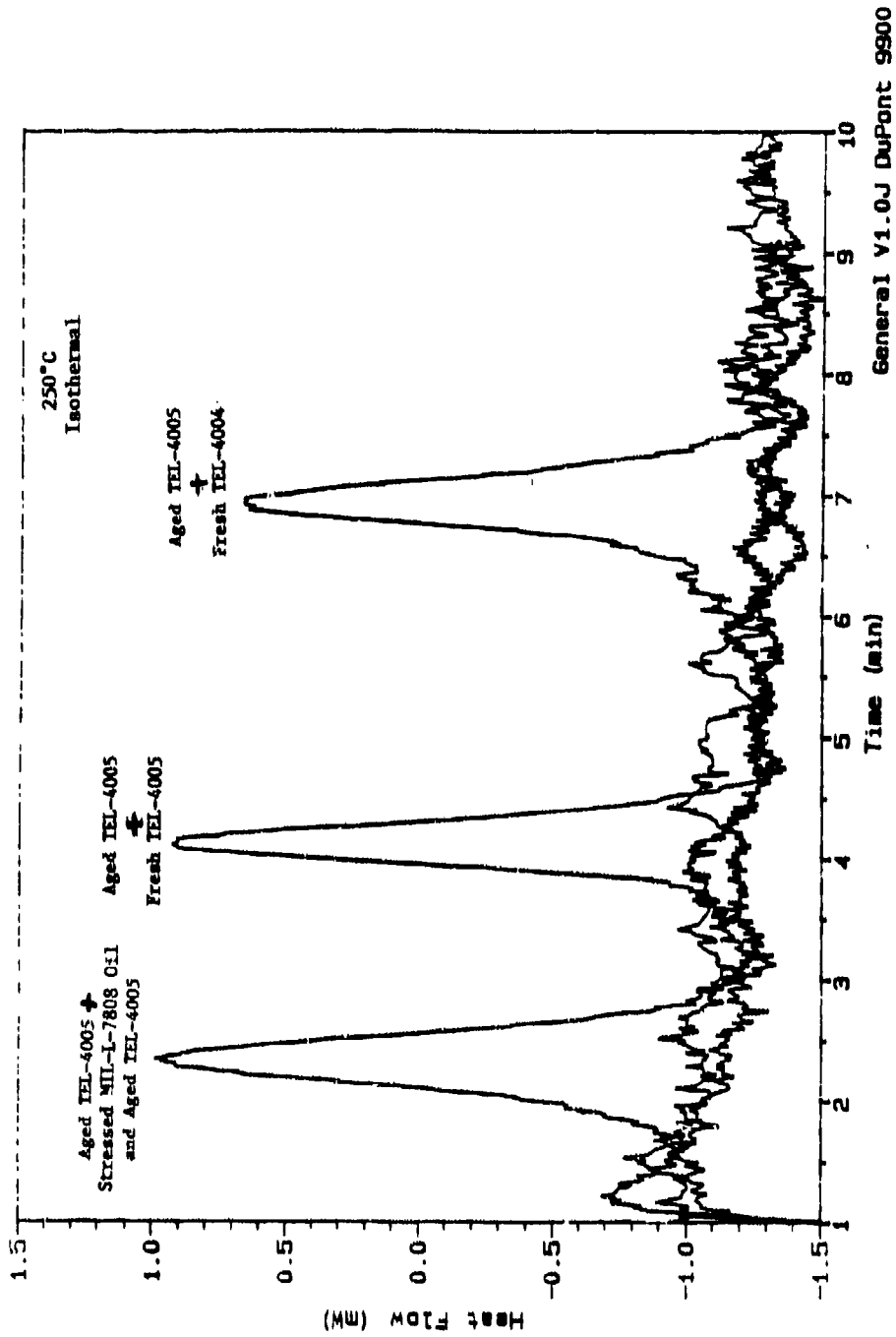


Figure 100. Effects of Fresh TEL-4004 and TEL-4005 MIL-L-7808 Oils on the Thermogram (250°C - Isothermal) of a Aged (180 Hours at 370°F) TEL-4005 MIL-L-7808 Oil.

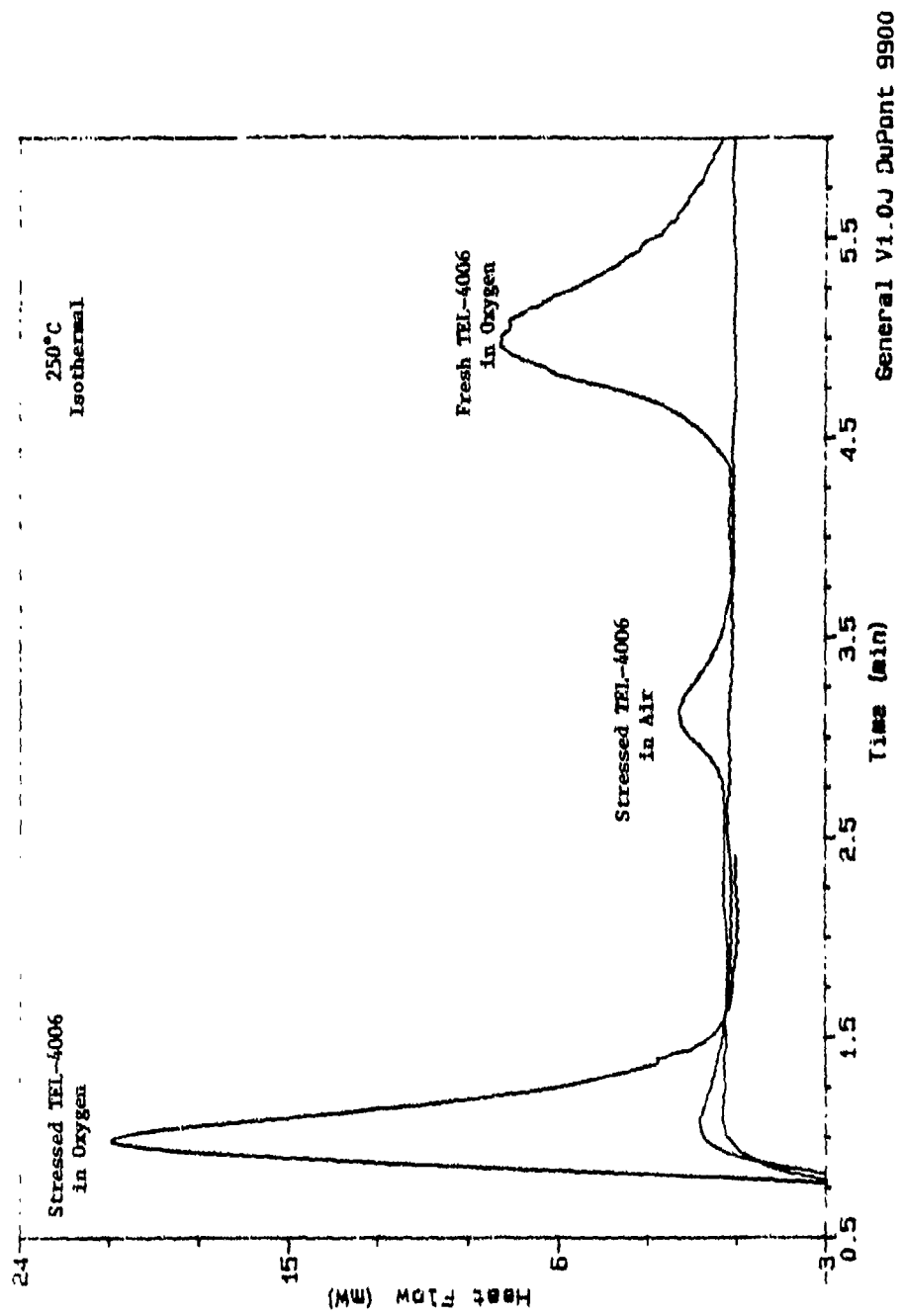


Figure 101. Effect of an Oxygen Atmosphere on the SP-DSC Thermograms (250°C) of Fresh and Stressed (194 Hours at 370°F) TEL-4006 MIL-L-7808 Oils.

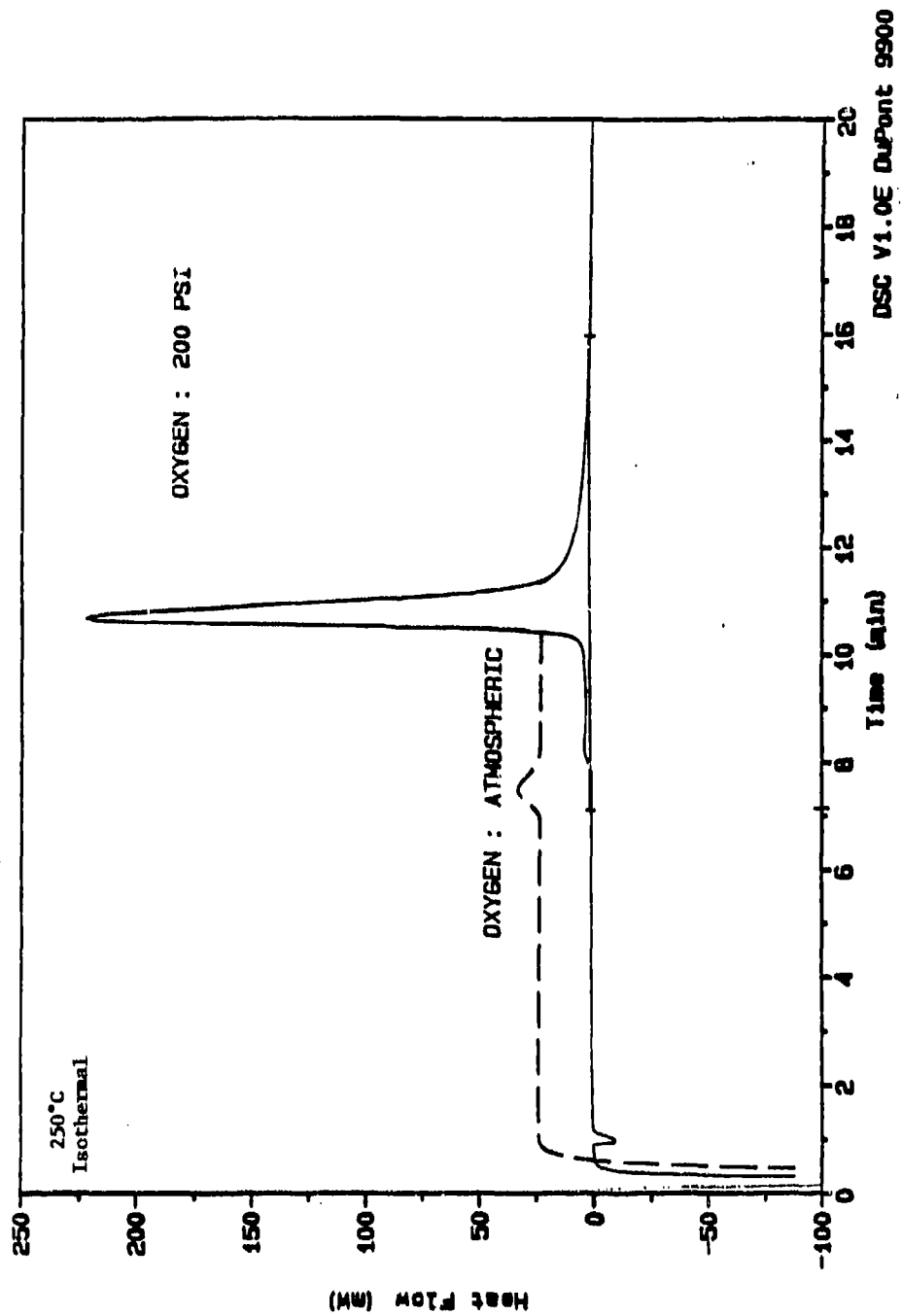


Figure 102. Effect of Oxygen Pressure on the Thermogram (250°C - Isothermal) of the Fresh TEL-4006 MIL-L-7808 Oil.

(f) Effect of Initial Temperature

Although the TEL-4006 oil stressed 194 hours at 370°F (stable life = 320 hours) still has RLL, it produces an exotherm at 250°C with an onset of oxidation time (Figure 101) of approximately 0.8 minutes. Also, the exotherm of fresh TEL-4006 oil (which has the longest stable life at 370°F) should occur at approximately 10 minutes to obtain the most accurate RLL assessments; however, it occurs at approximately 5 minutes. Therefore, the SP-DSC stressing temperature of 250°C is too high when an oxygen atmosphere is used.

To determine the effect of the initial temperature on the exotherm of the stressed (305 hours at 370°F) TEL-4006 oil with 0% RLL, the initial temperatures of 230, 235, and 240°C were studied. The exotherms produced by the stressed TEL-4006 oil at the different initial temperatures are shown in Figure 103.

The exotherms for the stressed TEL-4006 oil (Figure 103) indicate that an initial temperature of 230°C would increase the capability of the SP-DSC technique to distinguish between oil samples with limited RLL. However, an exotherm was not produced in the required 10 minutes for the fresh TEL-4006 oil at 230°C (isothermal). Therefore, a heating rate of 3°C/minute was used to shorten the onset of oxidation times for fresh MIL-L-7808 oils. After holding at 230°C for 1 minute, the temperature was increased at 3°C/minute to produce an exotherm for the fresh TEL-4006 oil with an onset of oxidation time of 9.6 minutes (Figure 104).

(g) Sealed Pan-Differential Scanning Calorimetric Analyses of the MIL-L-7808 Oils

To evaluate the SP-DSC technique with an oxygen atmosphere, fresh and stressed (370°F) MIL-L-7808 lubricating oils were analyzed using an initial temperature of 230°C (isothermal for 1 minute) followed by a 3°C/minute ramp for 10 minutes (230°

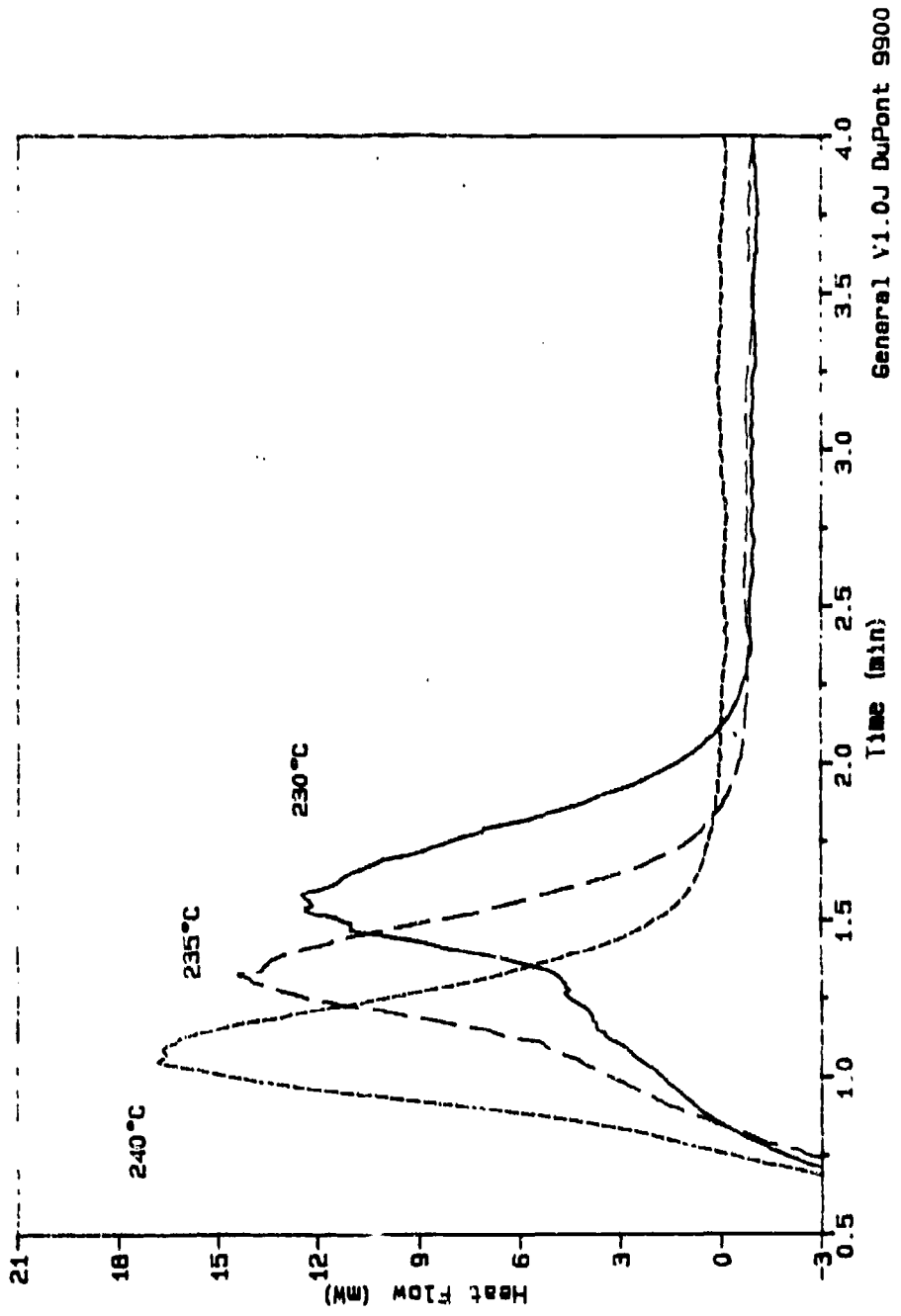


Figure 103. Effect of Initial Temperature on the SP-DSC (in Oxygen) Thermogram of a Stressed (305 Hours at 370°F) TEL-4006 MIL-L-7808 Oil.

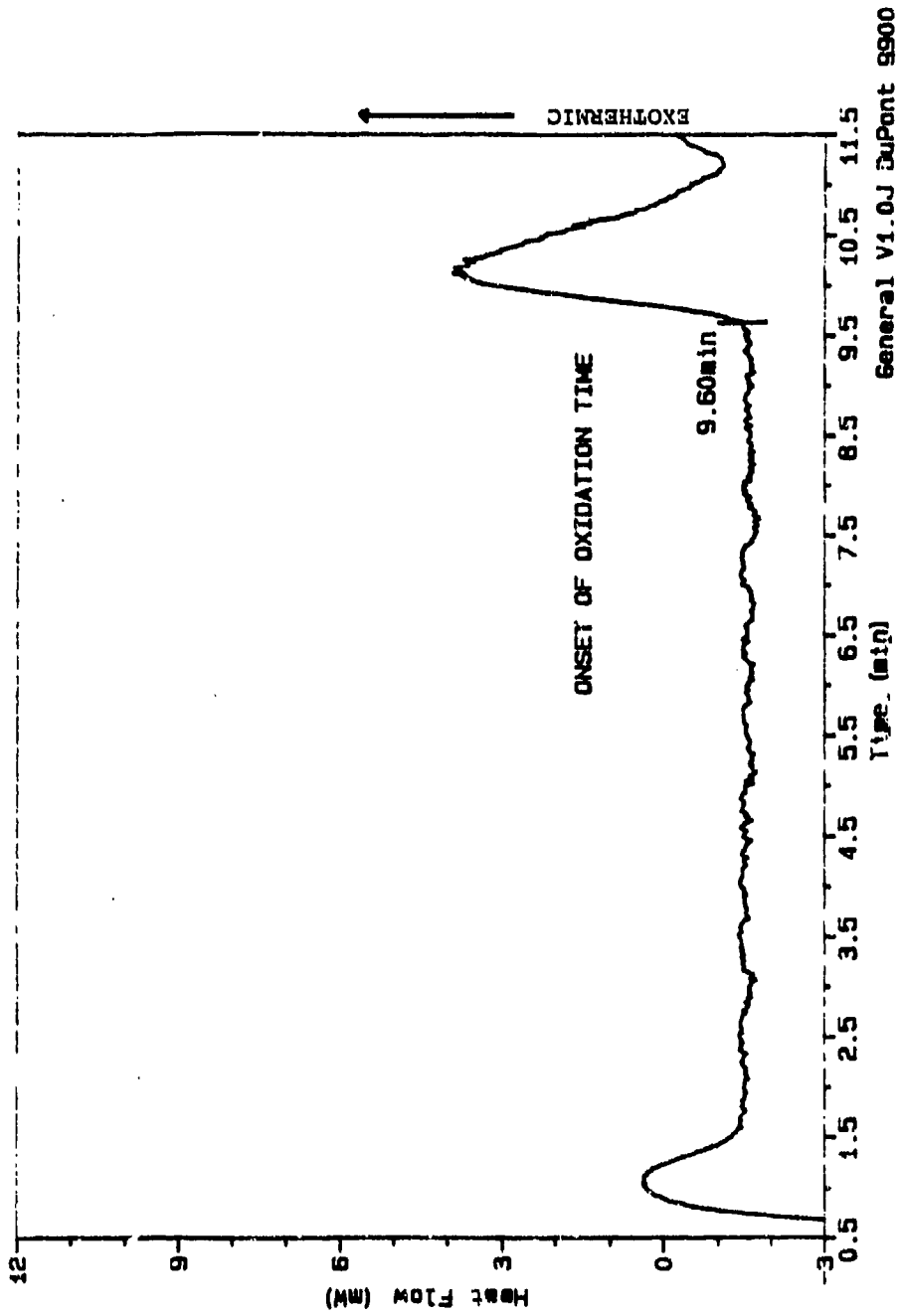


Figure 104. SP-DSC Thermogram (230°C - 3°C/Min.) of the Fresh TEL-4006 MIL-L-7808 Oil Demonstrating the Determination of the Onset of Oxidation Time.

to 260°C). The exotherms produced by the fresh and stressed TEL-4001 through TEL-4006 MIL-L-7808 oils are shown in Figures 105-110, respectively.

The exotherms shown in Figures 105-110 indicate that after the first 24 hours of stressing there is a direct relationship between the RLL of the MIL-L-7808 oil samples and the SP-DSC results, i.e., the onset of oxidation times decrease with stressing time at 370°F.

During the first 24 hours of stressing, the onset of oxidation times remain fairly constant for the TEL-4002 through TEL-4005 oils (Figures 106-109), but decrease for the TEL-4001 and TEL-4006 oils (Figures 105-110). Similar results were obtained by the HP-DSC (Figure 91). Therefore, it appears that the oils containing PANA and DODPA, TEL-4002 through TEL-4005 oils, actually increase in oxidative stability during the early stages of oxidation. While, the oxidative stabilities of the oils containing octyl-PANA and DODPA, TEL-4001 and TEL-4006 oils, decrease with stressing time regardless of the stage of oxidation.

To initially study the relationships which exist between the onset of oxidation times of the SP-DSC technique and the RLL of the MIL-L-7808 oils, the onset of oxidation time for each oil sample was plotted versus its corresponding stressing time at 370°F. The plots for the TEL-4001 through TEL-4006 MIL-L-7808 oils are shown in Figure 111.

The plots of the MIL-L-7808 oils' onset of oxidation times in Figure 111, show that the SP-DSC determined oxidation stabilities of the fresh MIL-L-7808 oils decrease in the order: TEL-4006>TEL-4003>TEL-4004\*TEL-4002>TEL-4005>TEL-4001. This order of oxidation stabilities agrees well with the results of the HP-DSC technique (Figure 91) and of the Federal Test Method Standard 791 Method 5307.1 (Appendix A).

The plots of the MIL-L-7808 oils' SP-DSC onset of oxidation times in Figure 111, also show that the onset of oxidation times for the MIL-L-7808 oil samples with 0% RLL (taken after end of stable life at 370°F) range between 0.9-1.6 minutes.

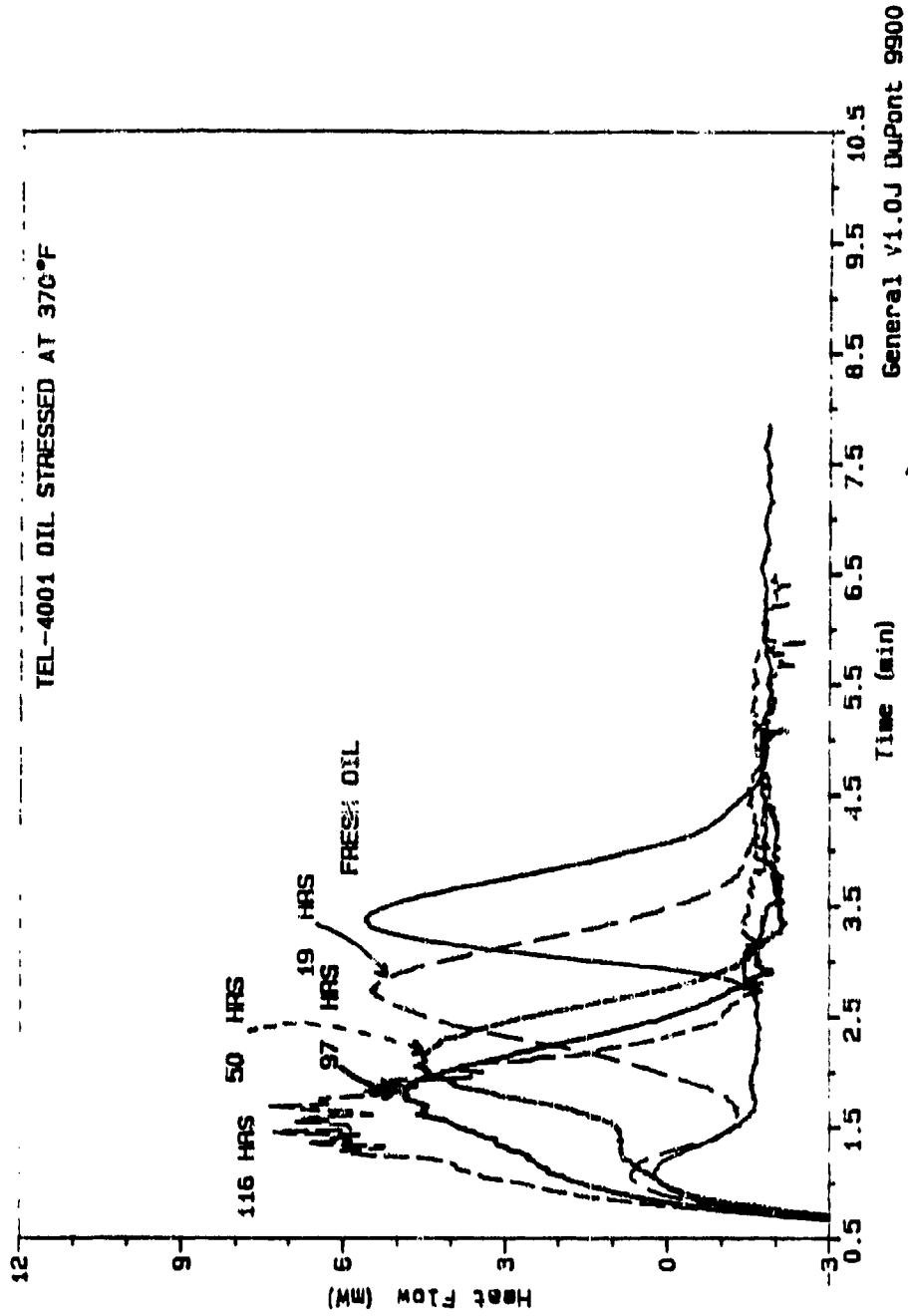


Figure 105. SP-DSC (in Oxygen) Thermograms (230°C - 3°C/Min.) of Fresh and Stressed (19-116 Hours at 370°F) TEL-4001 MIL-L-7808 Oils.

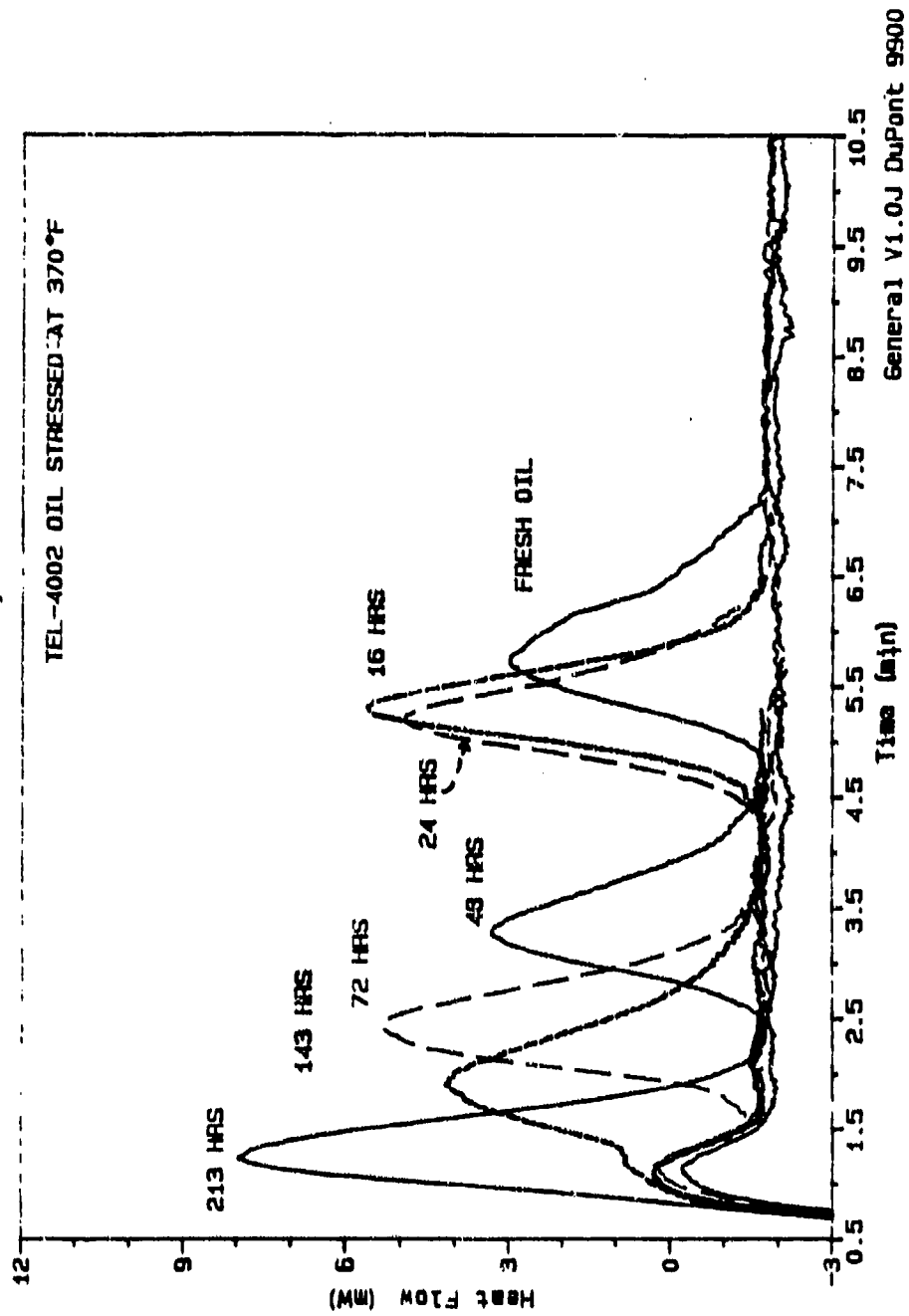


Figure 106. SP-DSC (in Oxygen) Thermograms (230°C - 3°C/Min.) of the Fresh and Stressed (16-213 Hours at 370°F) TEL-4002 MIL-L-7808 Oils.

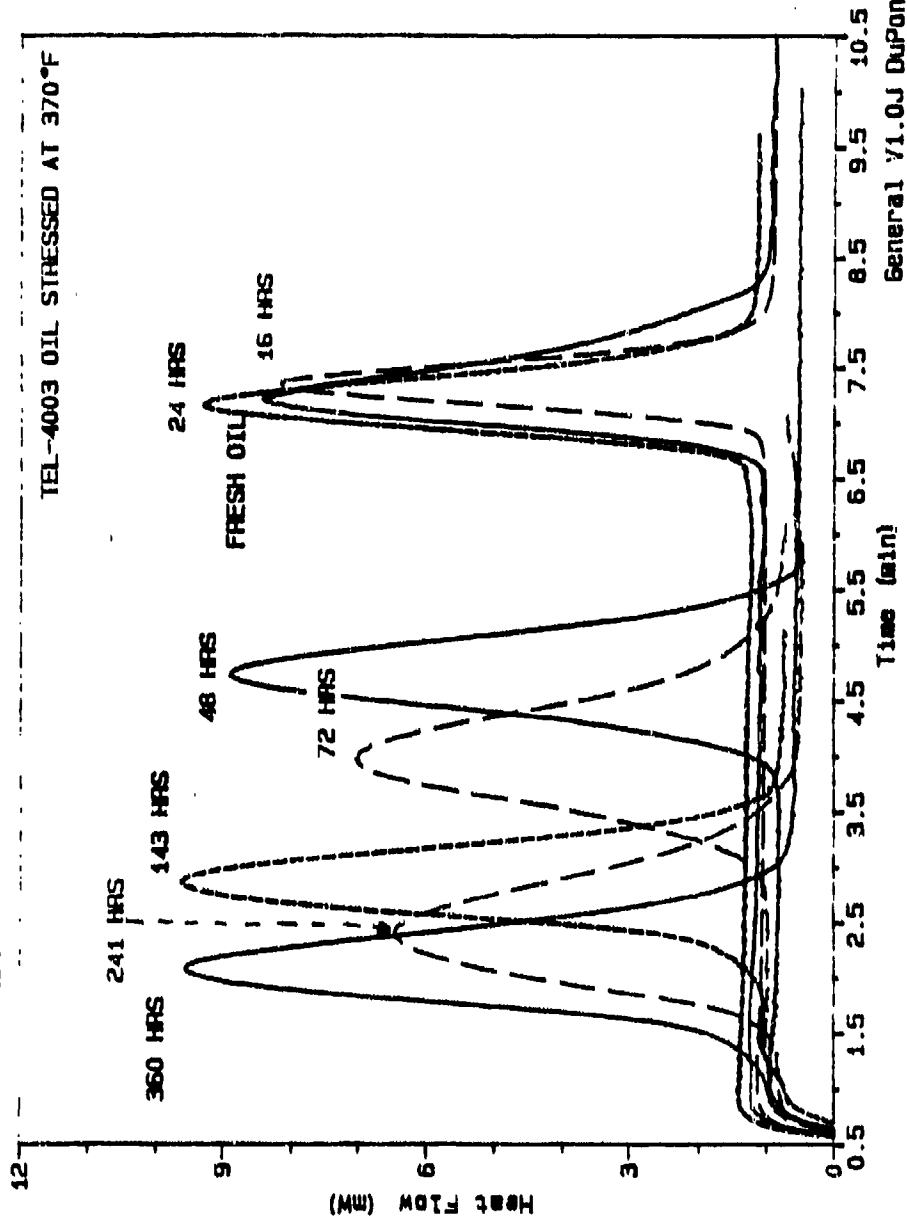


Figure 107. SP-DSC (in Oxygen) Thermograms (230°C - 3°C/Min.) of the Fresh and Stressed (16-360 Hours at 370°F) TEL-4003 MIL-L-7808 Oils.

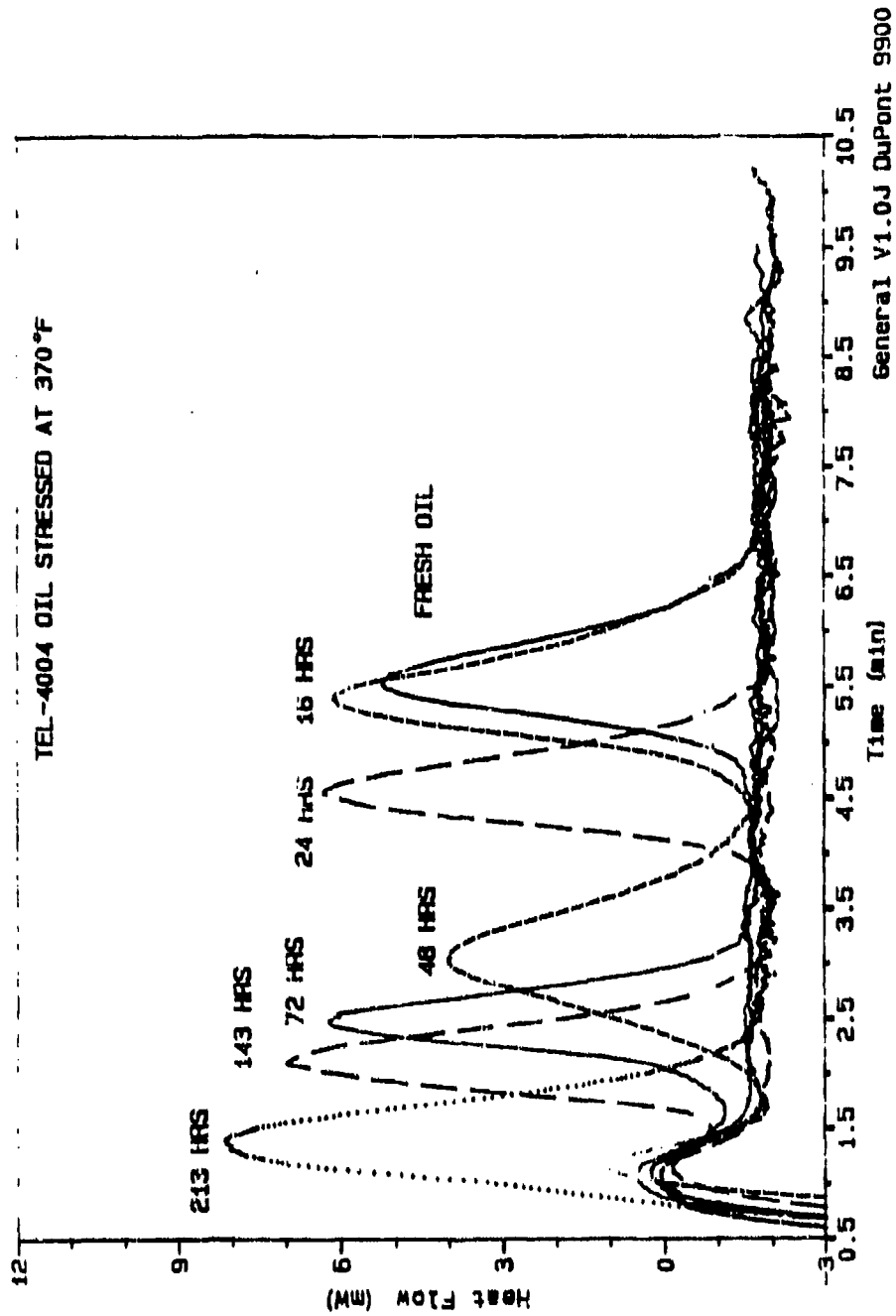


Figure 108. SP-DSC (in Oxygen) Thermograms (230°C - 3°C/Min.) of the Fresh and Stressed (16-213 Hours at 370°F) TEL-4004 MIL-L-7808 Oils.

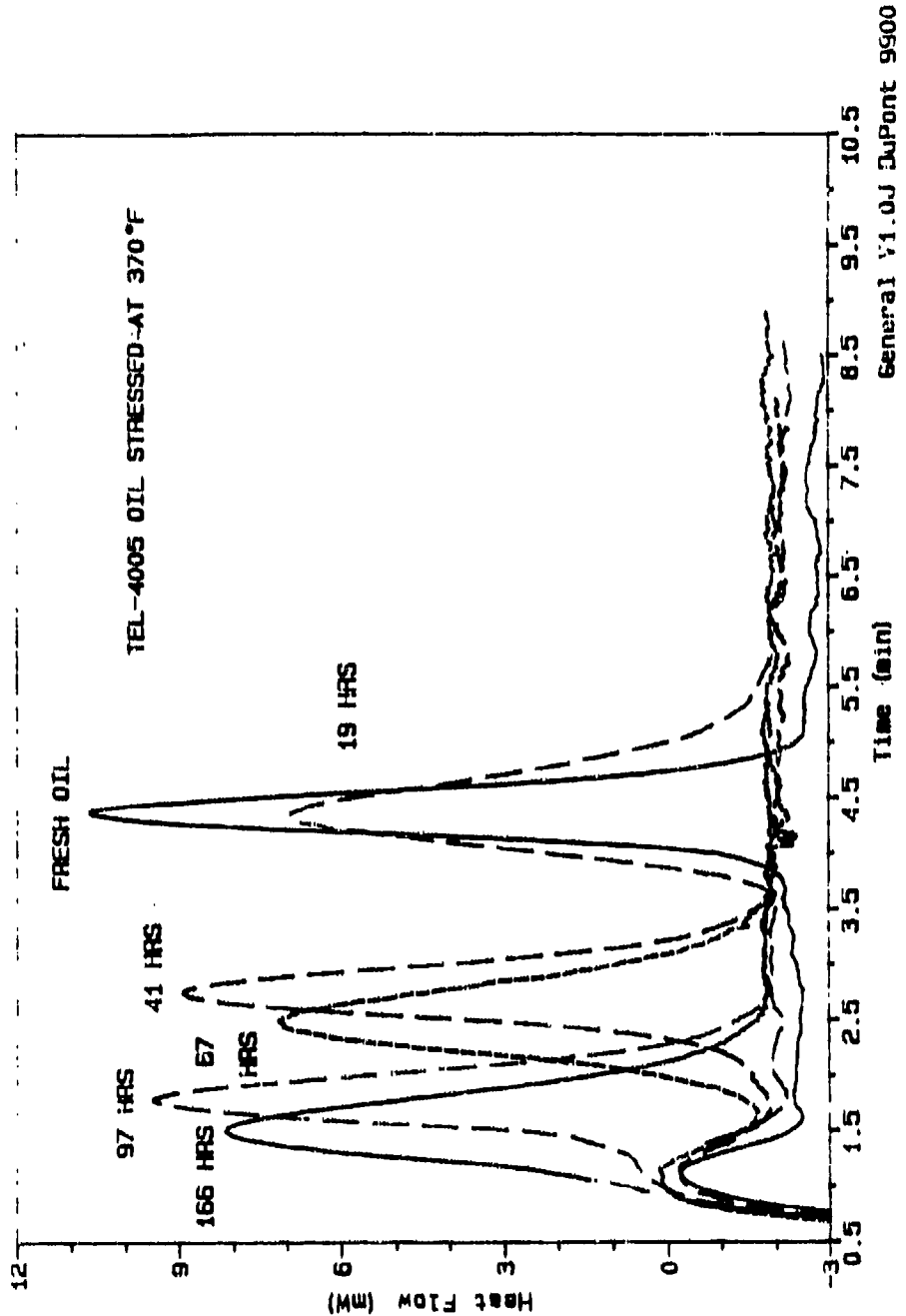


Figure 109. SP-DSC (in Oxygen) Thermograms (230°C - 3°C/Min.) of the Fresh and Stressed (19-166 Hours at 370°F) TEL-4005 MIL-L-7808 Oils.

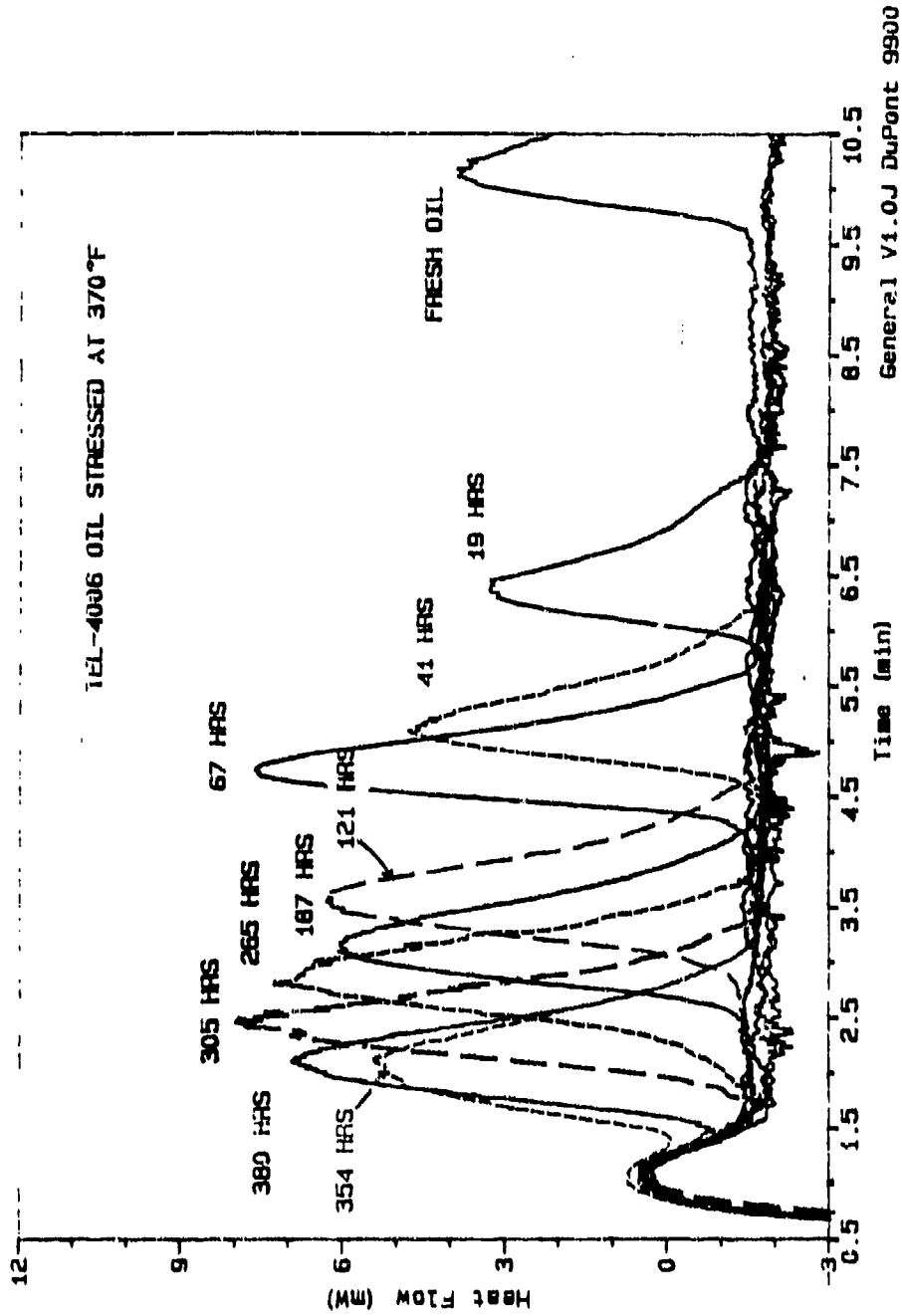


Figure 110. SP-DSC (in Oxygen) Thermograms (230°C - 2°C/Min.) of the Fresh and Stressed (19-380 Hours at 370°F) TEL-4006 MIL-L-7808 Oils.

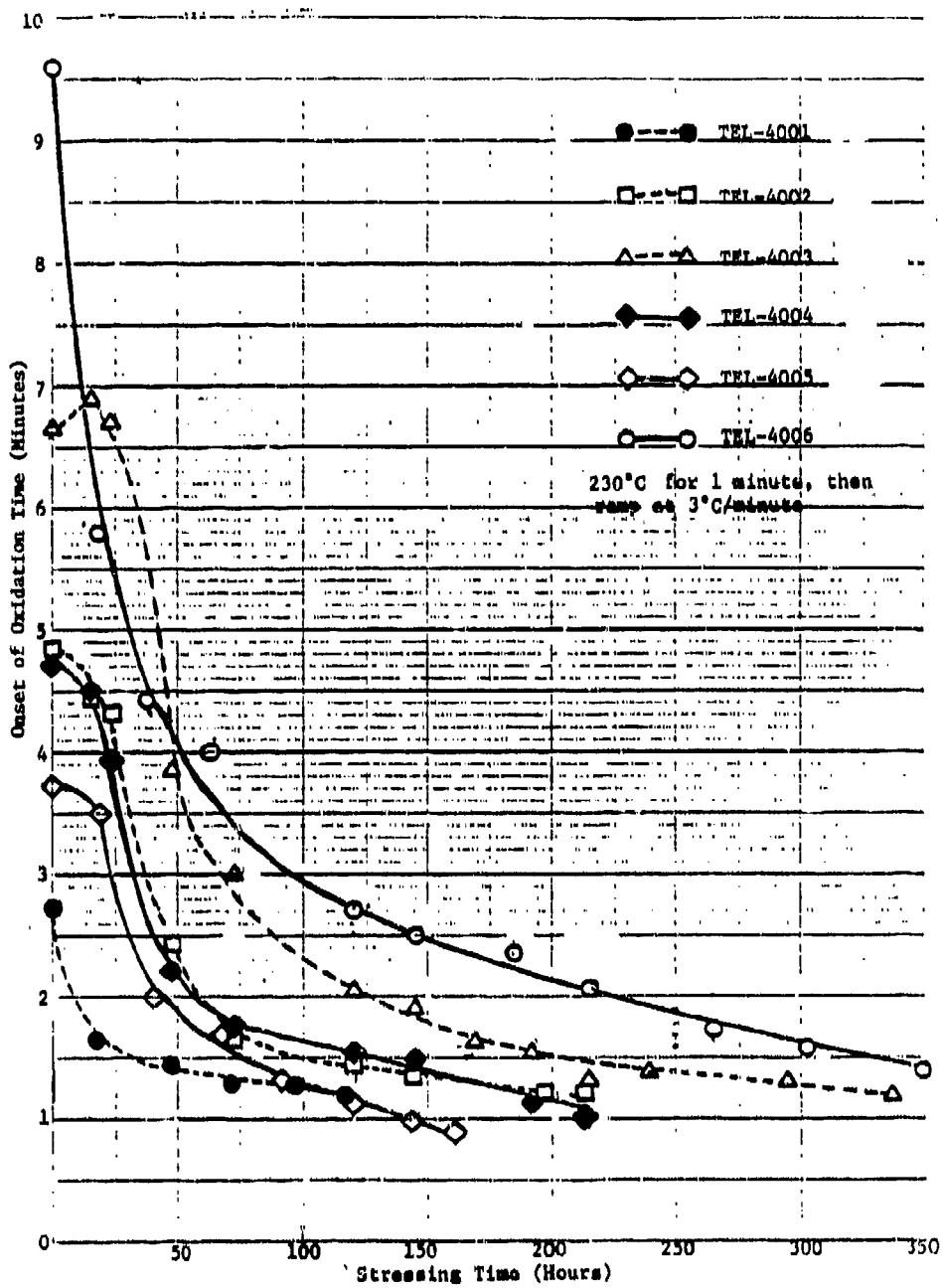


Figure 111. Plots of the SP-DSC (in Oxygen) Onset of Oxidation Time Versus Stressing Time at 370°F for the Fresh and Stressed MIL-L-7808 Oils.

The agreement of the different MIL-L-7808 oils' onset of oxidation times with 0% RLL for the SP-DSC technique is better than the agreement among the onset of oxidation times of the HP-DSC technique (1.0-2.4 minutes: Figure 91) and is worse than the agreement among the onset of reaction times of the HP-DSC technique (0.6-1.0 minutes: Figure 95).

Therefore, the results of the SP-DSC with an oxygen atmosphere are directly related to the RLL of the MIL-L-7808 oils and the results are slightly affected by formulation.

(h) Linearizing the SP-DSC Onset of Oxidation Time Plots

Since the SP-DSC onset of oxidation times are related to the RLL of MIL-L-7808 oils, an investigation to identify the mathematical expression which produced linear SP-DSC result versus RLL plots for the stressed MIL-L-7808 lubricating oil samples was performed.

Since the  $\ln$  values of the RCV (Figure 89) and of the HP-DSC (Figure 96) results produced linear plots versus the stressing times of the MIL-L-7808 oil samples, the  $\ln$  values of the SP-DSC onset of oxidation times were plotted. The  $\ln$  value of the SP-DSC onset of oxidation time versus hours of remaining lubricant life (370°F) plots are shown in Figure 112 for the TEL-4001 through TEL-4006 MIL-L-7808 oils.

As seen in Figure 112, the  $\ln$  value of the SP-DSC onset of oxidation time versus hours of remaining lubricant life plots of the MIL-L-7808 oil samples exhibit differing degrees of linearity. During the early stages of oxidation, the onset of oxidation times remain fairly constant for the TEL-4002 through TEL-4005 oils and decrease rapidly for the TEL-4001 and TEL-4006 oils. After the early stages of oxidation, the plots of the TEL-4001 and TEL-4006 oil samples are linear but contain inflection points. Similar inflection points were observed in the plots of the single scan-RCV results (Figure 76) but not in the plots of the multiple scan-RCV (Figure 89) and HP-DSC results (Figure 96).

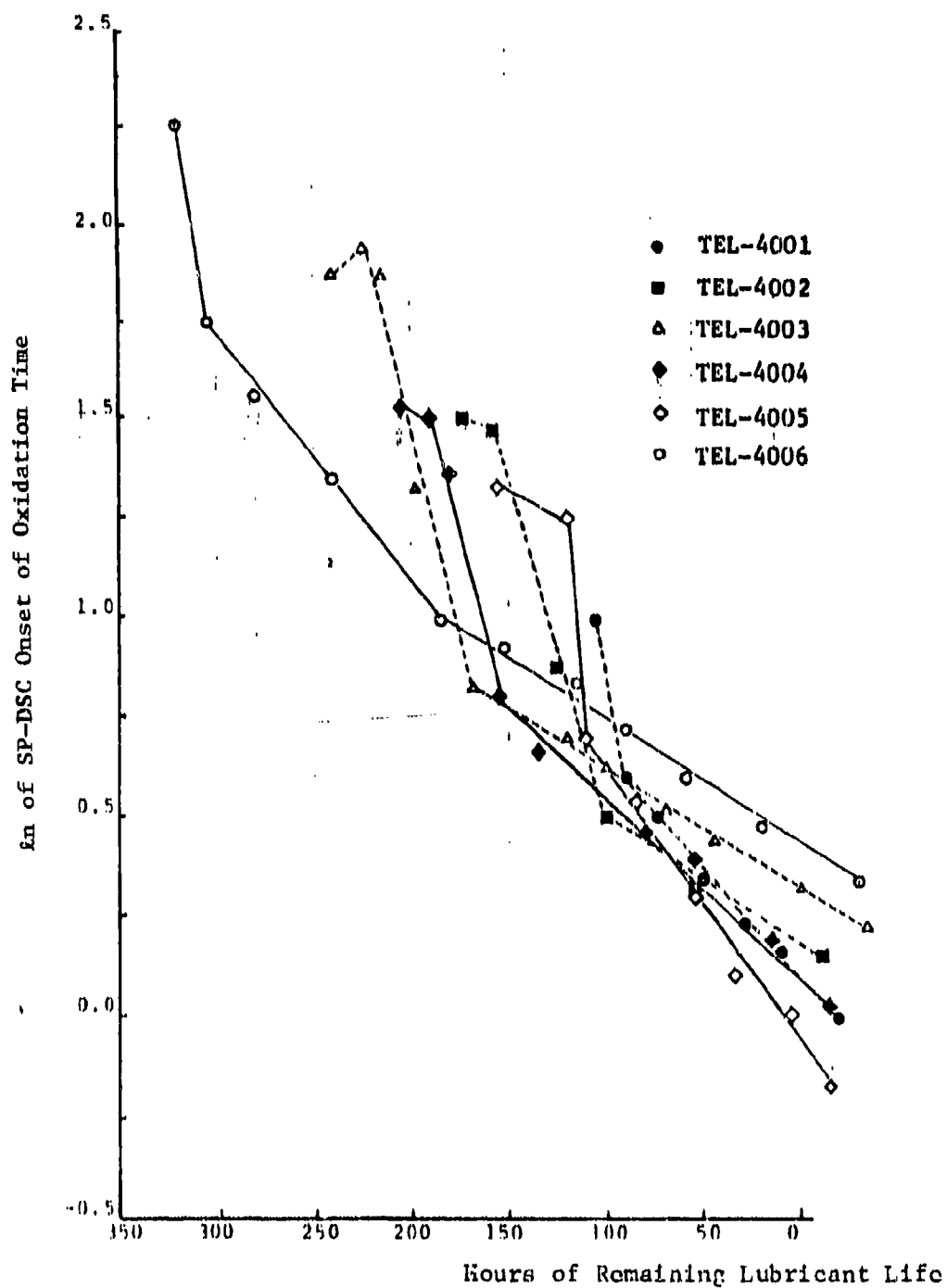


Figure 112. Plots of the  $\ln$  of the SP-DSC Onset of Oxidation Time Versus Hours of Remaining Lubricant Life at 370°F for the Fresh and Stressed MIL-L-7808 Oils.

Therefore, it appears that the SP-DSC technique determines the antioxidant capabilities of the species present in the oil sample (single scan CV analyzes only species present in oil sample). However, the HP-DSC technique determines, not only, the antioxidant capabilities of the species present in the oil sample, but also the capacities of the species present in the oil sample to generate new antioxidant species [multiple scan-CV, first generates new species, then measures the total concentration of species (original and generated) in the oil sample]. The fact that the agreement of the SP-DSC and HP-DSC results increases with stressing time (oil sample's capability to generate new species decreases with stressing time) supports this idea. Also, the DODPA concentration versus stressing time plots for the MIL-L-7808 oils contain similar inflection points (Appendix A).

The other interesting feature of the SP-DSC result versus stressing time plots in Figure 112 is that the onset of oxidation time decreases with hours of remaining lubricant life until the end of each oils' stable life. In contrast, the HP-DSC result versus hours of remaining lubricant life plots in Figure 96 show that the onset of reaction time decreases with stressing time until 60 (TEL-4003 oil) to 20 (TEL-4001 oil) hours prior to the end of the oils' stable lives. Therefore, it appears that the lower initial temperature (230°C) of the SP-DSC technique enables the SP-DSC to distinguish between oil samples with limited remaining lubricant lives better than the HP-DSC (initial temperature = 250°C).

#### (4) Comparison of the SP-DSC and HP-DSC Techniques

In order to determine the thermal stressing technique with the most potential for development into a RLLAT, Table 12 was prepared. The SP-DSC and HP-DSC techniques in Table 12 indicates, the thermal stressing technique best suited for development into RLLAT is not clear.

Although SP-DSC has lower instrumental cost and is simpler and safer to operate, HP-DSC has a lower operational cost and does not require sample preparation (shorter total analysis

TABLE 12  
SUMMARY OF SP-DSC AND HP-DSC TECHNIQUES

	<u>SP-DSC</u>	<u>HP-DSC</u>
<u>Cost</u>		
Instrumental	\$ 15-20K	\$ 20-25K
Operational	\$ 0.80	\$ 0.30
<u>Ease of Operation</u>		
Sample Preparation	Yes <sup>a</sup>	No
DSC Procedure	Simple	Complex
Safety Requirements	No	Yes
<u>Lubricant Life Prediction</u>		
Effect of Formulation on % Remaining Lubricant Life Value (Minutes)	1.2±0.3	0.8±0.2 <sup>b</sup> 1.7±0.7 <sup>c</sup>
Linear Relationship with Remaining Lubricant Life	No <sup>d</sup>	Yes
<u>Analysis Time (Minutes)</u>	1.2-10 <sup>e</sup>	0.8-10 <sup>b</sup> 1.7-11 <sup>c</sup>

<sup>a</sup> Seal DSC pan inside glove bag with oxygen atmosphere.

<sup>b</sup> Onset of reaction time.

<sup>c</sup> Onset of oxidation time.

<sup>d</sup> Linear between inflection points.

<sup>e</sup> Plus sample preparation time of 2-3 minutes.

time). The importance of the linear relationship between the technique's results and the RLL of an oil sample is lowered by the fact that operating jet engines require periodic oil additions, resulting in nonlinear relationships between the RLL of an oil sample and the operating time of the jet engine.

Therefore, for oil analysis labs analyzing a small number of oil samples taken from jet engines requiring frequent oil additions, the SP-DSC technique is better suited for RLL assessments. Whereas, for oil analysis labs analyzing a large number of oil samples taken from jet engines requiring limited oil additions, the HP-DSC technique is better suited for RLL assessments.

(d) Chemical Stressing Technique

(1) Introduction

As the results in Task 1 indicated, the colorimetric method is the chemical stressing technique best suited for development into a RLLAT candidate. The colorimetric method has the capability to differentiate between oil samples with varying degrees of thermal oxidative degradation. However, results of Task 1 also showed (Figure 38) that the experimental parameters of the colorimetric method need to be modified in order to complete the test in ten minutes. An additional problem with the colorimetric method is that fresh MIL-L-7808 lubricating oils do not exhibit BDN decoloration induction times (Figures 37 and 38).

Therefore, the experimental parameters capable of producing BDN decoloration induction times of less than 10 minutes were studied. The effects of reaction temperature and cumene hydroperoxide concentration on the induction time of the BDN decoloration reaction were studied. In order to compensate for the fresh MIL-L-7808 lubricating oils not producing BDN decoloration induction times, the time required to reach a preset decrease in absorbance was used to determine the end of the oils' BDN decoloration induction times. The developed colorimetric

method was then used to analyze fresh and stressed TEL-4001 through TEL-4006 MIL-L-7808 lubricating oils.

## (2) Effect of Sample Temperature

Since the rate of reaction between the antioxidant species in the oil sample and cumene hydroperoxide increases with temperature, i.e., BDN decoloration induction time decreases, the effect of sample temperature on the induction times of stressed TEL-4001 and TEL-4006 oil samples were studied. The MIL-L-7808 oils, TEL-4001 and TEL-4006, were chosen for this study since they produced the shortest and longest stable lives at 370°F, respectively. Therefore, a temperature which produced BDN decoloration induction times of less than ten minutes for the fresh TEL-4006 oil, but which allowed the differentiation between stressed TEL-4001 oil samples of varying degrees of thermal-oxidative degradation could be selected.

To determine the effects of reaction temperature on the induction time of the BDN decoloration reaction, 15  $\mu$ l samples of fresh and stressed (370°F) TEL-4001 and TEL-4006 oils were added to 0.75 ml of BDN solution and 0.5 ml of cumene hydroperoxide (optimum parameters from Task 1). The reaction temperatures of 25, 30, 35, and 40°C were studied and the absorbances of the BDN solution were plotted versus reaction time to determine the BDN decoloration induction times of the stressed TEL-4001 and TEL-4006 oils. The 24 hour stressed sample of the TEL-4006 oil produced BDN decoloration induction times of greater than 20 minutes at 25 and 30°C. At 40°C the experimental setup produced a signal to the X-Y plotter which was so erratic that the BDN decoloration induction times of the TEL-4006 oils could not be determined. However, the temperature of 35°C produced an BDN decoloration induction time of less than 15 minutes for the 19 hour stressed TEL-4006 oil and allowed the method to differentiate between the TEL-4001 oils with slightly different stressing times (Figure 113). Therefore, 35°C was used in all future research.

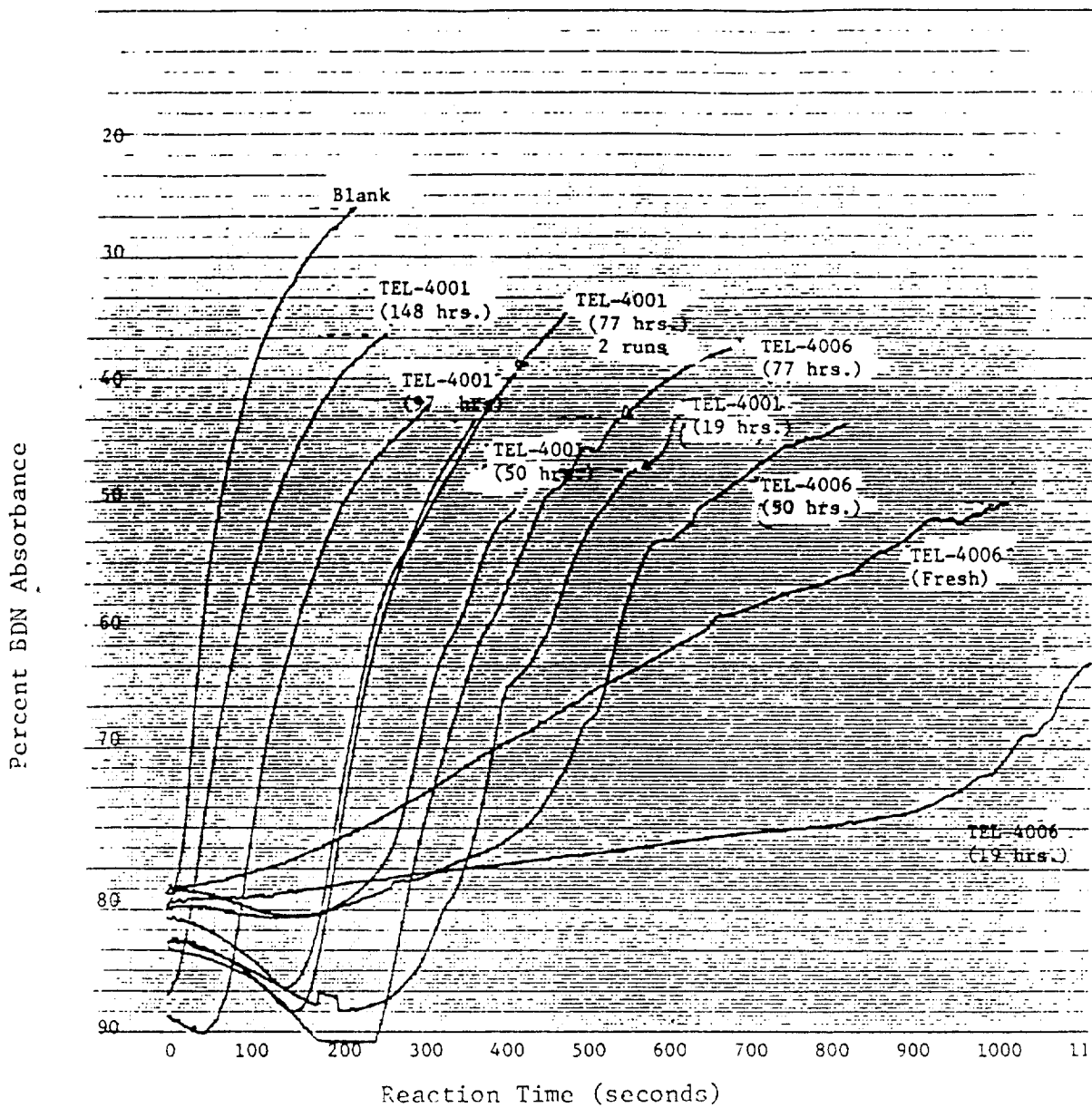


Figure 113. Plots of the Percent BDN Absorbance Versus Reaction Time at 35°C for the Fresh and Stressed TEL-4001 and TEL-4006 Oils.

### (3) Effect of Cumene Hydroperoxide Concentration

Since temperatures higher than 35°C produced erratic results and 35°C produces BDN decoloration induction times greater than 10 minutes for the slightly stressed TEL-4006 oil (Figure 113), the effect of cumene hydroperoxide concentration on the induction times of the TEL-4001 and TEL-4006 MIL-L-7808 oils was studied. To determine the effect of cumene hydroperoxide concentration on the induction time of the BDN decoloration method, 15 µl samples of fresh and stressed (370°F) TEL-4001 and TEL-4006 oils were added to 0.75 ml of BDN solution. By varying the amounts of cumene hydroperoxide added to the reaction system from 0.5 to 1.0 ml and plotting the absorbances of the BDN solution versus reaction time, it was determined that 0.75 ml of cumene hydroperoxide was capable of producing 10 minute or less BDN decoloration induction times for any of the fresh or stressed MIL-L-7808 oils.

However, the 0.75 ml of cumene hydroperoxide is not a fixed quantity, because different batches of cumene hydroperoxide produced different BDN decoloration induction times. When 0.75 ml of a new batch of cumene hydroperoxide was used during the research following the concentration study, BDN decoloration induction times of less than 7 minutes were obtained for the TEL-4006 oils and differentiation between stressed TEL-4001 oils became difficult. Another batch of cumene hydroperoxide required 1.0 ml to obtain induction times of less than 10 minutes for the TEL-4006 oils. Whether these differences are due to aging, to differing initial cumene hydroperoxide concentrations (80% purity), or to the species making up the remaining 20% of the obtained chemical is unknown. Therefore, the different batches were weakened or strengthened, by mixing the batches prior to use, in order to obtain a ten minute BDN decoloration induction time for the TEL-4006 oil sample which had been stressed 24 hours (sample with maximum BDN decoloration induction time).

#### (4) Colorimetric Analyses of MIL-L-7808 Oils

In order to determine the effects of formulation on the results of the colorimetric methods, the sets of fresh and stressed (370°F) TEL-4001 through TEL-4006 MIL-L-7808 lubricating oils were studied. The analyses were performed at 35°C using 15  $\mu$ l samples of oil, 0.75 ml of BDN solution and 0.75 ml of blended cumene hydroperoxide. The plots of the percent BDN absorbance versus reaction time at 35°C for the TEL-4001 through TEL-4006 oils are shown in Figures 114-119, respectively.

The plots of the percent BDN absorbance versus reaction time at 35°C shown in Figures 114-119 demonstrate the colorimetric method's capability to differentiate between varying degrees of thermal oxidation regardless of the MIL-L-7808 oils' formulation. However, in addition to the problem that new MIL-L-7808 lubricating oils do not produce induction periods, the shapes of the absorbance curves prior to the rapid BDN decoloration are dependent on formulation and degree of degradation. As the degradation of the oils increases, the absorbance curves exhibit a dramatic increase in absorbance prior to the rapid decrease in absorbance, especially the TEL-4001 oil. Also the absorbance curves for the 24 hour stressed TEL-4006 oil exhibits less rapid decoloration rates than the other oil samples. All of these factors decrease the accuracy of the BDN decoloration induction period determinations when the induction time is defined as the time at which rapid BDN decoloration occurs.

Therefore, a preset decrease in absorbance must be used to determine the BDN decoloration induction times of the different oil samples. The preset decrease in absorbance must be chosen so that reasonable BDN decoloration induction times for the new MIL-L-7808 oils are determined but the relationships between the stressed oils are not changed. The differences in the initial absorbance readings caused by the color variations of the oil samples must also be taken into account. The absorbance plots in Figures 114-119 indicate that the use of a 25% decrease in absorbance for determination of the BDN decoloration induction times

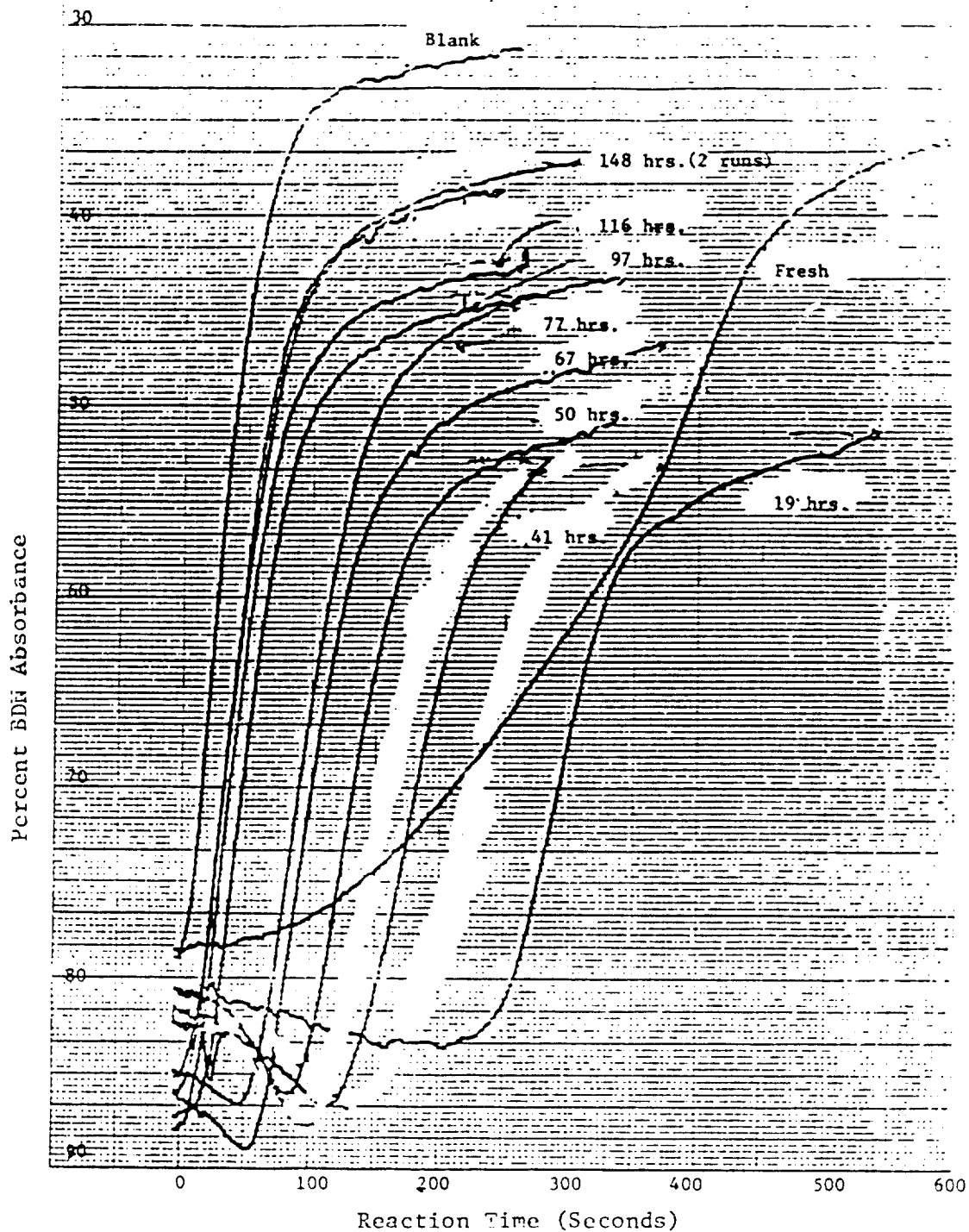


Figure 114. Plots of the Percent BDN Absorbance Versus Reaction Time at 35°C for the Fresh and Stressed (19-148 Hours at 370°F) TEL-4001 Oils.

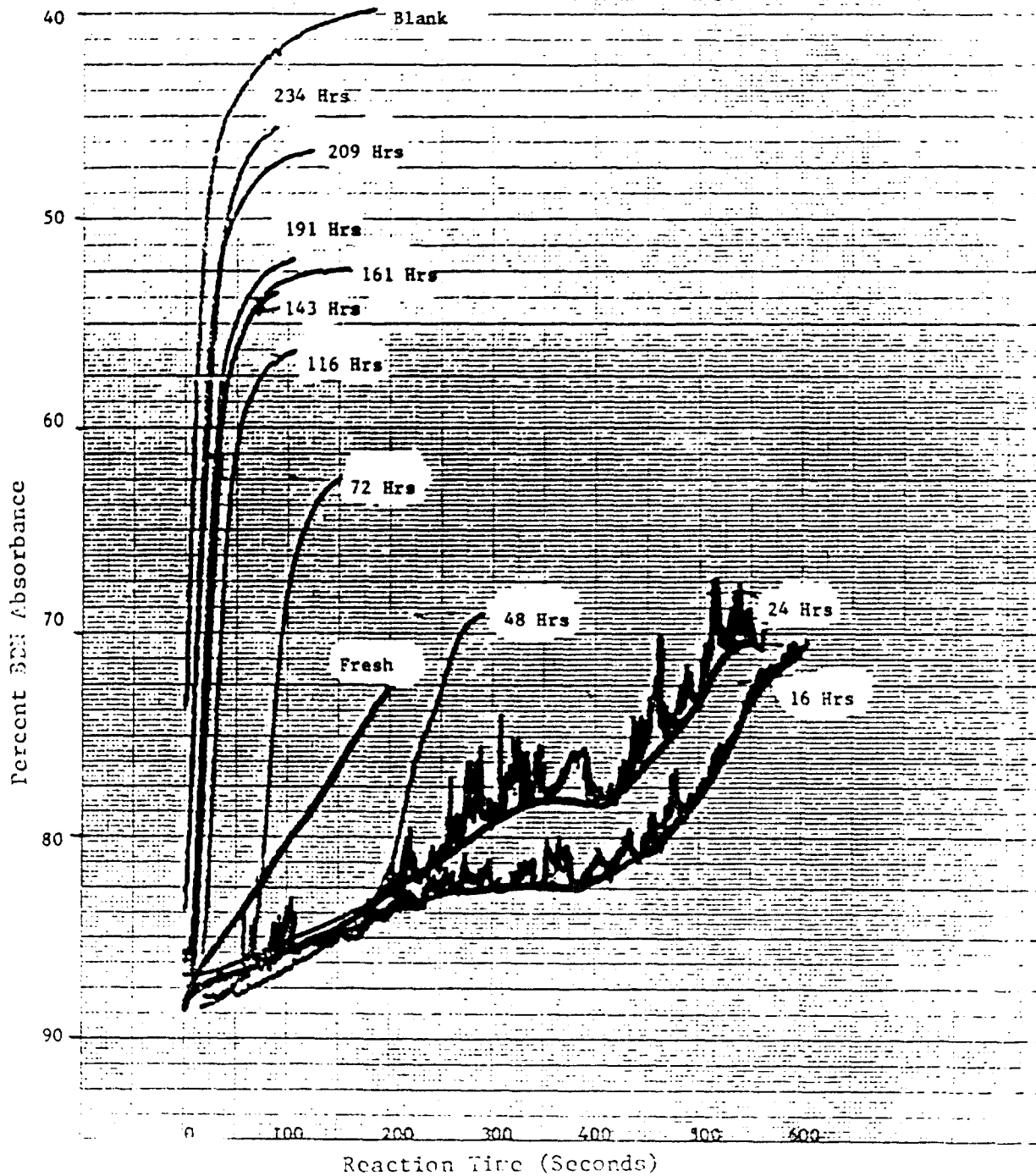


Figure 115. Plots of the Percent BDN Absorbance Versus Reaction Time at 35°C for the Fresh and Stressed (16-234 Hours at 370°F) TEL-4002 Oils.

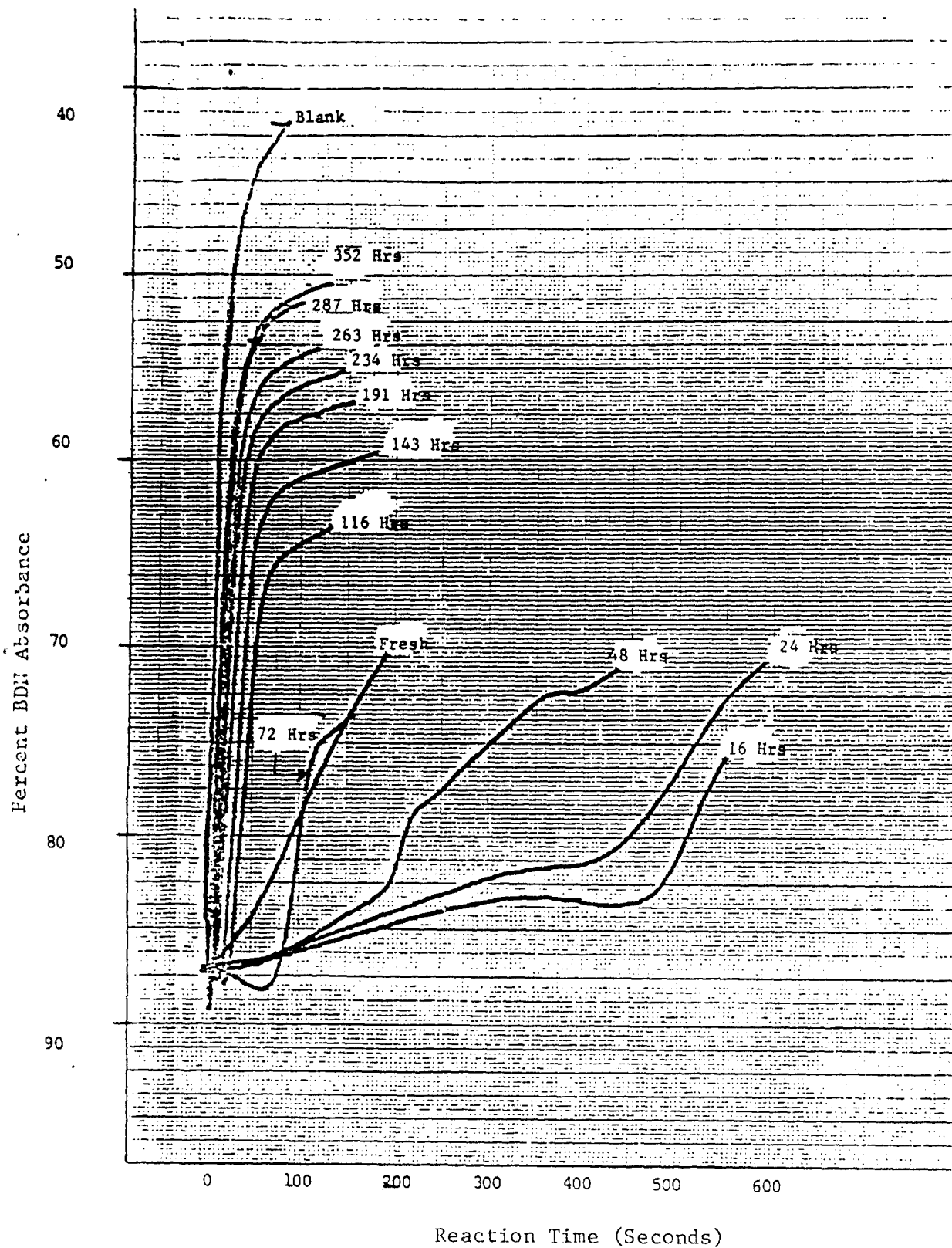


Figure 116. Plots of the Percent BDN Absorbance Versus Reaction Time at 35°C for the Fresh and Stressed (16-352 Hours at 370°F) TEL-4003 Oils.

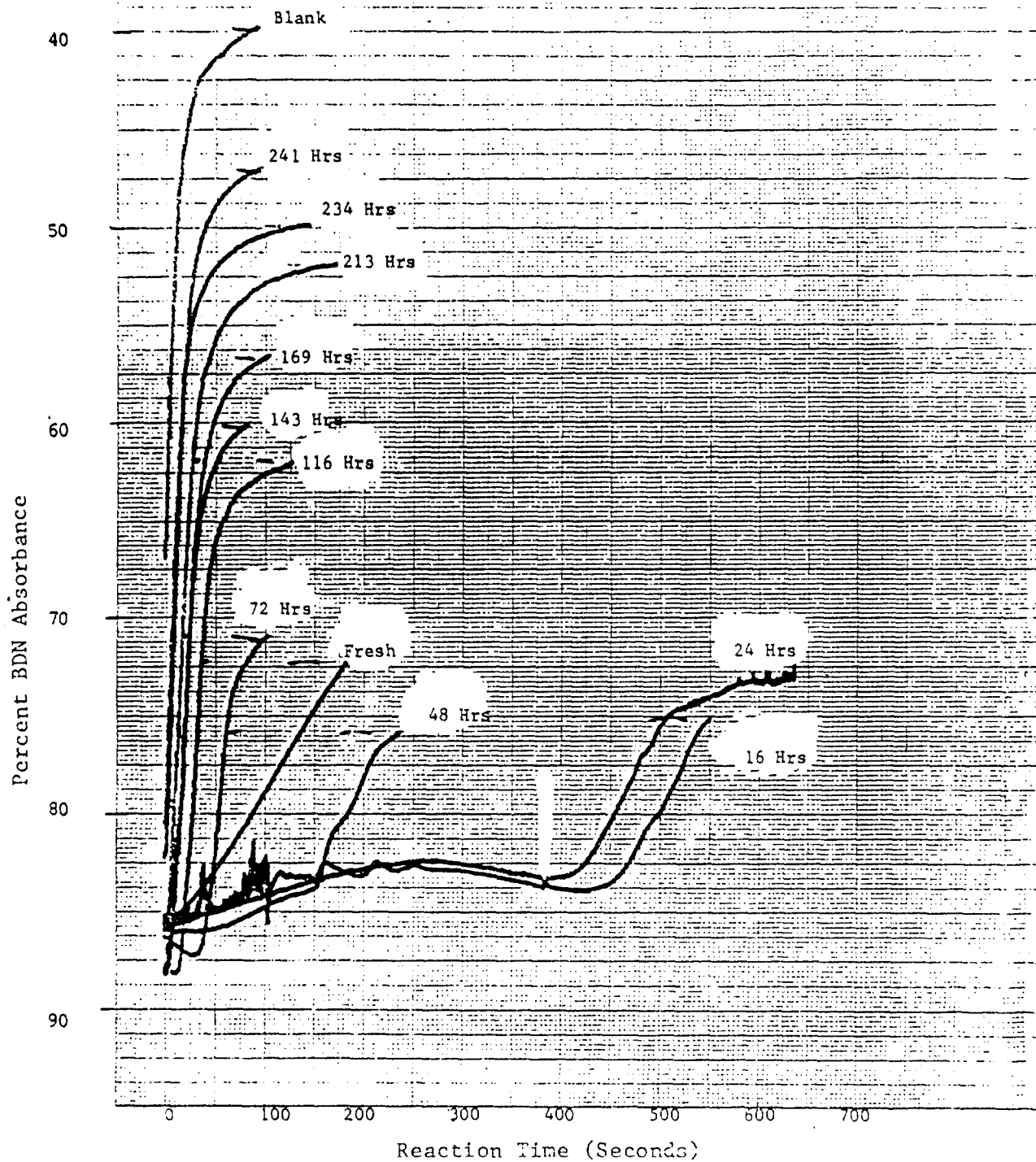


Figure 117. Plots of the Percent BDN Absorbance Versus Reaction Time at 35°C for the Fresh and Stressed (16-241 Hours at 370°F) TEL-4004 Oils.

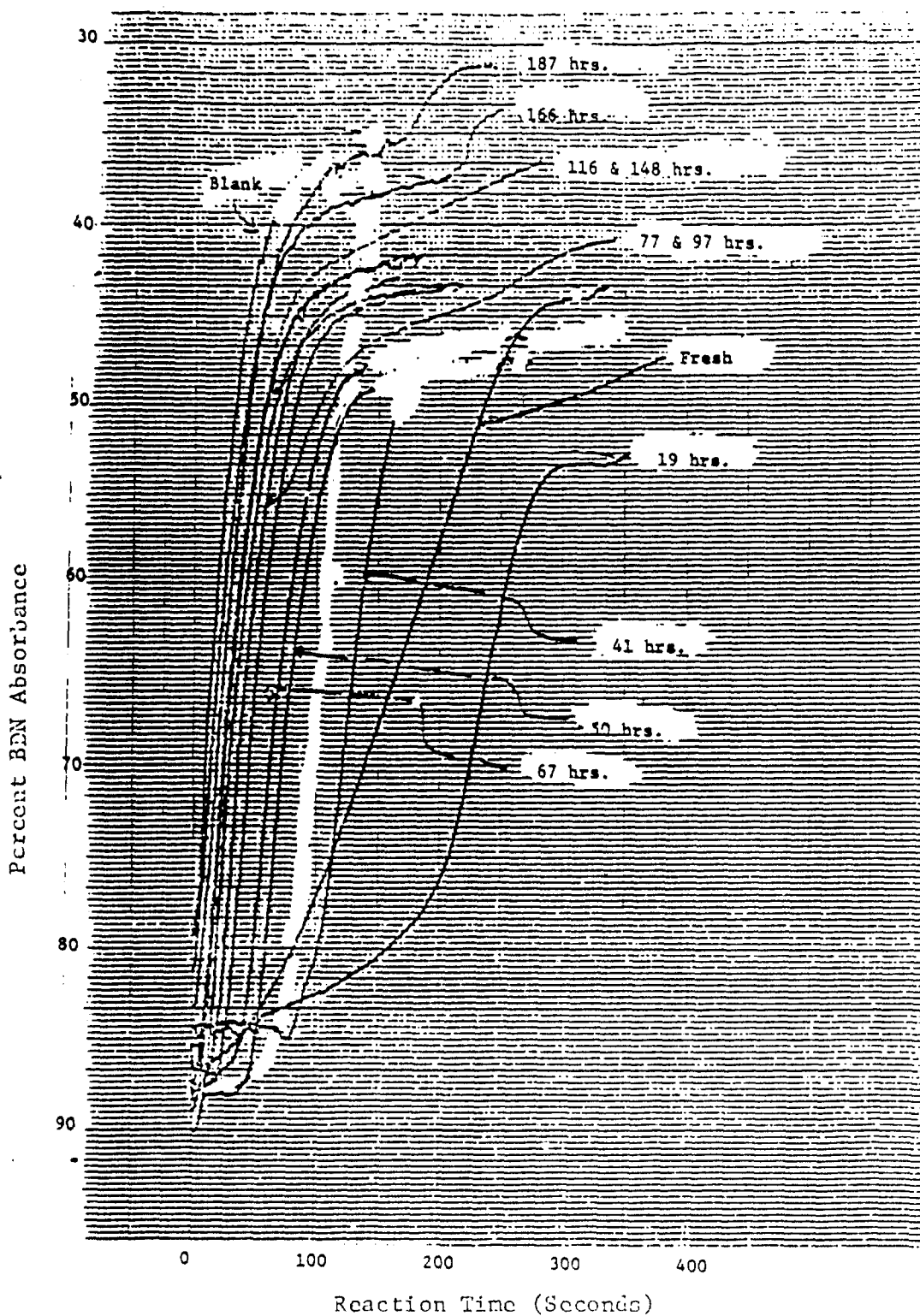


Figure 118. Plots of the Percent BDN Absorbance Versus Reaction Time at 35°C for the Fresh and Stressed (19-166 Hours at 370°F) TEL-4005 oils.

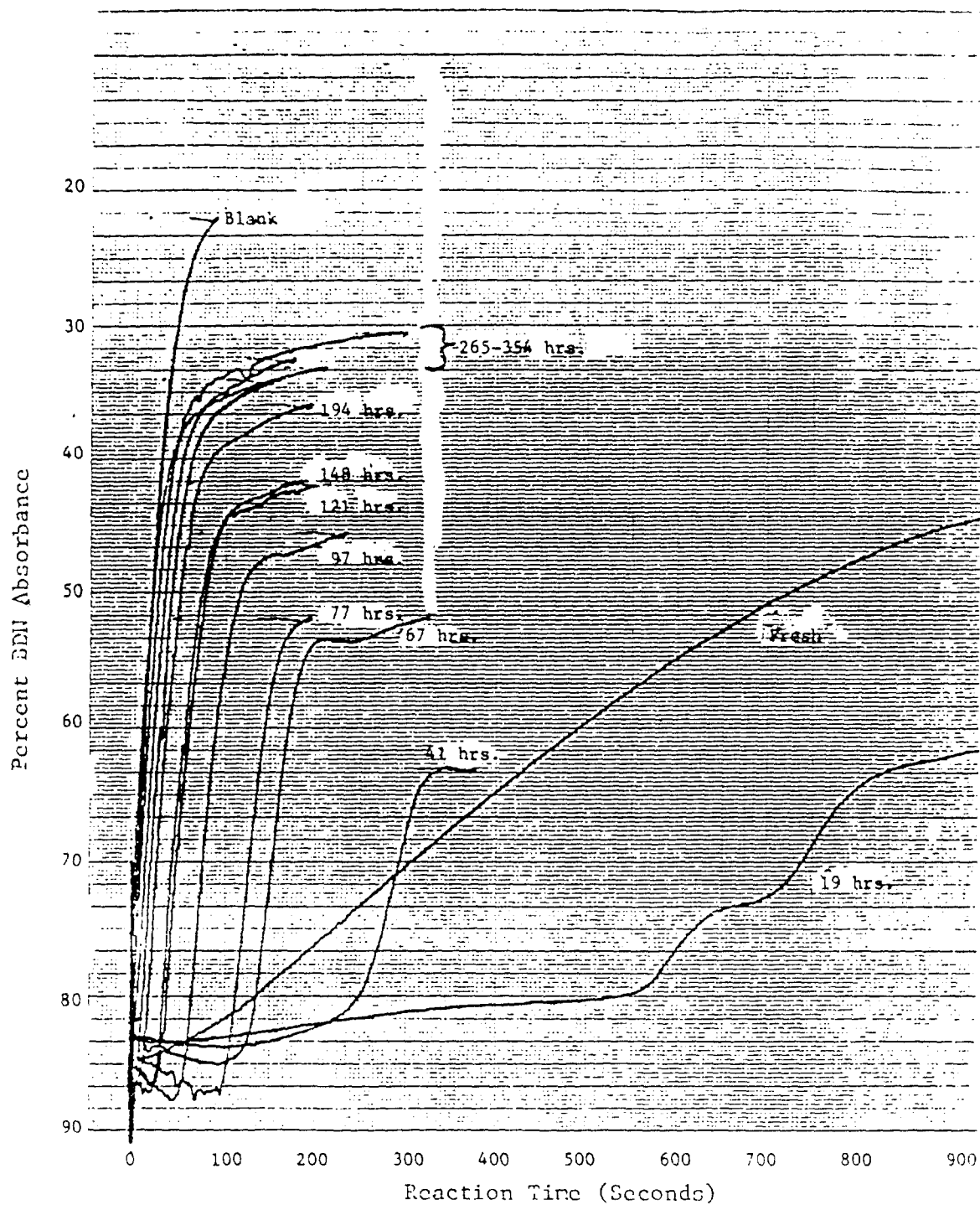


Figure 119. Plots of the Percent BDN Absorbance Versus Reaction Time at 35°C for the Fresh and Stressed (19-354 Hours at 370°F) TEL-4006 Oils.

produces reasonable BDN decoloration induction times for the fresh MIL-L-7808 oils, i.e., BDN decoloration induction time of fresh oil greater than oil sample 48 hours while less than or equal to oil stressed 24 hours.

The BDN decoloration induction times of the fresh and stressed (370°F) MIL-L-7808 oils determined using a 25% decrease in absorbance were plotted versus stressing time at 370°F and are presented in Figure 120.

The plots of BDN decoloration induction time versus stressing time at 370°F for the MIL-L-7808 oils shown in Figure 120 have shapes similar to the plots of the results of the other RLLAT candidates versus stressing time. However, in contrast to the other RLLAT candidates' results, the BDN decoloration induction time of every MIL-L-7808 oil increases dramatically during the first 24 hours of stressing at 370°F. These results indicate that the new antioxidant species generated by thermal-oxidation identified by cyclic voltammetry (Figures 58-67) and verified by HP-DSC (Figure 96) and SP-DSC (Figure 112), greatly improve the hydroperoxide decomposing capabilities of the antioxidant system in the stressed MIL-L-7808 oils.

(5) Linearizing the Colorimetric BDN Decoloration Induction Time Plots

Since the  $\ln$  values of the RCV (Figure 89), HP-DSC (Figure 96) and SP-DSC (Figure 112) results produced the most linear plots with the stressing times of the MIL-L-7808 oils, the log values of the BDN decoloration induction times were plotted. The log value of the colorimetric result versus hours of remaining lubricant life (370°F) plots are shown in Figure 121 for the TEL-4001 through TEL-4006 MIL-L-7808 lubricating oils.

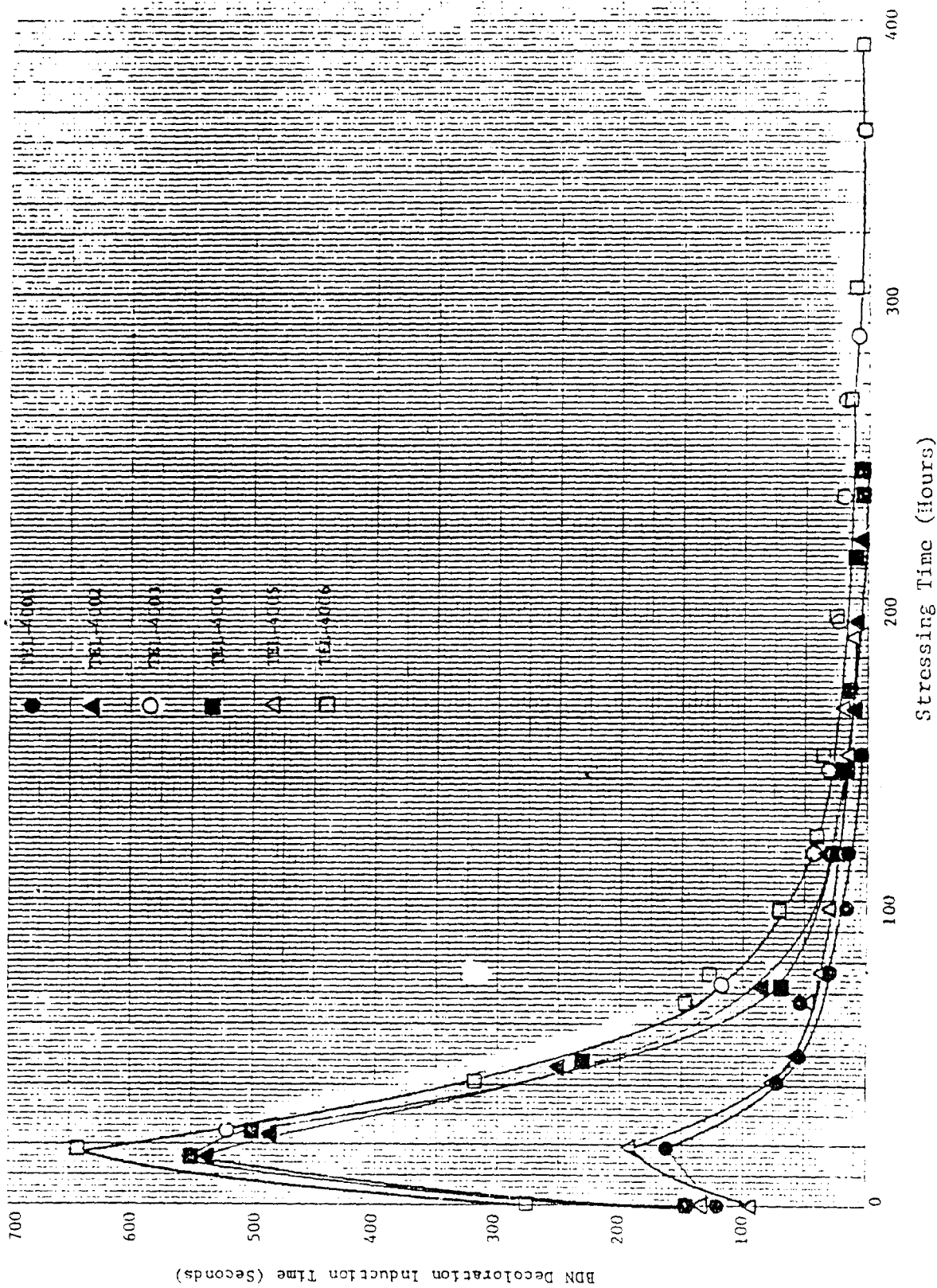


Figure 120. Plots of the BDN Decoloration Induction Time Versus Stressing Time at 370°F for the TEL-4001 Through TEL-4076 MIL-L-7808 Oils.

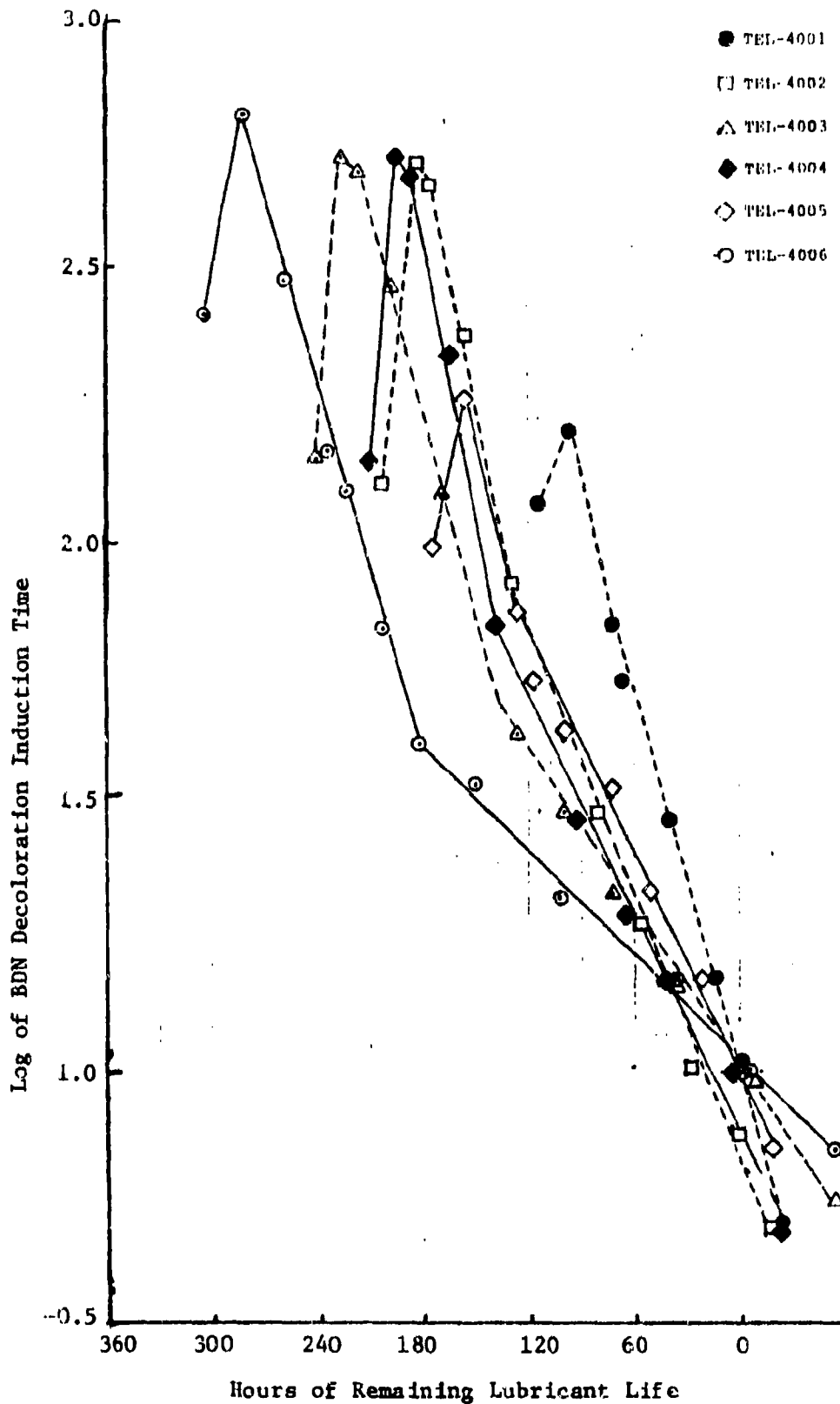


Figure 121. Plots of the Log of the BDN Decoloration Induction Time Versus Hours of Remaining Lubricant Life at 370°F for the Fresh and Stressed MIL-L-7808 Oils.

As seen in Figure 121, the log value of the BDN decoloration induction time versus hours of remaining lubricant life plots of the MIL-L-7808 oil samples exhibit differing degrees of linearity. During the first 24 hours of oxidation, the BDN decoloration induction times increase rapidly for all of the MIL-L-7808 oils. After the first 24 hours of oxidation, the log of the BDN decoloration induction time plots are linear, but contain inflection points similar to those observed for the SP-DSC (Figure 112), single scan-RCV (Figure 76), and DODPA concentration (Appendix A) plots.

Therefore, the colorimetric method determines the hydroperoxide decomposing capabilities of the antioxidant species present in the oil sample. Thus, the capacities of the antioxidant species present in the oil sample to generate new species with hydroperoxide decomposing capabilities are not measured by the colorimetric method.

The log value of the BDN decoloration induction time versus hours of remaining lubricant life plots in Figure 121 also show that the effect of formulation on the colorimetric method's results is small. At the ends of the MIL-L-7808 oils' stable lives at 370°F, the average BDN decoloration induction time is approximately  $8 \pm 3$  seconds.

(e) Comparison of Remaining Lubricant Life Assessment Test Candidates

The RLLAT candidates developed during this investigation have been categorized into three main groups and have been ranked in the following order: voltammetric > thermal stressing > chemical stressing. The three main groups and the criteria used to rank their potentials for development into RLLAT are listed in Table 13.

Of the RLLAT candidates developed during this investigation, the voltammetric techniques are the lowest in cost, easiest to operate, require the shortest analytical time, and produce the most accurate and precise RLL assessments (Table 13). The voltammetric techniques also can be used to identify the type

TABLE 13

## SUMMARY OF REMAINING LUBRICANT LIFE ASSESSMENT TEST CANDIDATES

	<u>Voltammetric</u>	<u>Thermal Stressing</u>	<u>Chemical Stressing</u>
<u>Cost</u>			
Instrumental	less than \$1,000 <sup>a</sup>	\$15-\$25K	less than \$1,000 <sup>a</sup>
Operational	\$0.08	\$0.30-0.80	\$0.10
<u>Ease of Operation</u>			
Sample size (µl)	50	0.2-1.0	15
Sample preparation	Simple	Simple	Moderate
Analytical procedure	Simple	Moderate	Moderate
Analysis of results	Simple	Simple- Moderate	Moderate
Safety Requirements	Normal	Normal- Moderate	Moderate
<u>Analysis Time</u>			
Sample preparation	less than 30 sec.	0.5-3 min.	less than 30 sec.
Analytical Procedure	less than 20 sec.	1-10 min.	0.2-10 min.
<u>Lubricant Life Prediction</u>			
Effect of Formulation on O% Life Value	Slight	Slight- Moderate	Slight
Relationship with Remaining Lubricant Life	Linear	Linear with inflection points	Linear with inflection points
<u>Additional Information</u>			
-- Identify antioxidant type		No	No
--- Estimate concentration of Hydro- peroxides			

<sup>a</sup> Plus cost of data acquisition system \$1,000-\$3,000.

of antioxidants used in the MIL-L-7808 oil formulation and to estimate the total concentration of hydroperoxides in the oil sample.

Therefore, the voltammetric techniques, in particular the reductive-cyclic voltammetric techniques, were the top candidates for development into a RLLAT.

Although the chemical stressing techniques are much lower in cost than the thermal stressing techniques, the thermal stressing techniques were ranked second for development into a RLLAT. The thermal techniques are easier to operate and do not require the toxic chemicals used by the chemical stressing techniques. Also the results of the chemical stressing techniques are more difficult to analyze than those of the thermal stressing techniques.

### 3. TASK 3. EVALUATION OF REMAINING LUBRICANT LIFE ASSESSMENT TEST BASED ON THE REDUCTIVE CYCLIC-VOLTAMMETRIC TECHNIQUE

#### a. Introduction

During Task 2 of this investigation, the RLLAT candidate based on the RCV technique was ranked as the best candidate for development into a RLLAT. In order to evaluate the RLLAT based on the RCV technique (RLLAT-RCV), the effects of stressing temperature, oil formulation and oil additions on its RLL assessments were studied. The RLL assessment capabilities of the RLLAT-RCV for actual used MIL-L-7808 and MIL-L-23699 oil samples were also studied.

#### b. Effect of Stressing Temperature

To determine the effects of stressing temperature on the RLLAT-RCV results, the TEL-4001 through TEL-4006 MIL-L-7808 oils were stressed at 392°F, characterized as described in Appendix A, and analyzed. The  $\ln$  values of the reduction wave heights were

then plotted versus hours of remaining lubricant life at 392°F. The  $\ln$  plots for the TEL-4001 through TEL-4006 oils are shown in Figure 122.

The  $\ln$  plots of the RLLAT-RCV results for the MIL-L-7808 oils stressed at 392°F (Figure 122) are in good agreement with the  $\ln$  plots for the MIL-L-7808 oils stressed at 370°F (Figure 89). For both temperatures, 370° and 392°F, the  $\ln$  plots are linear after only a few hours of stressing and the  $\ln$  plots have an approximate value of -0.70 (reduction wave height of 0.5  $\mu$ A) at the end of each oil's stable life. The only difference between the 370° and 392°F  $\ln$  plots is that the rate of decrease for the 392°F  $\ln$  plot is about double that for the 370°F  $\ln$  plot. The doubled rate of decrease for the 392°F  $\ln$  plot was expected, since the stable lives of the MIL-L-7808 oils stressed at 392°F oil are approximately half the stable lives of the oils obtained at 370°F (Appendix A).

Therefore, if the  $\ln$  value of -0.70 is assigned 0% RLL and an arbitrary  $\ln$  value of 3.44 is assigned 100% RLL, the RLLAT-RCV can be used to predict percent RLL regardless of stressing temperature or formulation. However, the remaining hours of life predictions can not be made from a single analysis since the rate of decrease is dependent on both the stressing temperature and oil formulation (Figures 89 and 122).

#### c. Effect of Oil Formulation

To further test the formulation independence of the RLLAT-RCV assessments, fresh candidate MIL-L-27502 lubricating oil was studied. The antioxidant system of the candidate MIL-L-27502 lubricating oil is unknown and thought to be unique. Therefore, candidate MIL-L-27502 oil is a good oil to test the formulation independence of the RLLAT-RCV. The cyclic and reductive-cyclic voltammograms of the candidate MIL-L-27502 lubricating oil are shown in Figure 123.

The voltammograms in Figure 123 show that cyclic voltammetry is able to detect antioxidant(s) in the candidate MIL-L-27502 oil and that the reduction wave B (Figure 123) is inhibited

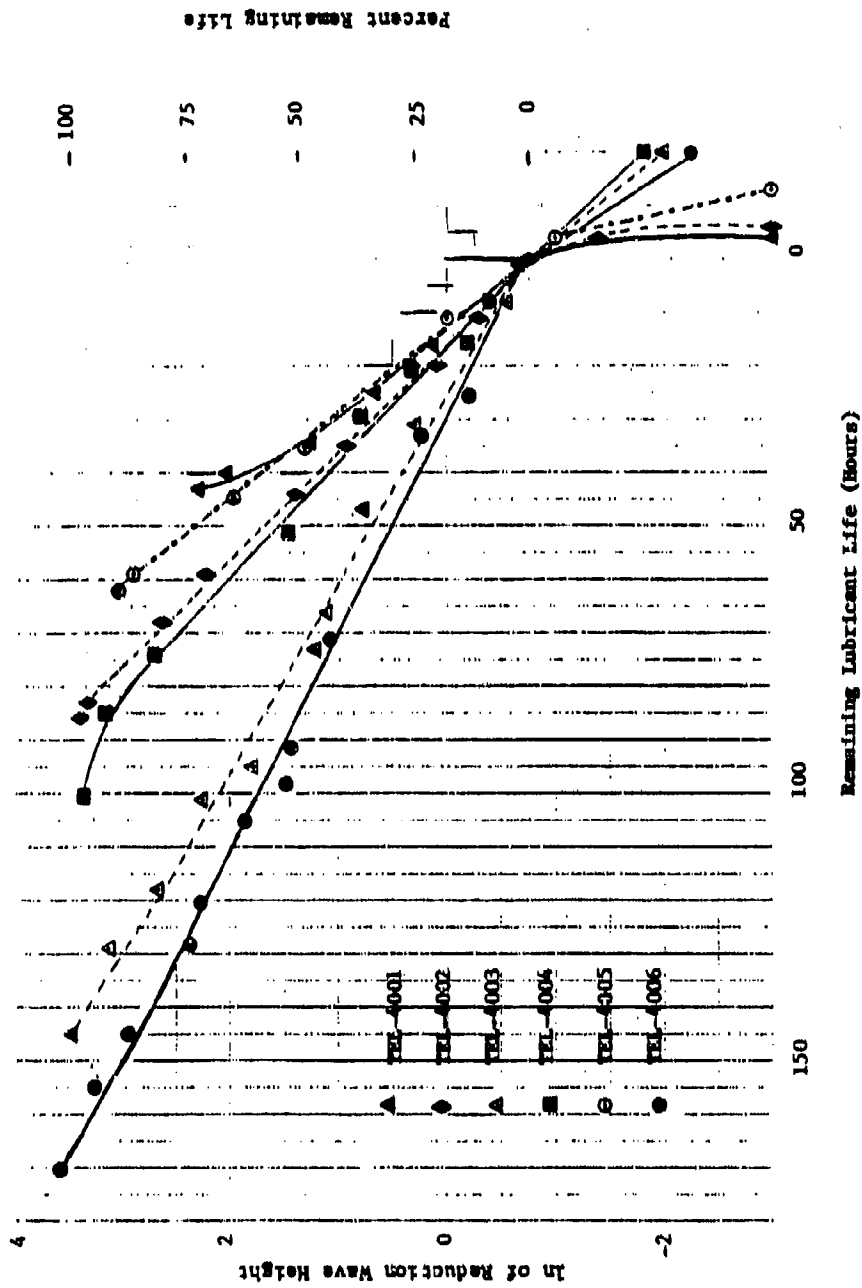


Figure 122. Plots of the ln of the Reduction Wave Height and Percent Remaining Life of the Reductive-Cyclic Voltammetric Technique Versus Hours of Remaining Lubricant Life at 392°F for the Fresh and Stressed MIL-L-7808 Oils.

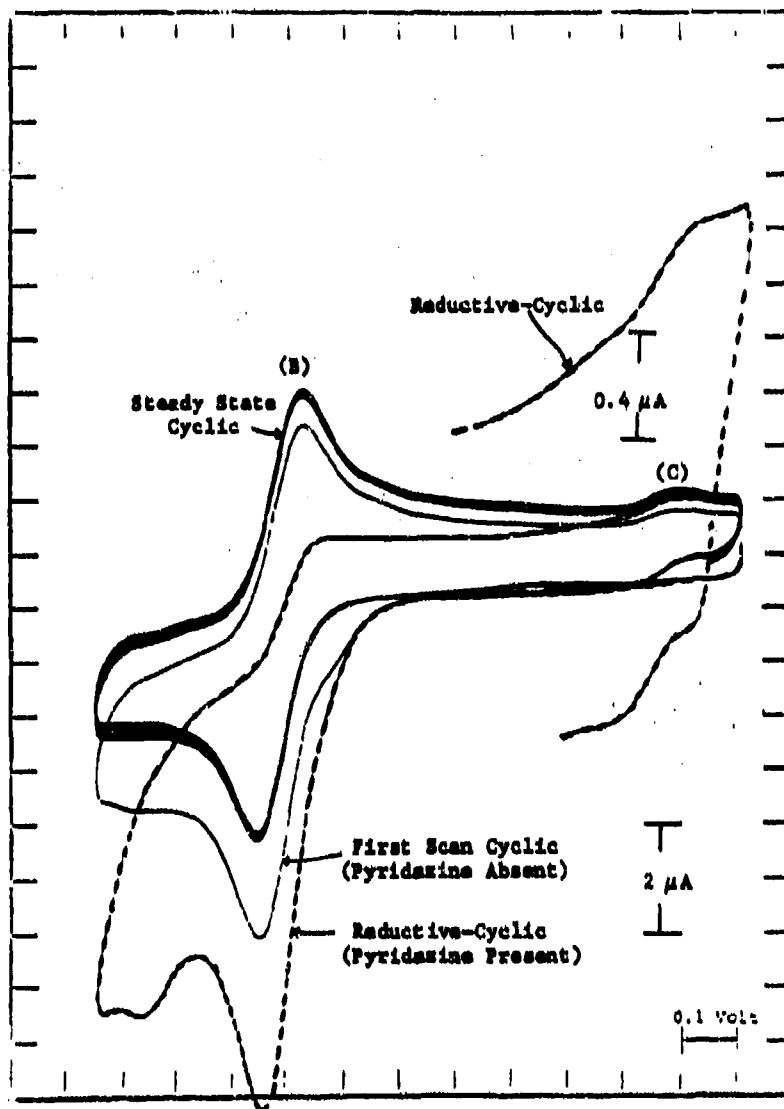


Figure 123. Cyclic (First Scan and Steady State) and Reductive-Cyclic Voltammograms of a Candidate MIL-L-27502 Oil in Acetone Using a GCE Electrode.

by the presence of pyridazine. Similar results were obtained for the MIL-L-7808 oils. The reduction wave C (Figure 123) is apparent even in the absence of pyridazine and increases when pyridazine is present.

These initial results indicate that cyclic voltammetry and RLLAT-RCV can be used to monitor at least one of the antioxidant species in this candidate MIL-L-27502 oil. The relationships between the RLLAT-RCV results and the RLL of the candidate MIL-L-27502 oil can only be established by studying sets of fresh and stressed MIL-L-27502 oils.

#### d. Analysis of Used MIL-L-7808 Oils

To further evaluate the RLLAT-RCV, used MIL-L-7808 oils (OP-232-1 through OP-232-43) obtained from AFWAL/POSL were studied by cyclic voltammetry. The cyclic voltammograms of the OP-232-1 through OP-232-43 oil samples are shown in Figures 124-128. The cyclic voltammogram of fresh TEL-4004 MIL-L-7808 oil is included in Figure 124 for reference.

The cyclic voltammograms in Figures 124-128 show that the OP-232-4 through OP-232-12 oils are fresh or negligibly stressed oils, while the OP-232-1 and OP-232-26 through OP-232-43 have undergone slight to moderate stressing. The estimation of stressing is based on the fact that fresh oils (TEL-4004 oil in Figure 124) do not produce the oxidation wave A (Figures 124-128) which has been assigned to antioxidant species generated during the early periods of thermal-oxidation.

The sizes and shapes of the cyclic voltammograms in Figures 124-128 also provide formulation information. The OP-232-4 through OP-232-12 oils produce cyclic voltammograms of similar size and shape indicating that the antioxidant systems of the oils are basically the same. The sizes and shapes of the cyclic voltammograms produced by the OP-232-26, OP-232-29, and OP-232-43 oils indicate that their original antioxidant systems were similar to those of the OP-232-4 through OP-232-12 oils. The OP-232-1 oil

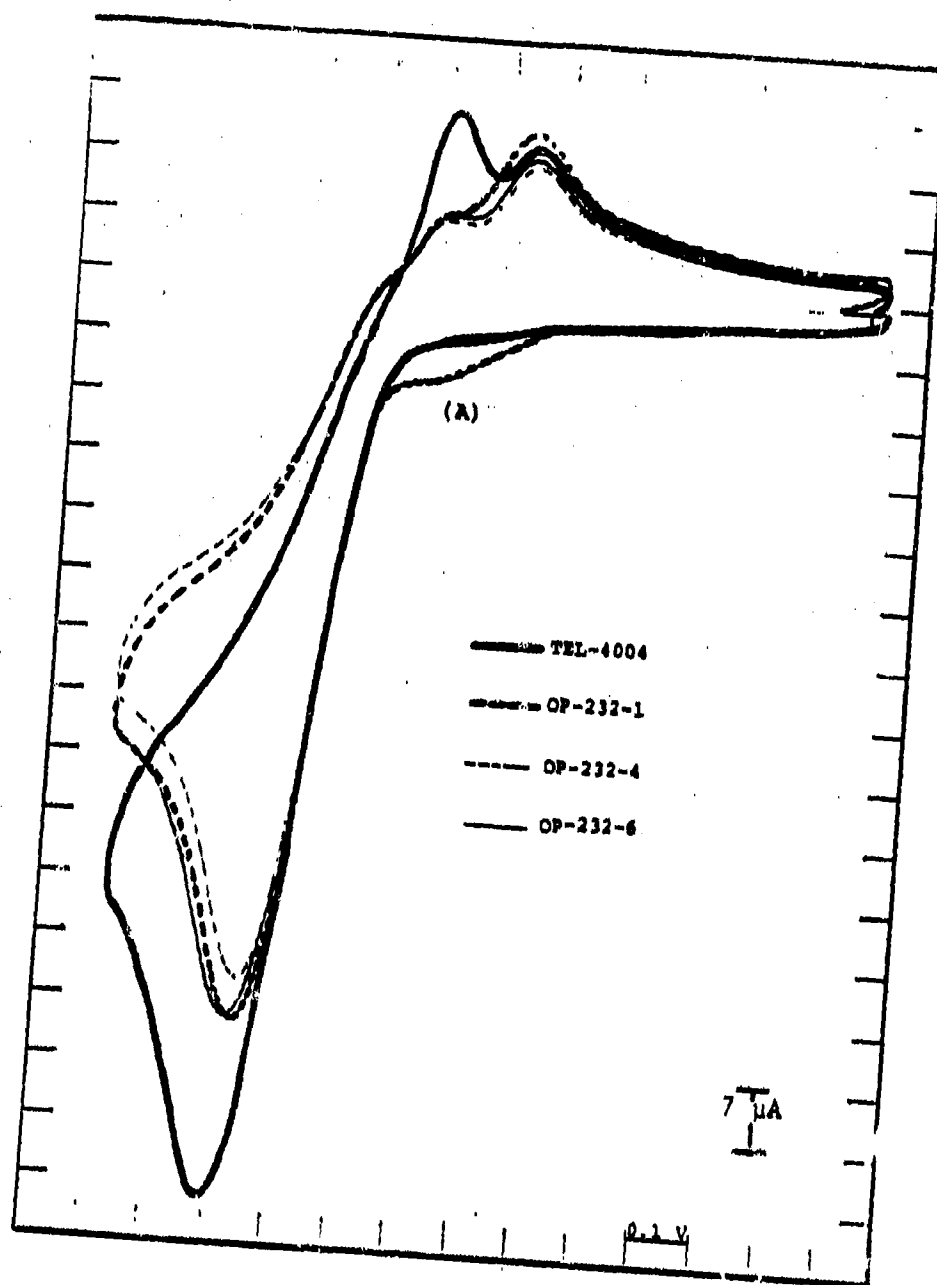


Figure 124. Cyclic (First Scan) Voltammograms of the Fresh TEL-4004 Oil and the OP-232-1, OP-232-4, and OP-232-6 MIL-L-7808 Oil Samples in Acetone Using a GCE Electrode.

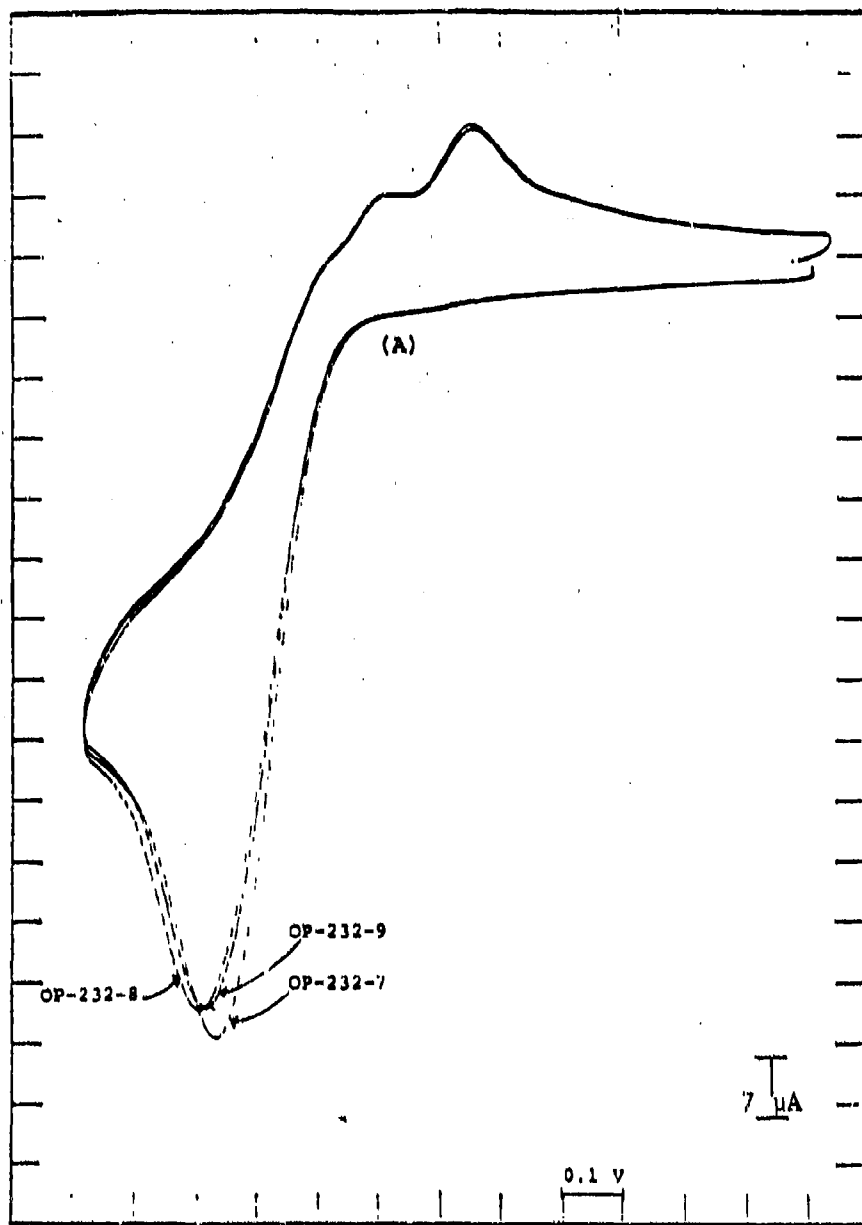


Figure 125. Cyclic (First Scan) Voltammograms of the OP-232-7, OP-232-8, and OP-232-9 MIL-L-7808 Oil Samples in Acetone Using a GCE Electrode.

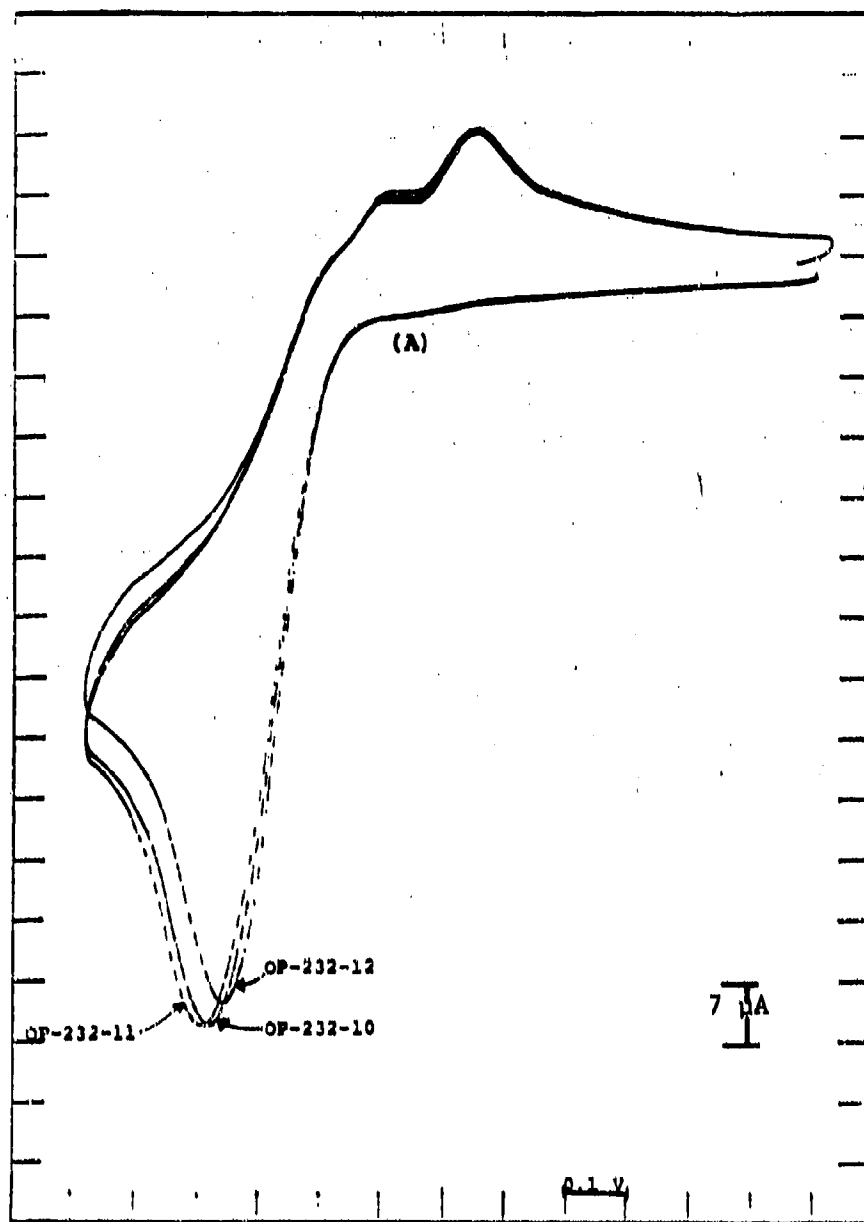


Figure 126. Cyclic (First Scan) Voltammograms of the OP-232-10, OP-232-11, and OP-232-12 MIL-L-7808 Oil Samples in Acetone Using a GCE Electrode.

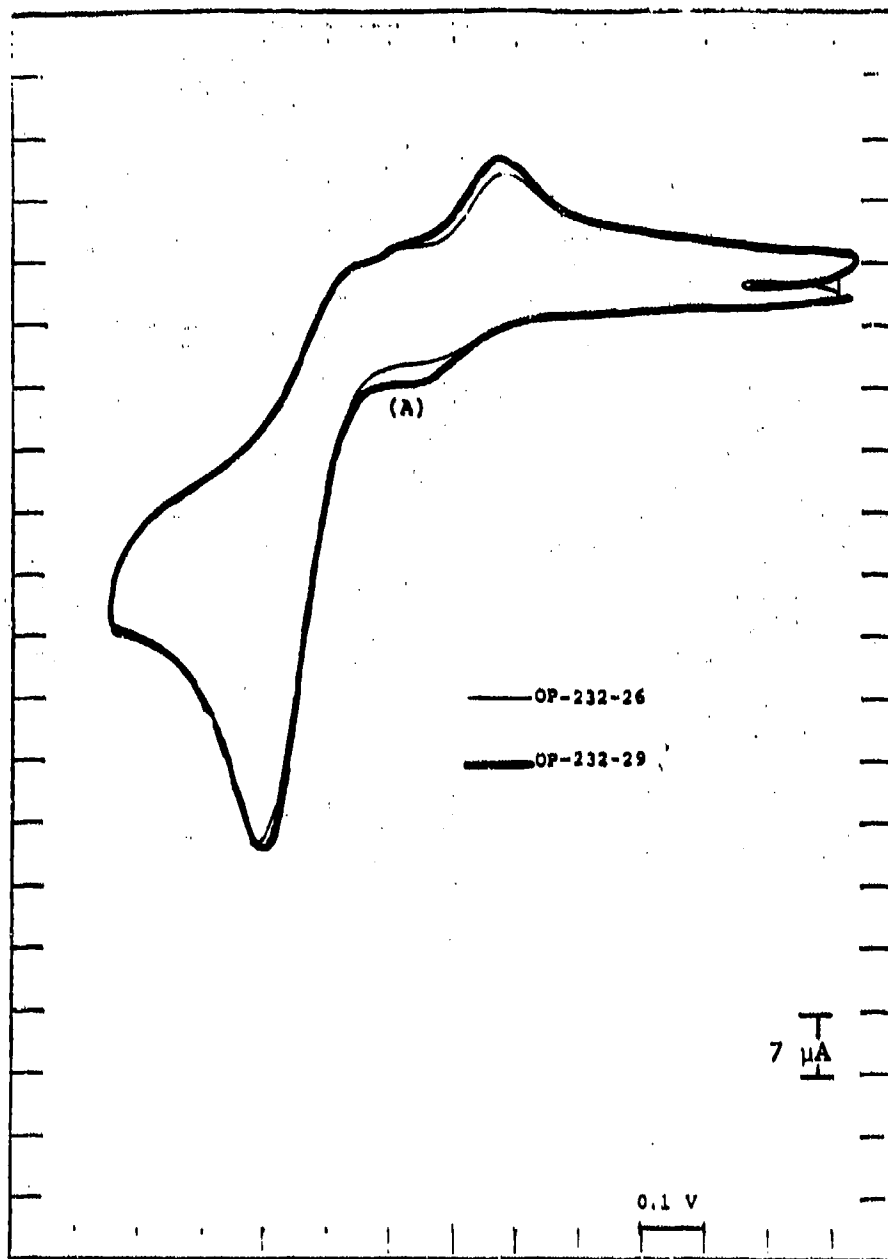


Figure 127. Cyclic (First Scan) Voltammograms of the OP-232-26 and OP-232-29 MIL-L-7808 Oil Samples in Acetone Using a GCE Electrode.

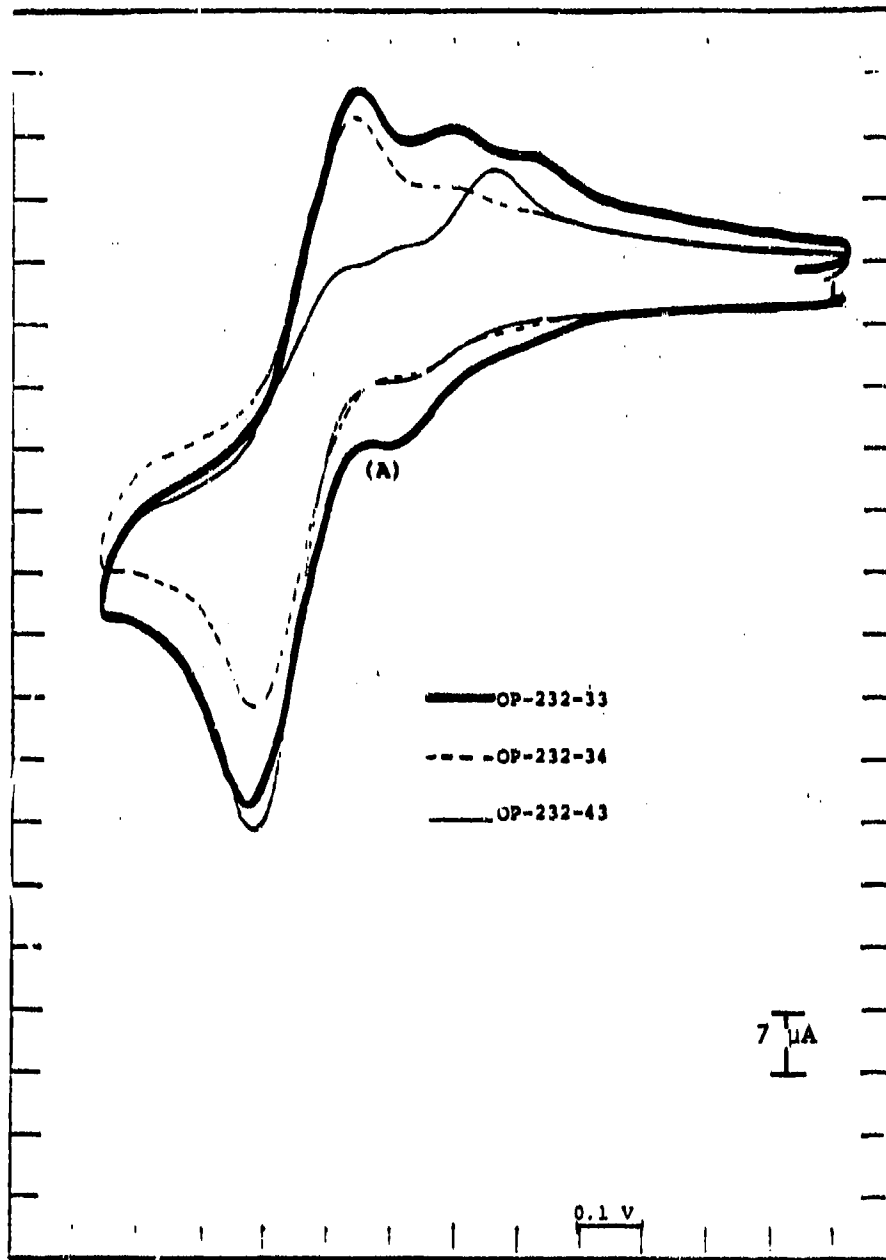


Figure 128. Cyclic (First Scan) Voltammograms of the OP-232-33, OP-232-34, and OP-232-43 MIL-L-7808 Oil Samples in Acetone Using a GCE Electrode.

contains an antioxidant system that is slightly different from the OP-232-4 through OP-232-29 and OP-232-43 oils.

The sizes and shapes of the OP-232-33 and OP-232-34 oils' cyclic voltammograms indicate that their antioxidant systems are similar and that their antioxidant systems are different from the OP-232-1 through OP-232-29 and OP-232-43 oils.

Although the cyclic voltammetric analyses provide valuable qualitative information, they are not capable of quantitative percent RLL assessments. Therefore, the OP-232-1 through OP-232-43 oils were also analyzed by the RCV technique. The RCV results, reduction wave heights and corresponding percent RLL, are listed in Table 14. The percent RLL assessments were made by assigning the reduction wave height  $\ln$  values of 3.44 and  $-.70$ , the percent RLL of 100 and 0%, respectively. These assignments resulted in a 97% RLL assessment for fresh TEL-4004 oil.

The RCV results in Table 14 agree well with the cyclic voltammetric analyses. The OP-232-4 through OP-232-12 oils have over 90% RLL (fresh oils) while the OP-232-26 through OP-232-43 oils have 88-60% RLL (stressed oils). However, the oil with the highest RLL, OP-232-1 oil, was shown by cyclic voltammetry to be a stressed oil, not a fresh oil.

In order to improve the RLL assessments of the RCV analyses, the D values were calculated for the OP-232-1 through OP-232-43 oils and are also listed in Table 14.

$D(\mu A) = \text{steady state reduction wave height} - \text{reduction wave height of first scan}$   
steady state = average of sixth through tenth scans

TABLE 14  
 REDUCTIVE-CYCLIC VOLTAMMETRIC RESULTS  
 FOR USED MIL-L-7808 OILS

	Reduction Wave Height ( $\mu$ A)	% Remaining Lubricant Life	D ( $\mu$ A)
OP-232-1	31.0	99.8	3.2
OP-232-4	24.0	93.4	6.0
OP-232-6	27.2	96.6	6.7
OP-232-7	28.0	97.3	7.8
OP-232-8	28.0	97.3	7.2
OP-232-9	28.0	97.3	8.0
OP-232-10	28.5	97.7	8.6
OP-232-11	28.5	97.7	8.2
OP-232-12	25.3	94.8	6.0
OP-232-26	17.4	85.0	3.2
OP-232-29	19.3	88.0	3.2
OP-232-33	10.2	72.3	2.0
OP-232-34	6.3	60.2	1.2
OP-232-43	20.6	88.1	3.0
Fresh TEL-4004	28.0	97.3	8.4

The D values in Table 14 are between 6.0 and 8.6 for the OP-232-4 through OP-232-12 oils indicating that they are fresh (D value of fresh TEL-4004 = 8.4), but are between 3.2 and 1.2 for the OP-232-1 and OP-232-26 through OP-232-43 oils, indicating that they are stressed oils (full agreement with cyclic voltammetric results). Therefore, by using both the  $\% RLL$  and the corresponding D value of the RCV analysis, a more comprehensive, accurate RLL assessment can be made by the RLLAT-RCV.

e. Analysis of Authentic Used MIL-L-7808 and MIL-23699 Oils

Although the used MIL-L-7808 oil samples provided by AFWAL/POSL were used to demonstrate the capability of the RLLAT-RCV to analyze used MIL-L-7808 oils with unknown formulations, the analyses could not be used to evaluate the RLL assessing capabilities of the RLLAT-RCV since the histories of the used MIL-L-7808 oil samples were unknown. Therefore, to further evaluate the RLLAT-RCV, authentic used MIL-L-7808 and MIL-L-23699 oil samples taken from abnormally operating engines were analyzed. The MIL-L-23699 oils were included in this study to further evaluate the formula independence of the RLLAT-RCV results. The plots of the  $\ln$  values of the RCV wave heights versus hours since oil change are shown in Figures 129-131. The Fe concentrations (SOAP determined: emission spectrometer) for each series of oil samples are also listed in Figures 129-131 to indicate the severity of wear occurring in the engine.

The plots in Figures 129-131 indicate that two main RLL-severity of wear relationships are represented by the series of oil samples. In the first case, the severity of wear increases resulting in a rapid decrease of the oil sample's RLL, e.g., sample series: H62, F51, and H99 (Figures 129 and 130). In fact, the sharp decrease in the RLL is a better indication of severe wear than the Fe concentrations for the sample series F51 and F52 (Figure 129) taken from the engines that failed before SOAP detection.

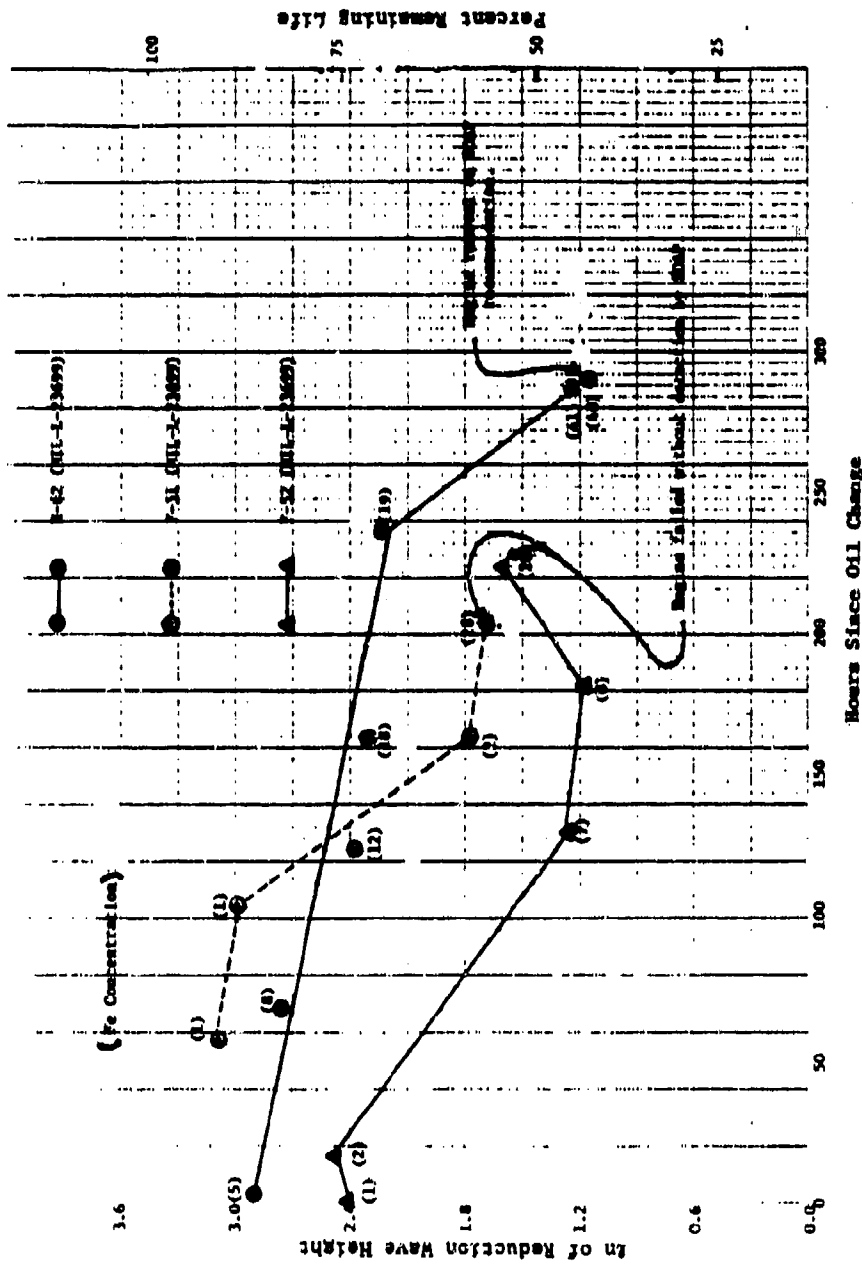


Figure 129. Plots of the  $\ln$  of the Reduction Wave Height and Percent Remaining Life of the Reductive-Cyclic Voltammetry Technique and the Fe Concentration (ppm) Versus Hours Since Oil Change for the Used Lubricating Oil Samples.

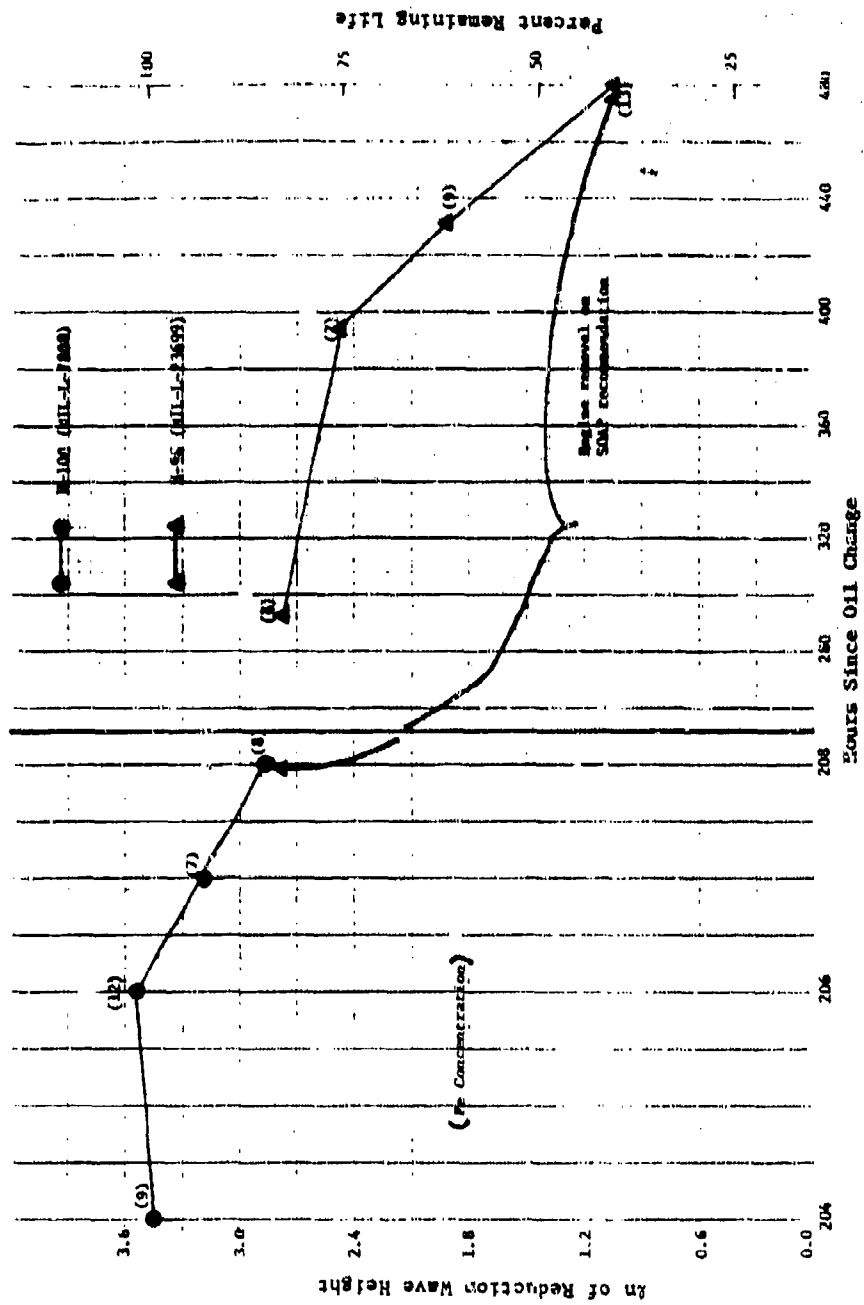


Figure 130. Plots of the  $\ln$  of the Reduction Wave Height and Percent Remaining Life of the Reductive-Cyclic Voltammetry Technique and the Fe Concentration (ppm) Versus Hours Since Oil Change for the Used Lubricating Oil Samples.

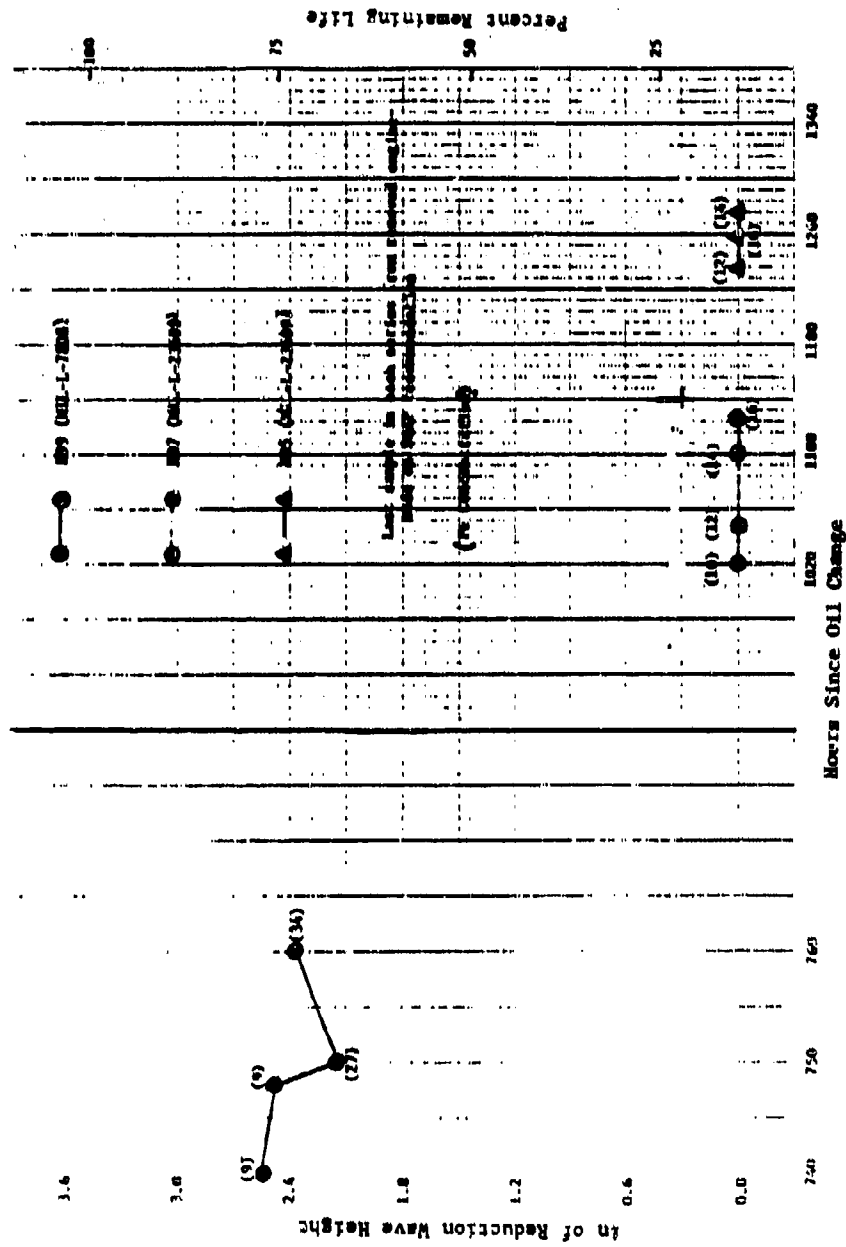


Figure 131. Plots of the  $\ln$  of the Reduction Wave Height and Percent Remaining Life of the Reductive-Cyclic Voltammetry Technique and the Fe Concentration (ppm) Versus Hours Since Oil Change for the Used Lubricating Oil Samples.

In the second case, it appears that the oil has reached the end of its stable life several hours prior to the occurrence of abnormal wear, e.g., H97 and H95 (Figure 131).

The plots in Figures 129-131 also indicate that oil additions were being performed causing the RLL of the oil samples to increase or reach a steady state value. Unfortunately, the times and amounts of the oil additions were not recorded so that the complete relationships between the RLL and severity of wear could not be determined. The oil additions also complicate the hours of RLL assessments.

One interesting fact obtained from Figures 129-131 is that the assignment of 0% RLL to a RCV wave height of  $0.5 \mu\text{A}$  appears to be too low for the MIL-L-23699 oils. Samples H97 and H95 (Figure 131) decreased to a RCV wave height of  $1.0 \mu\text{A}$  and then remained constant, even though the hours of use increased. Therefore, it appears that for MIL-L-23699 oils,  $1.0 \mu\text{A}$  ( $\ln$  value = 0.0) should be assigned 0% RLL. None of the used MIL-L-7808 oils appeared to reach the end of their stable lives (lowest value  $9.1 \mu\text{A}$ :  $\ln$  value = 2.20) so that an evaluation of the 0% RLL assignment of  $0.5 \mu\text{A}$  for the MIL-L-7808 oils could not be made.

Except for the slightly higher 0% RLL, the RCV results do not appear to be affected by the formula differences between the MIL-L-7808 and MIL-L-23699 oils. In fact, the higher 0% RLL may be a result of operating condition differences (bulk oil temperature, aeration rates, etc.) between the J79 and F-100 engines (MIL-L-7808 oil) and the T56 engine (MIL-L-23699 oil) rather than oil formulation differences.

#### f. Effect of Oil Addition

The RLLAT-RCV versus hours since oil changes plots (Figures 129-131) for the used MIL-L-7808 and MIL-L-23699 oil samples indicate that oil additions caused the RLL life of the oil samples to increase or reach a steady state value. Unfortunately, the times and amounts of the oil additions were not recorded so

that the effects of the oil additions on the RLL assessments of the RLLAT-RCV could not be determined.

Therefore, an oil addition study using Federal Test Method Standard 791 Method 5307.1 was performed. Samples of TEL-4004 MIL-L-7808 oil were stressed at 347°F and diluted with TEL-4001, TEL-4003, and TEL-4004 MIL-L-7808 oils at regular intervals. The RLLAT-RCV analyses of the diluted TEL-4004 oil samples were then plotted versus stressing time at 347°F to determine the effects of oil dilution and formulation mixing on the RLL assessments of the RLLAT-RCV (Appendix B).

Four different TEL-4004 oil samples stressed at 347°F were sampled and diluted at regular intervals. Two of the TEL-4004 oil samples, DIL-1 and DIL-2, were diluted with fresh TEL-4004 oil (20 ml) at differing intervals, 48 and 192 hours, respectively, to simulate jet engines undergoing rapid and slow oil losses, respectively. The other two TEL-4004 oil samples, DIL-3 and DIL-4, were diluted with fresh TEL-4001 and TEL-4003 oils, respectively, at 48 hour intervals to determine the effects of formulation mixing on the RLLAT-RCV results. The plots of the RLLAT-RCV analysis versus stressing time at 347°F for the DIL-1 through DIL-4 oil samples are shown in Figures 132-135, respectively. The COBRA reading versus stressing time at 347°F plots for the DIL-1 through DIL-4 oil samples are included in Figures 132-135 to estimate the oxidative degradation of the stressed oil samples.

As seen in Figures 132, 134, and 135, the oil additions of fresh TEL-4004, TEL-4001 and TEL-4003 oils cause the RLLAT-RCV analyses of the DIL-1, DIL-3, and DIL-4 oil samples, respectively, to obtain steady state values after the third or fourth additions of fresh oil. However, the steady state value attained by each sample is affected by the formulation of the oil being added. The TEL-4003 oil has the longest stable life (320 hrs at 370°F) and produces the highest steady state value of 12.5  $\mu$ A, while TEL-4001 oil has the shortest stable life (105 hrs at 370°F) and produces the lowest steady state value of 5  $\mu$ A. The TEL-4004 oil has a

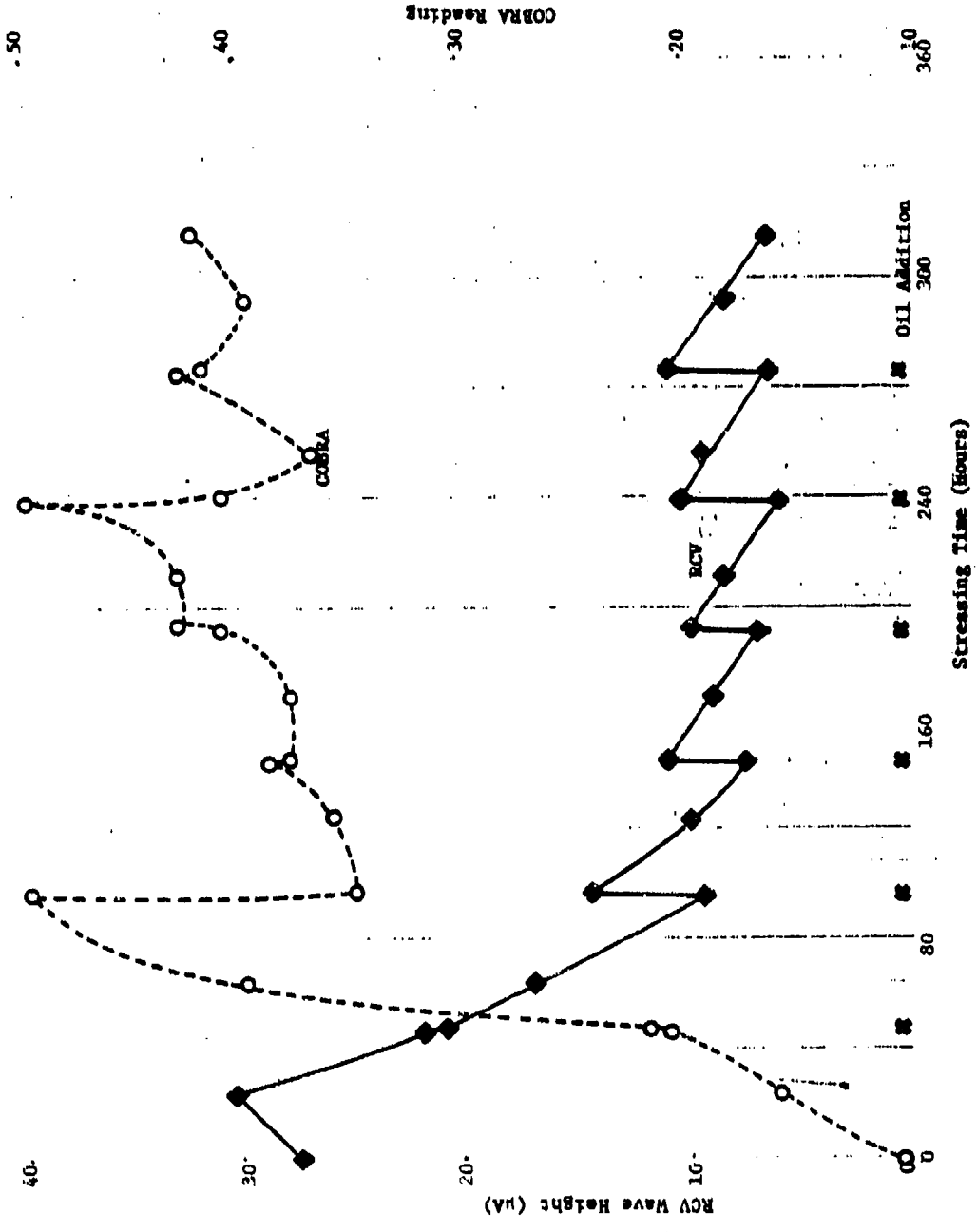


Figure 132. Plots of the RCV Wave Height and COBRA Reading Versus Stressing Time (347°F) for the DIL-1 Oil Samples.

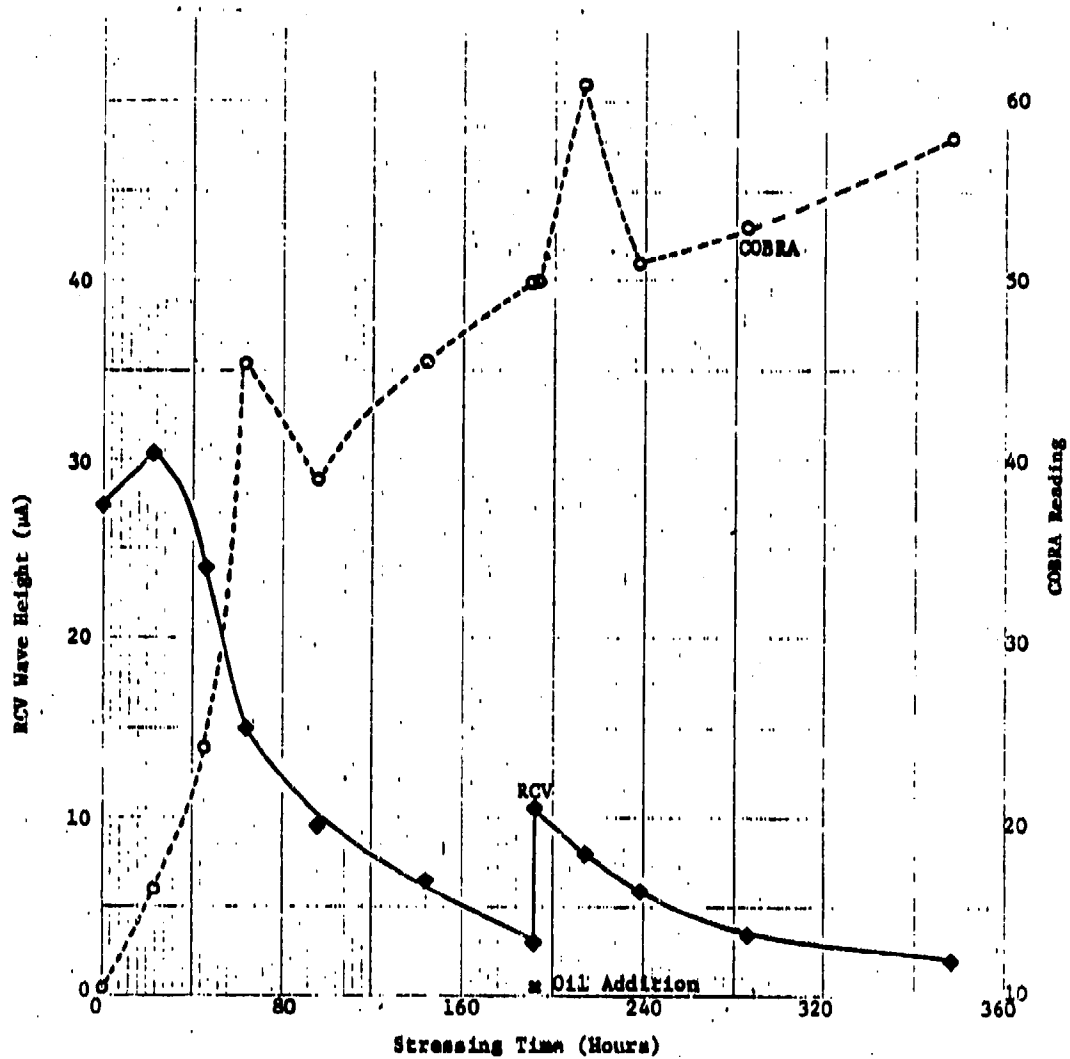


Figure 133. Plots of the RCV Wave Height and COBRA Reading Versus Stressing Time (347°F) for the DIL-2 Oil Samples.

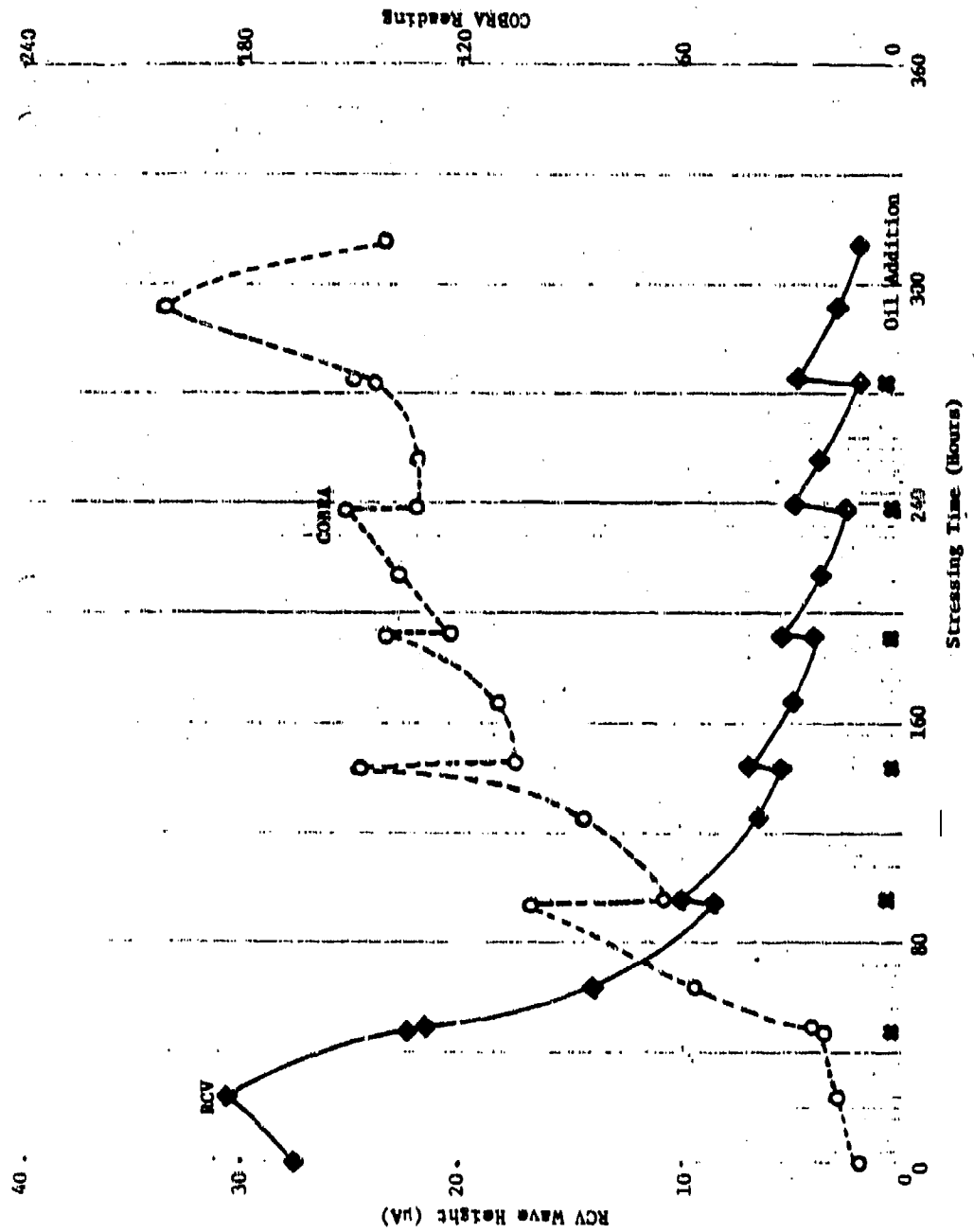


Figure 134. Plots of the RCV Wave Height and COBRA Reading Versus Stressing Time (347°F) for the DIL-3 Oil Samples.

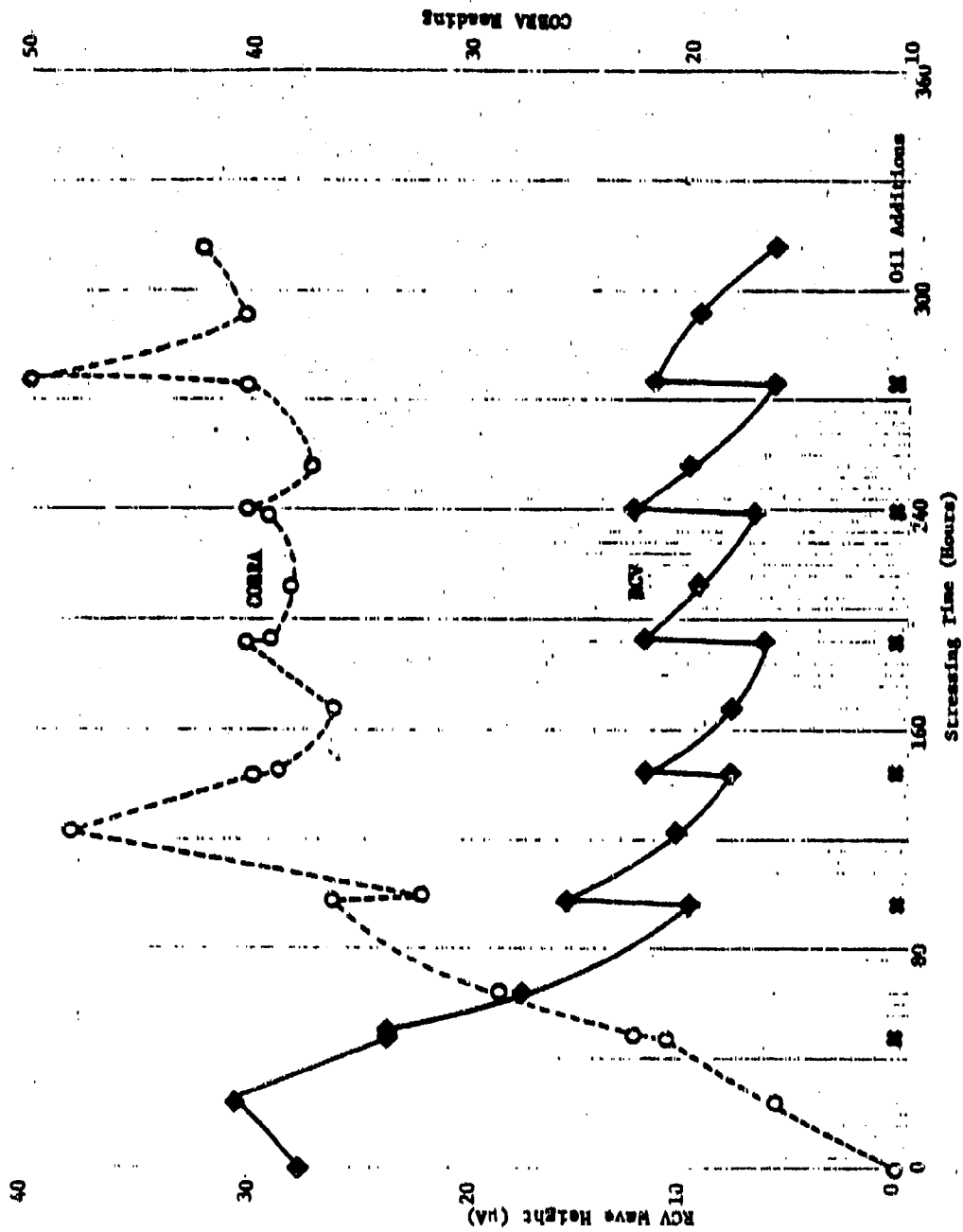


Figure 135. Plots of the RCV Wave Height and COBRA Reading Versus Stressing Time (347°F) for the DIL-4 Oil Samples.

stable life of 205 hrs at 370°F and produces a steady state value of 10  $\mu$ A.

The plots of the RLLAT-RCV results in Figures 132, 134 and 135 also show that the effect of the oil addition increases with stressing time. In fact, the first oil addition performed at 46 hours of stressing had no effect on the RLLAT-RCV results. After the first addition, the successive oil additions of the MIL-L-7808 oils produced fairly constant increases in the RCV results. The TEL-4003, TEL-4004, and TEL-4001 oils produced increases of 5.5, 4.5, and 2.0  $\mu$ A, respectively, in the RLLAT-RCV results; in full agreement with their respective stable lives periods (370°F) of 320, 205, and 105 hours.

The plots of the RLLAT-RCV results for the DIL-1 and DIL-2 oil samples shown in Figures 132 and 133, indicate that the effect of the oil addition on the RCV results may also be dependent on the time intervals at which the oil additions are made. For the oil addition intervals of 48 and 192 hours, the addition of TEL-4004 oil produced increases of 4.5 and 7.5  $\mu$ A, respectively in the RLLAT-RCV results of the DIL-1 and DIL-2 oil samples.

Since the RCV results decrease to a steady state value for the DIL-1, DIL-3, and DIL-4 oil samples, the increase in the RLLAT-RCV results caused by the oil additions must be equal to the decrease in the RLLAT-RCV results caused by the stressing between successive oil additions. Therefore, if the operating conditions of the jet engine change, causing an increase in the severity of the stressing conditions (temperature, air flow rate, etc.) of the lubricating oil, the decrease between successive oil additions will accelerate and a change in the steady state value of the RLLAT-RCV results will occur.

To simulate a jet engine in which the stressing conditions of the lubricating oil are becoming more severe, the stressing temperatures of the DIL-1 through DIL-4 oils were increased after 335 hours from 347 to 370°F. The  $\ln$  values of the RLLAT-RCV results of the DIL-1 through DIL-4 oils from 193 hours of stressing (347°F) to 400 hours of stressing (370°F) were plotted versus stressing time as shown in Figure 136.

The plots in Figure 136 show that the  $\ln$  of the RLLAT-RCV results of the DIL-1 through DIL-4 oils decrease at fairly constant rates between successive oil additions, and that, increasing the temperature from 347 to 370°F dramatically increases the rates at which the  $\ln$  of the RCV results decrease. The rates at which the  $\ln$  of the RCV results decrease between successive oil additions is approximately doubled by the 347° to 370°F temperature increase.

#### g. Summary of RLLAT Based on RCV

The initial investigation showed that the RLL assessment capabilities of the RLLAT-RCV were independent of temperature and that the RLLAT-RCV has potential for RLL assessments of lubricating oils other than MIL-L-7808 oils, e.g. MIL-L-23699 and MIL-L-27502 lubricating oils.

For jet engines which require infrequent oil additions, the RLLAT-RCV results can be used to assess the percent RLL of individual used oil samples and the rate at which the RCV results decrease with operating time can be used to predict the hours of RLL for the jet engine under normal operating conditions. When the jet engine's operating conditions become abnormal, the rates at which the RLLAT-RCV results decrease versus hours since oil change accelerate, enabling the detection of the abnormal operating conditions.

For jet engines which require frequent oil additions, the RLLAT-RCV results can be used to assess the percent RLL of individual used oil samples, but because frequent oil additions maintain the RLL of the used lubricating oil at an acceptable level, the hours of RLL predictions are meaningless. However,

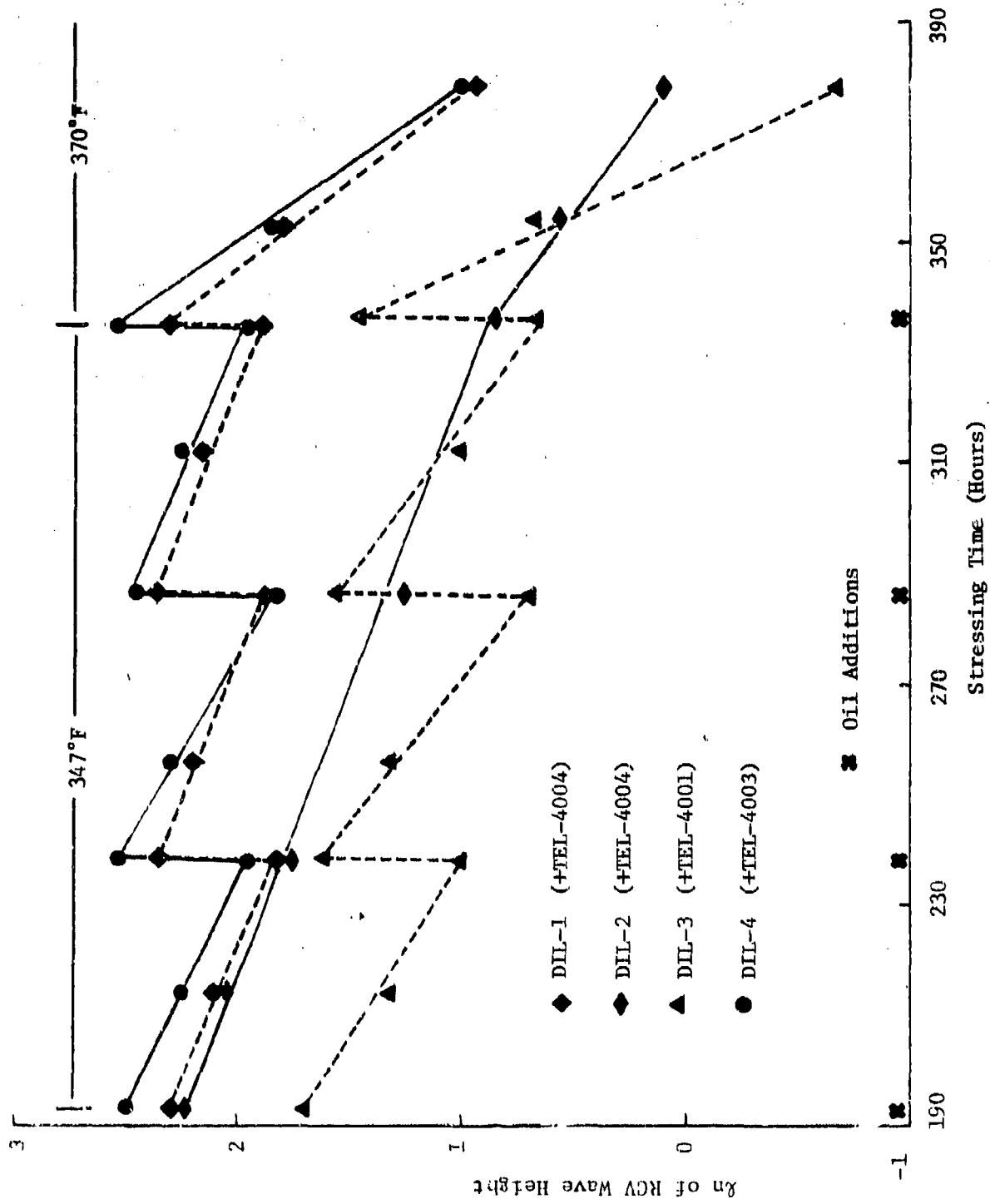


Figure 136. Plots of the  $\lambda n$  of the RCV Wave Height Versus Stressing Time at 347°F and 370°F for the DIL-1 through DIL-4 Oil Samples.

when the jet engine's operating conditions become abnormal, the rates at which the RLLAT-RCV results decrease between oil additions accelerate, enabling the detection of abnormal operating conditions.

SECTION III  
CONCLUSIONS AND RECOMMENDATIONS

During Task 1 of this investigation, numerous analytical techniques with potential for development into a RLLAT were identified (Table 2) and evaluated for use by the Air Force. Of the analytical techniques identified in Task 1, only the voltammetric, differential scanning calorimetric, and colorimetric techniques were capable of assessing the RLL of MIL-L-7808 oils. The modified Ford method was also capable of assessing RLL of MIL-L-7808 oils, but the use of the unstable free radical initiator solution and the length of the analysis time (>15 minutes for fresh MIL-L-7808 oils) made the modified Ford method unsuitable for use by the Air Force. The remaining analytical techniques listed in Table 2 had limited RLL assessing capabilities. Consequently, RLLAT candidates were developed from the voltammetric, differential scanning calorimetric, and colorimetric techniques in Task 2.

In Task 2, two voltammetric techniques, CV and RCV, were developed into RLLAT candidates and then evaluated using the criteria in Table 1. It was shown that the results of the CV technique could be used to identify the type of antioxidant(s) present in a fresh MIL-L-7808 oil and to estimate the oxidative degradation of a MIL-L-7808 oil. However, the CV technique could not be used to assess the RLL of MIL-L-7808 oils containing phenothiazine or other sulfur containing antioxidants. In contrast to the CV technique, the RLL assessments of the RCV technique were accurate (linear relationship between RCV results and RLL assessments) and formula independent. A microcomputer-based data acquisition system was incorporated into the RCV to produce a RLLAT candidate that had potential for base-level operation and RLL assessments.

Two differential scanning calorimetric techniques, HP-DSC and SP-DSC, were also developed into RLLAT candidates and then evaluated (criteria in Table 1) in Task 2. It was determined

that the formula dependence of the HP-DSC technique's RLL assessments was affected by the method used to interpret the HP-DSC results. The onset of reaction time resulted in the most accurate and the least formula dependent RLL assessments for the HP-DSC technique. The SP-DSC technique, which eliminated the high pressure requirements of the HP-DSC technique, also produced formula independent RLL assessments. However, inflection points in the SP-DSC result versus RLL plots of the different MIL-L-7808 oils reduced the accuracy of the SP-DSC RLL assessments. The development of the HP-DSC and SP-DSC techniques into RLLAT candidates was limited by the techniques' high instrumental and operational costs (Table 13).

The last analytical technique to be developed into a RLLAT candidate and then evaluated (criteria in Table 1) in Task 2 was the colorimetric technique. The colorimetric technique produced formula independent RLL assessments, but the accuracy of the RLL assessments was reduced by the inflection points in the colorimetric result versus RLL plots of the different MIL-L-7808 oils. Also, the fresh MIL-L-7808 oils did not produce induction times for the colorimetric technique making the interpretation of the results difficult. The development of the colorimetric technique into a RLLAT candidate was limited by the difficult interpretation of the results and by the toxicity of the cumene hydroperoxide used by the technique.

The results of Task 2 showed that the RLLAT candidate based on the RCV technique was the least expensive, most rapid, and easiest to operate RLLAT candidate and that the RCV technique produced the most accurate RLL assessments (Table 13). Therefore, a RLLAT based on the RCV technique was developed in Task 3.

The results in Task 3 showed that the RLLAT-RCV could be used to assess the RLL of MIL-L-7808 oils stressed at different temperatures, of different type lubricating oils, and of authentic used MIL-L-7808 and MIL-L-23699 oil samples. The results of

Task 3 also showed that the RLLAT-RCV was able to detect engines experiencing severe wear.

Therefore, a RLLAT based on the RCV technique has been developed which is capable of accurately assessing the RLL of MIL-L-7808 oils and has potential for use by the Air Force. The initial results of this investigation indicate that the RLLAT-RCV could be used to eliminate the need for scheduled oil changes and to improve the capability of the Air Force's Spectrometric Oil Analysis Program to detect engines experiencing severe wear. Thus, the RLLAT-RCV has the potential of providing the Air Force with increased fleet reliability in addition to savings in material and labor costs.

Due to the successful development of the RLLAT-RCV and the potential benefits to the Air Force, it is recommended that prototypes of the RLLAT-RCV be produced. The prototypes should then be field tested to evaluate their ability to eliminate scheduled oil changes and to detect engines experiencing severe wear. In order that the full potential of the RLLAT-RCV be attained, the RLL assessment capabilities of the prototype need to be evaluated for different types of lubricating oils, e.g., MIL-L-7808 and MIL-L-23699 oils.

## APPENDIX A - PREPARATION AND CHARACTERIZATION OF STRESSED MIL-L-7808 OIL SAMPLES

### A.1 Introduction

To develop the RLLAT candidates, sets of stressed oil samples were prepared from the TEL-4001 through TEL-4006, TEL-5001, and TEL-5002 MIL-L-7808 lubricating oils using Federal Test Method Standard 791 Method 5307.1 at stressing temperatures of 370°F and 392°F. The stressed oil samples were thoroughly characterized by viscosity (40°C), total acid number (TAN), COBRA measurement, and magnesium (Mg) concentration. The antioxidants in the stressed oil samples were identified and quantified by gas chromatography using a thermionic specific (nitrogen-phosphorous sensitive) detector.

The physical properties and antioxidant concentrations of the TEL-4001 through TEL-4006, TEL-5001, and TEL-5002 MIL-L-7808 oils were then plotted versus stressing time at 370°F and 392°F. The plots were used to determine the stable lives of the TEL-4001 through TEL-4006, TEL-5001, and TEL-5002 oils and to determine the relationships that exist among the physical properties, antioxidant concentrations, and the RLL of the MIL-L-7808 oils.

### A.2 Physical Properties of the TEL-4001 through TEL-4006 MIL-L-7808 Oils Stressed at 370°F

The plots of the COBRA reading, viscosity (40°C), TAN, and Mg concentration versus stressing time are shown in Figures A-1-A-6 for the TEL-4001 through TEL-4006 MIL-L-7808 lubricating oils, respectively.

As seen in Figures A-1-A-6, during the early hours of thermal-oxidative stressing the values of the physical properties increase at a moderate rate. After the initial rise, the values of the physical properties increase at a much slower, steady rate up to the time of the dramatic rate increase that occurs at the end of the oil's stable life.

To determine the stressing time at which the breakpoint occurs (oil's stable life ends), the flat portions of the physical property plots were extrapolated to a stressing time past the

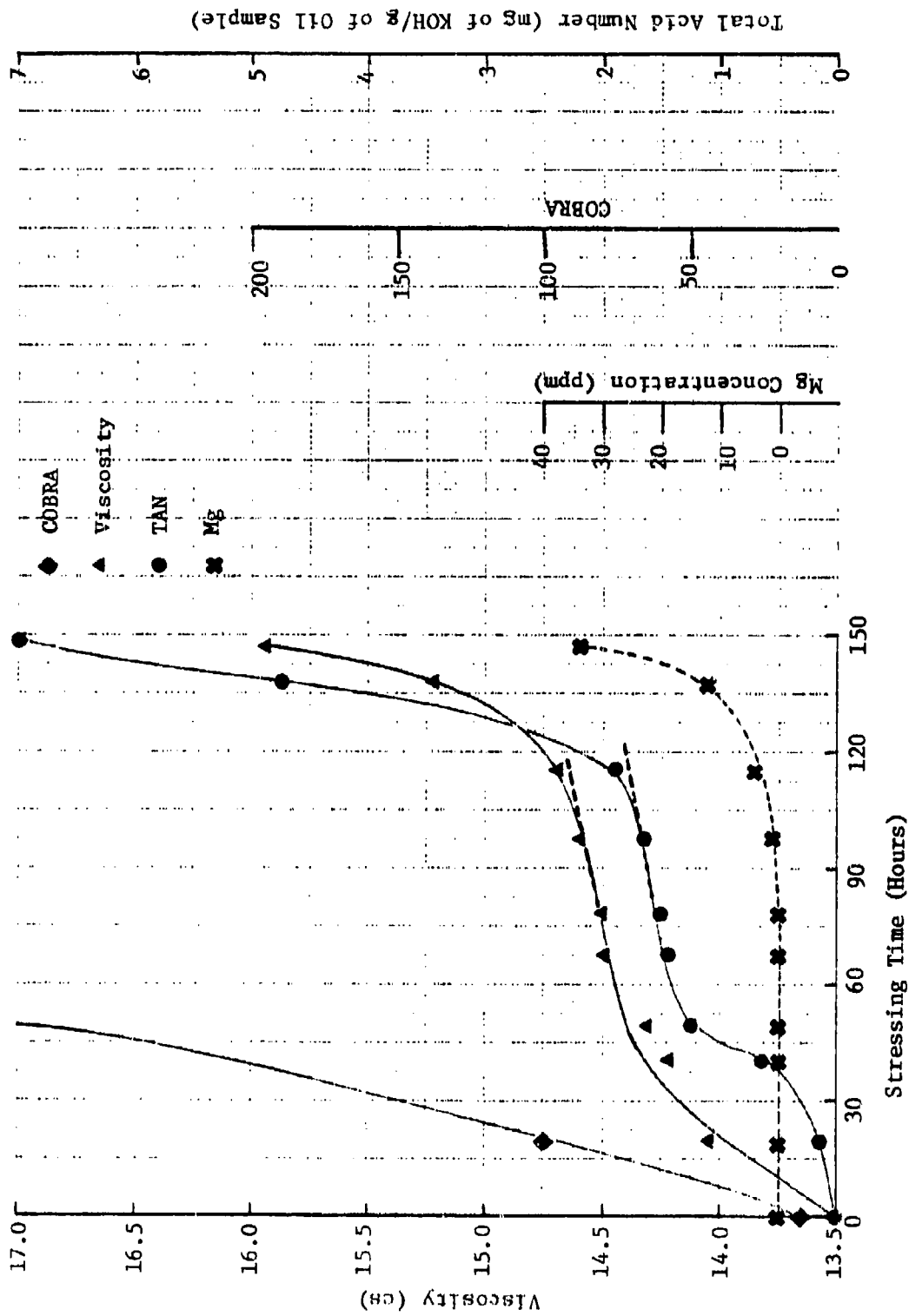


Figure A-1. Plots of the COBRA Reading, Viscosity (40°C), Total Acid Number (TAN), and Mg Concentration Versus Stressing Time at 370°F for the TEL-4001 MIL-L-7808 Oil.

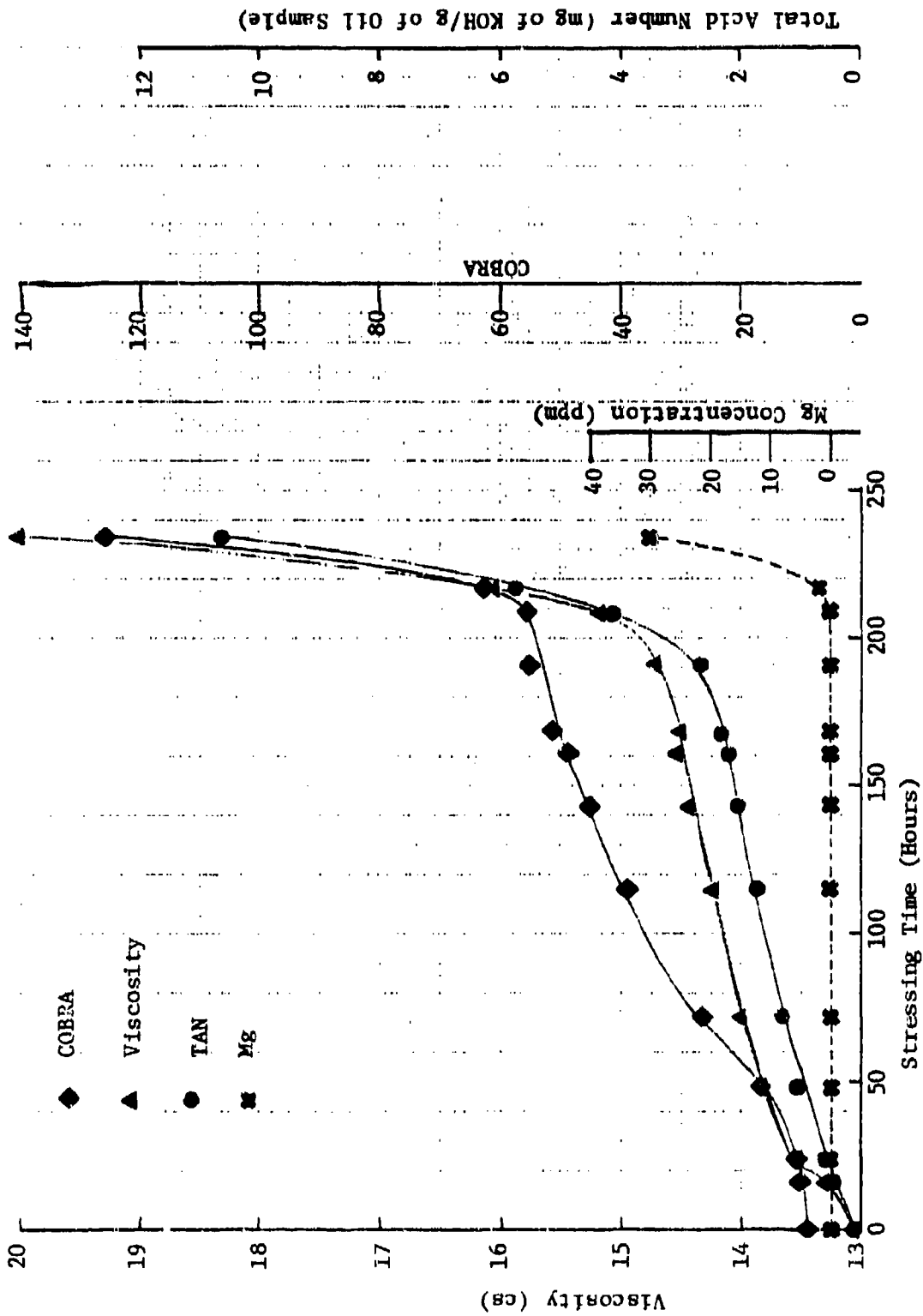


Figure A-2. Plots of the COBRA Reading, Viscosity (40°C), Total Acid Number (TAN), and Mg Concentration Versus Stressing Time at 370°F for the TEL-4002 MIL-L-7808 Oil.

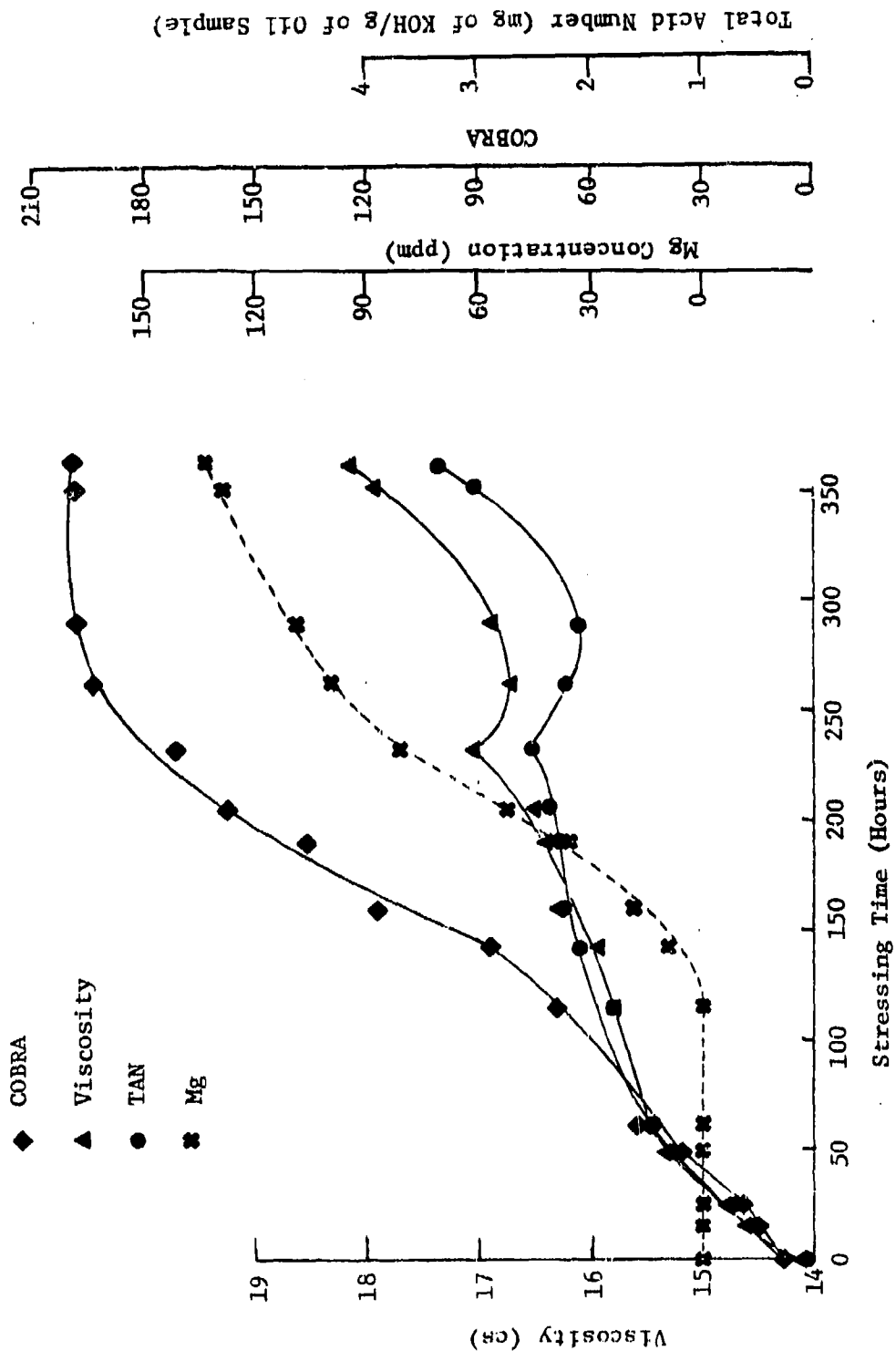


Figure A-3. Plots of the COBRA Reading, Viscosity (40°C), Total Acid Number (TAN), and Mg Concentration Versus Stressing Time at 370°F for the TEL-4003 MIL-L-7808 Oil.

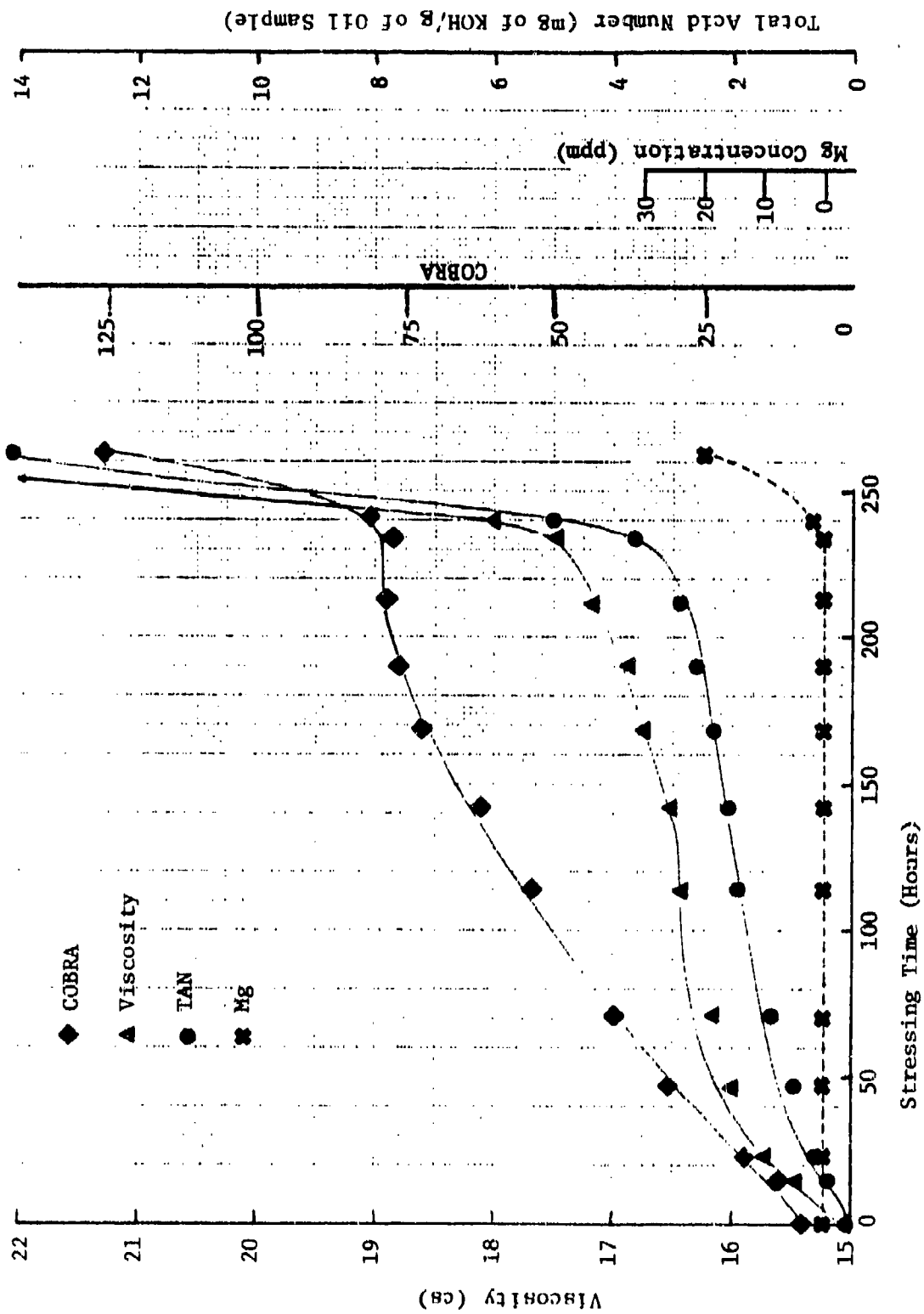


Figure A-4. Plots of the COBRA Reading, Viscosity (40°C), Total Acid Number (TAN), and Mg Concentration Versus Stressing Time at 370°F for the TEL-4004 MIL-L-7808 Oil.

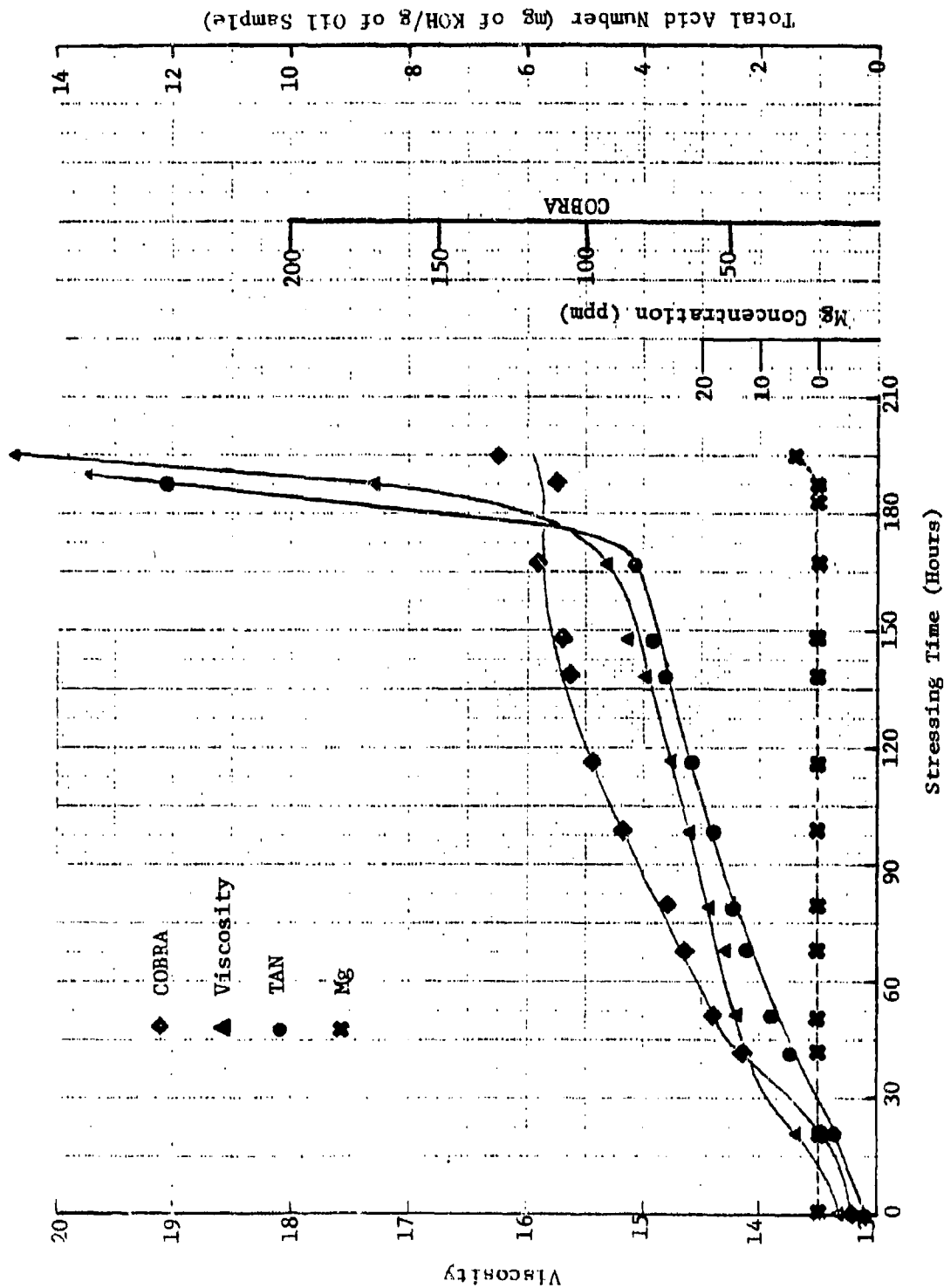


Figure A-5. Plots of the COBRA Reading, Viscosity (40°C), Total Acid Number (TAN), and Mg Concentration Versus Stressing Time at 370°F for the TEL-4005 MIL-L-7808 Oil.

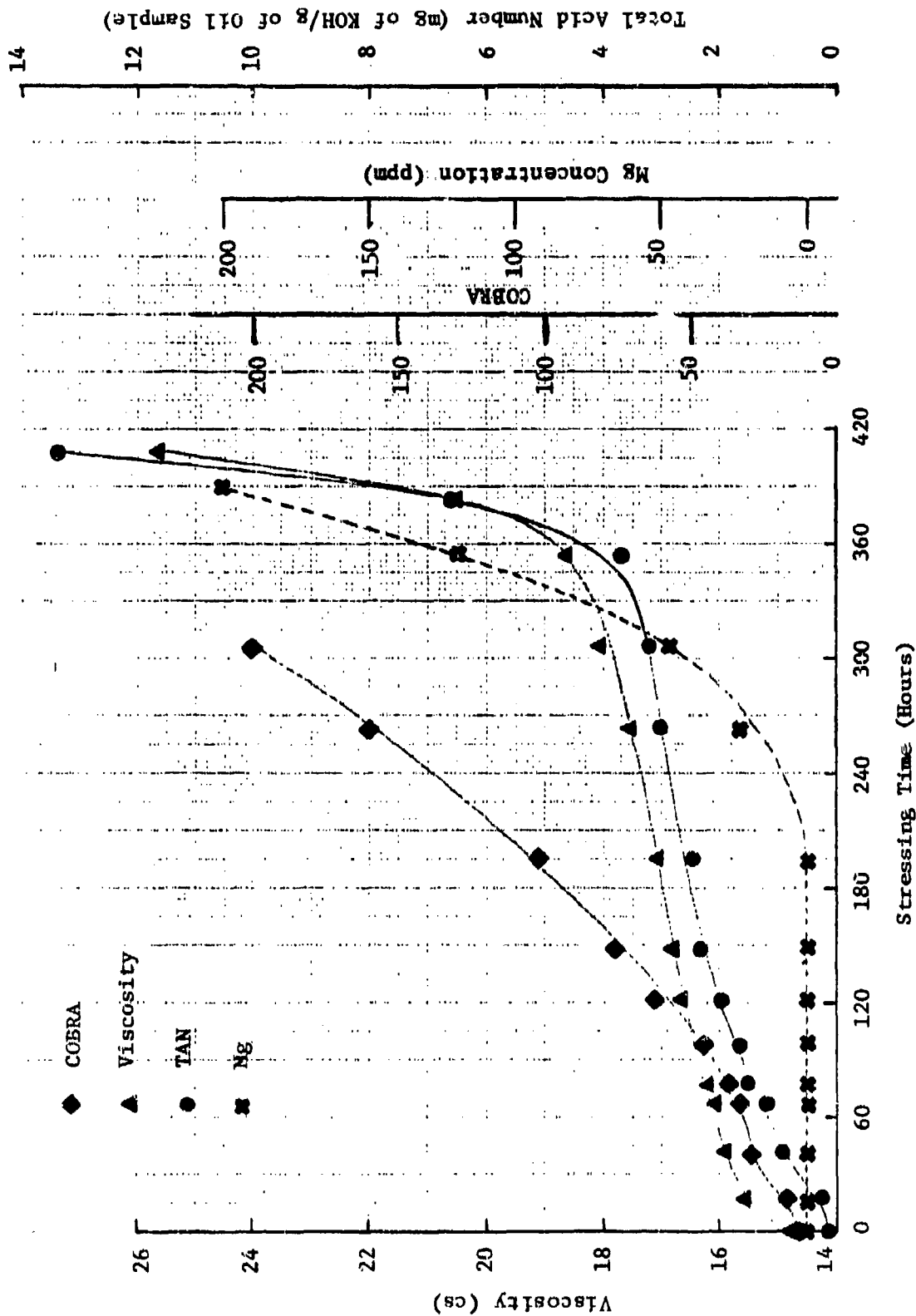


Figure A-6. Plots of the COBRA Reading, Viscosity (40°C), Total Acid Number (TAN), and Mg Concentration Versus Stressing Time at 370°F for the TEL-4006 MIL-L-7808 OIL.

dramatic rate increase as shown in Figure A-1. The stressing time at which the physical property plot diverges from the extrapolated plot is defined as the breakpoint of the physical property plot. The stable lives of the TEL-4001 through TEL-4006 MIL-L-7808 oils as defined by the breakpoints of the viscosity (40°C), TAN, COBRA reading, and Mg concentration versus stressing time plots in Figures A-1-A-6 are listed in Table A-1.

Except for the TEL-4003 oil, the viscosity (40°C) and TAN versus stressing time plots (Figures A-1-A-6) for the TEL-4001 through TEL-4006 MIL-L-7808 oils contain breakpoints which are well-defined and are in good agreement (Table A-1).

For the TEL-4003 oil, the viscosity (40°C) and TAN versus stressing time plots (Figure A-3) do not contain dramatic rate increases. In fact, the viscosity (40°C) and TAN plots each contain a rate decrease at approximately 240 hours.

Except for the TEL-4003 and TEL-4006 oils, the Mg concentration versus stressing time plots (Figures A-1-A-6) indicate that corrosion of the Mg specimen occurs soon after the dramatic rate increases in the viscosity (40°C) and TAN plots. For the TEL-4006 oil, Mg corrosion is significant 80 hours prior to the breakpoints of the viscosity (40°C) and TAN plots. For the TEL-4003 oil, Mg corrosion is significant after 170 hours of thermal oxidative stressing; rate decreases of viscosity (40°C) and TAN plots occurred at 240 hours.

Of the physical properties plotted, the COBRA plots are the least informative in determining stable lives (Figures A-1-A-6). The COBRA measurements for the TEL-4001, TEL-4003, and TEL-4006 oils went off scale (>200) before the oils' stable lives ended, while the COBRA measurements for the TEL-4002 and TEL-4004 oils did not increase dramatically until 24-48 hours after their stable lives had ended. The COBRA measurements for the TEL-4005 oil remained fairly constant 24 hours after its stable life had ended, even though the TAN had increased dramatically (Figure A-5).

TABLE A-1

BREAKPOINTS OF PHYSICAL PROPERTY VERSUS STRESSING TIME  
PLOTS FOR 370°F

	Breakpoints (Hours)			
	Viscosity (40°C)	TAN	COBRA	Mg Concentration
<u>MIL-L-7808 oil</u>				
TEL-4001	105	105	0 <sup>a</sup>	105
TEL-4002	170	180	210	210
TEL-4003	240	240	>270 <sup>b</sup>	140
TEL-4004	205	205	230	230
TEL-4005	155	165	>195 <sup>b</sup>	170
TEL-4006	315	325	>305 <sup>b</sup>	240
TEL-5001	240	>140 <sup>b</sup>	240	350
TEL-5002	110	>250 <sup>b</sup>	0 <sup>a</sup>	50

<sup>a</sup>No stable life.

<sup>b</sup>Went off scale prior to breakpoint.

### A.3 Physical Properties of the TEL-4001 through TEL-4006 MIL-7808 Oils Stressed at 392°F

In order that the effects of temperature on the results of the RLLAT candidates could be studied and because the physical property versus stressing time at 370°F plots did not produce a well-defined stable life for the TEL-4003 oil, the TEL-4001 through TEL-4006 MIL-L-7808 oils were stressed at 392°F. The plots of the COBRA reading, viscosity, TAN, and Mg concentration versus stressing time at 392°F are shown in Figures A-7-A-12 for the TEL-4001 through TEL-4006 oils, respectively.

Except for the TEL-4003 oil, the viscosity and TAN versus stressing time at 392°F plots for the TEL-4001 through TEL-4006 MIL-L-7808 lubricating oils exhibit breakpoints which are well defined and are in good agreement (Table A-2). Although the stable life of the TEL-4003 oil ends at 130-140 hours, the dramatic rate increase is suppressed due to Mg corrosion until 180-190 hours (Figure A-9).

As was the case for the oils stressed at 370°F, the COBRA measurements for the TEL-4001, TEL-4003, and TEL-4006 oils went off scale (>200) before their respective stable lives ended, while the COBRA measurements for the TEL-4002 and TEL-4004 oils did not increase dramatically until their stable lives had ended. The COBRA measurements for the TEL-4005 oil remained fairly constant 24 hours after its stable life had ended, even though the TAN had increased dramatically.

The results for the COBRA, viscosity, and TAN measurements are similar to those reported for the 370°F stressed samples except that the stable lives are approximately half as long at 392°F as they are at 370°F. The 50 percent decrease in stable life was expected since the rate of reaction approximately doubles when the stressing time is increased by 10°C (18°F). These results imply that the thermal-oxidation mechanisms of the MIL-L-7808 oils are not affected by the temperature increase.

However, it appears that the reactions of the degradation products are affected by the increase in temperature. Deposits

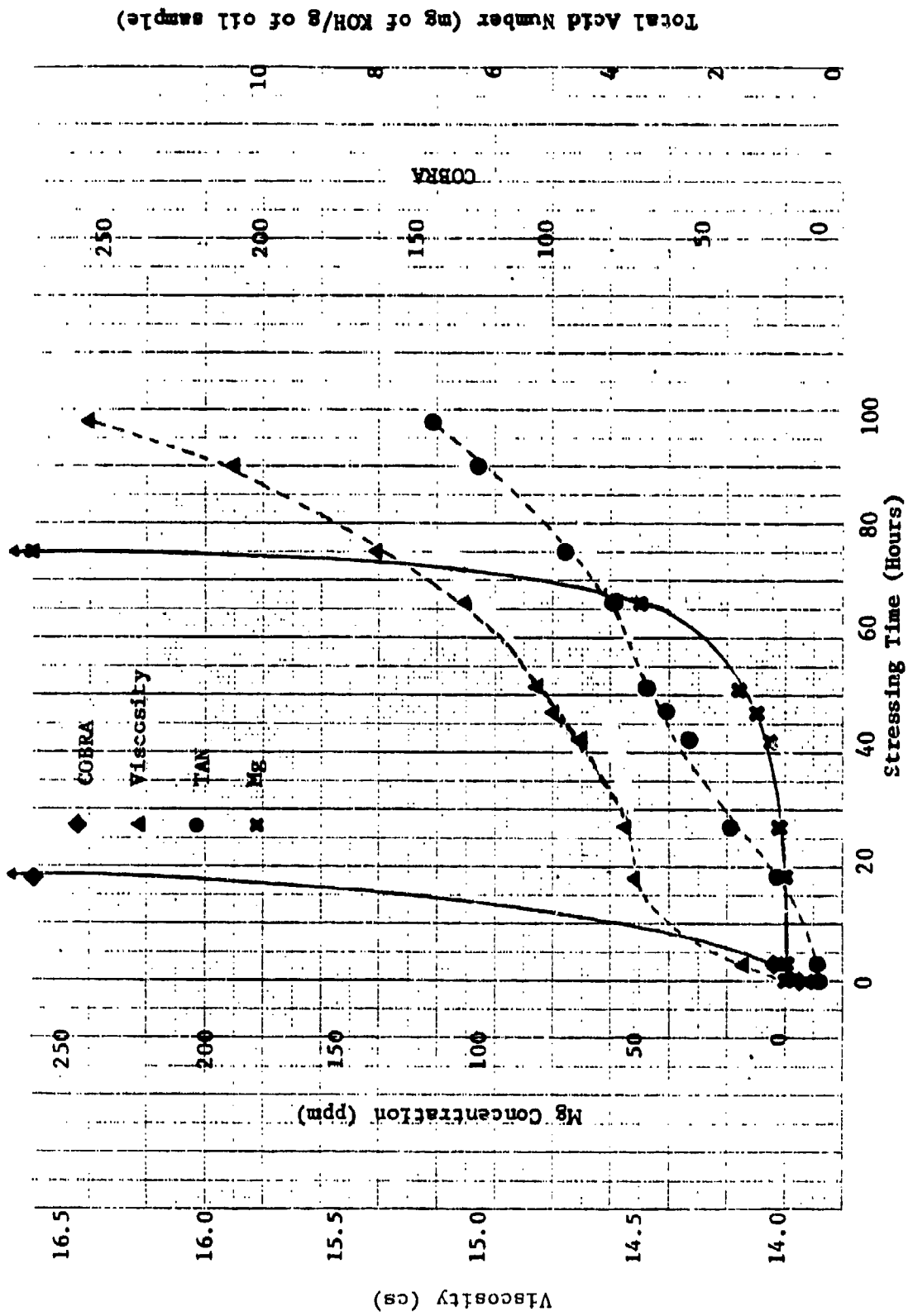


Figure A-7. Plots of the COBRA Reading, Viscosity (40°C), Total Acid Number (TAN), and Mg Concentration versus Stressing Time at 392°F for the TEL-4001 MIL-L-7808 Oil.

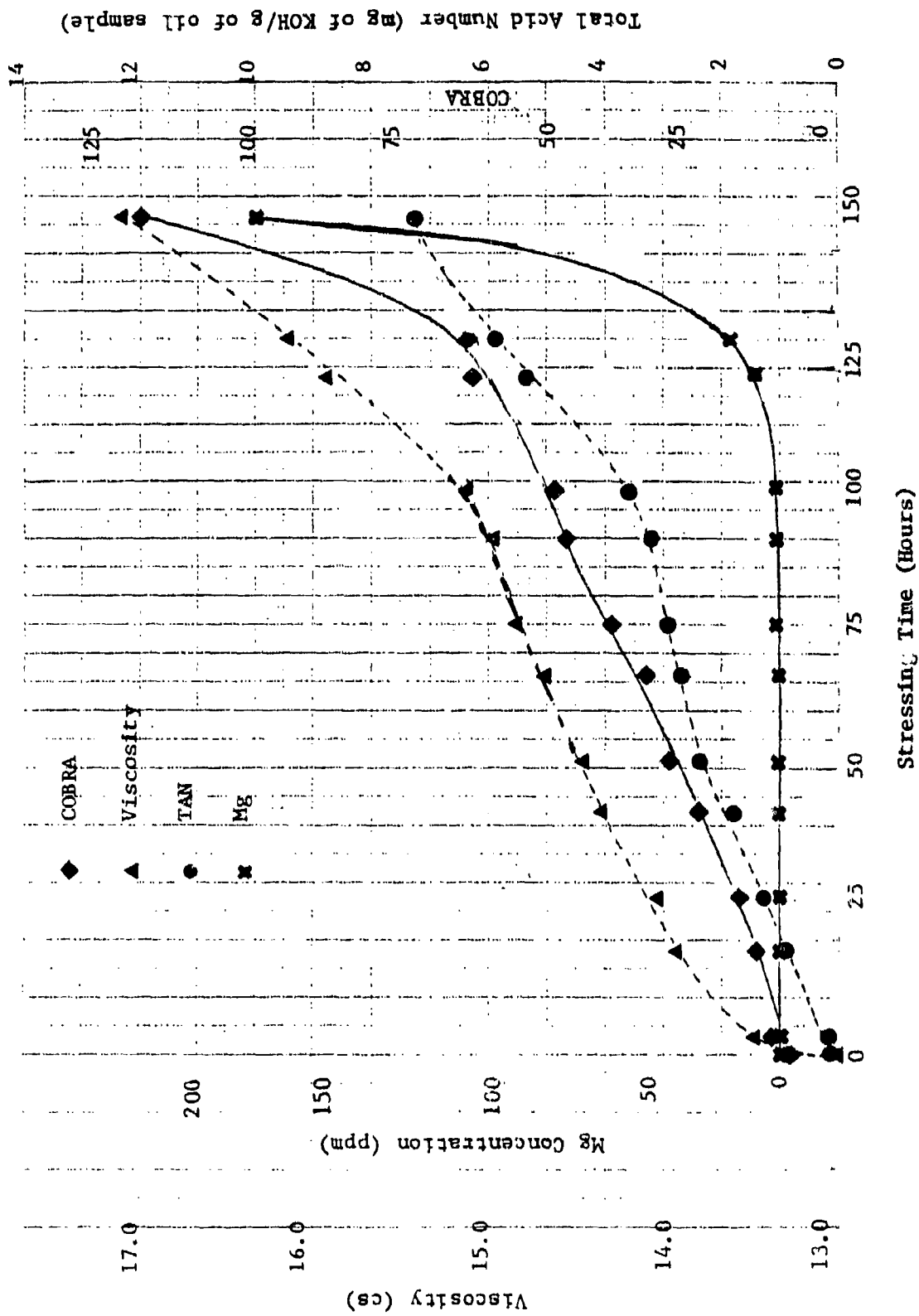


Figure A-8. Plots of the COBRA Reading, Viscosity (40°C), Total Acid Number (TAN), and Mg Concentration versus Stressing Time at 392°C for the TEL-4002 MIL-L-7808 Oil.

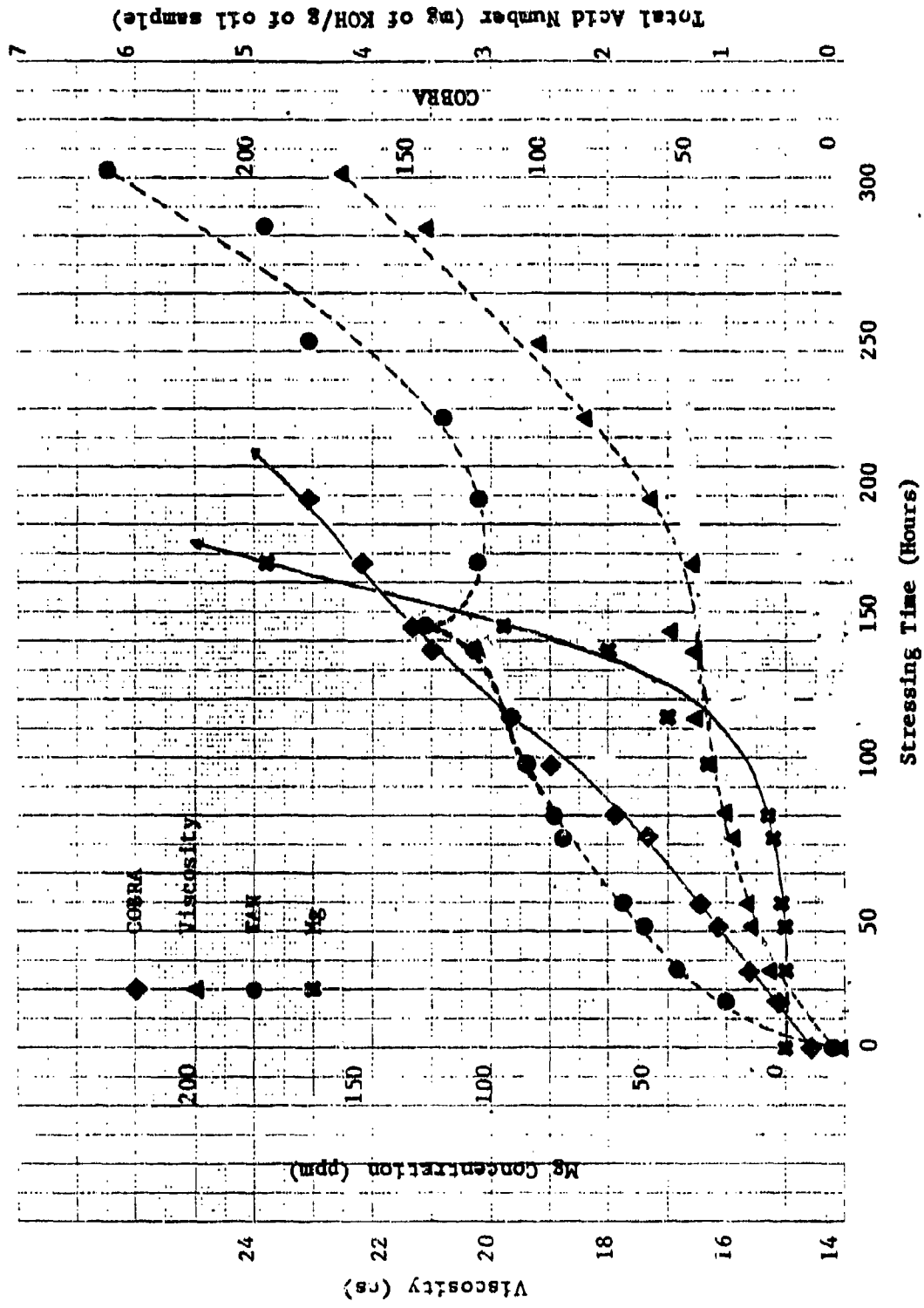


Figure A-9. Plots of the COBRA Reading, Viscosity (40°C), Total Acid Number (TAN), and Mg Concentration versus Stressing Time at 392°F for the iEL-4003 MIL-L-7808 OIL.

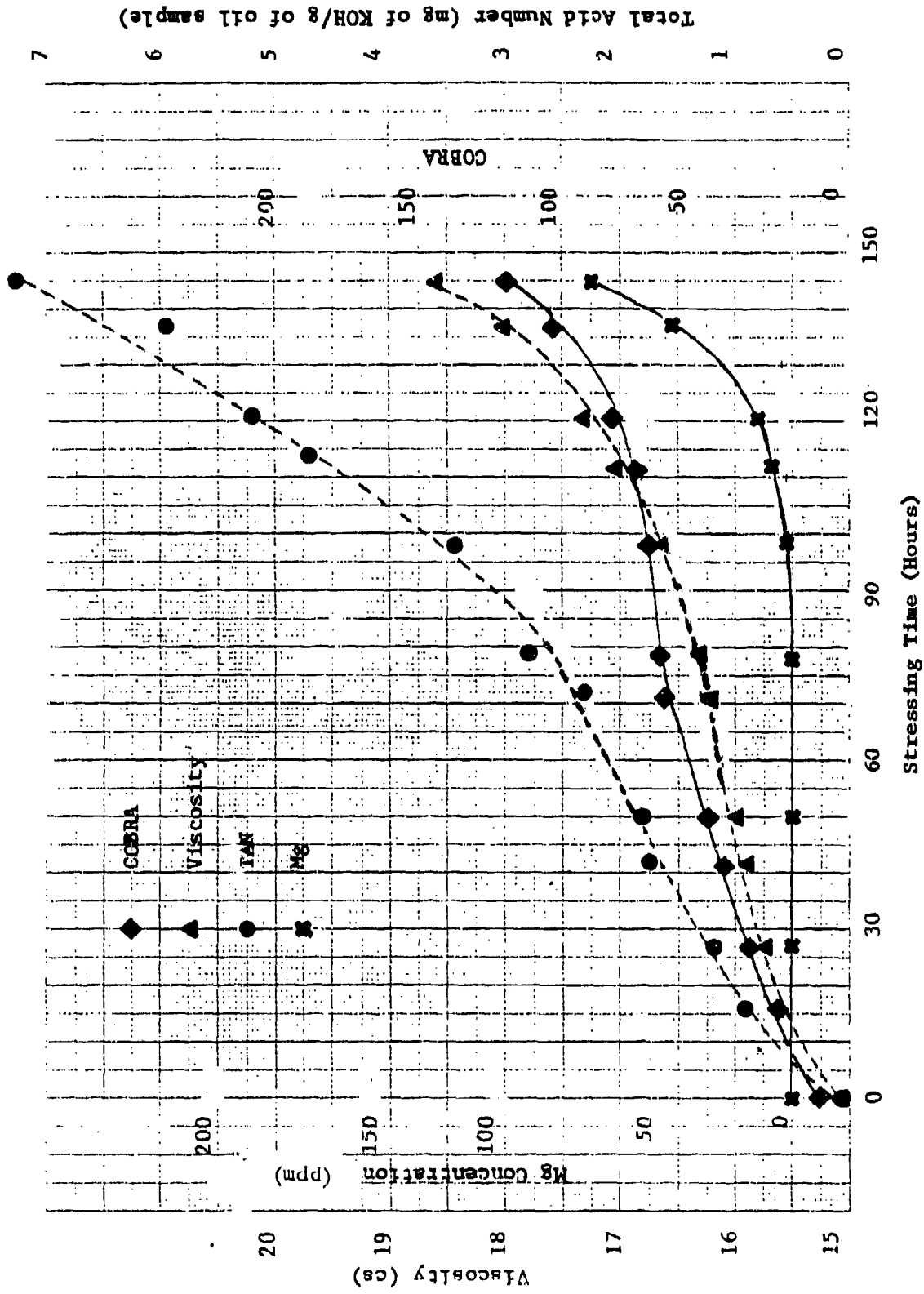


Figure A-10. Plots of the COBRA Reading, Viscosity (40°C), Total Acid Number (TAN), and Mg Concentration versus Stressing Time at 392°F for the TEL-4004 MIL-L-7808 Oil.

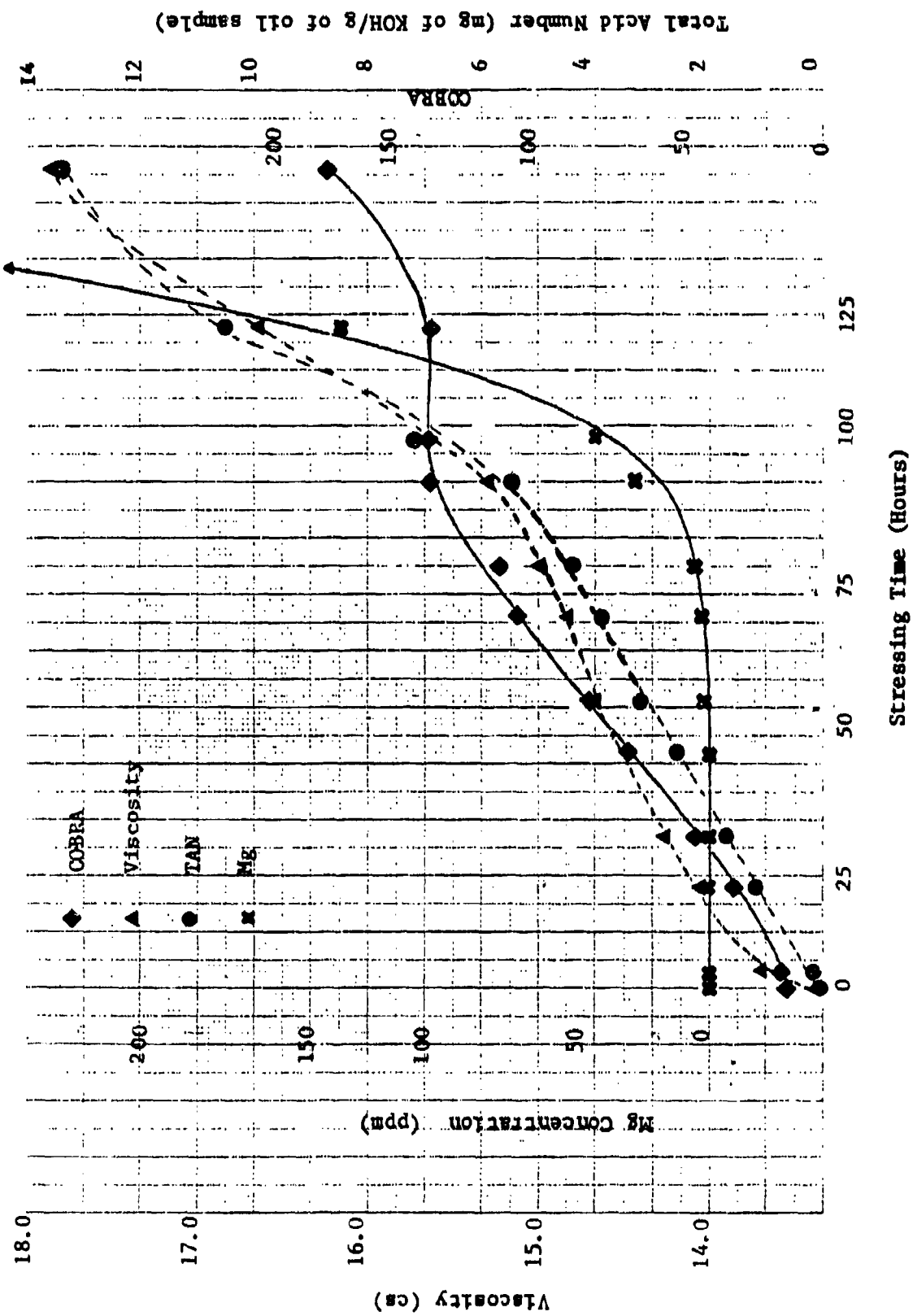


Figure A-11. Plots of the COBRA Reading, Viscosity (40°C), Total Acid Number (TAN), and Mg Concentration versus Stressing Time at 392°F for the TEL-4005 MIL-L-7808 Oil.

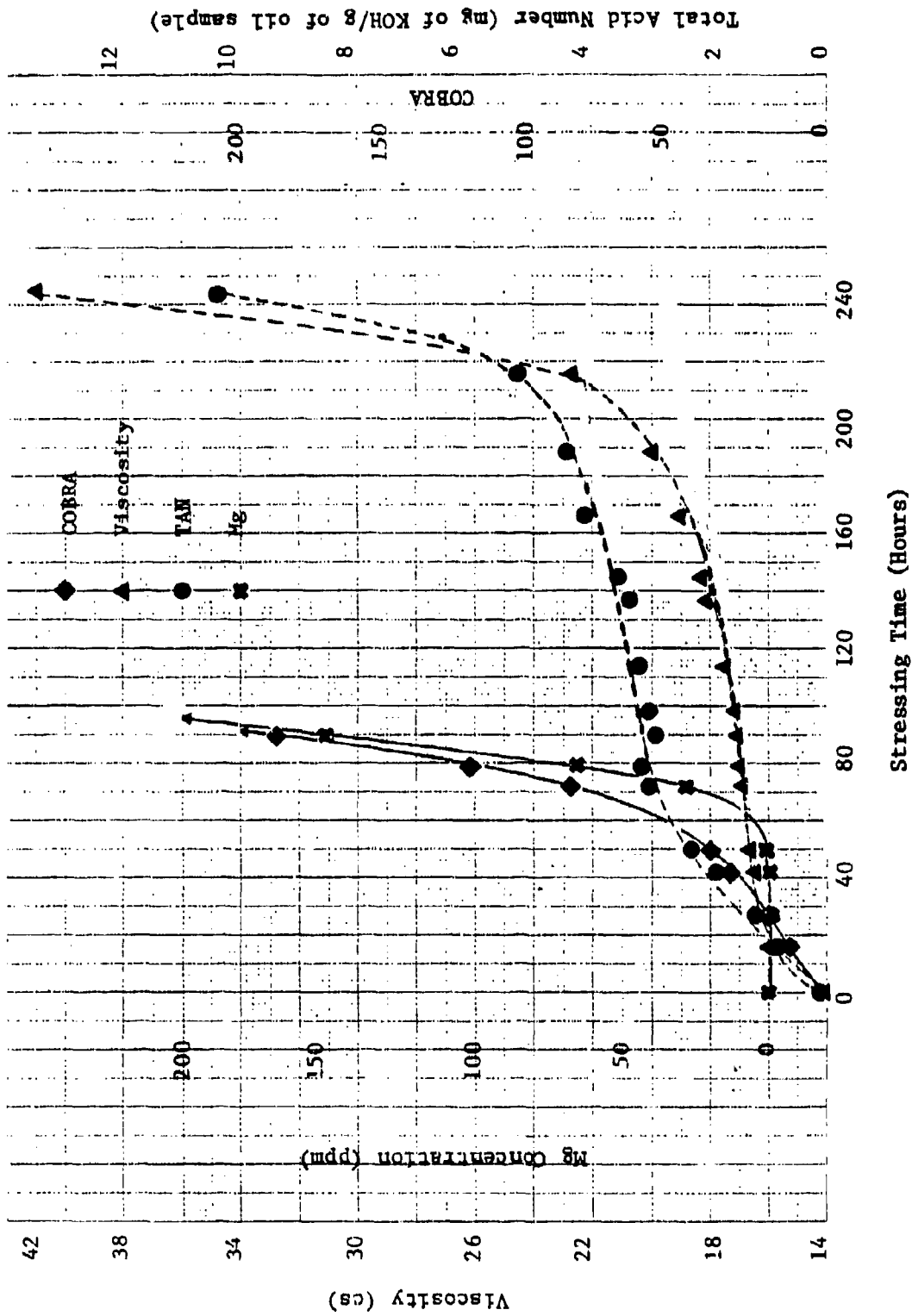


Figure A-12. Plots of the COBRA Reading, Viscosity (40°C), Total Acid Number (TAN), and Mg Concentration versus Stressing Time at 392°F for the TEL-4006 MIL-L-7808 Oil.

TABLE A-2

BREAKPOINTS OF PHYSICAL PROPERTY VERSUS STRESSING TIME  
PLOTS FOR 392°F

	Breakpoints (Hours)			Mg Concentration
	Viscosity (40°C)	TAN	COBPA	
<u>MIL-L-7808 Oil</u>				
TEL-4001	60	65	0 <sup>a</sup>	65
TEL-4002	90	90	125	140
TEL-4003	140	130	>200 <sup>b</sup>	135
TEL-4004	85	80	110	110
TEL-4005	75	80	125	90
TEL-4006	150	160	60	70

<sup>a</sup>No stable life.

<sup>b</sup>Went off scale prior to breakpoint.

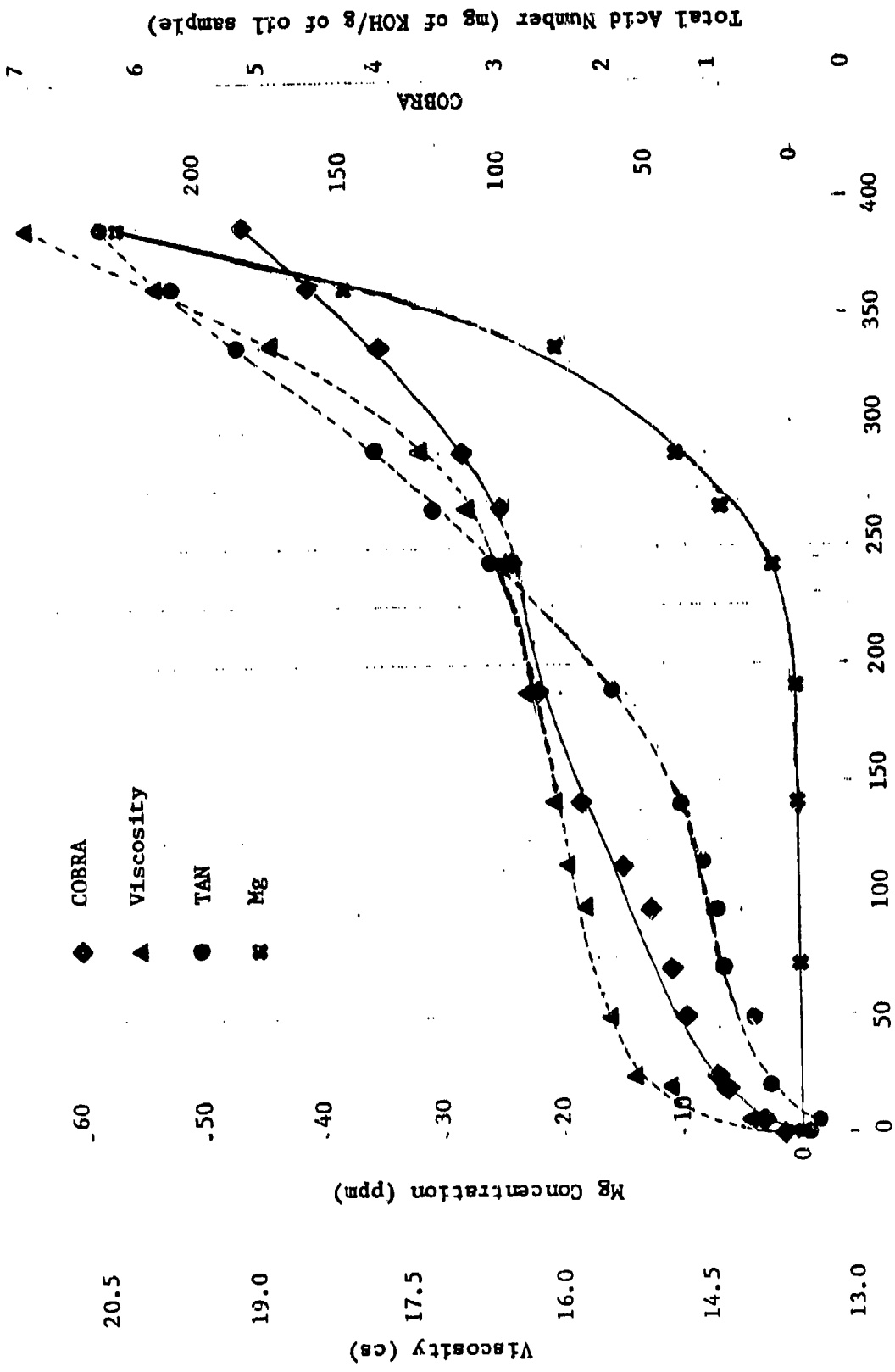
were observed on the inside of the TEL-4001 oil's reaction tube during the first 24 hours of stressing at 392°F, but not at 370°F. The deposition ended after 24 hours and did not reoccur for the rest of the test. Although the Mg corrosion characteristics of the TEL-4001 through TEL-4005 oils were similar at 370° and 392°F (Mg corrosion began after the stable lives for the TEL-4001 through TEL-4005 oils had ended) the Mg corrosion for the TEL-4006 oil initiated after only 50 hours (stable life = 150-160 hours) at 392°F, while Mg corrosion initiated just prior to the end of the oil's stable life at 370°F.

The results of the 392°F stressing temperature study indicate that basing the stable life determination of the TEL-4003 oil on the small inflections in the oil's viscosity and TAN plots (Figure A-3) was correct. The stable life of 130-140 hours determined for the TEL-4003 oil at 392°F is approximately half the 240 hours stable life determined for the TEL-4003 oil at 370°F using the small inflections in the viscosity and TAN plots (Figure A-3). Also, the Mg corrosion that suppressed the dramatic rate increase of the TEL-4003 oil's 392°F plots (Figure A-9) is also present at 370°F (Figure A-3), and is thought responsible for the absence of the dramatic rate increase at the end of the TEL-4003 oil's stable life at 370°F.

#### A.4 Physical Properties of the TEL-5001 and TEL-5002 MIL-7808 Oils Stressed at 370°F

The plots of the COBRA reading, viscosity (40°C), TAN, and Mg concentration versus stressing time are shown in Figures A-13-A-14 for the TEL-5001 and TEL-5002 oils, respectively.

The plots of the viscosity versus stressing time at 370°F for the TEL-5001 and TEL-5002 MIL-L-7808 lubricating oils (Figures A-13 and A-14) exhibit breakpoints at approximately 240 and 110 hours, respectively. However, the COBRA measurements for the TEL-5002 oil go off scale (>200) before 30 hours of stressing at 370°F, while the COBRA measurements of the TEL-5001 oil exhibit a breakpoint similar to that of the viscosity plot.



Stressing Time (Hours)

Figure A-13. Plots of the COBRA Reading, Viscosity (40°C), Total Acid Number (TAN), and Mg Concentration versus Stressing Time at 370°F for the TEL-5001 MIL-L-7808 Oil.

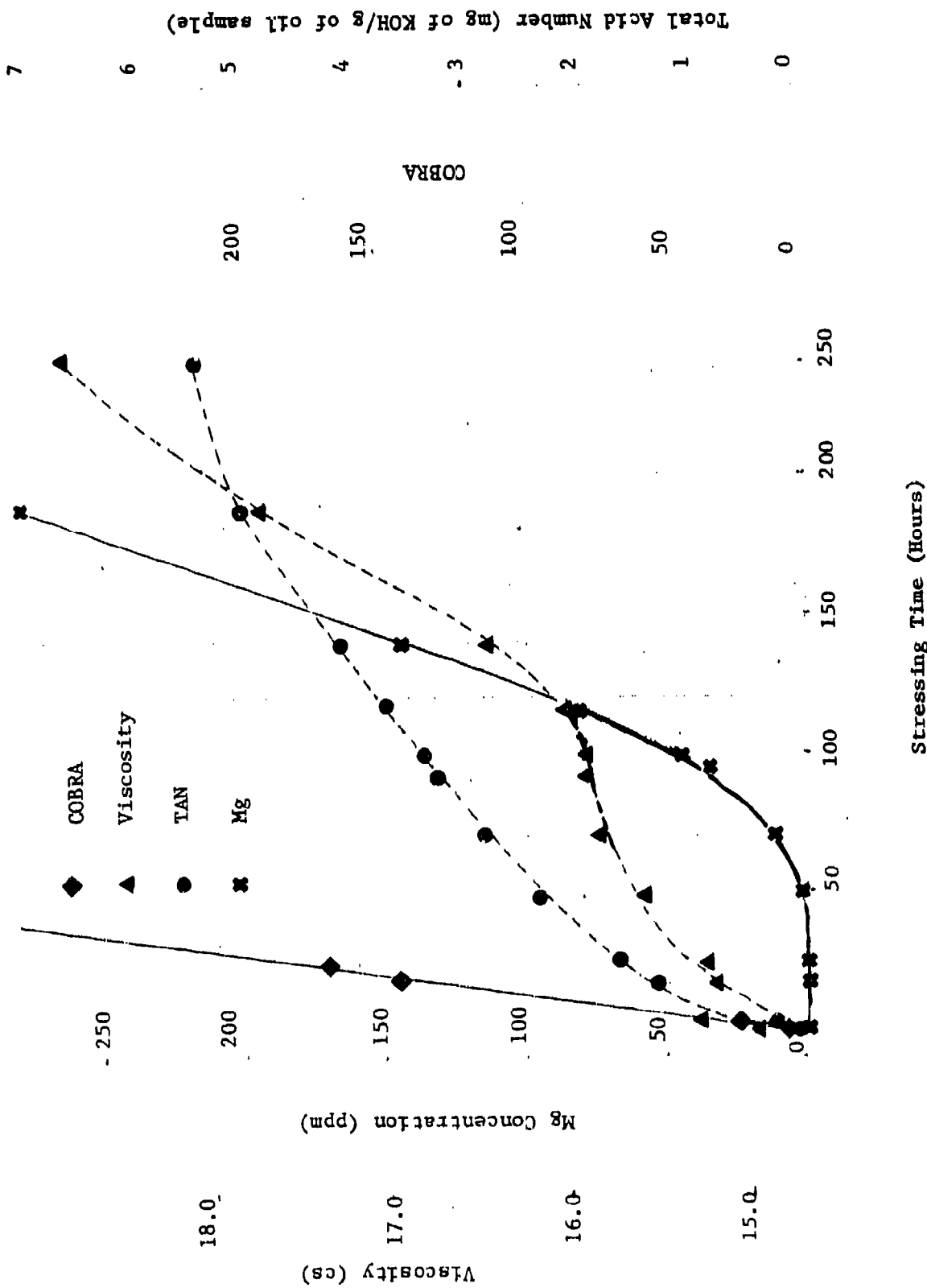


Figure A-14. Plots of the COBRA Reading, Viscosity (40°C), Total Acid Number (TAN), and Mg Concentration versus Stressing Time at 370°F for the TEL-5002 MIL-L-7808 Oil.

In contrast to the TAN plots of the TEL-4001 through TEL-4006 MIL-L-7808 oils stressed at 370°F, the TAN plots of the TEL-5001 and TEL-5002 oils do not exhibit well-defined breakpoints. The TAN plot of the TEL-5001 oil exhibits a slight rate increase at approximately 150 hours of stressing, but the rate of TAN increase remains slow throughout the remaining stressing time up to 400 hours. The slow increase in the TAN of the TEL-5001 oil versus stressing time is not due to suppression by Mg corrosion since the Mg concentration is only 60 ppm after 400 hours of stressing (viscosity plot breakpoint = 240 hours).

However, the absence of a breakpoint in the TAN plot of the TEL-5002 oil may be due to suppression by Mg corrosion, since Mg corrosion begins at 50 hours and the Mg concentration is approximately 100 ppm after 125 hours of stressing (viscosity plot breakpoint = 110 hours).

#### A.5 Identification of the Antioxidants Used in the MIL-L-7808 Lubricating Oils

The fresh and stressed lubricating oil samples of each MIL-L-7808 oil, TEL-4001 through TEL-4006, were analyzed by the gas chromatographic procedure employing the thermionic specific detector which is only responsive to nitrogen and phosphorus containing compounds. An internal standard (INT STAN in Figure A-15) was used to determine the concentration of the known antioxidants.

The MIL-L-7808 lubricating oils can be separated into three main groups (a) TEL-4002 through TEL-4005, (b) TEL-4001, TEL-4006, and TEL-5002, and (c) TEL-5001. The TEL-4002 through TEL-4005 oils contain differing amounts of PANA and DODPA. Examples of the chromatograms produced by the fresh and stressed TEL-4002 through TEL-4005 oils are shown in Figure A-15.

The chromatograms of the TEL-4002 through TEL-4005 oils contain peaks assigned to PANA and DODPA and also one large broad peak around 8 minutes (Figure A-15) which is assumed to be tricresyl phosphate (P containing). The other interesting feature displayed by the chromatograms of the TEL-4002 through

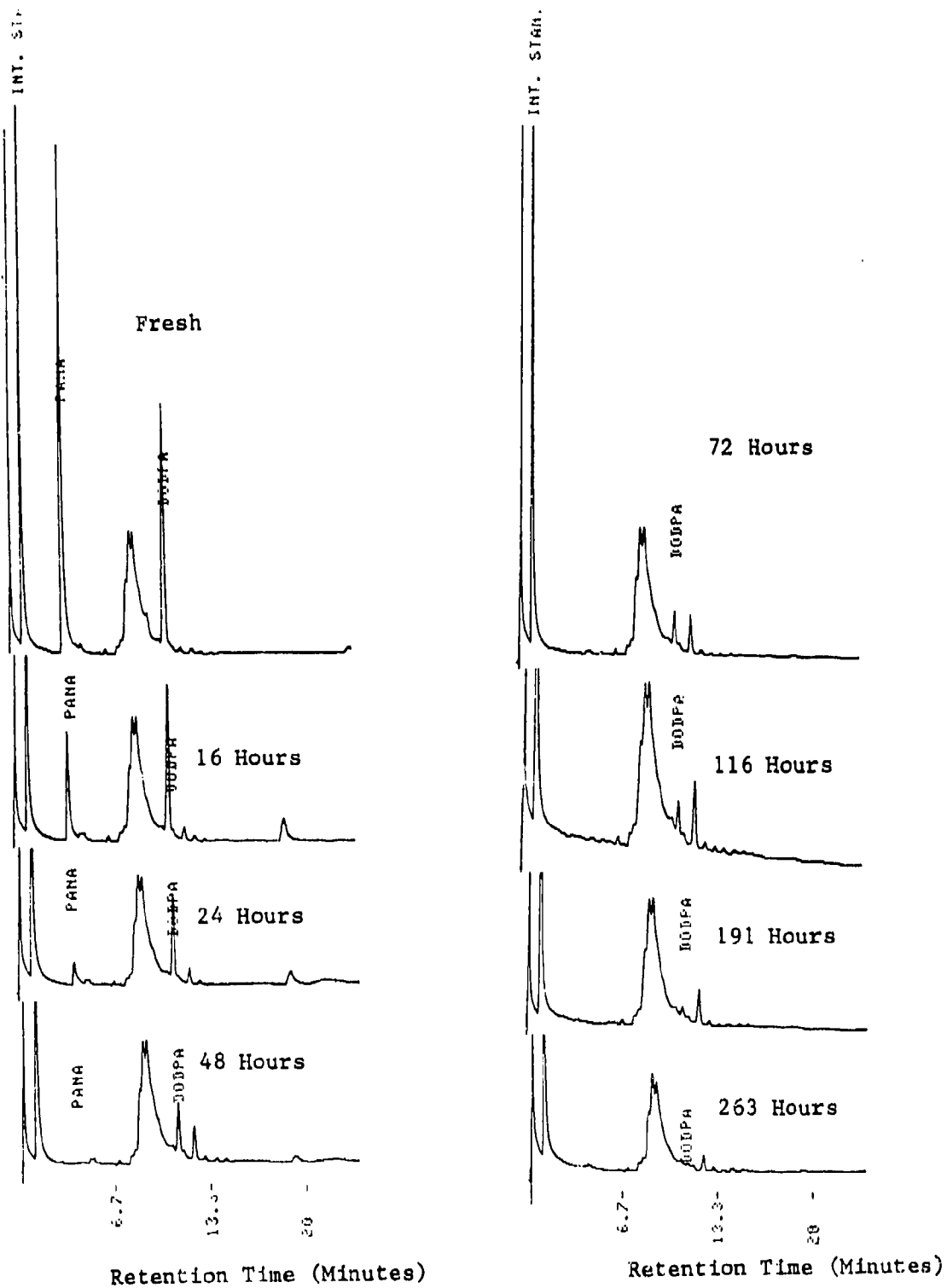


Figure A-15. Gas Chromatograms of the Fresh and Stressed (16-263 Hours at 370°F) TEL-4004 MIL-L-7808 Oils.

TEL-4005 oils is that peaks with retention times of 12 and 18 minutes (Figure A-15) are present in the stressed oil samples but not in the fresh oil. The peak at 18 minutes is at a maximum in the early stages of oxidation (16 hours at 370°F) and then decreases with stressing time. In contrast, the peak at 12 minutes increases with stressing time. Therefore, the peaks are assigned to oxidation products of PANA and DODPA. The peak at 18 minutes appears to have antioxidant capacity (decreases with stressing time), while the 12 minute peak does not appear to have antioxidant capacity (increases with stressing time).

In the second class of MIL-L-7808 oils, TEL-4001, TEL-4006, and TEL-5002, the principal antioxidants are identified as octyl-PANA and DODPA (Figures A-16-A-18). Unlike the first class of oils, the TEL-4001 and TEL-4006 oils also appear to contain other nitrogen (or phosphorus) containing compounds (Figures A-16 and A-17) while the TEL-5002 oil appears to contain only octyl-PANA and DODPA (Figure A-18). Also, the TEL-4001 and TEL-5002 oils appear to contain tricresyl phosphate (strong, broad peak at around 8 minutes in Figures A-16 and A-18), but the TEL-4006 oil does not contain any strong, broad peaks (Figure A-17).

The fresh TEL-4001 oil's chromatogram (Figure A-16) contains a very strong, broad peak that elutes at a retention time of 1.6 minutes just after the internal standard. The peak at 1.6 minutes decreases with stressing time and is no longer detectable at 137 hours (Figure A-16). The TEL-4006 oil's chromatograms (Figure A-18) contain three sharp peaks at 2.6, 5.0, and 8.1 minutes which decrease with stressing time. Since the unknown peaks in the TEL-4001 and TEL-4006 oils decrease with stressing time, they are speculated to have antioxidant capacities. The TEL-4001, TEL-4006, and TEL-5002 oils did not produce the new species seen in the chromatograms of the TEL-4002 through TEL-4005 oils (Figure A-15).

The third class of MIL-L-7808 oils consists of the TEL-5001 oil. The gas chromatogram of the fresh TEL-5001 oil in Figure A-19 contains peaks assigned to DODPA (10.3 minutes) and

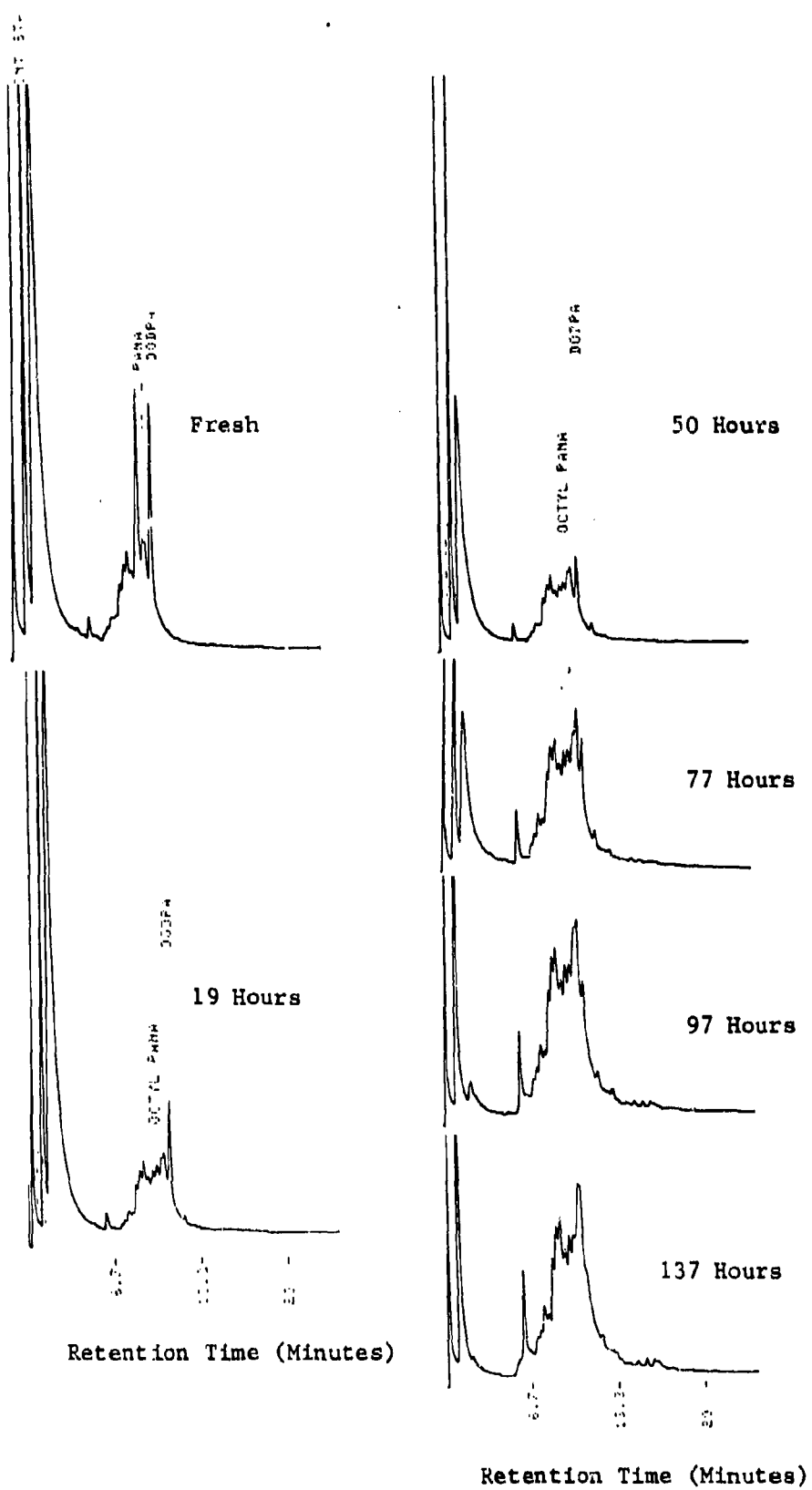
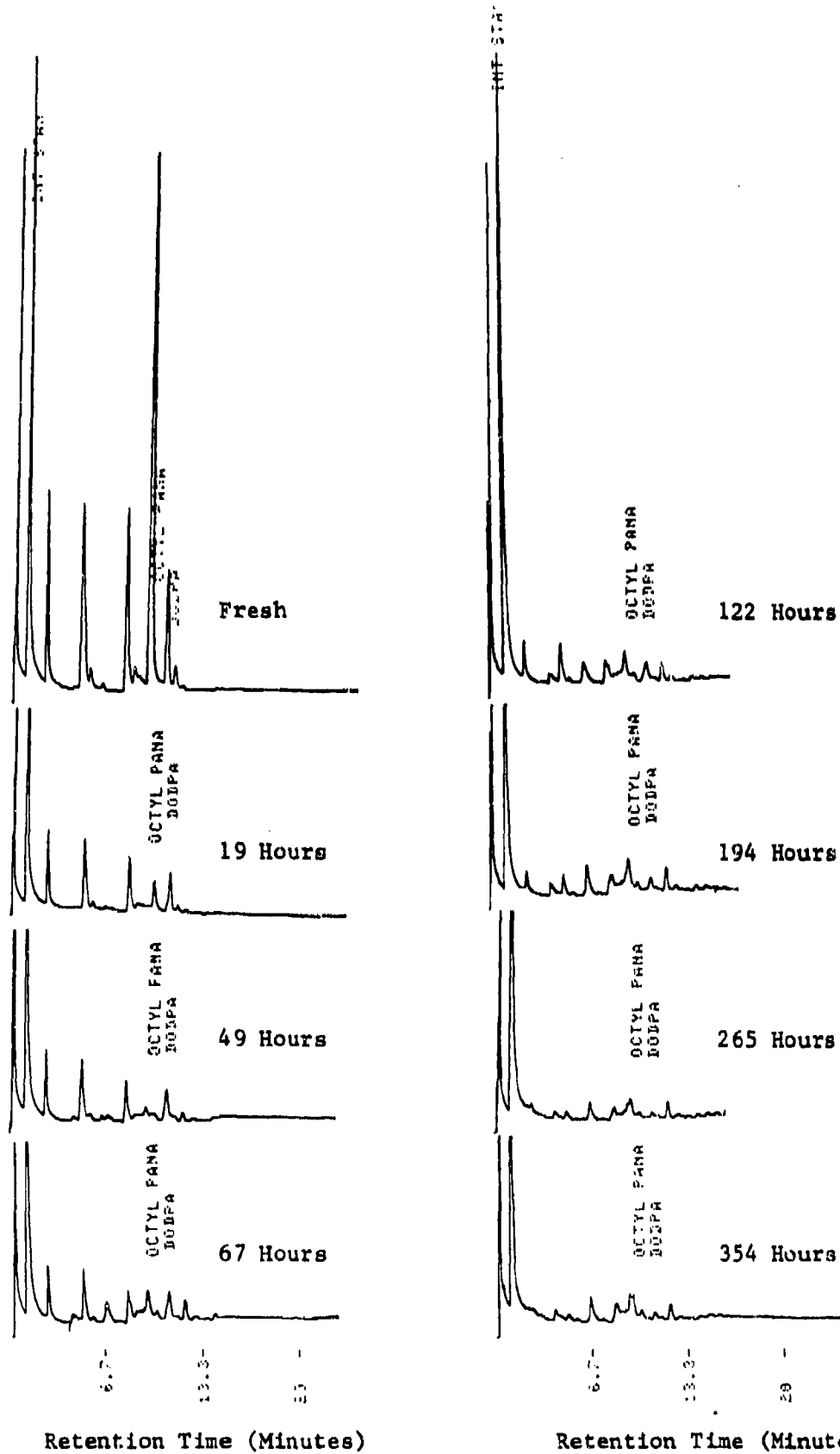


Figure A-16. Gas Chromatograms of the Fresh and Stressed (19-137 Hours at 370°F) TEL-4001 MIL-L-7808 Oils.



Retention Time (Minutes)                      Retention Time (Minutes)

Figure A-17. Gas Chromatograms of the Fresh and Stressed (19-354 Hours at 370°F) TEL-4006 MIL-L-7808 Oils.

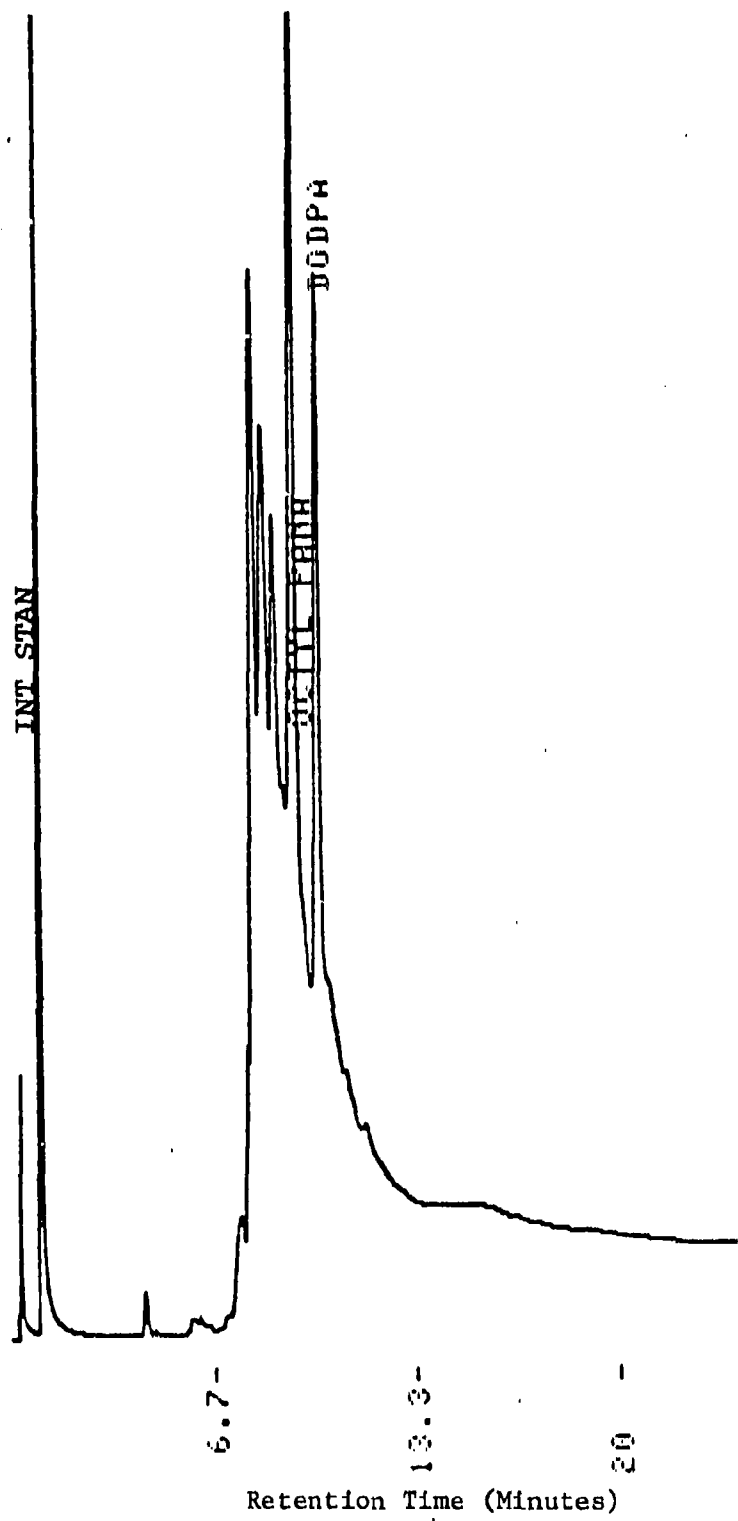


Figure A-18. Gas Chromatogram of the Fresh TEL-5002 MIL-L-7808 Oil.

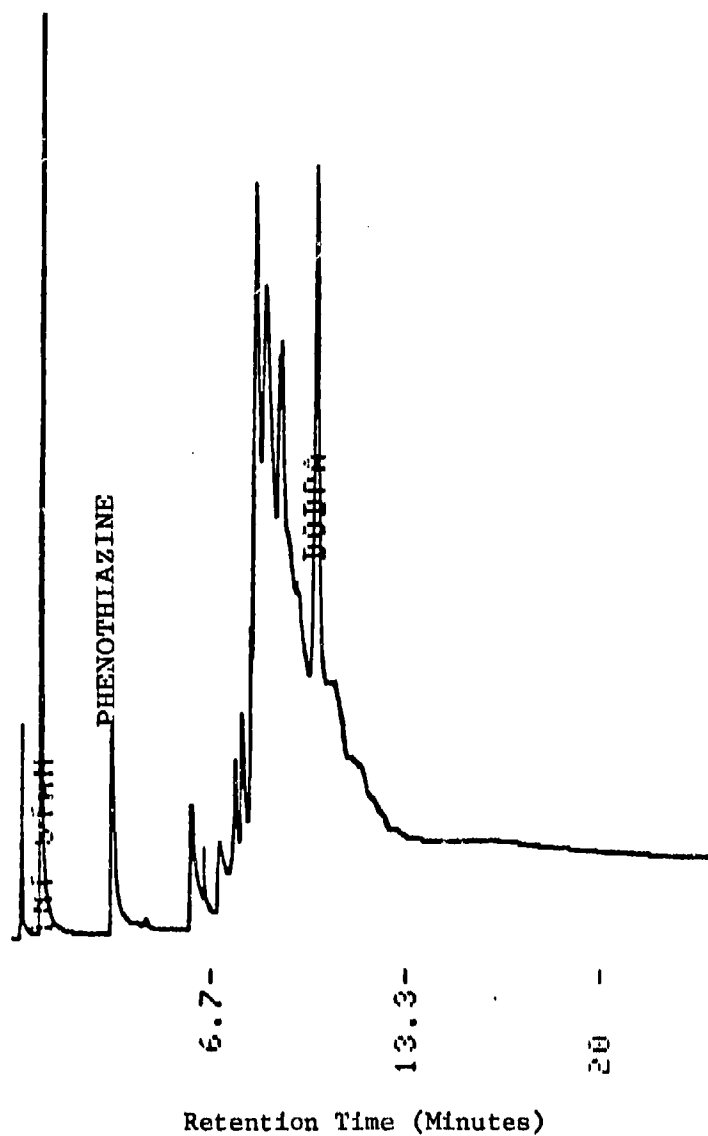


Figure A-19. Gas Chromatogram of the Fresh TEL-5001 MIL-L-7808 Oil.

phenothiazine (3.2 minutes). In contrast to the TEL-4001 through TEL-4006 and TEL-5002 oils, the TEL-5001 oil does not contain PANA or octyl-PANA. The compound at 3.2 minutes was identified as phenothiazine by adding phenothiazine to the fresh TEL-5001 oil and observing that the size of the peak at 3.2 minutes increased in size without the formation of a new peak. Therefore, the retention times of phenothiazine and the unknown compound are identical. Although the matching of gas chromatographic retention times can not be used for absolute identification of an unknown compound, the identification by gas chromatography was adequate for this investigation.

A.6 Antioxidant Concentration versus Stressing Time at 370°F  
Plots for the TEL-4002 through TEL-4005 MIL-L-7808 Oils

The plots of the PANA and DODPA concentrations versus stressing time at 370°F for the TEL-4002 through TEL-4005 oils shown in Figures A-20-A-23 are very similar. For each oil the concentration of PANA rapidly decreases during the early stages of oxidation and is no longer detectable (less than 0.01 percent) after approximately 30 hours of oxidation (Figures A-20-A-23) regardless of the PANA's original concentration or the oil's stable life. Although only a few points are available, the plots of the PANA concentration versus stressing time appear to be linear indicating that the PANA depletion reaction is zero order.

In contrast to PANA, the rate at which the concentration of DODPA depletes is nonlinear and the concentration of DODPA is detectable (greater than 0.01 percent) up to the end of the TEL-4002 through TEL-4005 oils' respective stable lives (Figures A-20-A-23). Since the plot of the concentration of DODPA versus stressing time is nonlinear,  $\ln$  of the DODPA concentration was plotted versus the stressing time at 370°F for each oil (Figures A-20-A-23).

The plots of the  $\ln$  of the DODPA concentration versus stressing time for the TEL-4002 through TEL-4005 oils shown in

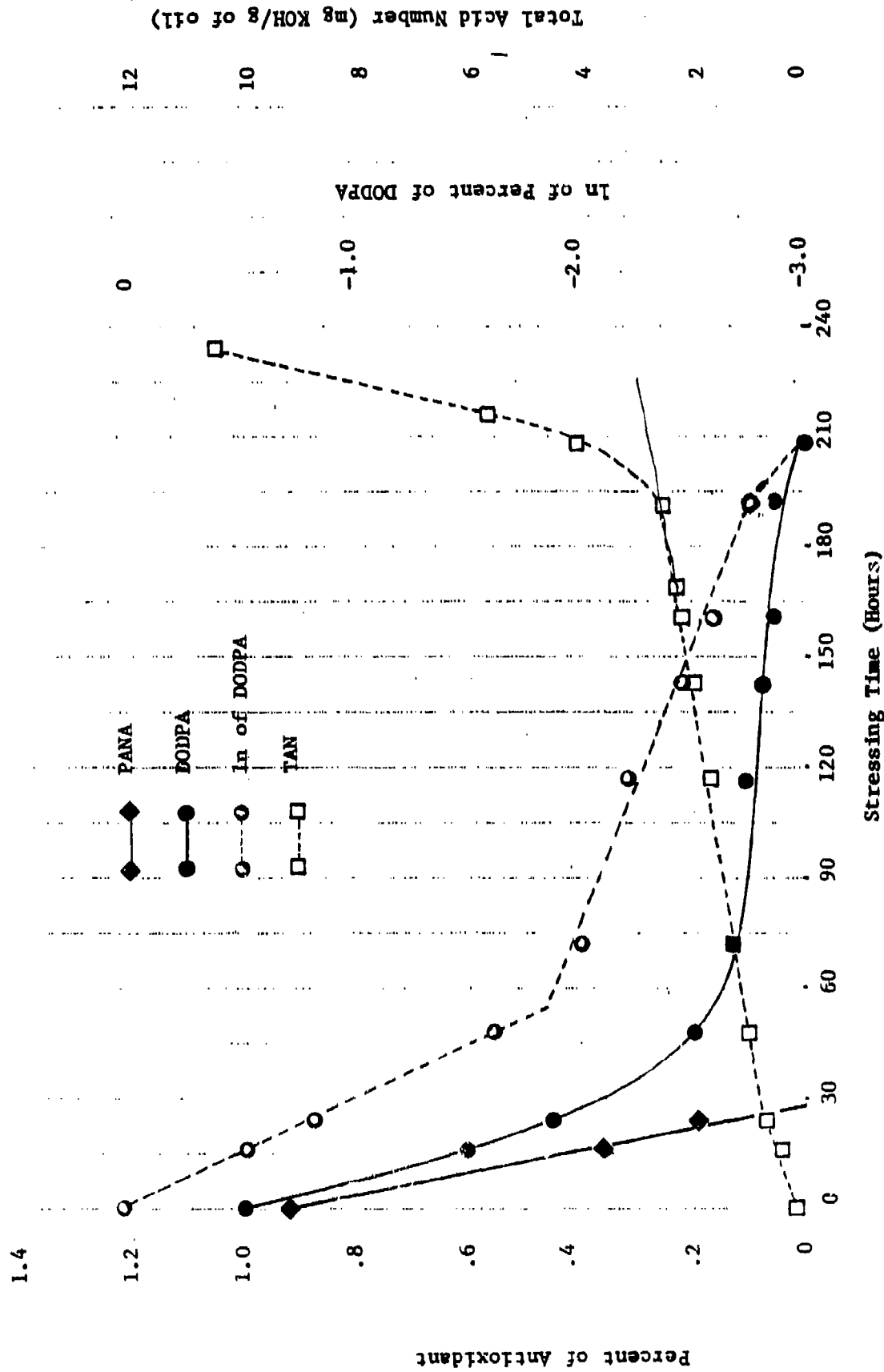


Figure A-20. The Plots of the Percent (by Weight) of the Antioxidants, PANA and DODPA, of the In of the Percent (by Weight) of DODPA, and of the Total Acid Number (TAN) versus Stressing Time at 370°F for the TEL-4002 MIL-L-7808 Oil.

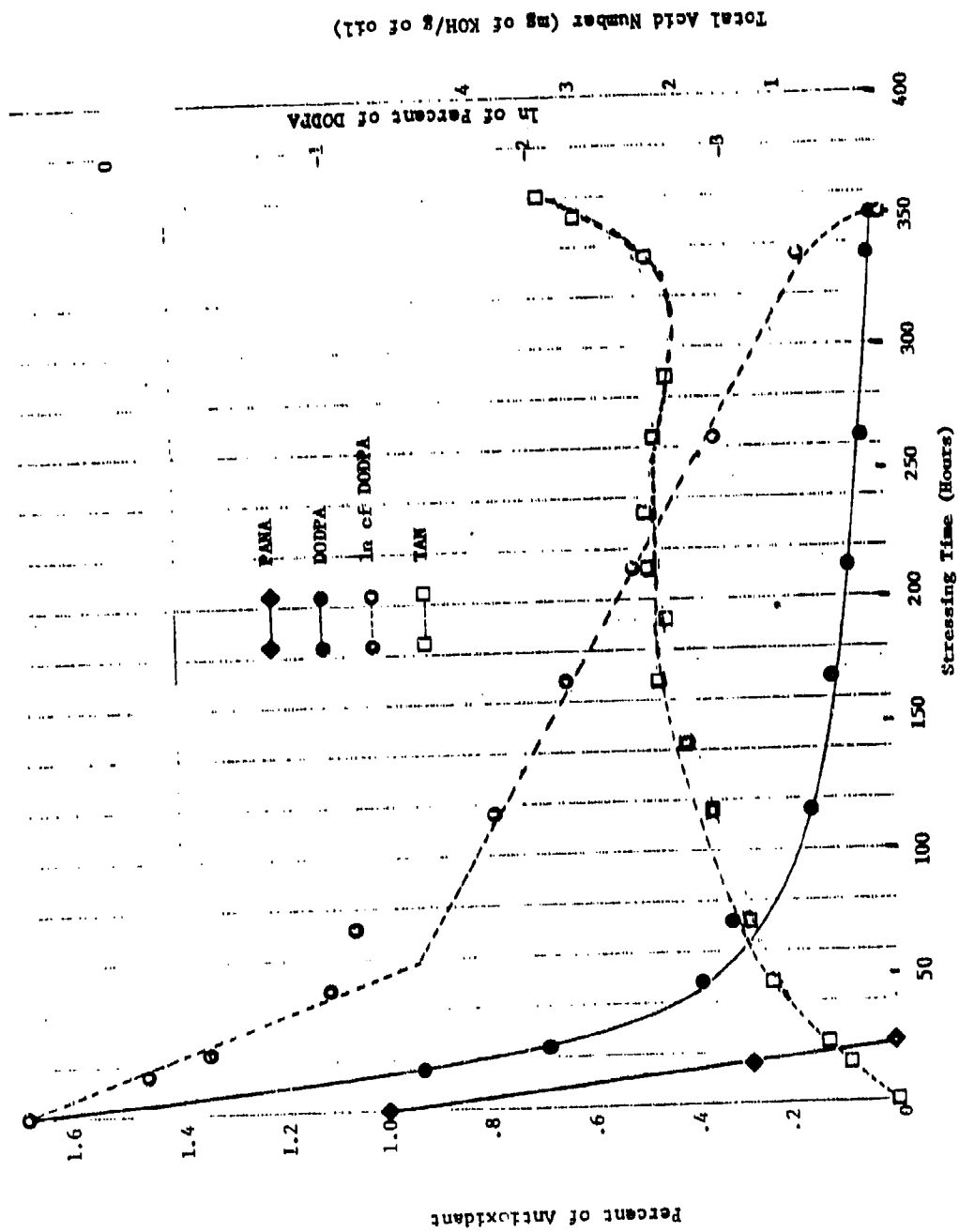


Figure A-21. Plots of Percent (by Weight) of Antioxidants, PANA and DODPA, of the ln of the Percent (by Weight) of DODPA, and of the Total Acid Number (TAN) versus Stressing Time at 370°F for the TEL-4003 MIL-L-7808 Oil.

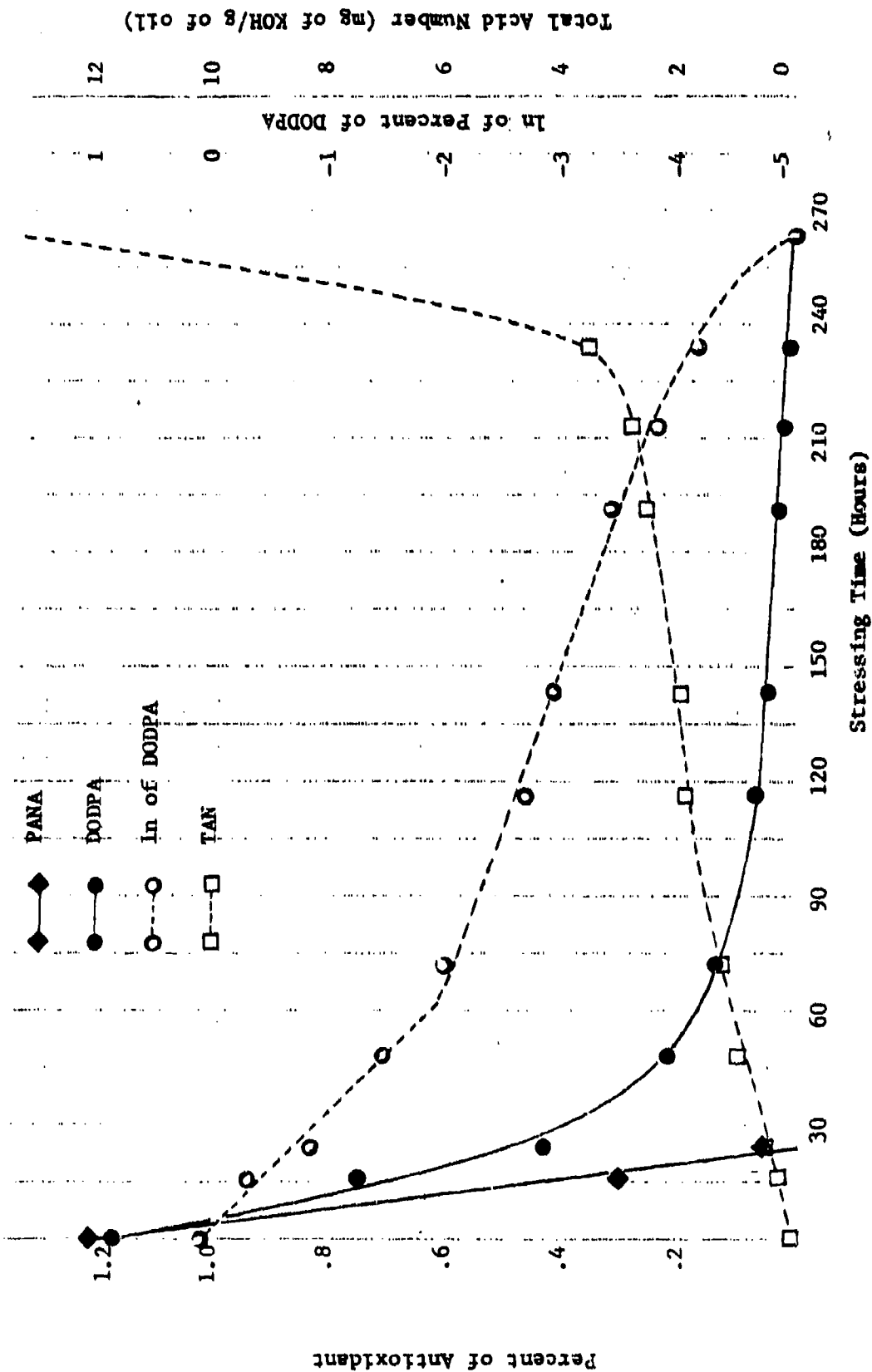


Figure A-22. Plots of Percent (by Weight) of Antioxidants, PANA and DODPA, of the ln of Percent (by Weight) of DODPA, and of the Total Acid Number (TAN) versus Stressing Time at 370°F for the TEL-4004 MIL-I-7808 Oil.

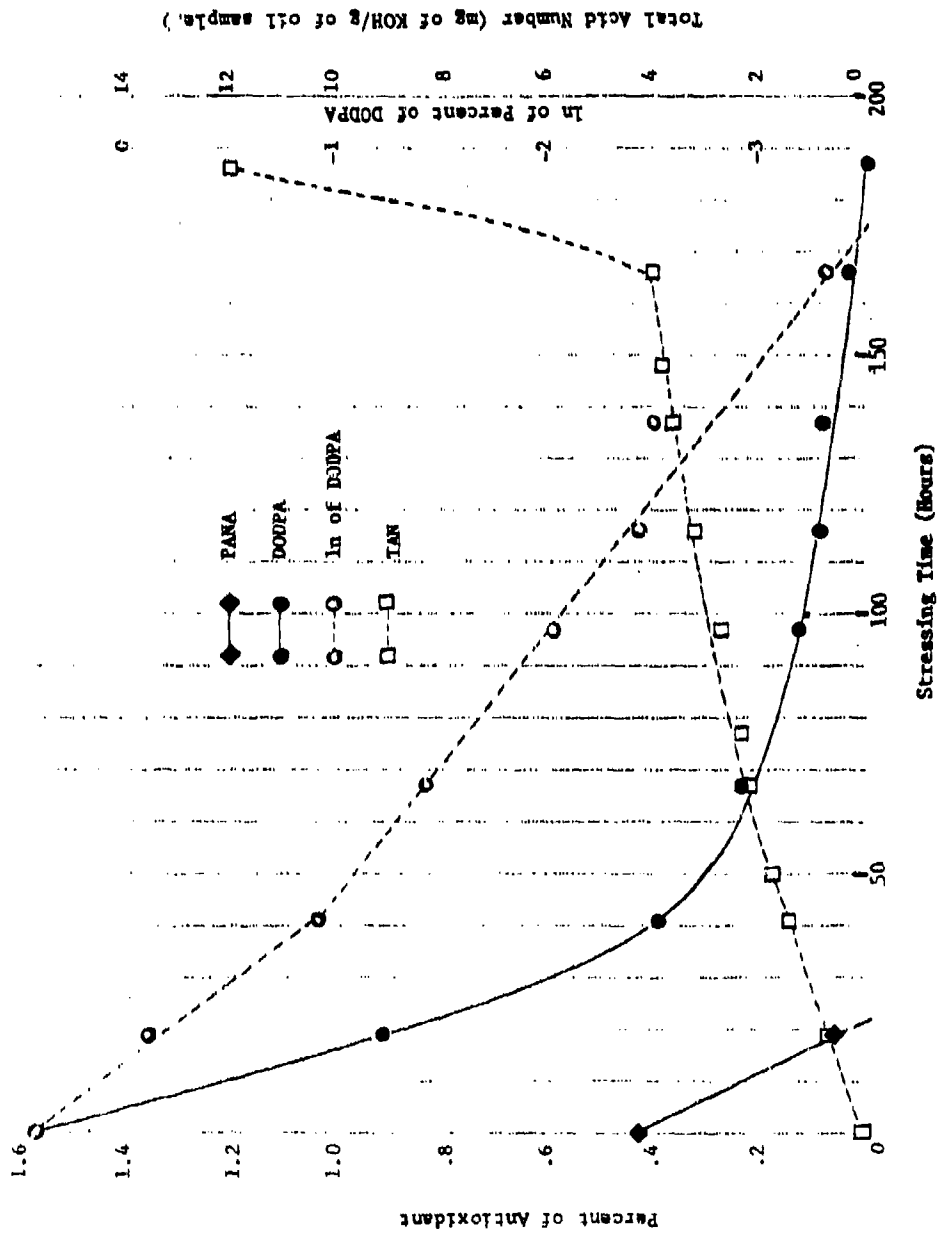


Figure A-23. Plots of Percent (by Weight) of Antioxidants, PANA and DODPA, of the ln of Percent (by Weight) of DODPA, and of the Total Acid Number (TAN) versus Stressing Time at 370°F for the TEL-4005 MIL-L-7808 Oil.

Figures A-20-A-23 consist of two linear sections with an inflection point occurring at about 40-50 hours of stressing time. The inflection point occurs about 10-30 hours after the PANA is no longer detectable. For the TEL-4002 through TEL-4005 oils, the linear section before the inflection point has a more negative slope (faster rate of depletion), than the linear section after the inflection point. Therefore, it appears that the DODPA depletion reaction(s) is first order, and the rate of the depletion is affected by the presence of PANA and/or the generated species with antioxidant capacity. However, since the original concentration of PANA has an effect on the rate at which the concentration of DODPA decreases with stressing time and on the concentration of the DODPA at the ends of the oils' stable lives (Figures A-20-A-23), the concentration of the DODPA cannot be directly related to the RLL of MIL-L-7808 oils without prior knowledge of the original PANA concentration.

A.7 Antioxidant Concentration versus Stressing Time at 370°F  
Plots for the TEL-4001 and TEL-4006 MIL-L-7808  
Oils

In comparison to the TEL-4002 through TEL-4005 oils, the antioxidant systems of the TEL-4001 and TEL-4006 oils are complicated by the presence of other nitrogen (possibly phosphorus) containing compounds which deplete with stressing time and thus appear to have antioxidant capacity. In the case of the TEL-4001 oil, there is one unknown (1.6 minutes in Figure A-16). In the TEL-4001 oil the octyl-PANA is no longer detectable after less than 30 hours of stressing at 370°F (Figure A-24). Since only two points were obtained, no conclusions on the order of the depletion reaction of octyl-PANA can be made.

In contrast to the octyl-PANA, the DODPA is detectable past the end of the TEL-4001 oil's stable life (105 hours at 370°F). The ln of the DODPA concentration was plotted versus the stressing time and as seen in Figure A-24 the ln of the DODPA depletion reaction is linear. Thus, the depletion reaction of DODPA is first order. However, the plot of the DODPA concentration for the TEL-4001 oil (Figure A-24) does not show an inflection point

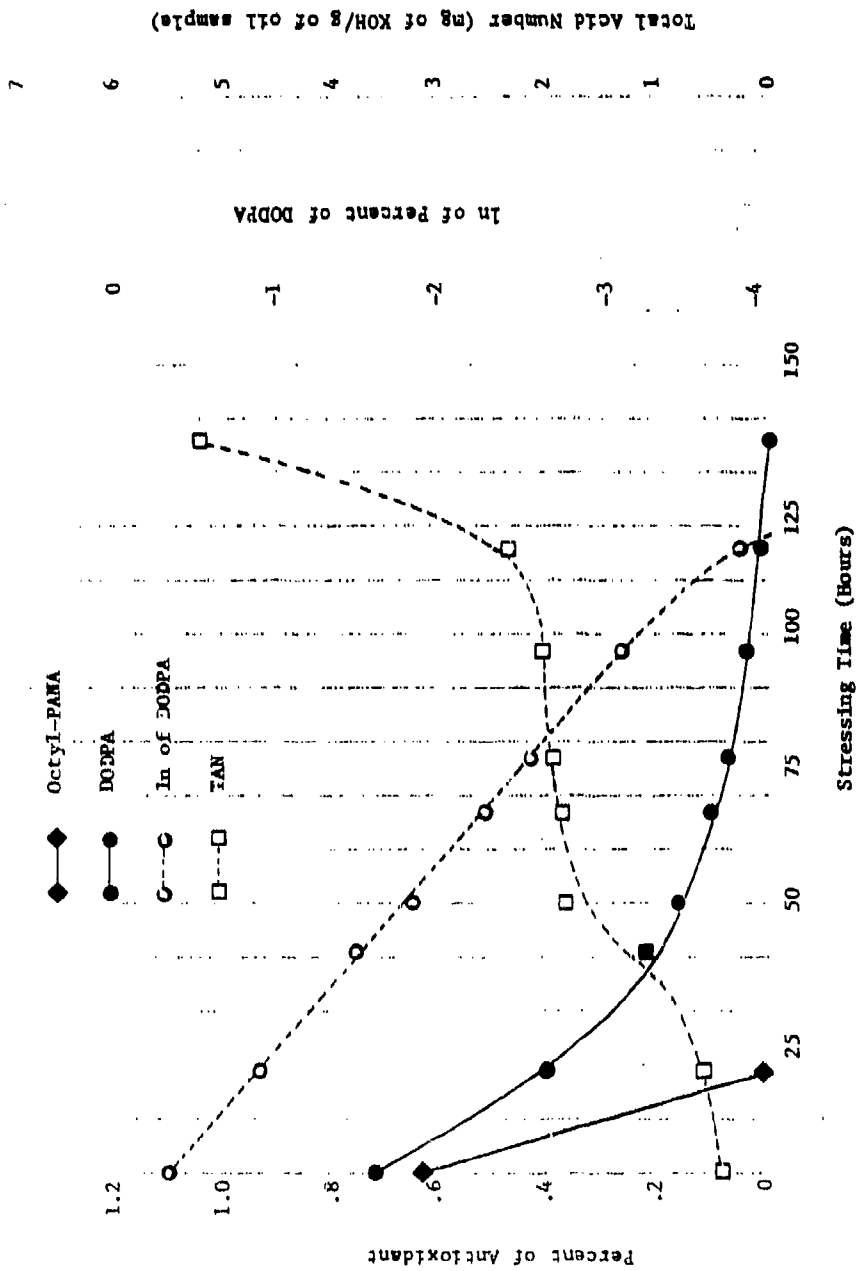


Figure A-24. Plots of Percent (by Weight) of Antioxidants, Octyl-PANA and DODPA, of the ln of Percent (by Weight) of DODPA, and of the Total Acid Number (TAN) versus Stressing Time at 370°F for the TEL-4001 MIL-L-7808 OIL.

as did the plots of the TEL-4002 through TEL-4005 oils (Figures A-20-A-23) and does not appear to be affected by the presence of octyl-PANA.

Since the nitrogen containing compound producing the peak at 1.6 minutes in the gas chromatogram of the TEL-4001 oil is unknown, the nitrogen to carbon ratio is unknown, which is needed in the calculation of the compound's concentration. Therefore, to study the relationship between the unknown compound and stressing time at 370°F, the weight fraction at each stressing time (t) was calculated by equation (6).

$$\text{weight fraction at time (t)} = \frac{\text{peak area of unknown at time (t)}}{\text{peak area of unknown in fresh oil}} \quad (6)$$

The plots of the weight fractions of the unknown, octyl-PANA, and DODPA for the TEL-4001 oil were plotted versus stressing time at 370°F and are presented in Figure A-25.

The plot of the unknown versus stressing time in Figure A-25 shows that for the first 20 hours, the weight fraction, and consequently, the concentration of the unknown remains constant. Once the octyl-PANA is depleted (20 hours at 370°F), the weight fraction of the unknown decreases with stressing time and becomes undetectable at the end of the TEL-4001 oil's stable life. The ln plot of the unknown versus stressing time is linear (Figure A-25) after the first twenty hours, and thus, the depletion reaction of the unknown is first order.

Therefore, the DODPA and unknown compound deplete by first order reactions, while the order of the octyl-PANA depletion reaction could not be determined due to a lack of data points. The DODPA depletion reaction is not affected by the presence of octyl-PANA, but the concentration of the unknown compound does not decrease until the octyl-PANA is depleted.

The TEL-4006 oil's gas chromatograms contain three peaks at retention times of 2.6, 5.0, and 8.1 minutes (Figure A-17). As in the TEL-4001 oil, the octyl-PANA is no longer detectable after less than 30 hours of stressing (Figure A-26), even though the

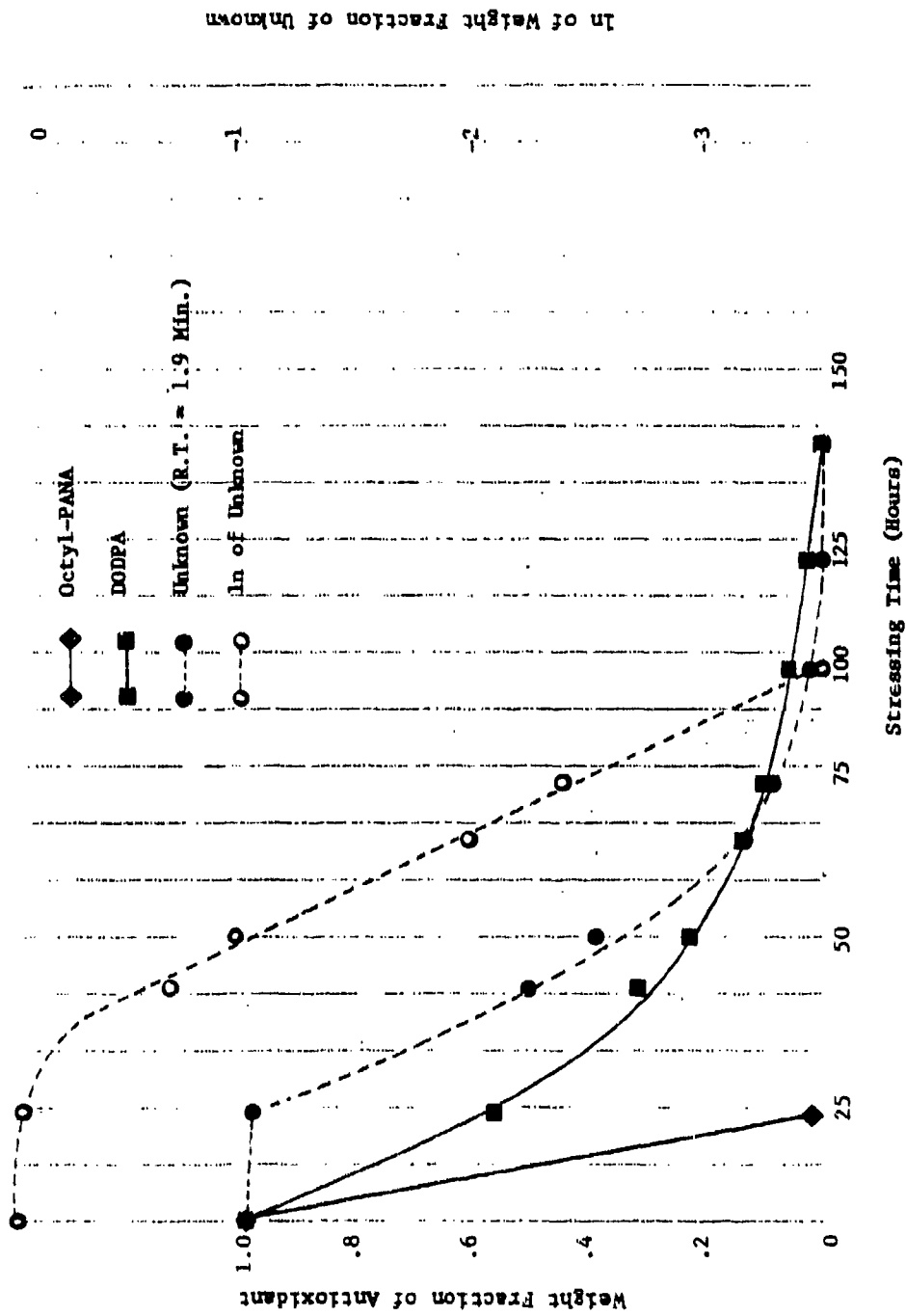


Figure A-25. Plots of Weight Fractions of Antioxidants, Octyl-PANA, DODPA, and Unknown (Retention Time = 1.9 Minutes), and of the ln of Weight Fraction of Unknown versus Stressing Time at 370°F for the TEL-4001 MIL-L-7808 Oil.

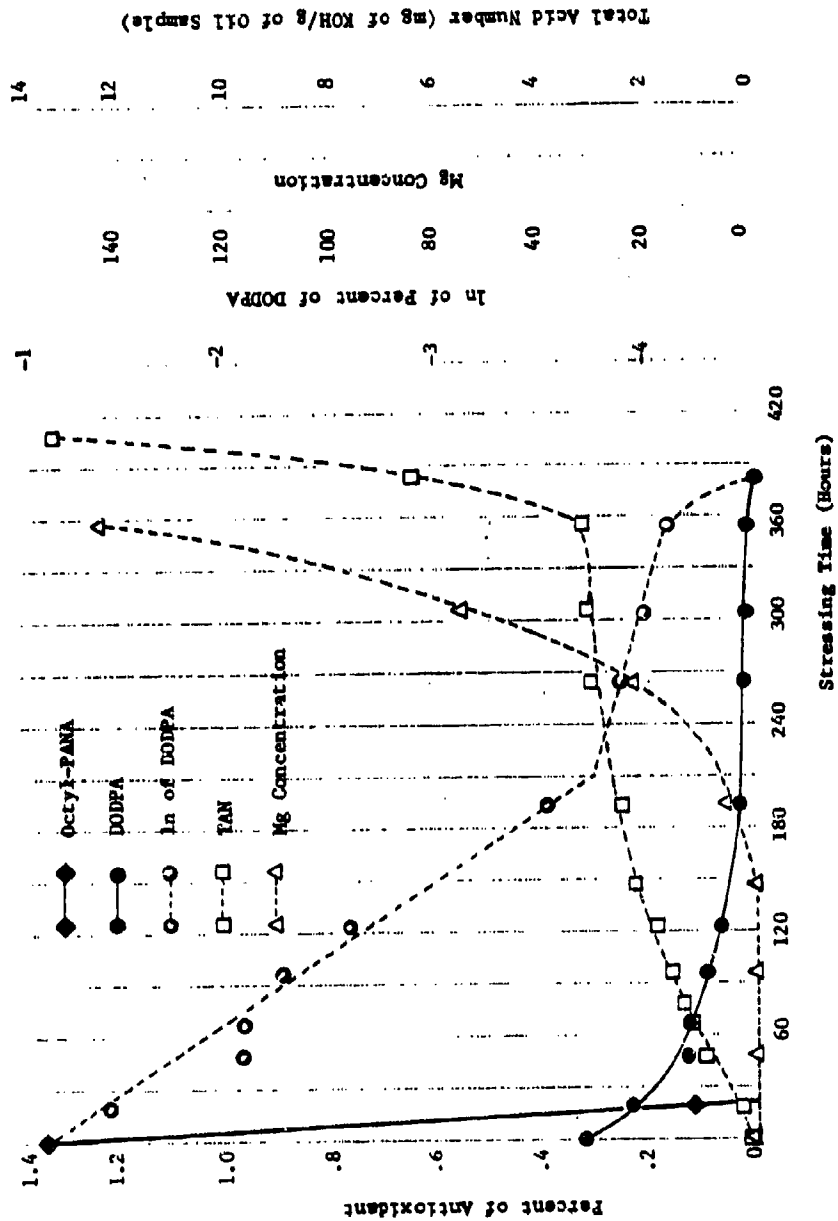


Figure A-26. Plots of Percent (by Weight) of Antioxidants, Octyl-PANA and DODPA, of the In of Percent of DODPA, of the Mg Concentration, and of the Total Acid Number (TAN) versus Stressing Time at 370°F for the TEL-4006 MIL-L-7808 Oil.

original concentrations of octyl-PANA in the TEL-4001 and TEL-4006 oils were 0.62 and 1.34 percent, respectively.

Again the DODPA is detectable at the end of the TEL-4006 oil's stable life. However, in contrast to the TEL-4001 oil (Figure A-24), the ln plot of the DODPA concentration versus stressing time for the TEL-4006 oil consists of two linear sections (Figure A-26). The ln plot of the DODPA concentration has an inflection point which occurs at 210 hours, long after the octyl-PANA is depleted. The inflection point coincides with the initiation of the Mg corrosion (Figure A-26).

As was the case for the TEL-4001 oil, the weight fractions of the unknown compounds at retention times of 2.6, 5.0, and 8.1 minutes were plotted versus stressing time. Since the plots of the unknown compounds are similar, only the weight fraction of the 5.0 minute peak was plotted with the weight fractions of octyl-PANA and DODPA versus the stressing time at 370°F (Figure A-27). As seen in Figure A-27 the plots of the unknown and DODPA are similar. Although the ln plots of the unknown and DODPA consist of linear sections, the inflection point of the unknown occurs at 40 hours, 10 hours after the octyl-PANA is depleted, while for DODPA the inflection point occurs at 210 hours (Figure A-26).

Therefore, the DODPA and unknown compound's depletion reactions are first order while the order of the octyl-PANA depletion reaction could not be determined due to the lack of data points. Although the DODPA depletion reaction is not affected by the presence of octyl-PANA, the depletion reactions of the unknown compounds are affected.

#### A.8 Antioxidant Concentration versus Stressing Time at 370°F Plots for the TEL-5001 MIL-L-7808 Oil

The antioxidant plots of the TEL-5001 oil are shown in Figure A-28. The plots of the DODPA concentration in the TEL-5001 oil (Figure A-28) show that DODPA depletes by a more complicated mechanism than the DODPA in the TEL-4001 through TEL-4006 oils (Figures A-20-A-27). For the first 90 hours of

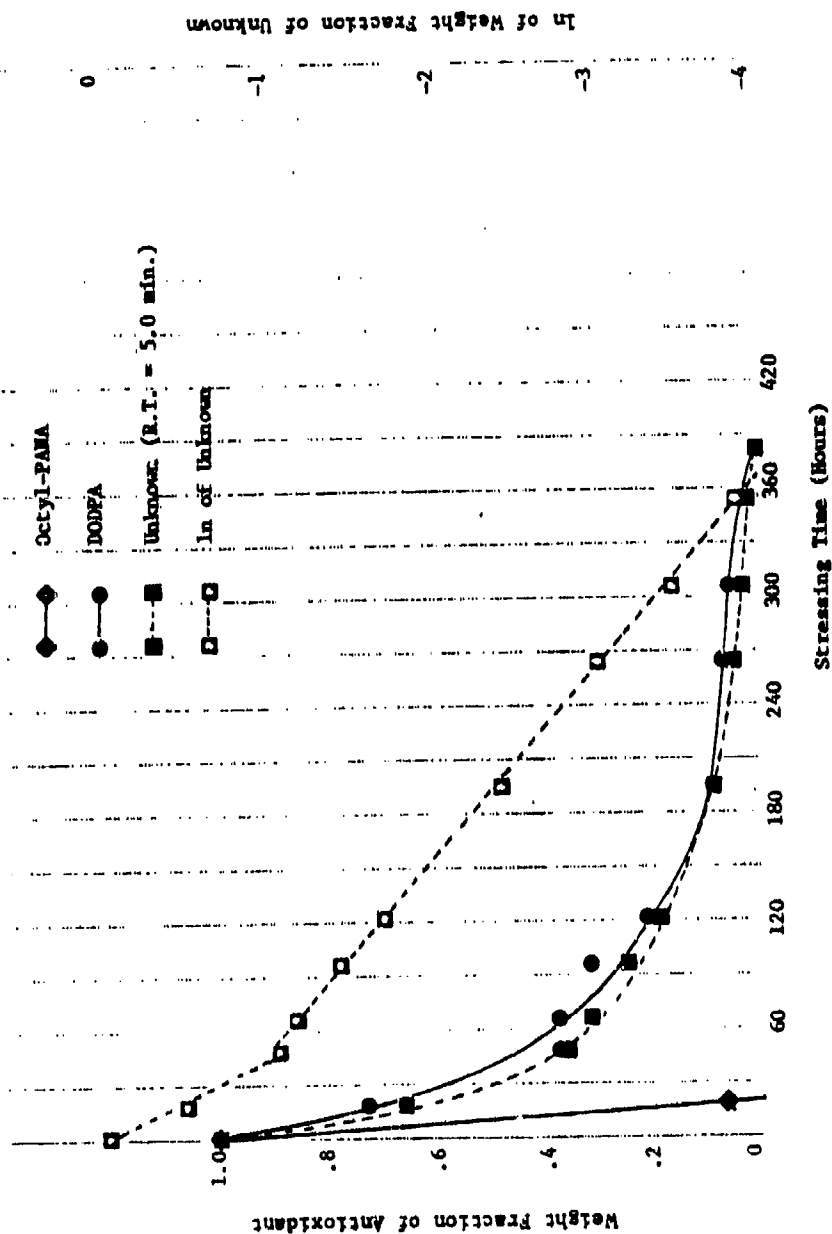


Figure A-27. Plots of Weight Fractions of Antioxidants, Octyl-PANA, DODPA, and Unknown (Retention Time = 5.0 Minutes), and of the ln of the Weight Fraction of the Unknown versus Stressing Time at 370°F for the TEL-4006 MIL-L-7808 Oil.

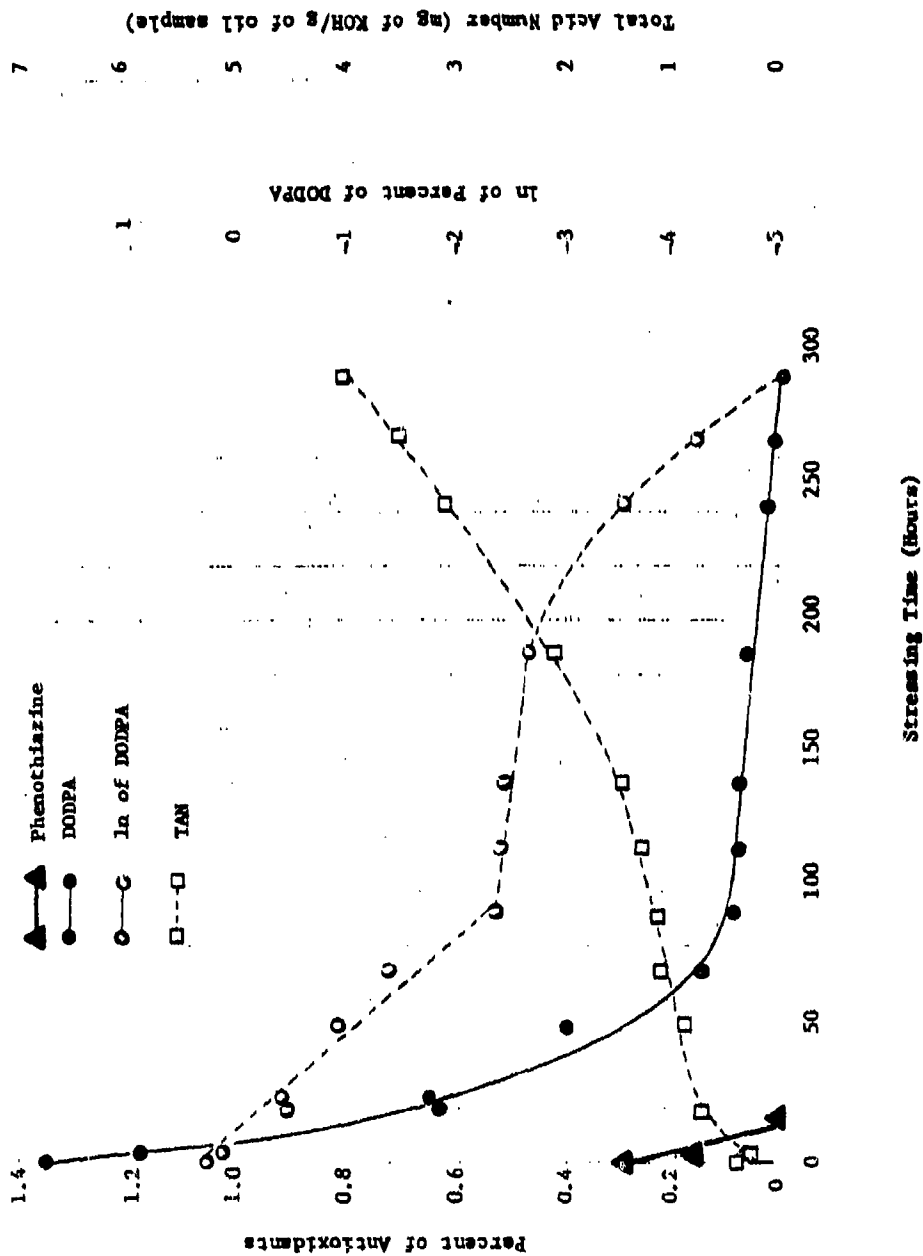


Figure A-28. Plots of Percent (by Weight) of Antioxidants, Phenothiazine and DODPA, of the ln of Percent (by Weight) of DODPA, and of Total Acid Number (TAN) versus Stressing Time at 370°F for the TEL-5001 MIL-L-7808 Oil.

stressing at 370°F the DODPA depletes rapidly, then from 90 to 190 hours of stressing the DODPA concentration remains fairly constant, and after 190 hours of stressing the DODPA again depletes rapidly until it is no longer detectable at 290 hours of stressing. The slight rate increase in the TAN plot corresponds with the stressing time (90 hours at 370°F) at which the DODPA concentration becomes constant.

In contrast to DODPA, phenothiazine depletes very rapidly and is no longer detectable after only 20 hours of stressing. The rapid depletion of the phenothiazine is similar to the rapid depletion of PANA and octyl-PANA in the TEL-4001 through TEL-4006 oils (Figures A-20-A-27). The lack of data points makes the determination of the order of the depletion reaction for phenothiazine unreliable.

#### A.9 Antioxidant Concentration versus Stressing Time at 370°F Plots for the TEL-5002 MIL-L-7808 Oil

The antioxidant plots of the TEL-5002 oil are shown in Figure A-29. The plots of the DODPA concentration in Figure A-29 show that the DODPA in the TEL-5002 oil depletes by a first order reaction. However, in contrast to the TEL-4001 and TEL-4006 oils (Figures A-24-A-27) which contain octyl-PANA, the plot of the DODPA for the TEL-5002 oil (Figure A-29) contains an inflection point at the stressing time the octyl-PANA is no longer detectable. Thus, the DODPA plot of the TEL-5002 oil is more similar to the DODPA plots of the PANA containing TEL-4002 through TEL-4005 oils (Figures A-20-A-23) than the octyl-PANA containing TEL-4001 and TEL-4006 MIL-L-7808 oils (Figures A-24-A-27). The DODPA is detectable past the end of the TEL-5002 oils' stable life (viscosity breakpoint) of 110 hours at 370°F.

As was seen for the TEL-4001 and TEL-4006 oils, the octyl-PANA in the TEL-5002 oil (Figure A-29) depletes very rapidly and is no longer detectable after only 15 hours of stressing. The lack of data points makes the determination of the order of the octyl-PANA depletion reaction unreliable.

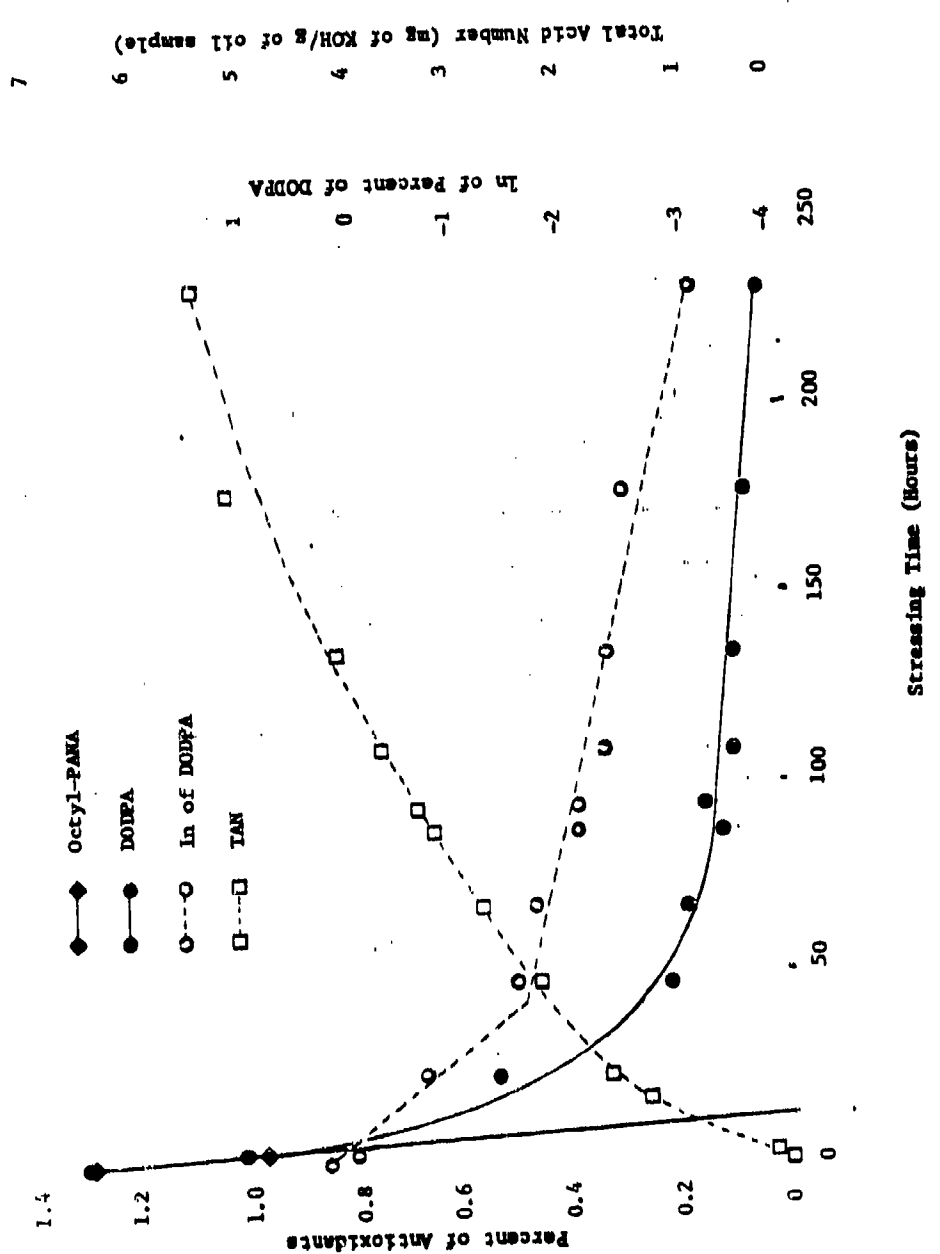


Figure A-29. Plots of Percent (by Weight) of the Antioxidants, Octyl-PANA and DODPA, of the ln of Percent (by Weight) of DODPA, and of Total Acid Number (TAN) versus Stressing Time at 379°F for the TEL-5002 MIL-L-7808 Oil.

A.10 Antioxidant Concentration versus Stressing Time at 392°F  
Plots for the TEL-4001 through TEL-4006 MIL-L-7808 Oils

As was seen for the MIL-L-7808 oils stressed at 370°F, the plots of the PANA in the TEL-4002 through TEL-4005 oils (Figures A-30-A-33) and octyl-PANA in the TEL-4001 and TEL-4006 oils (Figures A-34-A-35) deplete very rapidly. Regardless of the oils' stable lives (60-160 hours) at 392°F, the PANA and octyl-PANA could no longer be detected (less than 0.01 percent) in the stressed TEL-4001 through TEL-4006 oils (Figures A-30-A-35) after 20 hours of stressing.

The plots in Figures A-30-A-35 show that the DODPA depletes by a first order reaction and is detectable at the end of each oil's stable life. As with the stressed oils at 370°F, the DODPA plots show an inflection point soon after the PANA is depleted (TEL-4002 through TEL-4005 oils) and not when octyl-PANA is depleted (TEL-4001 and TEL-4006 oils). The DODPA plot of the TEL-4006 oil shows an inflection point near the end of its stable life as it did at 370°F.

The unknown compounds in the TEL-4001 and TEL-4006 oils (Figures A-36 and A-37) depleted by first order reactions at 392°F as they did at 370°F and are detectable up to the ends of the oils' stable lives.

A.11 Summary of the MIL-L-7808 Oils' Characteristics

The investigation to prepare and characterize the MIL-L-7808 oils showed that the TEL-4001 through TEL-4006, TEL-5001, and TEL-5002 MIL-L-7808 oils contain a variety of antioxidant systems resulting in a wide range of stable lives at stressing temperatures of 370° and 392°F. The TEL-4002 through TEL-4005 MIL-L-7808 oils contain differing amounts of PANA and DODPA and have stable lives (average of viscosity and TAN breakpoints in Tables A-1 and A-2) of 175, 240, 205, and 155 hours at 370°F and of 90, 135, 85, and 75 hours at 392°F, respectively.

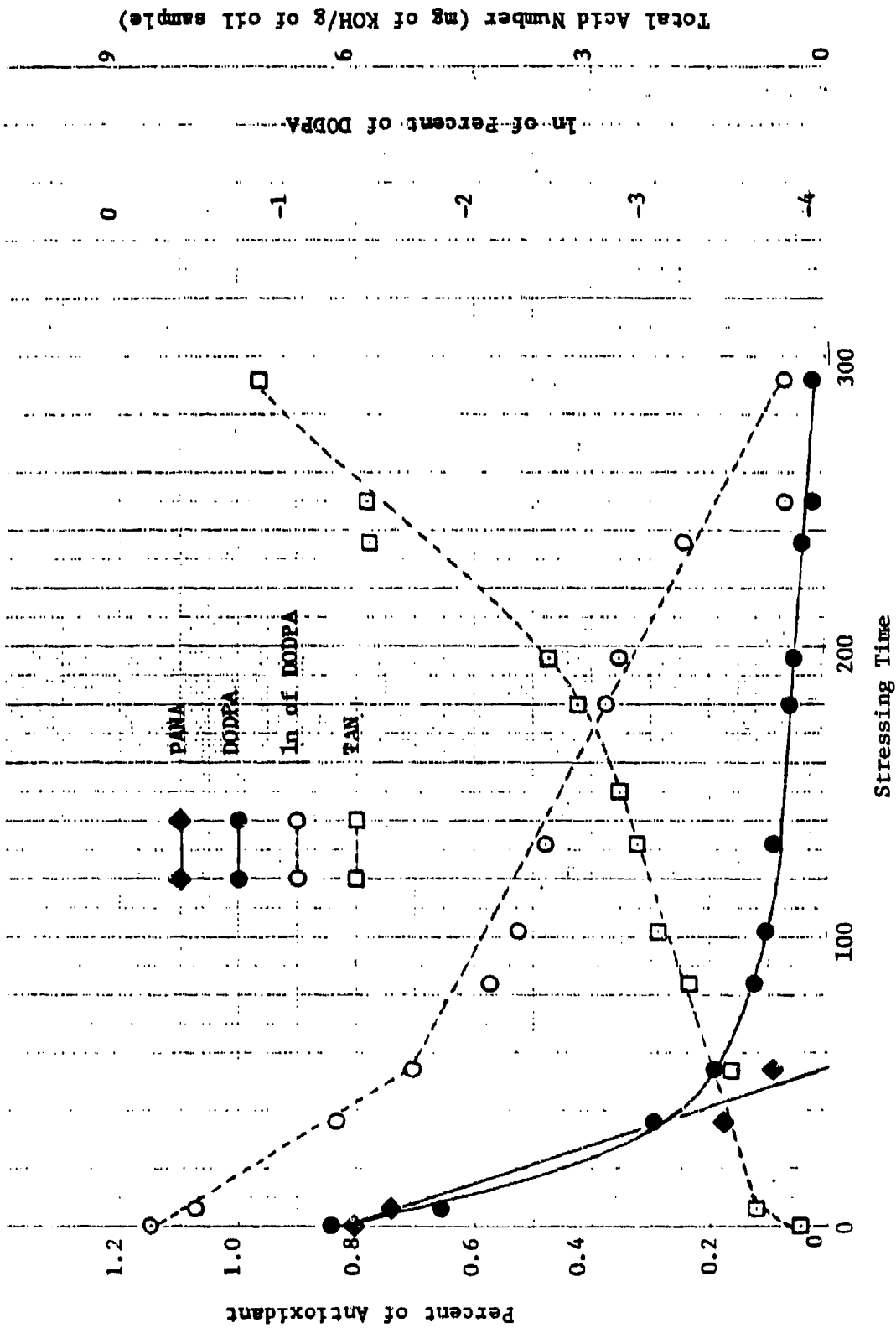
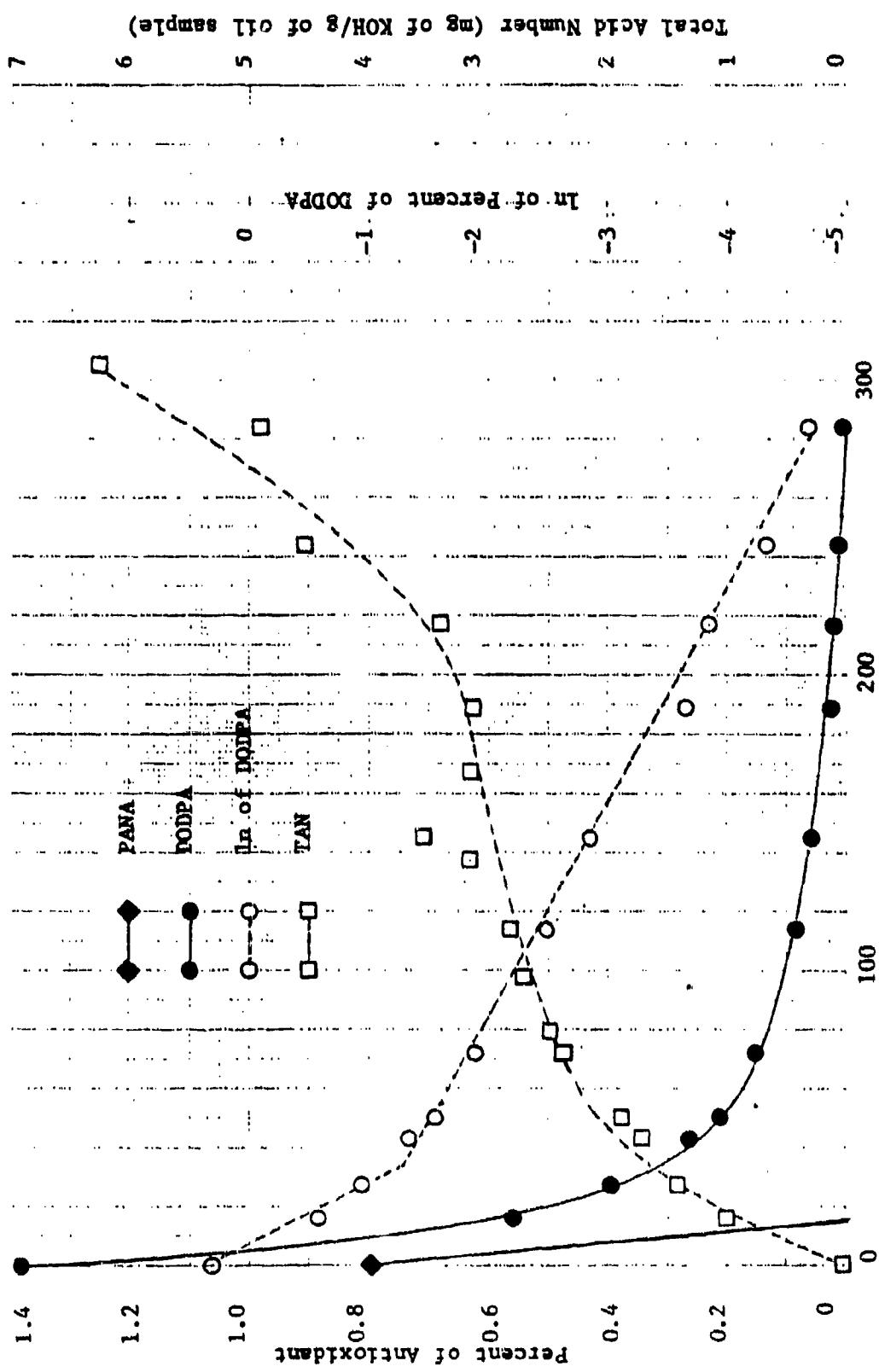


Figure A-30. Plots of Percent (by Weight) of Antioxidants, PANA and DODPA, of the In of the Percent (by Weight) of DODPA, and of the Total Acid Number (TAN) versus Stressing Time at 392°F for the TEL-4002 MIL-L-7808 Oil.



Stressing Time (Hours)

Figure A-31. The Plots of the Percent (by Weight) of the Antioxidants, PANA and DODPA, of the ln of the Percent (by Weight) of DODPA, and of the Total Acid Number (TAN) versus Stressing Time at 392°F for the TEL-4003 MIL-L-7808 Oil.

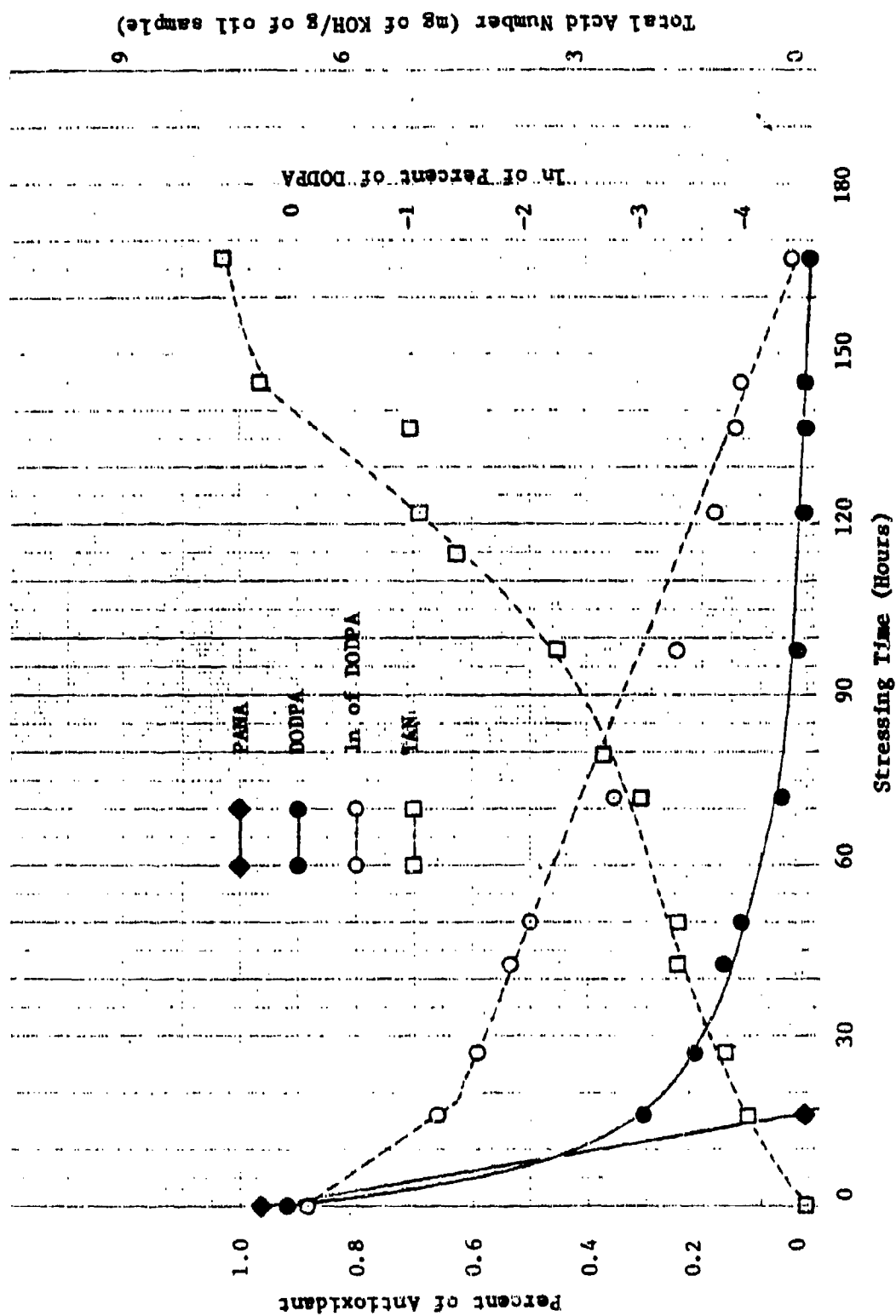


Figure A-32. Plots of Percent (by Weight) of Antioxidants, PANA and DODPA, of the ln of Percent (by Weight) of DODPA, and of the Total Acid Number (TAN) versus Stressing Time at 392°F for the TEL-4004 MIL-L-7808 OIL.

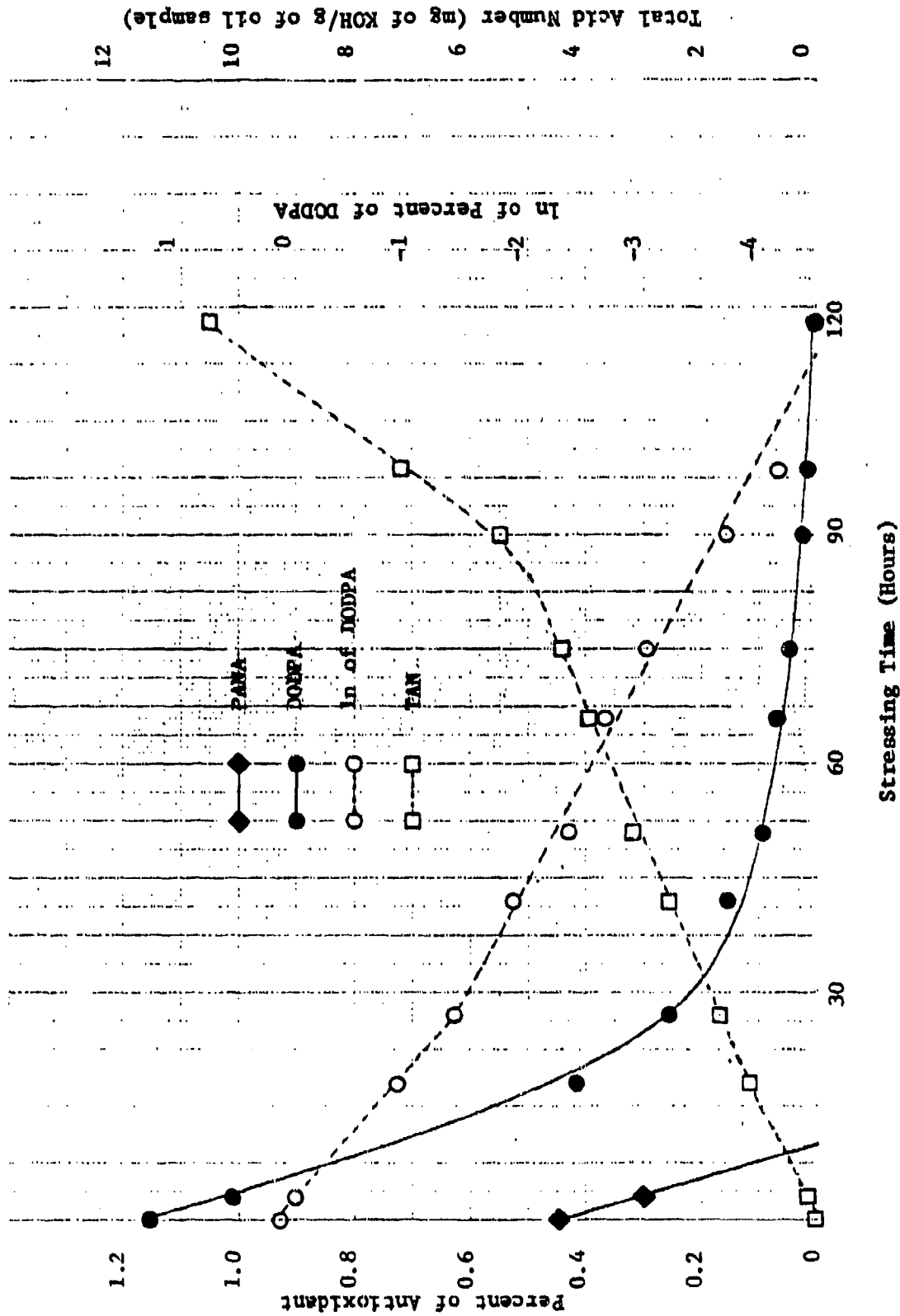


Figure A-33. Plots of Percent (by Weight) of Antioxidants, PANA and DODPA, of the ln of Percent (by Weight) of DODPA, and of the Total Acid Number (TAN) versus Stressing Time at 392°F for the TEL-4005 MIL-L-7808 Oil.

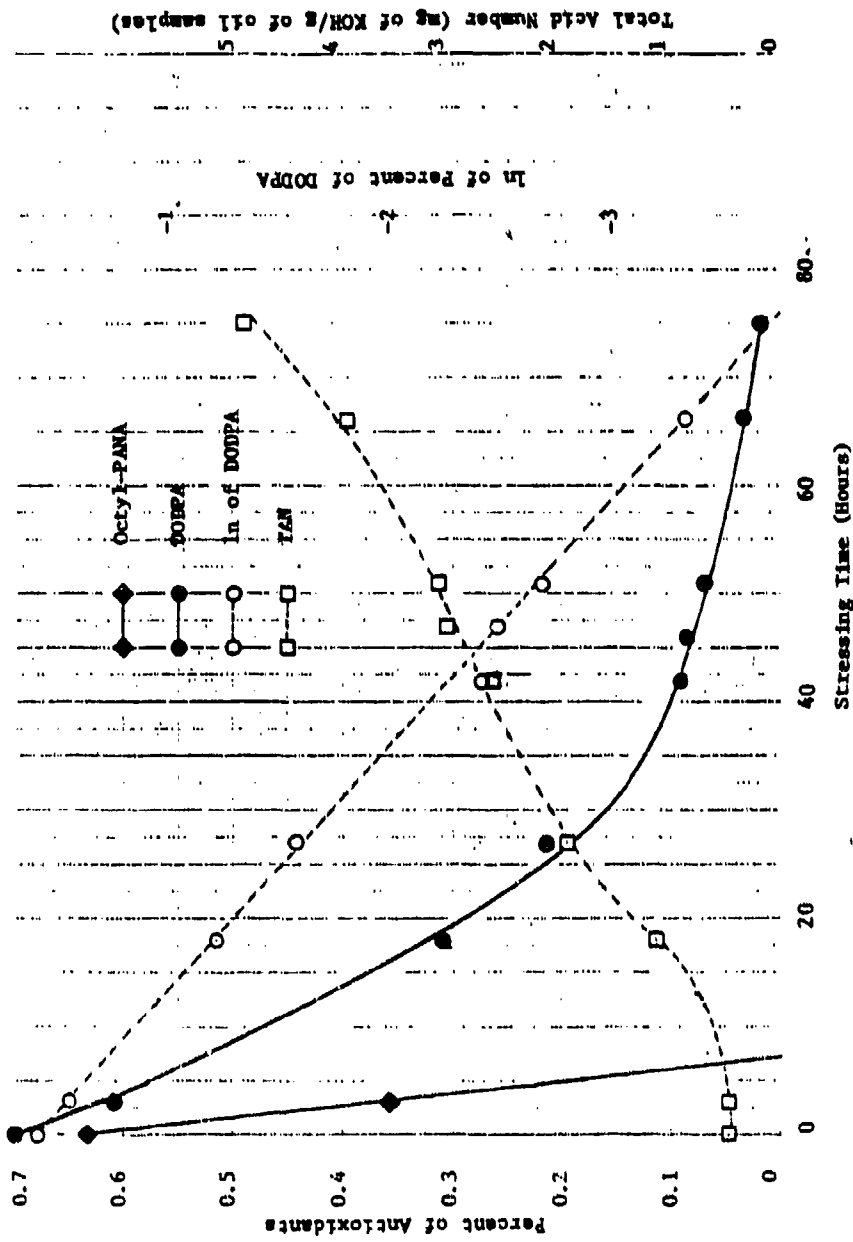


Figure A-34. Plots of Percent (by Weight) of Antioxidants, Octyl-PANA and DODPA, of the In of Percent (by Weight) of BODPA, and of the Total Acid Number (TAN) Versus Stressing Time at 392°F for the TEL-4001 MIL-L-7808 OIL.

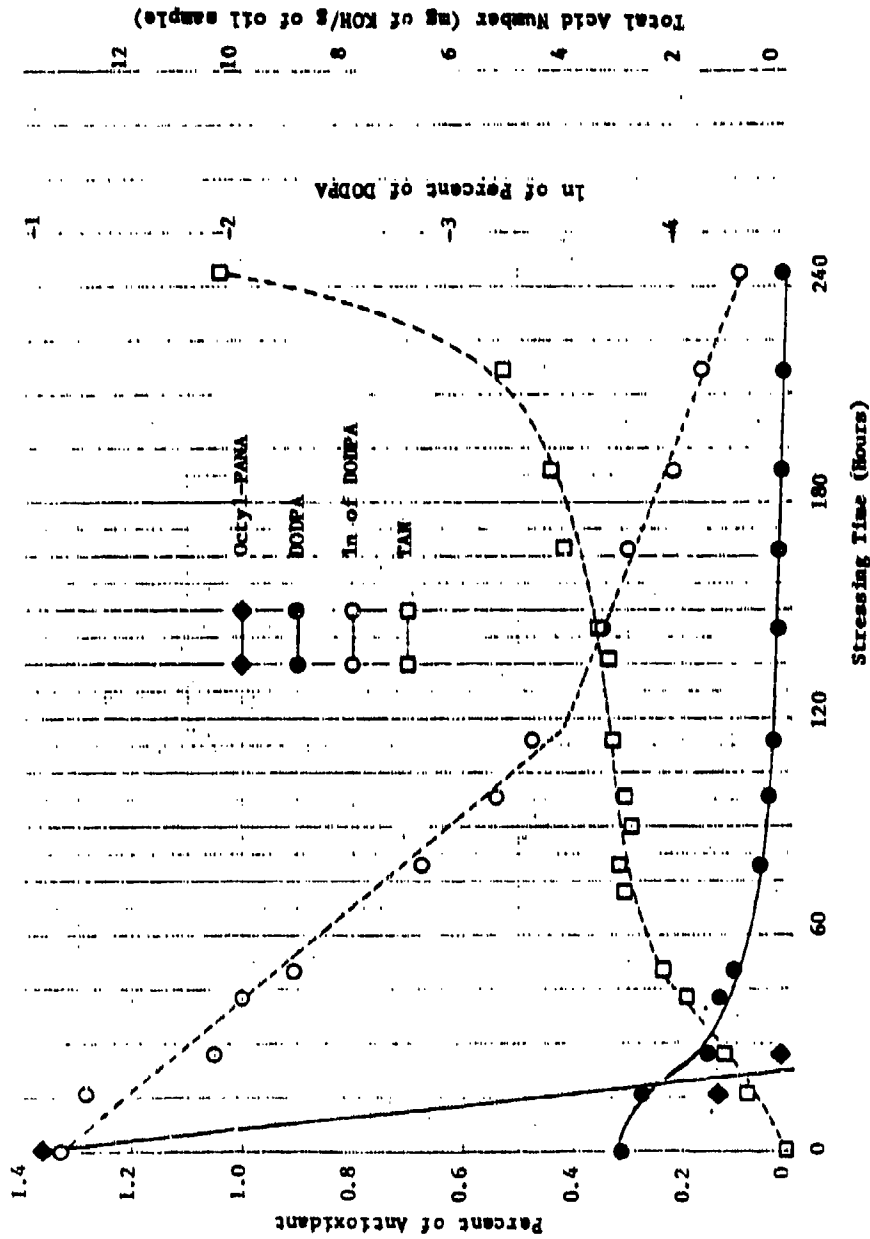


Figure A-35. Plots of Percent (by Weight) of Antioxidants, Octyl-PANA and DODPA, of the ln of Percent (by Weight) of DODPA, and of the Total Acid Number (TAN) Versus Stressing Time at 392°F for the TEL-4006 MIL-L-7808 Oil.

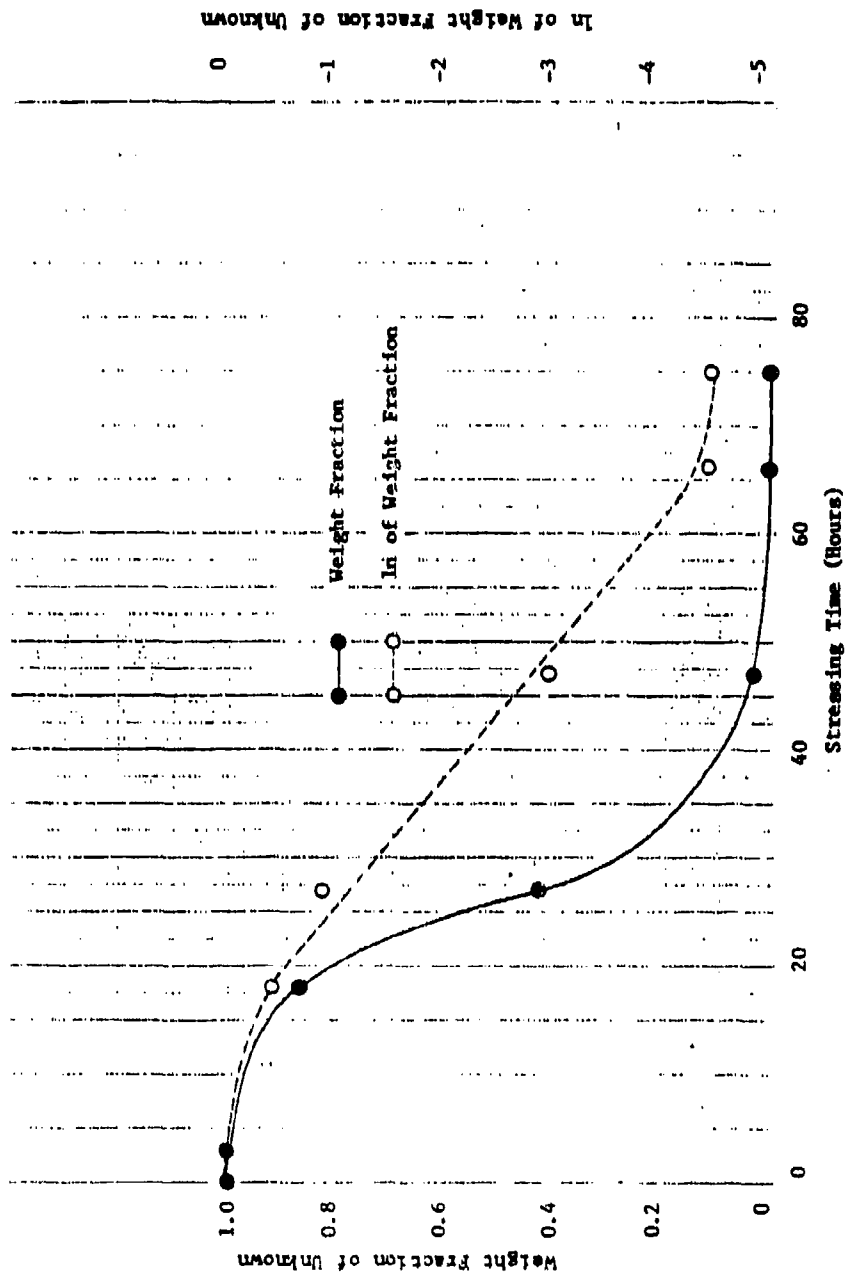


Figure A-36. Plots of Weight Fraction of Unknown (Retention Time = 1.9 Minutes) and of the ln of Weight Fraction of Unknown Versus Stressing Time at 392°F for the IFL-4001 MIL-L-7808 Oil.

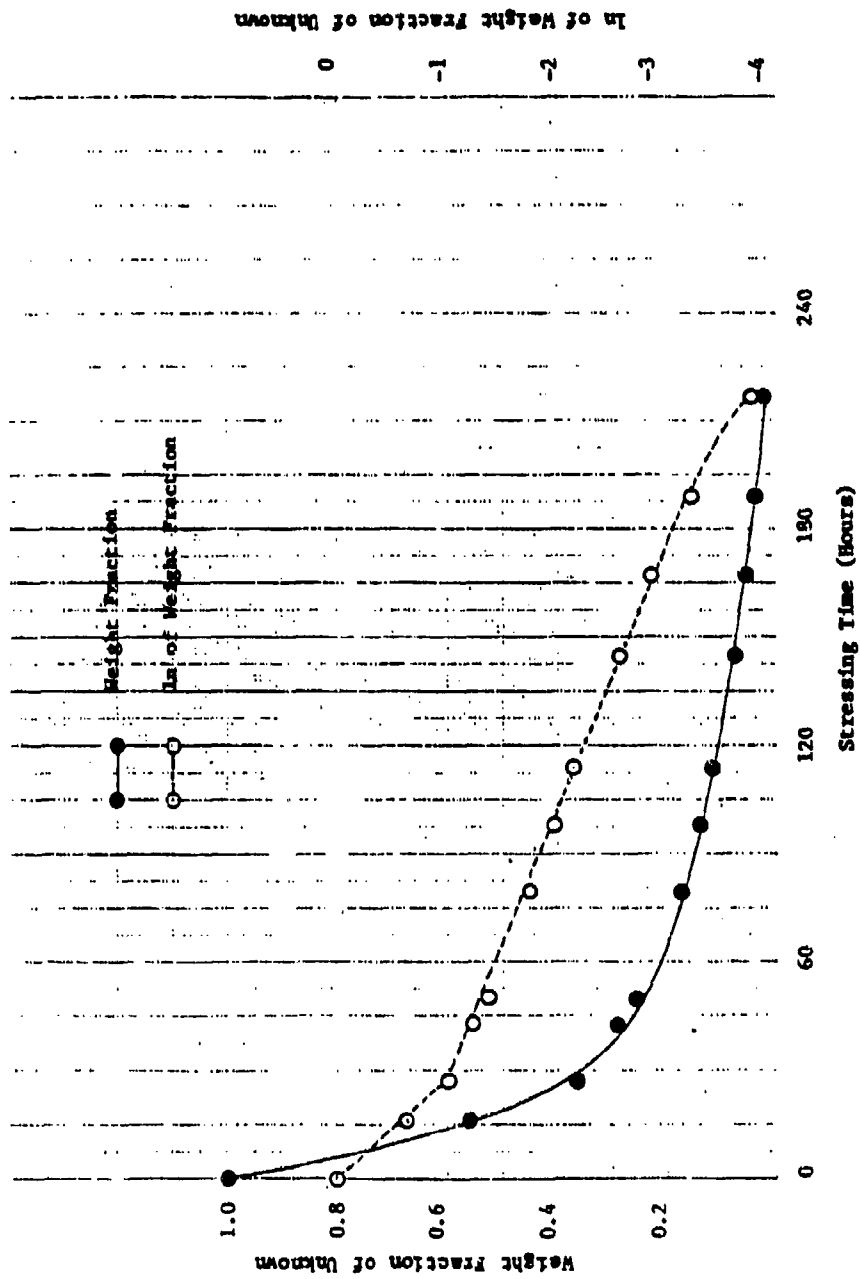


Figure A-37. Plots of Weight Fraction of Unknown (Retention Time = 5.0 Minutes) and of the ln of the Weight Fraction of the Unknown Versus Stressing Time at 392°F for the TEL-4006 MIL-L-7808 Oil.

In addition to the original antioxidants in the TEL-4002 through TEL-4005 oils, species are generated during thermal-oxidation stressing which appear to have antioxidant capacities, i.e., deplete with stressing time.

The TEL-4001, TEL-4006, and TEL-5002 MIL-L-7808 oils contain differing amounts of octyl-PANA and DODPA and have stable lives of 105, 320, and 110 (viscosity breakpoint for TEL-5002 oil) hours at 370°F, respectively, and the TEL-4001 and TEL-4006 oils have stable lives of 60 and 155 hours at 392°F (the TEL-5001 oil was not stressed at 392°F). The TEL-4001 and TEL-4006 oils also contain unknown compounds that appear to have antioxidant capacities.

The TEL-5001 MIL-L-7808 oil contains phenothiazine (preliminary determination) and DODPA and has a stable life of 240 hours (viscosity breakpoint) at 370°F. The stable lives of the MIL-L-7808 oils at 370°F and the concentrations of the antioxidants in the fresh MIL-L-7808 oils are listed in Table 5.

The PANA, octyl-PANA, and phenothiazine present in the different MIL-L-7808 oils deplete rapidly and are no longer detectable after 15-60 hours of stressing at 370°F and after 5-25 hours of stressing at 392°F regardless of the oils' stable lives. The order of the PANA, octyl-PANA, and phenothiazine depletion reactions could not be determined due to the lack of data points but appeared to be zero order.

The DODPA and the unknown compounds in the different oils deplete by first order reactions and are detectable up to the end of the oils' stable lives. The presence of PANA has a strong effect on the DODPA depletion reactions in the TEL-4002 through TEL-4005 oils. The presence of octyl-PANA has a strong effect on the DODPA depletion reaction in the TEL-5002 oil but does not have an effect on the DODPA depletion reactions in the TEL-4001 and TEL-4006 oils. The octyl-PANA does affect the depletion reactions of the unknown compounds in the TEL-4001 and TEL-4006 oils. The presence of phenothiazine has no effect on the DODPA depletion reaction in the TEL-5001 oil.

Since PANA, octyl-PANA, and phenothiazine deplete so rapidly there is no relationship between the concentration of PANA, octyl-PANA, or phenothiazine, and the RLL of a stressed MIL-L-7808 oil. Although DODPA is detectable up to the end of the each MIL-L-7808 oil's stable life, the rate of the DODPA depletion is dependent upon the original concentration of PANA or octyl-PANA in the fresh MIL-L-7808 oil. Also, the concentration of DODPA at the end of each MIL-L-7808 oil's stable life is different. Thus, there is no relationship between the concentration of the DODPA and the RLL of a stressed MIL-L-7808 oil.

on the Apple IIe monitor and printed on a  $\mu$ 92 Microline Printer, (Okidata, Mt. Laurel, New Jersey).

b. Differential Scanning Calorimetry

The high pressure and hermetically-sealable pan DSC studies were performed on a DuPont 9000/9900 Thermal Analysis System in conjunction with a 910 cell base and a DSC cell (atmospheric pressure) or a high pressure-DSC cell (DuPont Instrument Systems, Wilmington, Delaware). The 900 Computer/Thermal Analysis System is based on a Texas Instruments Professional computer, CRT display screen (to view data from current or previous experiments), floppy disk data storage, module interface and a two or six pen digital plotter.

The threaded-sealable pan DSC studies were performed on a Perkin Elmer 7 Series Thermal Analysis System in conjunction with a DSC 7 module (Perkin Elmer Corporation, Fairfield, Ohio). The Perkin Elmer 7 Series Thermal Analysis System is based on the PE7500 Professional Computer, CRT display screen (to view data from current or previous analysis), dual floppy disk drives, module interface, and a graphics plotter.

c. Fluorimetry

The fluorescence investigation was performed on a Farrad Spectrofluorimeter MK-1 with a mercury lamp as the radiant energy source. The wavelength of 351 nm was used to excite the samples.

d. Gas Chromatography

The gas chromatographic analyses were performed on a Varian Series 1860 Gas Chromatograph equipped with a Varian Thermionic Specific Detector (Varian Associates, Inc., Instrument Group, Palo Alto, California). The detector and injection ports were set at 350°C. The air and hydrogen flow rates used by the detector were set at 173 and 4.5 ml/minute, respectively. A helium flow rate of 31 ml/minute was established through the 6 ft. x 1/8 inch stainless steel column which was packed with 3 percent OV-1 on Chromosorb W (80/100 mesh) (Alltech Associates,

## APPENDIX B - EQUIPMENT AND PROCEDURES

### B.1 Introduction

This section describes the instrumentation, supplies and procedures used to develop the RLLAT candidates. The equipment and procedures used to prepare and characterize the thermally-oxidized MIL-L-7808 oils are also described herein.

### B.2 Instrumentation

#### a. Voltammetry

The voltammetry studies were performed on a CV-1B Voltammetry Electronics Control Module [Bioanalytical Systems, Inc. (BAS), West Lafayette, Indiana]. The auxiliary electrode was a platinum wire electrode and the reported potentials were referenced to a RE-1 Ag/AgCl reference electrode (BAS). The working electrode was a glassy carbon (GCE), platinum (PTE), or thin film mercury on gold (HG-AUE) voltammetry electrode (BAS). The HG-AUE electrode was produced by allowing a drop of mercury to sit on the polished surface of a gold voltammetry electrode for 2-3 minutes. The excess mercury was then wiped off and smoothed with a soft, dry tissue to produce the mirror-like finish of the mercury-gold amalgam surface.

The cyclic voltammograms were recorded on a X-Y Recorder (Hewlett-Packard, Mosley Division, Palo Alto, California). The reductive-cyclic voltammograms were sampled, analyzed, and displayed by a data acquisition system based on an Apple IIe microcomputer (Apple Computer, Inc., Cupertino, California). The output of the CV-1B module was converted to digital form by a 16 channel, 12 byte analog/digital converter, Model AII3 (Interactive Structures, Bala Cynwyd, Pennsylvania), which was interfaced with the Apple IIe microcomputer. The sampling rate was controlled by a Speed-Demon card (Microcomputer Technologies, Santa Monica, California). The reductive-cyclic voltammograms and the results of the data analyses were displayed

Inc., Deerfield, Illinois). The gas chromatograms were plotted and integrated by a Shimadzu C-R3A Computer Integator (Shimadzu Scientific Instruments, Columbia, Maryland). The chart speed was 3 cm/minute.

e. Electrochemistry

The electrochemical analyses were performed on a COBRA (NAECO Associates Inc., Arlington, Virginia).

f. Atomic Emission Spectrometry

The atomic emission spectrometric analyses were performed on a rotating disk electrode-spark source-atomic emission spectrometer, (Engine Oil Analysis Spectrometer, Baird Corporation, Bedford, Massachusetts). The spectrometer is capable of simultaneously analyzing for Ag, Al, Cr, Cu, Fe, Mg, Ni, Pb, Si, and Sn.

B.3 Supplies

a. Chemicals

The diphenylamine (99 + % purity), cumene hydroperoxide (~80 percent purity), dicumene peroxide (~70 percent purity), and the organic bases; pyridine, pyrazine, pyridazine, quinoxaline, and 2,2' dipyridyl (97-99+% purity) were obtained from Aldrich Chemical Corporation, Milwaukee, Wisconsin. The azobisisobutyronitrile (AIBN) (~98 percent purity) and benzoic peroxide (~80 percent purity) were obtained from Fisher Scientific (Cincinnati, Ohio). The bis[4-(dimethylamino) dithiobenzil] nickel (BDN) was obtained from Exciton Chemicals (Dayton, Ohio). All of the other chemicals used in this investigation were ACS certified and were obtained from Fisher Scientific.

b. Solvents

All of the solvents used in this investigation were obtained from Fisher Scientific and were ACS certified.

c. Electrolytes

The lithium perchlorate,  $[\text{LiClO}_4]$  (ACS certified) and tetrabutylammonium perchlorate  $[(\text{CH}_3\text{CH}_2\text{CH}_2\text{CH}_2)_4\text{NClO}_4]$  (~10 percent  $\text{H}_2\text{O}$ : polarographic grade) were obtained from Fisher Scientific. The tetraethylammonium perchlorate  $[(\text{CH}_3\text{CH}_2)_4\text{NClO}_4]$  (~10 percent  $\text{H}_2\text{O}$ : polarographic grade) was obtained from Southwestern Analytical Chemicals, Inc., Austin, Texas.

d. Antioxidants

The generic samples of the N-phenyl- $\alpha$ -naphthylamine (PANA) and dioctyl diphenylamine (DODPA) antioxidants were obtained from AFWAL/POSL. The N-(p-octylphenyl)- $\alpha$ -naphthylamine (octyl-PANA) antioxidant (Tradename: Irganox (LO-6) was obtained from CIBA-GEIGY Corporation, Hawthorne, New York, in commercial grade purity. The phenothiazine (98 + % purity) was obtained from Aldrich Chemical Company in ACS reagent grade.

e. Lubricating Oils

The fresh MIL-L-7808 lubricating oils (TEL-4001 through TEL-4006, TEL-5001, and TEL-5002) and the fresh candidate MIL-L-27502 lubricating oil were obtained from AFWAL/POSL. The used MIL-L-7808 lubricating oils, OP-232-1 through OP-232-43, were also obtained from AFWAL/POSL.

The authentic used MIL-L-7808 and MIL-L-23699 lubricating oil samples were obtained from gas turbine engines of Air Force aircraft. The oil samples consist of a series of oil samples taken from representative engines. The used MIL-L-7808 oil samples were taken from F-100 and J79 engines. The used MIL-L-23699 oil samples were all taken from T56 engines.

Each series of oil samples was taken from a selected engine and consists of the last 3-7 consecutive oil samples prior to engine removal. If the engine removal was due to engine failure without prior detection by the Spectrometric Oil Analysis Program (SOAP), the oil samples are referred to as failures (F).

However, if the engine removal was due to a maintenance recommendation of SOAP and abnormal wear was verified by inspection, the oil samples are referred to as hits (H).

#### B.4 Preparation and Characterization of Stressed TEL-4005 Oil Samples

To prepare the stressed oil samples used in Task 1 to initially evaluate the identified analytical techniques, 400 ml of fresh TEL-4005 oil was measured into a 1 liter, three neck round bottom flask. The flask was then fitted with an Allihn condensor, an air supply tube (supporting the metal specimens) and a thermocouple tube. The metal specimens (Metaspec Company, San Antonio, Texas) were placed on the air supply tube (separated by 9 mm glass spacers) in the order specified by Federal Test Method Standard 791 Method 5307.1: aluminum (402-C) (bottom position); silver (402-H); bronze, silicon (402-4616); steel, carbon, mild (402B); steel, M-50 (402-M50); magnesium (402D); and titanium (420G) (top position). The dry air supply was obtained from a compressed air cylinder, industrial grade (AIRCO, Murray Hill, New Jersey) and was controlled by a 602-flowmeter (Matheson, Dayton, Ohio).

The flask was then placed inside a 1 liter heating mantle to obtain an oil temperature of 175°C (heating mantle temperature 250°C). The oil sample required approximately one hour to equilibrate at 175°C. An air flow of 10 l/hr was established through the oil sample and the measurement of the stable life was started. Oil samples (30-40 ml) were withdrawn at 24 hour intervals to obtain a well defined stable life. Each withdrawn sample was characterized by viscosity (40°C). The values obtained for the viscosity were plotted versus the stressing time as shown in Figure B-1. The stable life of the TEL-4005 oil at 175°C under the described conditions is 96 hours (Figure B-1).

#### B.5 Preparation and Characterization of MIL-L-7808 Oils Stressed at 370° and 392°F

The aluminum block heating medium was manufactured so that it held four sample tubes as per specifications given in Reference 45. All of the glassware and metal specimens used in

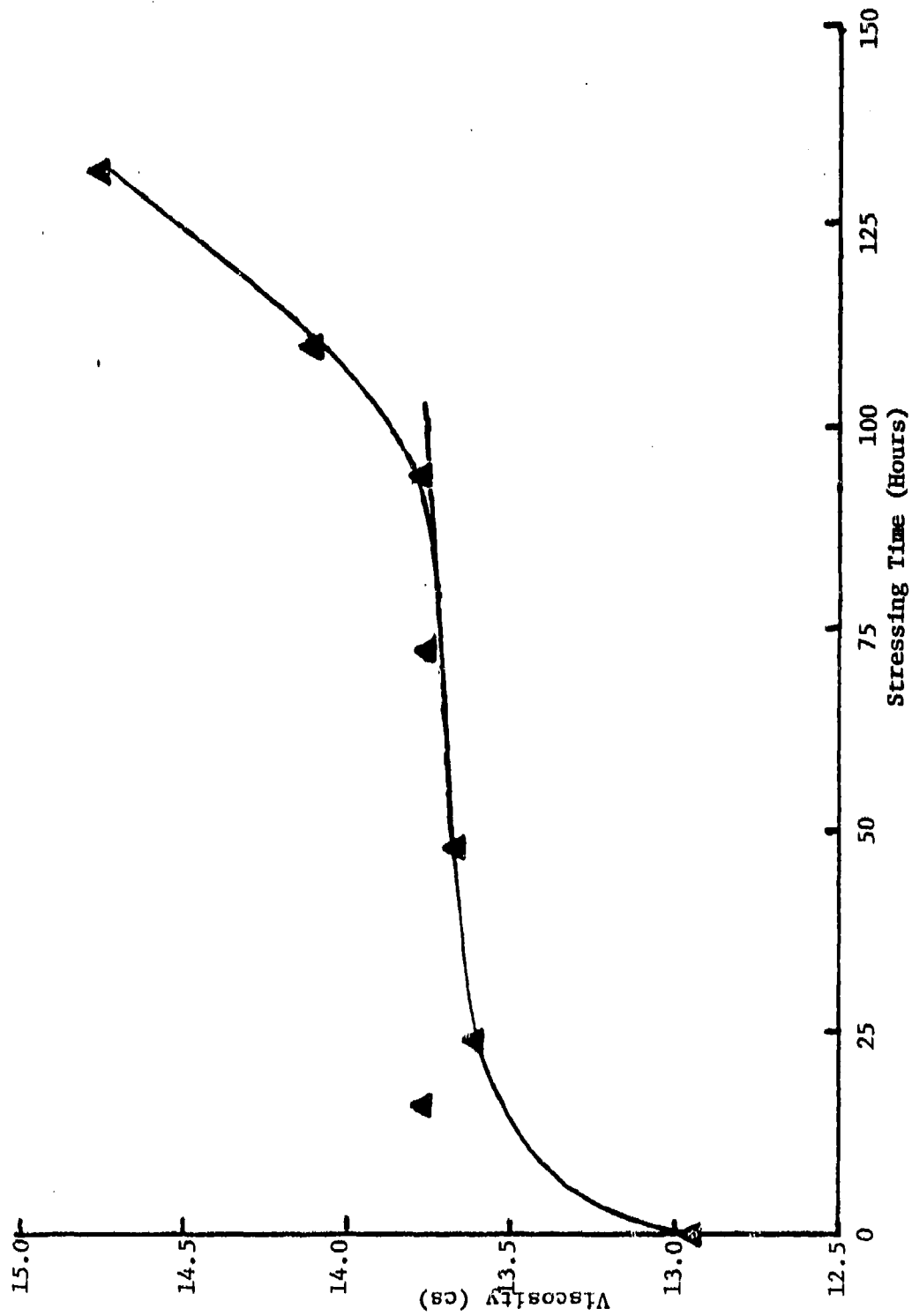


Figure B-1. Viscosity versus Stressing Time (175°C) Plot for the TEL-4005 Oil.

this investigation were manufactured to the specifications given in Federal Test Method Standard No. 791B Method 5307.1. The dry air supply for the oil samples heated in the aluminum block was obtained from a compressed air cylinder, industrial grade (AIRCO). The air supply was split into one separate line per oil sample and the flow rate of each line was controlled using a 602-flowmeter (Matheson).

After 450 ml of fresh MIL-L-7808 lubricating oil was measured into the four sample tubes, each sample tube was then fitted with a sample tube head, an Allihn condensor, an air supply tube (supporting the metal specimens) and a thermocouple tube as specified by Federal Test Method Standard No. 791B Method 5307.1. The sample tubes were then placed into the aluminum block heating medium. The temperature of each oil sample was monitored and each oil sample required approximately one hour to equilibrate at 370°F and approximately 90 minutes to equilibrate at 392°F. An air flow of 10 l/hr was then established through each oil sample and the measurement of the stable life of each oil sample was started.

Oil samples (30-40 ml) were withdrawn at 16-48 hour intervals at 370°F and at 3-24 hour intervals at 392°F so that a well defined stable life could be obtained for each MIL-L-7808 lubricating oil. Each withdrawn oil sample was characterized by COBRA (as described in Reference 35), viscosity (40°C), and total acid number (ASTM Method 664) measurements and by magnesium concentrations (atomic emission spectrometer as described in Reference 46).

The values obtained for the COBRA, viscosity, and total acid number measurements and the Mg concentrations were then plotted versus the stressing time to determine the stable lives of the MIL-L-7808 oils at 370° and 392°F as described in Appendix A.

B.6 Gas Chromatographic-Antioxidant Analyses of the MIL-L-7808 Oils Stressed at 370° and 392°F

In order to quantify the antioxidants present in the fresh and stressed MIL-L-7808 lubricating oils, an internal standard solution prepared from diphenylamine was used. A drop of the internal standard solution and a drop of the oil sample were placed in a vial. Each drop was weighed to the nearest 0.0001 g. Approximately 2 ml of acetone was then added to the vial, the vial was stoppered and shaken by hand until a homogenous solution was obtained. A 1  $\mu$ l sample of the solution was then injected into the GC. The column temperature was programmed to start at 200°C, increase at 8°C/minute to 325°C, and then hold at 325°C for 10 minutes. The concentration (percent by weight) of each antioxidant present in the fresh and stressed MIL-L-7808 lubricating oils was then calculated from the known weights of the internal standard and oil sample.

B.7 Preparation of Stressed TEL-4004 Oil Samples for the RCV Oil Dilution Study

The aluminum block heating medium was used to heat four 160 ml samples of TEL-4004 MIL-L-7808 lubricating oil using the glassware and metal specimens specified by Federal Test Method Standard 791 Method 5307.1. The TEL-4004 oil samples required approximately one hour to equilibrate at 347°F. An air flow of 10 l/hr was then established through each oil sample and the measurement of each oil sample's stable life was started.

Oil samples (4-7 ml) were withdrawn at 20-48 hour intervals until approximately 20 ml of oil had been withdrawn. Once 20 ml of TEL-4004 oil had been withdrawn, 20 ml of fresh TEL-4001, TEL-4003, or TEL-4004 MIL-L-7808 oil was added, the diluted TEL-4004 oil sample allowed to become homogeneous (approximately 30 minutes), and then an oil sample (2-7 ml) withdrawn. This procedure of withdrawing samples and adding oil was repeated for 340 hours to produce two stressed TEL-4004 oil samples with different

RLL, a mixed stressed oil sample consisting of TEL-4004 and TEL-4001 oils, and a mixed stressed oil sample consisting of TEL-4004 and TEL-4003 oils.

After 340 hours, the stressing temperature was increased from 347°F to 370°F to simulate an engine going from normal to abnormal operating conditions.

Due to the small sizes of the withdrawn samples, only COBRA measurements were obtained and plotted against stressing time to estimate the degree of oxidation of each oil sample. The withdrawn oil samples were then analyzed by RCV to determine the effects of oil dilution and formulation mixing on the RLL predictions of the RCV.

#### B.8 Procedure for Analytical Techniques Capable of Oxidative Degradation Estimations

##### a. Hydroperoxide Analyses

(1) Iodine Liberation Method - The modified procedures of the Mair and Graupner iodine liberation methods (Reference 23) are given in Table B-1. The only modification made in the iodine liberation methods are concerned with the titration of the reaction NaI solution and are denoted in Table B-1.

(2) Cyclic Voltammetric Method - The cyclic voltammetric peroxide determinations were performed with platinum and glassy carbon working electrodes on 300  $\mu$ l oil samples diluted with 10 ml of acetone (0.1 M LiClO<sub>4</sub>). The diluted oil samples were deaerated with a steady stream of nitrogen for 3 minutes prior to analysis. The potential range of +0.2 to -2.0 V was scanned at a rate of 500 mV/sec. The heights of the produced reduction waves (-1.0 to -1.7 V) were then used to quantitate the total hydroperoxide concentrations of the oil samples.

##### b. Permanganatometric Method

A 25 ml portion of 0.01 N KMnO<sub>4</sub> solution was added to a 250 ml glass erlenmeyer flask, along with 10 ml of an aqueous sulfuric acid solution (volume ratio: 5 parts H<sub>2</sub>SO<sub>4</sub>/1 part H<sub>2</sub>O) and 4 ml of an MIL-L-7808 oil sample. The flask was stoppered, then gently shaken and allowed to sit undisturbed or stirred

Table B-1

## IODINE LIBERATION METHODS I, II, AND III

METHOD I

1. Dissolve 2 g of NaI in 35 ml of isopropanol and 2.5 ml of acetic acid in a 250 ml erlenmeyer flask.
2. Add 4 ml of oil sample to flask with swirling.
3. Reflux for five minutes.
4. Add 20 ml of  $\text{CCl}_4^a$ .
5. Add 100 ml of distilled water.
6. Add 5 ml of starch indicator solution and titrate from dark purple to colorless with standardized 0.005 N sodium thiosulfate.

	<u>Method II</u>	<u>Method III</u>
1. Reflux 50 ml of glacial acetic acid briefly	Yes	Yes
2. Cool, dissolve 6 g of NaI	Yes	Yes
3. Add 3.0 ml of distilled water	Yes	No
4. Add 4 ml of oil sample	Yes	Yes
5. Add 2.0 ml of concentrated HCl acid	No	Yes
6. Reflux at least	20 min.	50 min.
7. Add 20 ml of $\text{CCl}_4^a$	Yes	Yes
8. Add 100 ml of distilled water	Yes	Yes
9. Titrate with 0.005 N sodium thio-sulfate and starch indicator	Yes	Yes

<sup>a</sup>Modification made in Mair and Graupner Methods I, II, and III to separate the colored oil sample from the aqueous layer so that the endpoint (blue to clear) could be determined.

vigorously with a magnetic stirring bar at room temperature for a predetermined period of time. After the predetermined period of reaction time, the flask was unstoppered, 2 g of KI was added, and the mixture was shaken until the KI was completely dissolved. After the KI was dissolved, 20 ml of chloroform and 65 ml of distilled water were added to the flask to produce a 100 ml aqueous layer (upper layer) containing the iodine liberated by unreacted  $\text{KMnO}_4$  and a 24 ml lower organic layer containing the used oil sample. The liberated iodine in the aqueous layer was then titrated with a standardized 0.005N sodium thiosulfate solution using a 0.5 percent aqueous starch solution as an indicator.

c. Electrical Property Measurements

To measure the resistance and capacitance of the selected MIL-L-7808 oils, a 100 ml oil sample was poured into a 250 ml beaker containing a tunable air capacitor. The voltage readings  $V_I$  and  $V$  (Figure 53) were recorded for input waveforms with frequencies of 10, 100, and 1,000 Hz to obtain the resistance, combined resistance and capacitance, and capacitance, respectively, of the oil sample.

d. Fluorescence Measurements

To measure the fluorescence of the MIL-L-7808 oils, the spectral range of 350 to 650 nm was monitored. The oil samples were analyzed neat in a 3 ml quartz cell with a 10 mm light path.

B.9 Procedure for Remaining Lubricant Life Assessment Test Candidates

a. Cyclic Voltammetric Techniques

The cyclic voltammetric techniques were performed with the CV-1B Voltammetry Electronics Control Module and recorded on a X-Y Recorder. After the initial evaluations of different working electrodes, the glassy carbon working electrode was used for all of the cyclic voltammetric techniques. The auxiliary

electrode was a platinum wire electrode and the reported potentials were referenced to the RE-1 Ag/AgCl reference electrode.

All of the cyclic voltammetric analyses were performed using an oil sample to acetone ratio of 1:50. The acetone contained  $\text{LiClO}_4$  (0.1M) as the electrolyte. The cyclic voltammograms were produced by scanning from 0.0 V to 1.1 V then back to 0.0 V at a rate of 500 mV/sec.

The cyclic voltammograms produced in the presence of organic bases were performed by adding the appropriate amount of a solution containing 5 percent organic base in acetone to the diluted oil sample. The cyclic voltammograms in the presence of an organic base were performed by applying a potential of +1.0 V to the working electrode and immediately decreasing the potential to 0.0 V at a rate of 500 mV/sec.

b. Reductive-Cyclic Voltammetric Techniques

The RCV technique was performed with a CV-1B Voltammetry Electronics Control Module. The working electrode was a glassy carbon voltammetry electrode and the auxiliary electrode was a platinum wire electrode. The reported potentials were referenced to a RE-1 Ag/AgCl reference electrode.

All of the RCV analyses were performed on a 60  $\mu\text{l}$  oil sample diluted with 3 ml of acetone containing 0.05M  $\text{LiClO}_4$  and 375 ppm of pyridazine. Except for the study to determine the effects of multiple scans on the results of the RCV technique, the RCV voltammograms were produced by scanning from 0.0 V to 1.0 V then back to 0.0 V at a rate of 0.5 to 1.0 V/sec.

For the effect of multiple scan study, the first scan was accomplished by applying a potential of 0.6 V to the working electrode and immediately decreasing the potential to 0.0 V at a rate of 500 mV/sec. The remaining scans were accomplished by scanning from 0.0 V to 1.0 V then back to 0.0 V at a rate of 500 mV/sec.

To record the RCV voltammograms on the Apple IIe microcomputer based data acquisition system, the Apple IIe

microcomputer was programmed to sample the CV-1B output at approximately 70 msec intervals. The signal of the oxidation wave was nullified by having the computer set its gain to zero. The computer recorded data was obtained by pushing the "A" key of the Apple IIe keyboard. The Apple IIe was programmed to simultaneously start the data acquisition procedure and close the scan switch (start scanning) of the CV-1B Module when the "A" key was pushed. The data requisition was performed for ten cycles at a scan rate of 1.0 V/sec. The maximum reduction wave height (minus the blank's reduction wave height), the  $\ln$  value of the maximum reduction wave height, and the percent RLL of the oil sample were then calculated and printed out on the  $\mu$ 92 Microline Printer. The computer program used to control the data acquisition of the Apple IIe microcomputer and to calculate the percent RLL of the oil sample was written in Basic language and is listed in Figure B-2.

c. Differential Scanning Calorimetric Techniques

(1) High Pressure-Differential Scanning Calorimetric Technique - Once the high pressure cell of the DuPont 9000/9900 Thermal System reached equilibrium at 200°-250°C (250°C optimum temperature) a weighed sample (approximately 2 mg equivalent to 2.5  $\mu$ l by volume) was placed in a Solid Fat Index (SFI) container which is an aluminum DSC pan with etched interior surfaces. The lid was laid on top of the SFI container and the SFI container was placed in the HP-DSC cell. The HP-DSC cell was immediately closed and then pressurized with oxygen to 100-500 psig (200 psig optimum). The moment the pan was placed in the cell is equal to 0.0 minutes. On average the pan reached temperature equilibrium (250°C) in 30 seconds and the pressure of the cell reached 200 psig in 60 seconds. The temperature was held at 250°C (isothermal) for up to 15 minutes to produce the thermogram of the oil sample (Figure 31). The thermogram was then analyzed as described in Section 2.

(2) Hermetically Sealed Pan-Differential Scanning Calorimetric Techniques - Once the DSC cell of the DuPont

```

80 POKE - 16295,0: REM OFF
90 N = 500
100 REM -----A113 INIT----- (INITIALIZE A/D CONVERTER)
110 HMEM: 38144
120 D% = CHR% (4): M = 1: SLOT = 5
130 PRINT D%: "LOAD GETA113, DELAY, A%9500"
140 DIM AX(1, M), DX(N), P(15)
150 AX(0, 0) = SLOT
160 AX(1, 0) = - M
200 REM -----A113 SET-----
210 GA = 1
220 AX(0, 1) = 0 + GA * 16
225 POKE 25, 0
230 REM -----PLOT SET-----
240 XO = 0: YO = 0: UO = 0: VO = 159
250 XM = N: YM = 4096: UM = 279: VM = 0
260 MX = (UO - UM) / (XO - XM)
270 MY = (VO - VM) / (YO - YM)
280 BX = UO - MX * XO
290 BY = VO - MY * YO
300 PR# 0: GOTO 430
390 IF L ( ) 0 THEN GOTO 1090
400 PRINT "RUN 100% LIFE STANDARD"
410 PRINT "HIT L"
420 GET C$: GOTO 2000
425 PR# 0
430 IF B ( ) 0 THEN GOTO 390
440 PRINT "RUN 0% LIFE STANDARD"
450 PRINT "HIT B"
460 GET C$: GOTO 2000
1090 PRINT "ENTER SAMPLE TYPE"
1092 PRINT "HIT 'B' IF 0% LIFE STANDARD"
1093 PRINT "HIT 'L' IF 100% LIFE STANDARD" (TYPE OF SAMPLE TO BE ANALYZED)
1094 PRINT "HIT 'S' IF OIL SAMPLE"
1095 GET C$
1096 IF C$ = "B" THEN B = 0
1097 IF C$ = "S" THEN PRINT "
ENTER SAMPLE IDENTIFICATION": INPUT
S$
2000 REM -----ACQUIRE-----
2005 HGR : HCOLOR= 3: HPLDT 0, VO
2006 POKE - 16295, 0: REM ON (START DATA ACQUISITION)
2020 FOR X = 0 TO N
2040 POKE 8, 1: CALL 38144
2050 DX(X) = AX(1, 1)
2060 U = MX * X + BX
2070 V = MY * DX(X) + BY
2090 NEXT X
2091 POKE - 16296, 1: REM OFF
2100 N = N - 1: TEXT : GOTO 4000
3000 REM -----SAVE-----
3010 INPUT "FILE NAME " : IF#
3020 PRINT D%: "OPEN " : IF#
3030 PRINT D%: "WRITE " : IF#
3040 FOR I = 0 TO N

```

Figure B-2. Computer Program Used to Acquire Data and Calculate the Remaining Lubricant Life on the Apple IIe Microcomputer.

```

3050 PRINT DX(I)
3060 NEXT I
3070 PRINT D$;"CLOSE "IF$
3100 RETURN
4000 REM -----INTEGRATE-----
4001 K = 1
4005 PR# 1;N0 = 0
4006 PRINT F#          (DETERMINE MAXIMUM WAVE HEIGHT OF EACH SCAN)
4010 FOR I = N0 TO N
4020 IF DX(I) > 0 THEN N1 = I: GOTO 4100
4030 NEXT I
4040 PR# 0; GOTO 7000
4100 FOR I = N1 TO N
4105 D = DX(I) / 4096
4110 SUM = SUM + D
4120 IF DX(I) < 0 THEN N0 = I: F(K) = DMAX: SUM = 0: DMAX = 0: K = K + 1
4130 IF D > DMAX THEN DMAX = D
4140 NEXT I
4170 PR# 0; GOTO 7000
5000 REM -----LOAD-----
5010 IS = ""
5020 PR# 1
5030 PRINT IS;"H"
5040 PR# 0
5050 RETURN
6000 REM -----LOAD-----
6010 INPUT "FILE NAME "IF$
6020 PRINT D$;"OPEN "IF$
6030 PRINT D$;"READ "IF$
6040 FOR I = 0 TO N
6050 INPUT DX(I)
6060 NEXT I
6070 PRINT D$;"CLOSE "IF$
6100 RETURN
7000 REM -----VIEW-----
7005 HGR : HCOLOR= 3: H$LOT 0,V0
7010 I = 0
7020 FOR K = 0 TO N
7030 U = MX + X + BX
7040 V = MY + DX(Y) + BY
7050 H$LOT TO U,V
7060 NEXT X
8000 PR# 1          (CALCULATE PERCENT REMAINING LUBRICANT LIFE)
8001 IF C# = "B" THEN B = 0
8005 AVE = (P(7) + P(8) + P(9) + P(10) - (4 * B)) / 4
8010 IF C# = "S" THEN GOTO 8080
8050 IF C# = "B" THEN B = AVE + .03
8060 IF C# = "L" THEN L = AVE
8065 PRINT "OX LIFE = "L
8066 IF L < 0 THEN PRINT "100% LIFE = "L
8070 IF C# = "B" OR C# = "L" THEN GOTO 425
8075 IF L < 0 THEN GOTO 8300
8080 W = 31.2 / L
8082 S = AVE + W
8085 IF S < 0 THEN GOTO 8900
8090 Y = LOG (S)
8100 PER = (Y + .56) / .04
8105 DEF FN A(Z) = W * (Z - B)
8107 PRINT : PRINT
8108 PRINT "SAMPLE 1:"IS$
8110 PRINT "7-10 PEAK HEIGHTS(UA) = " FN A(P(7));" " FN A(P(8));" " FN
A(P(9));" " FN A(P(10))
8120 PRINT "AVERAGE PEAK HEIGHT(UA) = "L
8135 PRINT "LN OF AVE. PEAK HEIGHT = "Y
8140 PRINT "PERCENT REMAINING LUBRICANT LIFE="PER;"%"
8150 GOTO 8900
8200 PRINT "ERROR---REPEAT ANALYSIS"
8210 GOTO '90
8220 PR# 0
8230 GOTO 1090

```

Figure B-2. Computer Program Used to Acquire Data and Calculate the Remaining Lubricant Life on the Apple IIe Microcomputer. (Concluded).

9000/9900 Thermal System reached equilibrium at the preset temperature, a 0.2-2.0  $\mu\text{l}$  sample (0.2  $\mu\text{l}$  optimum) was pipetted into the DSC pan. After the hermetic cover was placed into the DSC pan, the DSC pan was placed in the lower hermetic die. The DSC pan was then hermetically sealed using the preforming tool and sample encapsulating press.

In the case of the oxygen atmosphere, the DSC pan containing the sample, the hermetic cover, and the sample encapsulating press were placed inside a glove bag. The glove bag was purged of air by a strong flow of oxygen for about 5 minutes. The flap of the glove bag was then loosely folded and clipped, and the oxygen flow was adjusted to a rate that kept the glove bag slightly inflated during the sealing procedure. The DSC pan was then hermetically sealed as previously described.

The hermetically sealed pan was then placed in the DSC cell and the analysis time started immediately upon closure of the DSC cell. The temperature of the DSC cell was held at the initial temperature for 1 minute. The temperature was then held constant at the initial temperature until the completion of the test (isothermal) or increased at a rate of 3°C/minute until the completion of the test (ramped). The thermogram displayed in Figure 104 demonstrates the method used to determine the onset of oxidation time.

(3) Threaded Sealed Pan-Differential Scanning Calorimetric Technique - Once the DSC cell of the Perkin Elmer 7 Series Thermal System reached equilibrium at 100°C, a 2  $\mu\text{l}$  sample was pipetted into the lower half of the stainless steel, threaded DSC pan. A copper ring was placed on the guiding pins of the sealing tool. The upper and lower halves of the pan were screwed together to seal the pan. The sealed pan was then placed in the DSC cell and the temperature allowed to come to equilibrium for 1 minute. The analysis time was initiated by increasing the temperature from 100° to 250°C at 500°C/minute. Once the temperature of the sample reached 250°C, the temperature was held constant until the completion of the test.

d. Chemical Stressing Technique

(1) Colorimetric Technique

The appropriate amount (0.75 ml optimum) of a BDN solution ( $3.03 \times 10^{-4}$  M) prepared in toluene and 10-50  $\mu$ l (35  $\mu$ l optimum) MIL-L-7808 oil sample were pipetted into a 1 dram, flint glass vial. The cumene hydroperoxide (0.50 ml) was then added to the reaction system, the vial was stoppered, shaken by hand, and then placed inside an aluminum block heated to 25°-40°C (35°C optimum). The vial was positioned in front of a detector (UDT 10DP, United Detector Technology, Santa Monica, California). A 2 mm diameter, 2 mW beam from a Helium-Neon Laser (Spectrophysics Model 133, Mountain View, California) with a wavelength of 632.8 nm was aligned so that it passed through the vial onto the detector. In order to cancel signals from room light, the laser beam was passed through a chopper and associated lock-in-amplifier (PAR, Dynatrac 3, Stanford, Connecticut). The signal from the detector was amplified and then plotted versus time on a X-Y Recorder (Houston Instruments, Model 2000). The BDN decoloration induction time is defined as the length of reaction time required to obtain a 25 percent decrease in the absorption of the BDN solution.

(2) Modified Ford Method - Once the temperature of the reaction system stabilized at 60°C, a magnetic stirrer, 4 ml of the AIBN in chlorobenzene (0.2-0.5 M) (0.2 M optimum) solution, and 20  $\mu$ l of the oil sample were pipetted into the 25 ml flask. Oxygen was then bubbled rapidly through the reaction solution for one minute. After one minute the oxygen flow was stopped and the oxygen inlet tube removed. The reaction system was sealed off with a sleeve type serum bottle stopper and the temperature allowed to equilibrate for two minutes with continuous stirring. An easily oxidizable substance [benzaldehyde (0.5 ml) optimum] was then injected through the stopper into the stirred reaction solution. An equal volume of oxygen was removed with the syringe to set the pressure of the reaction vessel to atmospheric pressure (columns of acetone in the U-tube manometer level). The

reaction time of 0 minutes coincides with the leveling of the acetone columns. The pressure changes of the reaction system were monitored by recording the pressure every 30 to 60 seconds and then plotting the pressure changes versus reaction time (Figure 45). The induction time for this work is defined as the length of time required for the oxygen absorption to result in a pressure decrease of 18 Torr.

## REFERENCES

1. B. Conway and E. Rudd, Technique of Electroorganic Synthesis, Techniques of Chemistry, N. Weinberg, ed., John Wiley and Sons, Inc., New York, 1974.
2. A. Zeman, et al., Aging of Neopentyl Polyol Ester Oils. I. Evaluation of Aviation Turbine Oils by Determination of Residual Antioxidative Capacity, Tribol. Schmierungstech, 31: 72, 1984.
3. M. Braid, Process for Dimerizing Diarylamines, U.S. Patent No. 3,759,996, September 18, 1973.
4. S. Wawzonek and T. W. McIntyre, Electrolytic Oxidation of Aromatic Amines, J. Electrochem. Soc., 114: 1025, 1967.
5. J. Bacon and R. Adams, Anodic Oxidations of Aromatic Amines. III. Substituted Anilines in Aqueous Media, JACS, 90: 6596, 1968.
6. D. Clark, S. Weeks, and S. Hsu, Chemiluminescence of Fuels and Lubricants-A Critical Review, Lub. Eng., 39: 690, 1983.
7. H. Ravner and H. Wohltjen, The Determination of the Oxidative Stability of Several Deuterated Lubricants by an Electronic Gas Sensor, Lub. Eng., 39: 701, 1983.
8. M. Evans and R. Newton, Inverse Gas Chromatography in the Study of Polymer Degradation. Part 3. Study of the Inhibited Oxidation of Squalene as a Model for Antioxidant Protected, Natural Rubber Vulcanizates, Chromatographia, 12: 83, 1979.
9. T. Sarnavskaya and E. Lebedev, New Methods to Evaluate the Resistance of Synthetic Oils to Thermal Oxidative Destruction, Khim. Technol. Topliv Masel, 5: 61, 1975.
10. C. Ku and S. Hsu, A Thin-Film Oxygen Uptake Test for the Evaluation of Automotive Crankcase Lubricants, Lub. Eng., 40: 75, 1984.
11. E. Cvitkovic, E. Klaus, and F. Lockwood, A Thin-Film Test for Measurement of Oxidation and Evaporation of Ester-Type Lubricants, ASLE Trans., 22: 395, 1979.
12. E. Nikonorov, Evaluation of Thermal and Thermal-Oxidative Stability of Synthetic Lubricants by Derivatographic Method, Khim. Technol. Topliv Masel, 4:36, 1983.
13. R. Blaine, Thermal Analytical Characterization of Oils and Lubricants, American Laboratory, January 1974.

14. S. Hsu, A. Cummings, and D. Clark, Evaluation of Automotive Crankcase Lubricants by Differential Scanning Calorimetry, Society of Automotive Engineers, Special Pub, SP-526, Paper No. 821252, 1982.
15. I. Tiunova, et al., Use of Thermal Analysis for Predicting the Service Life of Lubricating Oils, Neftepererab. Neftekhim., 5: 21, 1975.
16. A. Zeman, Differential-Scanning-Kalorimetrie (DSC, PDSC)-Möglichkeiten bei der Beurteilung der Thermisch-Oxidativen Stabilität von Synthetischen Fluggasturbinölen, Schmiertechnik and Tribologie, 29: 55, 1982.
17. P. Bartl and A. Zeman, Quality Control of Used Synthetic Aviation Turbine Oils by Analytical Methods, JOAP International Symposium Proceedings, Pensacola, Florida, May 1983.
18. K. Enmanji, Estimation of Relative Efficiency of Antioxidants by Using the Decoloration Rates of the Nickel Dithiolate Complex, Nippon Kagaku Kaishi, 6: 796, 1979.
19. L. Mahoney, et al., Determination of the Antioxidant Capacity of New and Used Lubricants; Methods and Applications, Ind. Eng. Chem., Prod. Res. Div., 17: 250, 1978.
20. L. Mahoney, et al., Time-Temperature Studies of High Temperature Deterioration Phenomena in Lubricant Systems: Synthetic Ester Lubricants, Report No. AFOSR-TR-80-0065, Air Force Office of Scientific Research, Washington, D.C., 1980.
21. S. Korcek, et al., Antioxidant Consumption and Oxidative Degradation of Lubricants, NBS Special Publication 584, Proceedings of Joint Conference on Measurements and Standards for Recycled Oil/Systems Performance and Durability, Gaithersburg, Maryland, October, 1979.
22. M. Uri., Thermal and Photochemical Autooxidation., 8: 125, 1970.
23. R. Mair and A. Graupner, Determination of Organic Peroxides by Iodine Liberation Procedures, Anal. Chem., 36: 194, 1964.
24. E. Levin and A. Yamshchikov, Electrochemical Reduction of Organic Hydroperoxides, Elektrokhimiya, 4: 54, 1968.
25. C. Iditoru and D. Aikens, Cyclic Voltammetry Determination of ,'-Dimethylphenyl Hydroperoxide, Revue Roumaine de Chimie, 23: 959, 1978.
26. Y. Chertkov and T. Kirsanova, Oxidation Potential-A Common Characteristic for the Oxidizability of Engine Fuels, Khim. Tekhnol. Topliv Masel, 3: 57, 1976.

27. Y. Chertkov and A. Gorenkov, Oxidation of Distillate Engine Fuels by Permanganometric Method, Khim. Tekhnol. Topliv Masel, 1: 37, 1983.
28. Mobil Corporation, British Patent No. 1,117,714, June 19, 1968.
29. E. Jantzen, Early-Stage Detection of Oil Changes in Aircraft Engines, AGARD Conference Proceedings, 1971.
30. E. Jantzen, Investigation of Aircraft Turbine Oils from Aircraft Engines, Report No. DLR-FB-70-07, Deutsche Forschungs-Und Versuchsantalt Fuer Luft-und Raumfahrt, Munich, February, 1970.
31. F. Oehme, Dielectric Measurements in Hydrocarbon Oils. I. Determination of the Oxidation Tendency of Lubricating Oils by Dielectric Measurements, Erdol and Kohle, 13: 740, 1960.
32. F. Oehme, Dielectric Measurements in Hydrocarbon Oils. II. Conductivity Loss and d.c. Conductivity of Lubricating Oils, Erdol and Kohle, 14: 711, 1961.
33. G. Shor, et. al., Effect of Solid Phase Potential on Some Properties of Lubricating Oils, Khim. Technol. Topliv. Masel, 16: 26, 1970.
34. G. Shor and V. Lapin, Appearance of an Electrical Field During the Use of Lubricating Oils, Electrichestkiye Yavlianiya Treniya Pri Rezanii Metallov, 12: 108, 1969.
35. H.A. Smith, Evaluation of Complete Oil-Breakdown-Rate Analyzer (COBRA Instrument), Report No. AFAPL-TR68-121, Air Force Aero Propulsion Laboratory, Wright-Patterson Air Force Base, Ohio, November, 1968.
36. H.A. Smith, Complete Oil-Breakdown-Rate Analyzer (COBRA) for Identifying Abnormal Operating Turbine Engines, JOAP International Symposium Proceedings, Pensacola, Florida, May, 1983.
37. V. Alekseev and A. Tobolova, Applications of Luminescence Analysis Techniques in the Regeneration of Lubricating Oils, Zavod. Lab., 33: 992, 1967.
38. M. Khalupcvskii, Luminescent Analysis of Lubricating Oils, Ind. Lab., 28: 206, 1962.
39. J.B.F. Lloyd, Synchronized Excitation of Fluorescence Emission Spectra, Nature, Physical Sciences, 231: 64, 1971.
40. K. Masuko, Fluorescence of Oils II. Fluorescent Spectra of Lubricating Oils, Kagaku Keisatsu Kenkyusho Hokoku, 15: 325, 1962.

41. V. Krasnova, Luminescence Analysis of Petroleum and Lubricating Oils, Zavod. Lab., 11: 561, 1947.
42. P. Sniegowski, A Kinetic Study of Lubricant Antioxidant Depletion in Aircraft Gas Turbine Engines, Lub. Eng., 41: 11, 1985.
43. J. Walker and W. Tsang, Characterization of Lubricating Oils by Differential Scanning Calorimetry, Society of Automotive Engineers, Paper No. 801383, October 1980.
44. D. Clark, E. Klaus, and S. Hsu, The Role of Iron and Copper in the Oxidation Degradation of Lubricating Oils, Lub. Eng., 41: 280, 1985.
45. B. Baber, et al., Development of Lubricant Screening Tests and Evaluation of Lubricants for Gas Turbine Engines for Commercial Supersonic Transport, AFWAL Report No. ASD-TDR-63-264, March 1963.
46. W. Rhine, C. Saba, and R. Kauffman, Spectrometer Sensitivity Investigation on the Spectrometric Oil Analysis Program, Report No. NAEC-92-169, Naval Air Engineering Center, Lakehurst, New Jersey, 1982.